DEVELOPMENT AND APPLICATION OF A GROUND-COUPLED HEAT PUMP SIMULATION MODEL FOR RESIDENTIAL CODE-COMPLIANCE SIMULATION IN TEXAS

A Dissertation

by

SUNG LOK DO

Submitted to the Office of Graduate and Professional Studies of
Texas A&M University
in partial fulfillment of the requirements for the degree of

DOCTOR OF PHILOSOPHY

Chair of Committee,	Jeff S. Haberl
Committee Members,	Charles Culp
	Liliana Beltran
	Michael Pate
Head of Department,	Ward V. Wells

May 2014

Major Subject: Architecture

ABSTRACT

The intent of this study was to improve residential energy efficiency in Texas by developing an improved tool for home builders and code officers to use for evaluating their designs. It was achieved by developing a new ground-coupled heat pump (GCHP) model for residential systems to be used with the DOE-2.1e simulation program. To accomplish this, this study investigated closed-loop ground heat exchanger (GHX) models, including horizontal, surface water, and vertical GHX models.

This study selected a case-study house in Texas which has a custom-built GHX using a combination of a horizontal GHX and a surface water GHX. This study developed a custom-built GHX model for the case-study house to calculate the entering water temperatures (EWTs). The custom-built GHX model was then validated using the measured EWT data from the case-study house. The results showed the monthly average EWTs differences between the measured and calculated EWTs were observed to be about 2.2 F during the heating season and about 3.2 F during the cooling season. Therefore, this study concluded the slightly over-estimated EWTs were acceptable considering the other uncertainties of the field conditions.

In addition, a vertical GHX DOE-2.1e model was developed by using the DOE-2.1e FUNCTION command. The g-function values approximated in this study was used for the vertical GHX DOE-2.1e model. To develop a new DOE-2.1e GCHP simulation model, this study then incorporated the vertical GHX DOE-2.1e input FUNCTION within an air-source heat pump (ASHP) simulation module by modifying existing DOE-

2 calculation algorithms. To evaluate the new DOE-2.1e GCHP model, this study also developed simplified residential ASHP/GCHP base-case models for Houston and Dallas, using DOE-2.1e, eQUEST, IC3, REM/Rate, and EnergyGauge. The DOE-2.1e simulation results were then compared against the other programs to verify the accuracy of the new DOE-2.1e GCHP model. The comparison showed good agreement in the total site energy use within 3.3 MMBtu/yr (5.3%) differences. In addition, the simulation results showed the GCHP system benefits: for the total site energy savings, 9.7% in Houston and 13.1% in Dallas, and for the heating plus cooling energy savings, 27.3% in Houston and 35.3% in Dallas.

DEDICATION

To my loving father, mother, and wife,

Who have sacrificed so much for me

ACKNOWLEDGEMENTS

Completion of this doctoral dissertation was not possible without assistance, support, encouragement, and love of a great number of individuals around me. They have been a part of my Ph.D. journey over the past six years. No words come close to describing my gratitude to them, but I would love to express my sincere gratitude to all of them here. First and foremost, I would like to express my deepest appreciation to my advisor, Dr. Jeff Haberl. Without his invaluable advice and guidance, this study could not be achieved. Especially, I will always remember his humor and gesture which gave me relaxation and encouragement in the journey.

I would also like to thank my committee members: Dr. Charles Culp for his comments, encouragement, and support during this journey; Dr. Liliana Beltran for her advice and comments about architectural view points; and Dr. Michael Pate for his guidance and recommendation on the calculation methodology.

I would like to acknowledge Dr. Juan-Carlos Baltazar who continuously supported me in various ways. Especially, he spent a lot of time to listen my thoughts and ideas about the simulation methods in this study. My sincerely thanks go to Dr. Larry Degelman who allowed me to measure his system. I will not forget all of his kindness and help. In addition, regarding the field measurement, I am thankful to Kelly Milligan. Without his help, I could not start the field measurement on time.

Many thanks also go to all of my friends and colleagues who shared their ideas, discussed various issues with me, and encouraged me. In addition, special thanks go to

the Energy Systems Laboratory at Texas A&M University, which supported me financially.

I would love to express my appreciation to my loving family who gave me unconditioned love and continuous trust. My father, Choonho, always supported me at every stage of my life. My mother, Geumok, trusted and encouraged me whenever I was in trouble. My sisters took care of my parents all the time instead of me. My son, Hyunseung, gave me a lot of joy and peace during this journey. Finally, but by no means least, I would like to thank my wife, Youngha, who longed to see this achievement come true with incredible patience and love.

TABLE OF CONTENTS

Page

LIST OF FIGURES

Page

LIST OF TABLES

Page

CHAPTER I

INTRODUCTION

1.1. Background

Several major political issues worldwide are increasing non-renewable energy use, which contributes to atmospheric climate change (Bernstein et al., 2008). Increasing use of the fossil fuels (i.e., coal, natural gas, oil), which are non-renewable resources, may be contributing to worldwide climate change through increasing carbon dioxide (CO2) levels. Additionally, increased worldwide energy use has led to higher energy prices, which are a major concern for the world's economy.

Concerns about climate change and higher energy prices have created attention about improving the efficiency of heating and cooling systems. For example, the use of efficient ground source heat pump (GSHP) systems is increasing for heating and cooling buildings. GSHP systems utilize relatively constant ground temperatures instead of ambient temperatures for residential and commercial heat pump system applications, which take advantage of the fact that the ground is warmer than the ambient air in the winter and cooler than the ambient air in the summer, leading to higher heat pump system efficiency. Typical GSHP systems are equipped with water-source heat pumps and ground heat exchangers, where heat is extracted from the ground in the heating mode, or heat is rejected to the ground in the cooling mode. GSHP systems, therefore, reduce the amount of electricity used by the heat pump system by utilizing geothermal energy to more efficiently heat and cool buildings and/or provide domestic water

heating. The International Ground Source Heat Pump Association (IGSHPA) claims that GSHP systems are one of the most efficient residential heating and cooling systems available today, with heating efficiencies 50 to 70% higher and cooling efficiencies 20 to 30% higher than air-source heat pump systems (IGSHPA, 2011a). Due to this advantage in saving energy, the US Environmental Protection Agency (US EPA) has endorsed GSHP systems as the most energy-efficient, environmentally clean, and cost-effective space conditioning systems available (EPA, 1993). In addition, GSHP systems have another advantage in that the entire system can be located inside a house with only two insulated pipes connecting the heat pump (HP) system to the ground heat exchangers (GHXs). This feature gives a life expectancy of 20 years or more due the reduced wear and tear that a traditional air-source system experiences. This is a substantial improvement over air-source heat pump (ASHP) systems, which have a life expectancy of only 10 to 20 years (Beca, 2009).

GSHP systems are classified by ground heat exchanger configuration as follows: the ground-coupled heat pump (GCHP), groundwater heat pump (GWHP), and surface water heat pump (SWHP). Although different types of GSHP systems vary in the ways the ground temperatures are delivered to the heat pump, the main concept in utilizing the ground as a heat source/sink is the same. (ASHRAE, 2007b). The selection of the best GSHP system is largely dependent on the local, geological, and thermal characteristics of the soil at a site. The system used most widely is the GCHP system, which uses closed-loop GHXs since this technology can be applied virtually anywhere and has minimal disturbance to the ground water (i.e., aquifer). The GCHP system typically has

two types of closed-loop GHXs: a vertical closed-loop and a horizontal closed-loop. In residential use, the vertical closed-loop GHX is used more commonly than the horizontal loop GHX due to the reduced GHX installation area required (Lund et al., 2004).

In spite of their increasing popularity, various difficulties continue to exist regarding the utilization of the GCHP system. These include: the high initial cost of GCHP systems, limitations in GCHP design and installation infrastructure, and a lack of new technologies and designers to improve GCHP system performance. In addition, the analysis of GCHP systems requires a reliable, easy-to-use simulation tool for accurately predicting GCHP systems performance (Liu and Hellström, 2006), which is not always available with certified code-compliant simulation programs. RESNET[1] have accredited three International Energy Conservation Code (IECC) code-compliance software tools: Residential EnergyGauge, IC3, and REM/Rate. Two of the RESNET-certified software tools (Residential EnergyGauge and REM/Rate) have the GCHP system calculation. However, they provide approximated estimation of the GCHP system and do not provide any detailed technical reports for the estimation.

Hourly whole-building computer simulation programs are widely accepted for analyzing and evaluating complex building performance to achieve energy efficiency in building energy research. In 2007, the publicly funded International Code-Compliant Calculator (IC3) was created to help homeowners satisfy the Texas Building Energy Performance Standards (TBEPS). IC3 is currently used by builders, home energy raters,

[1] Residential Energy Services Network (RESNET) is an independent and non-profit organization for building energy efficiency rating and certification systems in U.S. founded in 1995

and code officials to calculate the energy performance of new single-family houses in Texas (Liu et al., 2008). IC3 is a free, RESNET-certified, web-based tool that uses the nationally recognized DOE-2 simulation program and Texas weather data to predict the energy performance of a residence (Gilman et al., 2008). The IC3 program can simulate most building features found in residences with the exception of GCHP systems. However, the DOE-2 program (DOE-2.1e) used by the current IC3 program does not have a GCHP model even though several other non-web-based computer simulation tools (e.g., EnergyPlus, eQUEST, TRNSYS, EnergyGauge, REM/Rate, etc.) have various types of GCHP system models. In addition, none of the RESNET-certified software tools can accurately predict GCHP systems performance and also provide detailed technical report about the GCHP performance calculation. Therefore, in order to simulate the performance of a residential GCHP system using RESNET-certified IC3, which is becoming a popular choice for homeowners who seek to build high performance houses (Liu and Hellström, 2006; Rybach, 2005), a new GCHP model for the DOE-2 simulation program (DOE-2.1e) needs to be developed.

1.2. Purpose and Objective

The purpose of this study is to improve residential energy use efficiency in Texas by developing an improved tool for home builders and code officers to use for evaluating their designs.

The objective is to develop a ground-coupled heat pump (GCHP) model with closed-loop ground heat exchangers for residential systems to be used with the DOE-

2.1e simulation program. This will be accomplished by reviewing existing technologies and methods to calculate GCHP performance, finding a reasonable method that simulates a GCHP system, and developing a GCHP simulation model for the DOE-2.1e program to be incorporated into the International Code-Compliant Calculator (IC3) program. Thus, the objectives of this study are:

1. Investigating and evaluating existing closed-loop ground heat exchanger (GHX) models using in whole-building simulation programs;
2. Developing a custom-built GHX model for a case-study residential building in Texas;
3. Validating the custom-built GHX model using measured data from the case-study residential building;
4. Developing a vertical GHX model for the DOE-2.1e simulation program with the DOE-2.1e FUNCTION commands;
5. Developing a GCHP simulation model for the DOE-2.1e simulation program using the vertical GHX input FUNCTION;
6. Developing simplified residential base-case simulation models with an air-source heat pump (ASHP) system, using the DOE-2.1e, eQUEST, IC3, EnergyGauge, and REM/Rate programs;
7. Developing simplified residential base-case simulation models with a GCHP system, using the DOE-2.1e, eQUEST, EnergyGauge, and REM/Rate programs; and

8. Verifying and testing the newly developed DOE-2.1e GCHP system simulation model against eQUEST, EnergyGauge, and REM/Rate.

1.3. Organization of the Dissertation

This chapter has discussed the background, purpose, and objectives of the research.

Chapter II discusses the previous research associated with this work to provide the basis for the development of this research. It provides existing residential building energy codes and standards, residential building certification software tools, the International Code-Compliant Calculator (IC3) code-compliant simulation program, the previous literature about ground source heat pump (GSHP) systems, previous work and methodologies on ground-coupled heat pump (GCHP) system simulations, and whole-building computer simulation programs used in the residential building energy analysis.

Chapter III discusses the importance of this study and contribution in this research area, and discusses the scope and limitation of the research.

Chapter IV discusses the methodologies to conduct this study. It includes description of the closed-loop ground heat exchanger (GHX) models, case-study house and system measurement, development of the custom-built GHX model for the case-study house, validation of the custom-built GHX model with measured data, development of the DOE-2.1e GCHP simulation model using the closed-loop vertical GHX models, simplified residential base-case simulation models using an air-source

heat pump (ASHP) system and a GCHP system, and verification of the DOE-2.1e GCHP simulation model with other GCHP simulation programs.

Chapter V provides results of this study. It is organized in two sections: the custom-built GHX model and the vertical GHX model. The results of the custom-built GHX model section include the measured data analysis of the case-study house and the Energy Systems Laboratory's Solar Test Bench (STB), the calculated temperatures using the custom-built GHX model, validation of the calculated entering water temperatures using the custom-built GHX model with the measured data. The results of the vertical GHX model section include the results of the residential ASHP base-case model, the results of the vertical GHX DOE-2.1e model, the results of the residential GCHP base-case model, and verification of the DOE-2.1e GCHP simulation model with other GCHP simulation programs.

Finally, Chapter VI summarizes this study and discusses future work for this study.

CHAPTER II

LITERATURE REVIEW

2.1. Introduction

In order to perform the literature review for this study, the following categories of literature were reviewed: 1) existing residential building energy codes and standards, 2) residential building certification software tools, 3) the IC3 code-compliant simulation program, 4) the previous literature about GSHP systems, 5) previous work and methodologies on GCHP simulations, and 6) whole-building computer simulation programs used in residential building energy analysis.

The sources of literature include the following: 1) the American Society of Heating and Air-Conditioning Engineers (ASHRAE) journal, the Solar Energy journal, the Energy and Buildings journal, the Building and Environment journal, the Building Performance Simulation journal, the Energy Research journal, the Renewable Energy journal, and the Applied Thermal Energy journal; 2) proceedings of the International Conference Energy Storage, the International Energy Agency Heat Pump Conference, and the Symposium on Improving Building Systems in Hot and Humid Climates; 3) building energy codes, including the International Energy Conservation Code (IECC), the International Residential Code (IRC), and ASHRAE Standard 90.2; 4) ASHRAE Handbooks: 5) publications of the Oak Ridge National Laboratory (ORNL), the International Ground Source Heat Pump Association (IGSHPA), the Geo-Heat Center, the US Department of Energy (DOE), the CanmetENERGY Technology Centre; and 6)

dissertations and theses related to GCHPs from Oklahoma State University, University of Lund in Sweden, Texas A&M University, and others.

2.2. Existing Residential Building Energy Codes and Standards

Energy codes and standards provide guidance and requirements to builders, designers, and energy modelers that are cost-effective in saving energy to lower monthly utility bills. A number of energy codes and standards have been developed and adopted to improve the energy performance of residential houses. The most relevant resources for this study include: the International Energy Conservation Code (IECC) (ICC, 2009a), the International Residential Code (IRC) (ICC, 2009b), and ASHRAE Standard 90.2-2007 (ASHRAE, 2007a). The main purpose of this review is to see applicable building energy codes requirements for a low-rise single-family residential building.

2.2.1. International Energy Conservation Code (IECC)

The IECC is a model energy building code based on experiences gained through decades of code development. The first IECC (1998) was based on the 1995 edition of the Model Energy Code (MEC). The MEC contained energy efficiency criteria for new residential and commercial buildings and additions to existing buildings. It set minimum insulation requirements for the building envelope (e.g., ceilings, walls, floors, and foundations) and performance requirements for the mechanical, lighting, and power systems (DOE, 1999). Since 1998, the IECC has been revised and improved several times. The latest version of the IECC, released in early 2011, was the 2012 IECC.

Almost 40 states in the United States have adopted the IECC or MEC. Some states such as Alabama, Hawaii, Kansas, Mississippi, Missouri, North Dakota, South Dakota, and Wyoming do not have mandatory codes. Five states (California, Florida, North Carolina, Oregon, and Washington) have developed their own mandatory codes (BECP, 2009).

The IECC has two separate categories: residential buildings (low-rise single-family and low-rise multi-family), and commercial buildings (including high-rise multi-family not defined as residential buildings) (DOE, 2009). The IECC applies to new construction and additions, alterations, renovations, and repairs of existing buildings (ICC, 2006, 2009a). The IECC promotes energy efficiently in buildings through minimum code requirements, including: insulation and fenestration, building thermal envelope, energy efficient mechanical systems, and requirements for efficient electrical power and lighting systems.

The requirements provided by the IECC must follow either the prescriptive path or the performance path approach. The code requirements for the envelope and the system in the IECC are assigned by climate zone which are listed by state, county, and territories. For example, the 2009 IECC defined the City of Houston as Climate Zone 2 and has prescriptive provisions for that climate zone classification such as fenestration U-factor of 0.65, glazed fenestration solar heat gain coefficient (SHGC) of 0.30, R-13 wood frame wall insulation, R-30 ceiling insulation, R-13 above-grade floor insulation[2], and others. For the HVAC system in the Climate Zone 2, a minimum of R-8 insulation is required for the supply ducts in attics whereas all other ducts shall be insulated to a

[2] In the IECC, a floor is an above-grade floor exposed to ambient condition.

minimum of R-6. In the IECC, air conditioner systems shall comply with Federal minimum standard, including a Seasonal Energy Efficient Rating (SEER) of 13, a furnace minimum Annual Fuel Utilization Efficiency (AFUE) of 78% or higher, and a heat pump Heating Seasonal Performance Factor (HSPF) of 7.7 or higher.

2.2.2. International Residential Code (IRC)

The 2009 IRC provides a comprehensive prescriptive requirements for single-family or duplexes and for townhouses (less than three stories above grade) to regulate the construction (ICC, 2009b). It is also a comprehensive, stand-alone residential building code that contains minimum code requirements for the building, plumbing, mechanical, electrical, and energy system as needed for home assembly.

Both the 2009 IRC and the 2009 IECC have provisions for residential construction. However, there are several differences in the 2009 IRC and the 2009 IECC. First, the 2009 IECC includes other low-rise multi-family buildings such a multi-family apartments, whereas the 2009 IRC does not. In addition, the 2009 IECC covers residential buildings, including R-3 type buildings[3], as well as R-2 and R-4 type buildings three stories or less in height above grade (ICC, 2009a). On the other hand, groups R-3 and R-4 may also comply with the requirements of the 2009 IRC.

---

[3] The R-1 classification includes transient type housing consisting of hotels and motels; R-2 includes permanent type housing more than two dwelling units consisting of apartment houses and dorms; R-3 includes single detached houses and duplexes, not classified as R-1 and R-2, as well as adult and child day-care facilities that provide accommodations for five or fewer persons for less than 24 hours; and R-4 includes residential care/assisted living facilities that have more than 5, but less than 16, occupants, including staff (Ching and Winkel, 2007).

The 2009 IECC also addresses only energy whereas the 2009 IRC addresses all codes requirements including: structural components, thermal insulation, mechanical systems, plumbing systems, and others. Finally, whereas the 2009 IECC offers both a prescriptive path and a performance path, the 2009 IRC offers only a prescriptive path.

There are also some other differences in the prescriptive requirements. For example, regarding fenestration requirements, the 2009 IECC requires a glazed fenestration SHGC of 0.30 or lower whereas the 2009 IRC requires the SHGC of 0.35 in Climate Zone 1 through 3 (Liu et al., 2010). Above-grade floor insulation requirements, which are installed to maintain permanent contact with the underside of the subfloor decking, are different. The 2009 IECC requires R-38 floor insulation in Climate Zone 7 and 8 whereas the 2009 IRC requires only R-30 for those zones.

In Texas, the prescriptive energy efficiency provisions of the 2009 IRC were adopted as the energy code in Texas for single-family residential construction (three stories or less) and became effective on January 1, 2012[4]. The 2009 IECC is the current state energy code for all other residential that don't meet the prescriptive requirements of the 2009 IRC, commercial, and industrial construction.

2.2.3. ASHRAE Standard 90.2-2007

ASHRAE Standard 90.2-2007 (Energy Efficient Design of New Low-Rise Residential Buildings) provides minimum requirements for the energy-efficient design

[4] Website for U.S. Department of Energy: http://www.energycodes.gov/states/state_info.php?stateAB=TX Date accessed: 2/15/2012.

of residential dwelling units, which include single-family houses and multi-family houses (of three stories or fewer, above grade) (ASHRAE, 2007a). In addition, manufactured houses (modular or mobile houses) are covered under ASHRAE Standard 90.2-2007, whereas they are not covered under the IECC and the IRC. ASHRAE Standard 90.2-2007 covers the building envelope, heating/air-conditioning systems and their equipment, and domestic hot water heating systems, as well as requirements for the overall building design alternatives and trade-offs. This standard also provides two optional methods for low-rise residential buildings to comply with it: a prescriptive path method and a performance path method, which is an annual energy cost budget method. In the prescriptive path, a proposed building must satisfies all applicable mandatory requirements of the residential building envelope and of the heating, ventilating, air-conditioning (HVAC) and service water heating equipment. On the other hand, in a performance path, which is the annual energy cost budget method, a proposed building can achieve performance compliance with this standard if the calculated (simulated) annual energy cost (AEC) of the proposed design is equal to or less than the AEC of the standard reference design. Even though this standard is not directly associated with this study, this standard is invaluable because it provides a comparative requirement for energy efficient design of residential dwelling units.

The energy codes and standards reviewed in this work are the 2009 IECC, the 2009 IRC, and the ASHRAE Standard 90.2-2007. For this study, the 2009 IECC will be used as the base line residential construction energy code for Texas since the 2009 IRC allows compliance with the 2009 IECC as an alternative to Chapter eleven, “Energy

Efficiency", and the ASHRAE Standard 90.2-2007 is not used for residential construction in Texas.

2.3. Residential Building Code-Compliant Software

IECC residential code-compliant software tools accredited by certification procedures of the Residential Energy Services Network (RESNET) are reviewed in this section. Several residential software tools have been developed to be used to determine if a building complies with the IECC residential code requirements. Residential code-compliant tools create different reports that are associated with the energy analysis, energy code compliance, energy rating, energy consumption, emissions reductions, and cost analysis. In some states, building code officials depend on certified, code-compliant simulations to determine if a home meets the state energy code requirements using the IECC performance-path approach.

In order to verify the accuracy and comparability of different IECC compliance software tools, RESNET has defined a suite of five software tests that are necessary for the software to perform to be RESNET certified, code-compliance software (Residential Energy Services Network, 2006), as follows:

- Test #1: Tier one of the Home Energy Rating Systems (HERS) Building Energy Simulation Test (BESTEST);
- Test #2: IECC code reference home auto-generation tests;
- Test #3: HVAC tests;
- Test #4: Duct distribution system efficiency (DSE) tests; and

- Test #5: Hot water system performance tests.

Tier one of the HERS BESTEST was developed by the National Renewable Energy Laboratory (NREL) for testing the building load prediction accuracy of simulation software. The IECC code reference home auto-generation tests verify the ability of the software tool to automatically generate the IECC Standard Reference Design Home. The HVAC tests verify the accuracy and consistency with which software tools predict the performance of the HVAC equipment. The DSE tests verify the accuracy with which software tools calculate the air distribution system loss. The hot water system performance tests determine the ability of the software to accurately predict hot water system energy use (Residential Energy Services Network, 2006). Regarding GSHP systems, testing of GSHP systems are indirectly included in the RESNET certification process through the use of the optional system types in the HVAC tests. However, in version of the RESNET certification procedures, there is a no direct test for GSHP systems.

Three IECC code-compliance software tools in 2013 have been accredited by RESNET[5]: EnergyGauge Version 2.8, the International Code Compliance Calculator (IC3) Version 3.12.4, and REM/Rate Version 12.91. OptiMiser was also accredited by RESNET as an IECC performance verification software tool in 2012, but its accreditation was expired in 2013. The four RESNET-certified (previously and currently) software tools are reviewed in the next section.

---

[5] Website for National Registry of Accredited IECC Performance Verification Software Tools: http://www.resnet.us/programs/iecc_programs
Date accessed: 02/10/2013.

2.3.1. OptiMiser

The OptiMiser software developed by EnergyLogic Inc. in Denver, Colorado, was a RESNET-certified IECC performance verification software tool to certify new homes including single- and multi-family in 2012. OptiMiser is also designed for an analysis of existing homes through the application of utility bill information (EnergyLogic, 2010). It complies with the 2006 IECC requirements only. It uses Variable-Base Degree Day (VBDD) Models for its energy estimating method. OptiMiser generates reports on home improvements including emissions reductions, energy savings, and cost effectiveness. It provides comprehensive results from historical energy usage of a home and provides financial analysis tools for users to help energy retrofit decisions. In addition, it also produces detailed cost estimates for major energy retrofit improvements, integrating material and labor costs.

However, The OptiMiser software does not have any renewable energy options like a solar photovoltaic (PV) system and does not appear to have the ability to evaluate GCHP system performance as well.

2.3.2. EnergyGauge

The Florida Solar Energy Center (FSEC) in Cocoa, Florida, developed EnergyGauge which is a home energy simulation software package (FSEC, 2011). It simulates building energy performance using the DOE-2.1e program. It has two main versions: USA Residential EnergyGauge and Commercial EnergyGauge. The USA Residential EnergyGauge is used for residential analysis including single- and multi-

family. EnergyGauge is also a RESNET-certified IECC software tool in 2013 (FSEC, 2011). It complies with the IECC requirements (i.e., the 1998, 2000, 2003 IECC, and 2004 IECC Supplement) whereas it does not comply with 2009 IECC requirements. One key feature of EnergyGauge is that it provides output for the Florida Building Energy Rating Guide, which provides HERS Index for the home (Fairey et al., 2002). In addition, it provides comprehensive reports including an Energy Star homes qualification analysis, annual and monthly energy use, a cost analysis, standard DOE-2 reports, and an air pollution reduction analysis.

It allows users to simulate home energy performance, which includes examining different energy saving and/or renewable energy options (i.e., a solar PV system and a solar hot water heating system), and to evaluates energy use and peak demand impacts of home energy-efficiency improvements.

The USA Residential EnergyGauge can calculate GCHP system performance with open and closed heat exchanger loops. However, it provides approximate GCHP system estimation. EnergyGauge utilizes the ground temperatures embedded in the DOE-2 weather files, which shows annual variations of monthly average ground temperatures at various depths. The ground temperatures were created with the equation developed by Kusuda and Achenbach (1965). In EnergyGauge, the monthly average ground temperatures are used directly in the GCHP system calculation by assuming that the monthly average values of the ground temperatures are equal to the values of the entering water temperatures (EWTs) from ground heat exchangers (GHXs) to the heat pump unit (D. Parker, personal communication, October 7, 2010). This method provides

a simplified estimation of the GCHP system because of several following reasons: 1) this method uses a RESYS (Residential System) subroutine (LBL, 1982a), with a refrigerant-to-air heat exchanger for the GCHP system calculation. However, the GCHP system is better modeled with a refrigerant-to-water heat exchanger, called Water-Source Heat Pump (WSHP), since the condenser in the GCHP system exchanges heat between water circulated in GHXs and refrigerant circulated in a Heat Pump (HP) unit; 2) this method is not more appropriate for vertical GHXs than horizontal GHXs. EnergyGauge may use annually same EWTs since the calculated ground temperatures have no variations when ground is deeper than around 35 ft from the ground level. This means that EnergyGauge assumes the vertical GHXs are infinitely long and EWTs are not affected by hourly/monthly/yearly system's heating and cooling loads. Therefore, this method is oversimplified. On the other hand, this method can predict some EWT variations affected by a weather basis when ground depth is less than 35 ft from the ground level. So, this method might be used more appropriately for horizontal GHXs; 3) this method uses monthly average temperatures embedded in the DOE-2 weather files. However, EnergyGauge performs an hourly annual computer simulation. This means that EnergyGauge should have approximately hourly GCHP system results, and not include hourly building loads to the GHXs; and 4) this method does not include the pump power consumption to circulate fluid through GHXs, which can significantly impact the GCHP system performance. Therefore, the method in EnergyGauge does not consider significant parameters such as building thermal loads, weather, and ground/ground heat exchangers thermal properties. That is, the GCHP system performance in EnergyGauge

does not vary depending on the significant parameters. In addition, EnergyGauge does not provide any technical reports about how their GCHP system calculation procedures were developed.

2.3.3. International Code Compliance Calculator (IC3)

The IC3 software was developed by the Energy Systems Laboratory (ESL) of the Texas A&M University System in College Station, Texas (ESL, 2010a). It is a publicly-funded, web-based, RESNET-certified, and IECC Performance Verification software tool that uses the DOE-2.1e simulation program. IC3 was designed to calculate the performance of new single- and multi-family residences according to the Texas Building Energy Performance Standards (TBEPS) (ESL, 2010b). It has been approved by the U.S. Environmental Protection Agency (EPA) and Texas Commission on Environmental Quality (TCEQ) for use in determining above-code compliance in support of statewide NOx emissions reductions credits (Liu et al., 2010). It is intended to cover new residences in Texas and works best with homes using wood framing, conventional systems, one or two stories, and homes that are under 10,000 square feet of conditioned floor space (ESL, 2010b). It complies with the IECC requirements (i.e., the 2000 IECC with the 2001 Supplement, the 2006 IECC Houston, the 2006 National Appliance Energy Conservation Act (NAECA) revisions, the 2009 IECC, and the 2009 IECC Austin requirements) for energy code compliance calculations and provides reports, including: an inspection list, energy analysis, % above code analysis, and a certificate.

However, the current IC3 does not have any renewable energy options and also does not have the ability to calculate GCHP performance.

2.3.4. REM/Rate

The REM/Rate software was developed by the Architectural Energy Corporation (AEC)[6] in Boulder, Colorado, for the Home Energy Rating Systems (HERS) providers. It is a software tool for residential energy analysis including single- and multi-family residences. REM/Rate is a RESNET-certified tool for code compliance, and can be used for home energy ratings (AEC, 2011). REM/Rate calculates residential system energy performance, annual energy costs, and annual net savings costs. It provides a comprehensive output by comparing the Rated Home to the Reference Home as defined in the "Mortgage Industry National Home Energy Rating Systems Standards" as promulgated by the RESNET, including: an energy analysis, cost analysis, air pollution reduction, and code compliance (AEC, 2011). It also calculates a HERS Index, and reports the results in tables and graphic format. REM/Rate performs the 1992, 1993, and 1995 MEC, the 1992 ASHRAE 90.2, and the IECC compliance analysis (i.e., 1998, 2000, 2003 IECC, and 2001, 2004 IECC Supplement, 2009).

REM/Rate even allows users to calculate the performance of a solar PV system, and can calculate the GCHP system performance with open and closed-loop ground heat exchangers using Air-Conditioning, Heating, and Refrigeration Institute (AHRI, formerly ARI) capacity and efficiencies. REM/Rate uses a neural network routine to

[6] Architectural Energy Corporation (AEC) is a division of United Technologies Corporation (UTC).

determine the overall efficiency of the heat pump and the ground loop given the equipment and ground loop characteristics. However, it is unknown how the neural network for the GCHP system operates due to it being a black box with no publications. Salcido who works at REM Software Technical Support Team said "…REM/Rate is probably not the best tool for GSHP modeling." and "… I am not sure of the accuracy." (R. Salcido, personal communication, August 15, 2012). In addition, REM/Rate is based on a climate similarity analysis, using heat balance equations on a seasonal basis. For example, REM/Rate aggregates hourly weather data into seasonal weather data and uses this to determine heating and cooling loads. It means REM/Rate presents approximate hourly simulation results and even peak load estimation of a building regardless a system type.

Table 2-1 provides a summary table that compares the IECC performance verification software tools accredited by RESNET. Four software tools were compared: OptiMiser, Residential EnergyGauge, International Code Compliance Calculator (IC3), and REM/Rate.

Table 2-1: Comparison of IECC Performance Verification Tools Accredited by RESNET

Software	OptiMiser	Residential EnergyGauge	IC3	REM/Rate
Developer	EnergyLogic	Florida Solar Energy Center	Energy Systems Laboratory	Architectural Energy Corporation
Location	Denver, CO	Cocoa, FL	College Station, TX	Boulder, CO
Target Building Type	Existing/New, SF/MF Residences	Existing/New, SF/MF Residences	New, SF/MF Residences	Existing/New, SF/MF Residences
Web-based	No	No	Yes	No
Free to Use	No	No	Yes	No
Application of Utility Bill Information	Yes	No	No	No
RESNET-certified 2006 IECC Code-compliant Software	No	Yes	Yes	Yes
Additional IECC Code-compliant	-	1998/2000/2003/ 2004* IECC	2000/2001*/ 2009 IECC; 2006 IECC Houston; 2009 IECC Austin	1998/2000/2001*/ 2003/2004*/2009/ 2012 IECC
Output	Energy Anlaysis; Cost Analysis; Pollution Analysis	Energy Analysis; Energy Star Homes Qualification; Cost Analysis; HERS Index; Standard DOE-2 Report; Pollution Analysis	Energy Analysis; % Above Code; Inspection List; Certificate	Energy Analysis; Cost Analysis; Code Compliance; HERS Index; Graphic Format Report
Renewable Energy Option	No	Yes (PV & Solar Thermal)	No	Yes (PV)
GSHP Calculation	No	Yes	No	Yes
Available GSHP Type	-	GCHP without open and closed loop	-	GCHP with open and closed loop
Technical Report for GSHP Calculation	-	No	-	No

Footnotes:

1. RESNET-certified code-compliant software is reviewed as of February 2013.
2. * means supplement
3. PV: Photovoltaic

In summary, four software tools were reviewed in this section: OptiMiser, EnergyGauge, IC3, and REM/Rate. OptiMiser was previously RESNET-certified and other three software tools are currently RESNET-certified. All of them comply with the 2004 supplement of the IECC and with the 2006 IECC. IC3 also complies with 2009 IECC and REM/Rate complies with 2009 and 2012 IECC additionally. Of four software tools, IC3 is only available program that is a free-to-use and has a web-based interface. Two software tools (EnergyGauge and REM/Rate) have the ability to calculate GCHP system performance, including: EnergyGauge which has a GCHP system without open/closed-loop design; and REM/Rate which has a GCHP system with open/closed-loop design. However, both software tools provide approximate estimation of the GCHP system and do not provide detailed technical reports for their GCHP system calculation.

2.4. The IC3 Code-Compliant Simulation Program

Residential energy codes and standards help to provide energy-efficient homes, which to reduce air pollution from electricity generated by fossil fuels (Liu et al., 2008). In May 2007, the Energy Systems Laboratory (ESL) released the International Code-compliant Calculator (IC3). The IC3 software is a publicly-funded, web-based, RESNET-certified, code-compliant software tool that builders, inspectors, architects, engineers, and others use to demonstrate the performance of proposed single-family residences according to the Texas Building Energy Performance Standards (TBEPS). The software is intended to simulate the code-compliance of the majority of site-built, single-family houses built in Texas (ESL, 2010a). IC3 is an easy-to-use tool that

calculates the code-compliance and above-code performance of a new home, and calculates the annual and Ozone Season Day (OSD) air pollution reductions due to the home's energy efficiency above code using the USEPA's eGRID[7] to convert energy savings to emissions reductions.

In the IC3 software, several simulation models have been created for different single-family configurations. During a simulation, one of the single-family configurations is modified for each house to accommodate the user's envelope, construction, and HVAC system. IC3 is based on the DOE-2.1e simulation program, which can be linked to a web-based graphical user interface or used in the DOE-2 Desktop Processor (DDP) to calculate the energy use from the code-compliant house and a proposed house (Liu et al., 2008).

In difference to IC3 where users can simulate only one house at a time in the web-based interface, the DDP allows users to run multiple simulations using an input spreadsheet. In both the IC3 and DDP program, the DOE-2.1e simulation program model is controlled by one large input file, which uses DOE-2's Building Description Language (BDL) and parametric inputs. The ESL faculty, staff, and graduate students created and tested IC3 using thousands of runs to simulate different types of configuration (Gilman et al., 2008). Presently, the current version of the BDL file[8] is 4.01.08. The BDL file used by the DOE-2.1e program has three major categories:

---

[7] eGRID is Emissions and Generation Resource Integrated Database of the United States Environmental Protection Agency (USEPA).

[8] This version is current as of 03/01/2012

LOADS, SYSTEMS, and PLANT[9]. The LOADS portion of the input file contains information about building, construction, space, and shading parameters.

Several major improvements to IC3 have been made to properly account for additional building energy performance features such as: the residential thermal distribution system (Kim, 2006); part-load performance calculations (Henderson et al., 2000); and the calculation of heating Energy Input Ratio (EIR) and cooling EIR values (Fairey et al., 2004). One of the major improvements to IC3 is the use of a duct model, which is based on ASHRAE Standard 152-2004[10] (Kim, 2006). Unfortunately, the DOE-2.1e (version 119) simulation program has simplified duct heat loss or gain calculation that represents a constant duct air loss or gain and a constant delta-T heat gain. As a result, the DOE-2.1e program does not predict duct heat loss or gain from an unconditioned space as accurately as a more complex model.

ASHRAE developed a more accurate duct model for ASHRAE Standard 152-2004 to determine the design and seasonal efficiencies of residential thermal distribution systems (ASHRAE, 2004). The ASHRAE duct model considers the impact of duct leakage, duct location, duct and attic insulation levels, and climate (Kim and Haberl, 2008). Subsequently, the ASHRAE duct model was incorporate into the DOE-2.1e input file for IC3 using FUNCTION commands in the SYSTEM portion of the BDL (Kim, 2006). Use of an ASHRAE Standard 152-2004 duct model allowed IC3 to more accurately predict duct heat loss or gain in an unconditioned space (i.e., attic). Another

---

[9] The Economics portion of DOE-2 is not used in IC3

[10] ASHRAE Standard 152-2004 is a method of test to determine the design and seasonal efficiencies of residential thermal distribution systems.

improvement to IC3 involved the Residential System (RESYS) routine, which provides more accurate part load energy use calculation and humidity predictions (Henderson et al., 2000). Regardless of the previous improvements, IC3 still needs additional improvements, including the ability to evaluate GCHP system performance.

In this section, the IC3 code-compliant simulation program is reviewed. IC3 is based on the DOE-2.1e simulation program, which does not have an accurate GCHP system performance calculation. Therefore, there is a need to develop a new GCHP system simulation model in the DOE-2.1e which will be an important improvement for IC3.

2.5. Ground Source Heat Pump (GSHP) Systems

The concept of a ground source heat pump (GSHP) system was first described in 1852 by Lord Kelvin at the University of Glasgow in Scotland (Lund et al., 2004) although his concept was based on extracting heat from outdoor air, not from the ground. In 1912, the Swiss turbine engineer, Heinrich Zoelly, patented the idea of using a heat pump to extract heat from the ground (rivers or groundwater) instead of outdoor air (Zogg, 2008; Spitler, 2005). However, their ideas were not implemented successfully until 1940's. Around 1945, Robert C. Webber in Indianapolis, Indiana, installed the first experimental residential system with his deep freezer, which used a closed-loop heat exchanger having a carrier fluid or refrigerant circulating through a pipe (Banks, 2012; IGSHPA, 2012b). In 1946, J. Donald Krocker built the first commercial ground source heat pump to heat a Commonwealth Building in Portland, Oregon, and in 1948 Professor

Carl Nielsen of Ohio State University designed the first residential ground source heat pump in his home (AES 2012).

GSHP systems utilize relatively steady ground temperatures (between 46˚F and 80˚F at 30 ft. below the ground surface throughout the year) as a heat source/sink for the heat pump to provide space heating, space cooling, and hot water (ASHRAE, 2007c). The GSHP system is more efficient than the Air-Source Heat Pump (ASHP) system because the ground temperatures are lower than ambient temperatures during the cooling season and higher than the ambient temperatures during the heating season. Using the ground as a heat source/sink rather than the ambient air increases the temperature difference between the heat source/sink and the condenser, which allows the GSHP compressor to be operated at a lower discharge pressure than the ASHP compressor. As the result, the GSHP system can be equipped with a smaller compressor than an ASHP system with a similar cooling capacity, resulting in less electricity consumption.

Figure 2-1 shows vapor-compression refrigeration cycle and description. Figure 2-2 shows a conceptual pressure enthalpy (P-h) diagrams for comparison of a typical ASHP and GCHP system.

However, the GSHP system analysis must also consider the additional pump electricity required to circulate water through ground heat exchanger (GHX). Fortunately, even though the pump power is added to the GSHP system power consumption, a GSHP system with a properly-sized pump uses less electricity for the overall system operation than an ASHP system (Hwang et al., 2009).

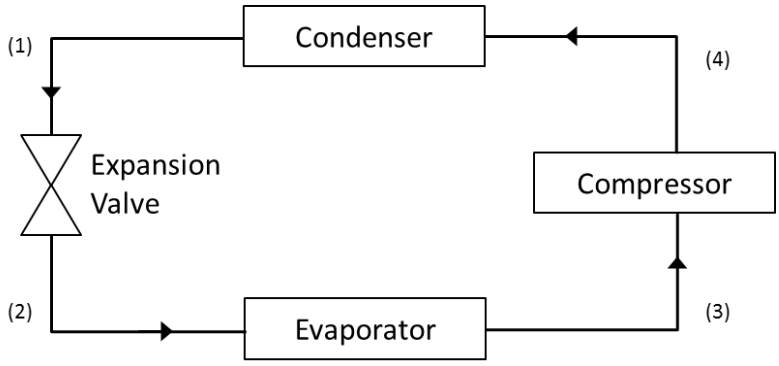

Vapor-Compression Refrigeration Cycle Process Description

3-4 Isentropic compression

4-1 Constant pressure heat rejection in the condenser

1-2 Throttling in an expansion valve

2-3 Constant pressure heat addition in the evaporator

Figure 2-1: Vapor-Compression Refrigeration Cycle and Description

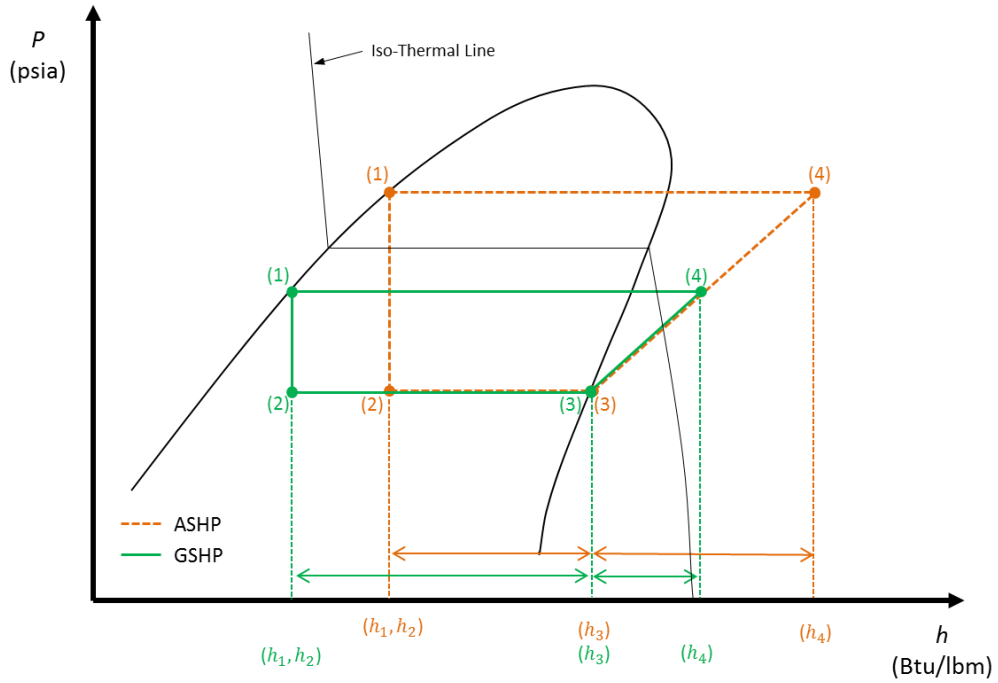

Figure 2-2: P-h Diagrams for an ASHP and GCHP System

The GSHP system is the general term that includes ground-coupled heat pumps (GCHP), groundwater heat pumps (GWHP), and surface water heat pumps (SWHP) (ASHRAE, 2007c). Although each of these systems utilizes the ground as a heat source/sink, they vary in the different ways the ground temperatures are delivered to the heat pump. The GCHP system has a closed-loop GHX that circulates a fluid through tubes buried in the ground. The GWHP has an open-loop GHX that extracts and returns fluid to wells in the ground. The SWHP has a closed-loop or open-loop GHX that has piping placed in lakes, river, or bodies of water. The selection of the best GSHP system is largely dependent on the local, geological, and thermal characteristics of the soil at a site. Figure 2-3 shows conceptual schematic diagrams for different GSHP systems and for components of a typical GCHP system.

GSHP systems have received considerable attention in the recent decades due to their improved energy efficiency when compared to air-coupled systems (Hughes, 2008). World-wide applications of GSHP systems have been growing at a rate of 10 percent annually over the past ten years (Rybach, 2005). With a majority of this growth for residential application, it is estimated that 84 percent of GSHP systems use closed-loop earth connection (46 percent vertical well, 38 percent horizontal trenches) and 15 percent of GSHP systems use open-loop GHX systems (Lund et al., 2004).

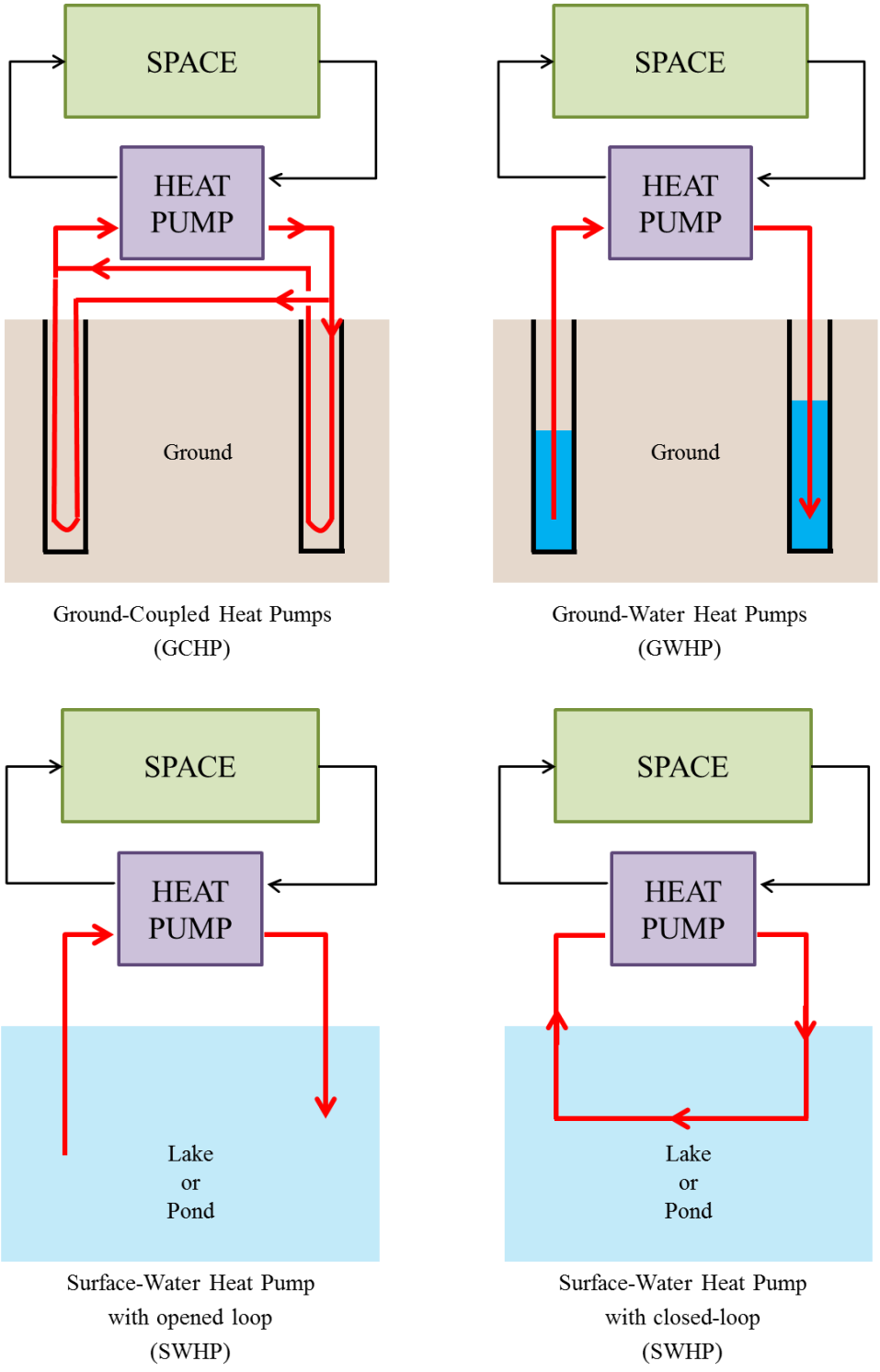

Figure 2-3: Diagrams of Different GSHP System Types

In general, a growing interest has been focused on GCHP systems that use a closed-loop for the ground heat exchanger over systems that use to an open-loop. The major reason for the shift toward GCHP systems is that the technology can be applied virtually anywhere soil conditions are appropriate. On the other hand, other GSHP systems (i.e., GWHP and SWHP) may not be applicable to all sites and may be restricted by local environmental regulations (ASHRAE, 2007c). Of all types of GSHP systems that could be applied, the GWHP systems would be the most energy efficient and cost effective when ample ground water is available on a site.

2.5.1. Ground-Coupled Heat Pump (GCHP) Systems

In the late 1970s, mathematical models for the GCHP technology were developed and tested by Dr. Jim Bose, of Oklahoma State University, and Dr. Harry Braud, of Louisiana State University (Sukup and Johnson, 1989; Wagers and Wagers, 1985). Their GCHP systems have a series of buried pipes, which circulates heat in a closed ground heat exchanger loop. Similar to GSHP systems, GCHP systems can also be operated at a lower discharge pressure, using a downsized compressor. Therefore, GCHP systems use less electricity for the system operation compared to ASHP systems, resulting in reduced utility charges. For this reason, CanmetENERGY projects that such systems could achieve significant energy savings of 30% to 70% in the heating mode and 20% to 50% in the cooling mode (CANMET, 2005). In addition, Karr showed annual Energy Use Intensities (EUI) and percent savings of a GCHP system with horizontal Ground Heat Exchangers (GHXs) compared to an ASHP system for a 26

multi-unit assisted living building at ten different locations, using the EnergyPro[11] software developed by EnergySoft Inc., in California (Karr 2011). Based on the results of his study, Table 2-2 shows the comparison of the annual EUI and percent savings and Figure 2-4 shows the location of the cities in the 2009 IECC climate zone. His study showed that, in general, the cold climates (i.e., Fargo and Billings) had the largest energy savings (about 10%) versus the hot climates (i.e., Dallas and Phoenix). The average annual EUI savings for ten cities is about 27%. Dallas, Texas had a 19% savings of the annual EUI, which is the lowest of all the cities.

Table 2-2: Average Annual Energy Use and Percent Savings for Horizontal GCHP System Compared to ASHP System

City	2009 IECC Climate Zone	ASHP	GCHP	
		kBtu/sqft	kBtu/sqft	% Savings
Billings	Zone 6	65.3	46.0	30%
Phoenix	Zone 2	65.9	51.8	21%
Denver	Zone 5	59.5	44.3	26%
Salt Lake	Zone 5	60.7	45.4	25%
Fargo	Zone 7	72.8	48.2	34%
Lincoln	Zone 5	72.9	49.3	32%
Dallas	Zone 3	65.2	52.8	19%
Kansas City	Zone 4	73.5	49.3	33%
Seattle	Zone 4	54.9	43.9	20%
Portland	Zone 5	56.5	44.6	21%
Average Energy Use & Savings		64.7	47.6	27%

[11] EnergyPro is certified for use with the Title 24 Standards and it is a Window based program for Residential and Non-residential buildings.

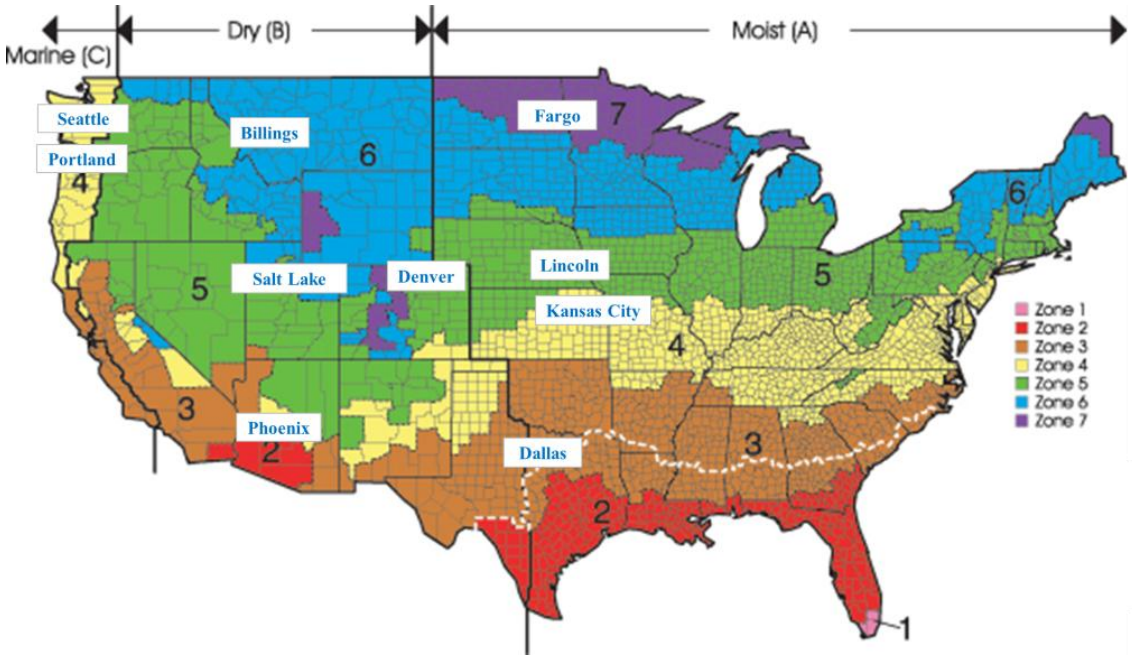

Figure 2-4: Map of the Cities in the 2009 IECC Climate Zone

The heat pump (HP) unit in the GCHP system uses the refrigeration cycle to raise or lower the temperature of the energy delivered from ground heat exchangers (GHXs) before distributing it in a building through conventional means. The GHX is where the heat transfer occurs between the HP and the ground. Thus, the GHX is an important component in determining the GCHP systems thermal efficiency.

Figure 2-5 and Figure 2-6 show diagrams of typical components of a GCHP system with a vertical GHX, circulation loops, and refrigerant state in the cooling and heating operation cycle.

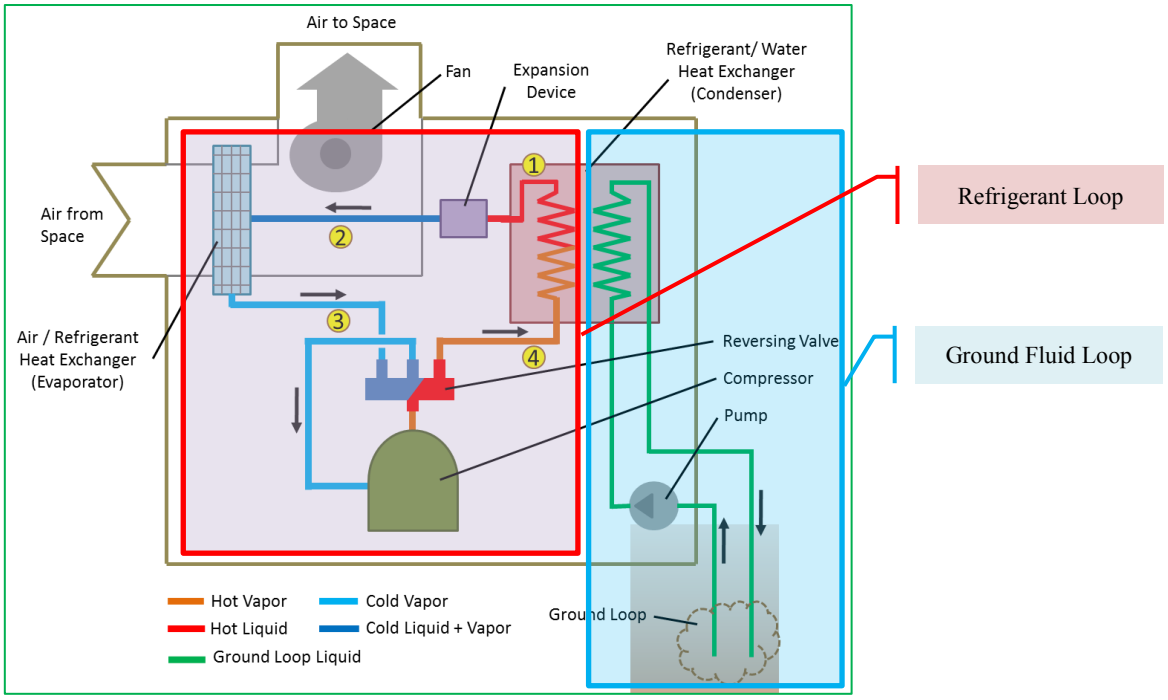

Figure 2-5: Components of a Typical GCHP System for Cooling Cycle

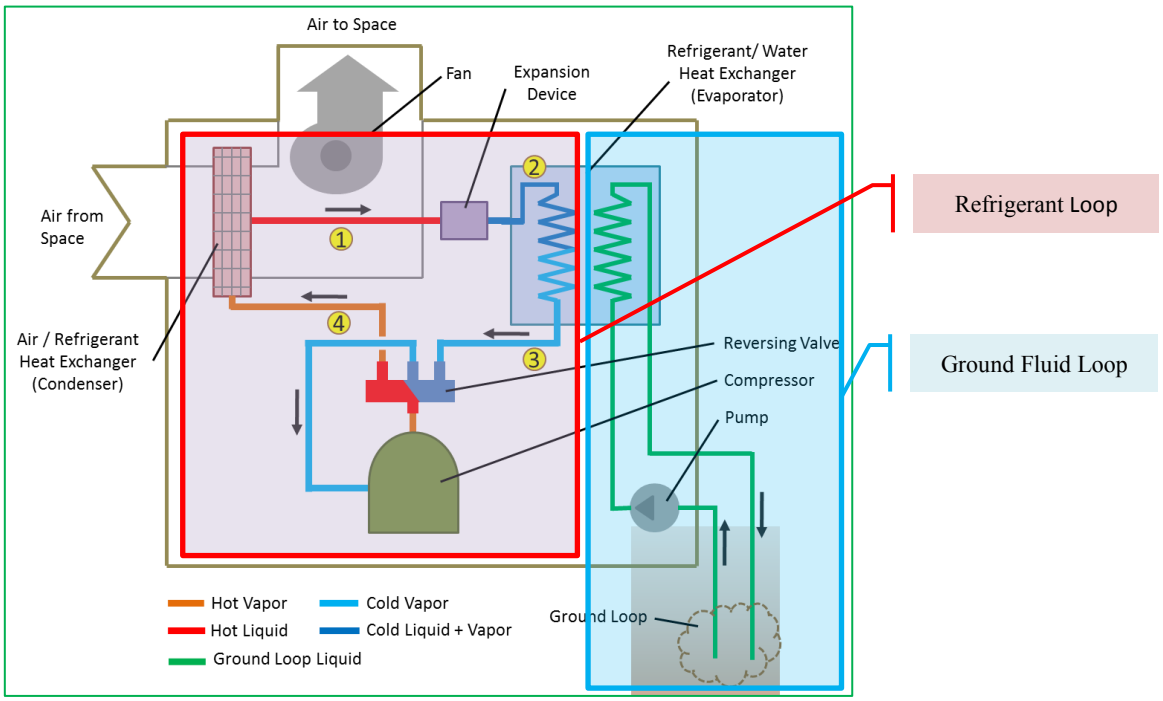

Figure 2-6: Components of a Typical GCHP System for Heating Cycle

In the cooling operation cycle (Figure 2-1, Figure 2-2, and Figure 2-5), for example, a circulating refrigerant enters the compressor as a vapor (point 3). The compressor compresses the vapor to a high pressure. Then, the high pressure vapor enters the condenser (point 4). Condenser condenses the vapor into a liquid by transferring heat to the ground fluid loop. The condensed liquid flows through the expansion device (point 1) where the liquid experiences large pressure decreases, resulting in a phase change to a mixture of liquid and vapor at a lower temperature and pressure. Then, the mixture enters the evaporator coil (point 2) and becomes vapor by absorbing heat from the space warm air. The circulated refrigerant vapor returns to the compressor again (point 3). The cooling cycle repeats during cooling operation. And, the heating operation has simply reversible cycle to the cooling cycle.

The applications of GCHP systems are generally classified according to two types of GHX designs: vertical and horizontal. Vertical GHXs are normally more efficient than horizontal GHXs and require less piping since the annual average ground temperature in a vertical well is more uniform than in a horizontal trench. However, closed-loop GHXs with a vertical well are generally more expensive to install than closed-loop GHXs with a horizontal trench (CANMET, 2005).

Vertical GHXs consist of two, small-diameter high-density polyethylene (HDPE) tubes (pipes) that are inserted into vertical boreholes. After being inserted, the boreholes are then grouted with a solid medium (such as a bentonite/cement-based material) and the connecting trench back-filled. Grouting improves the heat transfer and help to prevent the surface water from draining into the borehole and contaminating the

groundwater. Also grouting prevents one borehole from leaking into an adjacent borehole. Following the grouting and backfilling, all the wells (vertical pipes) are connected to the horizontal underground header supply and return pipes. The header pipes that connect to and from the heat pump are used to carry the GHX heat transfer fluid from the vertical pipes to the heat pump (CANMET, 2005). Once all of the boreholes are connected to the header pipes, the header trench containing the pipes is then filled.

The HDPE tubes are thermally fused at the end that is inserted into the bottom of the bore to form a continuous length of pipe that includes a supply, return, and U-bend. Vertical tubes range from 0.75 to 1.5 in. in diameter. Borehole depths range from 50 to 600 feet (ASHRAE, 2007c), depending on local soil conditions, depth of the water table, and available drilling equipment. To reduce thermal interference between individual boreholes, a minimum borehole separation distance of 20 feet is recommended when boreholes are place in a grid pattern (ASHRAE, 2007c).

The horizontal GHXs are generally suitable for smaller applications such as residential and light commercial buildings since a larger land area is required for large HVAC systems. The piping in a horizontal GHX can be buried relatively near the surface of the ground and still benefit from the moderate temperatures that the earth provides. Ground temperatures may fluctuate as much as ±10˚F at a depth of six feet, which can fall below freezing temperatures in a cold climate. Therefore, the circulating fluid is generally mixed with an antifreeze solution (i.e., propylene glycol, denatured alcohol, or methanol) in heating-dominated regions (ASHRAE, 2007c). However the

antifreeze solution lowers the overall system efficiency because the addition of the antifreeze reduces the fluid overall heat transfer (decreased system capacity) and requires additional pumping power due to added weight (increased fluid concentration).

In this section, GSHP systems were reviewed. In general, three types of GSHP systems are commonly used, including: GCHP, GWHP, and SWHP. Similarly, ground heat exchangers have two main types: vertical and horizontal heat exchangers. Both ground heat exchangers may have an open-loop or a closed-loop heat exchanger configuration. The GCHP system that has a vertical GHX with a closed-loop is found as the most popular type of GSHP system in residential applications due to its applicability to almost any location and the fact that it generally requires fewer restrictions by local environmental regulations. Thus, the GCHP system equipped with a closed, vertical GHX will be studied in this work.

2.6. Previous Work and Methodologies on Ground-Coupled Heat Pump (GCHP) System Simulations

To simulate a GCHP system, a vertical closed-loop ground heat exchanger model is used to calculate the return water temperature from the GHX to the heat pump. The return water temperature depends on the properties, depth and length of the ground loops, the time-of-year, the operating hours, the ground thermal properties, and the building thermal load. The size of the GHX influences the return water temperature, which plays an important role in the heat pump's performance. Therefore, the main objective of the GHX simulation model is to accurately determine the return water

temperatures based on the building heating/cooling load, surrounding ground temperatures, and GHX properties.

The GHX simulation model usually has two separate heat transfer analysis. One analysis is outside the borehole, while the other analysis is inside the borehole. The analysis outside the borehole must account for the heat transfer through the surrounding medium (i.e., soil, rock, sand). The wall temperature inside the borehole is determined by the analysis outside the borehole. The analysis inside the borehole must account for the heat transfer through the grout, through the high-density polyethylene (HDPE) pipe, and into the fluid. This analysis generally considers the thermal properties and resistance of materials such as grout, U-tube pipes, and fluid.

2.6.1. Ground Heat Exchanger (GHX) Simulation Models

A number of simulation models have been developed to explain the thermal behavior of the GHX. Most of these models were based on either an analytical or a numerical methodology or a hybrid methodology combining analytical and numerical models. With regard to the analytical methodology, two representative models are generally used for the design for the GHX: one is Lord Kelvin's infinite line-source model (Gehlin, 1998; Kelvin, 1882) and the other is a cylinder source model (Carslaw and Jaeger, 1947; Ingersoll and Zobel, 1954). Most of the GHX models used in simulation programs are based on one of these two analytical methodologies.

Analytical models are usually based on a number of assumptions, which include simplifications in order to solve the complicated sequence of equation. As a result, the

required computation time of analytical models is usually much less than the time required for numerical models. In addition, the straightforward, simplified algorithms used in an analytical model can be readily integrated into a whole-building, energy simulation program (Yang et al., 2010).

On the other hand, numerical models may have fewer approximations than the analytical models. Compared with the analytical models, the numerical models calculate more realistically the performance of the system which means they can better estimate the nearness of a calculation to the actual value. However, most of the numerical models use polar or cylindrical grids, which can be computationally slow due to the large number of grid points used in a real system. In addition, numerical models can be inconvenient to incorporate directly into a whole-building energy analysis program since numerical models require a significant number of inputs for each location and generate large quantities of output that may need post processing (Yang et al., 2010).

In addition, it should be noted that a reasonable estimation using both analytical and numerical models can be made by assuming/defining reasonable values of the model's variables.

2.6.2. Analytical Solution

The line-source model is a classic solution that calculates the temperature distribution around an imaginary line that represents the vertical borehole. The earliest application of this approach was developed by Lord Kelvin to calculate the thermal performance through ground heat exchanger pipes. Hence, this model is also called

"Kelvin's line-source theory" (Lamarche et al., 2010). In this model, the soil or ground is assumed as an infinite medium with a uniform and constant initial temperature. Ingersoll and Plass (1948) used this model to calculate ground-loop heat exchangers. Unfortunately, this method neglects the heat transfer in the vertical direction of the borehole axis. In addition, this method assumes that a temperature difference from the ground surface and down to the bottom of the borehole does not exist. Therefore, the heat conduction process in the ground is simplified as a one-dimensional problem. This approach has been widely utilized in analytical design methods. A number of improvements to this approach have been proposed to account for these simplifying factors to enhance the accuracy of the calculation of the GHX temperature. For example, one major improvement to this method was proposed by Hart and Couvillion (1986) who considered an undisturbed far-field temperature by introducing a far-field radius (r_∞), which estimated the amount of heat transfer from the line-source to the ground. With this improvement, the line-source model could be used to estimate continuous time-dependent heat transfer between a line-source and the ground (Murugappan, 2001).

Another analytical solution is the use of a cylindrical source model, which treats the two legs of the U-tube as a single isolated pipe surrounded by an infinite solid medium with constant thermal properties (Carslaw and Jaeger, 1947). This solution assumed that the heat throughout the GHX is transferred by conduction and ground water movement. Heat transfer between nearby boreholes was neglected in this method. Ingersoll and Zobel (1954) modified this model to solve for the required borehole length.

Kavanaugh[12] (1985) further refined the model by developing correction factors to consider the non-uniform heat flow around a buried pipe and varying the number of U-tubes. In addition, Kavanaugh modified the model to calculate the interference of the two legs of the U-tube. More recently, Young (2004) considered the cylindrical borehole as a buried electrical cable model that accounts for the thermal capacity of borehole elements, including: grout and fluid. To do this, Young described the elements of a buried electrical cable as the borehole, the core as the circulating fluid, and the sheath as the grout. Young also introduced a fluid multiplication factor. His study showed that increased fluid circulated in a GHX results in better system performance. Young's model was referred to as the Borehole Fluid Thermal Mass Model (BFTM model).

2.6.3. Numerical Solution

Numerical models have been developed to more realistically examine the nature of heat transfer around the borehole heat exchangers for research purposes. In addition, numerical models have been used in system simulations to more accurately evaluate field data. From GCHP experiments, a number of numerical models have been developed to calculate the temperature distribution around the U-tube boreholes. Breger et al. (1996) developed a "one-quarter horizontal cross-section model" using a finite element model (FEM) to examine the performance of a U-tube heat exchanger. Muraya

[12] Steve Kavanaugh has been a Professor of Mechanical Engineering at the University of Alabama since 1985. He conducted various studies associated with design and installation of GCHP system. He also wrote a guideline for the GCHP system (Kavanaugh, 1991; Kavanaugh & Rafferty, 1997; Kavanaugh, Lambert, & Messer, 2002), and conducted field tests for ground thermal properties (Kavanaugh, 2000 and 2001).

et al. (1996) studied the thermal interference that occurs between two legs of a U-tube. Rottmayer et al. (1997) developed a transient, quasi-three-dimensional finite difference model for a vertical U-tube borehole. In this model, the vertical conduction was neglected, but a number of horizontal slices were used that discretized the borehole in the vertical direction, allowing for a vertical temperature variation of the heat transfer fluid in the U-tube.

Shonder and Beck (1999) developed a radial one-dimensional numerical model of heat transfer around a U-tube borehole. This model was used to determine ground thermal properties from in-situ test data. In order to simplify the problem, they used an equivalent diameter approach and a finite difference method. In addition, Zeng et al. (2003) established a new quasi-three-dimensional model for vertical GHXs. This model took into account the thermal interference between U-tube legs and the fluid axial convective heat transfer by considering a borehole with a finite length. Whereas previously, both line-source models and cylindrical models using analytical solutions neglected that the axial heat transfer in the direction of the borehole axis by considering a borehole with infinite length. Finally, Rees et al. (2004) developed a numerical model of groundwater flow and heat transfer in and around standing column wells. This model was able to identify the most significant design parameters of a standing column well performance (i.e., well depth, borehole diameter, ground properties, and "bleed" rate[13]) and their effect on well performance.

---

[13] In a groundwater heat pump (GWHP) with an open-loop ground heat exchanger, all water extracted from the well is circulated through the heat pump. Then, the circulated water returns to the well to be

Of the various numerical GHX models that have been developed, one numerical approach is the most common: the duct ground heat storage (DST) model developed by Hellström (Hellström, 1989). Hellström's "Duct Ground Heat Storage" simulation model uses densely packed, vertical, closed-loop heat exchangers for seasonal thermal energy storage (Yang et al., 2010). In Hellström's model, the DST is defined as a system where heat is stored directly in the ground. A duct or channel system is then used to exchange the heat between a heat carrier fluid, which is circulated through the duct and the storage region. The thermal process in the storage region deals with three separate problems: the global heat flow problem, the local thermal problem, and the steady-flux problem. The global heat flow problem describes the interaction between the storage volume and the surrounding ground called the far-field. The local thermal problem presents the thermal process around the individual ducts (i.e., the boreholes). The steady-flux problem explains heat pulses around a pipe for a constant injection or extraction rate. The DST model was implemented using the TRNSYS simulation program (ECW, 2012).

2.6.4. Hybrid Solution

A hybrid model combines the advantages of numerical and analytical solutions. The most well-known hybrid model is the g-function model developed by Eskilson (Eskilson, 1987; Fossa, 2009). In Eskilson's model, a two-dimensional numerical calculation was used for a single borehole in homogeneous ground with constant initial

---

discharged into the ground. However, not all the water gets return to the well. To account for the water not return to the well, a "Bleed" rate is used to represent the portion of the discharged flow from the heat pump system to some other well or water source (Rees et al., 2004).

and boundary temperatures. In Eskilson's model, the thermal capacitance of the borehole elements, such as the pipe wall and the grout, are neglected. The concept of a g-function was introduced by Eskilson to explain the dimensionless temperature response factors at the borehole wall. Eskilson's g-function calculates the temperature change at the borehole wall in response to a stepped heat input for a unit time.

The disadvantage of Eskilson's approach, however, is that it is time-consuming, and it can hardly be incorporated directly into an hourly, whole-building design and energy analysis program for practical applications. This is because the g-functions of the GHXs with different configurations have to be pre-computed and stored as a database (Yang et al., 2010). The pre-computed and stored database then allows a g-function model to be used like the analytical solution in hourly, whole-building simulation tools (i.e., eQUEST and EnergyPlus). Use of a g-function model with a pre-calculated GHX database allows for less computational time and better accuracy. Unfortunately, the g-function model developed by Eskilson does not calculate the thermal resistance effects of the borehole elements, such as the pipe wall, the grout, and the fluid flow.

Yavuzturk and Spitler (1999) enhanced Eskilson's g-function algorithm to account for the effects of the thermal properties of the grouting material and of the anti-freeze in the GHX model's heat transfer performance (Yavuzturk, 1988). The enhanced g-function model by Yavuzturk and Spitler is called the short time-step g-function model.

In summary, this section reviewed vertical closed-loop, ground heat exchanger models to calculate the return water temperature from the GHX to the heat pump in

GCHP systems. The models have three types of approaches: analytical (the line-source model and the cylindrical source model), numerical (the duct ground heat storage system model and others), and hybrid (the Eskilson's g-function model).

2.7. Whole-Building Computer Simulation Programs Used in Residential Building Energy Analysis

In building energy research, whole-building computer simulation programs are widely and extensively used for analyzing and evaluating complex building performance to improve building energy efficiency. The U.S. Department of Energy (DOE) currently provides information on 393 building software tools[14] for evaluating energy efficiency, renewable energy, and sustainability in buildings. Of these 393 tools, five simulation programs related to whole-building energy simulation were selected for this study: the DOE-2.1e program, eQUEST, EnergyPlus, TRNSYS, and EnergyGauge.

The DOE-2.1e program (DOE-2) is a well-known hourly building energy analysis program which uses DOE-2's building description language (BDL) to describe the building layout, construction, schedules, HVAC systems, plant, and utility rates. The origin of the DOE-2 began with the Post Office Program which was the loads program (i.e., computational procedure) developed by the General American Research Division (GARD)[15] in the late 1960s (Oh, 2013). The Computation Consultants Bureau (CCB)

---

[14] Website for Building Energy Software Tools Directory from U.S. Department of Energy: http://apps1.eere.energy.gov/buildings/tools_directory/
Date accessed: 03/05/2013.

[15] GARD was one of the divisions in the General American Transportation Corporation (GATX), which was a subcontractor for the Post Office facilities division (Stamper 1995; Oh, 2013).

developed the CAL-ERDA program in the late 1970s. CAL-ERDA was based on the load algorithms used in the Post Office Program and utilized the equations of the ASHRAE algorithms (i.e., weighting factor method) and the NECAP program (i.e., NASA's Energy Cost Analysis Program) to develop the calculation procedure (Graven and Hirsch, 1977). CAL-ERDA used the Building Description Language (BDL)[16] and improved calculation speed by recompiling the code (Graven and Hirsch, 1977; Oh, 2013). In 1978, the DOE-1 was released[17], which was a slightly enhanced version of CAL-ERDA (ANL, 1978 as cited in LASL, 1980; Oh, 2013). DOE-2.0a in 1979 and DOE-2.1a in 1980 were released by LBL and LASL. These DOE-2 series had a new BDL to more easily control the LOADS, SYSTEMS, PLANT, and ECONOMICS analysis program. In 1982, DOE-2.1b which had an option to choose metric or English units for inputs and outputs was released by LBL and LANL (LBL, 1982b). In addition, DOE-2.1b included the split flux method for daylight calculation. In 1984, LBL released DOE-2.1c which included algorithms for sunspace analysis (LBL, 1984). In 1989, LBL released DOE-2.1d which improved the calculation method for diffuse solar radiation shading (LBL, 1989). In 1993, LBL and James J. Hirsch & Associates (JJH) released DOE-2.1e which is the most recent version. In this version, more HVAC system models were added including: water loop heat pump systems, water-cooled condenser for packaged units, electric and fuel meters, packaged variable volume temperature (PVVT)

[16] BDL is a user-friendly computer input language to be used in the building's load, systems, plant, and economic sub-programs.

[17] DOE-1 was released by CCB, the Lawrence Berkeley Laboratory (LBL, now Lawrence Berkeley National Laboratory (LBNL)), the Los Alamos Scientific Laboratory (LASL, now Los Alamos National Laboratory (LANL)), and the Argonne Nation Laboratory (ANL).

system, and gas heat pumps. DOE-2.1e-121, the latest version through updates and improvements from DOE-2.1e-087 in 1995, has been used for an hourly building energy analysis program since 2003. DOE-2.1e can be categorized two versions: the standard DOE-2.1e and the enhanced DOE-2.1e (Oh, 2013). The standard DOE-2.1e series includes the versions before Version e-110, which were developed by LBNL and JJH together. On the other hand, the enhanced DOE-2.1e series includes the versions after Version e-110, which were developed by JJH solely; and improved by fixing existing bugs and having new features. The features of the enhanced DOE-2.1e contributed to the development of DOE-2.2 (JJH, 2012)

The DOE-2.2 program was based on DOE-2.1e and publically created by James J. Hirsch & Associates (JJH) in collaboration with LBNL in 1996. However, the DOE-2.2 has been privately supported for version update by JJH. eQUEST, also created by JJH in 1999, uses the DOE-2.2 program. eQUEST provides input/output wizards and a graphical user interface (GUI) for easy-of-use (RMI, 2011). eQUEST also has new features such as GCHP systems. The current release version is eQUEST 3.64[18].

EnergyPlus is based on Building Loads Analysis and System Thermodynamics (BLAST) developed by the U.S. Army Construction Engineering Research Laboratory (CERL) and DOE-2.1e. EnergyPlus is a stand-alone hourly or sub-hourly simulation program. EnergyPlus basically reads an input file and writes output as text files. However, a number of third party graphical interfaces are available. For example, a Google SketchUp plugin is used for quickly creating building geometry. A

[18] The version of the eQUEST program is 3.64 as of September, 2013.

DesignBuilder provides a GUI to most EnergyPlus HVAC system types (DesignBuilder, 2012). A Simergy, released by Lawrence Berkeley National Laboratory (LBNL) in 2012, provides an easy and effective GUI to EnergyPlus, including HVAC system template, component shapes, schedules and calendar libraries, geometry, and result visualization (Simergy, 2013).

TRNSYS, developed by the Solar Energy Laboratory (SEL) at the University of Wisconsin in 1975, is a commercially available transient simulation program (Klein et al., 2010). TRNSYS has a modular structure to solve complex energy system problems by breaking the problem down into a series of smaller components.

EnergyGauge developed by the Florida Solar Energy Center (FSEC) has two separate simulation tools: EnergyGauge USA for code-compliance and home energy rating and EnergyGauge Summit for the Florida commercial energy code-compliance. EnergyGauge can be used as a fast and easy to use evaluation of whole-building energy simulation, but does not easily provide room-by-room HVAC sizing. Recently, FSEC announced that a multiple-conditioned zones simulation is now possible for Version 3.0.01 by entering multiple HVAC systems and assigning them to a single block. It means that a user does not need to break up the house into multiple spaces for each HVAC system (FSEC, 2012).

Of the five simulation tools that were previously mentioned, the DOE-2.1e program, eQUEST, and EnergyPlus have been used by a number of individuals and organizations since those programs can simulate most of the building features found in today's buildings. The DOE-2.1e program, EnergyPlus, and TRNSYS provide complete

documentation for users, including a description of the system functions. However, eQUEST and EnergyGauge do not. Regarding the availability to edit input files, the DOE-2.1e, EnergyPlus, and TRNSYS allow users to edit the input files, whereas, eQUEST and EnergyGauge do not. When comparing simulation run time, EnergyPlus takes a relatively long time to simulate the annual energy performance of a building model. Regarding a RESNET-certified software tool, as mentioned in Section 2.3, DOE-2.1e is used for the calculation tool (simulation engine) of the IC3 and the EnergyGauge software, which are accredited by RESNET.

2.7.1. Computer Simulation Programs with Ground-Coupled Heat Pump (GCHP) Model

Four of the selected five tools have the capability to simulation GCHP systems: eQUEST, EnergyPlus, TRNSYS, and EnergyGauge. However, not all of these programs have published documentation about their detailed algorithms. In addition, only two of the four tools allow users to customize input files. Finally, the EnergyGauge program evaluates the GCHP system performance for residential use only.

The eQUEST/DOE-2.2 program simulates the performance of a GCHP system at a particular hour using a modified version of DOE-2.2's water source heat pump system simulation module. DOE-2.2 is the simulation program used by eQUEST. The eQUEST/DOE-2.2 program uses an enhanced g-function algorithm, which is based on the g-function algorithm developed by Eskilson (1987) at Lund University, Sweden, for fast calculation of the borehole wall temperature. The eQUEST/DOE-2.2 enhanced g-

function model also uses the procedures developed by Yavuzturk & Spitler (1999). Liu & Hellström (2006) presented the verification and validation results of the enhanced GHX model implemented into the eQUEST/DOE-2.2 and developed a dedicated interface for the eQUEST Graphical User Interfaced (GUI) for GCHP simulations.

The EnergyPlus program contains the water source heat pump model with a ground-loop heat exchanger in their whole-building GCHP annual energy simulation. This program also uses the enhanced (short time step) g-function model developed by the Yavuzturk & Spitler (1999) as the ground heat exchanger model. However, users must input appropriate g-function values into the program according to desired GHXs configurations when this program runs simulation. Fisher et al. (2006) claimed that the simulation results, using the g-function model in the EnergyPlus program, showed an average error of less than 6% to predict ground heat transfer rate when compared with measured data for continuous heat pump operation.

TRNSYS calculates water source heat pump performance with a ground heat exchanger for its GCHP system. This simulation program uses the duct ground heat storage (DST) model by Hellström as the ground-loop heat exchanger (Hellström, 1989). Thornton et al. (1997) used Hellström's approach as a part of a detailed component-based simulation model which was later implemented in TRNSYS by Mazzarella in 1993 (Shonder and Hughes, 1993). The DST model implemented in TRNSYS was tested with monitored data from a family housing unit by adjusting input parameters such as the far-field temperature and the ground formation thermal properties (Yavuzturk, 1988).

Yavuzturk (1988) claimed that the calibrated DST model accurately estimates measured entering water temperatures from a ground heat exchanger.

EnergyGauge simulates the GCHP system performance with a simplified method. As mentioned in Section 2.3.2, the simplified method assumes that ground temperatures in a Typical Meteorological Year (TMY) type weather file are same as the entering fluid temperature from GHXs to the heat pump unit. In the TMY type weather file, ground temperatures are calculated using the algorithm developed by Kusuda and Achenbach (1965). As a result of this assumption, EnergyGauge provides only a rough evaluation of a GCHP system performance that can potentially over/under predict the system performance savings, depending on how close the performance of the actual GHX comes to the theoretical TMY ground temperatures.

In summary, GCHP models used in the whole-building energy simulation programs reviewed in this section have three models: the response factor model (g-function) in eQUEST and EnergyPlus; the DST model in TRNSYS; and a simplified model in EnergyGauge. Most of these programs use a water source heat pump with a GHX unit except for EnergyGauge, which uses its own GCHP unit developed by the Florida Solar Energy Center (FSEC).

2.7.2. Other Programs for Ground-Coupled Heat Pump (GCHP) Design/Simulation

Other programs that focus solely on GCHP system design, especially on Ground Heat Exchanger (GHX) design, have been developed. This study reviewed three GCHP

simulation tools based on the finite line-source model and cylindrical source model: the Earth Energy Designer (EED) program, GLHEPRO, and GshpCalc. The EED program developed by BLOCON, Lund, Sweden (BLOCON, 2008), , and GLHEPRO developed by International Ground Source Heat Pump Association (IGSHPA), Stillwater, Oklahoma (IGSHPA, 2012), use the finite line-source model, which is also referred as the Eskilson's approach (Yang et al., 2010). On the other hand, the GshpCalc program developed by GeoKISS, Northport, AL (GeoKISS, 2013), uses a cylindrical source model.

The EED program originated from the Lund program, which was the PC-program for sizing vertical GHXs developed by Lund University, Sweden. It uses algorithms based on the Eskilson's approach. The Lund program has a stored data file for pre-calculated g-function values which allow the Lund program to retrieve g-function values rapidly. However, the Lund program was difficult to use due to the number of inputs required and the complexity of input parameters (Yang et al., 2010). As a result, the EED program was developed to be a more user-friendly program version of the Lund program (Hellström and Sanner, 2001).

The GLHEPRO program (Spitler, 2000) was developed primarily to design vertical GHXs used in commercial or institutional buildings, based on the Eskilson's approach. Yang et al. (2010) described that the GLHEPRO program was developed "… in order to make the 'Swedish' methodology developed by Eskilson tractable for American users.". Spitler claimed the Eskilson's approach was the best currently available methodology (IGSHPA, 2012c).

On the other hand, the GshpCalc program, for the design of vertical GCHP systems, implements the method developed by Kavanaugh (1984), which is based on the cylindrical model. The method uses cyclic load pulses (i.e., daily, monthly, and annual) for the heat extraction/addition to the ground. And, the method uses a steady-state heat solution to predict the required borehole length and effective thermal ground resistance corresponding to each pulse (Yang et al., 2010). Kavanaugh and Rafferty claimed the method has been used widely within the United States for design of GCHP systems (Kavanaugh and Rafferty, 1997).

In summary, whole-building energy simulation programs (the DOE-2.1e program, eQUEST, EnergyPlus, TRNSYS, and EnergyGauge) were reviewed in this section. The review determined that none of the five simulation programs satisfied the following features together: 1) detailed system description; 2) editable input files; 3) short simulation run time; and 4) accurate GCHP system simulation capability. A review of the GCHP analysis used in the most popular simulation programs showed that the DOE-2.1e program does not have the capability to simulate the GCHP system but other four simulation programs do. The g-function method is used in eQUEST and EnergyPlus, the DST model is used in TRNSYS, and EnergyGauge uses its own very simplified GCHP algorithm. In addition, three additional programs (EED, GLHEPRO, and GshpCalc) were reviewed that focused solely on GCHP system design based on the Eskilson's approach (EED and GLHEPRO) and on program that used the cylindrical source model (GshpCalc).

2.8. Summary of the Literature Review

A number of energy codes and standards have been adopted to improve the energy performance of residential houses by offering guidance to users such as builders, building official, designers, and energy modelers. This study reviewed the IECC, the IRC, and ASHRAE Standard 90.2-2007 to identify the similarities and/or differences. The IECC and IRC are the building energy codes that Texas has currently adopted as Texas Building Energy Performance Standards (TBEPS) for all residential buildings. The prescriptive energy efficiency provisions of the 2009 IRC were adopted as the energy code in Texas for single-family residential construction (three stories or less) and the 2009 IECC is the current state energy code for all other residential that don't meet the prescriptive requirements of the 2009 IRC, commercial, and industrial construction.

Several residential building certification software tools have been developed to simplify and clarify code compliance, and to estimate a building's energy performance. The five code-compliant software tools reviewed in this study were the OptiMiser program, REM/Rate, EnergyGauge, IC3, and REScheck. Only one tool, the IC3 software, can be used as a free, web-based tool that is RESNET-certified.

The IC3 software, developed by the ESL, is code-compliant software that allows users to check the code compliance of proposed single-family residences and multi-family residences according to the TBEPS. The simulation model in IC3 uses the DOE-2.1e simulation program. In order to account for building energy performance more properly, there have been on-going efforts to improve the DOE-2.1e simulation model, including the addition of a residential thermal distribution system (i.e., a duct model) and

others. However, the current IC3 does not have the ability to simulate the GCHP system. Therefore, there is a need to develop the ground-coupled heat pump (GCHP) system module in the IC3.

The use of the ground source heat pump (GSHP) system in high performance, energy-efficient buildings is becoming a popular option for building system designers. Of the GSHP system models reviewed, the GCHP model with a vertical closed-loop ground heat exchanger (GHX) is the most widely used in residential systems (Lund et al., 2004).

Various GCHP models have been developed. All of the GCHP models focused on modeling the GHX loop to calculate GCHP system performance. The GHX models surveyed used either an analytical, numerical, or a hybrid modeling approach. Regardless of the approach, the primary purpose of those GHX models is to accurately estimate the hourly return fluid temperature from the GHXs to the heat pump.

This study reviewed vertical closed-loop GHX models, including analytical (i.e., the line-source model and the cylindrical source model), numerical (i.e., the duct ground heat storage system model and others), and hybrid models (i.e., the Eskilson's g-function model). In general, analytical solutions use simplified models whereas numerical solutions use detailed calculations. These features can lead analytical solutions to be less accurate when compared to numerical solutions. However, analytical solutions provide faster computational time than numerical solutions. The hybrid solutions take advantages of both analytical and numerical solutions.

Five whole-building simulation programs (i.e., the DOE-2.1e program, eQUEST, EnergyPlus, TRNSYS, and EnergyGauge) were reviewed in this study. Four of these programs have the capability to simulation GCHP systems; the exception is the DOE-2.1e program. However, none had well-documented GCHP models that could easily model complex building shapes with acceptable run times and modifiable input files.

Therefore, there is a need for a free, web-based, and RESNET-certified, code-compliant software, such as IC3, to have the capability to calculate the GCHP system performance together with the whole-building simulation program using a vertical closed-loop GHX.

CHAPTER III

SIGNIFICANCE AND LIMITATION OF THIS STUDY

3.1. Significance of This Research

This research is expected to provide the following benefits:

a. The development of a custom-built ground heat exchanger (GHX) model for a case-study house in Texas;
b. Calibration and installation of temperature sensors to measure the entering water temperatures (EWTs) for the case-study house;
c. Validation of the custom-built GHX model using field measurements from the case-study house;
d. The development of a simplified residential base-case model using the step-by-step input change method;
e. The development of a vertical GHX FUNCTION model, which is more sophisticated than the other models currently used in the IECC performance verification software tools accredited by RESNET;
f. The development of g-function approximation for residential applications to be used for the vertical GHX DOE-2.1e input FUNCTION;
g. The development of a ground-coupled heat pump (GCHP) system model with vertical GHX units to be used for the DOE-2.1e program; and
h. Comparison of the DOE-2.1e GCHP system model to other models used in whole building energy simulation program.

3.2. Limitations of This Research

The limitations of this study include the following:

a. This study is solely focused on the GCHP system with the closed-loop GHX;
b. Only single-family IECC code-compliant, detached houses in hot and humid climates were considered;
c. This study is restricted to a 2009 IECC code-compliant standard design for a residence;
d. The developed custom-built GHX model is validated with field measurements from an actual single-family house located in Texas, not with lab tests;
e. The developed g-function approximation can be used for residential application only.
f. The developed DOE-2.1e GCHP system model using a vertical GHX is verified by comparing simulation results against other whole-building energy simulation programs, which have the capability to simulate a GCHP system.
g. This study is restricted to an energy simulation analysis only. Any costs associated with implementing a GCHP system in a residence are not provided; and
h. This study does not provide an analysis of the long-term GCHP system energy use changes caused by long-term ground temperature rise/drop.

CHAPTER IV

RESEARCH METHODOLOGY

This chapter discusses the methodology used in this study. The methodology includes the development of a custom-built ground heat exchanger (GHX) model, validation of the custom-built GHX model with measured data from a case-study house, the development of a simplified residential base-case model using the 2009 IECC requirements, development of a DOE-2.1e ground-coupled heat pump (GCHP) simulation model using a vertical GHX FUNCTION, and comparison of the developed DOE-2.1e GCHP simulation model to results from other simulation program.

Section 4.1 introduces study objectives, tasks, and overall research methodology. Section 4.2 describes equations used for closed-loop GHX models, which include horizontal, surface water, and vertical GHX models in this study. Section 4.3 presents description to develop a custom-built GHX model for the case-study house and its validation with the measured data. Section 4.4 describes methodology to develop the DOE-2.1e GCHP simulation model with a vertical GHX, including: development for a simplified residential ASHP base-case model, development of the vertical GHX FUNCTION, and comparative study against other code-compliant programs.

4.1. Introduction

The primary objective of this study is to develop a ground-coupled heat pump (GCHP) simulation model, using a vertical ground heat exchanger (GHX), for single-

family residential systems to be used with the DOE-2.1e simulation program. In addition, this study is to develop a custom-built GHX model which has a combination of the horizontal GHX and the surface water GHX. Figure 4-1 shows a diagram of the methodology used to accomplish these objectives in this study. The methodology includes several major tasks as follow:

a. *Review a closed-loop GHX calculation method*: This task will investigates existing calculation methods for types of the closed-loop GHXs including horizontal, surface water, and vertical GHXs.
b. *Develop a custom-built GHX model*: This task develops a custom-built GHX model to calculate the EWTs of the GCHP system installed in the case-study house. The custom-built GHX model will be developed by combining the horizontal GHX model and the surface water GHX model and it will calculate the EWTs. This section includes a description of the case-study house, measurement, and data collection of the GHX temperatures. In addition, in order to measure outdoor environmental condition, this study uses local weather data from the Solar Test Bench (STB) of the Energy Systems Laboratory (ESL), which is built on the roof of the Langford building at Texas A&M University.
c. *Validate the custom-built GHX model against the measured data*: The custom-built GHX model will be validated using the measured EWT data from the case-study house, in which a GCHP system is installed.
d. *Develop a DOE-2.1e ground-coupled heat pump (GCHP) simulation model*: This task is to develop a DOE-2.1e GCHP simulation model using a vertical ground heat

exchanger (GHX). The development of the GCHP system model will be focused on calculating the performance of vertical GHX units. The vertical GHX calculation model will be defined by creating FUNCTION commands for the DOE-2.1e input file. The RESYS system (i.e., ASHP simulation module in DOE-2.1e) will be modified using the created vertical GHX FUNCTION, and then the modified DOE-2.1e RESYS system will work like a GCHP system. It calls DOE-2.1e GCHP simulation model in this study.

e. *Develop simplified residential base-case simulation models in hot and humid climate*: This task is to develop simplified residential base-case simulation models using air-source heat pump (ASHP) and ground-coupled heat pump (GCHP) systems. To accomplish this task, the DOE-2.1e, eQUEST, and other code-compliant programs (i.e., IC3 only for ASHP, EnergyGauge, and REM/Rate) were used. These base-case models will be developed using residential home characteristics compliance with the 2009 IECC code requirements. The base-case model will be located in Houston and Dallas, Texas to represent a hot and humid climate. The simulations throughout this study will be performed with using Typical Meteorological Year version 2 (TMY2) weather data for Houston and Dallas.

f. *Verify the DOE-2.1e GCHP simulation model*: This task is to verify the developed DOE-2.1e GCHP system simulation model with a vertical GHX. The simulation results of the DOE-2.1e GCHP base-case simulation model will be compare to the simulation results from the other GCHP base-case simulation models: eQUEST, and other code-compliant programs.

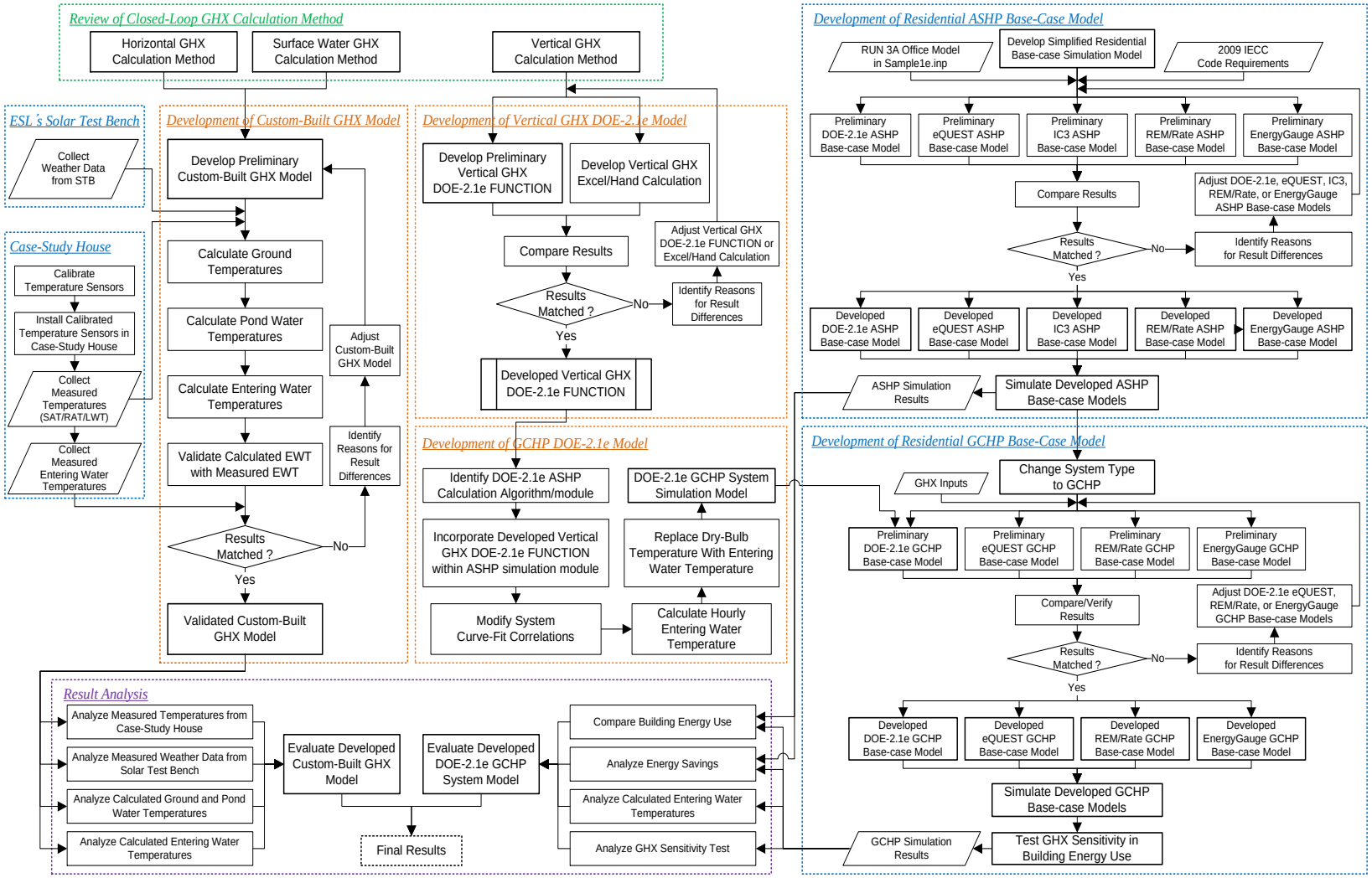

Figure 4-1: Diagram of Research Methodology

4.2. Closed-Loop Ground Heat Exchanger Model

A ground heat exchanger (GHX) model is used to determine the entering water temperature (EWT) from GHX to the heat pump. The EWTs have an effect on the heat transfer between the GHX and the surrounding heat source/sink (i.e., soil, aquifer, and others), as shown in Figure 4-2. Therefore, In order to determine the EWT, the calculations for the source/sink temperature and temperature change are required. Based on these calculations, the EWT is predicted for each hour of the simulation. This chapter describes the closed-loop GHX models used for the calculations, which include the horizontal GHX, the surface water GHX, and the vertical GHX.

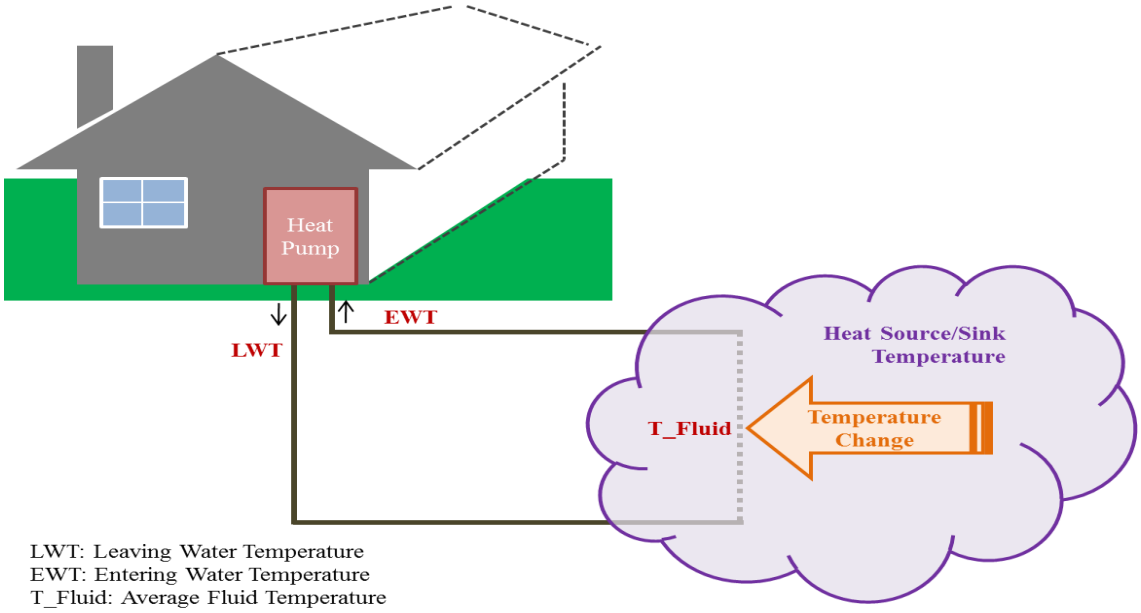

Figure 4-2: Conceptual Diagram for the Ground Heat Exchanger Model

4.2.1. Horizontal Ground Heat Exchanger Model

A horizontal GHX consists of pipes buried in the ground that are used for transferring heat between the ground and the circulating fluid through the horizontal

GHX. The surrounding ground temperatures are used as the heat source/sink temperatures in the horizontal GHX model. The fluid temperature changes are a result from the heat transfer to/from the ground.

The horizontal GHX model in this study requires a leaving water temperature, a GHX thermal load, and the time of the year. In addition, it also requires parameters which include the mean ground temperature, the amplitude of the ground temperature variation, the phase angle of the ground temperature, the GHX length and depth, the fluid flow rate, the thermal properties of ground/pipe/water, and the undisturbed ground depth. Figure 4-3 presents a diagram of the input and output parameters for the horizontal GHX model.

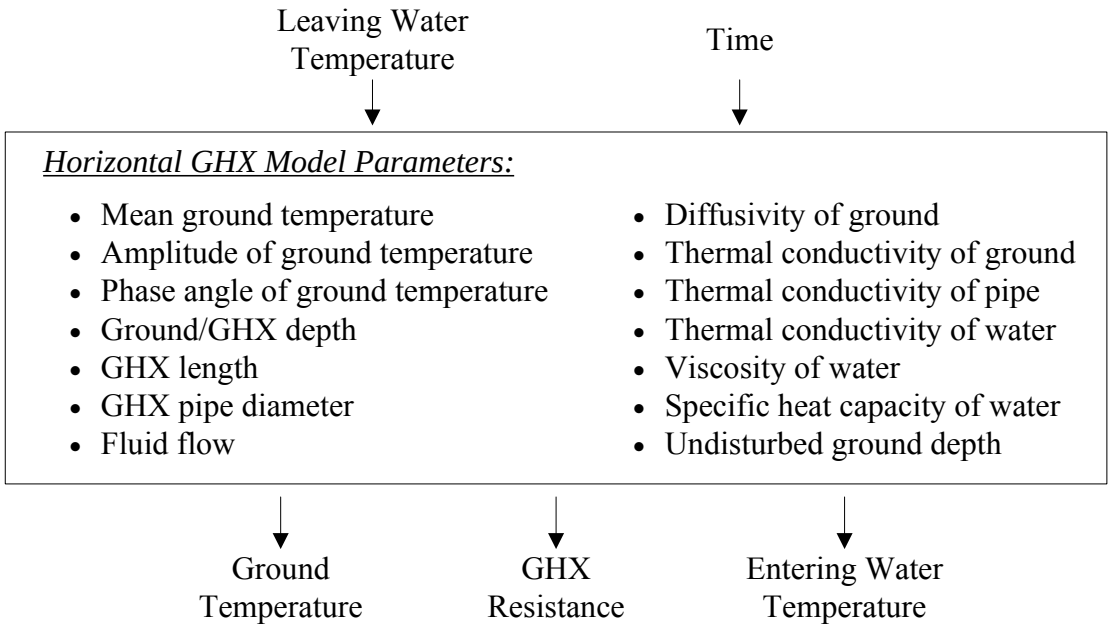

Figure 4-3: Horizontal GHX Model Input and Output Parameters

4.2.1.1. Ground Temperature

In simulations where the ground temperatures are not known, the ground temperatures are calculated, using their algorithm developed by Kusuda and Achenbach (1965). The algorithm gives a sinusoidal variation of the mean ground temperature. The following equation[19] shows the algorithm to calculate the ground temperature.

$$\mathrm{T}(Z_{depth}, t_{year}) = T_{mean} - T_{amp} \times \exp\left\{-Z_{depth}\left(\frac{\pi}{8760\times\alpha_{ground}}\right)^{\frac{1}{2}}\right\} \times \cos\left\{\frac{2\pi}{8760}\left[t_{year} - t_{phase} - \frac{Z_{depth}}{2}\left(\frac{8760}{\pi\times\alpha_{ground}}\right)^{\frac{1}{2}}\right]\right\} \quad (4.1)$$

Where,

Z_{depth}	is the depth of ground (ft),
t_{year}	is the time of the year (hours or days),
T_{mean}	is the mean ground surface temperature over year (F),
T_{amp}	is the amplitude of ground surface temperature variation (F),
α_{ground}	is the thermal diffusivity of ground (ft^2/hour or ft^2/day), and
t_{phase}	is the phase angle (hours or days).

The ground temperature in equation 4.1 depends on four parameters: 1) the mean ground surface temperature over the year (i.e., the undisturbed ground temperature), 2) the amplitude of ground surface temperature, 3) the thermal diffusivity of the ground, 4) the phase angle (i.e., the time shift between the beginning of year and the time of the minimum surface temperature). In addition, the ground temperatures are calculated as a

[19] When using daily values, 8,760 hours should be replaced with 365 days in the algorithm.

function of the ground depth and the time of the year with correlations for a given location. The exponential term accounts for ground depth and the cosine term accounts for annual temperature variation.

For example, the ground temperatures in Houston can be predicted assuming the following correlations[20]: 1) the mean ground temperature is 71 F, 2) the amplitude of ground surface temperature variation is 15.7 F, 3) the phase angle is 792 hours (33 days), 4) the thermal diffusivity of ground is 0.025 ft^2/hour (0.6 ft^2/day). The ground temperatures calculated from the algorithm of Kusuda and Achenbach are shown in Figure 4-4 and Figure 4-5.

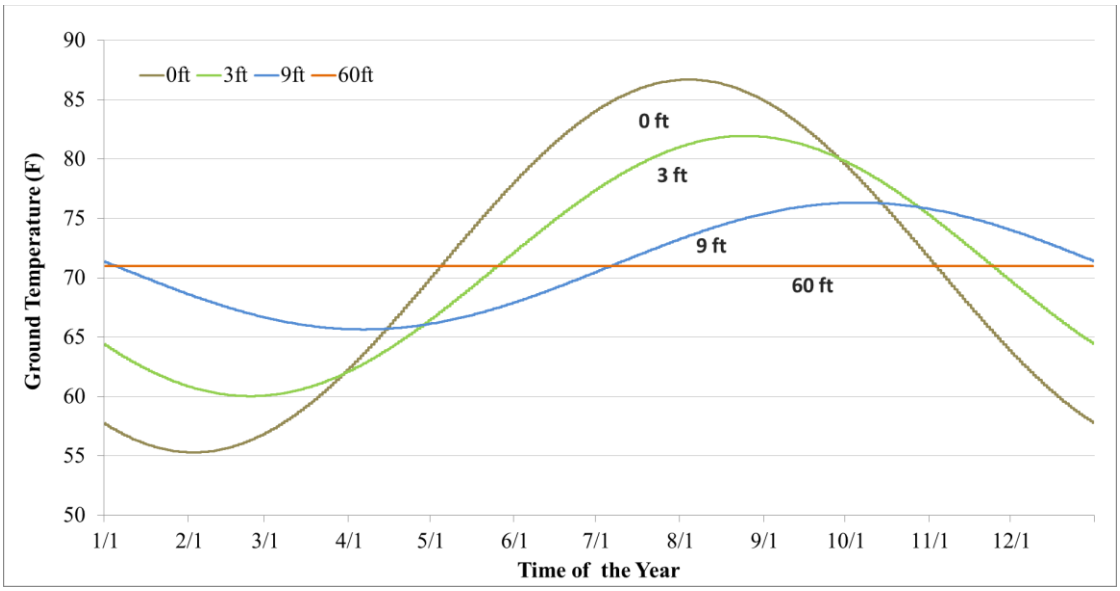

Figure 4-4: Annual Ground Temperatures at Different Depth in Houston

[20] The GeoDesigner software developed by ClimateMaster provided the mean ground temperature, the amplitude of ground surface temperature variation, the phase angle for 14 cities in Texas, including Amarillo, Austin, Corpus Christi, Dallas, El Paso, Houston, and others. This software is available from the following web address: http://www.bryantgeo.com/geodesigner.htm (Bryant, 2013)

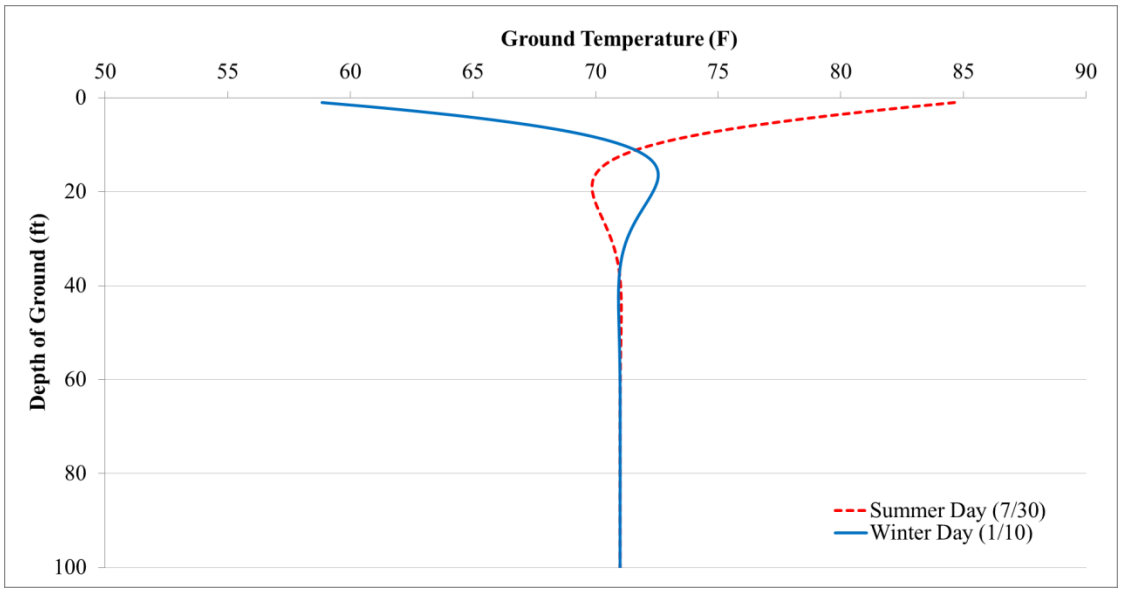

Figure 4-5: Summer and Winter Ground Temperatures at Different Depths in Houston

As shown in Figure 4-4 and Figure 4-5, the ground temperatures change according to the time of the year and depth of the ground. Specifically, temperatures deeper in the ground experience less variation in temperatures and have a time lag farther behind those of ground temperatures at a shallow depth. At ground depths greater than about 35 feet below the surface, the ground temperatures are constant at 71 F.

4.2.1.2. Horizontal GHX Resistance

The total horizontal GHX thermal resistance is calculated using the convective resistance in the fluid, the conductive resistance of the pipe wall, and the resistance of the soil between the pipe and the surrounding ground. Figure 4-6 presents the diagram of the thermal resistance for the horizontal GHX model.

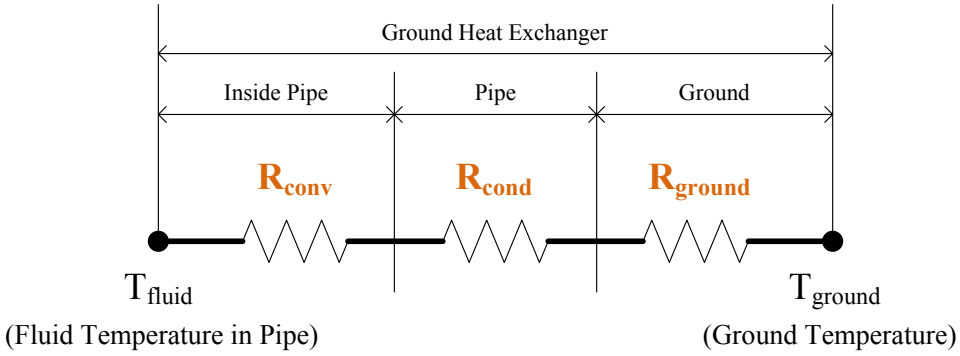

Figure 4-6: Thermal Resistance Diagram for the Horizontal GHX Model

To calculate the total resistance (R_{total}), first, the thermal resistances of each material section are calculated, and then the total resistance is calculated by the summation of the each material resistance. The total horizontal GHX thermal resistance is calculated as follows:

$$R_{total} = R_{conv} + R_{cond} + R_{ground} \tag{4.2}$$

Where,

R_{total}	is the total thermal borehole resistance (F-hr-ft/Btu),
R_{conv}	is the convective resistance of the inner pipe (fluid) (F-hr-ft/Btu),
R_{cond}	is the conductive resistance of the pipe (F-hr-ft/Btu), and
R_{ground}	is the resistance between the pipe and the ground (F-hr-ft/Btu).

To accomplish this, the thermal resistances for each material section must be calculated. First, the convective resistance of the pipe (R_{conv}), which is the convection heat transfer due to internal flow, is estimated, using the following equations (Incropera & De Witt, 2001):

$$Re_D = \frac{4\,\dot{m}}{\pi\, D_{in,pipe}\,\mu} \tag{4.3}$$

$$P_r = \frac{C_p\,\mu}{k_{fluid}} \tag{4.4}$$

$$\mathrm{f} = (0.790 ln Re_D - 1.64)^{-2} \tag{4.5}$$

$$\mathrm{Nu}_D = 4.36 \qquad \mathrm{Re}_D < 2{,}300 \tag{4.6}$$

$$\mathrm{Nu}_D = \frac{(f/8)Re_D P_r}{1.07+12.7(f/8)^{1/2}\left({P_r}^{2/3}-1\right)} \qquad 2{,}300 \le \mathrm{Re}_D < 10{,}000 \tag{4.7}$$

$$\mathrm{Nu}_D = 0.023 {Re_D}^{4/5} {P_r}^{n} \qquad 10{,}000 \le \mathrm{Re}_D \tag{4.8}$$

$$\mathrm{h} = \frac{Nu_D\, k_{fluid}}{D_{in,pipe}} \tag{4.9}$$

$$R_{conv} = \frac{1}{\pi\, D_{in,pipe}\, h} \tag{4.10}$$

Where,

$D_{in,pipe}$	is the pipe inner diameter (ft),
Re_D	is the Reynolds number (non-dimensional),
ṁ	is the rate of fluid flow through the pipe (lb/s),
μ	is the viscosity of fluid (lb/ft-hr),
P_r	is the Prandtl number (non-dimensional),
C_p	is the specific heat of fluid (Btu/lb-F),
k_{fluid}	is the fluid thermal conductance (Btu/hr-ft-F),
f	is the friction factor[21] to approximate the smooth surface condition,
Nu_D	is the Nusselt number (non-dimensional),
n	is the coefficient of the exponential term, approximated with 0.35 for both heating and cooling modes (non-dimensional), and
h	is the convection coefficient of fluid (Btu/hr-ft^2-F).

[21] The friction factor developed by Petukhov is a single correlation that encompasses a large Reynolds number range (Incropera & De Witt, 2001)

Where, the Nusselt number equations vary based on the fluid flow characteristics inside the pipe of the ground heat exchanger: 1) the constant Nusselt number of 4.36 is used for the laminar flow condition ($\mathrm{Re}_D < 2{,}300$), using equation 4.6. 2) the Nusselt number is calculated for the transition region between laminar flow and turbulent flow ($2{,}300 \leq \mathrm{Re}_D < 10{,}000$), using equation 4.7. 3) the Nusselt number is calculated for the fully turbulent flow ($10{,}000 \leq \mathrm{Re}_D$), using equation 4.8.

Second, the conductive resistance of the pipe (R_{cond}) is estimated, using following equation (Lee, 2008):

$$R_{cond} = \frac{ln\left(\frac{D_{out,pipe}}{D_{in,pipe}}\right)}{2\pi k_{pipe}} \tag{4.11}$$

Where,

$D_{out,pipe}$ is the pipe outer diameter (ft),
$D_{in,pipe}$ is the pipe inner diameter (ft), and
$\mathrm{k_{pipe}}$ is the pipe thermal conductance (Btu/hr-ft-F).

Third, the conductive resistance of the ground is calculated by the following equation (Lee, 2008):

$$R_{ground} = \frac{1}{2\pi k_{ground}}\left[ln\left(\frac{D_{in,pipe}+D_{out,pipe}+d_{constant}}{D_{in,pipe}+D_{out,pipe}}\right)\right] \tag{4.12}$$

Where,

k_{ground} is the ground thermal conductance (Btu/hr-ft-F),
$D_{in,pipe}$ is the pipe inner diameter (ft),
$D_{out,pipe}$ is the pipe outer diameter (ft), and

$d_{constant}$ is the distance between the pipe surface and the undisturbed ground (ft).

4.2.1.3. Entering Water Temperature for the Horizontal GHX

The differential heat transfer equation for the horizontal GHX can be written as:

$$\frac{\Delta T_{out}}{\Delta T_{in}} = \frac{T_{ground} - T_{out}}{T_{ground} - T_{in}} = exp\left[-\frac{l}{\dot{m}\, c_p\, R_{total}}\right] \quad (4.13)$$

Where,

T_{ground} is the ground temperature, using equation 4.1 (F),
T_{in} is the leaving fluid temperature from a heat pump (F),
T_{out} is the entering fluid temperature to a heat pump (F),
ṁ is the rate of fluid flow through the pipe (lb/hr),
C_p is the specific heat of the fluid (Btu/lb-F),
l is the length of the ground heat exchanger (ft), and
R_{total} is the total thermal borehole resistance (F-hr-ft/Btu),

Solving equation 4.13, the EWT for the horizontal GHX is given by:

$$EWT = T_{ground} + \left(T_{in} - T_{ground}\right) \times exp\left[-\frac{l}{\dot{m}\, c_p\, R_{total}}\right] \quad (4.14)$$

4.2.2. Surface Water Ground Heat Exchanger Model

The surface water GHX consists of pipes buried in the aquifer (i.e., pond) and is used for transferring heat between the aquifer and the GHX. In the surface water GHX model, the prediction of the pond water temperatures throughout the year is important to the design and evaluation of the surface water GHX. The dominant energy transfer

mechanisms for the pond water temperature calculation are absorbed solar radiation, pond thermal radiation, convection of the pond surface, heat transfer to/from the ground contacted with the pond, evaporation of the pond surface, and heat transfer between the fluid in the pipe and the pond. The pond water temperatures are used as the heat source/sink temperatures in the surface water GHX model. The fluid temperature changes result from the heat transfer between the leaving water and the pond water temperatures.

The surface water GHX model in this study required weather data to be used for the pond water temperature calculation, including the outdoor temperature, relative humidity, wind speed, solar radiation, leaving water temperature, and GHX thermal load. In addition, the model required parameters which include: the pond geometry, GHX geometry, fluid flow rate, pond latitude and longitude, thermal properties of ground/pipe/water, index of refraction, extinction coefficient, and Stefan-Boltzmann constant. Figure 4-7 presents diagram of input and output parameters for the surface water GHX model.

4.2.2.1. Surface Water Temperature

A shallow pond (less than 30 ft of water depth) was considered as the aquifer (surface water) in this study. The pond water temperatures were calculated using the energy transfer mechanisms by Pezent and Kavanaugh (1990), Chiasson (1999), and Hayes et al. (2011).

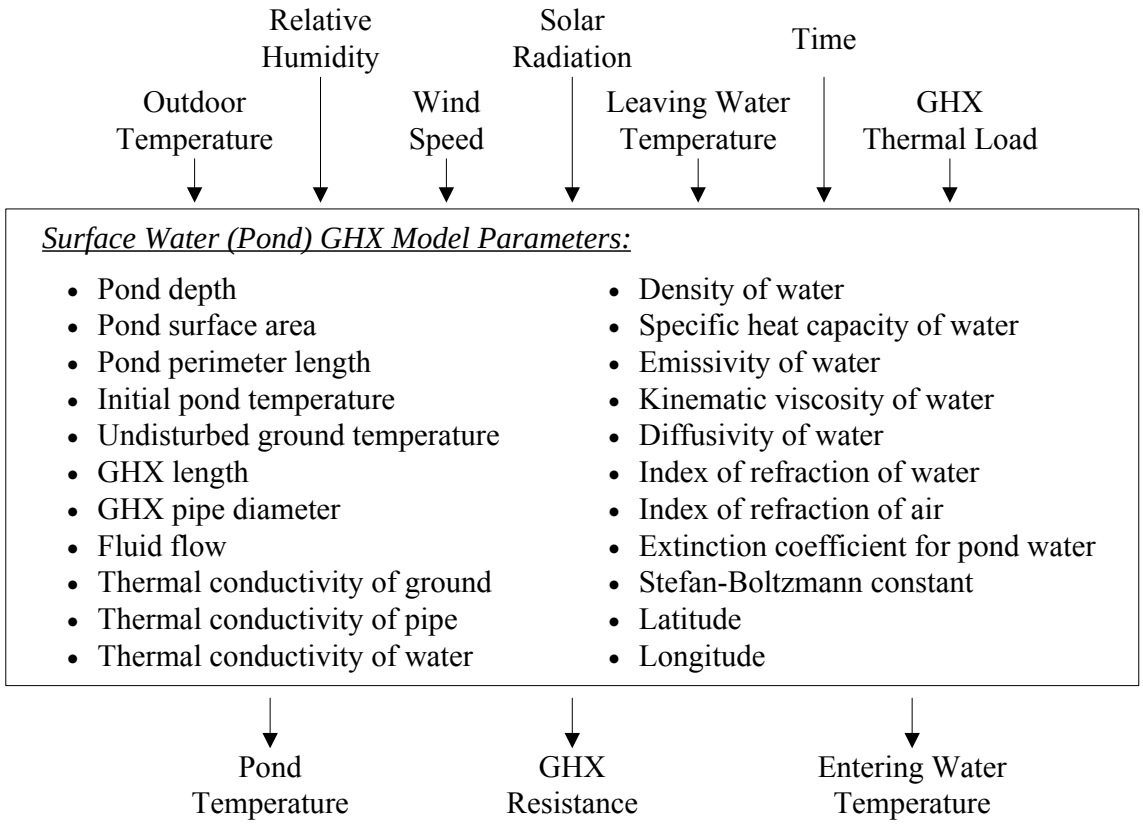

Figure 4-7: Surface Water GHX Model Input and Output Parameters

The schematic diagram for the energy transfer mechanisms used in this study is shown in Figure 4-8. The energy transfer mechanisms[22] include: the absorbed solar radiation, the pond thermal radiation by the sky, the convection of the pond's surface, the heat transfer to/from the pond's ground, the evaporation of water from the pond's surface, and the heat transfer between the fluid in the pipe and the pond.

[22] This study does not consider the heat transfer due to ground water seepage which accounts for the inflows and outflows of ground water to the pond since the ground water seepage may not always be expected in shallow ponds (Chiasson, 1999).

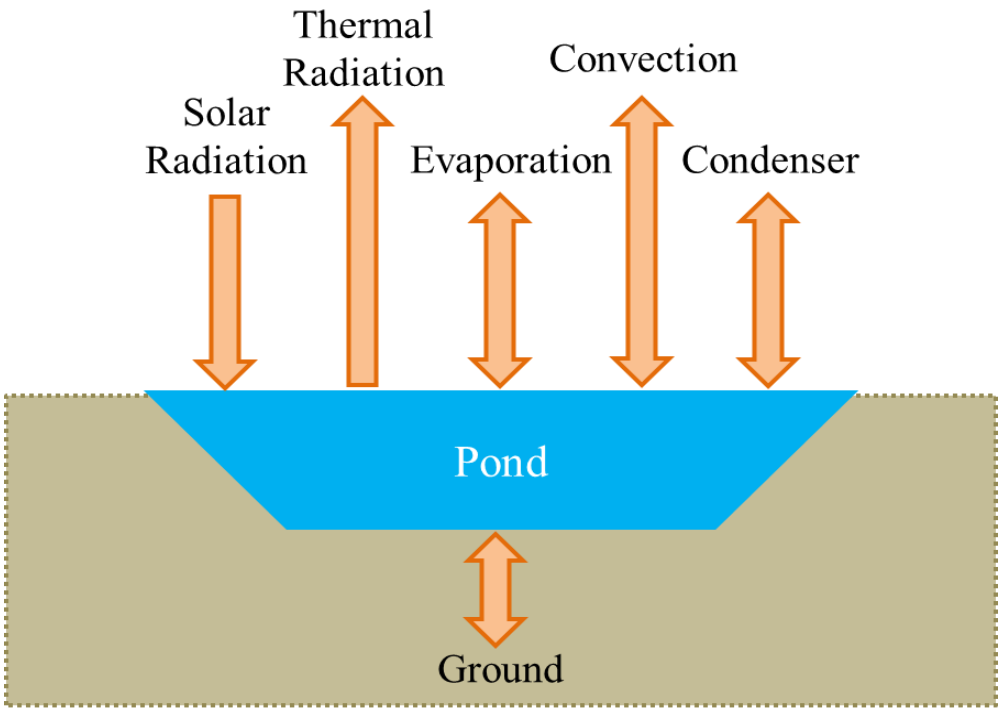

Figure 4-8: Energy Transfer Mechanism for the Pond

Using the above mechanisms, the temperature change in the pond can be calculated with the following mathematical expression, which assumes that the pond water body has a uniform temperature at a given time (i.e., no temperature gradients):

$$\frac{dT}{dt} = \left(Q_{solar} + Q_{rad} + Q_{evap} + Q_{conv} + Q_{ground} + Q_{fluid}\right)/(V\rho C_p) \qquad (4.15)$$

Where,

Q_{solar} is the solar radiation absorbed by the pond water (Btu/hr),

Q_{rad} is the thermal radiation from water to sky (Btu/hr),

Q_{evap} is the evaporation at the pond surface (Btu/hr),

Q_{conv} is the convection at the pond surface (Btu/hr),

Q_{ground} is the heat transfer to/from the ground contacted with the pond (Btu/hr),

Q_{fluid} is the heat transfer between the fluid in the pipe and the pond (Btu/hr),

V is the pond volume (ft^3),

ρ is the density of the pond water (lb/ft^3), and

C_p is the specific heat capacity of the pond water (Btu/lb-F).

First, the solar radiation absorbed by the pond (Q_{solar}) represents all solar radiation on the pond surface, excluding the reflected solar radiation. In order to calculate the amount of the absorbed solar radiation, the angle of incidence of solar beam radiation on a surface is first determined, given by the following equation:

$$\cos\theta = \cos\emptyset \cos\delta \cos\omega + \sin\emptyset \sin\delta \quad (4.16)$$

Where,

θ is the angle of incidence (degrees),

$\emptyset$ is the pond's latitude, south negative, north positive (degrees),

δ is the solar declination (degrees), and

ω is the hour angle, morning negative, afternoon positive (degrees).

Once the angle of incidence is calculated, the refraction angle of the direct solar radiation at the pond surface is given by the following equation, using Snell's Law:

$$\cos\theta_r = \frac{n_{air}}{n_{water}} \sin\theta \quad (4.17)$$

Where,

θ_r is the angle of refraction of sun's rays (degrees),

n_{air} is the index of refraction of air, 1 (non-dimensional),

n_{water} is the index of refraction of water, 1.33 in the visible spectrum (non-dimensional), and

θ is the angle of incidence (degrees).

Then, the reflectance of solar radiation off the pond's surface is calculated by the following equations:

$$r_{\parallel} = \frac{\tan^2(\theta_r + \theta)}{\tan^2(\theta_r + \theta)} \quad (4.18)$$

$$r_{\perp} = \frac{\sin^2(\theta_r + \theta)}{\sin^2(\theta_r + \theta)} \quad (4.19)$$

$$\tau_a = \exp(-\frac{Kd}{\cos\theta_r}) \quad (4.20)$$

$$\tau = \frac{1}{2}\left(\frac{1-r_{\parallel}}{1+r_{\parallel}} + \frac{1-r_{\perp}}{1+r_{\perp}}\right) \times \tau_a \quad (4.21)$$

$$\rho = \tau_a - \tau \quad (4.22)$$

Where,

θ_r is the angle of refraction of sun's rays (degrees),

θ is the angle of incidence (degrees),

$r_{\parallel}$ is the parallel component of unpolarized radiation (non-dimensional),

$r_{\perp}$ is the perpendicular component of unpolarized radiation (non-dimensional),

τ_a is the transmittance of solar radiation, considered absorption losses (non-dimensional),

k is the extinction coefficient for pond[23], (1/ft),

d is the depth of the pond, (ft),

τ is the transmittance of solar radiation (non-dimensional), and

ρ is the reflectance of solar radiation (non-dimensional).

[23] Lamoureux J. (2003) presents that the average light extinction coefficient for the ponds was 0.13 cm^{-1}

Finally, the amount of the solar radiation absorbed by the pond is given by the equations:

$$I = I_b \times \cos\theta + I_d \quad (4.23)$$

$$Q_{solar} = I(1-\rho) \times A_{pond} \quad (4.24)$$

Where,

I	is the incident solar radiation on the pond surface (Btu/hr-ft^2),
I_b	is the beam solar radiation (Btu/hr-ft^2),
I_d	is the diffuse solar radiation (Btu/hr-ft^2),
θ	is the angle of incidence (degrees),
A_{pond}	is the surface area of the pond (ft^2), and
Q_{solar}	is the solar radiation absorbed by the pond water (Btu/hr).

Second, the thermal radiation (Q_{rad}) is to account for longwave thermal radiation from water to sky at the pond's surface. The amount of the thermal radiation is determined, given by the following equations:

$$T_{sky} = T_{oa}\left[0.711 + 0.0056T_{dp} + 0.000073T_{dp}^2 + 0.013\cos(15t)\right]^{1/4} \quad (4.25)$$

$$Q_{rad,SI} = \varepsilon\,\sigma\left(T_{pond}^4 - T_{sky}^4\right) \quad (4.26)$$

$$Q_{rad,IP} = 0.316998331 \times Q_{rad,SI} \quad (4.27)$$

$$Q_{rad} = A_{pond}\,Q_{rad,IP} \quad (4.28)$$

Where,

T_{sky}	is the sky temperature (K),
T_{oa}	is the outdoor air temperature (K),
T_{dp}	is the outdoor air dew point temperature (K),
t	is the hour from midnight (hour),

ε is the emissivity of the pond water[24] (non-dimensional),

σ is the Stefan-Boltzmann constant, 5.670373 x 10^{-8} (W/m^2-K^4),

$Q_{rad,SI}$ is the thermal radiation per unit area (W/m^2),

$Q_{rad,IP}$ is the thermal radiation per unit area (Btu/hr-ft^2),

A_{pond} is the surface area of the pond (ft^2), and

Q_{rad} is the thermal radiation of the pond (Btu/hr).

Third, the evaporation of the pond's surface (Q_{evap}) that accounts for the heat removed from the pond is dependent on: the velocity of the air, the pond surface area, and the difference between the saturation pressure at the outdoor air dew point and the saturation vapor pressure at the pond surface temperature. The saturation vapor pressure can be calculated using the following equations (ASCE, 2005):

$$e_{pond} = 0.6108 \exp\left(\frac{17.27 \times T_{pond}}{T_{pond}+237.3}\right) \quad (4.29)$$

$$e_{oa} = 0.6108 \exp\left(\frac{17.27 \times T_{dp}}{T_{dp}+237.3}\right) \quad (4.30)$$

$$P_{pond} = \mathrm{e_{pond}} \times 0.2953 \quad (4.31)$$

$$P_{oa} = \mathrm{e_{oa}} \times 0.2953 \quad (4.32)$$

Where,

e_{pond} is the saturation vapor pressure at the pond surface (kPa),

T_{pond} is the pond water temperature (C),

e_{oa} is the saturation pressure at the outdoor air dew point (kPa),

T_{dp} is the outdoor air dew point temperature (C),

P_{pond} is the saturation vapor pressure at the pond surface (in. Hg), and

[24] The value of 0.96 for the emissivity of water was from Incropera and De Witt (2001).

P_{oa} is the saturation pressure at the outdoor air dew point (in. Hg).

Then, the evaporative heat transfer that accounts for the evaporation of water from the pond's surface is determined, given by the following equation (ASHRAE, 2011):

$$Q_{evap} = A_{pond}\,(a + bv)(P_{oa} - P_{pond}) \tag{4.33}$$

Where,

A_{pond} is the surface area of the pond (ft^2),
a is 95 of the constant (Btu/h-ft^2-in.Hg),
b is 0.425 of the constant (Btu-min/h-ft^3-in.Hg),
v is the wind speed (ft/min),
P_{oa} is the saturation pressure at the outdoor air dew point (in. Hg),
P_{pond} is the saturation vapor pressure at the pond surface (in. Hg), and
Q_{evap} is the evaporative heat transfer at the pond surface (Btu/hr).

Fourth, the convection of the pond surface (Q_{conv}) accounts for the heat removed from the pond surface due to cold air passing over the pond surface. The convective heat transfer coefficient from the wind can be calculated using the following equation (Kishore and Joshi, 1984; Pezent and Kavanaugh, 1990):

$$h_{conv} = 1.004 + 0.3\,\nu \tag{4.34}$$

Where,

ν is the wind speed (mile/hr), and
h_{conv} is the convective heat transfer coefficient by wind (Btu/hr-ft^2-F).

Then, the convective heat transfer is determined, given by the following equation:

$$Q_{conv} = h_{conv} A_{pond} (T_{oa} - T_{pond}) \quad (4.35)$$

Where,

h_{conv} is the convective heat transfer coefficient by wind (Btu/hr-ft^2-F),
A_{pond} is the surface area of the pond (ft^2),
T_{oa} is the outdoor air temperature (F),
T_{pond} is the pond water temperature (F), and
Q_{conv} is the convective heat transfer at the pond surface (Btu/hr).

Fifth, the conductive heat transfer to/from the ground contacted with the pond (Q_{ground}) accounts for the heat transferred from pond water body to the pond surrounding perimeter and to the pond bottom surface. The ground heat transfer can be written as (Chiasson, 1999):

$$Q_{ground} = \left(0.999 \frac{K_g}{d_g - d_{pond}} + 1.37 \frac{K_g P_{pond}}{A_{pond}}\right) A_{pond} (T_{pond} - T_{ground}) \quad (4.36)$$

Where,

k_{ground} is the thermal conductivity of ground (Btu/hr-ft-F),
d_g is an assumed ground depth at a constant ground temperature (ft),
d_{pond} is the pond depth (ft),
P_{pond} is the perimeter length of the pond (ft),
A_{pond} is the surface area of the pond (ft^2),
T_{pond} is the pond water temperature (F),
T_{ground} is the undisturbed ground temperature, using equation 4.1 (F), and
Q_{ground} is the heat transfer at the pond perimeter and bottom surface (Btu/hr).

Finally, the heat transfer between the fluid in the pipe and the pond (Q_{fluid}) accounts for the pond thermal load due to heat exchanger fluid. The amount of the fluid heat transfer is given by:

$$Q_{\text{fluid}} = \dot{m}\, c_p \left(T_{in} - T_{pond}\right) \tag{4.37}$$

Where,

$\dot{m}$	is the rate of fluid flow through the pipe (lb/hr),
C_p	is the specific heat of the fluid (Btu/lb-F),
T_{in}	is the leaving fluid temperature from a heat pump (F),
T_{pond}	is the pond water temperature (F), and
Q_{fluid}	is the fluid heat transfer to the pond (Btu/hr).

Using the heat transfer mechanisms, the pond water temperature at the current hour can be calculated using the following expression:

$$T_{pond} = T_{pre,pond} + \frac{dT}{dt} \tag{4.38}$$

Where,

$T_{pre,pond}$	is the pond water temperature for the previous hour (F),
$\frac{dT}{dt}$	is the pond water temperature change at current hour, using equation 4.15 (F), and
T_{pond}	is the pond water temperature at the current hour (F).

4.2.2.2. Surface Water GHX Resistance

The total surface water GHX thermal resistance is calculated using the convective resistance in the fluid, the conductive resistance of the pipe wall, and the resistance between the pipe and the pond. Figure 4-9 presents the diagram of the thermal resistance for the surface water GHX model.

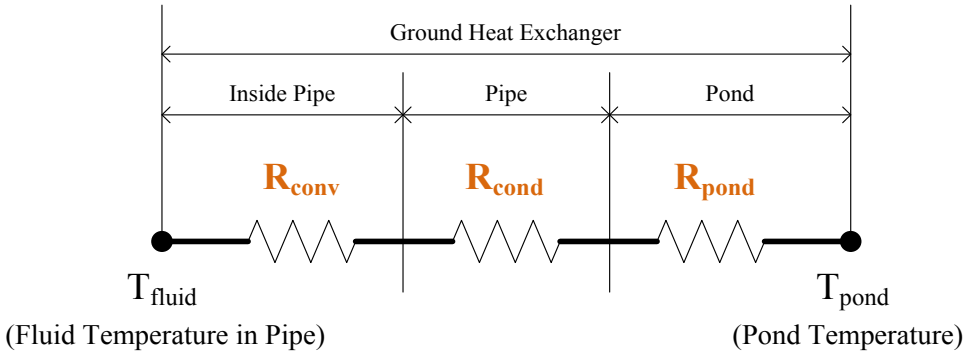

Figure 4-9: Thermal Resistance Diagram for the Surface Water GHX Model

First, the thermal resistances of each material section are calculated. The total resistance is calculated by the summation of the each material resistance. The total surface water GHX thermal resistance is calculated as follows:

$$R_{total} = R_{conv} + R_{cond} + R_{pond} \tag{4.39}$$

Where,

R_{total} is the total thermal borehole resistance (F-hr-ft/Btu),
R_{conv} is the convective resistance of the inner pipe (fluid) (F-hr-ft/Btu),
R_{cond} is the conductive resistance of the pipe wall (F-hr-ft/Btu), and
R_{pond} is the convective resistance between the outer pipe surface and the pond water body (F-hr-ft/Btu).

The convective resistance of the inner pipe (R_{conv}) and the conductive resistance of the pipe wall (R_{cond}) are calculated, following with same equations (eq. 4.10 and eq 4.11) for the horizontal GHX thermal resistance described in Section 4.2.1.2. However, the convective resistance at the outer pipe surface in the pond water needs to be calculated. That is, the convective heat transfer due to internal flow (R_{conv}) which uses the Nusselt number as a function of the Reynolds and Prandtl numbers whereas the convective heat transfer at the outer pipe surface uses the Nusselt number as a function of the Rayleigh numbers. The outer pipe surface is assumed as external free convection boundary layer and the long horizontal cylinder surrounded by pond water. The convective heat transfer at the outer pipe surface can be calculated by using following expressions (Incropera & De Witt, 2001):

$$\beta = 1/(\frac{T_{pond} + T_{pipe}}{2}) \tag{4.40}$$

$$Ra_D = \frac{g\,\beta\,(\Delta T)D^3}{v\,\alpha} \tag{4.41}$$

$$P_r = \frac{C_p\,\mu}{k_{fluid}} \tag{4.42}$$

$$Nu_D = \left(0.60 + \frac{0.387\,Ra_D^{1/6}}{\left[1+(0.559/P_r)^{9/16}\right]^{8/27}}\right)^2 \tag{4.43}$$

$$\mathrm{h} = \frac{Nu_D\,k_{fluid}}{D} \tag{4.44}$$

$$R_{pond} = \frac{1}{\pi\,D\,h} \tag{4.45}$$

Where,

β is the volumetric thermal expansion coefficient of water (k^{-1}),

T_{pond} is the pond water temperature (K),

T_{pipe} is the pipe surface temperature (K),

ΔT is the temperature difference between the pond and the pipe surface (K),

g is the acceleration due to gravity, g is 32.174 (ft/s^2),

D is the outer diameter of the pipe (ft),

v is the kinematic viscosity of water (ft^2/hr),

α is the thermal diffusivity of water (ft^2/hr),

Ra_D is the Rayleigh number (non-dimensional),

C_p is the specific heat of fluid (Btu/lb-F),

μ is the viscosity of fluid (lb/ft-hr),

k_{fluid} is the fluid thermal conductance (Btu/hr-ft-F),

P_r is the Prandtl number (non-dimensional),

h is the convection coefficient of fluid (Btu/hr-ft^2-F), and

R_{pond} is the convective resistance between the outer pipe surface and the pond water body (F-hr-ft/Btu).

4.2.2.3. Entering Water Temperature for the Surface Water GHX

The differential heat transfer equation for the horizontal GHX can be written as:

$$\frac{\Delta T_{out}}{\Delta T_{in}} = \frac{T_{pond} - T_{out}}{T_{pond} - T_{in}} = exp\left[-\frac{l}{\dot{m}\, c_p\, R_{total}}\right] \quad (4.46)$$

Where,

T_{pond} is the pond water temperature (F) using equation 4.38,

T_{in} is the leaving fluid temperature from a heat pump (F),

T_{out} is the entering fluid temperature to a heat pump (F),

ṁ is the rate of fluid flow through the pipe (lb/hr),

C_p is the specific heat of the fluid (Btu/lb-F),

l is the length of the ground heat exchanger (ft), and

R_{total} is the total thermal borehole resistance (F-hr-ft/Btu).

Solving equation 4.46, the EWT for the surface GHX is given by:

$$EWT = T_{pond} + \left(T_{in} - T_{pond}\right) \times exp\left[-\frac{l}{\dot{m}\, c_p\, R_{total}}\right] \quad (4.47)$$

4.2.3. Vertical Ground Heat Exchanger Model

The vertical ground heat exchanger (GHX) model is used to determine the entering water temperature (EWT) from GHX to the heat pump. In order to determine the EWT, the average borehole wall temperature is calculated using an enhanced g-function algorithm (Eskilson, 1987; Yavuzturk and Spitler, 1999). Then, the average fluid (water) temperature inside the pipe in the borehole is calculated using a total thermal borehole resistance. Finally, the EWT is determined.

Therefore, the vertical GHX model in this study has several calculation processes, including determination of the: 1) ground temperature, 2) total thermal borehole resistance, 3) g-function approximation, 4) average borehole wall temperature, 5) average borehole fluid (water) temperature, and 6) entering water temperature (EWT).

Figure 4-10 shows the simplified calculation flow diagram for the vertical ground heat exchanger model to determine the EWT.

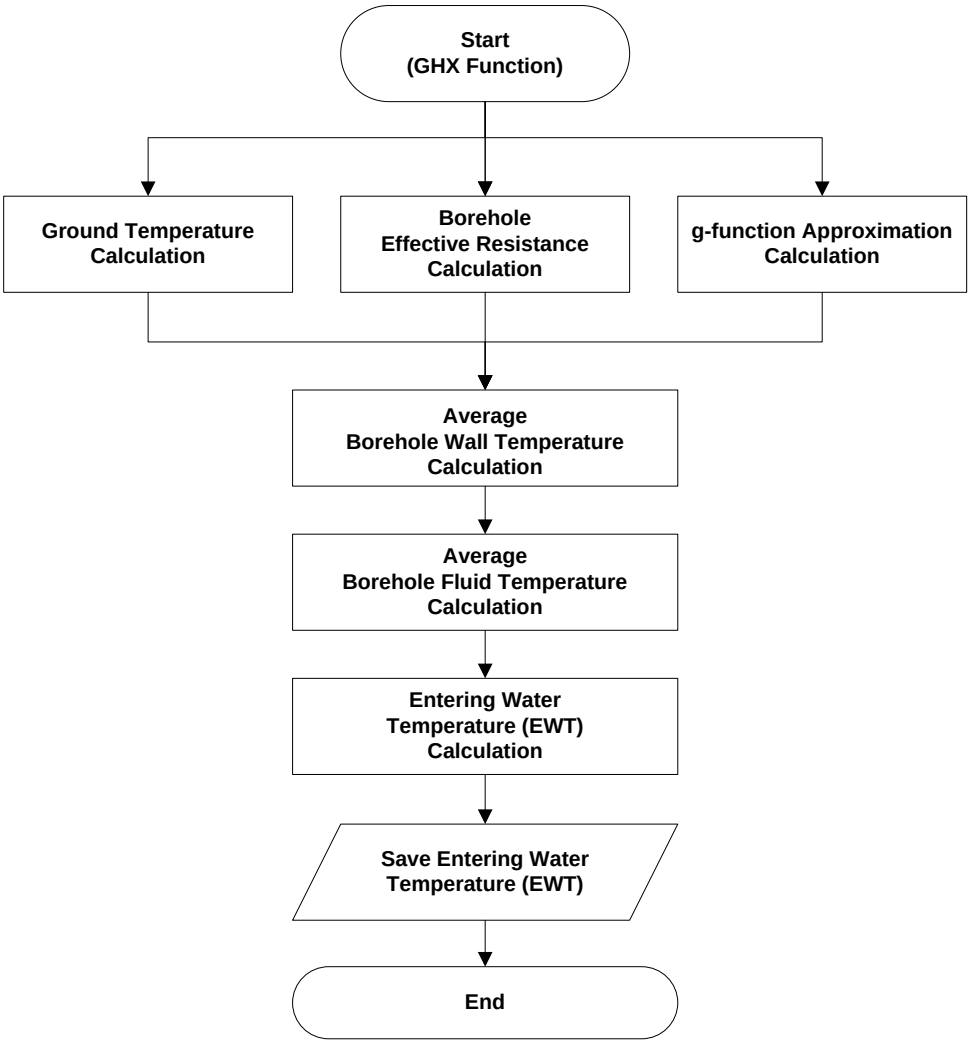

Figure 4-10: Flow Diagram for Vertical Ground Heat Exchanger Model

The vertical GHX model in this study requires leaving water temperature, GHX thermal load, time of the year, g-function value. In addition, it also requires parameters which are the mean ground temperature, amplitude of the ground, phase angle of the ground, GHX length, depth, number, shank space and configuration, fluid flow rate, and

thermal properties of ground/pipe/water. Figure 4-11 presents diagram of input and output parameters for the vertical GHX model.

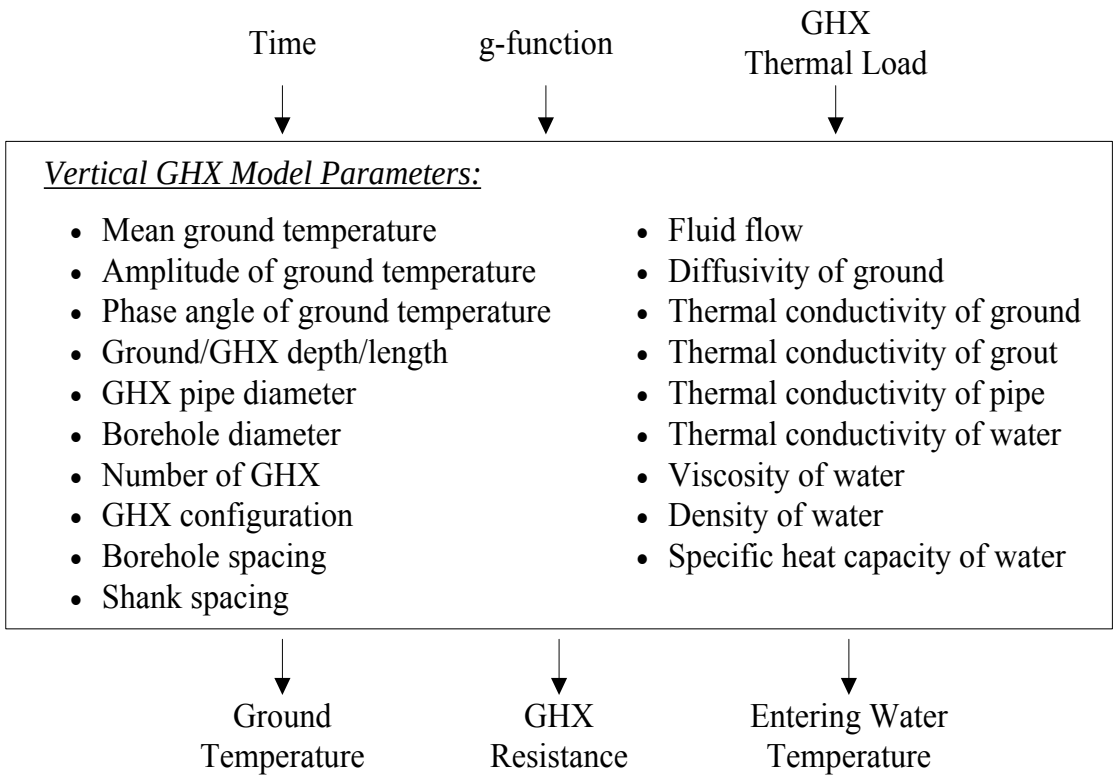

Figure 4-11: Vertical GHX Model Input and Output Parameters

4.2.3.1. Ground Temperature

The undisturbed ground temperature is calculated, using the algorithm developed by Kusuda and Achenbach (1965), described in the Section 4.2.1.1. At ground depths greater than about 35 feet below the surface, the undisturbed ground temperature at the bottom of the vertical GHX is assumed to be same as the mean ground surface temperature over year (e.g., 71F in Houston).

4.2.3.2. Vertical Ground Heat Exchanger (Borehole) Resistance

The total thermal borehole resistance is calculated by combining the conductive resistance of the grout, the conductive resistance of the pipe, and the convective resistance of the fluid at the pipe wall.

Figure 4-12 shows a diagram of a thermal resistance circuit for the borehole and the equation 4.48 describes the calculation of the total thermal borehole resistance.

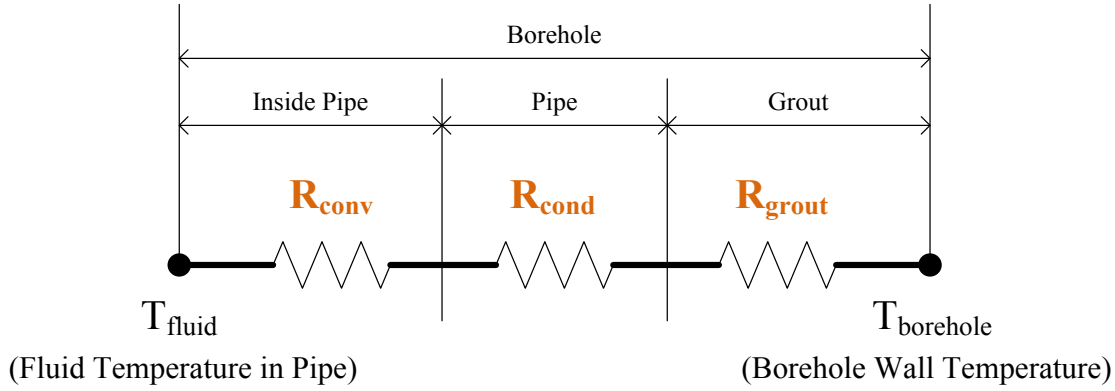

Figure 4-12: Thermal Resistance Diagram for the Vertical GHX Model

$$R_{total} = R_{grout} + R_{cond} + R_{conv} \tag{4.48}$$

Where,

R_{total} is the total thermal borehole resistance (F-hr-ft/Btu),
R_{grout} is the conductive resistance of the grout (F-hr-ft/Btu),
R_{cond} is the conductive resistance of the pipe (F-hr-ft/Btu), and
R_{conv} is the convective resistance of the inner pipe (i.e., fluid) (F-hr-ft/Btu).

First, in order to calculate the total thermal borehole resistance, the conductive resistance of the grout (R_{grout}) is estimated using a multipole method. Bennet et al. (1987) proposed the multipole method to solve steady-state heat conduction problems between pipes in a borehole and the multipole method is used in the EED design software (Hellström and Sanner, 2000). Larmarche et al. (2010) claimed the multipole solution gives the best estimate by comparing several methods for dimensionless borehole resistance for different shank spacing. In this study, using the multipole method, the conductive resistance of the grout is calculated by the following equations:

$$\sigma = \frac{k_{grout} - k_{ground}}{k_{grout} + k_{ground}} \tag{4.49}$$

$$\lambda_1 = \frac{D_{borehole}}{D_{out,pipe}} \tag{4.50}$$

$$\lambda_2 = \frac{D_{borehole}}{2X_c} \tag{4.51}$$

$$\lambda_3 = \frac{\lambda_2}{2\lambda_1} \tag{4.52}$$

$$R_{grout} = \frac{1}{4\pi k_{grout}} \left[ln\left(\frac{\lambda_1 \lambda_2^{1+4\sigma}}{2\left(\lambda_2^4 - 1\right)^{\sigma}} \right) - \frac{\lambda_3^2 \left(1 - \left(4\sigma / \left(\lambda_2^4 - 1\right)\right)\right)^2}{1 + \lambda_3^2 \left(1 + \left(16\sigma / \left(\lambda_2^2 - 1/\lambda_2^2\right)^2\right)\right)} \right] \tag{4.53}$$

Where,

$\sigma,\ \lambda_1,\ \lambda_2,\ \lambda_3$	are dimensionless parameters,
k_{grout}	is the grout thermal conductance (Btu/hr-ft-F),
k_{ground}	is the ground thermal conductance (Btu/hr-ft-F),
$D_{borehole}$	is the borehole diameter (ft),
$D_{out,pipe}$	is the pipe outer diameter (ft), and
X_c	is the shank spacing, defined as half of the center-to-center distance between the two legs of the U-tube pipes (ft).

Second, the conductive resistance of the pipe (R_{cond}) is estimated, using following equation:

$$R_{cond} = \frac{ln\left(\frac{D_{out,pipe}}{D_{in,pipe}}\right)}{4\pi k_{pipe}} \tag{4.54}$$

Where,

$D_{out,pipe}$ is the pipe outer diameter (ft),

$D_{in,pipe}$ is the pipe inner diameter (ft), and

k_{pipe} is the pipe thermal conductance (Btu/hr-ft-F).

Third, the convective resistance of the pipe (R_{conv}) is estimated, using following equations:

$$A_c = \frac{\pi {D_{in,pipe}}^2}{4} \tag{4.55}$$

$$Re_D = \frac{4\dot{m}}{\pi D_{in,pipe}\mu} \tag{4.56}$$

$$P_r = \frac{C_p\mu}{k_{fluid}} \tag{4.57}$$

$$f = (0.790 ln Re_D - 1.64)^{-2} \tag{4.58}$$

$$Nu_D = 4.36 \qquad Re_D < 2{,}300 \tag{4.59}$$

$$Nu_D = \frac{(f/8)Re_D P_r}{1.07+12.7(f/8)^{1/2}\left({P_r}^{2/3}-1\right)} \qquad 2{,}300 \le Re_D < 10{,}000 \tag{4.60}$$

$$Nu_D = 0.023 {Re_D}^{4/5} {P_r}^{n} \qquad 10{,}000 \le Re_D \tag{4.61}$$

$$h = \frac{Nu_D k_{fluid}}{D_{in,pipe}} \tag{4.62}$$

$$R_{conv} = \frac{1}{2\pi D_{in,pipe} h} \tag{4.63}$$

Where,

A_c	is the cross-sectional area of the pipe (ft^2),
$D_{in,pipe}$	is the pipe inner diameter (ft),
Re_D	is the Reynolds number (non-dimensional),
ṁ	is the rate of fluid flow through the pipe (lb/s),
μ	is the viscosity of fluid (lb/ft-hr),
P_r	is the Prandtl number (non-dimensional),
C_p	is the specific heat of fluid (Btu/lb-F),
k_{fluid}	is the fluid thermal conductance (Btu/hr-ft-F),
f	is the friction factor[25] to approximate the smooth surface condition,
Nu_D	is the Nusselt number (non-dimensional),
n	is the coefficient of the exponential term, approximated with 0.35 for both heating and cooling modes (non-dimensional), and
h	is the convection coefficient of fluid (Btu/hr-ft^2-F).

The Nusselt number equations vary based on the fluid flow characteristics inside the pipe of the ground heat exchanger: 1) the constant Nusselt number of 4.36 is used for the laminar flow condition ($\mathrm{Re}_D < 2{,}300$), using equation 4.59. 2) the Nusselt number is calculated for the transition region between laminar flow and turbulent flow ($2{,}300 \leq \mathrm{Re}_D < 10{,}000$), using equation 4.60. 3) the Nusselt number is calculated for the fully turbulent flow ($10{,}000 \leq \mathrm{Re}_D$), using equation 4.61.

[25] The friction factor developed by Petukhov is a single correlation that encompasses a large Reynolds number range (Incropera & De Witt, 2001)

4.2.3.3. g-Function Approximation

This study uses the enhanced g-function approach which was previously discussed in Section 2.6.4. The g-function is a set of tabulated non-dimensional temperature response factors[26], which can determine the temperature change at the borehole wall corresponding to a change in the heat extraction/rejection input for a time step. Whereas Eskilson's g-function model is often called 'a long time-step g-function', the enhanced g-function model is called the short time-step g-function model (Yavuzturk, 1988) since the short time-step g-function model determines temperature response factors for shorter time periods (i.e., hourly or less). To generate both the short and long time-step g-function models, this study uses a curve-fitting method to approximate the g-function, which provides a fast evaluation that does not require a numerical solution.

First, this study considers seventeen borehole field configurations for residential applications, which include: line type, rectangle type, and L-shape type borehole configurations. The maximum number of boreholes in the considered configuration types is ten boreholes, assuming that a general rule-of-thumb is 250 feet of borehole length per ton of GCHP capacity (Chiasson, 1999). Table 4-1 presents the borehole field configuration types, array, and borehole numbers corresponding to the borehole field configurations.

---

[26] The tabulated g-function values are available from the Bdllib.dat file in the eQUEST program. The file includes g-function values for 42 well configurations. In addition, Eskilson has presented curves of the g-function values for 38 borehole configurations, which can be tabulated (Eskilson, 1987)

Table 4-1: Borehole Field Configuration for Residential Application

Configuration	Array	# of Borehole
Line Type 	Line 1x1 (Single)	1
	Line 1x2	2
	Line 1x3	3
	Line 1x4	4
	Line 1x5	5
	Line 1x6	6
	Line 1x7	7
	Line 1x8	8
Rectangle Type 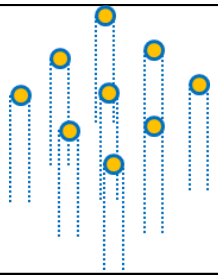	Rec 2x2	4
	Rec 2x3	6
	Rec 2x4	8
	Rec 2x5	10
	Rec 3x3	9
L-Shape Type 	L 2x2	3
	L 2x3	4
	L 2x4	5
	L 2x5	6

Second, the tabulated long time-step g-function, developed by Eskilson, is often displayed using graphs. For example, Figure 4-13 shows the long time-step temperature response factor (g-function) curves, which use non-dimensional time for boreholes that have line type and rectangle type configurations. The g-function values corresponding to

each borehole configuration have a ratio of 0.1 between the borehole space and depth[27]. Figure 4-14 presents long time-step g-function values corresponding to different center-to-center borehole spacing for 3×3 rectangle type borehole configuration. Figure 4-13 and Figure 4-14 indicate that temperature changes at the borehole wall increases as the number of boreholes increase, time of system operation increases, and borehole spacing decreases.

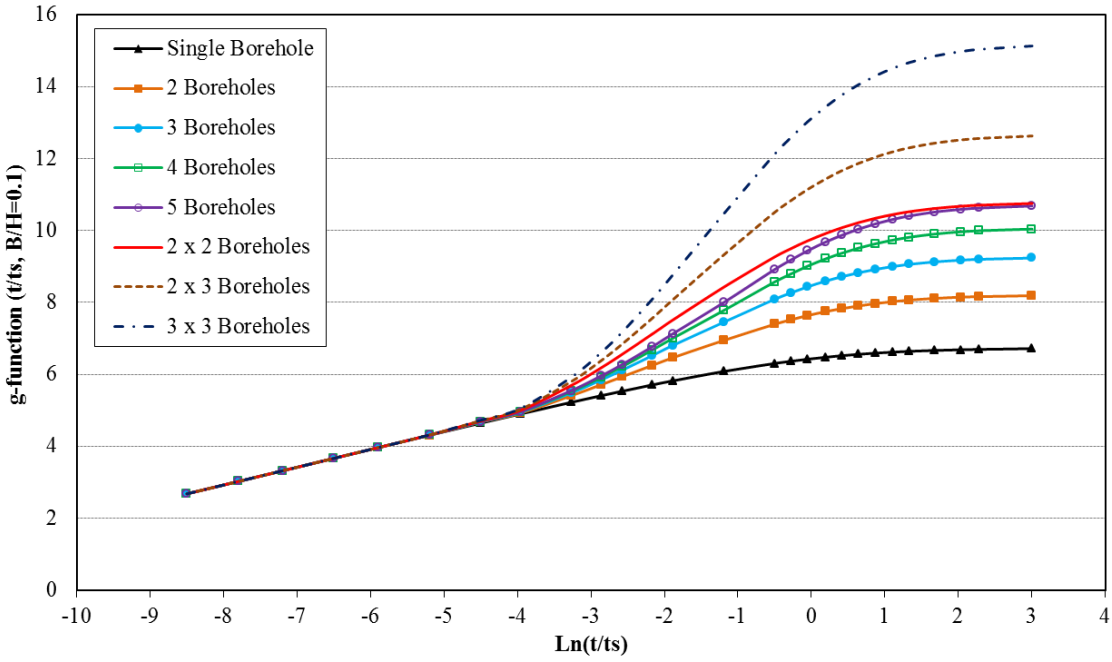

Figure 4-13: Long Time-Step g-Function Curves for Straight Line Type and Rectangle Type Borehole Configurations (Eskilson, 1987)

[27] t is time, ts is time scale, B is the borehole space, and H is the borehole depth in Figure 4-13.

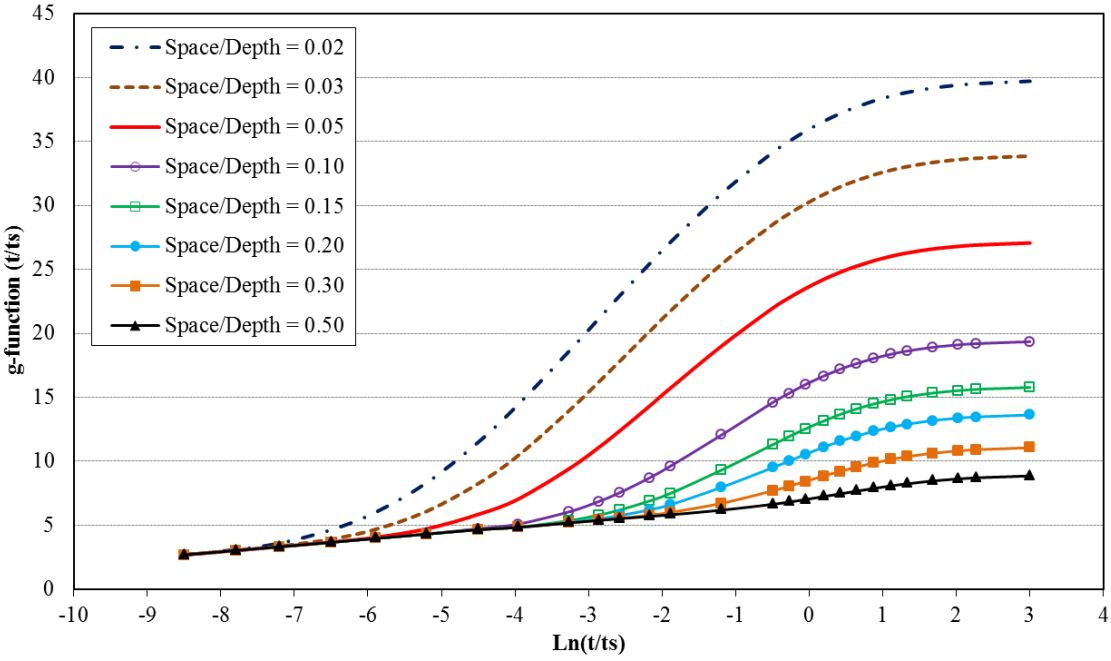

Figure 4-14: Long Time-Step g-Function Curves for 3×3 Rectangle Type Borehole Configurations (Eskilson, 1987)

Third, short time-step g-function values were developed by Yavuzturk and Spitler from the long time-step g-function values by using linear interpolation, which allows shorter time periods. Figure 4-15 shows the result plot for the short time-step g-function values with the long time-step g-function values for a single borehole and a 3×3 rectangle type borehole field.

Fourth, this study approximates g-function values for a single borehole and multiple boreholes (i.e., borehole field). The g-function approximation utilizes polynomial curve-fitting method to generate the g-function values for both short time-step and long time-step. Figure 4-16 shows the simplified diagram to approximate the g-function values in this study.

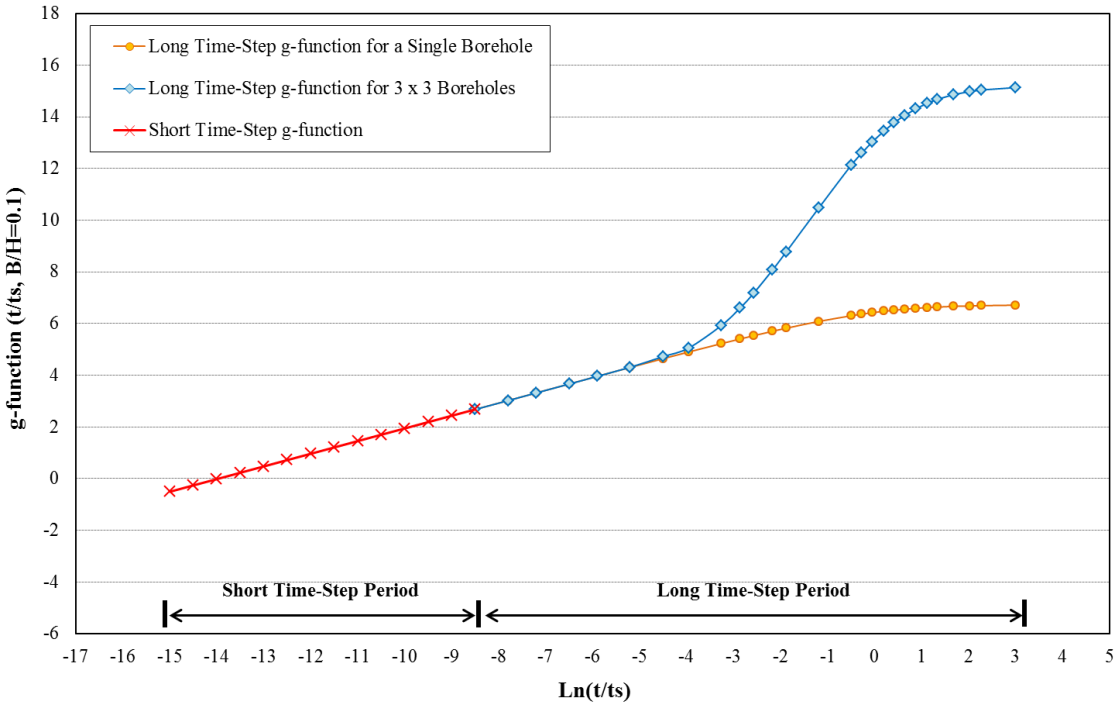

Figure 4-15: Plot of Short and Long Time-Step g-Function Curve

First, g-function values for a single borehole are calculated using polynomial curve-fitting method according to non-dimensional time. The g-function values for a single borehole are calculated with the following equation:

$$g_{single} = ax^3 + bx^2 + cx + d - \ln(\frac{r_b *}{r_b}) \quad (4.64)$$

Where,

g_{single}	is the g-function values for a single borehole,
x	is the non-dimensional time ($\ln(^t/_{t_s})$),
$r_b *$	is the borehole outer radius (ft),
r_b	is the borehole inner radius (ft), and
a, b, c, d	are the coefficients.

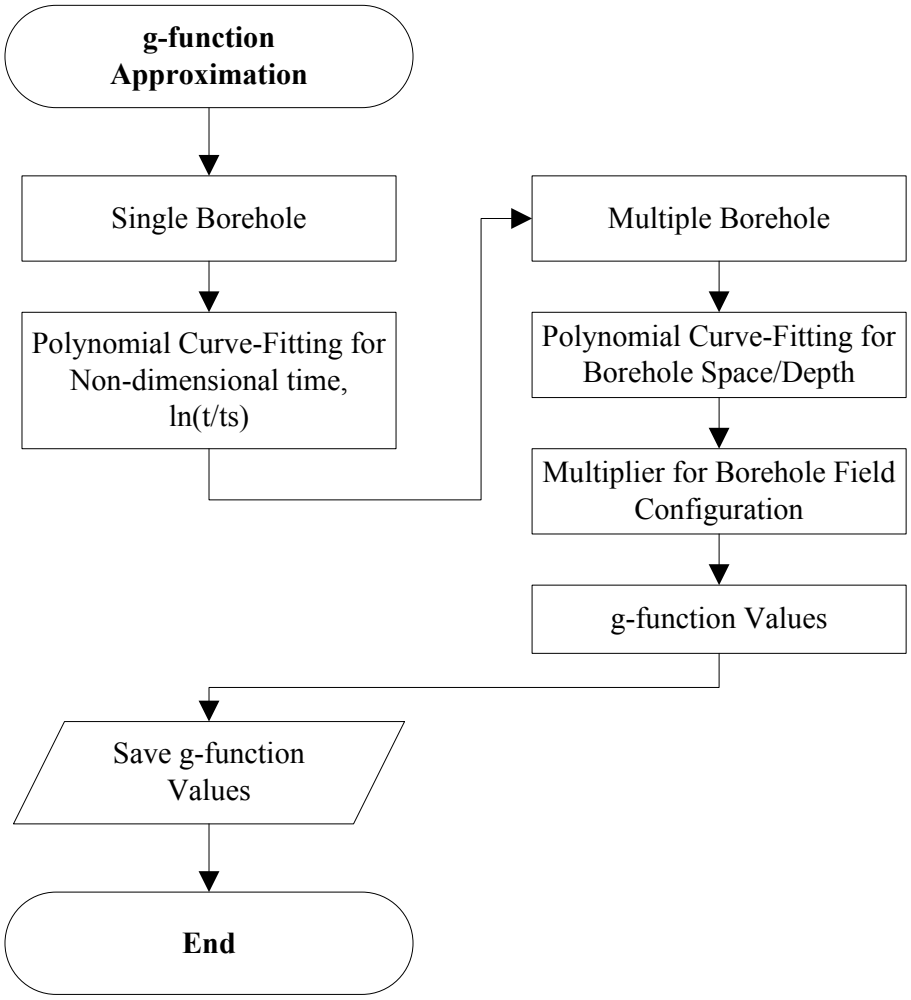

Figure 4-16: Diagram of g-Function Approximation Procedure

The coefficients used in the equation 4.64 are presented in the Table 4-2. If the g-function value is negative, the g-function value reset to zero by assuming that the borehole wall does not have any temperature change. In Figure 4-15, for example, when the non-dimensional time reaches to -14, the g-function value becomes negative. In this case, the g-function value set to zero.

Table 4-2: Coefficients for a Single Borehole g-Function Approximation

Non-Dimensional Time	Coefficients			
	a	b	c	d
ln(t/ts) < -8.5	0	0	0.49	6.846
-8.5 ≤ ln(t/ts) < -5.6		0.0016	0.5173	6.9588
-5.6 ≤ ln(t/ts) < 1.9	-0.0038	-0.0528	0.2364	6.4306
1.9 ≤ ln(t/ts) < 3.003		-0.0161	0.1138	6.5184
3.003 ≤ ln(t/ts)	0	0	0	6.716

Second, g-function values for multiple boreholes are calculated, also using polynomial curve-fitting method according to the ratio of a borehole space and borehole depth (B/H). In addition, the calculated g-function values are corrected using a multiplier according to a borehole field configuration and array. Using the curve-fit equation and multipliers, the g-function values for multiple boreholes are approximated with the following equation:

$$g_{multiple} = M(ax^5 + bx^4 + cx^3 + dx^2 + ex + f) + g_{single} \quad (4.65)$$

Where,

g_{single} is the g-function values for a single borehole, given by equation 4.64,

x is the non-dimensional time ($\ln(t/t_s)$),

M is the multiplier for borehole field configuration, and

a, b, c, d, e, f are the coefficients.

The coefficients and multipliers used in the equation 4.65 are presented in the Table 4-3 and Table 4-4, respectively.

Table 4-3: Coefficients for the Ratio of a Borehole Space and Depth

Borehole Space and Depth (B/H)	Coefficients					
	a	b	c	d	e	f
0.02	0.0008	0.0119	-0.0031	-0.4532	1.6505	17.9850
0.03	0.0011	0.0143	-0.0101	-0.4624	1.6359	14.8710
0.05	0.0015	0.0157	-0.0279	-0.4412	1.6389	11.1280
0.10	0.0026	0.0171	-0.0640	-0.3679	1.6011	6.6682
0.15	0.0030	0.0142	-0.0814	-0.2665	1.4844	4.4937
0.20	0.0032	0.0098	-0.0869	-0.1710	1.3268	3.1786
0.30	0.0043	0.0022	-0.0946	-0.0318	1.0363	1.6583
0.50	0.0050	-0.0118	-0.0634	0.0970	0.5528	0.5355

Table 4-4: Multipliers for the Borehole Configuration and Array

Configuration	Array	Number of Borehole	Multiplier
Line-Type	Line 1x2	2	0.174
	Line 1x3	3	0.297
	Line 1x4	4	0.387
	Line 1x5	5	0.471
	Line 1x6	6	0.530
	Line 1x7	7	0.589
	Line 1x8	8	0.632
Rectangle-Type	Rec 2x2	4	0.466
	Rec 2x3	6	0.698
	Rec 2x4	8	0.867
	Rec 2x5	10	1.015
	Rec 3x3	9	0.996
L-Type	L 2x2	3	0.320
	L 2x3	4	0.411
	L 2x4	5	0.496
	L 2x5	6	0.564

4.2.3.4. Average Borehole Wall Temperature

The calculation for the average borehole wall temperatures is based on a hybrid approach using the g-function developed by Eskilson. The approximated g-function values, described in Section 4.2.3.3, will be used to calculate the borehole wall temperatures. In addition, Yavuzturk and Spitler (1999) described the step heat extraction/rejection input to each time step, based on the graphical description of the superposition process. The step heat extraction/rejection input will be also used for the borehole wall temperature calculation.

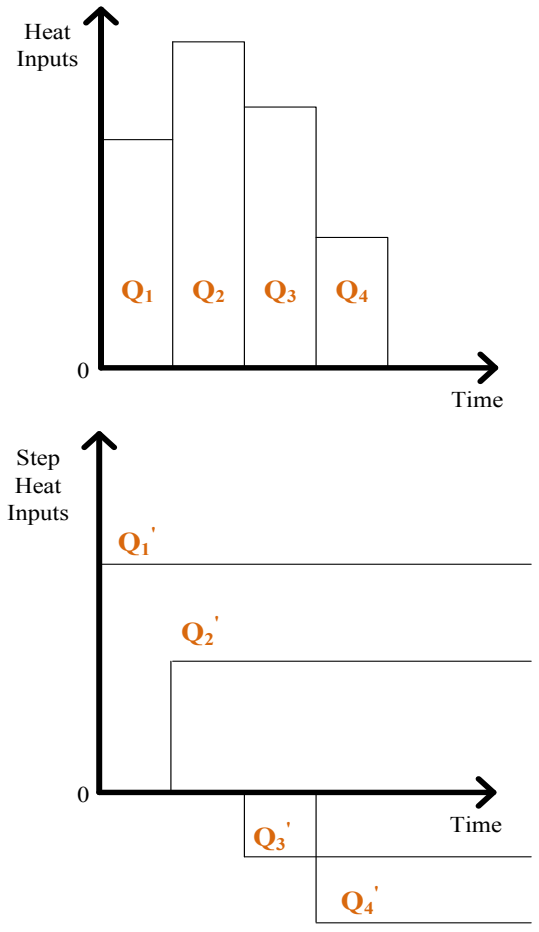

Figure 4-17: Superposition Method of Step Heat Inputs (Yavuzturk and Spitler, 1999)

Figure 4-17 shows the conceptual diagram of the superposition method. In the Figure 4-17, Q_1 is the basic heat input used for the entire period. Q_2, Q_3, and Q_4 are the heat inputs for each time step. Q_1', Q_2', Q_3', and Q_4' are the subsequent step heat inputs. That is, $Q_1' = Q_1$ for first time step, $Q_2' = Q_2 - Q_1$ for second time step, $Q_3' = Q_3 - Q_2$ for third time step, and $Q_4' = Q_4 - Q_3$ for fourth time step.

The average borehole wall temperatures ($T_{borehole}$ in Figure 4-18 which shows a conceptual diagram of a GHX), using the g-function approach with a single step heat pulse, are calculated with the following equation:

$$T_{borehole} = T_{ground} + \sum_{i=1}^{n} \frac{Q_i'}{2\pi k_{ground}} g\left(\frac{t_n - t_{i-1}}{t_s}, \frac{r_b}{H}, \frac{B}{H}, Borefield\right) \quad (4.66)$$

Where,

$T_{borehole}$	is the borehole wall temperature at the end of n^{th} time period (F),
T_{ground}	is the undisturbed ground temperature which is calculated from equation 4.1 (F),
Q_i'	is step heat extraction/rejection input per unit length (Btu/hr-ft),
k_{ground}	is the ground thermal conductance (Btu/hr-ft-F),
t	is time (hr),
t_s	is time scale = $H^2/9\alpha$,
α	is the thermal diffusivity of ground (ft^2/hour),
r_b	is the borehole radius (ft),
H	is the borehole depth (ft),
B	is the space between adjacent boreholes (ft), and
$Borefield$	is the borehole configuration and number.

The borehole wall temperatures are calculated by adding a temperature change (associated with sigma term in the equation 4.66 and in response to the step heat input at the time, ground thermal diffusivity, and borehole configuration) to the undisturbed ground temperature.

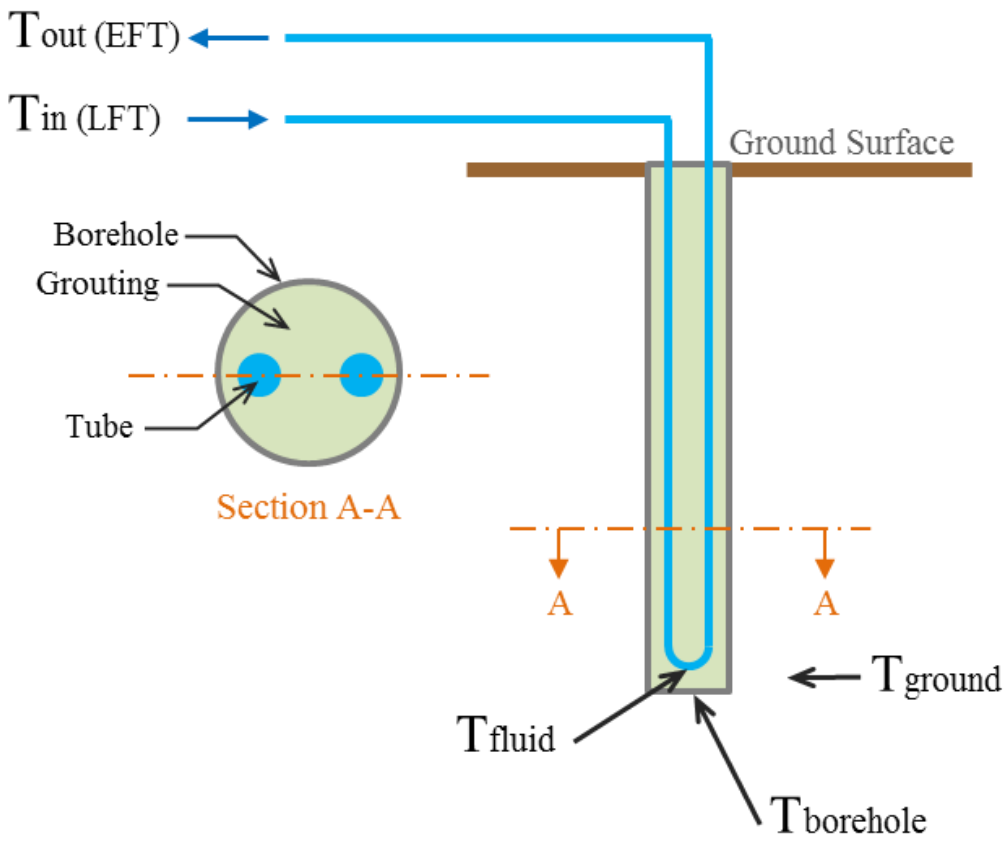

Figure 4-18: Conceptual Diagram of Ground Heat Exchanger

4.2.3.5. Average Fluid (Water) Temperature in the Borehole

Once the borehole resistance in Section 4.2.3.2 and average borehole wall temperature in Section 4.2.3.4 have been determined, the average fluid temperature

(Figure 4-18) inside the U-tube pipe can be computed. The average fluid temperature (T_{fluid}) can be determined, using the following expressions:

$$Q'_n = \frac{T_{fluid} - T_{borehole}}{R_{total}} \tag{4.67}$$

Where,

Q'_n is the heat extraction/rejection input per unit length at the n^{th} time period (Btu/hr-ft),

T_{fluid} is the average fluid temperature at the n^{th} time period (F),

$T_{borehole}$ is the average borehole wall temperature at the n^{th} time period, given by equation 4.66 (F), and

R_{total} is the total thermal borehole resistance, given by equation 4.48 (F).

If we solve for T_{fluid} from equation 4.67, it follows that

$$T_{fluid} = T_{borehole} + R_{total} \times Q'_n \tag{4.68}$$

Using this equation, the average fluid temperatures may be determined, based on the average borehole wall temperature, considering the convective resistance between the fluid and U-tube pipe, conductive resistance at the U-tube pipe, conductive resistance of the grout, and the step heat inputs at the desired time period as well.

4.2.3.6. Entering Water Temperature

The average fluid temperature determined from equation 4.68 is the mean fluid temperature at the halfway point between the borehole inlet and borehole outlet. If one

assumes that the temperature change between the inlet and outlet is linear. This can be expressed by the following equation:

$$T_{fluid} = \frac{T_{in} + T_{out}}{2} \tag{4.69}$$

Where,

T_{fluid}	is the average fluid temperature (F),
T_{in}	is the leaving fluid temperature from a heat pump (F), and
T_{out}	is the entering fluid temperature to a heat pump (F).

Therefore, the heat transfer rate through the half length of the borehole can be expressed by:

$$Q = 2 \times \dot{m} \times C_p \times \left(T_{out} - T_{fluid}\right) \tag{4.70}$$

Where,

Q	is the heat transfer rate (Btu/hr),
ṁ	is the rate of fluid flow through the pipe (lb/hr),
C_p	is the specific heat of the fluid (Btu/lb-F),
T_{out}	is the entering fluid temperature to a heat pump (F), and
T_{fluid}	is the average fluid temperature (F).

The Entering Water Temperature (EWT) circulated from a borehole to the heat pump is T_{out} in equations 4.69 and 4.70. Finally, if we solve for T_{out} from equations 4.69 and 4.70, it follows that

$$EWT = T_{fluid} + \frac{Q}{2\dot{m}C_p} \tag{4.71}$$

4.3. Custom-Built Ground Heat Exchanger Model

A custom-built GHX model is developed for the case-study house to calculate the ETWs by combining the horizontal GHX model and the surface water GHX model, which were described in Sections 4.2.1 and 4.2.2, respectively. The custom-built GHX model will be validated using the measured EWT data from the case-study house. This section includes a description of the case-study house, measurement, and data collection of the GHX temperatures. In addition, this study uses local weather data from the Solar Test Bench (STB) of the Energy Systems Laboratory (ESL), which is built on the roof of the Langford building at Texas A&M University.

4.3.1. Description of the Case-Study House

The case-study house, in which a GCHP system is installed, is located in College Station, Texas. It is a two-story residential house built in 1997. This house has one living room, one family room, one dining room, one kitchen, three bedrooms, two bathrooms, one pantry room, one utility (solar hot water heater) room, and one greenhouse on the first floor. In addition, the house has additional spaces on the second floor, including: one bedroom, one bathroom, one sewing room, three lofts, and one den (office). The total area is 3,075 ft^2, including 2,175 ft^2 for 1st floor and 900 ft^2 for 2nd floor. The HVAC system consists of a water-source heat pump (WSHP) system[28] (3.5 tons) for the whole house and a solar energy domestic hot water system.

---

[28] The case-study house has one additional WSHP system (1 ton) for the bedroom on the 2nd floor. However, this study does not consider it for the analysis, since this system is rarely operated by residents.

Figure 4-19: Front-Left Side of the Case-Study House (Facing Northeast)

Figure 4-20: Front-Right Side of the Case-Study House (Facing Northwest)

Figure 4-21: Back-Left Side of the Case-Study House (Facing Southwest)

Figure 4-22: Back-Right Side of the Case-Study House (Facing Southeast)

Figure 4-23: Back Side of the Case-Study House (Facing South)

The WSHP system utilizes custom-built ground heat exchangers (GHXs), which use a combination of horizontal GHXs and surface water (pond) GHX. The WSHP system is connected with the first horizontal GHX, the surface water GHX, and the second horizontal GHX, in sequence.

Figure 4-19 through Figure 4-23 show the pictures of the case-study house and Figure 4-24 presents the diagram of the GHX connection used in the case-study house.

The first GHX is the horizontal type which has 450 ft in length and 5 ft in depth. The second GHX is the surface water type which has 1,040 ft in length and 6 ft in depth. The third GHX is the horizontal type which has 920 ft in length and 6 ft in depth. The total length of all the GHXs is 2,410 ft, including 1,040 ft of surface water type GHX and 1,370 ft of horizontal type GHXs.

Figure 4-24: Installation of the GHXs Used in the Case-Study House

The GHXs uses polyethylene (PE) throughout the GHX unit. The PE pipe is two inches in diameter. A single pump is used to circulate the water from the WSHP to the GHXs. The pump has a single speed, 1/6 HP motor (about 4.28 gpm which is estimated based on the manufacture specification[29]).

Figure 4-25 shows the Water-Source Heat Pump system in the case-study house. Figure 4-26 shows the ground field, in which the horizontal GHX is installed and Figure 4-27 shows the pond which the surface water GHX is installed.

Figure 4-25: Water-Source Heat Pump of the Case-Study House

[29] The specification can be found in the following web link, http://www.fhp-mfg.com/files/download/Literature%20Archives/Discontinued%20Products/EM/EM_Install.pdf

Figure 4-26: Photo of the Pond for the Surface Water GHX

Figure 4-27: Photo of the Ground Field for the Horizontal GHX

4.3.2. Measurement and Data Collection from the Case-Study House

This section discusses the equipment and the sensors used for monitoring temperatures of the GHX and the case-study house. This includes the temperature sensor calibration and installation of the sensors.

4.3.2.1. Temperature Sensor Calibration

Ten thermocouple sensors (T-type) were used to measure the temperatures for the supply air, the return air, leaving water, and entering water. Before installing the thermocouple sensors in the ground-coupled heat pump system, the thermocouple sensors were calibrated to improve the accuracy of the measurement (Nicholas and White, 1994). To develop the correction factor, a calibrated scale and offset must be calculated. To implement the calibration of the thermocouple sensors, the American Society for Testing and Materials (ASTM) Standards E77-07 2007 was used.

The calibration methodology used in this study compares the temperature readings of the thermocouple sensors with the reference temperature readings. In order to calibrate the ten thermocouple sensors, two ASTM certified liquid-in-glass thermometers, two spirit-filled glass thermometers[30], three Resistance Temperature Detector (RTD) temperature sensors, a Campbell data logger model CR1000 (Campbell Scientific, 2013b), and a portable Synergistic data logger model C180 (Synergistic Control Systems, 1994) were used.

---

[30] National Institute of Standards and Technology (NIST)-certified spirit-filled glass thermometers were used.

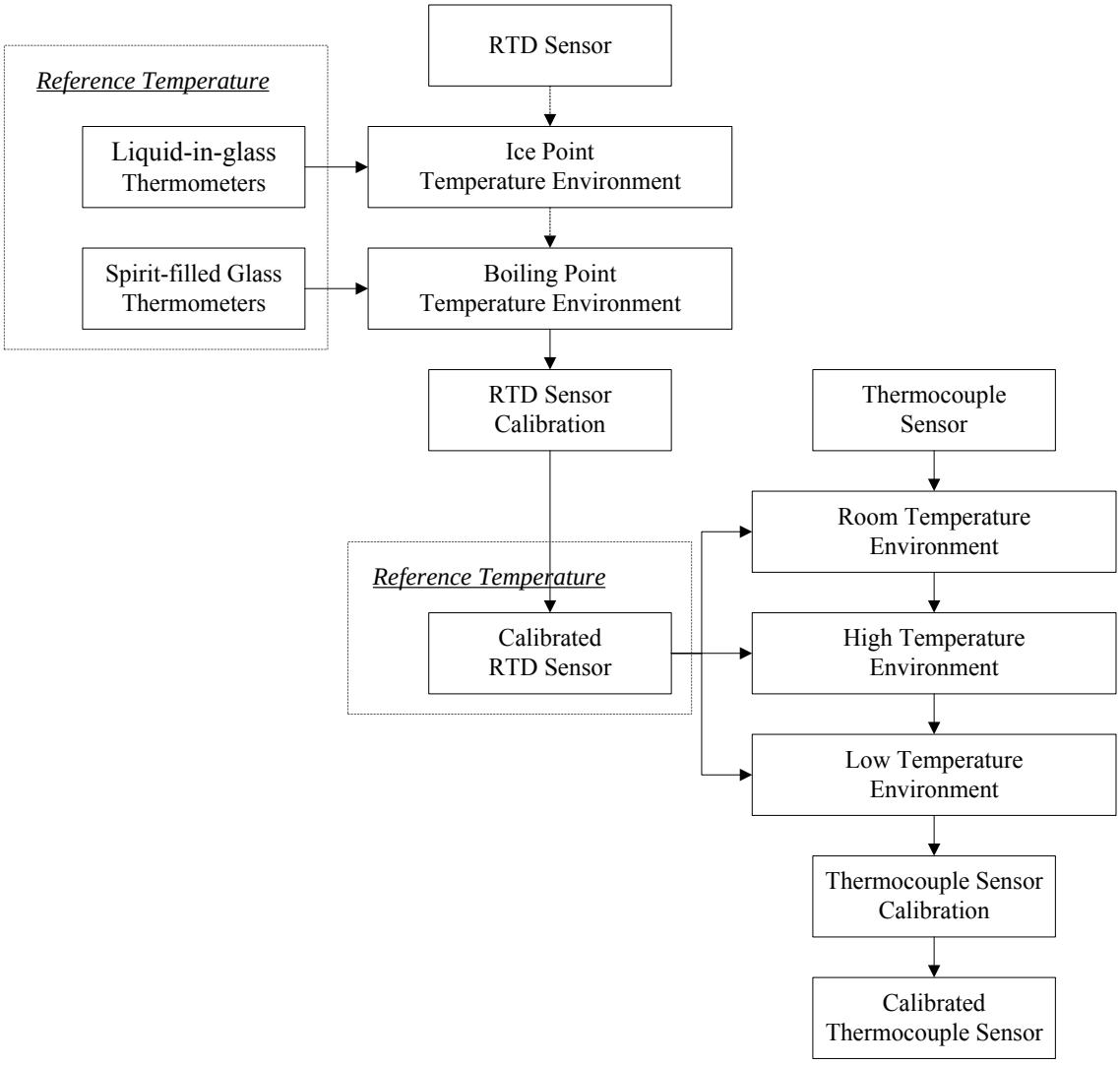

Figure 4-28: Calibration Procedure for the Thermocouple Sensors

Figure 4-28 shows the procedure used to calibrate the thermocouple sensors. First, the RTD temperature sensors were calibrated against ASTM certified liquid-in-glass thermometers and spirit-filled glass thermometer. The RTD temperature sensors were connected with a portable Synergistic data logger to read temperatures (Figure 4-29). The calibration was conducted under controlled temperature environments including

an ice point and a boiling point (Figure 4-29 and Figure 4-30), using distilled water. Scales and offsets were then determined, based on the RTD temperature readings and the reference temperature readings. The RTD sensors were calibrated according to the scales and offsets. The scales and offsets determined from the calibration can be found in the Appendix A. In addition, the calibration results of the RTD temperature sensors, including temperature corrections and residual plots before and after the calibration can be also found in the Appendix A.

After calibrating three RTD temperature sensors, the RTD sensors became the reference temperature sensors for the thermocouple sensors. The thermocouple sensors were then calibrated against the calibrated RTD temperature sensors[31].

The calibration for the thermocouple sensors was conducted under three different controlled temperature environments, which are general interest in this study: high temperature, room temperature, and low temperature. To control the temperature environments, the calibrated RTD temperature sensors and the thermocouple sensors were placed in a glass container. Then, the container was placed inside a refrigerator, which was used for a test chamber (Figure 4-31). The thermocouple sensors were connected to a Campbell data logger (CR1000) to read the temperatures (Figure 4-32).

[31] Two RTD sensors (RTD #1 and RTD #2) of three calibrated RTD sensors were used for the thermocouple sensor calibration since one RTD sensor had bad sensor readings.

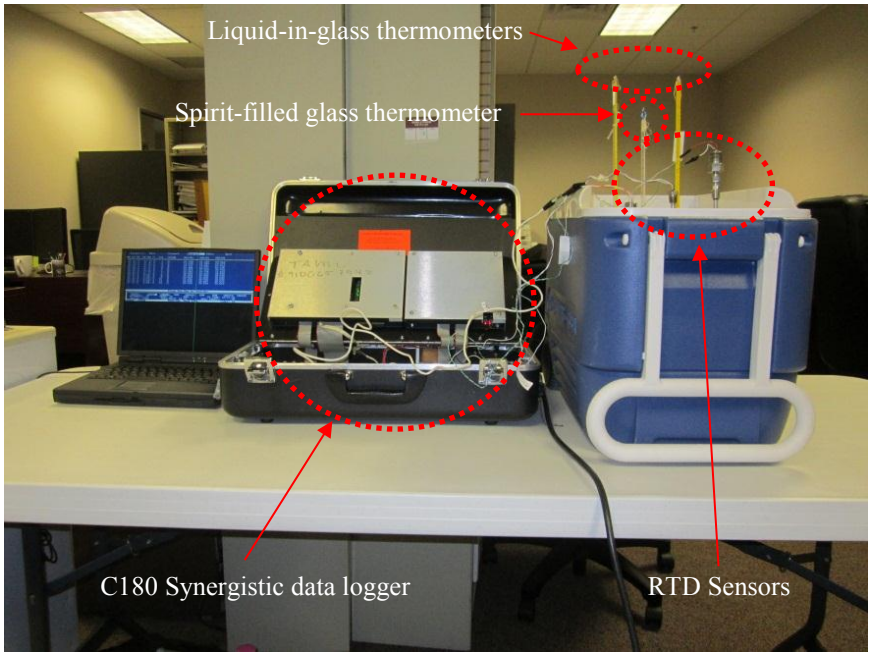

Figure 4-29: Ice Point Experiment Setting for the RTD Sensor Calibration

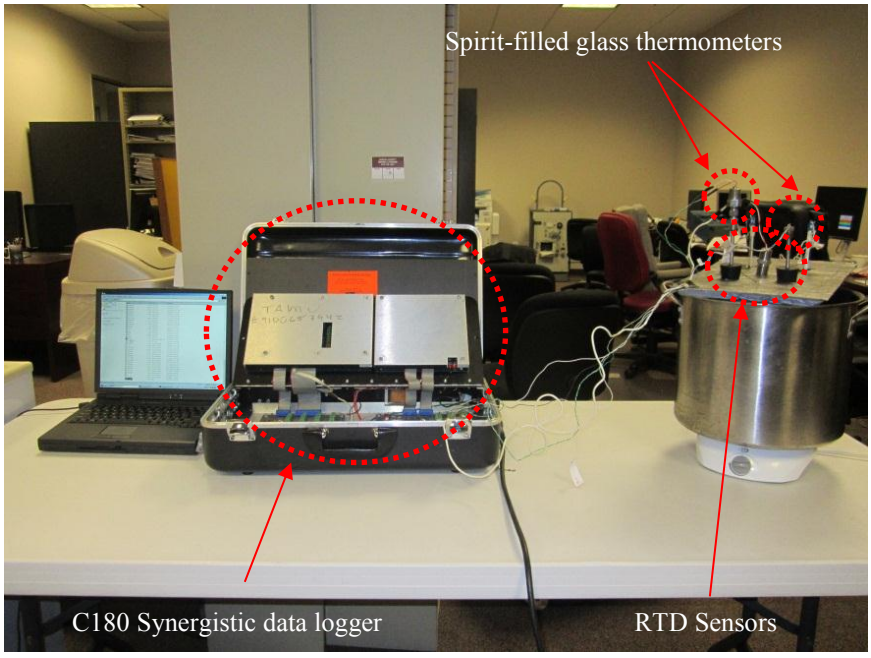

Figure 4-30: Boiling Point Experiment Setting for the RTD Sensor Calibration

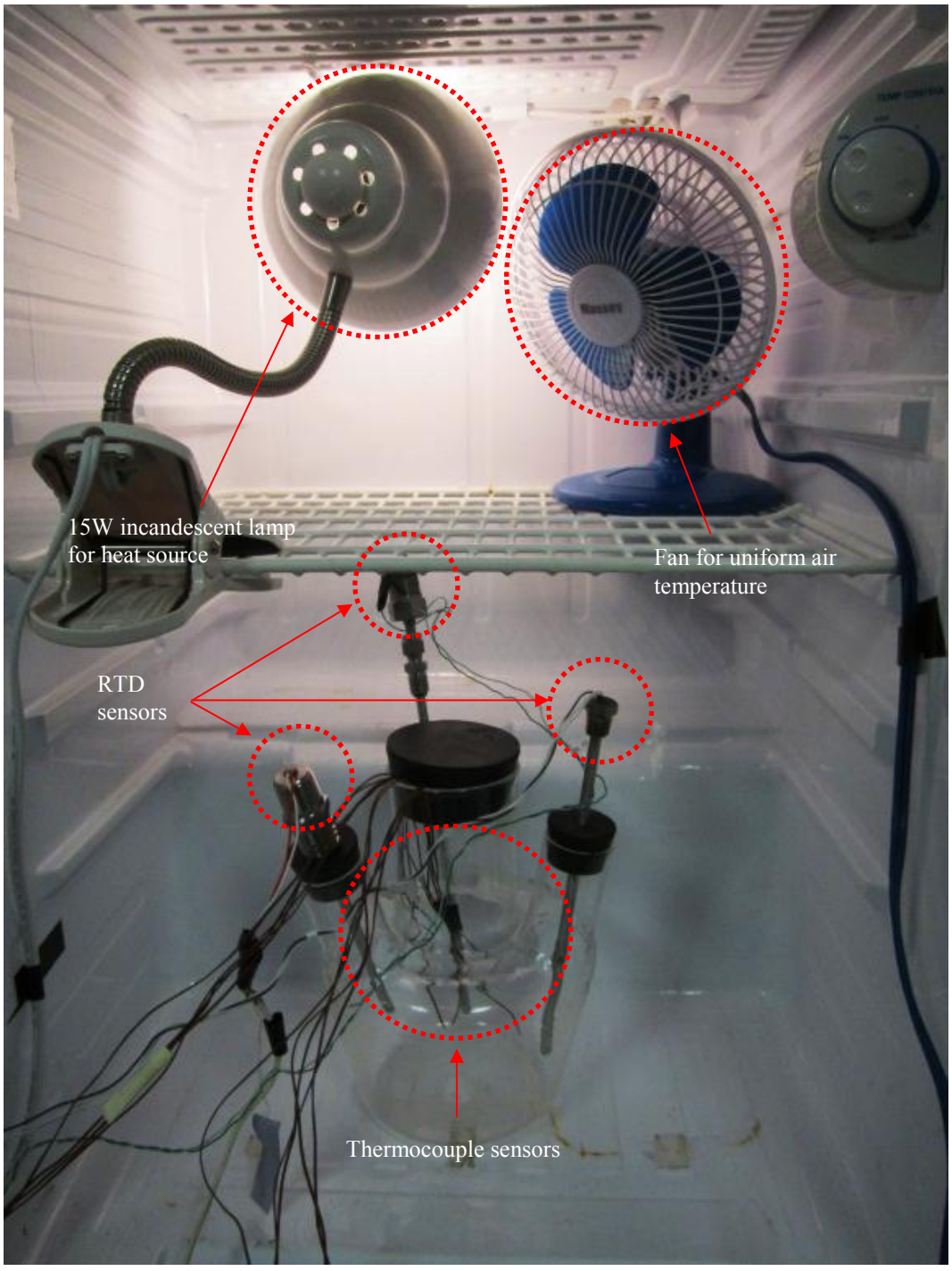

Figure 4-31: Experimental Setting inside Test Chamber

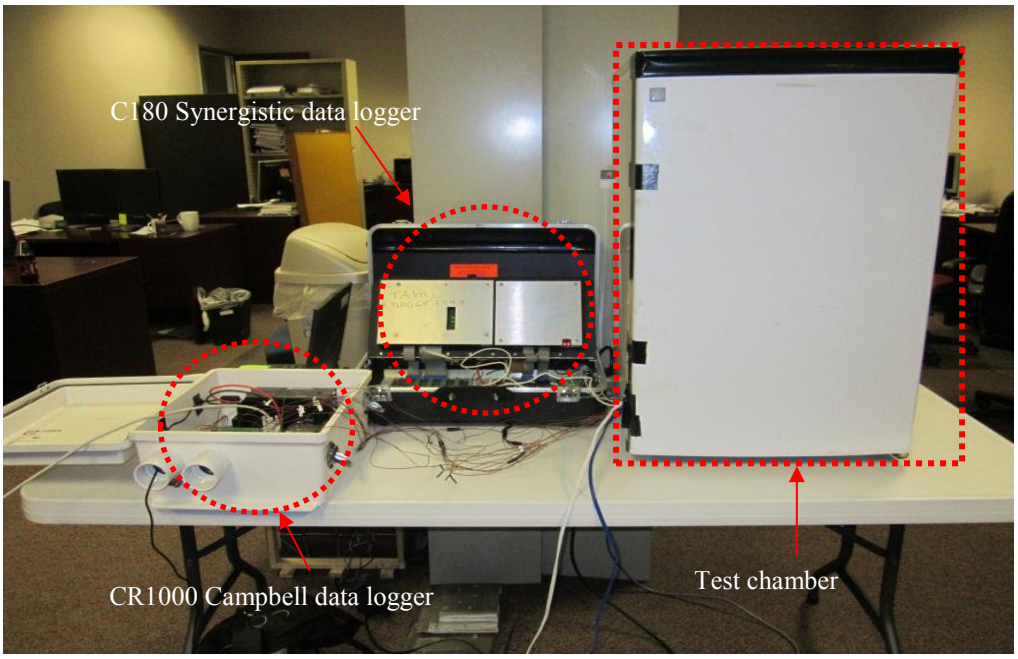

Figure 4-32: Experimental Setting for the Thermocouple Sensor Calibration

The room temperature and the low temperature environments were created by turning off the refrigerator and turning on the refrigerator, respectively. The high temperature environment was created by turning off the refrigerator and turning on a 15W incandescent lamp to produce heat inside the refrigerator. In addition, a small fan was used to maintain uniform thermal temperature inside the refrigerator and the refrigerator door were sealed with the duct tape tightly to minimize air leakage. Using scales and offsets based on the thermocouple temperature readings and the RTD temperature readings, the thermocouple sensors were calibrated.

The scales and offsets determined by the measurement can be found in the Appendix A. In addition, the calibration results of the thermocouple temperature sensors,

including temperature corrections and residual plots before and after calibration can be also found in the Appendix A.

4.3.2.2. Installation of Sensors

In order to measure the supply air, return air, entering water, and leaving water temperatures, ten thermocouple[32] sensors were used. Figure 4-33 shows the diagram for the installation of the sensors to measure the air and water temperatures.

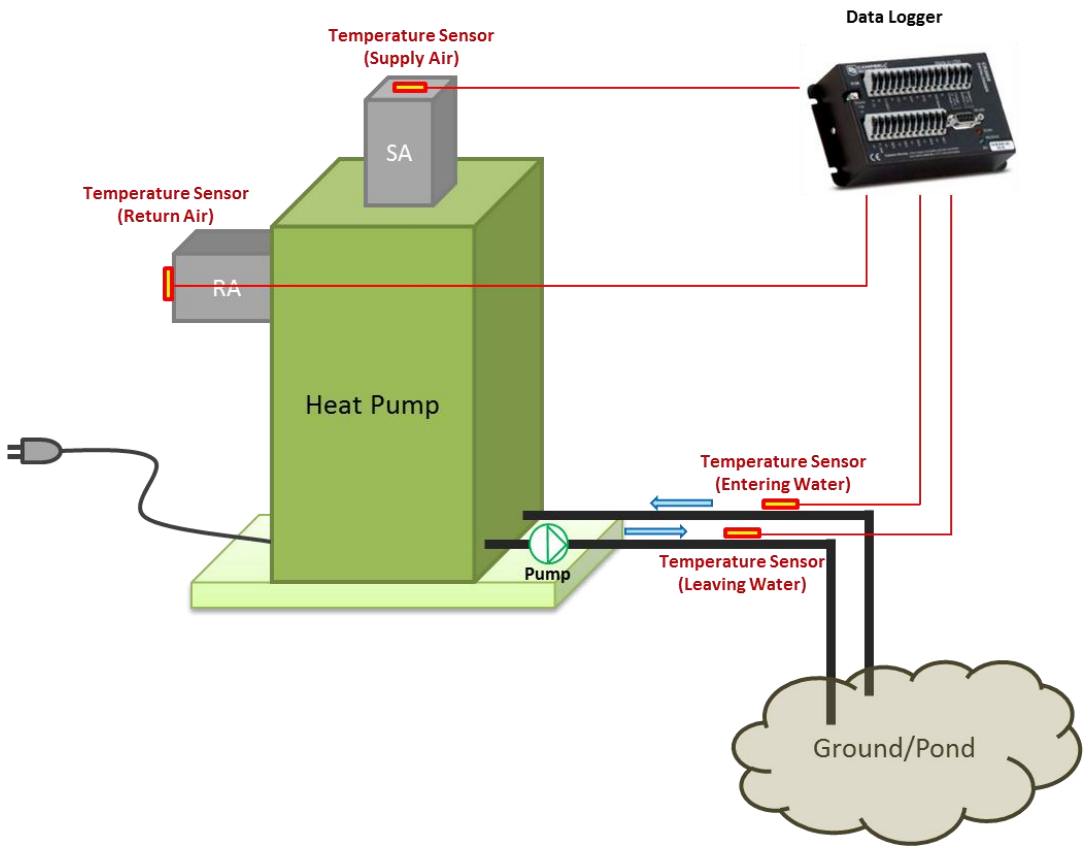

Figure 4-33: Diagram for Temperature Sensor Installation

[32] The thermocouple sensors used in this study are the T-type thermocouple made with a positive copper leg and a negative constantan leg, color coded is blue for positive and red for negative

Five thermocouple sensors were installed to measure the supply air temperature, three thermocouple sensors were installed to measure the return air temperature, one thermocouple sensor was installed to measure the Entering Water Temperature (EWT), and one thermocouple sensor was installed to measure the Leaving Water Temperature (LWT). Table 4-5 shows the summary table of the thermocouple sensors used for air and water temperatures.

Table 4-5: Thermocouple Sensors Used for Measurement

Measured Temperature	Sensor	Measure Point
Supply Air	Thermocouple Grid	5
Return Air	Thermocouple Grid	3
Entering Water	Single Thermocouple	1
Leaving Water	Single Thermocouple	1

The supply air and return air temperatures were measured using multiple thermocouples (i.e., a thermocouple grid) to account for air temperature variations that can occur in the supply/return duct. The thermocouple grid for the return air consists of three thermocouples and the thermocouple grid for the supply air consists of five thermocouples. The average air temperatures for the supply air and return air were calculated from multiple temperatures in the thermocouple grid. Figure 4-34 and Figure 4-35 show the photos of the thermocouple grid to measure return air temperatures and supply air temperatures, respectively.

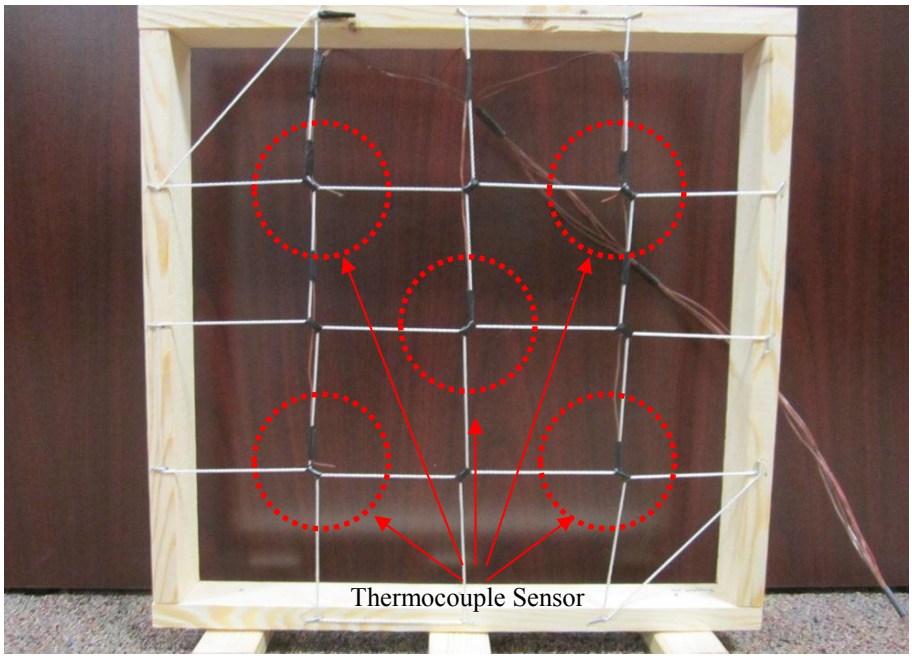

(a) Thermocouple Grid before Installation

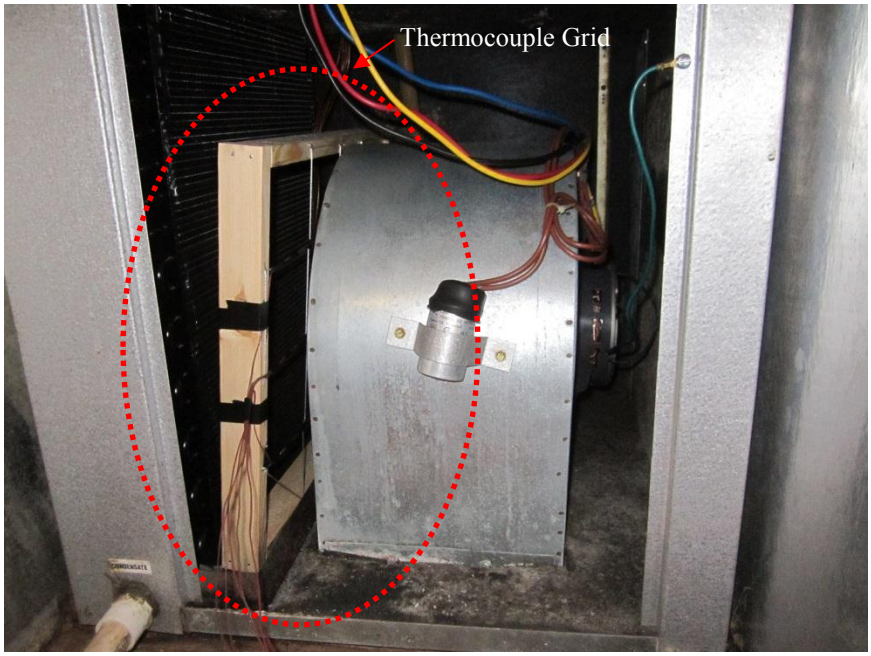

(b) Thermocouple Grid Installed in the Unit

Figure 4-34: Thermocouple Grid for the Supply Air Temperature Measurement

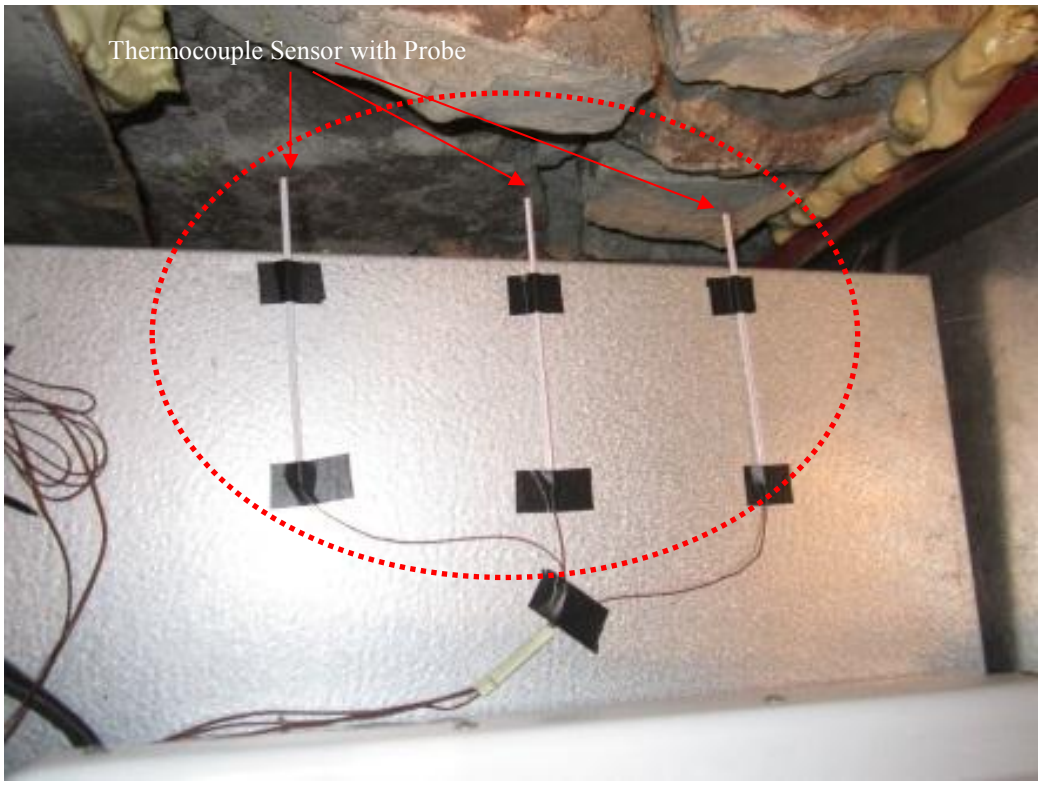

Figure 4-35: Thermocouple Grid for the Return Air Temperature Measurement

In order to measure the entering water and leaving water temperatures, the thermocouple sensors were attached to the return/supply pipe surfaces. Figure 4-36 shows the photos of the procedure used for the thermocouple sensor installation (ASTM, 1981 and Azbil, 2011). The procedure is described as follows:

- First, the pipe surface was cleaned with the sandpaper shown in Figure 4-36 (a);
- Second, the thermocouple sensor was attached to the cleaned pipe surface shown in Figure 4-36 (b). The sensing point of the sensor was covered with an aluminum tape to attach on the pipe surface; and the sensor cable was hold onto the pipe with a duct tape and cable tie tightly;

- Third, a double side tape covered the aluminum tape to remove air gap between the aluminum tape and the insulation material shown in Figure 4-36 (c); and
- Lastly, the insulation material covered the double side tape and pipe and the insulation material was sealed together with duct tape completely shown in Figure 4-36 (d).

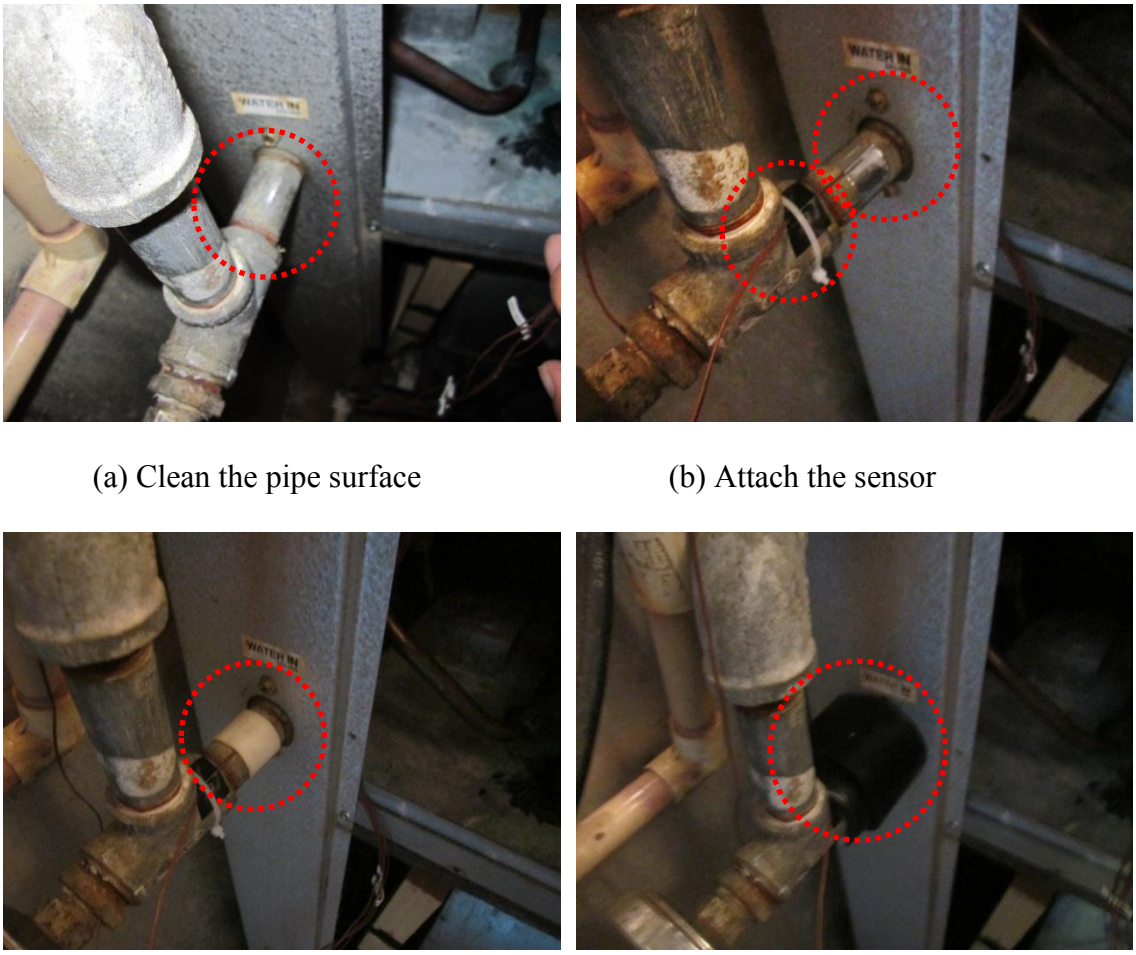

(a) Clean the pipe surface (b) Attach the sensor

(c) Cover the sensor (d) Add insulation

Figure 4-36: The Procedure to Water Temperature Sensor Installation

All of the installed thermocouple sensors were connected to the Campbell data logger (CR1000). The data logger was equipped with the multiplexer, which increases the number of sensors that can be measured[33]. The data logger records the supply air, return air, EWT, and LWT measured every minute. The hourly averaged temperature data calculated from the measured temperature data, when the system is on, will be used for the model validation. Figure 4-37 shows the photos of the WSHP system without and with the sensor installation. Figure 4-38 shows the photo of the data logger and multiplexer, which were connected with the thermocouple temperature sensors.

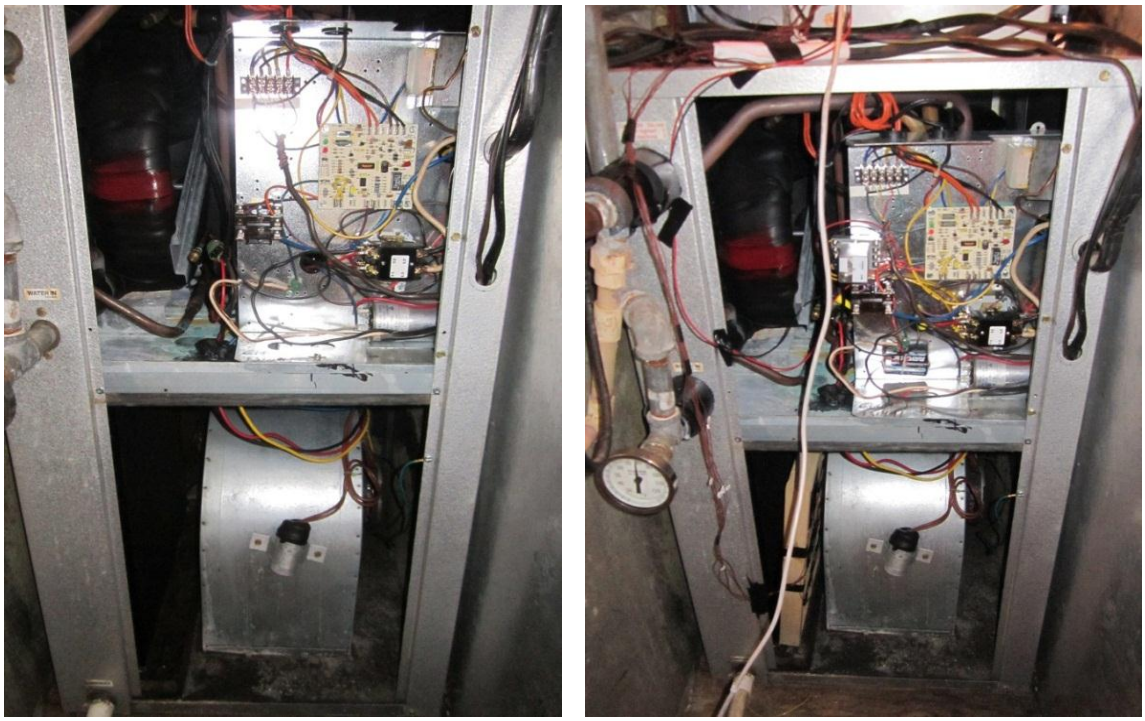

(a) Before (b) After

Figure 4-37: Photo of the WSHP Before and After the Sensor Installation

[33] In "2x32" mode, the multiplexer can scan 32 sensor input channels. In "4x16" mode, it can scan 16 input channels. This study used the "2x32" mode (Campbell Scientific, 2013a).

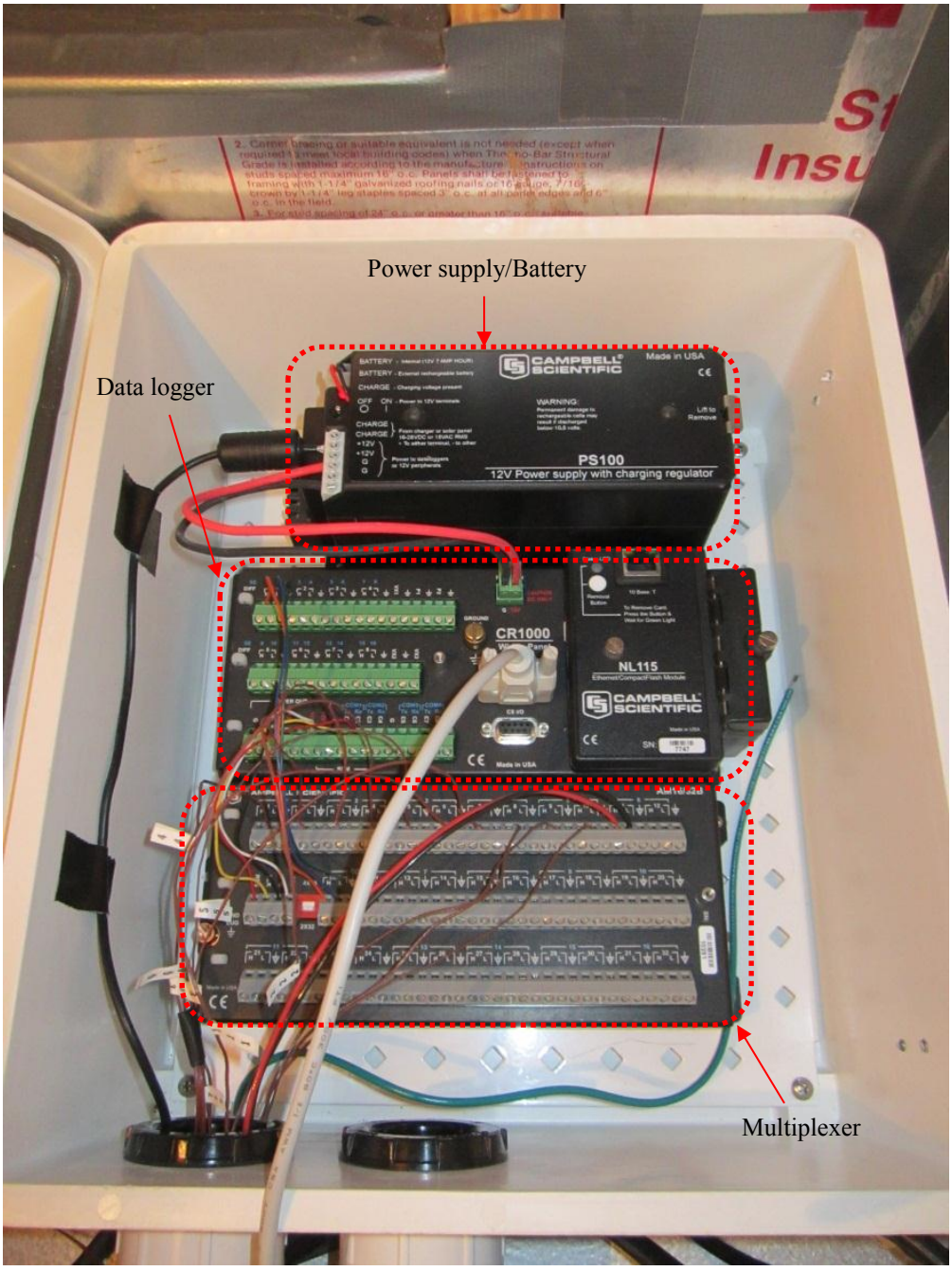

Figure 4-38: Photo of the Data Logger Connected with the Thermocouple Sensors

4.3.3. Description of the Solar Test Bench

Solar Test Bench (STB)[34] created by Energy Systems Laboratory (ESL) is located on the roof of the Langford Architecture building at Texas A&M University, which is about three mile from the case-study house. Sensors were installed at the STB to measure the weather data, including outdoor temperature and relative humidity, wind speed and direction, global, normal incidence, and diffuse solar radiation. The STB collects the measured data every one minute. The sensors installed at the STB were summarized in Table 4-6. In addition, Figure 4-39 shows a picture of the STB sensors.

Table 4-6: Summary of Sensors Installed at the Solar Test Bench

Sensor	Number of Sensors	Measured Quantity	Make/ Model	Reference
Temperature & Relative Humidity	2	Temperature & Relative Humidity	Vaisala/ HMP45A	Vaisala, 2013
Anemometer	2	Wind Speed & Wind Direction	Metone/ 034B	Campbell Scientific, 2013f
Pyranometer	3	Global Solar Radiation	Li-cor/ LI200	LI-COR, 2013
Normal Incidence Pyrheliometer	2	Normal Incidence Solar Radiation	Eppley/ NIP	EPLAB, 2013a
Precision Spectral Pyranometer	2	Global Solar Radiation	Eppley/ PSP	EPLAB, 2013b
Black and White Pyranometer	2	Diffused Solar Radiation	Eppley/ 8-48	EPLAB, 2006

The STB system consists of three main system clusters, as shown in Figure 4-40: the roof cluster (Figure 4-39), the mechanical room cluster (Figure 4-41), and the Energy Systems Lab cluster.

[34] The STB was built in 2006. Since then, the ESL staff and students have continuously adjusted and upgraded the STB.

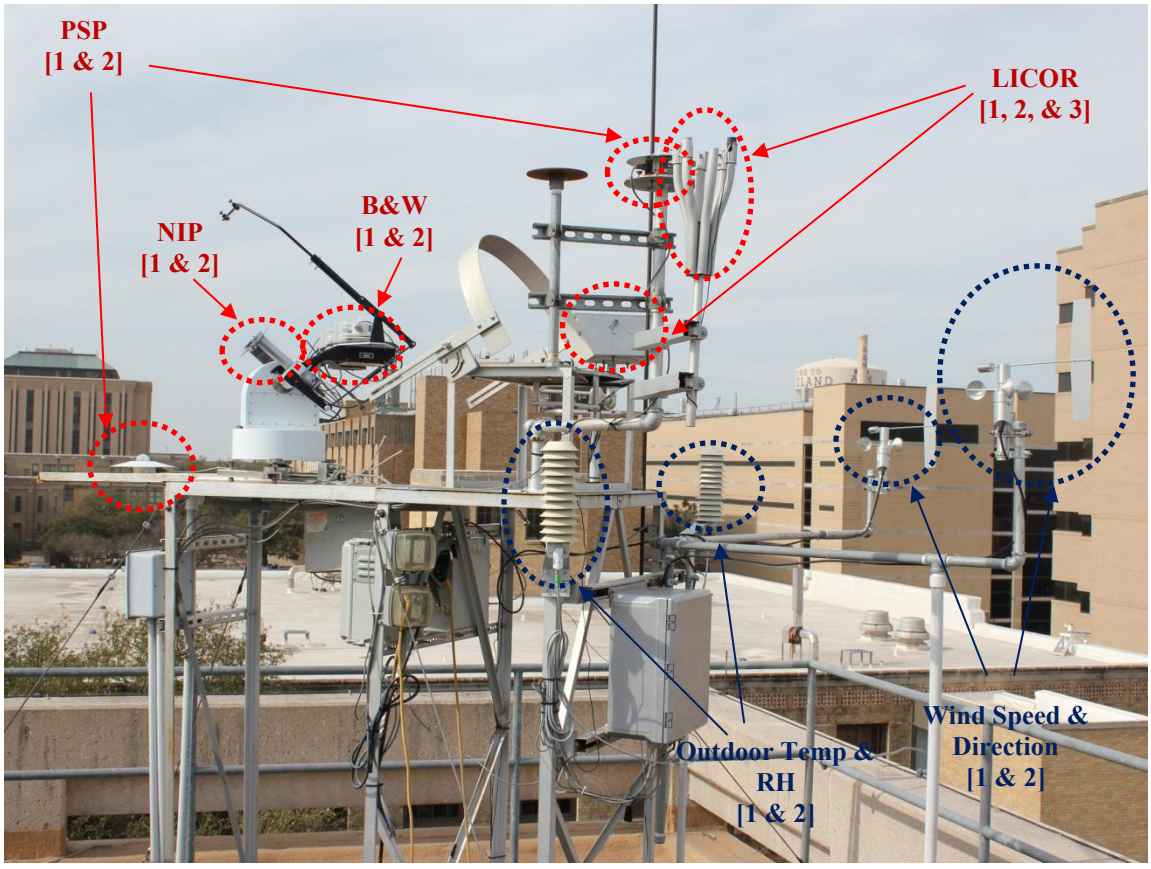

Figure 4-39: Photo of the Solar Test Bench

The roof cluster is the physical structure holding all the measurement devices, including all of the sensors and instruments (i.e., junction boxes) installed on the roof of the Langford Architecture building. The roof cluster provides power supply, lightning protection, and cable connections to the junction boxes. The output of the sensors is wired to the mechanical cluster. This cluster contains the surge protectors, the data logger, the multiplexer, Ethernet module, and power system. The output from the roof cluster passes through the surge protectors before entering into the data logger. The data logger collects the output measured at the roof cluster. The Ethernet module enables

communication between the mechanical room cluster and the ESL cluster. Finally, the data collected in the data-logger are automatically downloaded at ESL computer, which calls the ESL cluster. The ESL cluster plots/displays the results of the measurement on the STB website[35], using the Loggernet software (Campbell Scientific, 2013c), RTMC pro software (Campbell Scientific, 2013d), and RTMC web server software (Campbell Scientific, 2013e). The Loggernet software allows that the collected data is automatically downloaded to the computer in ESL office. The RTMC pro software is used to access the data files and generates result plots. The RTMC web server software is used to post the real-time plots on the STB website.

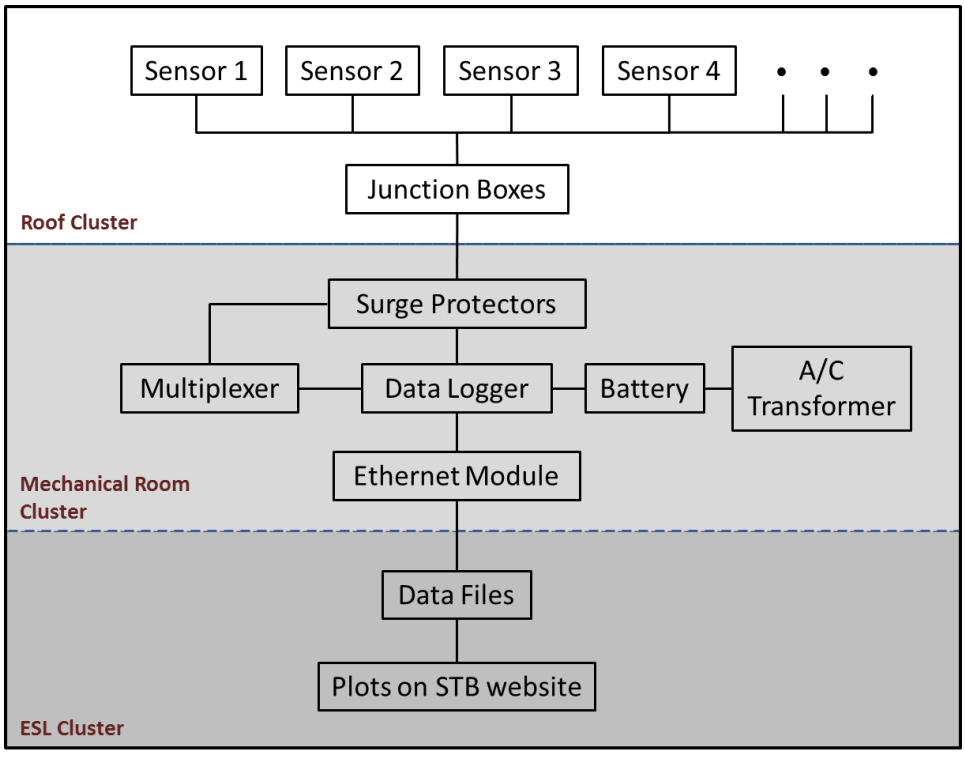

Figure 4-40: Schematic Diagram of the STB System Cluster

[35] The STB website is, as of May 9 2013, http://165.91.141.95:6785/

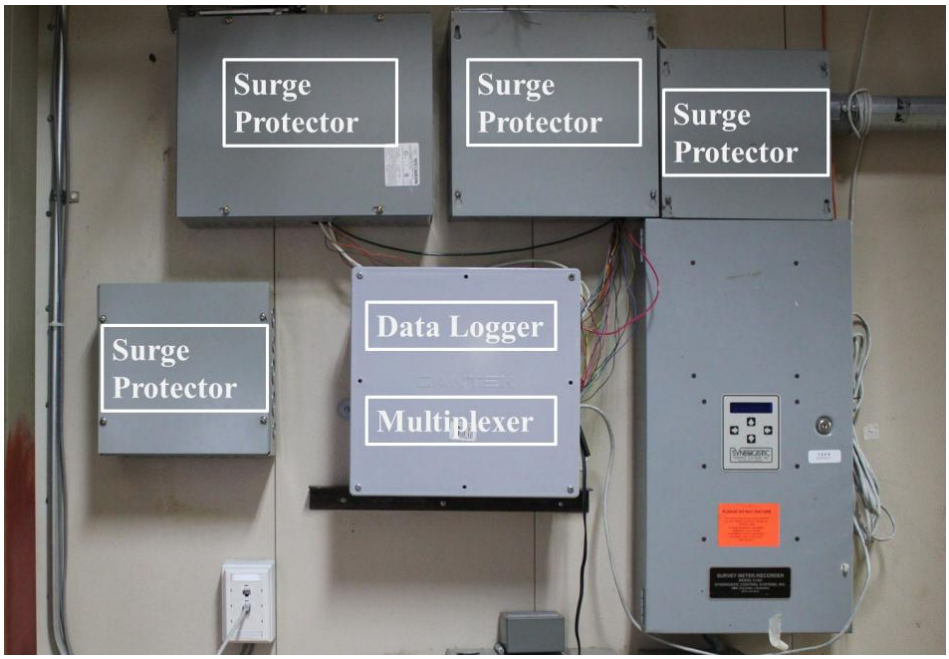

(a) With Panel Cover

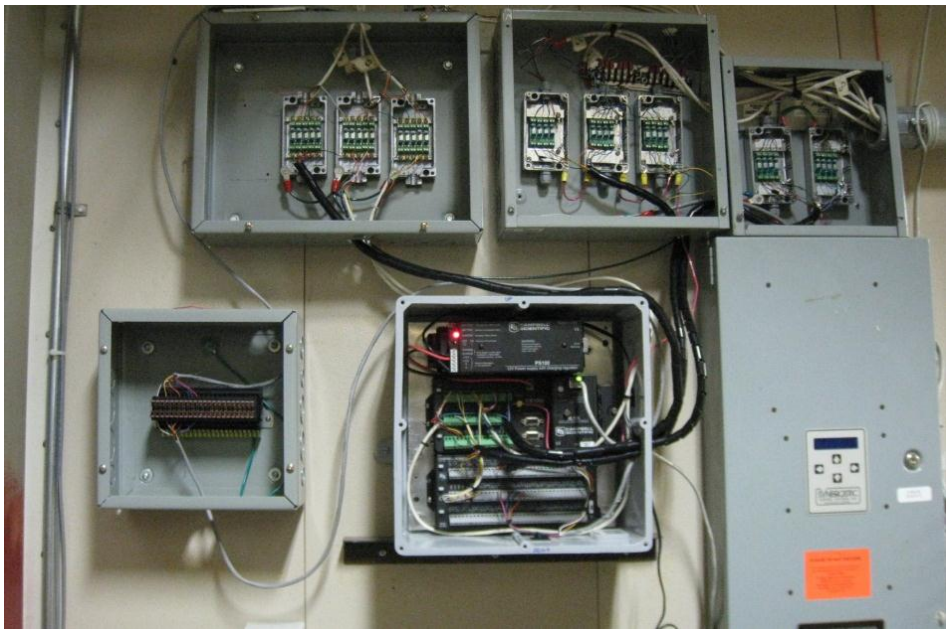

(b) Without Panel Cover

Figure 4-41: Photo of the Mechanical Room Cluster

The following screen shots (Figure 4-42 through Figure 4-47) show example plots displayed from the STB website. The STB plots have the results of the current measurement and the seven-day measurement, updating the data every minute.

Figure 4-42 is the screen shot for the Current Conditions tab in the STB website, which presents measurement summary for the current and the last 24 hours weather conditions, including outside temperature and relative humidity (RH), wind speed and direction, and solar radiation. Figure 4-43 is the screen shot for the Last 7 Days tab in the STB website, which shows weather conditions for the last seven-days, including outdoor temperature, RH, wind speed, and solar radiation, using 15 minutes average values. Figure 4-44 and Figure 4-45 are the screen shots for the Solar Radiation-LICOR tab and Solar Radiation-PSP tab in the STB website. The Solar Radiation-LICOR tab provides global solar radiation values, measured from three LICORs, for the current measurement using every minute reading and the last seven days measurement using 15 minutes average. The Solar Radiation-PSP tab also provides global solar radiation values, measured from two PSPs, for the current measurement using every minute reading and the last seven days measurement using 15 minutes average. In addition, the PSP tab provides the comparison of reading difference between two PSPs, using time series and x-y plots. Figure 4-46 and Figure 4-47 are the screen shots for the Solar Radiation-NIP and Solar Radiation-B&W in the STB website, which show the seven-day normal incidence solar radiation and diffuse solar radiation measured from, two NIPs and two B&Ws, respectively. These tabs also provide the measurement difference like the Solar Radiation-PSP tab.

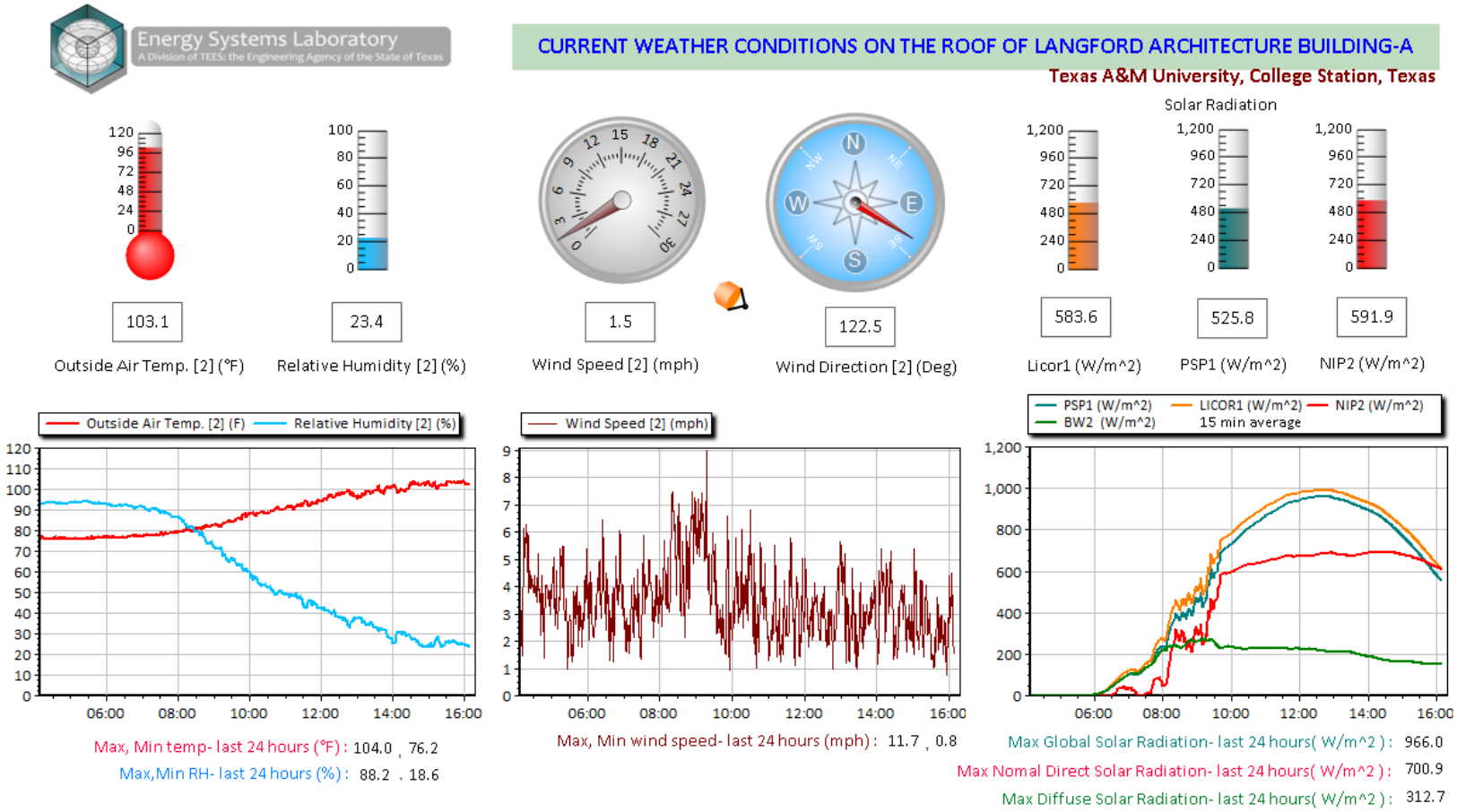

Figure 4-42: Screen Shots for the Current Condition in STB website

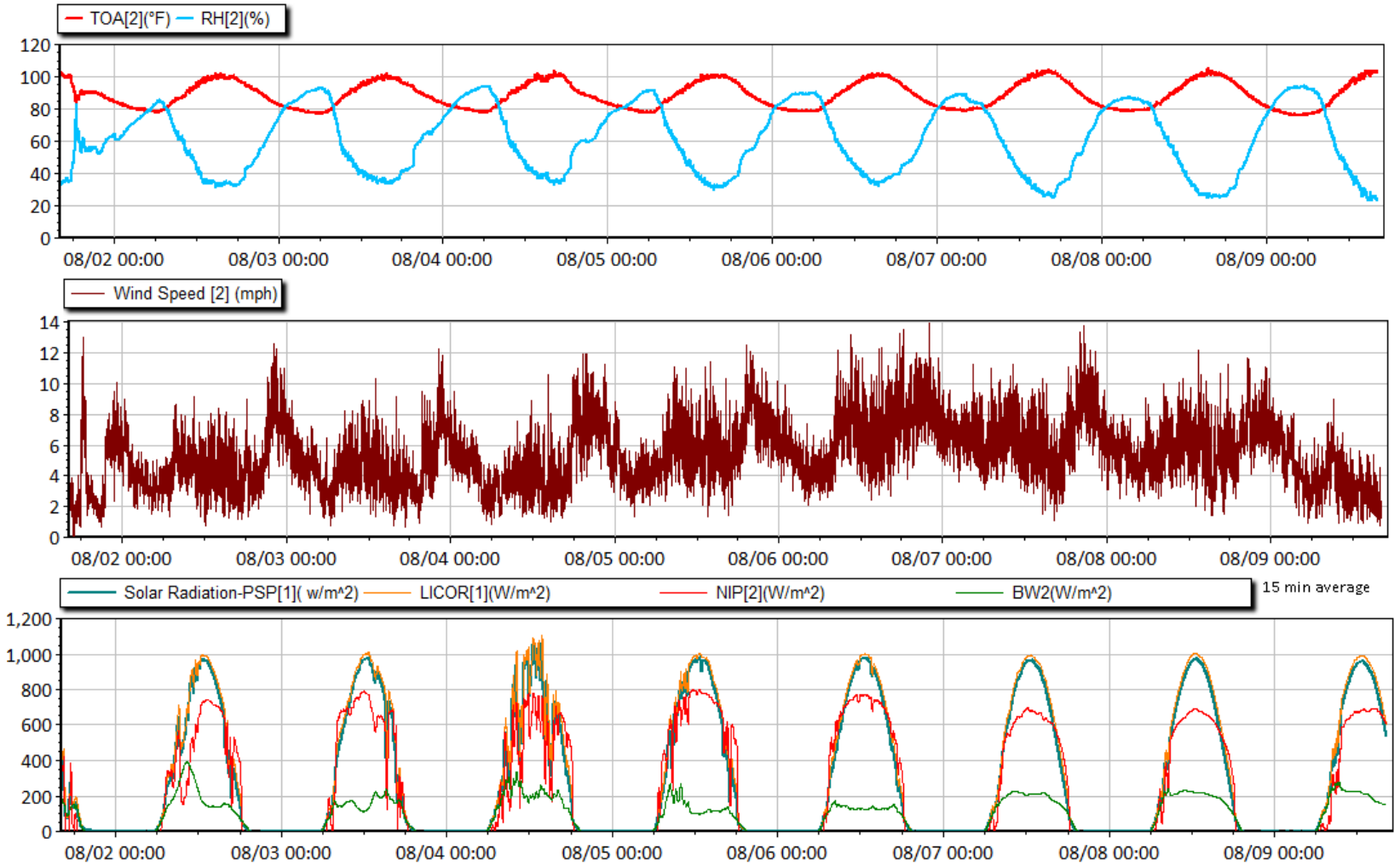

Figure 4-43: Screen Shots for the Last 7 Days in STB website

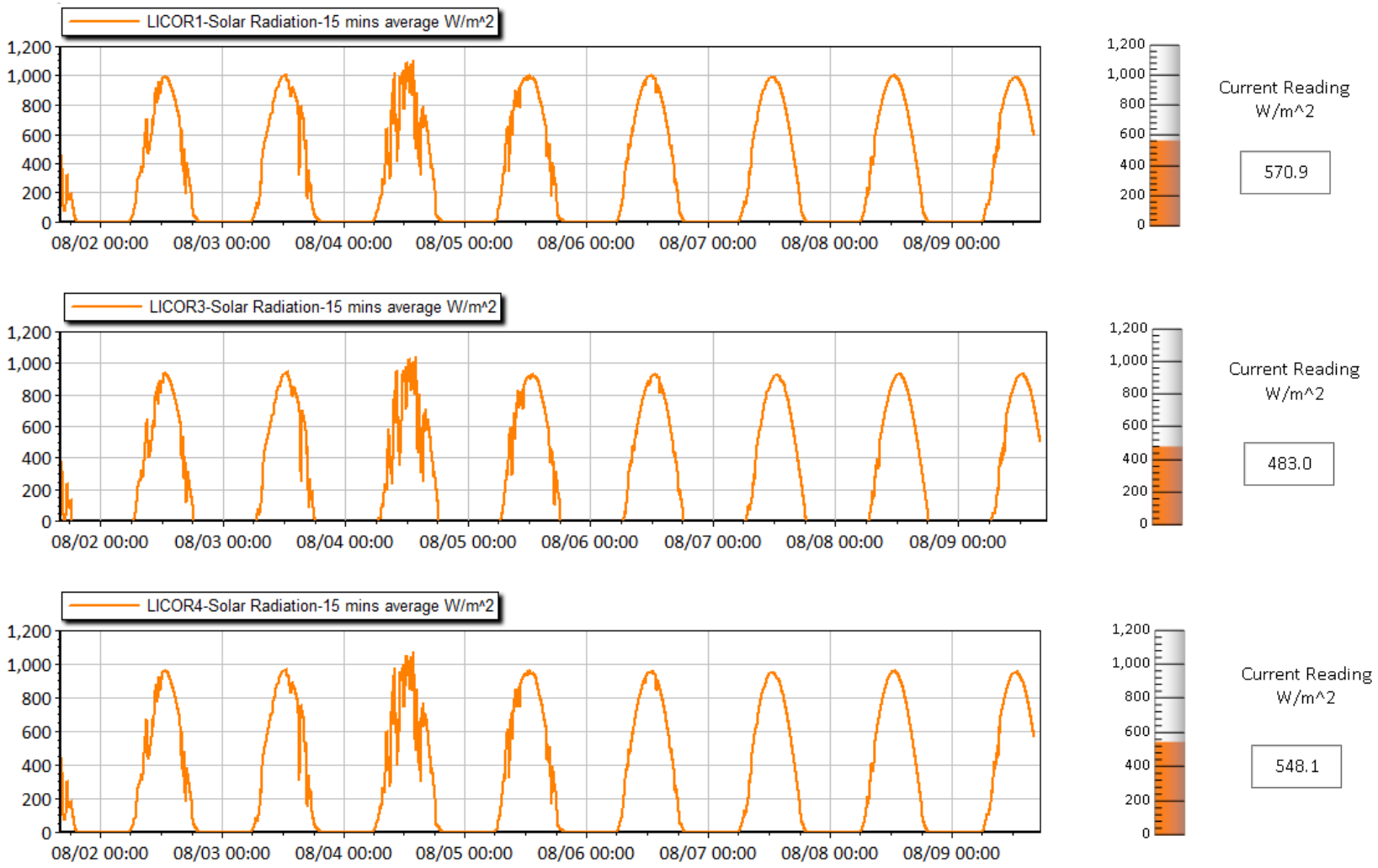

Figure 4-44: Screen Shots for the Solar Radiation-LICOR in STB website

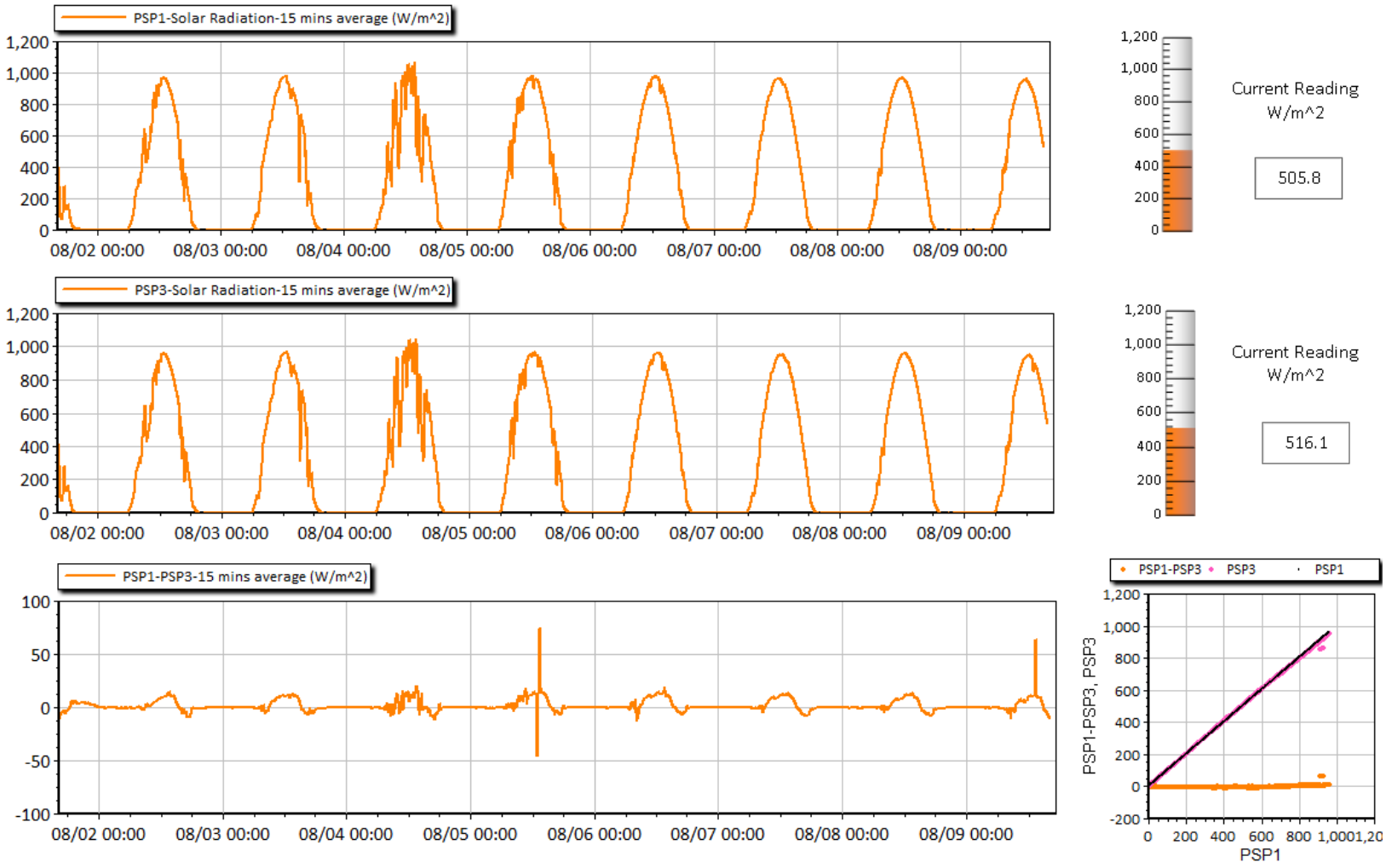

Figure 4-45: Screen Shots for the Solar Radiation-PSP in STB website

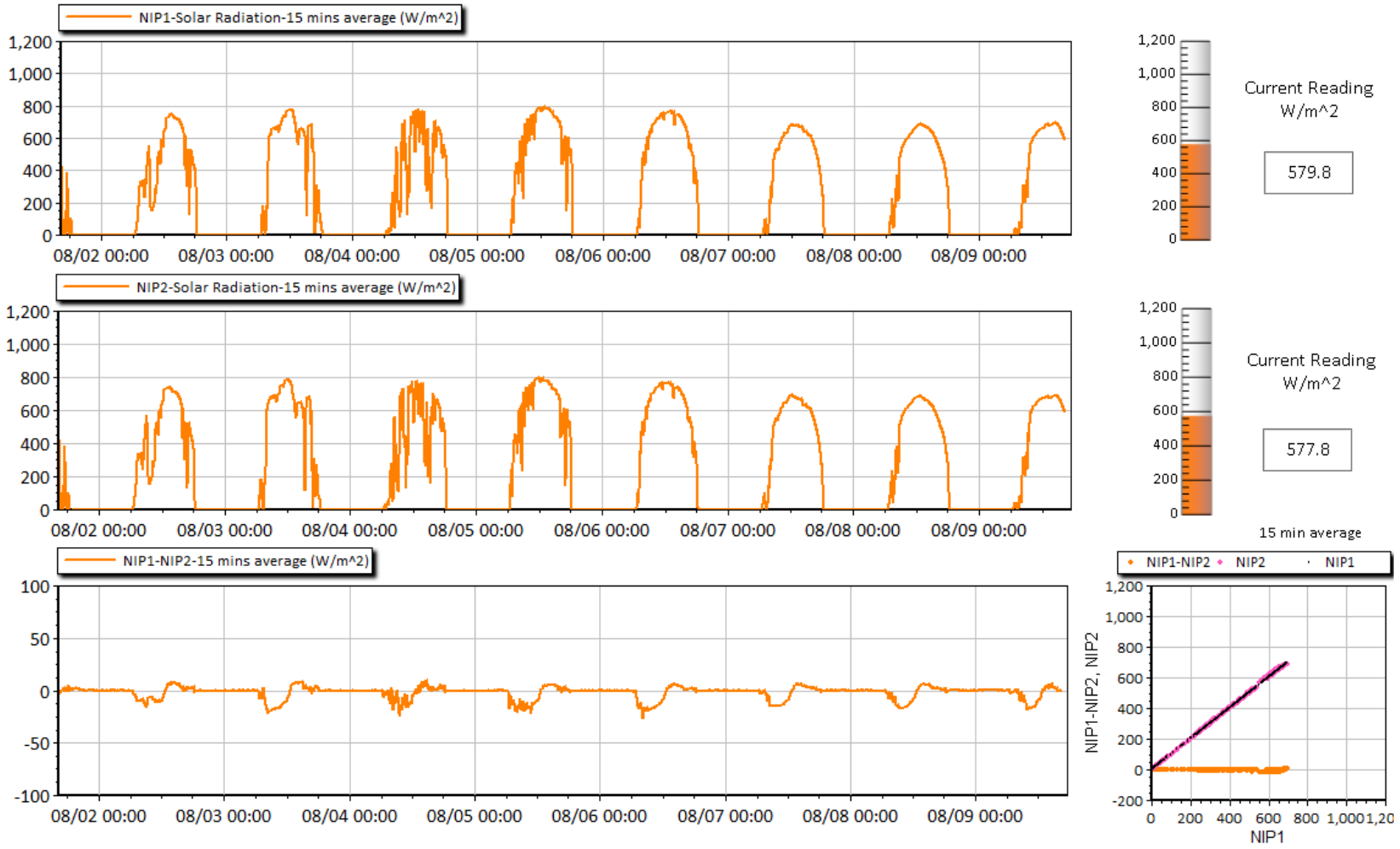

Figure 4-46: Screen Shots for the Solar Radiation-NIP in STB website

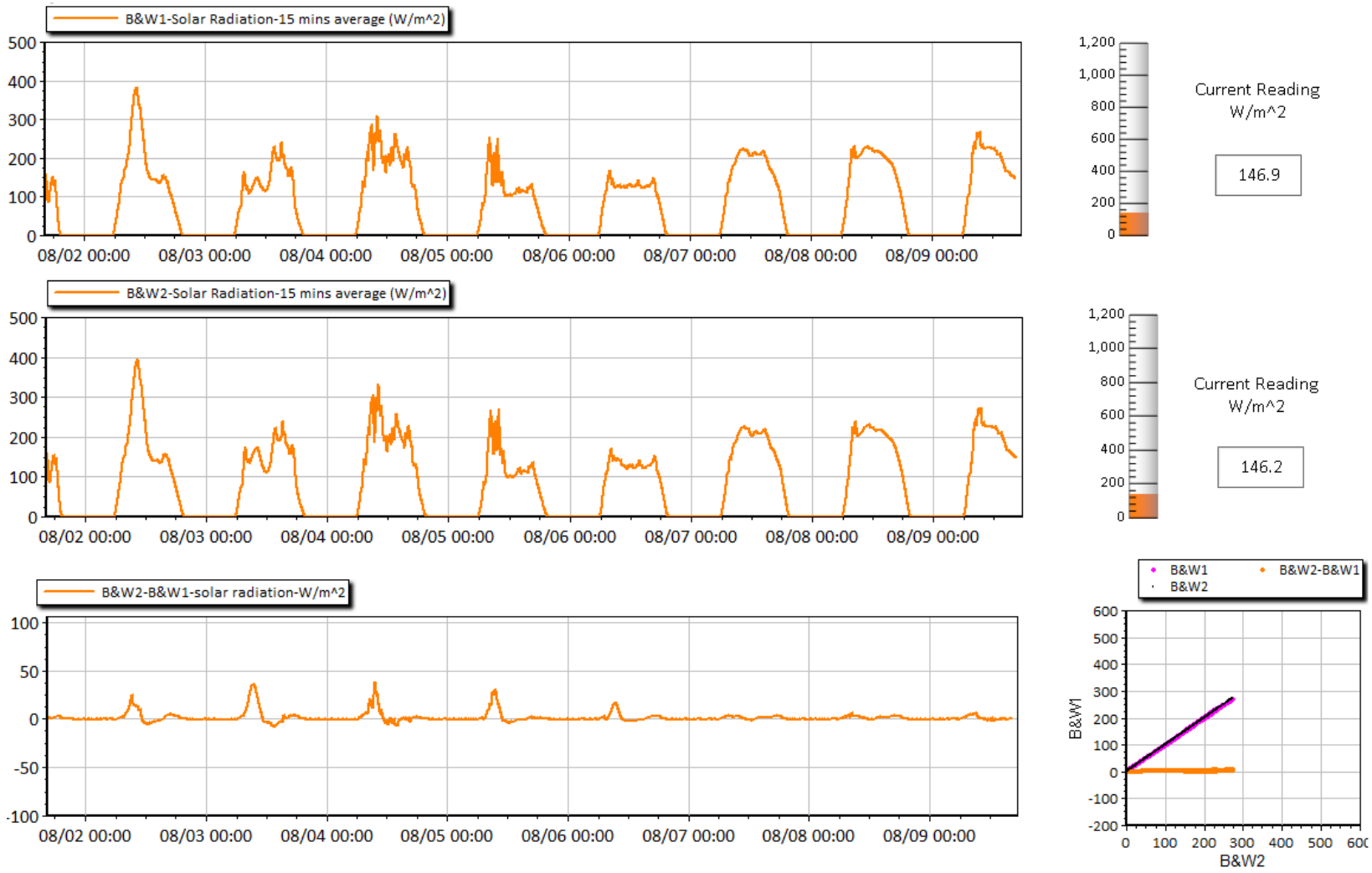

Figure 4-47: Screen Shots for the Solar Radiation-B&W in STB website

4.3.4. Data Collection from the Solar Test Bench

The weather data collected from the STB are the outdoor temperature and relative humidity, the wind speed and direction, and the solar radiations. With the exception of the wind direction data, all the weather data will be used for the case-study house GHX model. The collected STB weather data, which has one-minute interval, were averaged to one-hour interval to be used for the pond water temperature calculations, including calculations for the absorbed solar radiation, pond thermal radiation, convection of the pond surface, heat transfer to/from the ground, and evaporation of the pond surface, which are described in the Section 4.2.2.1. Table 4-7 presents the summary of the STB weather data list to be used for this study.

Table 4-7: List of the STB Weather Data Used for the Pond Temperature Calculation

Pond Temperature Calculation	STB Data
Absorbed Solar Radiation	• Global Solar Radiation, and • Diffuse Solar Radiation
Thermal Radiation	• Outdoor Temperature, and • Relative Humidity
Ground Heat Transfer	• Outdoor Temperature, • Relative Humidity, • Wind Speed, • Global Solar Radiation, and • Diffuse Solar Radiation
Convective Heat Transfer	• Outdoor Temperature, and • Wind Speed
Evaporative Heat Transfer	• Outdoor Temperature, • Relative Humidity, and • Wind Speed

4.3.5. Custom-Built GHX Model for Case-Study House

The WSHP system in the case-study house utilizes custom-built ground heat exchangers (GHXs), which use a combination of horizontal GHXs and surface water (pond) GHX. The WSHP system is connected with the first horizontal GHX, the surface water GHX, and the second horizontal GHX, in sequence (Figure 4-24). As a result, the custom-built GHX model is developed to calculate the EWTs for the case-study house.

The custom-built GHX model uses both the horizontal GHX model and the surface water GHX model which were described in Sections 4.2.1 and 4.2.2, respectively. The horizontal GHX model is used for the first GHX and the third GHX and the surface water GHX model is used for the second GHX. Figure 4-48 presents the conceptual diagram for the custom-built GHX model to be used for the case-study house.

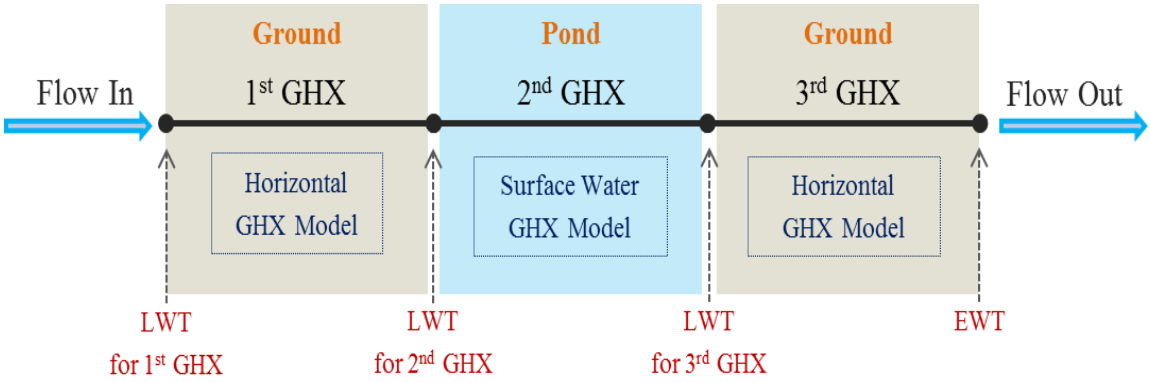

Figure 4-48: Diagram of the Custom-Built GHX Model for the Case-Study House

The leaving water temperature (LWT) from the heat pump flows through the first GHX pipe. The water temperature at the end of the first GHX pipe is calculated using

the horizontal GHX model and then the calculated water temperature becomes the leaving water temperature for the second GHX pipe. The water temperature at the end of the second GHX pipe is calculated using the surface water GHX model and then the calculated water temperature becomes the leaving water temperature for the third GHX pipe. In the same manner, the water temperature at the end of the third GHX pipe is calculated using the horizontal GHX model. Finally, the calculated water temperature becomes the entering water temperature (EWT) to the heat pump system.

4.4. Vertical Ground Heat Exchanger Model

This section describes the methodology to develop a simplified residential base-case simulation model, using an air-source heat pump (ASHP) system and a ground-coupled heat pump (GCHP) system with the vertical GHX model developed in this study. In addition, this section includes description of developing the vertical GHX DOE-2.1e model.

This study initially develops a simplified residential ASHP base-case model to apply a vertical GHX model developed in this study, which is used to determine the entering water temperatures (EWTs). Then, the ASHP system in the base-case model is modified to be a GCHP system using the vertical GHX model.

The simplified residential ASHP base-case simulation model is referenced residential home characteristics compliance with the 2009 International Energy Conservation Code (IECC) requirements. The residential base-case model is located in Houston and Dallas, Texas to represent a hot and humid climate. The simulations

throughout this study are performed with using Typical Meteorological Year version 2 (TMY2) weather data for Houston and Dallas. First, to develop the simplified residential ASHP base-case simulation model for Houston, this study uses a step-by-step procedure that changes various inputs to determine the impact of the changes. The DOE-2.1e program and the eQUEST program are used for the procedure. Second, using the developed base-case simulation model for Houston, this study develops the residential ASHP base-case model for Dallas by modifying input parameters for the 2009 IECC requirements from Houston to Dallas. The simulation results of the residential ASHP base-case models developed in this study are compared against the results from other code-compliant simulation programs (i.e., IC3, EnergyGauge, and REM/Rate).

The DOE-2.1e GCHP base-case model using a vertical GHX is then developed by modifying the DOE-2.1e ASHP base-case model. This study also compares the simulation results of the DOE-2.1e GCHP base-case model against eQUEST, EnergyGauge, and REM/Rate.

Section 4.4.1 describes the procedure to develop a simplified residential ASHP base-case model for Houston and Dallas in Texas, using DOE-2.1e and eQUEST. Section 4.4.2 describes a method to develop the residential GCHP base-case model with the vertical GHX to be used in the DOE-2.1e program. Section 4.4.2.3 provides a description of the comparison study for the residential DOE-2.1e ASHP and GCHP base-case models, against eQUEST, and the other code-compliance simulation programs.

4.4.1. Development of Simplified Residential ASHP Base-Case Models

This section provides the procedure to develop simplified residential ASHP base-case models located in Houston and Dallas, TX. The ASHP base-case models are based on the standard reference design and requirements as defined in Chapter 4 of the 2009 IECC. First, this study uses a step-by-step procedure to develop the simplified residential ASHP base-case simulation model for Houston. Then, using the developed base-case simulation model for Houston, a residential ASHP base-case model for Dallas is developed by modifying input parameters for the 2009 IECC requirements from Houston to Dallas. The DOE-2.1e and eQUEST simulation programs are used to develop the simplified residential ASHP base-case models.

4.4.1.1. Simplified Residential ASHP Base-Case Model for Houston

The ASHP base-case model development procedure for Houston began with the "RUN 3A" which is one of the example models for a simple structure included in the samp1e.inp file in the DOE-2.1e program package. Figure 4-49 shows the 3-D geometry view of the RUN 3A model, which is a single-story, an office building, 30 degrees azimuth, 5,000 ft^2 of the floor area with an 8 feet floor-to-ceiling height, and 2 feet of the plenum height. Through the step-by-step procedure, the RUN 3A office model was modified to become the simplified residential ASHP base-case model (i.e., RUN_30 in the procedure) which is a single-story, a single-family, a south-facing and detached house, that has 2,500 ft^2 of the floor area with an 8 feet floor-to-ceiling height without a

plenum (Figure 4-50). In addition, the ASHP base-case model has a simplified structure with a rectangular geometry, a flat roof, and no attic space.

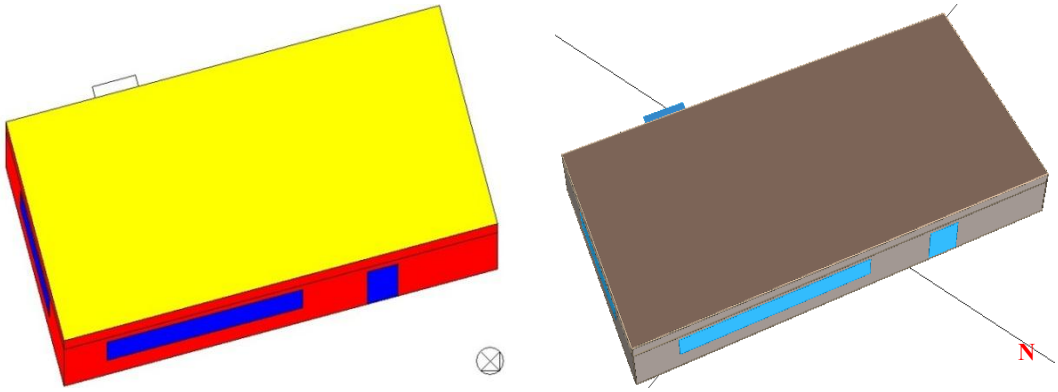

(a) DOE-2.1e (b) eQUEST

Figure 4-49: 3-D Geometry View of RUN 3A Office Model

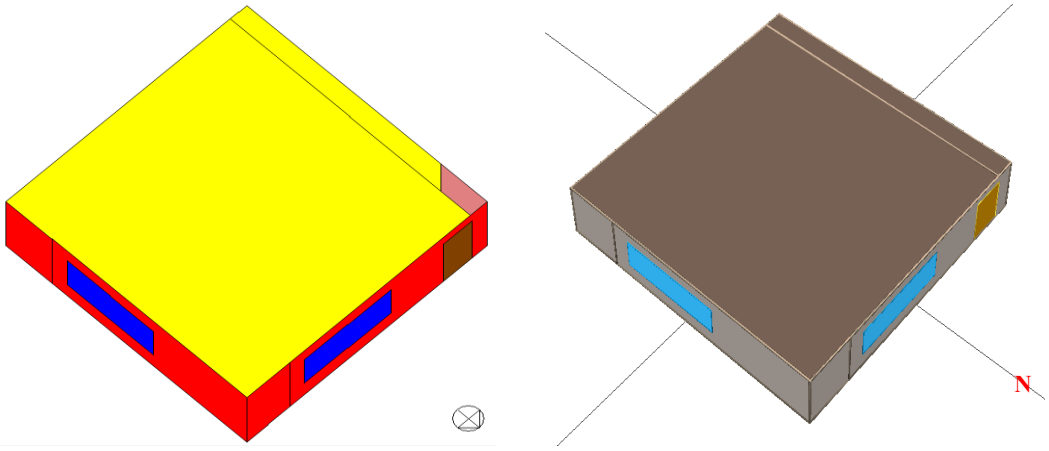

(b) DOE-2.1e (b) eQUEST

Figure 4-50: 3-D Geometry View of RUN_30 Residential Base-Case Model

The construction and system characteristics of the residential base-case model were determined from the climate-specific characteristics in the 2009 IECC (ICC,

2009a). In order to develop simplified residential simulation model, the schedules for space condition (i.e., lighting and equipment) and system operation (i.e., heating, cooling, fan, and infiltration) were set to be continuously on. A residential electric Domestic Hot Water (DHW) heater was also installed.

A step-by-step input change procedure is used to develop an ASHP base-case model located in Houston, TX (Do et al., 2013). The procedure starts from the RUN 3A office model to develop the residential ASHP model by changing selected inputs, which consists of six categories (30 simulation runs), including categories for the *Project* (7 simulation runs), the *ASHP System* (7 simulation runs), the *Construction* (9 simulation runs), the *Internal Gain* (2 simulation runs), the *Schedule* (4 simulation runs), and the *DHW* (1 simulation run).

Table 4-8 presents the entire simulation procedure to develop the simplified residential ASHP base-case model for Houston and summarizes the input parameters for the base-case model. The modified inputs for each simulation run are the yellow shaded inputs in the table. The input changes for each simulation run also include the previously modified inputs. For example, RUN_5 includes all of the modified inputs from RUN_1 to RUN_5.

Section 4.4.1.1.1 presents the *Project* category which defines general structures for the simplified residential building model. Section 4.4.1.1.2 gives a description of the *ASHP System* category which defines input parameters for the ASHP system. Section 4.4.1.1.3 describes the *Construction* category which defines input parameters for the residential building envelope based on the 2009 IECC requirements. Section 4.4.1.1.4

describes the *Internal Gain* category to define input parameters for the energy use of the lighting and equipment, the *Schedule* category to define input parameters for simplified building schedules for lighting, equipment, infiltration, and interior shading, and presents the *DHW* category to define a residential electric DHW system.

4.4.1.1.1. *Project Category*

The first of the six categories, the *Project* category, defines the general building structures for the simplified house, such as a number of spaces, area, fenestration, overhang, and orientation. Table 4-9 shows seven runs in the *Project* category and summarizes the input changes, which are yellow shaded in each row.

The modified inputs for each simulation in the *Project* category are described as follows:

- "RUN 3A", which is included in the DOE-2 program package, is the initial step in the procedure. The RUN_3A simulation modified the building location from Chicago to Houston. To accomplish this, the latitude was changed to 29.5˚, the longitude was changed to 95˚, and the altitude set to 68 ft. for Houston.
- The RUN_1 simulation changed the building space from five zones to a single zone.
- The RUN_2 simulation reduced the building space area from 5,000 ft^2 to 2,500 ft^2 for a typical single-family house. In addition, the fenestration was modified: the Window-to-Floor Ratio (WFR) was modified from 22 % to 15 %, and the door area reduced from 113 ft^2 to 40 ft^2, based on Table 405.5.2(1) in the 2009 IECC.

Table 4-8: Simulation Procedure for Simplified Residential ASHP Base-Case Model

SIMPLIFIED RESIDENTIAL BASE-CASE MODEL																																				
	PROJECT									ASHP SYSTEM							CONSTRUCTION											INTERNAL GAIN		SCHEDULE				DHW
Run Name	# of Spaces	Area	Fenestration (WFR)	Overhang	Azimuth	# of People	Plenum	Return-Air-Path	Door Location	System Change	SEER	HSPF	Fan Schedule	Thermostat Heat Schedule	Thermostat Cool Schedule	Air Flow Rate	Floor U-Value (Slab-on-Grade)	Roof U-Value	Roof Absorptance	Wall U-Value	Wall Absorptance	Door U-Value	Glazing U-Value	Window Frame	Glazing SHGC	Infiltration ACH	Ground Reflectance	Lighting (w/sqft)	Equip. (w/sqft)	Lighting	Equip.	Infiltration	Interior Shading	DHW System
	5 to 1	5,000 to 2,500	22% to 15%	Yes to No	30 to 0	52 to 0	Removed	Plenum to Direct	Two (S/N) to Single (N)	VAVS to RESYS	7.3 to 13	5.4 to 7.7	Schedule to Always	Schedule to 72	Schedule to 75	7,366 cfm to 1,800 cfm	0.05 to 0.088	0.048 to 0.035	0.7 to 0.75	0.069 to 0.082	0.7 to 0.75	1.142 to 0.5	0.516 to 0.65	None to Frame	0.87 to 0.3	0.25 to 0.35	0/0.2 to 0.24	1.5 to 0.1951	1.0 to 0.2632	Schedule to Always	Schedule to Always	Schedule to Always	None to Schedule	None to DHW
RUN_3A	5	5,000	22% WFR	Yes	30	52	Default	Plenum	Two (S/N)	VAVS	7.3	5.4	Schedule	Schedule	Schedule	7,366 cfm	0.05	0.048	0.7	0.069	0.7	1.47	0.574	None	0.87	0.25	0 (Wall) 0.2 (Roof)	1.5	1.0	Schedule	Schedule	Schedule	None	None
RUN_1	**1**	5,000	22% WFR	Yes	30	52	Default	Plenum	Two (S/N)	VAVS	7.3	5.4	Schedule	Schedule	Schedule	7,366 cfm	0.05	0.048	0.7	0.069	0.7	1.47	0.574	None	0.87	0.25	0 (Wall) 0.2 (Roof)	1.5	1.0	Schedule	Schedule	Schedule	None	None
RUN_2	1	**2,500**	**15% WFR**	Yes	30	52	Default	Plenum	Two (S/N)	VAVS	7.3	5.4	Schedule	Schedule	Schedule	7,366 cfm	0.05	0.048	0.7	0.069	0.7	1.47	0.574	None	0.87	0.25	0 (Wall) 0.2 (Roof)	1.5	1.0	Schedule	Schedule	Schedule	None	None
RUN_3	1	2,500	15% WFR	**No**	30	52	Default	Plenum	Two (S/N)	VAVS	7.3	5.4	Schedule	Schedule	Schedule	7,366 cfm	0.05	0.048	0.7	0.069	0.7	1.47	0.574	None	0.87	0.25	0 (Wall) 0.2 (Roof)	1.5	1.0	Schedule	Schedule	Schedule	None	None
RUN_4	1	2500	15% WFR	No	**0**	52	Default	Plenum	Two (S/N)	VAVS	7.3	5.4	Schedule	Schedule	Schedule	7,366 cfm	0.05	0.048	0.7	0.069	0.7	1.47	0.574	None	0.87	0.25	0 (Wall) 0.2 (Roof)	1.5	1.0	Schedule	Schedule	Schedule	None	None
RUN_5	1	2500	15% WFR	No	0	**0**	Default	Plenum	Two (S/N)	VAVS	7.3	5.4	Schedule	Schedule	Schedule	7,366 cfm	0.05	0.048	0.7	0.069	0.7	1.47	0.574	None	0.87	0.25	0 (Wall) 0.2 (Roof)	1.5	1.0	Schedule	Schedule	Schedule	None	None
RUN_6	1	2500	15% WFR	No	0	0	**Removed**	**Direct**	Two (S/N)	VAVS	7.3	5.4	Schedule	Schedule	Schedule	7,366 cfm	0.05	0.048	0.7	0.069	0.7	1.47	0.574	None	0.87	0.25	0 (Wall) 0.2 (Roof)	1.5	1.0	Schedule	Schedule	Schedule	None	None
RUN_7	1	2500	15% WFR	No	0	0	Removed	Direct	**Single (N)**	VAVS	7.3	5.4	Schedule	Schedule	Schedule	7,366 cfm	0.05	0.048	0.7	0.069	0.7	1.47	0.574	None	0.87	0.25	0 (Wall) 0.2 (Roof)	1.5	1.0	Schedule	Schedule	Schedule	None	None
RUN_8	1	2500	15% WFR	No	0	0	Removed	Direct	Single (N)	**RESYS**	7.3	5.4	Schedule	Schedule	Schedule	7,366 cfm	0.05	0.048	0.7	0.069	0.7	1.142	0.516	None	0.87	0.25	0 (Wall) 0.2 (Roof)	1.5	1.0	Schedule	Schedule	Schedule	None	None
RUN_9	1	2500	15% WFR	No	0	0	Removed	Direct	Single (N)	RESYS	**13**	5.4	Schedule	Schedule	Schedule	7,366 cfm	0.05	0.048	0.7	0.069	0.7	1.142	0.516	None	0.87	0.25	0 (Wall) 0.2 (Roof)	1.5	1.0	Schedule	Schedule	Schedule	None	None
RUN_10	1	2500	15% WFR	No	0	0	Removed	Direct	Single (N)	RESYS	13	**7.7**	Schedule	Schedule	Schedule	7,366 cfm	0.05	0.048	0.7	0.069	0.7	1.142	0.516	None	0.87	0.25	0 (Wall) 0.2 (Roof)	1.5	1.0	Schedule	Schedule	Schedule	None	None
RUN_11	1	2500	15% WFR	No	0	0	Removed	Direct	Single (N)	RESYS	13	7.7	**Always**	Schedule	Schedule	7,366 cfm	0.05	0.048	0.7	0.069	0.7	1.142	0.516	None	0.87	0.25	0 (Wall) 0.2 (Roof)	1.5	1.0	Schedule	Schedule	Schedule	None	None
RUN_12	1	2500	15% WFR	No	0	0	Removed	Direct	Single (N)	RESYS	13	7.7	Always	**72**	Schedule	7,366 cfm	0.05	0.048	0.7	0.069	0.7	1.142	0.516	None	0.87	0.25	0 (Wall) 0.2 (Roof)	1.5	1.0	Schedule	Schedule	Schedule	None	None
RUN_13	1	2500	15% WFR	No	0	0	Removed	Direct	Single (N)	RESYS	13	7.7	Always	72	**75**	7,366 cfm	0.05	0.048	0.7	0.069	0.7	1.142	0.516	None	0.87	0.25	0 (Wall) 0.2 (Roof)	1.5	1.0	Schedule	Schedule	Schedule	None	None
RUN_14	1	2500	15% WFR	No	0	0	Removed	Direct	Single (N)	RESYS	13	7.7	Always	72	75	**1,800 cfm**	0.05	0.048	0.7	0.069	0.7	1.142	0.516	None	0.87	0.25	0 (Wall) 0.2 (Roof)	1.5	1.0	Schedule	Schedule	Schedule	None	None
RUN_15	1	2500	15% WFR	No	0	0	Removed	Direct	Single (N)	RESYS	13	7.7	Always	72	75	1,800 cfm	**0.088**	0.048	0.7	0.069	0.7	1.142	0.516	None	0.87	0.25	0 (Wall) 0.2 (Roof)	1.5	1.0	Schedule	Schedule	Schedule	None	None
RUN_16	1	2500	15% WFR	No	0	0	Removed	Direct	Single (N)	RESYS	13	7.7	Always	72	75	1,800 cfm	0.088	**0.035**	0.7	0.069	0.7	1.142	0.516	None	0.87	0.25	0 (Wall) 0.2 (Roof)	1.5	1.0	Schedule	Schedule	Schedule	None	None
RUN_17	1	2500	15% WFR	No	0	0	Removed	Direct	Single (N)	RESYS	13	7.7	Always	72	75	1,800 cfm	0.088	0.035	**0.75**	0.069	0.7	1.142	0.516	None	0.87	0.25	0 (Wall) 0.2 (Roof)	1.5	1.0	Schedule	Schedule	Schedule	None	None
RUN_18	1	2500	15% WFR	No	0	0	Removed	Direct	Single (N)	RESYS	13	7.7	Always	72	75	1,800 cfm	0.088	0.035	0.75	**0.082**	0.7	1.142	0.516	None	0.87	0.25	0 (Wall) 0.2 (Roof)	1.5	1.0	Schedule	Schedule	Schedule	None	None
RUN_19	1	2500	15% WFR	No	0	0	Removed	Direct	Single (N)	RESYS	13	7.7	Always	72	75	1,800 cfm	0.088	0.035	0.75	0.082	**0.75**	1.142	0.516	None	0.87	0.25	0 (Wall) 0.2 (Roof)	1.5	1.0	Schedule	Schedule	Schedule	None	None
RUN_20	1	2500	15% WFR	No	0	0	Removed	Direct	Single (N)	RESYS	13	7.7	Always	72	75	1,800 cfm	0.088	0.035	0.75	0.082	0.75	**0.65**	0.516	None	0.87	0.25	0 (Wall) 0.2 (Roof)	1.5	1.0	Schedule	Schedule	Schedule	None	None
RUN_21	1	2500	15% WFR	No	0	0	Removed	Direct	Single (N)	RESYS	13	7.7	Always	72	75	1,800 cfm	0.088	0.035	0.75	0.082	0.75	0.65	**0.65**	**Frame**	**0.3**	0.25	0 (Wall) 0.2 (Roof)	1.5	1.0	Schedule	Schedule	Schedule	None	None
RUN_22	1	2500	15% WFR	No	0	0	Removed	Direct	Single (N)	RESYS	13	7.7	Always	72	75	1,800 cfm	0.088	0.035	0.75	0.082	0.75	0.65	0.65	Frame	0.3	**0.35**	0 (Wall) 0.2 (Roof)	1.5	1.0	Schedule	Schedule	Schedule	None	None
RUN_23	1	2500	15% WFR	No	0	0	Removed	Direct	Single (N)	RESYS	13	7.7	Always	72	75	1,800 cfm	0.088	0.035	0.75	0.082	0.75	0.65	0.65	Frame	0.3	0.35	**0.24**	1.5	1.0	Schedule	Schedule	Schedule	None	None
RUN_24	1	2500	15% WFR	No	0	0	Removed	Direct	Single (N)	RESYS	13	7.7	Always	72	75	1,800 cfm	0.088	0.035	0.75	0.082	0.75	0.65	0.65	Frame	0.3	0.35	0.24	**0.1951**	1.0	Schedule	Schedule	Schedule	None	None
RUN_25	1	2500	15% WFR	No	0	0	Removed	Direct	Single (N)	RESYS	13	7.7	Always	72	75	1,800 cfm	0.088	0.035	0.75	0.082	0.75	0.65	0.65	Frame	0.3	0.35	0.24	0.1952	**0.2632**	Schedule	Schedule	Schedule	None	None
RUN_26	1	2500	15% WFR	No	0	0	Removed	Direct	Single (N)	RESYS	13	7.7	Always	72	75	1,800 cfm	0.088	0.035	0.75	0.082	0.75	0.65	0.65	Frame	0.3	0.35	0.24	0.1952	0.2632	**Always**	Schedule	Schedule	None	None
RUN_27	1	2500	15% WFR	No	0	0	Removed	Direct	Single (N)	RESYS	13	7.7	Always	72	75	1,800 cfm	0.088	0.035	0.75	0.082	0.75	0.65	0.65	Frame	0.3	0.35	0.24	0.1952	0.2632	Always	**Always**	Schedule	None	None
RUN_28	1	2500	15% WFR	No	0	0	Removed	Direct	Single (N)	RESYS	13	7.7	Always	72	75	1,800 cfm	0.088	0.035	0.75	0.082	0.75	0.65	0.65	Frame	0.3	0.35	0.24	0.1952	0.2632	Always	Always	**Always**	None	None
RUN_29	1	2500	15% WFR	No	0	0	Removed	Direct	Single (N)	RESYS	13	7.7	Always	72	75	1,800 cfm	0.088	0.035	0.75	0.082	0.75	0.65	0.65	Frame	0.3	0.35	0.24	0.1952	0.2632	Always	Always	Always	**Schedule**	None
RUN_30	1	2500	15% WFR	No	0	0	Removed	Direct	Single (N)	RESYS	13	7.7	Always	72	75	1,800 cfm	0.088	0.035	0.75	0.082	0.75	0.65	0.65	Frame	0.3	0.35	0.24	0.1952	0.2632	Always	Always	Always	Schedule	**DHW**

- The RUN_3 simulation removed the overhang for the south-facing door.
- The RUN_4 simulation rotated the building orientation faced south.
- The RUN_5 simulation changed the occupancy number from 52 to 0.
- The RUN_6 simulation removed the plenum for the simplified residential model.
- The RUN_7 simulation modified the door size and location, from two doors (on the south wall and the north wall) to a single door (on the north wall only), based on the standard reference design of Table 405.5.2(1) of the 2009 IECC.

Table 4-9: Input Summary for the Project Category

Run Name	PROJECT								
	# of Spaces	Area	Fenestration (WFR)	Overhang	Azimuth	# of People	Plenum	Return-Air-Path	Door Location
	5 to 1	**5,000 to 2,500**	**22% to 15%**	**Yes to No**	**30 to 0**	**52 to 0**	**Removed**	**Plenum to Direct**	**Two (S/N) to Single (N)**
RUN_3A	5	5,000	22% WFR	Yes	30	52	Default	Plenum	Two (S/N)
RUN_1	**1**	5,000	22% WFR	Yes	30	52	Default	Plenum	Two (S/N)
RUN_2	1	**2,500**	**15% WFR**	Yes	30	52	Default	Plenum	Two (S/N)
RUN_3	1	2,500	15% WFR	**No**	30	52	Default	Plenum	Two (S/N)
RUN_4	1	2500	15% WFR	No	**0**	52	Default	Plenum	Two (S/N)
RUN_5	1	2500	15% WFR	No	0	**0**	Default	Plenum	Two (S/N)
RUN_6	1	2500	15% WFR	No	0	0	**Removed**	**Direct**	Two (S/N)
RUN_7	1	2500	15% WFR	No	0	0	Removed	Direct	**Single (N)**

4.4.1.1.2. *ASHP System Category*

The second of the six categories, the *ASHP System* category defines the input parameters for the Air-Source Heat Pump (ASHP) system model from the Variable Air Volume system (VAVS) used in "RUN 3A" of the samp1e.inp file. The input parameters include system efficiency, supply air fan, and thermostat setting. The ASHP system can be modeled with the residential system type, which is the RESYS system in the DOE-2.1e program. The RESYS system model was created to represent a residential air-to-air heat pump (i.e., ASHP) for a single-zone constant-volume system intended for homes or small office. Table 4-10 shows seven runs in the *ASHP System* category and summarizes the input changes, which are yellow shaded in each row.

Table 4-10: Input Summary for the ASHP System Category

Run Name	ASHP SYSTEM						
	System Change	SEER	HSPF	Fan Schedule	Thermostat Heat Schedule	Thermostat Cool Schedule	Air Flow Rate
	VAVS to RESYS	**7.3 to 13**	**5.4 to 7.7**	**Schedule to Always**	**Schedule to 72**	**Schedule to 75**	**7,366 cfm to 1,800 cfm**
RUN_3A	VAVS	7.3	5.4	Schedule	Schedule	Schedule	7,366 cfm
RUN_8	**RESYS**	7.3	5.4	Schedule	Schedule	Schedule	7,366 cfm
RUN_9	RESYS	**13**	5.4	Schedule	Schedule	Schedule	7,366 cfm
RUN_10	RESYS	13	**7.7**	Schedule	Schedule	Schedule	7,366 cfm
RUN_11	RESYS	13	7.7	**Always**	Schedule	Schedule	7,366 cfm
RUN_12	RESYS	13	7.7	Always	**72**	Schedule	7,366 cfm
RUN_13	RESYS	13	7.7	Always	72	**75**	7,366 cfm
RUN_14	RESYS	13	7.7	Always	72	75	**1,800 cfm**

The modified inputs for each simulation in the *ASHP System* category are described as follow:

- The RUN_8 simulation run changed the system model, from the Variable Air Volume system (VAVS) to the Residential system (RESYS) model.
- The RUN_9 simulation defined the cooling efficiency of the ASHP system, from SEER 7.3 to SEER 13, based on Table 503.2.3(2) in the 2009 IECC. The cooling Energy Input Ratio (EIR), which excludes the supply air fan energy, was calculated using equation 4.72 and equation 4.73 (Fairey et al., 2004). As a result, 0.211695 of the cooling EIR was used for the input.

$$SEER_{nofan} = 1/(1/SEER - FAN_{sa}) \quad (4.72)$$

$$EIR_{cooling} = 0.941 \times \left[1/\left(SEER_{nofan}/3.41\right)\right] \quad (4.73)$$

Where,

$SEER_{nofan}$	is the seasonal energy efficiency ratio, excluding supply fan energy,
$SEER$	is the seasonal energy efficiency ratio (e.g., SEER in the 2009 IECC),
FAN_{sa}[36]	is the supply air fan energy (Wh/Btu), and
$EIR_{cooling}$	is the cooling energy input ratio.

- The RUN_10 simulation defined the heating efficiency of the ASHP system, from 5.4 HSPF to 7.7 HSPF, based on Table 503.2.3(2) in the 2009 IECC. The heating

[36] The supply air fan energy was calculated, assuming the supply fan power is 0.365 w/cfm, by the following expression: 0.01095 Wh/Btu = (0.365 W/cfm) × (360 cfm/ton) × (1 ton/12,000 Btu/h)

EIR, which excludes the supply air fan energy, was calculated using equation 4.74 and equation 4.75 (Fairey et al., 2004). As a result, 0.236011 of the heating EIR was used for the input.

$$HSPF_{nofan} = 1/(1/HSPF - FAN_{sa}) \quad (4.74)$$

$$EIR_{heating} = 0.582 \times \left[1/\left(HSPF_{nofan}/3.41\right)\right] \quad (4.75)$$

Where,

$HSPF_{nofan}$	is the heating seasonal performance factor, excluding supply fan energy,
HSPF	is the heating seasonal performance factor (e.g., HSPF in the 2009 IECC),
FAN_{sa}	is the supply air fan energy (Wh/Btu), and
$EIR_{heating}$	is the heating energy input ratio.

- The RUN_11 simulation set the system fan to run when the system runs (Figure 4-51).
- The RUN_12 simulation set the heating thermostat at a constant 72 F (Figure 4-52), based on Table 405.5.2(1) in the 2009 IECC.
- The RUN_13 simulation set the cooling thermostat at a constant 75 F (Figure 4-53), based on Table 405.5.2(1) in the 2009 IECC.
- The RUN_14 simulation set the supply air flow from 7,366 cfm to 1,800 cfm, which assumes 360 cfm/ton and 500 ft^2/ton.

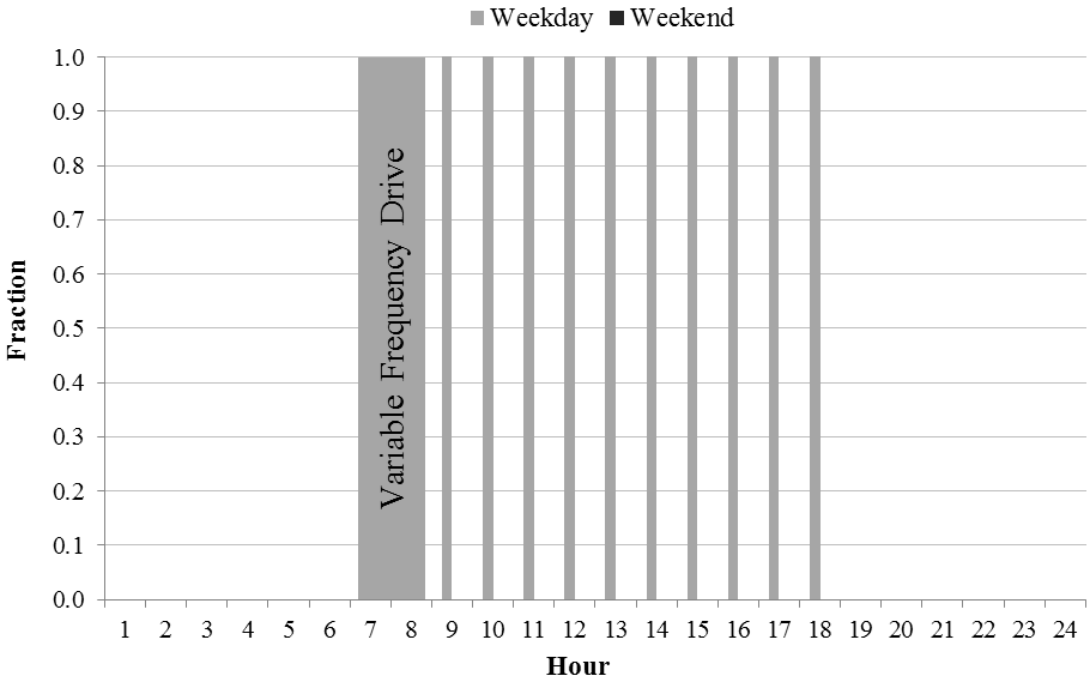

(a) Before Modification

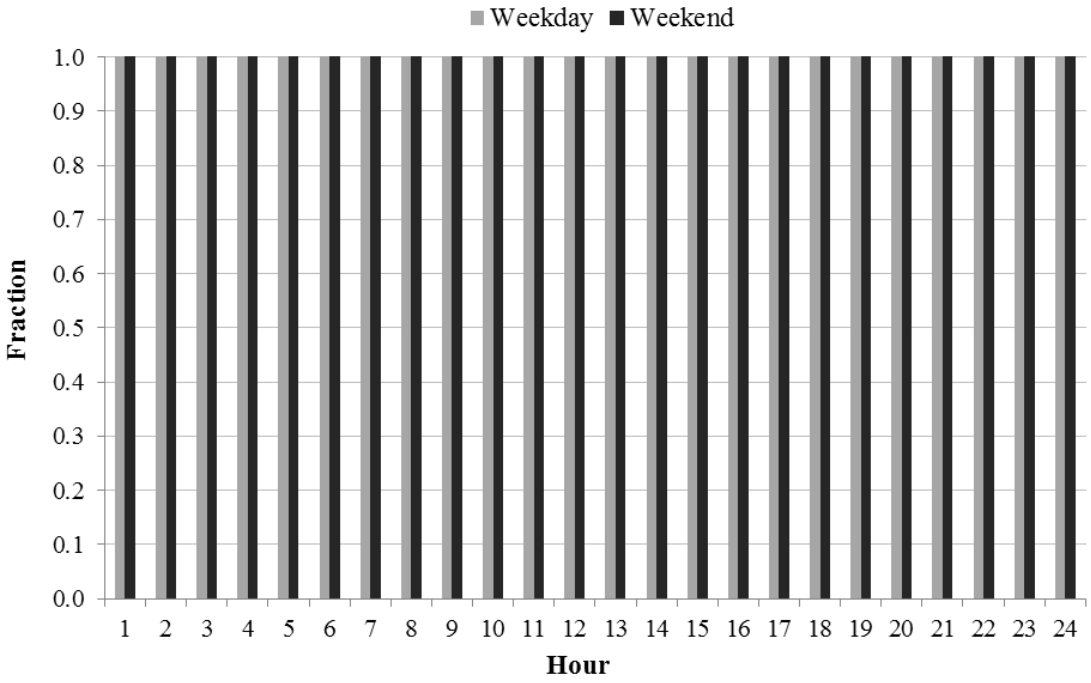

(b) After Modification

Figure 4-51: Modification of System Fan Schedule in RUN_11

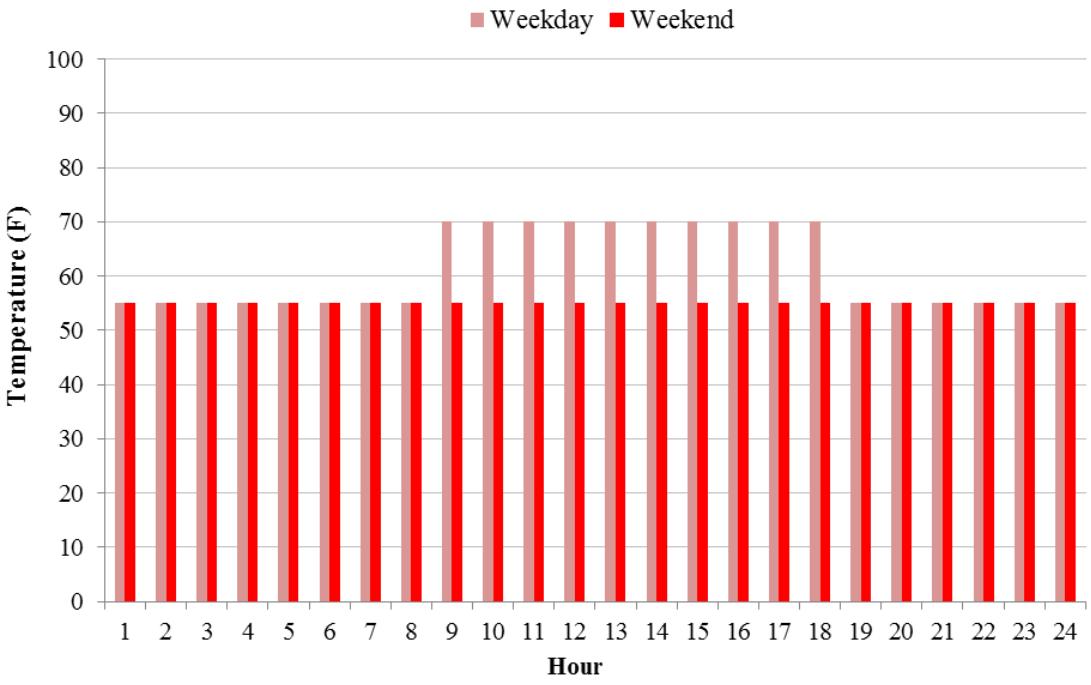

(a) Before Modification

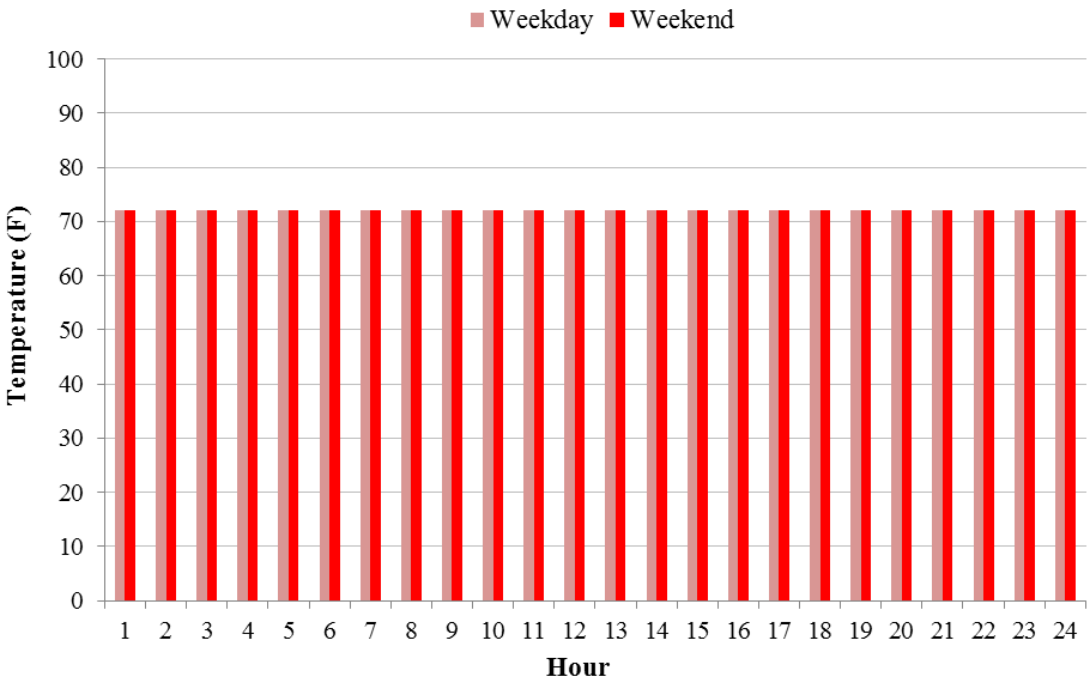

(b) After Modification

Figure 4-52: Modification of Heating Thermostat Schedule in RUN_12

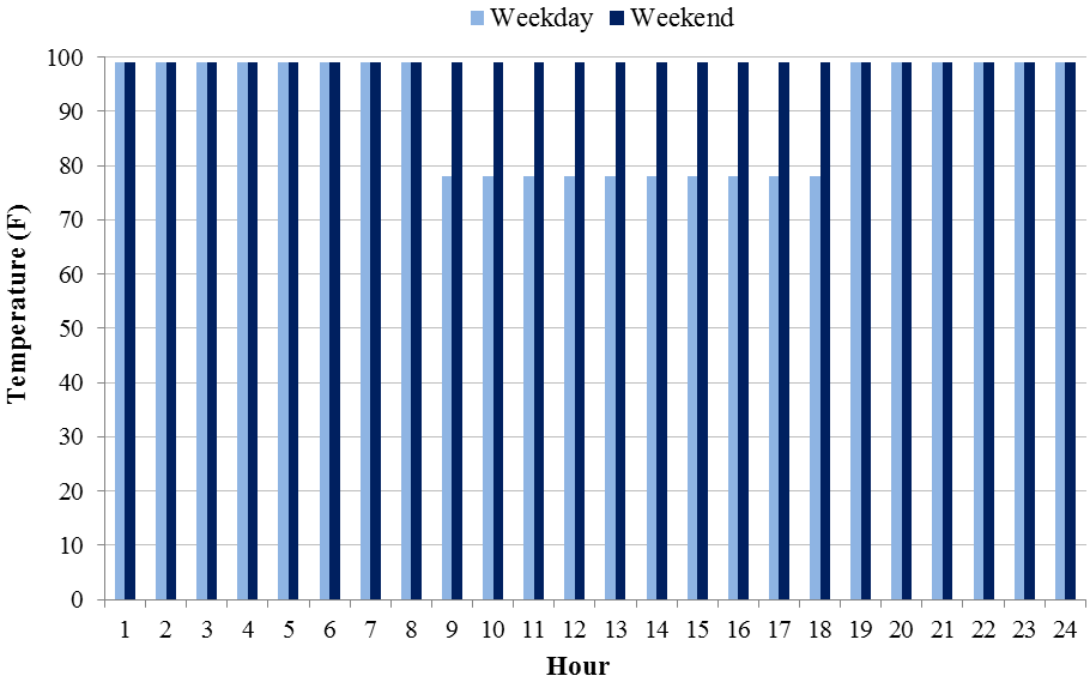

(a) Before Modification

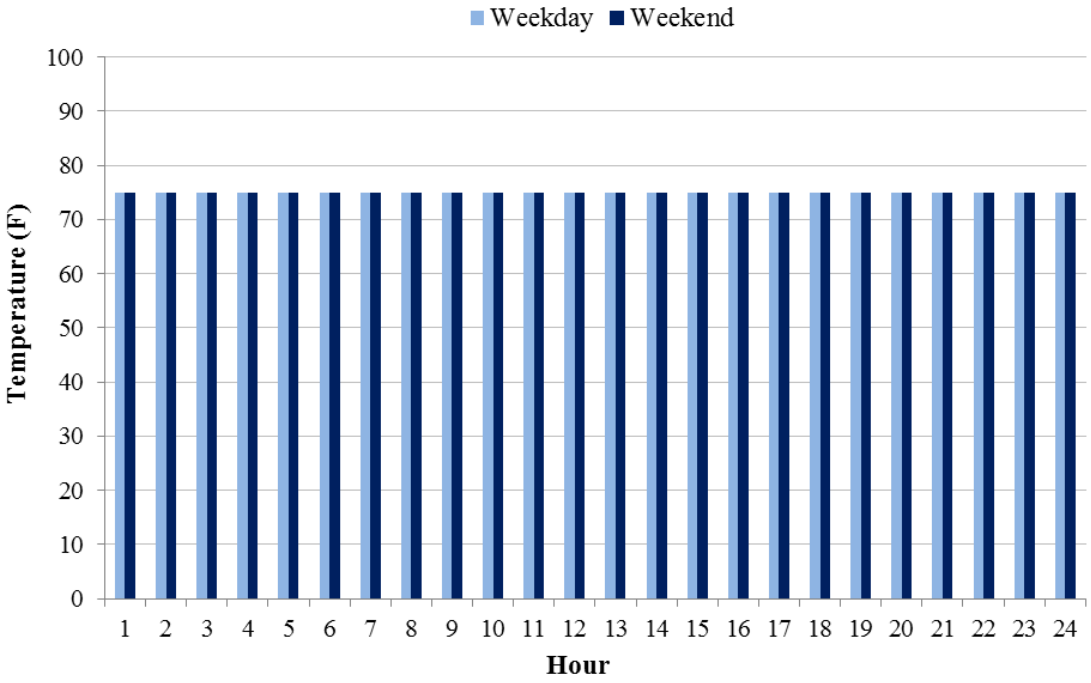

(b) After Modification

Figure 4-53: Modification of Cooling Thermostat Schedule in RUN_13

4.4.1.1.3. *Construction Category*

The third of the six categories, the *Construction* category modifies input parameters for the residential building envelope according to the the 2009 IECC requirements. The inputs include thermal insulation and solar absorptance/reflectance for the building envelope such as the floor, the roof, walls, the door, the windows, and the ground. Table 4-11 shows nine runs in the *Construction* category and summarizes the input changes, which are yellow shaded in each row.

Table 4-11: Input Summary for the Construction Category

Run Name	CONSTRUCTION										
	Floor U-Value (Slab-on-Grade)	**Roof U-Value**	**Roof Absorptance**	**Wall U-Value**	**Wall Absorptance**	**Door U-Value**	**Glazing U-Value**	**Window Frame**	**Glazing SHGC**	**Infiltration ACH**	**Ground Reflectance**
	0.05 to 0.088	**0.048 to 0.035**	**0.7 to 0.75**	**0.069 to 0.082**	**0.7 to 0.75**	**1.142 to 0.5**	**0.516 to 0.65**	**None to Frame**	**0.87 to 0.3**	**0.25 to 0.35**	**0/0.2 to 0.24**
RUN_3A	0.05	0.048	0.7	0.069	0.7	1.47	0.574	None	0.87	0.25	0 (Wall) 0.2 (Roof)
RUN_15	**0.088**	0.048	0.7	0.069	0.7	1.142	0.516	None	0.87	0.25	0 (Wall) 0.2 (Roof)
RUN_16	0.088	**0.035**	0.7	0.069	0.7	1.142	0.516	None	0.87	0.25	0 (Wall) 0.2 (Roof)
RUN_17	0.088	0.035	**0.75**	0.069	0.7	1.142	0.516	None	0.87	0.25	0 (Wall) 0.2 (Roof)
RUN_18	0.088	0.035	0.75	**0.082**	0.7	1.142	0.516	None	0.87	0.25	0 (Wall) 0.2 (Roof)
RUN_19	0.088	0.035	0.75	0.082	**0.75**	1.142	0.516	None	0.87	0.25	0 (Wall) 0.2 (Roof)
RUN_20	0.088	0.035	0.75	0.082	0.75	**0.65**	0.516	None	0.87	0.25	0 (Wall) 0.2 (Roof)
RUN_21	0.088	0.035	0.75	0.082	0.75	0.65	**0.65**	**Frame**	**0.3**	0.25	0 (Wall) 0.2 (Roof)
RUN_22	0.088	0.035	0.75	0.082	0.75	0.65	0.65	Frame	0.3	**0.35**	0 (Wall) 0.2 (Roof)
RUN_23	0.088	0.035	0.75	0.082	0.75	0.65	0.65	Frame	0.3	0.35	**0.24**

The modified inputs for each simulation in the *Construction* category are described as follow:

- The RUN_15 simulation in this category modified the floor thermal insulation. R-0 which was used for the slab-on-glade floor in Climate Zone 2, based on Table 402.1.1 in the 2009 IECC, using the Winkelmann method (Winkelmann, 1998).
- The RUN_16 simulation modified the roof thermal insulation. R-30 was used for the roof, based on Section 402.2.2 in the 2009 IECC. IECC. The U-0.035 value was applied to use the layer input method, including 7% of the framing factor[37]. The roof was divided into two different parts: 93% of the roof area was used for the cavity part, and 7% of the roof area was used for the stud part.
- The RUN_17 simulation modified the roof solar absorptance from 0.7 to 0.75, based on Table 405.5.2(1) in the 2009 IECC.
- The RUN_18 simulation modified the wall thermal insulation for Climate Zone 2 from U-0.069 to U-0.082, based on Table 402.1.3 in the 2009 IECC. The U-0.082 was applied to use the layer input method, including 25% of the framing factor. Each exterior wall was divided into two different parts: 75% of the wall area was used for the cavity part, and 25% of the wall area was used for the stud part.
- The RUN_19 simulation modified the wall solar absorptance from 0.7 to 0.75, based on Table 405.5.2(1) in the 2009 IECC.
- The RUN_20 simulation modified the door thermal insulation from U-1.142 to U-0.65, based on Table 303.1.3(2) in the 2009 IECC.

[37] Framing factor represents the percentage of stud or joist area.

- The RUN_21 simulation modified the window glass thermal conductance and Solar Heat Gain Coefficient[38] (SHGC) for Climate Zone 2 from U-0.516 to U-0.65 and from 0.87 to 0.3 (Table A-21), based on Table 402.1.3 in the 2009 IECC. In addition, an aluminum window frame was added.
- The RUN_22 simulation modified the infiltration rate from 0.2916 Air Changes per Hour (ACH) to 0.35 ACH, based on Table 405.5.2(1) in the 2009 IECC. In order to input the infiltration, this study used 0.0004321 of the Specific Leakage Area (SLA) value, which was calculated by the following equation (EnergyGauge, 2013):

$$ACH = SLA \times 1{,}000 \times W \times NS^{0.3} \tag{4.76}$$

Where,

ACH	is the air change per hour,
SLA	is the specific leakage area,
W	is the weather factor[39], and
NS	is the number of stories above grade.

- The RUN_23 simulation modified the ground reflectance from 0 for the exterior walls and 0.2 for the roof to 0.24 for both the walls and roof. 0.24 of the ground reflectance represents the base-case house model is surrounded by grass.

[38] Shading Coefficient (SC) = SHGC / 0.87
[39] 0.81of the weather factor was used for Houston (ASHRAE, 2010).

4.4.1.1.4. *Internal Gain, Schedule, and DHW Categories*

The other categories are the *Internal Gain, Schedule,* and *DHW* categories. These categories include two runs in the *Internal Gain* category, four runs in *Schedule* category, and one run in *DHW* category. Table 4-12 summarizes the input changes for each run, which are yellow shaded in each row.

Table 4-12: Input Summary for the Internal Gain, Schedule, and DHW Categories

Run Name	INTERNAL GAIN		SCHEDULE				DHW
	Lighting (w/sqft)	Equipment (w/sqft)	Lighting	Equipment	Infiltration	Interior Shading	DHW System
	1.5 to 0.1951	1.0 to 0.2632	Schedule to Always	Schedule to Always	Schedule to Always	None to Schedule	None to DHW
RUN_3A	1.5	1.0	Schedule	Schedule	Schedule	None	None
RUN_24	**0.1951**	1.0	Schedule	Schedule	Schedule	None	None
RUN_25	0.1952	**0.2632**	Schedule	Schedule	Schedule	None	None
RUN_26	0.1952	0.2632	**Always**	Schedule	Schedule	None	None
RUN_27	0.1952	0.2632	Always	**Always**	Schedule	None	None
RUN_28	0.1952	0.2632	Always	Always	**Always**	None	None
RUN_29	0.1952	0.2632	Always	Always	Always	**Schedule**	None
RUN_30	0.1952	0.2632	Always	Always	Always	Schedule	**DHW**

The *Internal Gain* category defines input parameters for the energy use of lighting and equipment. To determine the power density (W/ft^2) for lighting and equipment, the total internal gains were calculated, using the following equation from Table 405.5.2(1) in the 2009 IECC.

$$IG_{ain} = 17{,}900 + 23.8 \times CFA + 4{,}104 \times N_{BR} \quad (4.77)$$

Where,

IG_{ain} is the internal gains per dwelling unit (Btu/day),
CFA is the conditioned floor area (ft^2), and
N_{BR} is the number of bedrooms; four bedrooms were used.

As a result, the total internal gains were calculated as 89,712 Btu/day (27.49 kWh/day), which is equivalent to 3,738 Btu/hr (1.145 kWh/hr). The ratio to distribute the calculated total internal gains to lighting and equipment was then calculated, referencing the annual appliance and equipment loads in the Building America Research Benchmark (NREL, 2005). Assuming 100% incandescent interior lighting, 42.6% of the total internal gains was used for lighting and the rest of the total internal gains was used for equipment. Based on the distribution ratio, lighting power density and equipment power density for the residential model were determined as 0.1951 W/ft^2 and 0.2632 W/ft^2, respectively. The modified inputs in the *Internal Gain* category are described as follow:

- The RUN_24 simulation in this category modified the lighting power density from 1.5 W/ft^2 to 0.1951 W/ft^2.
- The RUN_25 simulation in this category modified the equipment power density from 1.0 W/ft^2 to 0.2632 W/ft^2.

The *Schedule* category defines input parameters for the residential model to have constant schedules for lighting, equipment, infiltration, and interior shading. The modified inputs for each simulation in the *Schedule* category are described as follow:

- The RUN_26 simulation in this category set the lighting system to be always on (Figure 4-54).
- The RUN_27 simulation in this category set the equipment system to be always on (Figure 4-55).
- The RUN_28 simulation in this category set the infiltration to be always on (Figure 4-56). However, it should be noted that the infiltration schedule does not work for the Sherman-Grimsrud (S-G) infiltration method in the DOE-2.1e program, and causes severe errors in the eQUEST program.
- The RUN_29 simulation in this category set the schedule of the interior shading[40] (Figure 4-57) for the windows based on Table 405.5.2(1) in the 2009 IECC. The standard reference design in the 2009 IECC requires that 0.85 and 0.7 of the multiplier in the interior shading schedule were used for winter and summer interior shading, respectively.

[40] Interior shading represents percentage of light transmitted from outside to inside through the blinds or drapes operation. The multipliers in the interior shading schedule are specified in terms of: 1.0 means no shading, 0.0 means full shading.

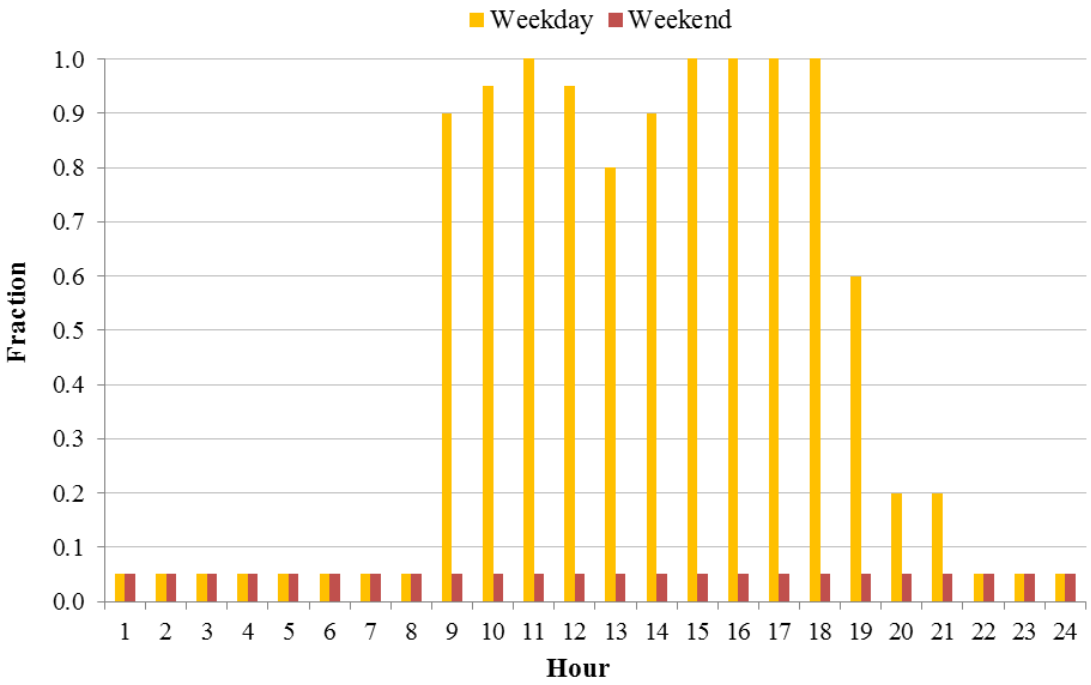

(a) Before Modification

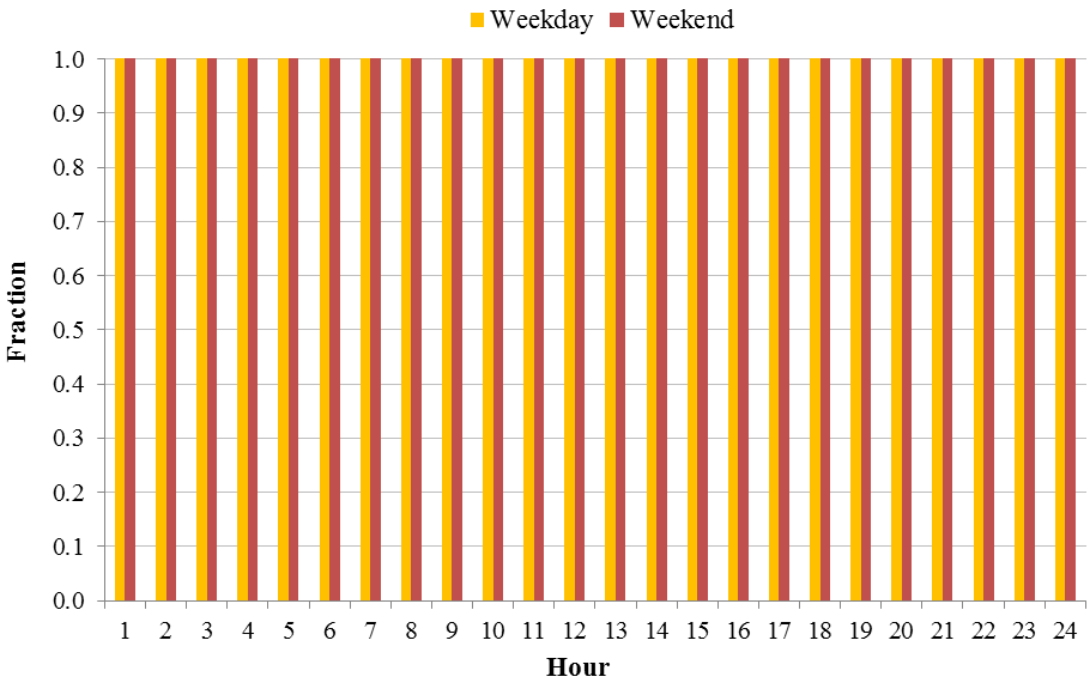

(b) After Modification

Figure 4-54: Modification of Lighting Schedule in RUN_26

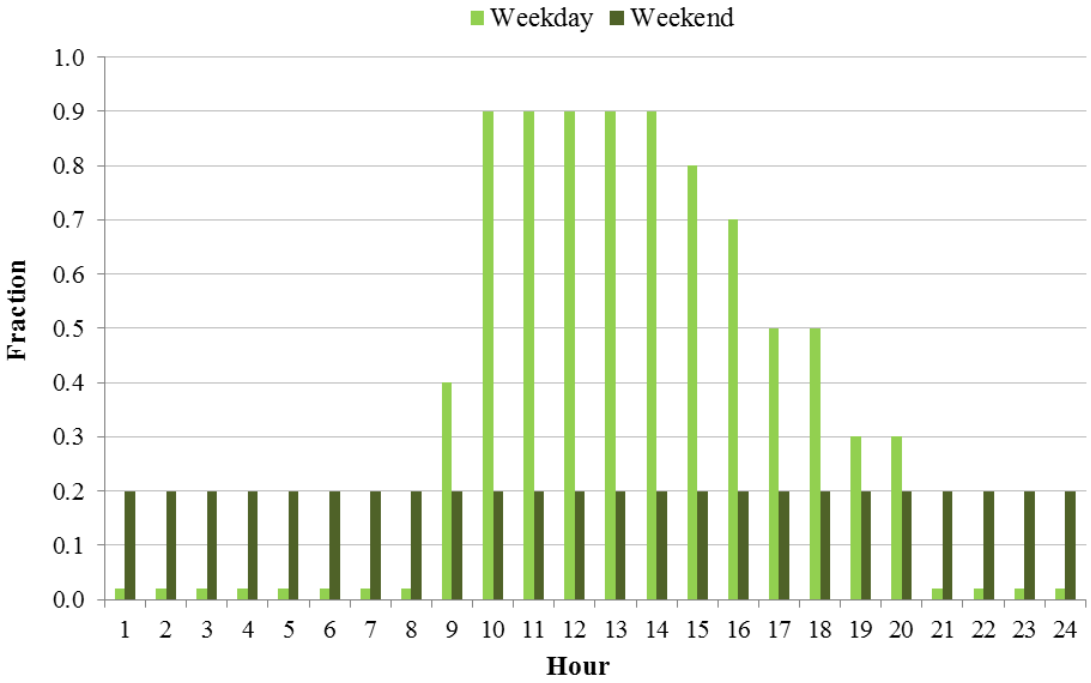

(a) Before Modification

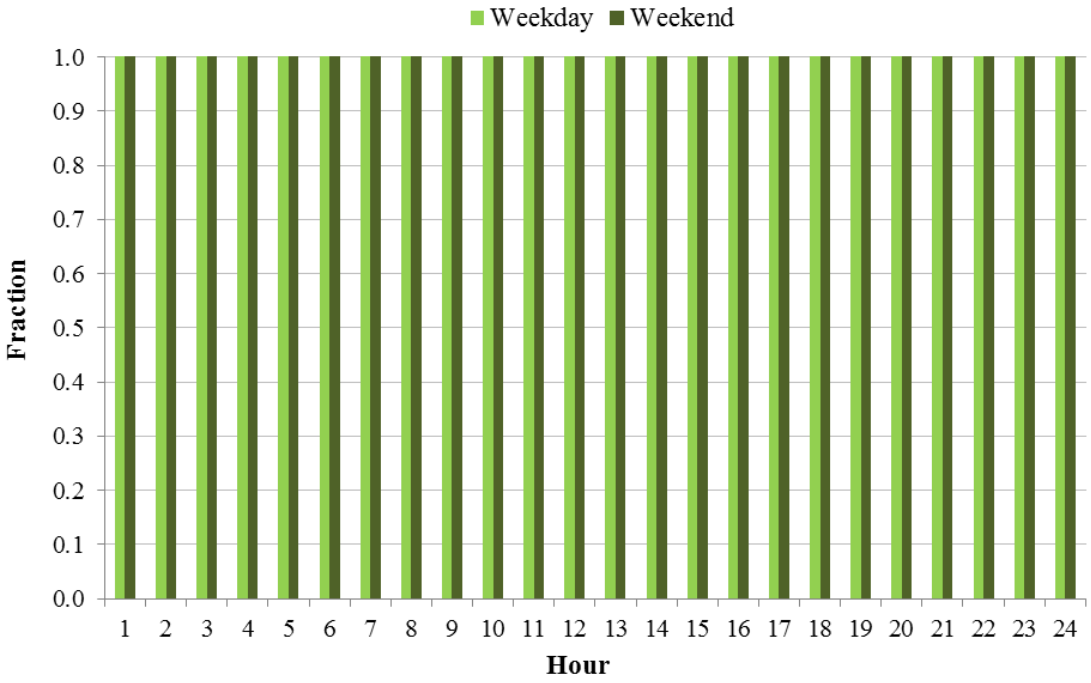

(b) After Modification

Figure 4-55: Modification of Equipment Schedule in RUN_27

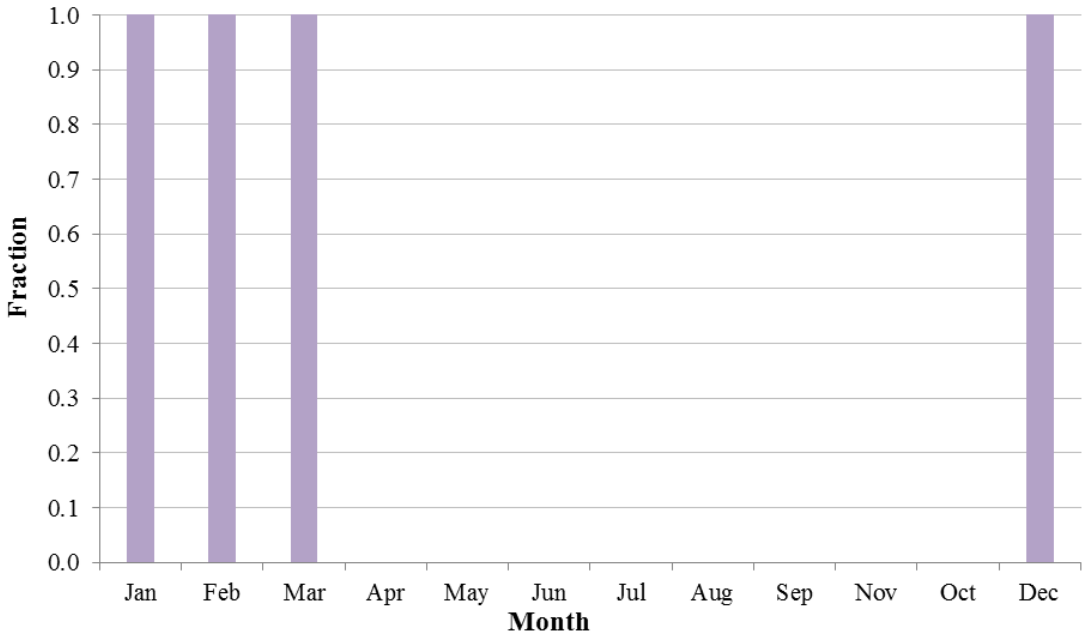

(a) Before Modification

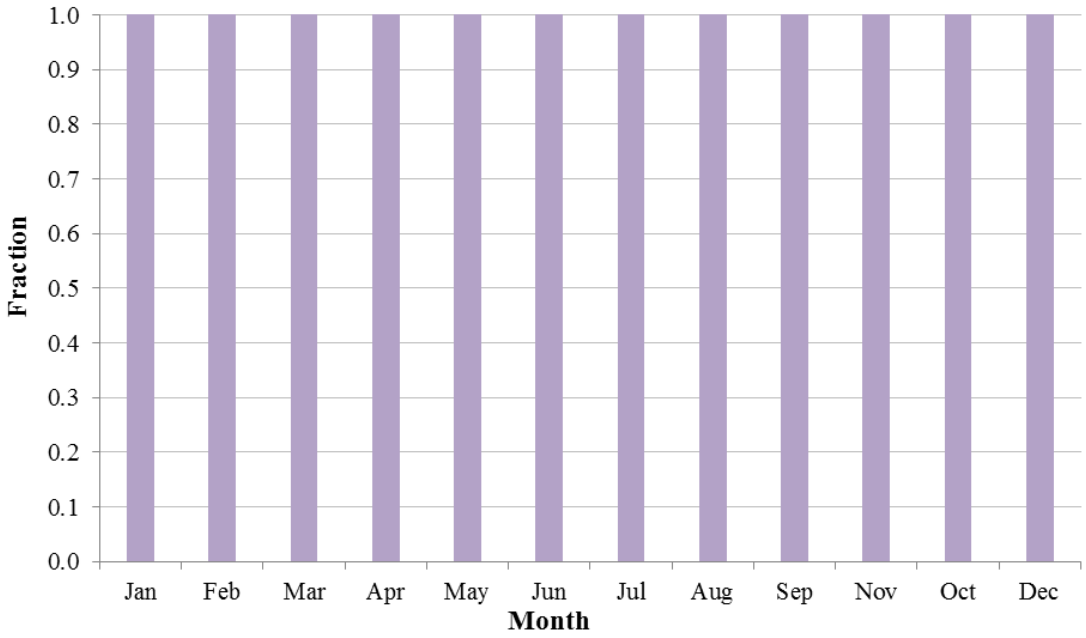

(b) After Modification

Figure 4-56: Modification of Infiltration Schedule in RUN_28

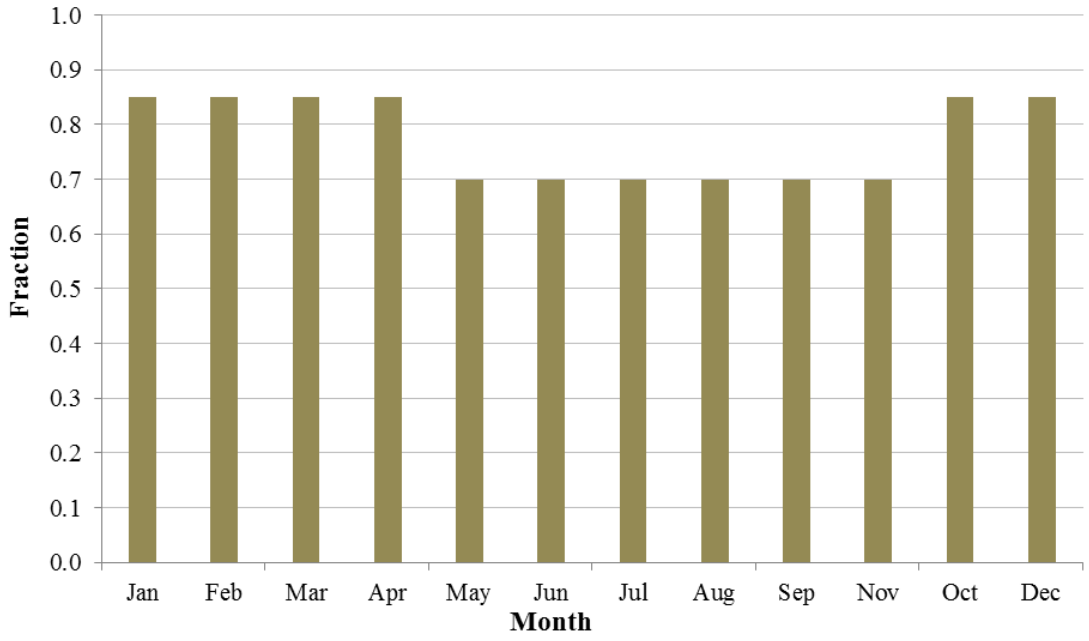

Figure 4-57: Interior Shading Schedule in RUN_29

Finally, the *DHW* category defines input parameters for a residential electric domestic hot water (DHW) heater system. The residential electric DHW heater model in this study had 50 gallons of the hot water tank size and 18,766 Btu/hr of the burner capacity (NREL, 2008). A 1.0 was used for the energy factor for the electric water heater, which is the default value of the DOE-2.1e program. To estimate the hot water consumption, the following equation was used. As a result, 0.0486 gal/min of the hot water consumption was determined.

$$HW_{use} = [30 + (10 \times N_{BR})]/1{,}440 \quad (4.78)$$

Where,

HW_{use} is the hot water use (gal/min), and

N_{BR} is the number of bedrooms; four bedrooms were used.

In addition, the IC3 DHW inlet water temperatures, which was calculated using the NREL report (NREL, 2004), were referenced. The resulted inlet water temperatures are shown in Figure 4-58. The modified input in the *DHW* category is described as follows:

- The RUN_30 simulation in this category defined the residential electric DHW system which has 50 gallons of the hot water tank size, 18,766 Btu/hr of the burner capacity, a 1.0 of the energy factor, and 0.0486 gal/min of the hot water consumption.

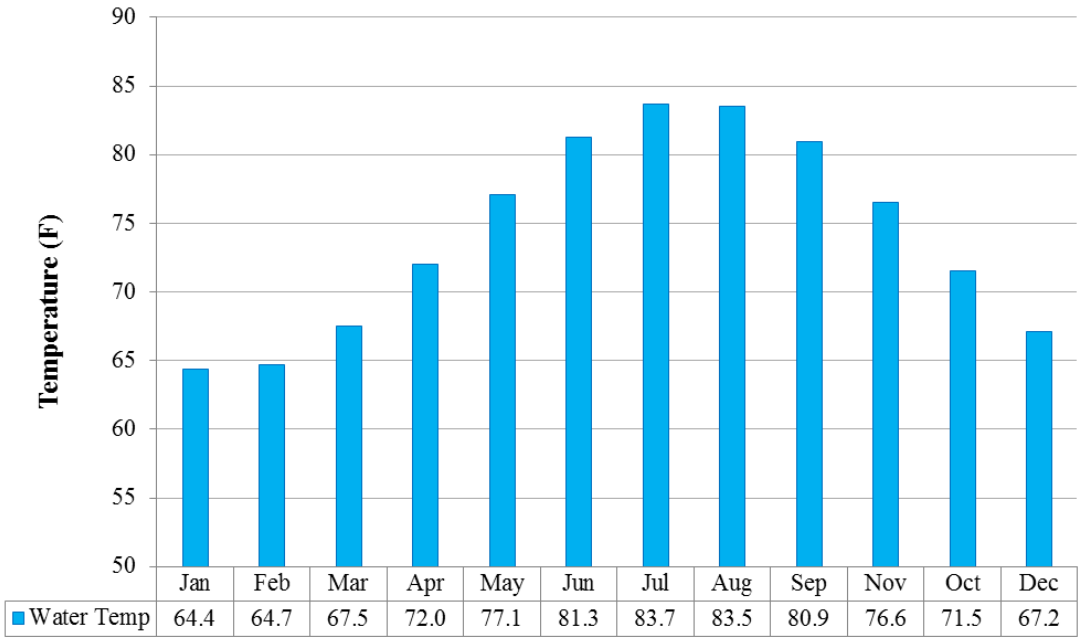

Figure 4-58: DHW Inlet Water Temperatures

4.4.1.2. Simplified Residential ASHP Base-Case Model for Dallas

This study also developed a simplified residential ASHP base-case simulation model located in Dallas, TX, which represents Climate Zone 3 in the 2009 IECC. Using the base-case simulation model for Houston (i.e., RUN_30 in Section 4.4.1.1), the residential ASHP base-case model for Dallas was developed by modifying input parameters for the 2009 IECC requirements from Houston to Dallas. The modified input parameters include the TMY2 weather data, location, DHW inlet temperatures, and fenestration requirements. Other input parameters (e.g., building geometry, schedules, HVAC systems, and others) were not changed.

4.4.2. Development of the Simplified Residential DOE-2.1e GCHP Base-Case Model

This section describes the method used to develop a residential DOE-2.1e ground-coupled heat pump (GCHP) base-case simulation model using a vertical Ground Heat Exchanger (GHX) model. The vertical GHX model, which is based on the equations in Section 4.2.3, was developed using the DOE-2.1e input FUNCTION method. The vertical GHX DOE-2.1e input FUNCTION was incorporated within the air-source heat pump simulation module (i.e., RESYS) by modifying the calculation algorithm (i.e., the input file). In this way, the modified ASHP system module works like the GCHP system model that includes a vertical GHX. To apply the vertical GHX DOE-2.1e input FUNCTION, this study used the simplified residential ASHP base-case models for Houston and Dallas, which are described in Section 4.4.1.

4.4.2.1. Method Used to Develop DOE-2.1e GCHP System

This section describes the method used to develop the DOE-2.1e ground-coupled heat pump (GCHP) system, using the DOE-2 FUNCTION command for a vertical GHX model. DOE-2 (DOE-2.1e) users are able to modify DOE-2 LOADS or SYSTEMS calculation algorithms without recompiling the DOE-2 program using the input FUNCTION feature (LBL, 1993a). This feature expands the modeling capability of DOE-2. The DOE-2 FUNCTION is written as FORTRAN-like routines that are included in a regular DOE-2 input file. DOE-2 users specify the values to be calculated, using the FUNCTION command, and specify where these values are to be used in the hourly simulation. The values to be replaced can be found by accessing the LOADS and SYSTEMS simulation variables in the looping structure of LOADS and SYSTEMS. The FUNCTION command is referenced within the hourly loop of the DOE-2 program and will be calculated each hour of the input run period.

In order to modify the DOE-2.1e calculation algorithm, the GHX FUNCTION will be written in the SYSTEMS section of the DOE-2 input file. Figure 4-59 shows an overall diagram of the DOE-2 calculation flow (LBNL, 2013) and the insertion point of the GHX FUNCTION command into the DOE-2 program calculation loop.

A water-source heat pump (WSHP) system incorporating the GHX model within the PLANT loop is the widely used method for a GCHP system in a whole-building energy program, as described in Section 2.7.1. However, this study implements the GHX model as a FUNCTION command within the air-source heat pump (ASHP) system

simulation module[41]. The reason for using the ASHP is that the DOE-2.1e program has a limitation in using the FUNCTION command in the PLANT loop. Specifically, the DOE-2.1e program does not allow users to modify the PLANT calculation algorithms even if users can access variables used in the PLANT loop (LBL, 1993a).

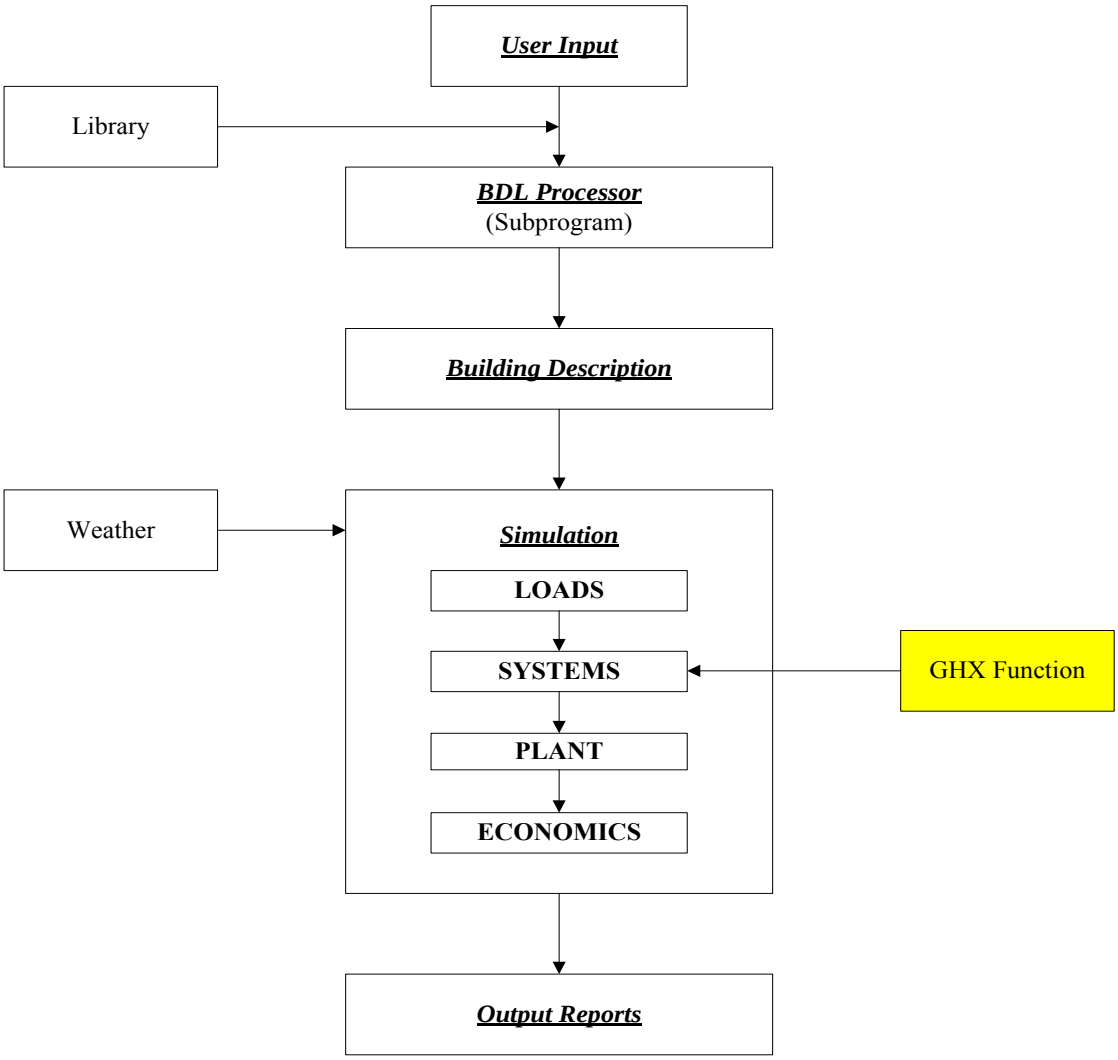

Figure 4-59: Diagram of GHX FUNCTION Located in the DOE-2 Flowchart

[41] The Air-Source Heat Pump system is named as Residential System in the DOE-2 BDL Summary (LBL, 1993b). Its subroutine name is RESYS.

The GHX FUNCTION calculates the entering water temperature (EWT), which is the circulated water temperatures through the GHX, for each hour of the run period. In the FUNCTION command, the Entering Dry-Bulb (EDB) temperatures at the condenser in the ASHP system simulation module will be replaced with the calculated EWTs. Figure 4-60 and Figure 4-61 show the conceptual diagram of the ASHP system and the GCHP system with a vertical GHX unit.

When transferring a system from the ASHP to the GCHP using the vertical GHX FUNCTION, it is noted that the electric power consumption for the fan in the outdoor condenser unit in the ASHP system has to be eliminated and the pump electric power to circulate the fluid through a GHX unit has to be included in the GCHP system model. However, this study did not manipulate the electric power consumption for the outdoor fan and the circulation pump separately since ordinary rated efficiencies (e.g., SEER and HSPF for an ASHP; EER and COP for a GCHP) already include the electric power consumption for an outdoor condenser fan in an ASHP system (AHRI, 2008) and for a GHX circulation pump in a GCHP system (AHRI, 1998). Therefore, this study assumed that the system's heating/cooling electric input ratio (EIR)[42] values already included the electric power consumption for the ASHP outdoor fan and the GCHP circulation pump. Otherwise, it was felt that double counting for outdoor fan energy or circulation pump energy could occur.

[42] The Electric Input Ratio (EIR) is the ratio of the electric energy input (in Btu/hr) to the rated capacity (in Btu/hr).

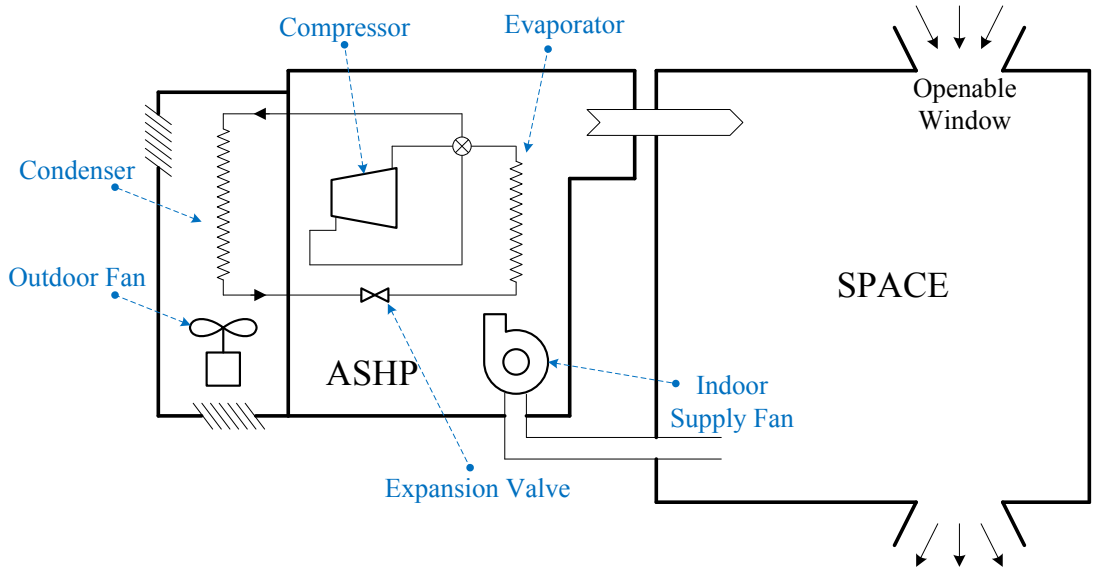

Figure 4-60: Diagram of an Air-Source Heat Pump System (LBL, 1994)

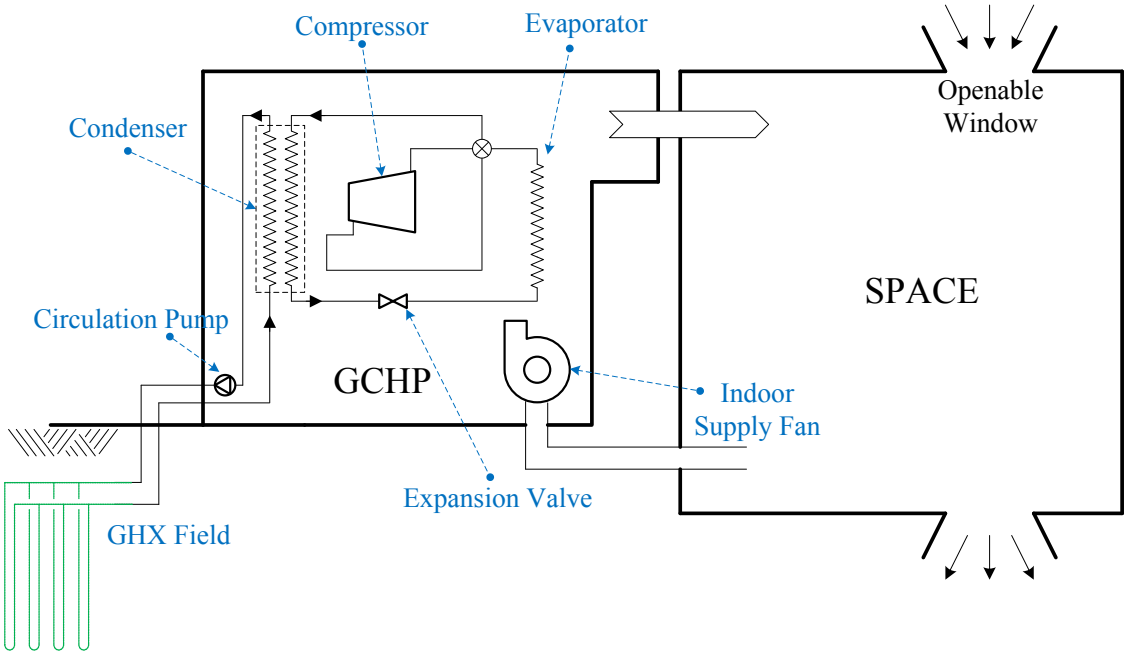

Figure 4-61: Diagram of a Ground-Coupled Heat Pump System

In addition, DOE-2 uses an empirical curve-fit method to estimate performance of the HVAC system under part load conditions. Therefore, the default RESYS system equipment curves in DOE-2.1e needed to be modified to represent the GCHP system equipment. Table 4-13 shows the default system correlations used for RESYS (i.e., ASHP) and GCHP systems[43]. These correlations were modified using the curve-fit command from the SYSTEMS section of the DOE-2.1e input file.

Table 4-13: System Curve-Fit Correlations for ASHP and GCHP

	Type of Curve	a	b	c	d	e	f
DOE-2.1e RESYS							
COOL-CAP-FT = SDL-C1	BI-QUAD	0.60034040	0.00228730	-0.00001280	0.00138980	-0.00008060	0.00014120
COOL-EIR-FT = SDL-C11	BI-QUAD	-0.96177870	0.04817750	-0.00023110	0.00324390	0.00014880	-0.00029520
COOL-EIR-FPLR = SDL-C16	LINEAR	0.12500000	0.87500000	0.00000000	0.00000000	0.00000000	0.00000000
COOL-SH-FT = SDL-C21	BI-QUAD	6.52756980	-0.12613750	0.00056880	0.00907570	-0.00004830	-0.00000880
HEAT-CAP-FT = SDL-C51	CUBIC	0.29495690	0.01425360	-0.00001170	0.00000060	0.00000000	0.00000000
HEAT-EIR-FT = SDL-C56	CUBIC	2.18554780	-0.04947180	0.00070420	-0.00000400	0.00000000	0.00000000
HEAT-EIR-FPLR = SDL-C61	CUBIC	0.08565220	0.93881370	-0.18343610	0.15897020	0.00000000	0.00000000
DOE-2.1e GCHP[1]							
COOL-CAP-FT-GSHP	BI-LINEAR	0.36674020	0.01540058	0.00000000	-0.00517634	0.00000000	0.00000000
COOL-EIR-FT-GSHP	BI-LINEAR	0.49878043	-0.00786524	0.00000000	0.01335313	0.00000000	0.00000000
COOL-SH-FT-GSHP	BI-QUAD	1.01813138	0.04775910	-0.00066600	-0.00810620	0.00001850	0.00005371
HEAT-CAP-FT-GSHP	BI-LINEAR	0.65710455	-0.00300010	0.00000000	0.01727820	0.00000000	0.00000000
HEAT-EIR-FT-GSHP	BI-LINEAR	0.64566398	0.00798015	0.00000000	-0.00638358	0.00000000	0.00000000
COOLHEAT-EIR-FPLR-GSHP	CUBIC	0.00988125	1.08033000	-0.10526700	0.01514030	0.00000000	0.00000000

Note: 1. The curve-fit correlations were obtained from the eQUEST simulation program (JJH, 2013).

[43] Forms of the System Curve-Fit Equations (LBL, 1993a):
Linear: $z = a + bx$
Cubic: $z = a + bx + cx^2 + dx^3$
Bi-Quadratic: $z = a + bx + cx^2 + dy + ey^2 + fxy$

4.4.2.2. Structure of Vertical GHX DOE-2.1e Input FUNCTION

The vertical GHX input FUNCTION in the DOE-2.1e program, which is used for a GCHP system, includes two subroutines. First, a THERMALLOAD subroutine (Figure 4-62) calculates the system's thermal loads before the ASHP system operates for cooling and heating. The system's cooling loads are the sum of the sensible part of the cooling coil load and the latent part cooling load. The system's heating loads are the sensible loads only (LBL, 1982a). The calculated system loads pass through another subroutine, GHXCALC. Second, a GHXCALC subroutine (Figure 4-63) calculates the EWTs based on the system's thermal loads. Then, the calculated EWTs replace the Entering Dry-Bulb (EDB) temperatures at the condenser in the DOE-2.1e ASHP system simulation module.

The two subroutines, consisted in the structure of the vertical GHX input FUNCTION, are called in the DOE-2 SYSTEMS loop. The THERMALLOAD subroutine is called at the DAYCLS-2 SUBR-FUNCTIONS (Figure 4-62) since the system's thermal load has to be calculated before system's operation. The GHXCALC subroutine is called at the RESYS-0, which is one of the six SUBR-FUNCTIONS included in a RESYS system[44] (Figure 4-63), since the RESYS-0 declares the EDB for the first time in the RESYS system loop. The calculated GHX temperatures are replaced with the EDB. Figure 4-64 shows an entire process flowchart of the vertical GHX input FUNCTION to develop a GCHP model implemented in the DOE-2.1e RESYS system.

---

[44] The RESYS system in DOE-2.1e has six SUBR-FUNTIONS: RESYS-0, RESYS-1Z, RESYS-2Z, RESYS-3Z, RESYS-4Z, and RESYS-5.

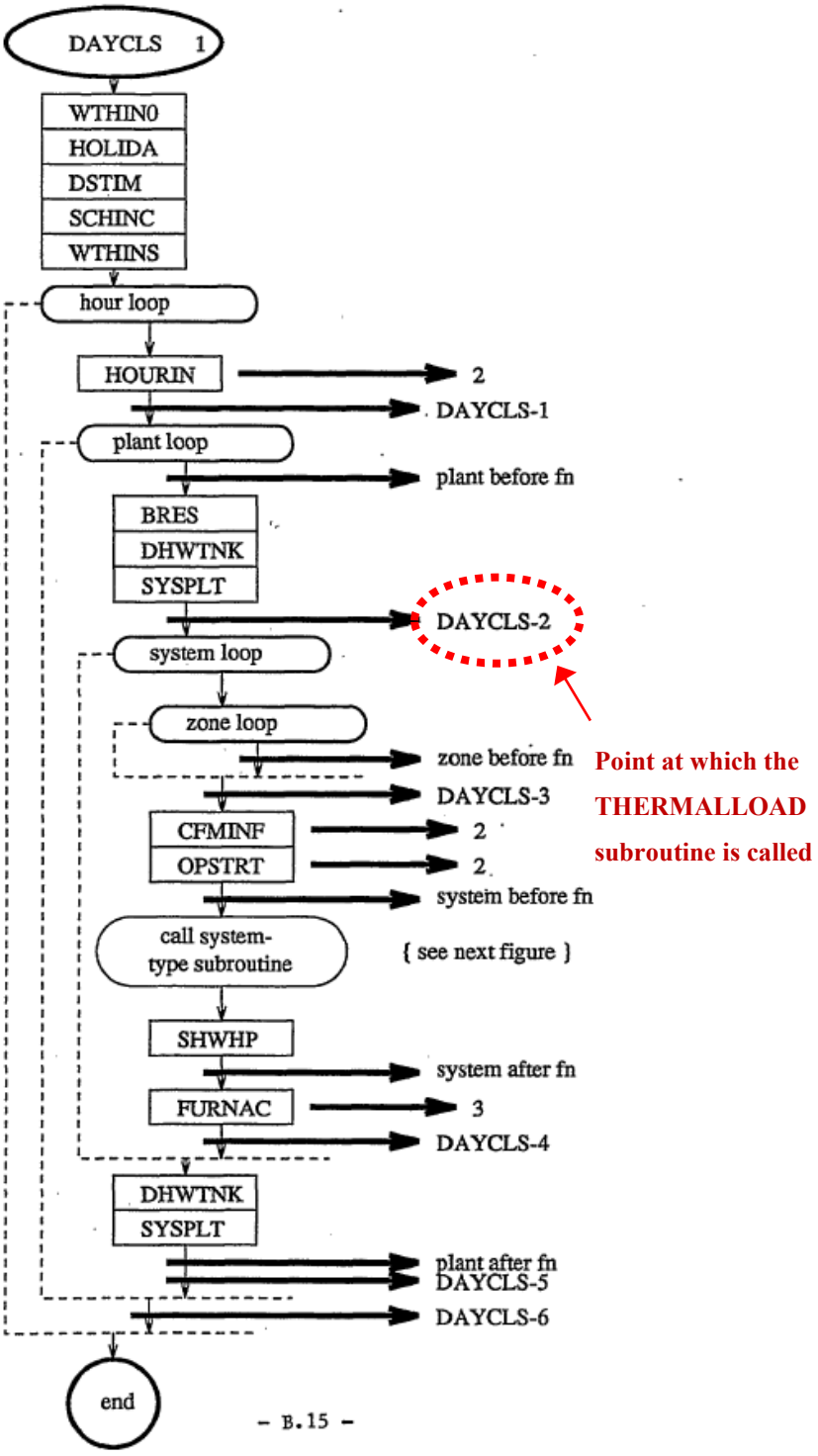

Figure 4-62: Diagram of DOE-2 SYSTEMS Flowchart (LBL, 1993a)

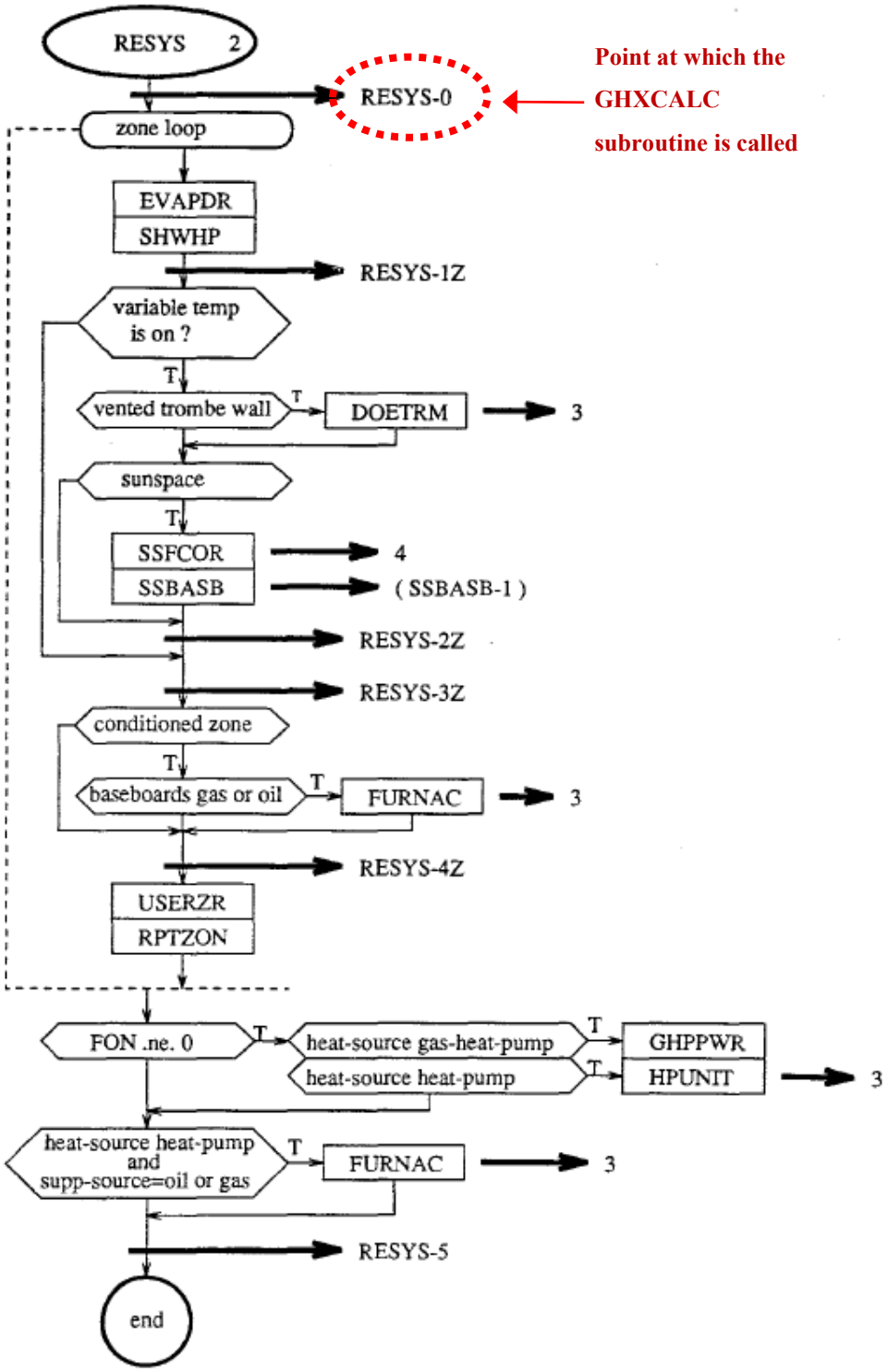

Figure 4-63: Diagram of DOE-2 RESYS Flowchart (LBL, 1993c)

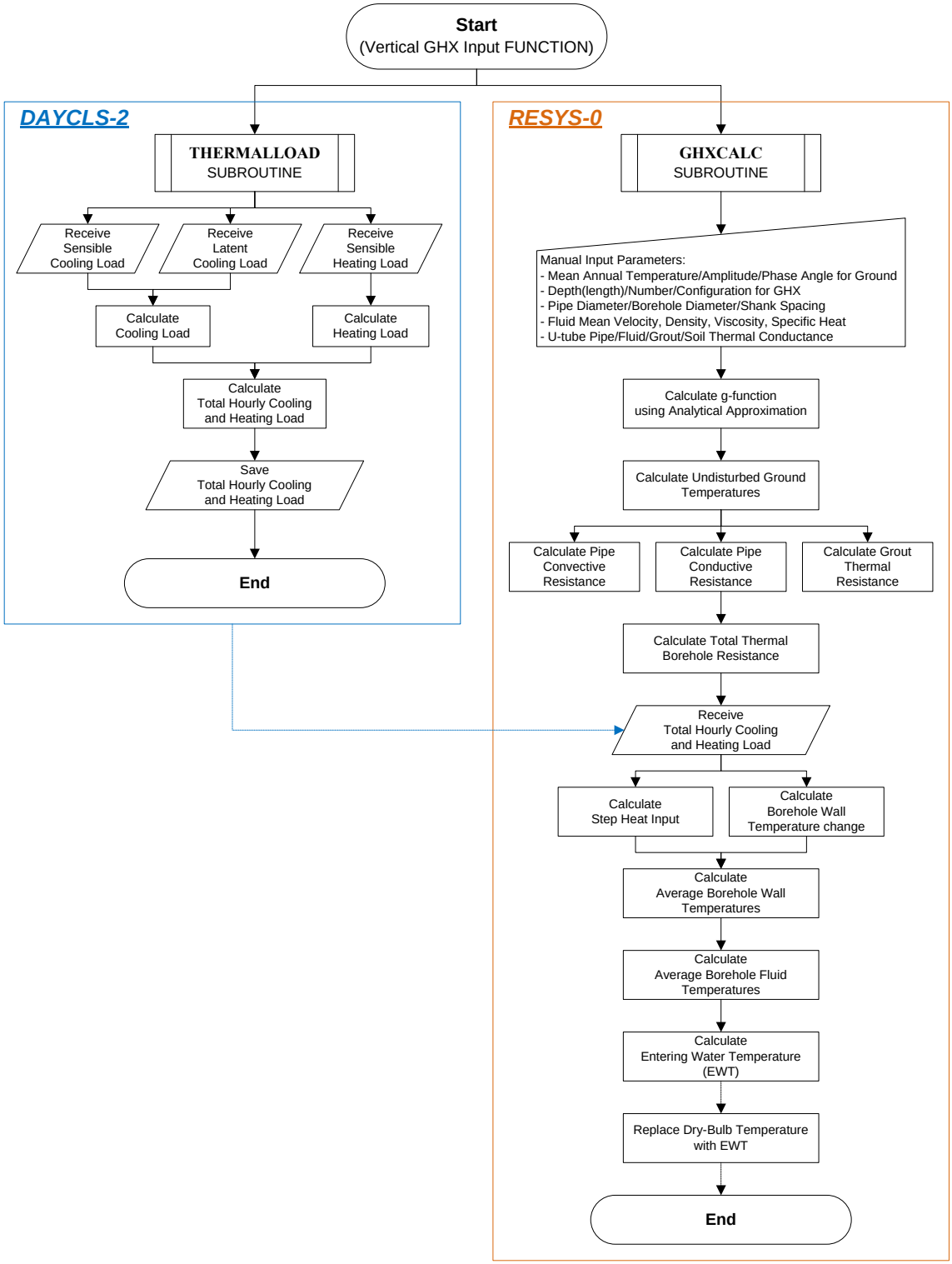

Figure 4-64: Flowchart of Vertical GHX Input FUNCTION in DOE-2.1e

4.4.2.3. Simplified Residential GCHP Base-Case Model

The developed vertical GHX DOE-2.1e input FUNCTION was incorporated within the air-source heat pump (ASHP) simulation module (i.e., RESYS) by modifying the calculation algorithm (i.e., the input file). To accomplish this, the simplified residential ASHP base-case models for Houston and Dallas, which were developed in Section 4.4.1, were used. Then, the DOE-2.1e input file for the ASHP base-case model was modified to become the GCHP system model using a vertical GHX DOE-2.1e model. The vertical GHX model requires various input parameters to define the GHX characteristics. Therefore, this section describes the input parameters used for the developed residential DOE-2.1e GCHP base-case simulation model.

First, it was necessary to define the ground conditions, including: the mean ground temperature, the amplitude of ground temperatures, and the phase angle (i.e., the time shift between the beginning of year and the time of the minimum surface temperature). In general, ground conditions are different for each location. Ground conditions for different cities in Texas are shown in Table 4-14.

Second, this study defined the GHX parameters, including the GHX length/depth, a number of the GHX field, and GHX configuration. To determine the GHX parameters, this study assumed 250 ft of GHX length per ton of air-conditioning, 3 gpm of GHX circulation fluid flow per ton, and 20 ft of borehole spacing which is recommended in the Geothermal Energy Chapter in the ASHRAE Handbook (ASHRAE 2007b). In addition, this study used 3/4 inch GHX pipe (i.e., u-tube) size, which has a 1.05 inch

nominal outer diameter, a 0.859 inch inner diameter, a 3.9 inch U-tube leg separation, and a 6 inch borehole diameter.

Table 4-14: Ground Conditions for Cities in Texas (Bryant, 2013)

	Mean Temperature (F)	Amplitude (F)	Phase Angle (Hours)
Abilene	67.0	21.0	816
Amarillo	62.0	19.9	672
Austin	72.0	16.0	792
Brownsville	73.0	14.0	744
Corpus Christi	72.0	15.7	768
Dallas	68.0	21.0	816
Del Rio	72.0	15.7	768
El Paso	66.0	20.0	672
Houston	71.0	15.7	792
Lubbock	63.0	21.0	816
Midland	66.0	21.0	816
San Antonio	72.0	15.7	768
Waco	69.0	18.0	792
Wichita Falls	65.6	21.0	816

Third, this study defined the thermal properties of the ground, grout, pipe, and the circulation fluid. This study assumed 0.75 Btu/hr-ft-F of the ground thermal conductivity[45] and 0.025 ft^2/hr of diffusivity[46]. The grout[47] was assumed to be a mixture of 20% bentonite and 40% quartzite, which has 0.85 Btu/hr-ft-F of thermal conductivity.

[45] The ground thermal conductivity was assumed based on the Texas thermal conductivity values (O'Neal et al., 1994) and the eQUEST defaults (JJH, 2013).
[46] The ground diffusivity assumed value from the ground-loop heat pump design basics (Niles, 2012) and the eQUEST defaults (JJH, 2013).
[47] The grout thermal conductivity was assumed based on study of geothermal systems design (Kavanaugh and Rafferty, 1997) and the eQUEST defaults (JJH, 2013).

A polyethylene pipe was used for the vertical GHX, which has a thermal conductivity of 0.23 Btu/hr-ft-F. Water is used for the circulation fluid. Table 4-15 shows the GHX input parameters used for the DOE-2.1e GCHP base-case simulation model in this study.

Table 4-15: GHX Input for DOE-2.1e GCHP Base-Case Simulation Model

		Houston	Dallas
Ground			
Mean Temperature	(F)	71.0	68.0
Amplitude	(F)	15.7	21.0
Phase Angle	(Hours)	792	816
Ground Heat Exchanger (GHX)			
GHX Length/Depth	(ft)	250	
Number of GHX		5	
GHX Configuration		Line-Type with 1 x 5	
Number of Field		1	
GHX Pipe Outer Diameter	(ft)	0.087500	
GHX Pipe Inner Diameter	(ft)	0.071667	
Borehole Diameter	(ft)	0.5	
Shank Spacing	(ft)	0.162500	
Borehole Spacing	(ft)	20	
Fluid Flow Rate	(gpm)	15	
Thermal Property			
Diffusivity of Ground	(ft^2/hr)	0.025	
Thermal Conductivity of Ground	(Btu/hr-ft-F)	0.750	
Thermal Conductivity of Grout	(Btu/hr-ft-F)	0.850	
Thermal Conductivity of Pipe	(Btu/hr-ft-F)	0.230	
Thermal Conductivity of Water	(Btu/hr-ft-F)	0.334	
Viscosity of Water	(lb/s-ft)	0.00076	
Density of Water	(lb/ft^3)	62.340	
Specific Heat Capacity of Water	(Btu/lb-F)	1	

4.4.3. Comparative Study of the ASHP and GCHP Base-Case Models

DOE-2.1e base-case models for ASHP and GCHP systems were developed as discussed in Section 4.4.1 and Section 4.4.2. In addition, an eQUEST base-case model for an ASHP system was also developed as discussed in Section 4.4.1. The DOE-2.1e ASHP base-case model and the eQUEST ASHP base-case model were compared against several code-compliance simulation programs including: IC3, REM/Rate, and EnergyGauge. The DOE-2.1e GCHP base-case model was also compared against eQUEST, REM/Rate, and EnergyGauge. However, the IC3 program was excluded since the IC3 program did not have the capability to simulation a GCHP system.

Table 4-16 and Table 4-17 summarize the inputs for the ASHP base-case simulation models, using IC3, DOE-2.1e, REM/Rate, EnergyGauge, and eQUEST, for Houston and Dallas, TX, respectively. In addition, Table 4-18 and Table 4-19 summarize the inputs for the GCHP base-case simulation models, using DOE-2.1e, REM/Rate, EnergyGauge, and eQUEST, for Houston and Dallas, TX, respectively. In general, it was observed that the four different programs used for the GCHP system comparison required significantly different inputs. For example, REM/Rate requires simplified inputs for the GCHP system including the GHX well type (i.e., vertical or horizontal), number of wells, well depth, and loop flow. However, REM/Rate does not require inputs such as GHX configuration, GHX pipe, shank/borehole spacing, and thermal properties. In a similar fashion, EnergyGauge requires limited inputs for rated GCHP heating and cooling efficiencies. On the other hand, eQUEST requires detailed inputs for ground, GHX, and thermal properties.

Table 4-16: ASHP Base-Case Input for Houston in Different Software

Input/Default (Houston)		IC3	DOE-2.1e (RUN_30)	REM / Rate	EnergyGauge	eQUEST (RUN_30)
PROJECT						
# of Bedrooms		4				
# of People		0	0	-	0	0
# of Stories		1				
Building Azumith		South	South	-	South	South
Conditioned Area	(sqft)	2,500				
Average Wall Height	(ft)	8				
Conditioned Volume	(cuft)	20,000				
Housing type		Single Family Detached				
CLIMATE						
Location		Houston				
Weather File		TMY2	TMY2	Combination of TMY2 & TMY3	TMY2	TMY2
FLOORS						
Type		Slab-on-grade				
R-value	(hr-sqft-F/Btu)	R-0				
Floor Covering		20% Tile, 80% Carpet	20% Tile, 80% Carpet	100% Carpet	20% Tile, 80% Carpet	20% Tile, 80% Carpet
Area	(sqft)	2,500				
Full Perimeter	(ft)	200				
Depth below Grade	(ft)	0				
Total Exposed Perimeter	(ft)	200				
On-Grade Exposed Perimeter	(ft)	200				
ROOF						
Roofing Material		Composition Shingle				
Roof Emissivity		0.9	0.9	-	White	0.9
Absorptance		0.75	0.75	0.75 (Medium Color)	0.75	0.75
Radiant Barrier		No				
Roof Insulation	(hr-sqft-F/Btu)	R-0				
Slope	(Degrees)	0				
Clay or Concrete Roofing		-	-	No	-	-
Sub-Tile Ventilation		-	-	No	-	-
CEILING						
Type		Cathedral	-	-	Cathedral	-
R-value[1]	(hr-sqft-F/Btu)	R-27.8	R-27.8	R-28.0	R-25.7	R-27.8
Equivalent U-value	(Btu/hr-sqft-F)	U-0.035				
Framing Factor		0.07				
Area	(sqft)	2,500				
WALLS						
Insulation[1]	(hr-sqft-F/Btu)	R-11.8	R-11.8	R-12.1	R-14.6	R-11.8
Equivalent U-value	(Btu/hr-sqft-F)	0.082				
Framing Factor		0.25				
Sheathing R-value	(hr-sqft-F/Btu)	0	-	-	R-0	-
Absorptance		0.75	0.75	0.75 (Medium Color)	0.75	0.75
(Width x Height) x Number	(sqft)	(50 x 8) x 4				
Exterior Finish		Brick	Brick	Brick	Wood	Brick
Location		Between Conditioned Space and Ambient				
DOORS						
Orientation		North, South	North	North	North	North
Area for each	(sqft)	20	40	40	40	40
R-value	(hr-sqft-F/Btu)	-	1.54	1.54	-	1.54
Equivalent U-value	(Btu/hr-sqft-F)	0.65				
Storm Door		No				
WINDOWS & SHADING						
U-value	(Btu/hr-sqft-F)	0.65				
SHGC		0.3				
No. of Panes		1	1	-	1	1
Frame Type		Aluminum	Aluminum	-	Metal	Aluminum
Frame Conductance	(Btu/hr-sqft-F)	3.037	3.037	-	-	3.037
Window Area	(sqft)	93.75 x 4				
Orientation		East, West, South, & North				
Overhang		None				
Interior Shade Winter		0.85				
Interior Shade Summer		0.7				
Adjacent Shading		None				

Table 4-16: Continued

Input/Default (Houston)		IC3	DOE-2.1e (RUN_30)	REM / Rate	EnergyGauge	eQUEST (RUN_30)
INFILTRATION						
Measurement Type		Blower Door	-	Blower Door	-	-
Specific Leakage Area		0.0004321				
Shielding Coefficient		0.24	0.24	0.24 (Shelter Class 3)	Suburban	0.24
2009 IECC Verification		-	-	Tested	-	-
Mechanical Ventilation		No				
COOLING						
Type		Electric	Electric	Electric	Central Unit	Electric
System Type		ASHP				
SHR (SV-A)		0.652				
Efficiency		SEER 13				
Capacity	(kBtu/hr)	60				
Location		Conditioned Space				
Supply CFM	(CFM/ ton)	360	360	-	360	360
HEATING						
Fuel Type		Electric				
Heating Type		ASHP				
Efficiency		7.7 HSPF				
Capacity	(kBtu/hr)	60				
Location		Conditioned Space				
Auxiliary Energy Source		Electric				
Auxiliary Energy Use	(kWh)	-	-	Default	-	-
DUCTS						
Supply R-value	(hr-sqft-F/Btu)	8	-	8	8	-
Return R-value	(hr-sqft-F/Btu)	6	-	6	8	-
Supply Duct Area	(sqft)	675	-	675	675	-
Return Duct Area	(sqft)	125	-	125	125	-
# Return		1	-	1	1	-
Duct Location		Conditioned Space				
Use Measured Leakage		-	-	Yes (CFM@25Pa)		-
Leakage to Outside		-	-	0	-	-
Total Duct Leakage		-	-	0	0	-
HOT WATER						
Type		Electric				
Rated Input	(Btu/hr)	18,766	18,766	-	-	18,766
Capacity	(Gallons)	50				
Water Usage	(Gallons/Day)	70				
Energy Factor[2]		1	1	0.98	0.87	1
Temperature Settings	(F)	120	120	-	120	120
THERMOSTAT SETTING						
Cooling	(F)	75				
Heating	(F)	72				
APPLIANCES & LIGHTS						
Schedule		Constant				
Lighting	(kW)	0.49				
Equipment	(kW)	0.66				

Notes:

1. Different R-values in REM/Rate and EnergyGauge are used to match the equvalent U-value of IC3.

2. Different Energy Factors in REM/Rate and EnergyGauge are used to match the annual hot water consumption in IC3.

Table 4-17: ASHP Base-Case Input for Dallas in Different Software

Input/Default (Dallas)		IC3	DOE-2.1e	REM / Rate	EnergyGauge	eQUEST
PROJECT						
# of Bedrooms		4				
# of People		0	0	-	0	0
# of Stories		1				
Building Azumith		South	South	-	South	South
Conditioned Area	(sqft)	2,500				
Average Wall Height	(ft)	8				
Conditioned Volume	(cuft)	20,000				
Housing type		Single Family Detached				
CLIMATE						
Location		Dallas (DFW)				
Weather File		TMY2	TMY2	Combination of TMY2 & TMY3	TMY2	TMY2
FLOORS						
Type		Slab-on-grade				
R-value	(hr-sqft-F/Btu)	R-0				
Floor Covering		20% Tile, 80% Carpet	20% Tile, 80% Carpet	100% Carpet	20% Tile, 80% Carpet	20% Tile, 80% Carpet
Area	(sqft)	2,500				
Full Perimeter	(ft)	200				
Depth below Grade	(ft)	0				
Total Exposed Perimeter	(ft)	200				
On-Grade Exposed Perimeter	(ft)	200				
ROOF						
Roofing Material		Composition Shingle				
Roof Emissivity		0.9	0.9	-	White	0.9
Absorptance		0.75	0.75	0.75 (Medium Color)	0.75	0.75
Radiant Barrier		No				
Roof Insulation	(hr-sqft-F/Btu)	R-0				
Slope	(Degrees)	0				
Clay or Concrete Roofing		-	-	No	-	-
Sub-Tile Ventilation		-	-	No	-	-
CEILING						
Type		Cathedral	-	-	Cathedral	-
R-value	(hr-sqft-F/Btu)	R-27.8	R-27.8	R-28.0	R-25.7	R-27.8
Equivalent U-value	(Btu/hr-sqft-F)	U-0.035				
Framing Factor		0.07				
Area	(sqft)	2,500				
WALLS						
Insulation	(hr-sqft-F/Btu)	R-11.8	R-11.8	R-12.1	R-14.6	R-11.8
Equivalent U-value	(Btu/hr-sqft-F)	0.082				
Framing Factor		0.25				
Sheathing R-value	(hr-sqft-F/Btu)	0	-	-	R-0	-
Absorptance		0.75	0.75	0.75 (Medium Color)	0.75	0.75
(Width x Height) x Number	(sqft)	(50 x 8) x 4				
Exterior Finish		Brick	Brick	Brick	Wood	Brick
Location		Between Conditioned Space and Ambient				
DOORS						
Orientation		North, South	North	North	North	North
Area for each	(sqft)	20	40	40	40	40
R-value	(hr-sqft-F/Btu)	-	2.0	2.0	-	2.0
Equivalent U-value	(Btu/hr-sqft-F)	0.5				
Storm Door		No				
WINDOWS & SHADING						
U-value	(Btu/hr-sqft-F)	0.5				
SHGC		0.3				
No. of Panes		1	1	-	1	1
Frame Type		Aluminum	Aluminum	-	Metal	Aluminum
Frame Conductance	(Btu/hr-sqft-F)	3.037	3.037	-	-	3.037
Window Area	(sqft)	93.75 x 4				
Orientation		East, West, South, & North				
Overhang		None				
Interior Shade Winter		0.85				
Interior Shade Summer		0.7				
Adjacent Shading		None				

Table 4-17: Continued

Input/Default (Dallas)		IC3	DOE-2.1e	REM / Rate	EnergyGauge	eQUEST
INFILTRATION						
Measurement Type		Blower Door	-	Blower Door	-	-
Specific Leakage Area		0.0004321				
Shielding Coefficient		0.24	0.24	0.24 (Shelter Class 3)	Suburban	0.24
2009 IECC Verification		-	-	Tested	-	-
Mechanical Ventilation		No				
COOLING						
Type		Electric	Electric	Electric	Central Unit	Electric
System Type		ASHP				
SHR (SV-A)		0.678				
Efficiency		SEER 13				
Capacity	(kBtu/hr)	60				
Location		Conditioned Space				
Supply CFM	(CFM/ ton)	360	360	-	360	360
HEATING						
Fuel Type		Electric				
Heating Type		ASHP				
Efficiency		7.7 HSPF				
Capacity	(kBtu/hr)	60				
Location		Conditioned Space				
Auxiliary Energy Source		Electric				
Auxiliary Energy Use	(kWh)	-	-	Default	-	-
DUCTS						
Supply R-value	(hr-sqft-F/Btu)	8	-	8	8	-
Return R-value	(hr-sqft-F/Btu)	6	-	6	8	-
Supply Duct Area	(sqft)	675	-	675	675	-
Return Duct Area	(sqft)	125	-	125	125	-
# Return		1	-	1	1	-
Duct Location		Conditioned Space				
Use Measured Leakage		-	-	Yes (CFM@25Pa)		-
Leakage to Outside		-	-	0	-	-
Total Duct Leakage		-	-	0	0	-
HOT WATER						
Type		Electric				
Rated Input	(Btu/hr)	18,766	18,766	-	-	18,766
Capacity	(Gallons)	50				
Water Usage	(Gallons/Day)	70				
Energy Factor[2]		1	1	0.98	0.87	1
Temperature Settings	(F)	120	120	-	120	120
THERMOSTAT SETTING						
Cooling	(F)	75				
Heating	(F)	72				
APPLIANCES & LIGHTS						
Schedule		Constant				
Lighting	(kW)	0.49				
Equipment	(kW)	0.66				

Notes:

1. Different R-values in REM/Rate and EnergyGauge are used to match the equvalent U-value of IC3.

2. Different Energy Factors in REM/Rate and EnergyGauge are used to match the annual hot water consumption in IC3.

Table 4-18: GCHP Base-Case Input for Houston in Different Software

Input/Default (Houston)		DOE-2.1e	REM / Rate	EnergyGauge	eQUEST
PROJECT					
# of Bedrooms		4			
# of People		0	-	0	0
# of Stories		1			
Building Azumith		South	-	South	South
Conditioned Area	(sqft)	2,500			
Average Wall Height	(ft)	8			
Conditioned Volume	(cuft)	20,000			
Housing type		Single Family Detached			
CLIMATE					
Location		Houston			
Weather File		TMY2	Combination of TMY2 & TMY3	TMY2	TMY2
FLOORS					
Type		Slab-on-grade			
R-value	(hr-sqft-F/Btu)	R-0			
Floor Covering		20% Tile, 80% Carpet	100% Carpet	20% Tile, 80% Carpet	20% Tile, 80% Carpet
Area	(sqft)	2,500			
Full Perimeter	(ft)	200			
Depth below Grade	(ft)	0			
Total Exposed Perimeter	(ft)	200			
On-Grade Exposed Perimeter	(ft)	200			
ROOF					
Roofing Material		Composition Shingle			
Roof Emissivity		0.9	-	White	0.9
Absorptance		0.75	0.75 (Medium Color)	0.75	0.75
Radiant Barrier		No			
Roof Insulation	(hr-sqft-F/Btu)	R-0			
Slope	(Degrees)	0			
Clay or Concrete Roofing		-	No	-	-
Sub-Tile Ventilation		-	No	-	-
CEILING					
Type		-	-	Cathedral	-
R-value	(hr-sqft-F/Btu)	R-27.8	R-28.0	R-25.7	R-27.8
Equivalent U-value	(Btu/hr-sqft-F)	U-0.035			
Framing Factor		0.07			
Area	(sqft)	2,500			
WALLS					
Insulation	(hr-sqft-F/Btu)	R-11.8	R-12.1	R-14.6	R-11.8
Equivalent U-value	(Btu/hr-sqft-F)	0.082			
Framing Factor		0.25			
Sheathing R-value	(hr-sqft-F/Btu)	-	-	R-0	-
Absorptance		0.75	0.75 (Medium Color)	0.75	0.75
(Width x Height) x Number	(sqft)	(50 x 8) x 4			
Exterior Finish		Brick	Brick	Wood	Brick
Location		Between Conditioned Space and Ambient			
DOORS					
Orientation		North	North	North	North
Area for each	(sqft)	40	40	40	40
R-value	(hr-sqft-F/Btu)	1.54	1.54	-	1.54
Equivalent U-value	(Btu/hr-sqft-F)	0.65			
Storm Door		No			
WINDOWS & SHADING					
U-value	(Btu/hr-sqft-F)	0.65			
SHGC		0.3			
No. of Panes		1	-	1	1
Frame Type		Aluminum	-	Metal	Aluminum
Frame Conductance	(Btu/hr-sqft-F)	3.037	-	-	3.037
Window Area	(sqft)	93.75 x 4			
Orientation		East, West, South, & North			
Overhang		None			
Interior Shade Winter		0.85			
Interior Shade Summer		0.7			
Adjacent Shading		None			

Table 4-18: Continued

Input/Default (Houston)		DOE-2.1e	REM / Rate	EnergyGauge	eQUEST
INFILTRATION					
Measurement Type		-	Blower Door	-	-
Specific Leakage Area		0.0004321			
Shielding Coefficient		0.24	0.24 (Shelter Class 3)	Suburban	0.24
2009 IECC Verification		-	Tested	-	-
Mechanical Ventilation		No			
COOLING					
Type		Electric	Electric	Central Unit	Electric
System Type		GCHP w/ vertical GHX			
SHR (SV-A)		0.722			
Efficiency		EER 13.4 for 2009 IECC Requirements / EER 14.1 for ORNL Recommendation			
Capacity	(kBtu/hr)	60			
Location		Conditioned Space			
Supply CFM	(CFM/ ton)	360	-	360	360
HEATING					
Fuel Type		Electric			
Heating Type		GCHP w/ vertical GHX			
Efficiency		3.1 COP for 2009 IECC Requirements / 3.3 COP for ORNL Recommendation			
Capacity	(kBtu/hr)	60			
Location		Conditioned Space			
Auxiliary Energy Source		Electric			
Auxiliary Energy Use	(kWh)	-	Default	-	-
Ground Heat Exchanger					
GHX Type		Vertical	Vertical	-	Vertical
GHX Length/Depth	(ft)	250	250	-	250
Number of GHX		5	5	-	5
GHX Configuration		Line-Type (1 x 5)	-	-	Line-Type (1 x 5)
Number of Field		1	-	-	1
GHX Pipe Outer Diameter	(ft)	0.0875	-	-	0.0875
GHX Pipe Inner Diameter	(ft)	0.071667	-	-	0.071667
Borehole Diameter	(ft)	0.5	-	-	0.5
Shank Spacing	(ft)	0.1625	-	-	0.1625
Borehole Spacing	(ft)	20	-	-	20
Fluid Flow Rate	(gpm)	15	15	-	15
Ground		Amphibolite	-	-	Amphibolite
Grout		20% Bentonite/40% Quartzite	-	-	20% Bentonite/40% Quartzite
Pipe		Polyethylene	-	-	Polyethylene
Circulation Fluid		Water	-	-	Water
DUCTS					
Supply R-value	(hr-sqft-F/Btu)	-	8	8	-
Return R-value	(hr-sqft-F/Btu)	-	6	8	-
Supply Duct Area	(sqft)	-	675	675	-
Return Duct Area	(sqft)	-	125	125	-
# Return		-	1	1	-
Duct Location		Conditioned Space			
Use Measured Leakage		-	Yes (CFM@25Pa)		-
Leakage to Outside		-	0	-	-
Total Duct Leakage		-	0	0	-
HOT WATER					
Type		Electric			
Rated Input	(Btu/hr)	18,766	-	-	18,766
Capacity	(Gallons)	50			
Water Usage	(Gallons/Day)	70			
Energy Factor[2]		1	0.98	0.87	1
Temperature Settings	(F)	120	-	120	120
THERMOSTAT SETTING					
Cooling	(F)	75			
Heating	(F)	72			
APPLIANCES & LIGHTS					
Schedule		Constant			
Lighting	(kW)	0.49			
Equipment	(kW)	0.66			

Notes:

1. Different R-values in REM/Rate and EnergyGauge are used to match the equvalent U-value of IC3.

2. Different Energy Factors in REM/Rate and EnergyGauge are used to match the annual hot water consumption in IC3.

Table 4-19: GCHP Base-Case Input for Dallas in Different Software

Input/Default (Dallas)		DOE-2.1e	REM / Rate	EnergyGauge	eQUEST
PROJECT					
# of Bedrooms		4			
# of People		0	-	0	0
# of Stories		1			
Building Azumith		South	-	South	South
Conditioned Area	(sqft)	2,500			
Average Wall Height	(ft)	8			
Conditioned Volume	(cuft)	20,000			
Housing type		Single Family Detached			
CLIMATE					
Location		Dallas (DFW)			
Weather File		TMY2	Combination of TMY2 & TMY3	TMY2	TMY2
FLOORS					
Type		Slab-on-grade			
R-value	(hr-sqft-F/Btu)	R-0			
Floor Covering		20% Tile, 80% Carpet	100% Carpet	20% Tile, 80% Carpet	20% Tile, 80% Carpet
Area	(sqft)	2,500			
Full Perimeter	(ft)	200			
Depth below Grade	(ft)	0			
Total Exposed Perimeter	(ft)	200			
On-Grade Exposed Perimeter	(ft)	200			
ROOF					
Roofing Material		Composition Shingle			
Roof Emissivity		0.9	-	White	0.9
Absorptance		0.75	0.75 (Medium Color)	0.75	0.75
Radiant Barrier		No			
Roof Insulation	(hr-sqft-F/Btu)	R-0			
Slope	(Degrees)	0			
Clay or Concrete Roofing		-	No	-	-
Sub-Tile Ventilation		-	No	-	-
CEILING					
Type		-	-	Cathedral	-
R-value	(hr-sqft-F/Btu)	R-27.8	R-28.0	R-25.7	R-27.8
Equivalent U-value	(Btu/hr-sqft-F)	U-0.035			
Framing Factor		0.07			
Area	(sqft)	2,500			
WALLS					
Insulation	(hr-sqft-F/Btu)	R-11.8	R-12.1	R-14.6	R-11.8
Equivalent U-value	(Btu/hr-sqft-F)	0.082			
Framing Factor		0.25			
Sheathing R-value	(hr-sqft-F/Btu)	-	-	R-0	-
Absorptance		0.75	0.75 (Medium Color)	0.75	0.75
(Width x Height) x Number	(sqft)	(50 x 8) x 4			
Exterior Finish		Brick	Brick	Wood	Brick
Location		Between Conditioned Space and Ambient			
DOORS					
Orientation		North	North	North	North
Area for each	(sqft)	40	40	40	40
R-value	(hr-sqft-F/Btu)	2.0	2.0	-	2.0
Equivalent U-value	(Btu/hr-sqft-F)	0.5			
Storm Door		No			
WINDOWS & SHADING					
U-value	(Btu/hr-sqft-F)	0.5			
SHGC		0.3			
No. of Panes		1	-	1	1
Frame Type		Aluminum	-	Metal	Aluminum
Frame Conductance	(Btu/hr-sqft-F)	3.037	-	-	3.037
Window Area	(sqft)	93.75 x 4			
Orientation		East, West, South, & North			
Overhang		None			
Interior Shade Winter		0.85			
Interior Shade Summer		0.7			
Adjacent Shading		None			

Table 4-19: Continued

Input/Default (Dallas)		DOE-2.1e	REM / Rate	EnergyGauge	eQUEST
INFILTRATION					
Measurement Type		-	Blower Door	-	-
Specific Leakage Area		0.0004321			
Shielding Coefficient		0.24	0.24 (Shelter Class 3)	Suburban	0.24
2009 IECC Verification		-	Tested	-	-
Mechanical Ventilation		No			
COOLING					
Type		Electric	Electric	Central Unit	Electric
System Type		GCHP w/ vertical GHX			
SHR (SV-A)		0.759			
Efficiency		EER 13.4 for 2009 IECC Requirements / EER 14.1 for ORNL Recommendation			
Capacity	(kBtu/hr)	60			
Location		Conditioned Space			
Supply CFM	(CFM/ ton)	360	-	360	360
HEATING					
Fuel Type		Electric			
Heating Type		GCHP w/ vertical GHX			
Efficiency		3.1 COP for 2009 IECC Requirements / 3.3 COP for ORNL Recommendation			
Capacity	(kBtu/hr)	60			
Location		Conditioned Space			
Auxiliary Energy Source		Electric			
Auxiliary Energy Use	(kWh)	-	Default	-	-
Ground Heat Exchanger					
GHX Type		Vertical	Vertical	-	Vertical
GHX Length/Depth	(ft)	250	250	-	250
Number of GHX		5	5	-	5
GHX Configuration		Line-Type (1 x 5)	-	-	Line-Type (1 x 5)
Number of Field		1	-	-	1
GHX Pipe Outer Diameter	(ft)	0.0875	-	-	0.0875
GHX Pipe Inner Diameter	(ft)	0.071667	-	-	0.071667
Borehole Diameter	(ft)	0.5	-	-	0.5
Shank Spacing	(ft)	0.1625	-	-	0.1625
Borehole Spacing	(ft)	20	-	-	20
Fluid Flow Rate	(gpm)	15	15	-	15
Ground		Amphibolite	-	-	Amphibolite
Grout		20% Bentonite/40% Quartzite	-	-	20% Bentonite/40% Quartzite
Pipe		Polyethylene	-	-	Polyethylene
Circulation Fluid		Water	-	-	Water
DUCTS					
Supply R-value	(hr-sqft-F/Btu)	-	8	8	-
Return R-value	(hr-sqft-F/Btu)	-	6	8	-
Supply Duct Area	(sqft)	-	675	675	-
Return Duct Area	(sqft)	-	125	125	-
# Return		-	1	1	-
Duct Location		Conditioned Space			
Use Measured Leakage		-	Yes (CFM@25Pa)		-
Leakage to Outside		-	0	-	-
Total Duct Leakage		-	0	0	-
HOT WATER					
Type		Electric			
Rated Input	(Btu/hr)	18,766	-	-	18,766
Capacity	(Gallons)	50			
Water Usage	(Gallons/Day)	70			
Energy Factor[2]		1	0.98	0.87	1
Temperature Settings	(F)	120	-	120	120
THERMOSTAT SETTING					
Cooling	(F)	75			
Heating	(F)	72			
APPLIANCES & LIGHTS					
Schedule		Constant			
Lighting	(kW)	0.49			
Equipment	(kW)	0.66			

Notes:

1. Different R-values in REM/Rate and EnergyGauge are used to match the equvalent U-value of IC3.

2. Different Energy Factors in REM/Rate and EnergyGauge are used to match the annual hot water consumption in IC3.

CHAPTER V

RESULTS: GROUND HEAT EXCHANGER MODELS

Ground heat exchanger (GHX) models (i.e. a horizontal GHX, surface water GHX, and vertical GHX,) are used to calculate the entering water temperatures (EWTs) from the GHX to the heat pump system. This study analyzed several closed-loop GHX models including: a horizontal GHX, a surface water GHX, and a vertical GHX.

The custom-built GHX model was developed for the case-study house, using the horizontal and surface water GHX model. Then, the EWTs calculated from custom-built GHX model were compared with the measured EWTs from the case-study house. The vertical GHX model was developed to be implemented in the DOE-2.1e program so that the ground-coupled heat pump (GCHP) system is used in the DOE-2.1 program. The results of the GCHP model with the vertical GHX were then compared against the GCHP simulation results using other programs (i.e., eQUEST, EnergyGauge, and REM/Rate), which have the feature of the vertical GHX calculation.

This chapter presents the results of this study, including: Section 5.1 gives analysis of the measured data from the ESL's Solar Test Bench and the case-study house, and comparison between the measured EWTs and calculated EWTs using the custom-built GHX model; and Section 5.2 presents analysis of the residential base-case models comparing an air-source heat pump (ASHP) system and GCHP system using the vertical GHX.

5.1. Custom-Built Ground Heat Exchanger Model

The custom-built ground heat exchanger (GHX) model, using the horizontal and surface water (i.e., pond) GHX models, was used to determine the entering water temperatures (EWTs) from the custom-built GHX to the heat pump at the case-study house. The observations showed the EWTs had an effect on the heat transfer between the GHX and the surrounding heat source/sink. Based on the calculation methodologies described in Sections 4.2.1, 4.2.2, and 4.3.5, the EWT was predicted for each hour and compared to the measured data. This chapter presents the calculated results of the custom-built GHX model using the measured data from the Energy Systems Laboratory's Solar Test Bench (STB), and compared them against the measured data from the case-study house.

5.1.1. Measured Data from the Solar Test Bench and the Case-Study House

The sensors installed at the ESL's STB to measure the weather data include outdoor temperature and relative humidity, wind speed and direction, global/normal incidence/diffuse solar radiation, which were described in Sections 0 and 4.3.4.

5.1.1.1. Measured Data from the ESL's Solar Test Bench

The ESL's STB weather data were collected from the middle of December 2012 to the end of July 2013, which corresponds to the period when the case-study house temperature measurements were taken. The STB weather data were collected at one-minute intervals, and averaged to one-hour intervals for the analysis. The hourly

averaged data were then used to predict the hourly pond water temperatures, using calculations for the absorbed solar radiation, pond thermal radiation, convection of the pond surface, heat transfer to/from the ground, and evaporation of the pond surface, which are described in the Section 4.2.2.1.

Figure 5-1 through Figure 5-5 show the plots of the hourly and daily average STB weather data from the middle of December, 2012 to the end of July 2013.

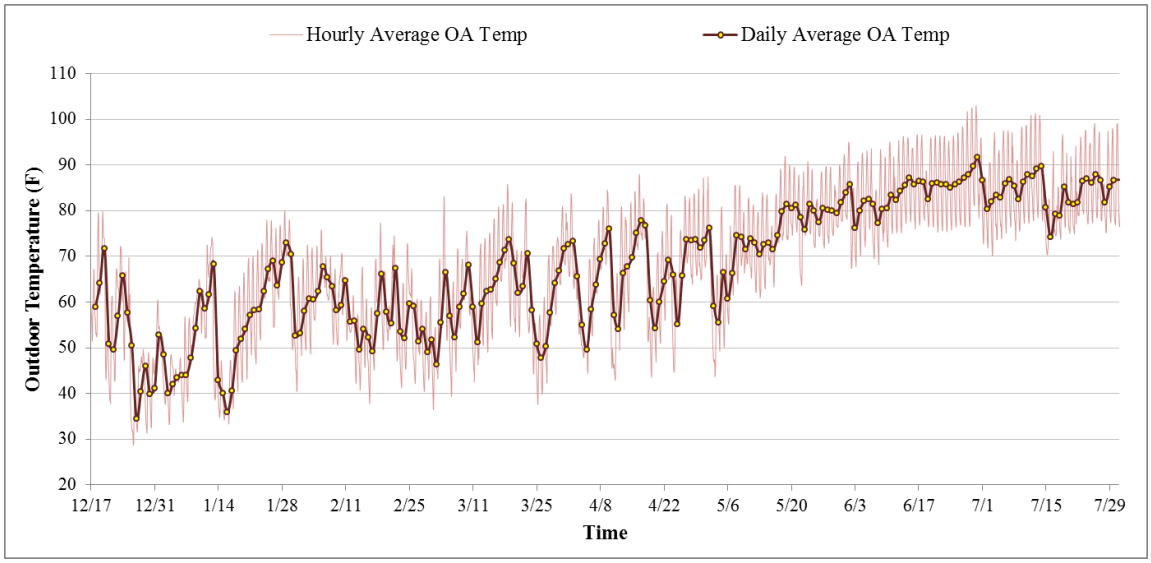

Figure 5-1: Hourly and Daily Average Outdoor Air Temperature (from the middle of December, 2012 to the end of July 2013)

Figure 5-1 shows the hourly and daily average Outdoor Air (OA) temperatures. The lowest daily average OA temperature was 34.5 F on 25th of December, 2012. The highest daily average OA temperature was 91.6 F on 30th of June, 2013. The coldest period of the year was observed from the end of the December to the middle of January. During February and March, the OA daily average temperatures stayed around 60 F. The

OA daily average temperatures had rapid temperature fluctuation (e.g., more than 20 F of daily average temperature change in one week) during March and April. Then, the OA daily average temperatures steadily increased from May, reaching an 87 F daily average temperature in the middle of June.

Figure 5-2 shows the hourly and daily average Relative Humidity (RH). The highest daily average RH was 94.9 % on 10th of January, 2013 and the lowest daily average RH was 22.9 % on the 22nd of December, 2012.

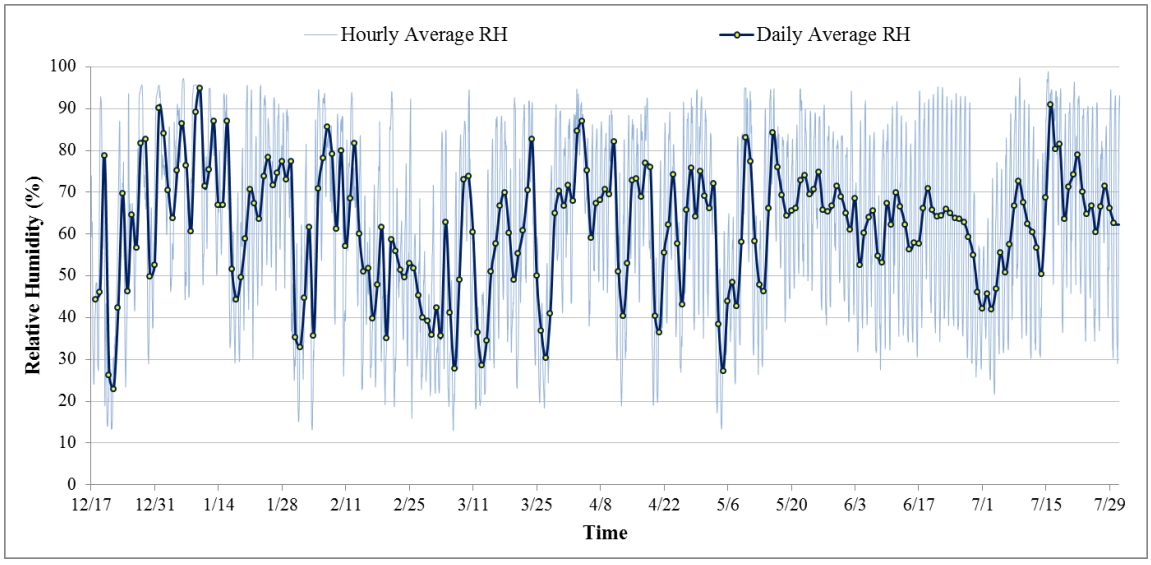

Figure 5-2: Hourly and Daily Average Relative Humidity (from the middle of December, 2012 to the end of July 2013)

Figure 5-3 shows the hourly and daily average wind speed. The highest daily average wind speed was 12.2 mph on 25th of March, 2013 and the highest hourly average wind speed was 20.1 mph on 25th of December, 2012. The daily average wind speed from the measured data was 5.6 mph for the observation period.

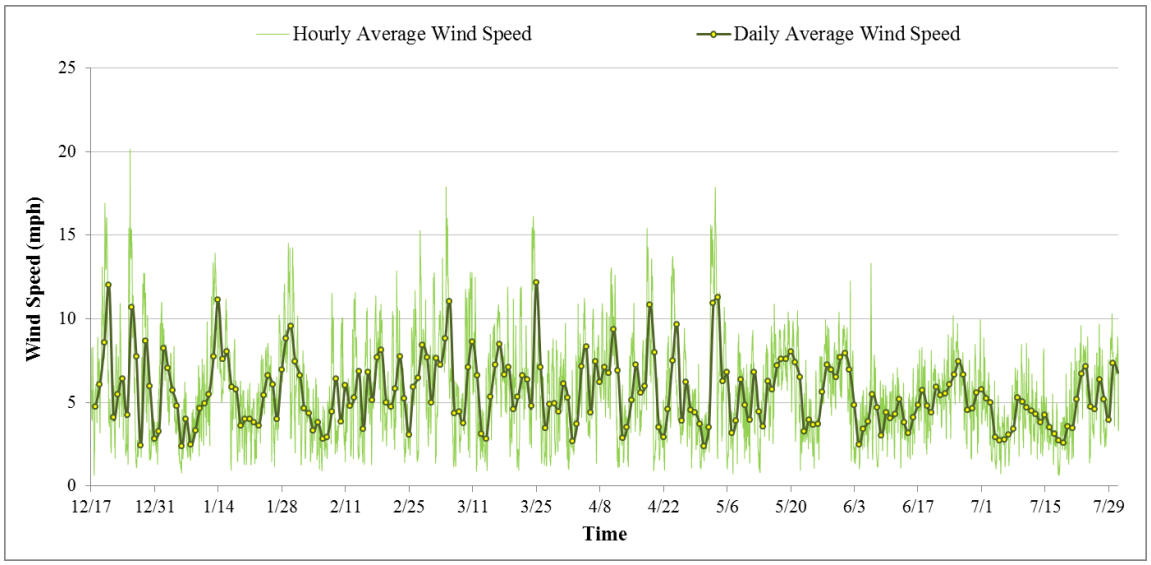

Figure 5-3: Hourly and Daily Average Wind Speed (from the middle of December, 2012 to the end of July 2013)

Solar radiation is an important component to predict the pond water temperature. Figure 5-4 and Figure 5-5 showed measured global and diffuse solar radiation on a horizontal surface during the monitoring period, including: global and diffuse radiation, respectively. Both of the global and diffuse solar radiation values had a trend, which was lower in the winter season, increased with large fluctuation in the spring season, then changed to higher and constant values in the summer season. In addition, Figure 5-6 shows the measurement results of the direct normal incidence solar radiation using the solar tracker which tracks the sun to allow the measurement of beam solar radiation. However, the measured beam solar radiation values were not used for the GHX model.

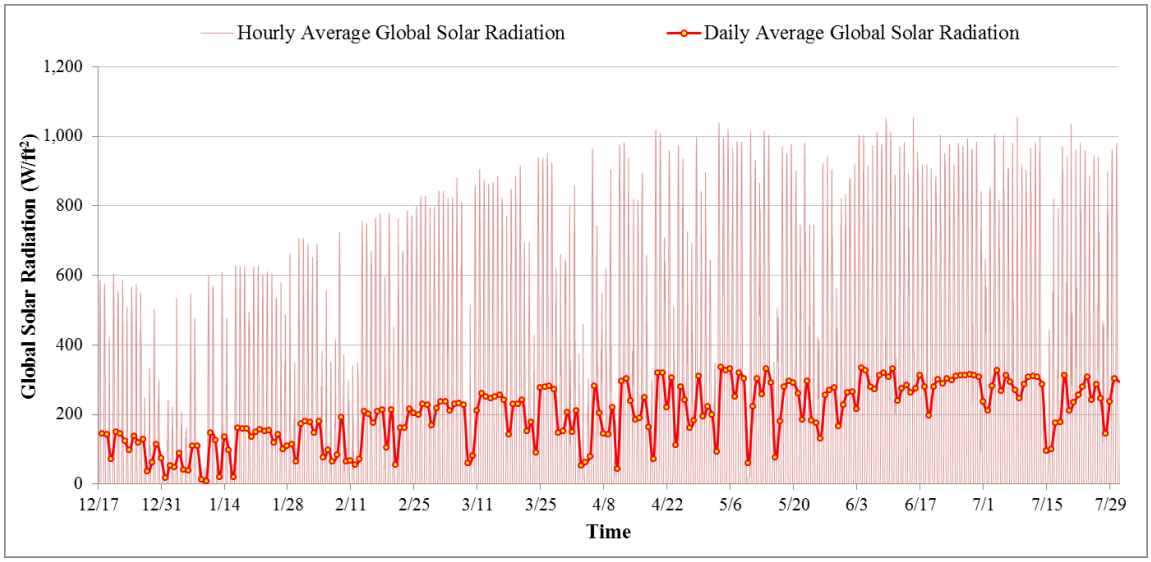

Figure 5-4: Hourly and Daily Average Global Solar Radiation (from the middle of December, 2012 to the end of July 2013)

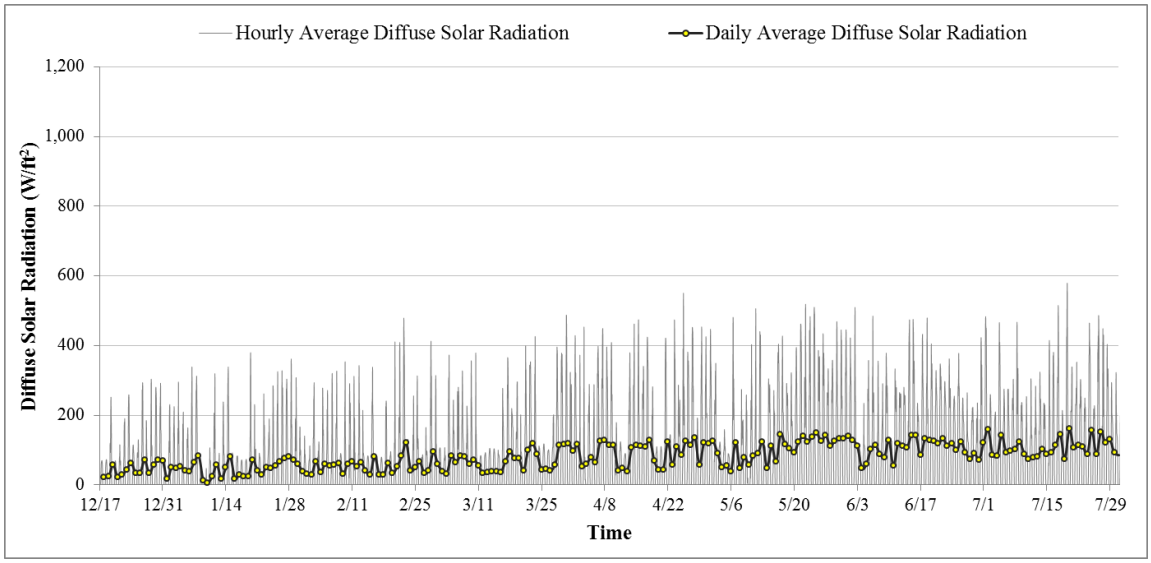

Figure 5-5: Hourly and Daily Average Diffuse Solar Radiation (from the middle of December, 2012 to the end of July 2013)

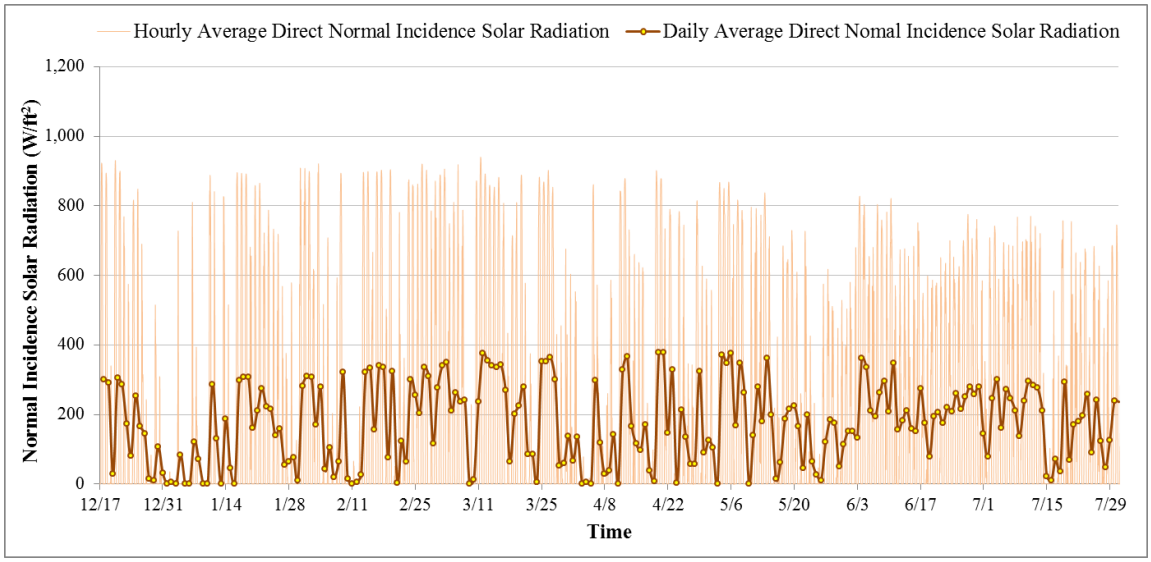

Figure 5-6: Hourly and Daily Average Direct Normal Incidence Solar Radiation (from the middle of December, 2012 to the end of July 2013)

5.1.1.2. Measured Data from the Case-Study House

The WSHP system for the case-study house utilizes a custom-built ground heat exchanger (GHX), which uses a combination of horizontal GHXs and a surface water (pond) GHX shown in Figure 4-24. The WSHP system is connected with the first horizontal GHX, the surface water GHX, and the second horizontal GHX, in sequence. The details of the case-study house can be found in the Section 4.3.1.

The measured data from the case-study house are the Entering Water Temperatures (EWTs), the Leaving Water Temperatures (LWTs), the Supply Air Temperatures (SATs), and the Return Air Temperatures (RATs). These data were used to validate the horizontal and surface water GHX models. The temperature measurement started from the middle of December, 2012 and ended in July, 2013. The measurement period included days during both the heating and cooling seasons.

The data were collected using one minute readings and converted to hourly average data to use for the horizontal and surface water GHX models, and to compare the measured EWT against the calculated EWT results for the heating or cooling operation periods.

Figure 5-7 through Figure 5-10 show plots of the hourly data and daily average data measured from December, 2012 to July, 2013. Figure 5-7 and Figure 5-8 show the measured data for the supply and return air temperatures. The average supply air temperatures were about 111 F for the heating operation and 55 F for the cooling operation. On the other hand, the average return air temperatures, which would be the thermostat setting, were about 75 F for the heating operation and 80 F for the cooling operation.

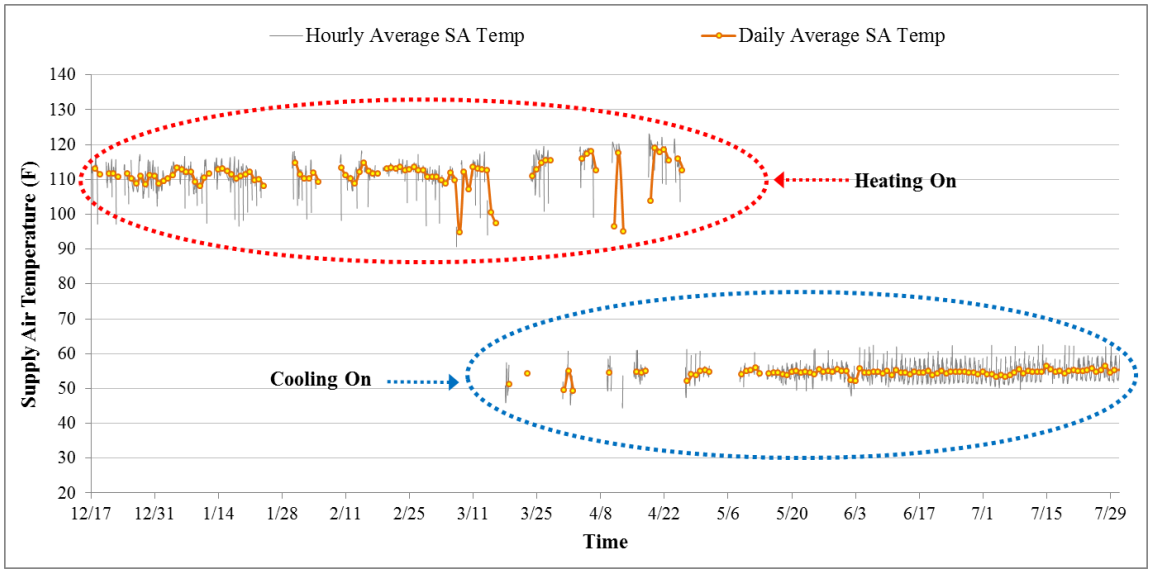

Figure 5-7: Hourly and Daily Measured Average SAT during System On

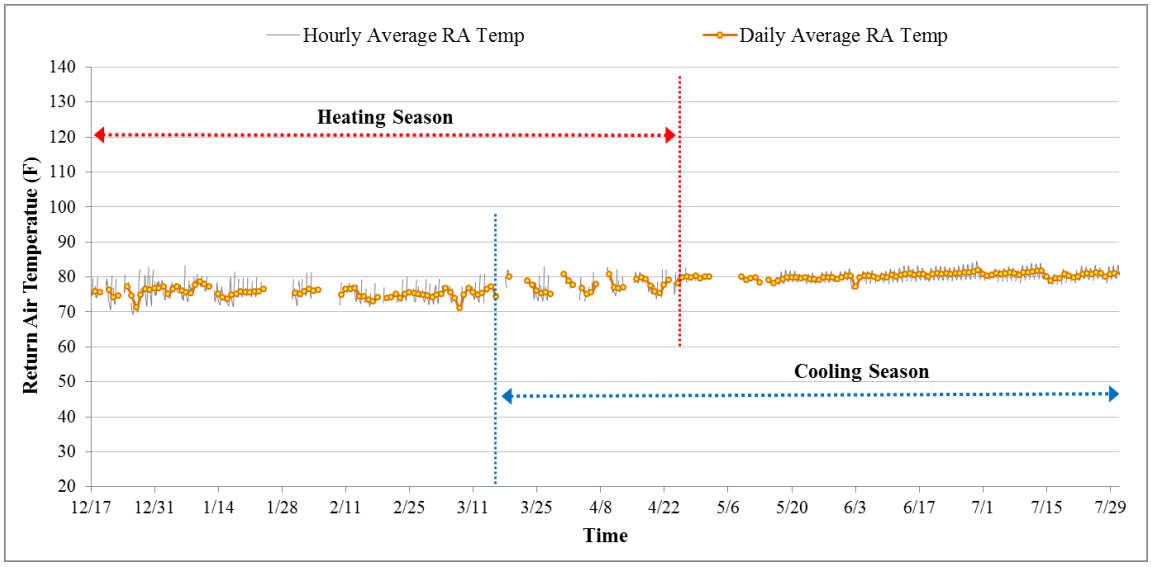

Figure 5-8: Hourly and Daily Measured Average RAT during System On

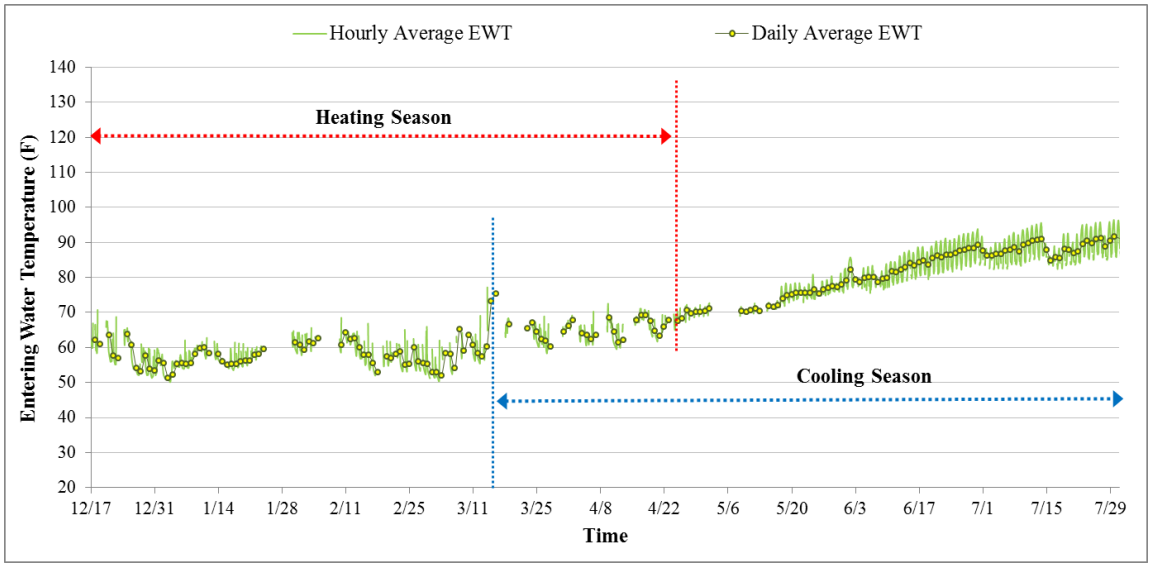

Figure 5-9: Hourly and Daily Measured Average EWT during System On

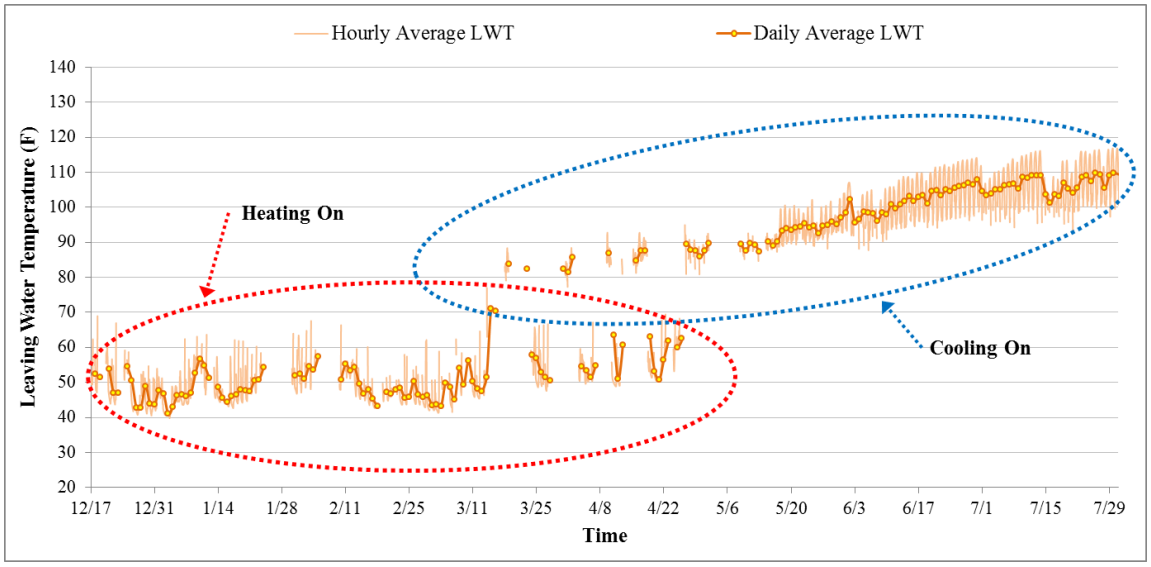

Figure 5-10: Hourly and Daily Measured Average LWT during System On

Figure 5-9 and Figure 5-10 presents the measured data for entering and leaving water temperature. The daily average entering water temperatures were about 57 F for the heating operation and 88 F for the cooling operation. On the other hand, the daily average leaving water temperatures were about 48 F for the heating operation and 108 F for the cooling operation.

Figure 5-11 presents the calculated system cooling and heating loads of the case-study house based on the measured EWT and LWT, and GHX fluid mass flow rate[48]. The calculation was conducted using the following equation:

[48] The fluid flow rate in gpm was estimated using the following equation: $GPM = \mathrm{Q}/(500 \times \Delta T)$. Q is the rated heat pump system capacity (39,000 Btu/hr for cooling and 28,000 Btu/hr for heating) from the system specification. ΔT is the temperature difference between the measured LWT and measured EWT (about 12 F for heating and 20 F for cooling). As a result, 4.28 gpm of average flow rate (4.67 gpm for heating and 3.9 gpm for cooling) was taken in this study.

$$Q = \dot{m} \times C_p \times (LWT - EWT) \quad (5.1)$$

Where,

Q	is the system load (Btu/hr),
ṁ	is the rate of fluid flow through a GHX (lb/hr),
C_p	is the specific heat of the water (Btu/lb-F),
LWT	is the leaving water temperature from a heat pump (F), and
EWT	is the entering water temperature to a heat pump (F).

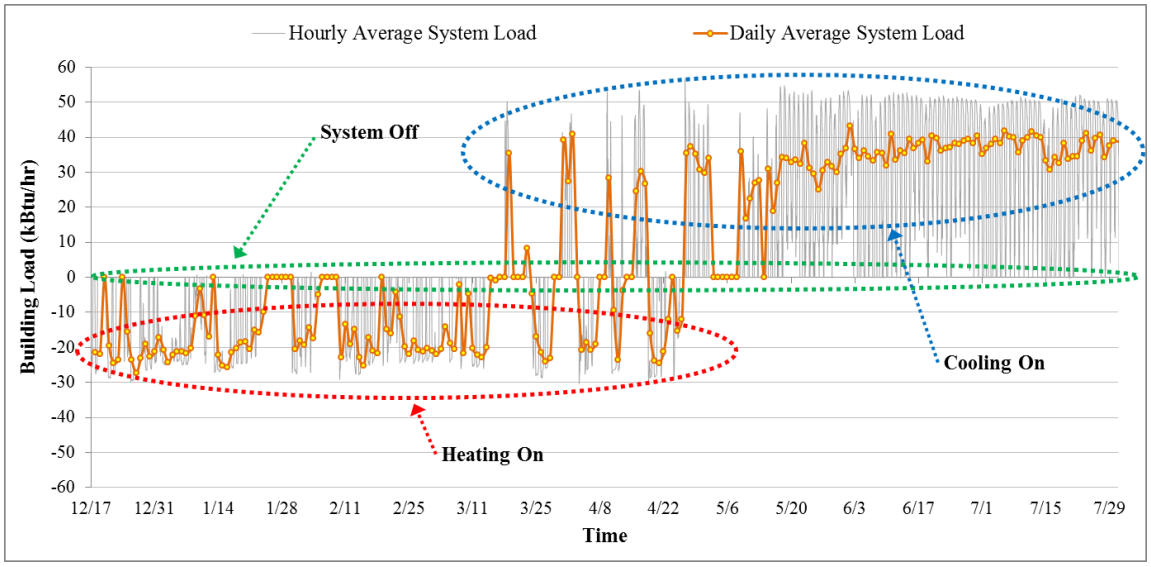

Figure 5-11: Hourly and Daily Calculated Average System Cooling and Heating Load

In Figure 5-11, when the system load is negative, the system operated to provide heating to the house; on the other hand, when the system load was positive, the system operated to provide cooling to the house. During the period from December 2012 to February 2013, the system in the case-study house did not have any cooling loads. From March to the end of April 2013, both the heating and cooling operation were observed;

the periods were identified as alternating periods. After May 2013, only the cooling operation was observed.

5.1.2. Horizontal and Surface Water Ground Heat Exchanger Model

To calculate the Entering Water Temperatures (EWTs) for the case-study house, the custom-built GHX model, which combines the horizontal GHX model and the surface water GHX model, was used. The custom-built GHX model calculated the EWTs, based on energy transfer mechanisms to account for the effect between the GHX and the surrounding heat source/sink. The calculation methodologies were described in Sections 4.2.1 and 4.2.2 for the horizontal GHX and surface water GHX, respectively. This study calculated the ground temperature, the pond water temperature, and the EWT for each hour of the simulation.

5.1.2.1. GHX Model Input Parameters

To use the custom-built GHX model which combines the horizontal and surface water GHX models for the case-study house, various input parameters were defined. Table 5-1 shows the summary table for the input parameters, including: the thermal properties of the ground (soil), circulation fluid, and GHX pipes; the GHX length and depth; the weather input; and the pond geometry and pond water thermal properties. The measured data from the Solar Test Bench were used for the values for the weather input parameters.

Table 5-1: Input Parameters Used for Horizontal and Surface Water GHX Models

Input Parameters		First GHX (Horizontal Type)	Second GHX (Surface Water Type)	Third GHX (Horizontal Type)
Ground	Mean Temperature (F)	72	72	72
	Temperature Amplitude (F)	21	-	21
	Phase Angle (hours)	792 hours (33 Days)	-	792 hours (33 Days)
	Thermal Diffusivity (ft^2/hour)	0.41	-	0.41
	Thermal Conductance (Btu/hr-ft-F)	0.71	-	0.71
Fluid	Flow Rate (gpm)	4.28		
	Viscosity (lb/hr-ft)	2.73		
	Specific Heat (Btu/lb-F)	1		
	Thermal Conductance (Btu/hr-ft-F)	0.334		
Pipe	Inner Diameter (ft)	0.16667 ft (2 inches)		
	Outer Diameter (ft)	0.19792 ft (2.375 inches)		
	Thermal Conductance (Btu/hr-ft-F)	0.2117		
Weather	Outdoor Air Temperature (F)	Measured		
	Relative Humidity (%)	Measured		
	Wind Speed (mph)	Measured		
	Global Solar Radiation (Btu/hr-ft^2)	Measured		
	Diffuse Solar Radiation (Btu/hr-ft^2)	Measured		
GHX	Length (ft)	450	1,040	920
	Depth (ft)	5	6	6
Pond	Surface Area (ft^2)	-	10,913	-
	Pond Perimeter (ft)	-	564	-
	Volume (ft^3)	-	65,480	-
	Water Density (lb/ft^3)	-	62.34	-
	Water Emissivity (Non-dimensional)	-	0.96	-
	Water Specific Heat (Btu/lb-F)	-	1	-
	Latitude (Degrees)	-	-30.628	-
	Longitude (Degrees)	-	96.334	-

5.1.2.2. Ground Temperatures

The ground temperatures to be used in the horizontal GHX model were calculated, using the algorithm developed by Kusuda and Achenbach (1965). The algorithm was described in the Section 4.2.1.1. The calculated ground temperatures used for both the first GHX and the third GHX installed in the case-study house, which are

the horizontal GHX type. To calculate the ground temperatures, a ground depth of 5 ft and 6 ft were used for the first GHX and the third GHX, respectively. Figure 5-12 shows the predicted hourly ground temperatures for the measurement period from the Kusuda and Achenbach model. For the first GHX model, the minimum ground temperature was 62.5 F and the maximum ground temperature was 78.3 F. On the other hand, for the third GHX model, the minimum ground temperature was 63.8 F and the maximum ground temperature was 76.3 F. As shown in Figure 5-12, the ground temperatures changed according to the time of the year. Temperatures deeper in the ground, which is the third GHX, experienced less variation in temperatures and have a time lag farther behind those of ground temperatures at a shallow depth.

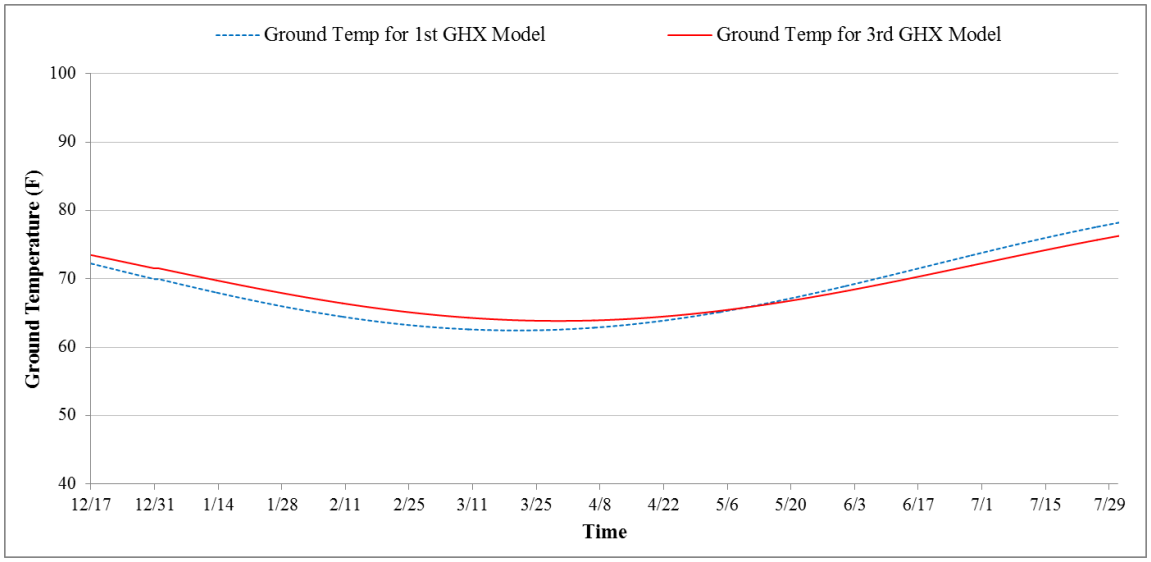

Figure 5-12: Predicted Hourly Ground Temperature for Horizontal GHX Models

5.1.2.3. Pond Temperatures

The pond water temperatures to be used for the surface water GHX model in the case-study house were estimated using the energy transfer mechanisms, which were previously described in the Section 4.2.2.1. The energy transfer mechanisms included the solar radiation absorbed by the pond at the pond's surface (Q_{solar}), the thermal radiation from the pond water to the sky at the pond's surface (Q_{rad}), the evaporation of the pond (Q_{evap}), the convection at the pond's surface (Q_{conv}), the conductive heat transfer to/from the ground in contact with the pond (Q_{ground}), and the heat transfer between the fluid in the pipe and the pond (Q_{fluid}). Figure 5-13 through Figure 5-18 showed the calculation results of the energy transfer mechanisms using the measured ESL's STB weather data. The negative and positive heat transfer values account for the heat loss and heat gain in the pond water, respectively.

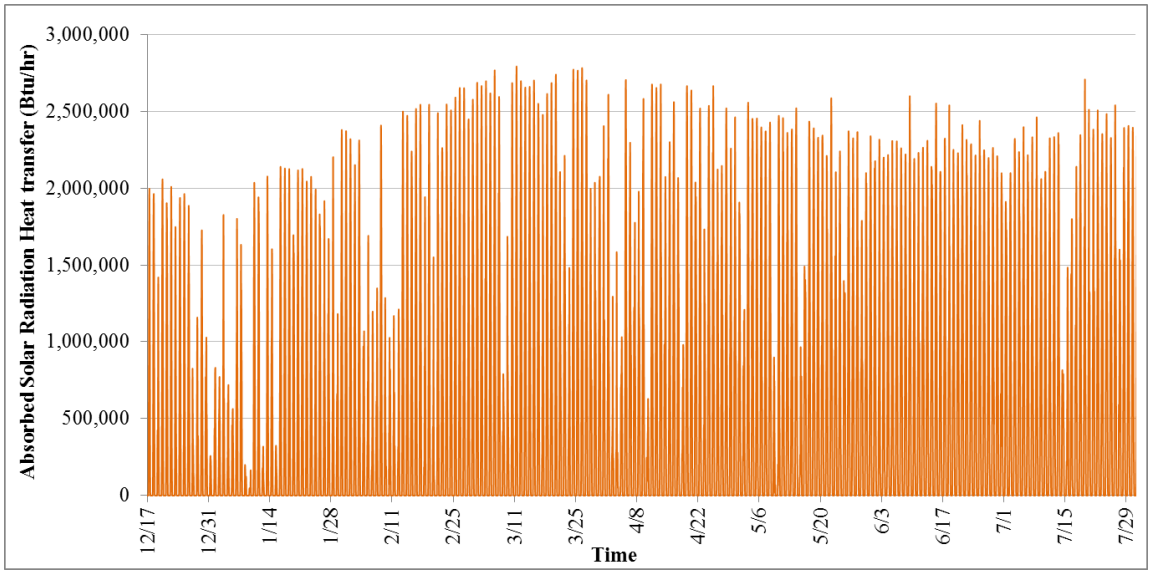

Figure 5-13: Hourly Solar Radiation Absorbed by the Entire Pond's Surface

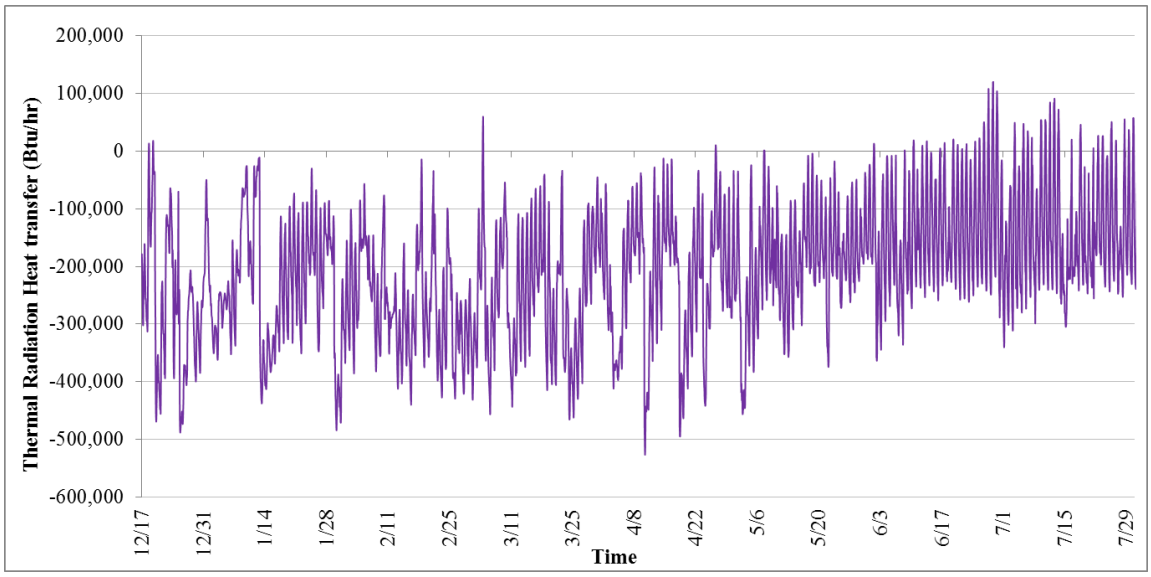

Figure 5-14: Hourly Thermal Radiation from Water to Sky at the Entire Pond's Surface

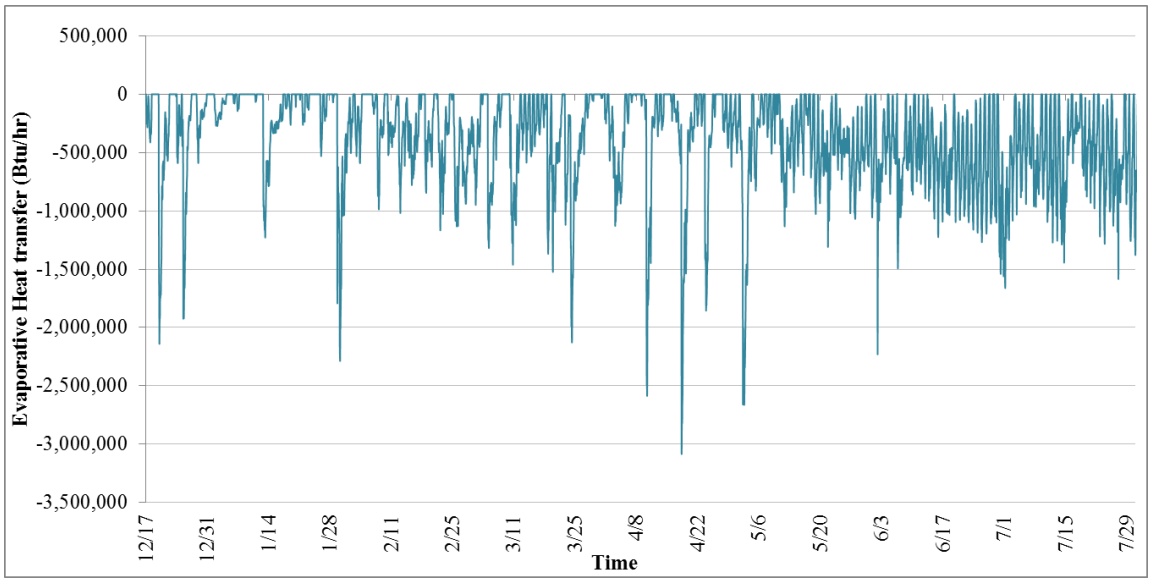

Figure 5-15: Hourly Evaporation of the Entire Pond's Surface

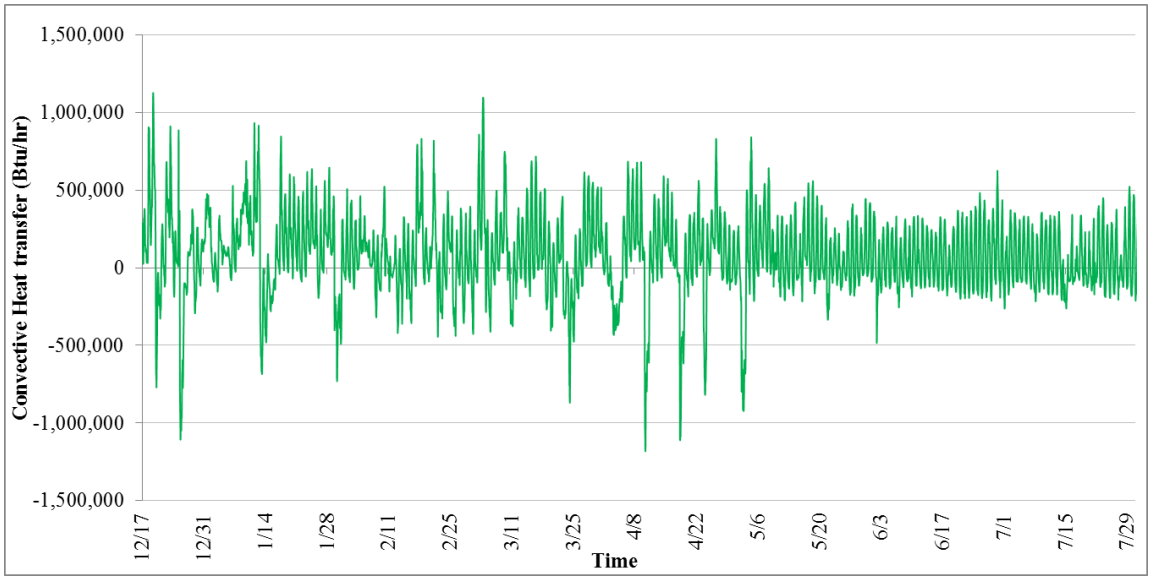

Figure 5-16: Hourly Convection of the Entire Pond's Surface

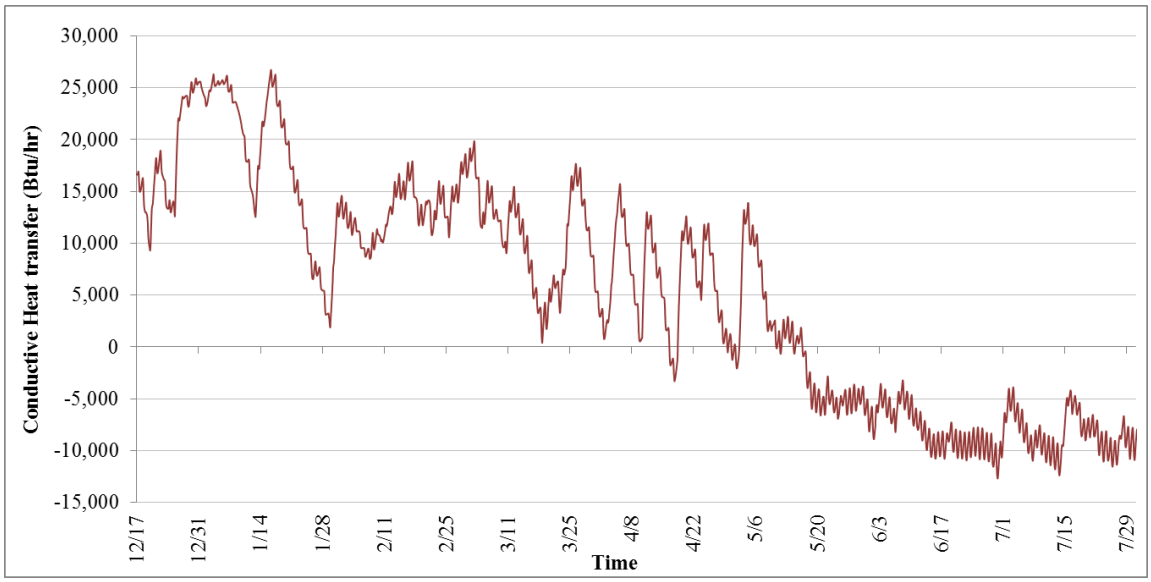

Figure 5-17: Hourly Conduction to/from the Pond Ground

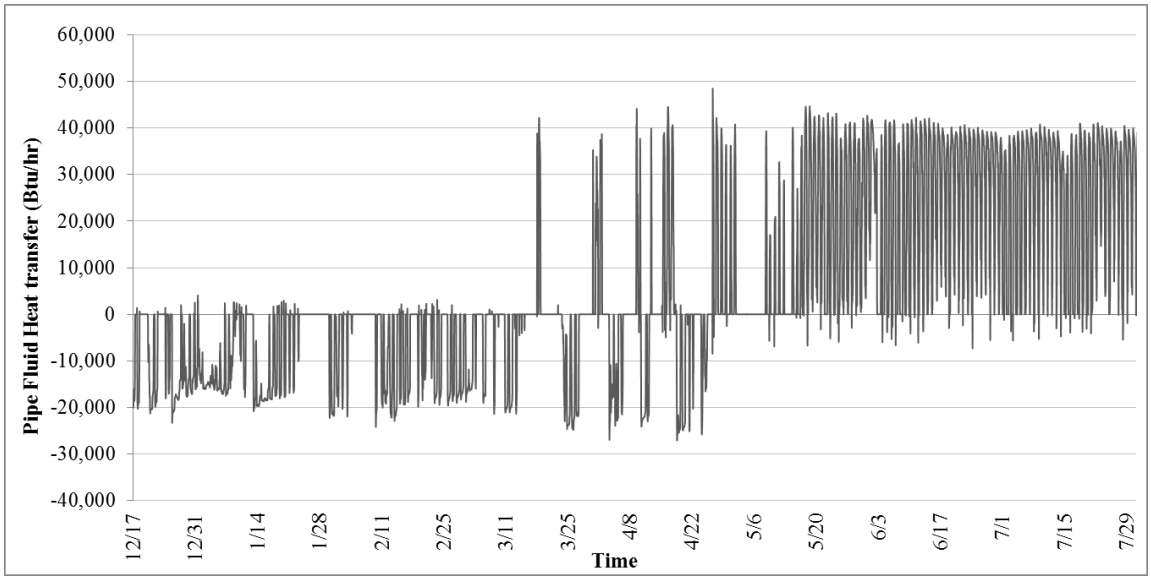

Figure 5-18: Hourly Heat Transfer between the Fluid in the Pipe and the Pond

Table 5-2 presents the monthly hourly average heat transfer to the pond. It was observed that the absorbed solar radiation was the largest heat transfer amount (about 43 % of total heat transfer amount, shown in Figure 5-19) which affected on the pond water temperature. The absorbed solar radiation and convective heat transfer were observed as the continuous heat gain to the pond water whereas the thermal radiation and the evaporation were observed as the continuous heat loss. The conductive heat transfer and the pipe fluid heat transfer, which represents the system loads after the first GHX, were observed as both heat gain and loss to the pond water. The monthly average total heat transfer had the negative values in December 2012 and February 2013 whereas the other months had the positive values.

Table 5-2: Monthly Hourly Average Heat Transfer to the Entire Pond

Monthly Hourly Average (Btu/hr-sqft)	Energy Transfer Mechanisms for the Entire Pond						
	Solar Radiation Q_{solar}	Thermal Radiation Q_{rad}	Evaporation Q_{evap}	Convection Q_{conv}	Conduction Q_{ground}	Fluid Q_{fluid}	Total Heat Transfer
December, 2012	31.1	-23.8	-28.0	9.2	1.7	-0.8	-10.7
January, 2103	31.0	-21.3	-15.9	12.6	1.6	-0.7	7.3
February, 2103	42.0	-24.1	-28.0	6.7	1.2	-0.5	-2.8
March, 2103	53.9	-22.8	-32.1	9.4	1.0	-0.3	9.2
April, 2103	49.2	-20.3	-31.6	4.6	0.6	0.0	2.6
May, 2103	53.6	-17.3	-39.9	6.6	0.0	1.2	4.2
June, 2103	58.1	-12.6	-51.1	5.6	-0.7	2.2	1.4
July, 2103	55.1	-12.7	-47.4	4.3	-0.8	2.2	0.8
Sum	374.1	-154.9	-274.0	59.1	4.5	3.2	12.0
Sum of Absolute Values	374.1	154.9	274.0	59.1	4.5	3.2	869.9
% of Sum of Absolute Values	43.0%	17.8%	31.5%	6.8%	0.5%	0.4%	100%

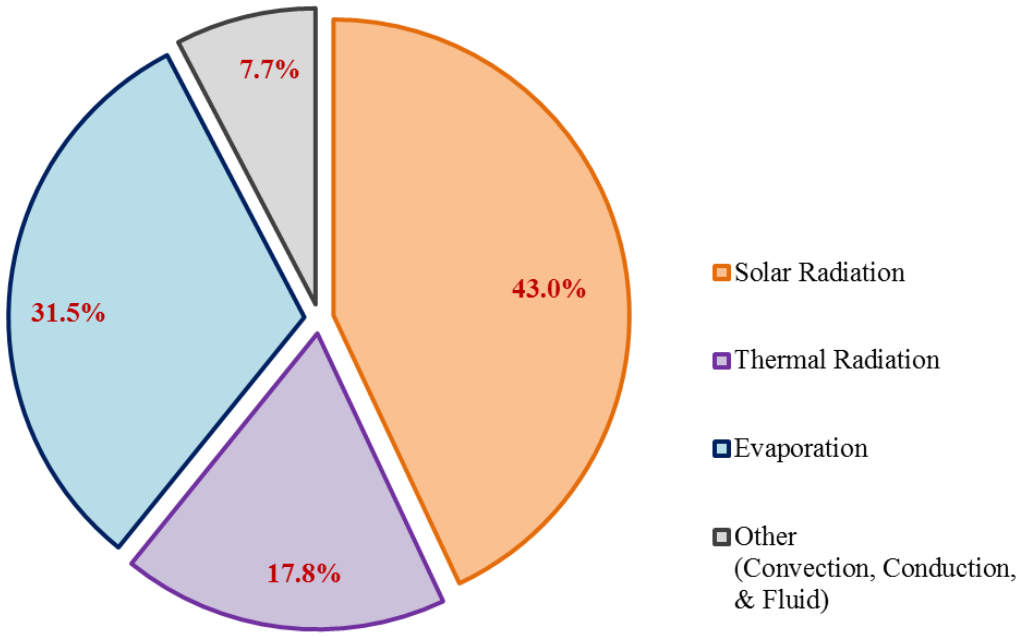

Figure 5-19: % Effect of Different Heat Transfer on Pond Water Temperature

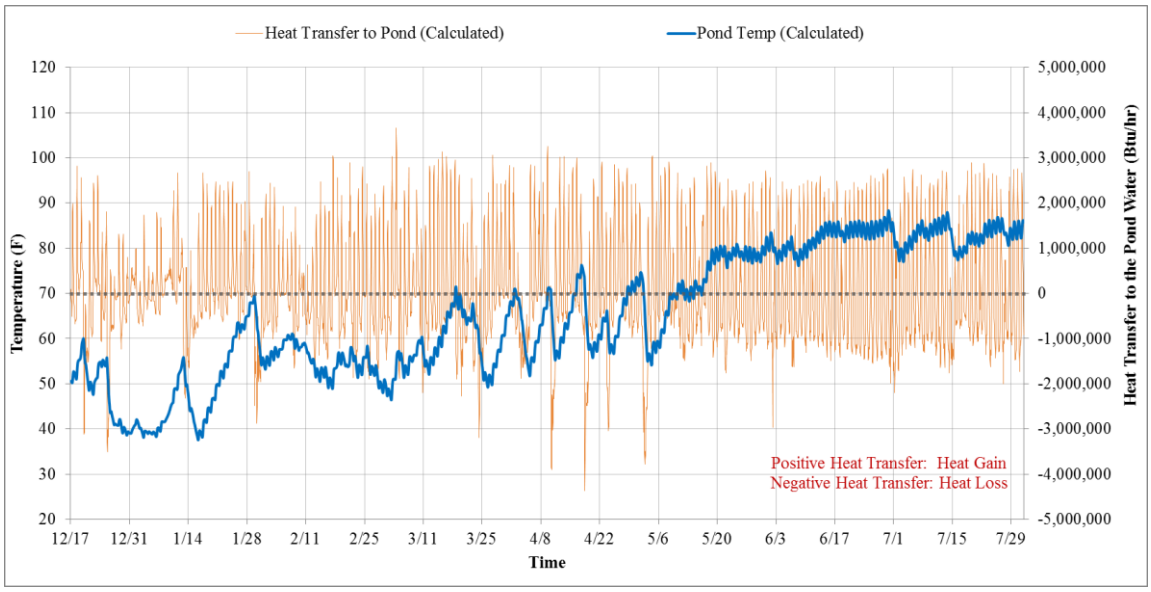

(a) Pond Water Temperature against Heat Transfer Amount

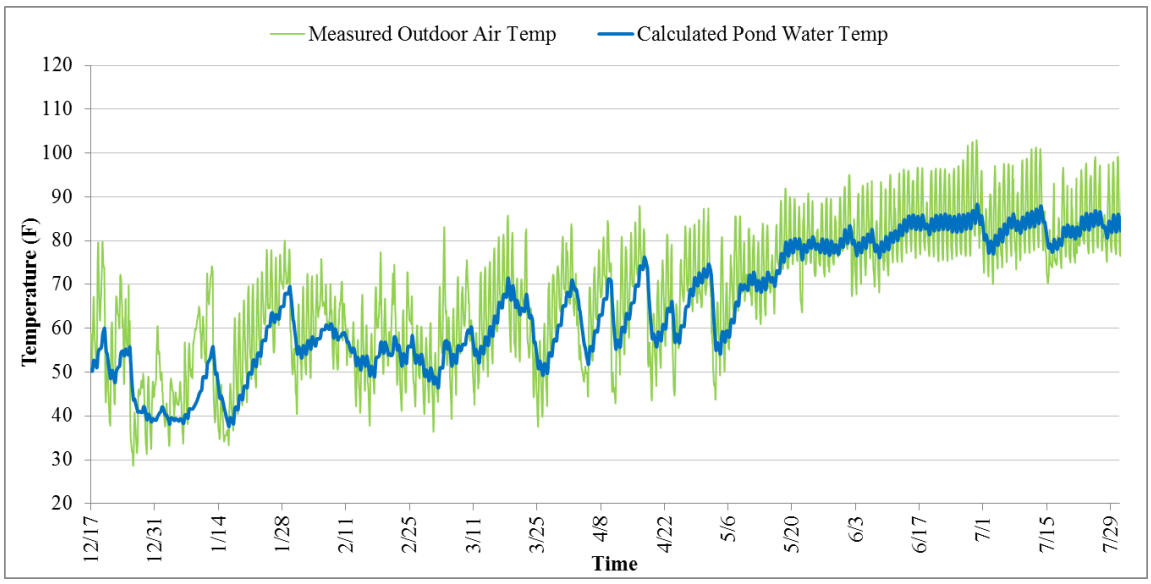

(b) Pond Water Temperature against Outdoor Temperature

Figure 5-20: Predicted Hourly Pond Water Temperature for Surface Water GHX Models

The pond water temperatures were predicted based on the energy transfer mechanisms. Figure 5-20 presents the resulted pond water temperatures, comparing with the calculated heat transfer amount to the pond water and comparing with the outdoor air temperatures. The lowest pond water temperature was 37.6 F on 16th of January, 2013. The highest pond water temperature was 88.3 F on 29th of June, 2013. The coldest period of the year was observed from the end of the December to the middle of January. During February, the pond water temperatures stayed around 55 F. The pond water temperatures had temperature fluctuations (e.g., about 19 F of hourly average temperature change in one week) during the middle of March and the early of the May. Then, the pond water temperatures had steadily increased until the end of June and reached to about 87 F on the early of July.

5.1.3. EWT Validation of Custom-Built GHX Model

The WSHP system at the case-study house utilizes custom-built GHXs, which use a combination of a horizontal GHXs and a surface water (i.e., pond) GHX. The WSHP system is connected with three GHXs: the first horizontal GHX, the surface water GHX, and the second horizontal GHX, in sequence. The custom-built GHX model in this study, which combines the horizontal GHX model and the surface water GHX model, was developed for the case-study house to calculate the EWTs described in Section 4.3.5.

Figure 5-21 shows the comparison of the calculated water temperatures in the three GHX pipes, including the ground temperatures and the pond water temperatures.

Based on the resultant temperatures for each GHX, it is interesting to note that the pond for the surface water GHX utilized in the case-study house did not work well as a heat source during the heating season (December and January). The reason was the pond is only 6 feet deep; therefore, the pond water temperatures are easily changed by the environment conditions (i.e., outdoor temperatures); as a result, the pond water temperatures were lower than the water temperatures at the end of the first GHX pipe. On the other hand, during other periods, the pond worked well as a heat source or sink. The calculated water temperatures at the end of the third GHX pipe in Figure 5-21 corresponds to the calculated EWTs to the WSHP at the case-study house.

Figure 5-22 shows the comparison of the calculated EWTs against the measured EWTs and the measured LWTs from the case-study house. The temperature difference between the measured LWT and measured EWT were observed about 12 F during the heating season and about 20 F during the cooling season.

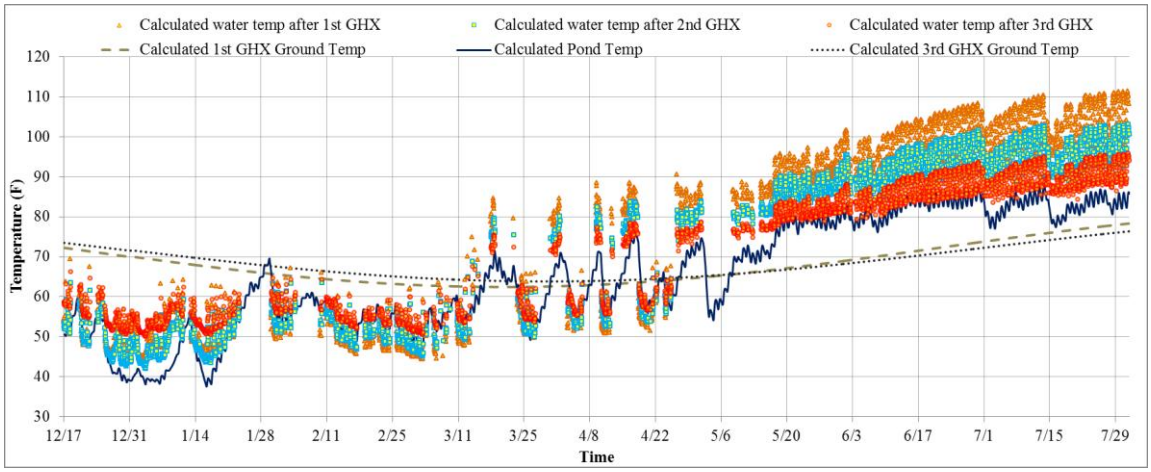

Figure 5-21: Calculated Water Temperature in Three GHXs used for Case-Study House

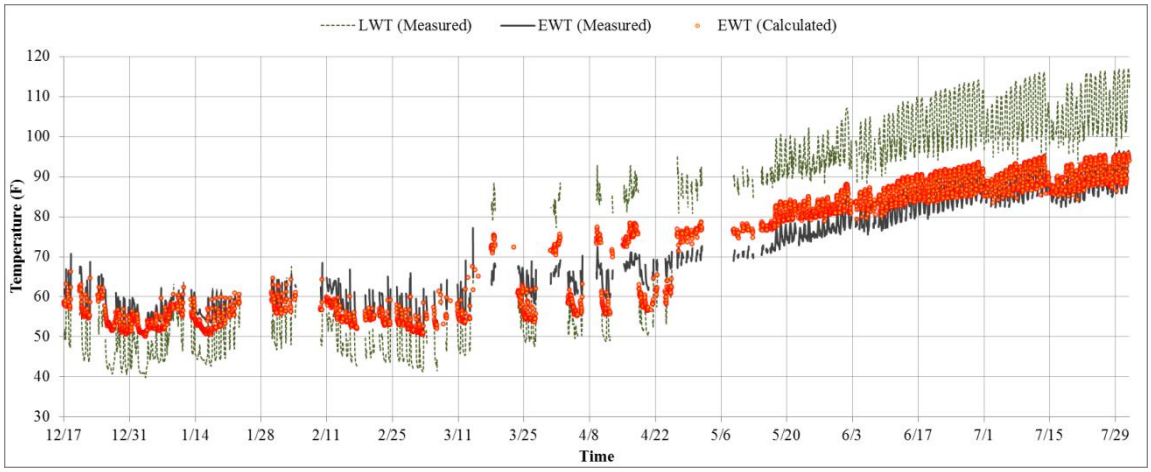

Figure 5-22: Hourly Average Measured LWT and EWT, and Calculated EWT

The calculated EWTs were compared to the measured EWTs data from the case-study house. This comparison allowed a validity check of the custom-built GHX model. The calculated and measured EWTs were compared for the hours when the heat pump system at the case-study house was operated from the middle of December 2012 to the end of July 2013. Figure 5-23, Figure 5-24, and Figure 5-25 show the comparison plots between measured EWTs and calculated EWTs for the monthly average, daily average and hourly average EWTs, respectively.

In Figure 5-23, the monthly average EWTs difference between the measured EWTs and the calculated EWTs was observed to be about 2.2 F during the heating season (December, January, and February) and about 3.2 F during the cooling season (May, June, and July). The calculated EWTs were lower than the measured EWTs for the heating season and the calculated EWTs were higher than the measured EWTs for the cooling season.

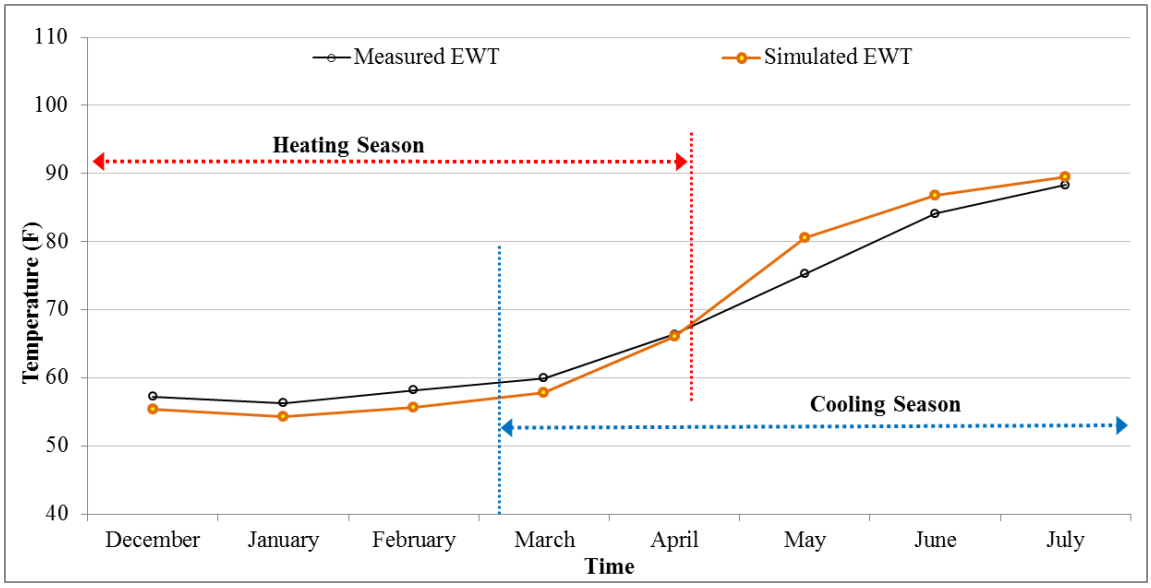

Figure 5-23: Monthly Average EWT Comparison between Measured and Calculated Values

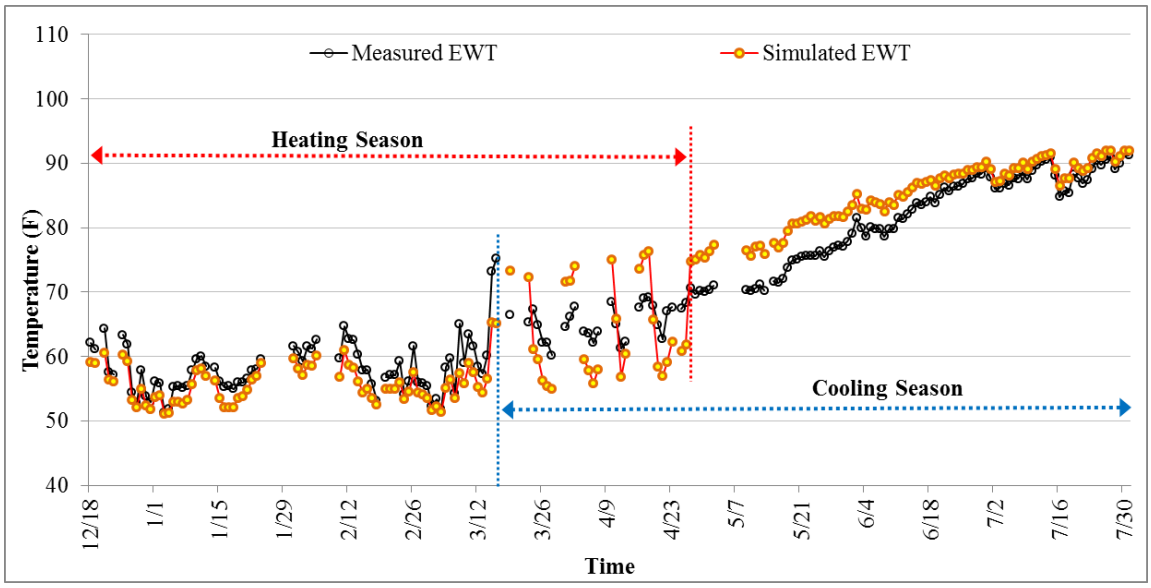

Figure 5-24: Daily Average EWT Comparison between Measured and Calculated Values

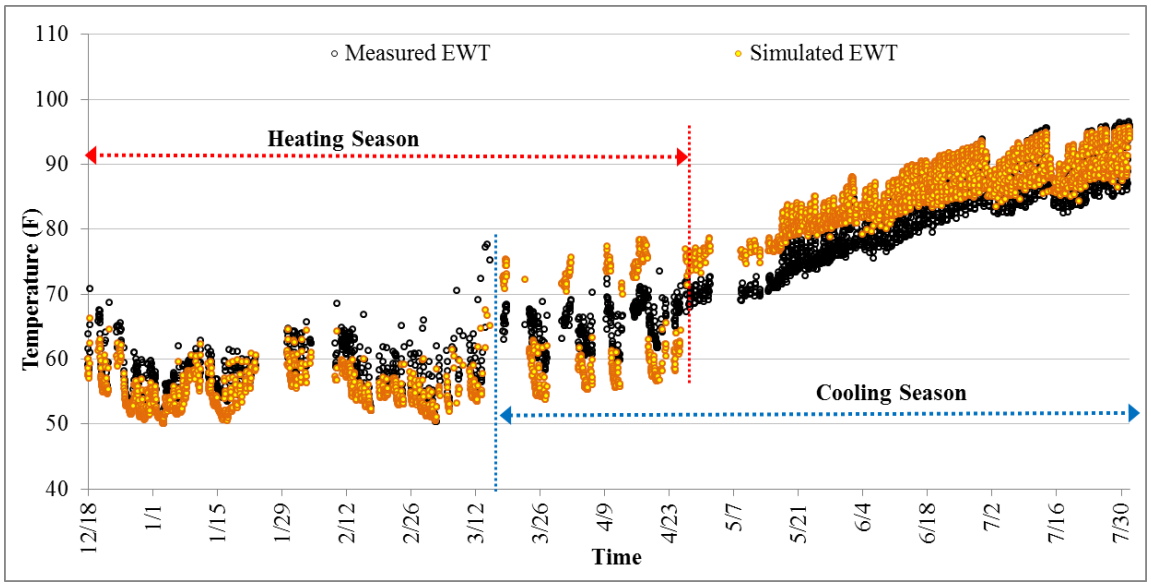

Figure 5-25: Hourly Average EWT Comparison between Measured and Calculated Values

In Figure 5-24, and Figure 5-25, the daily average and hourly average EWTs were compared between the measured EWTs and the calculated EWTs. The daily average and hourly average EWTs differences during the heating season and the cooling season were observed to be about 2.9 F for heating and 3.1 F for cooling (also shown in Figure 5-27), which was similar to the temperature difference of the monthly average EWTs in Figure 5-23. On the other hand, larger EWTs differences were observed to be about 5 F to 9 F during the alternating periods from March to the end of April 2013, which had both the heating and cooling operation. In addition, Figure 5-26 and Figure 5-27 presents plots of the measured and calculated EWTs versus the outdoor temperatures and the EWTs differences, which were subtracted from the measured EWTs to the calculated EWTs, corresponding the outdoor temperatures, respectively.

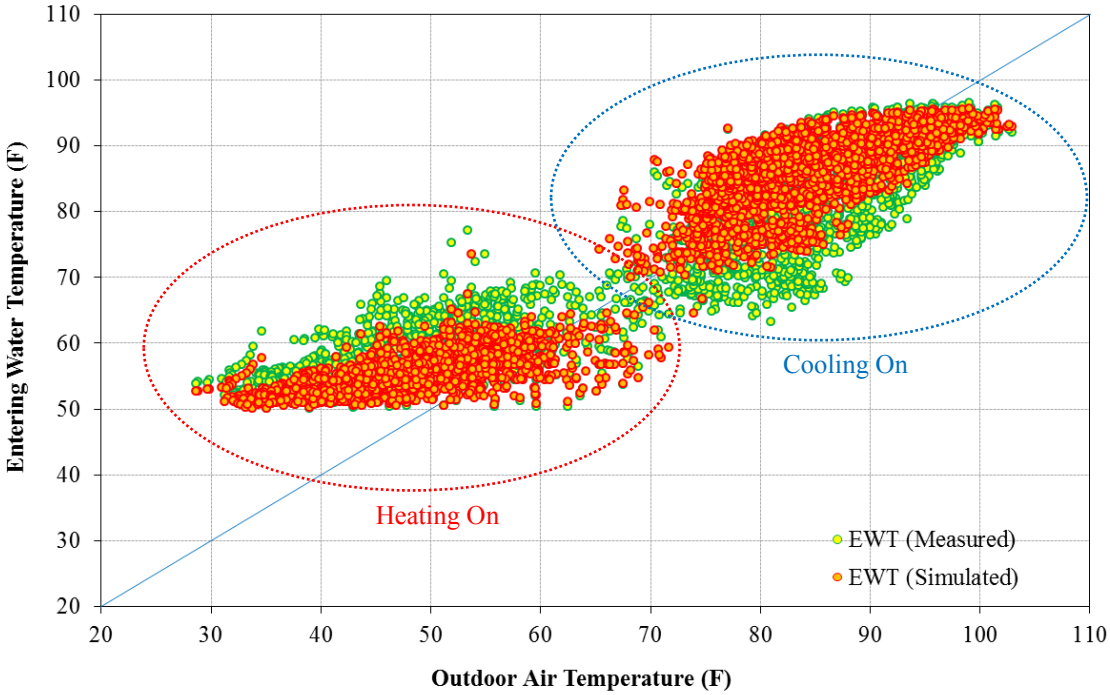

Figure 5-26: Hourly Average EWT against Outdoor Air Temperature

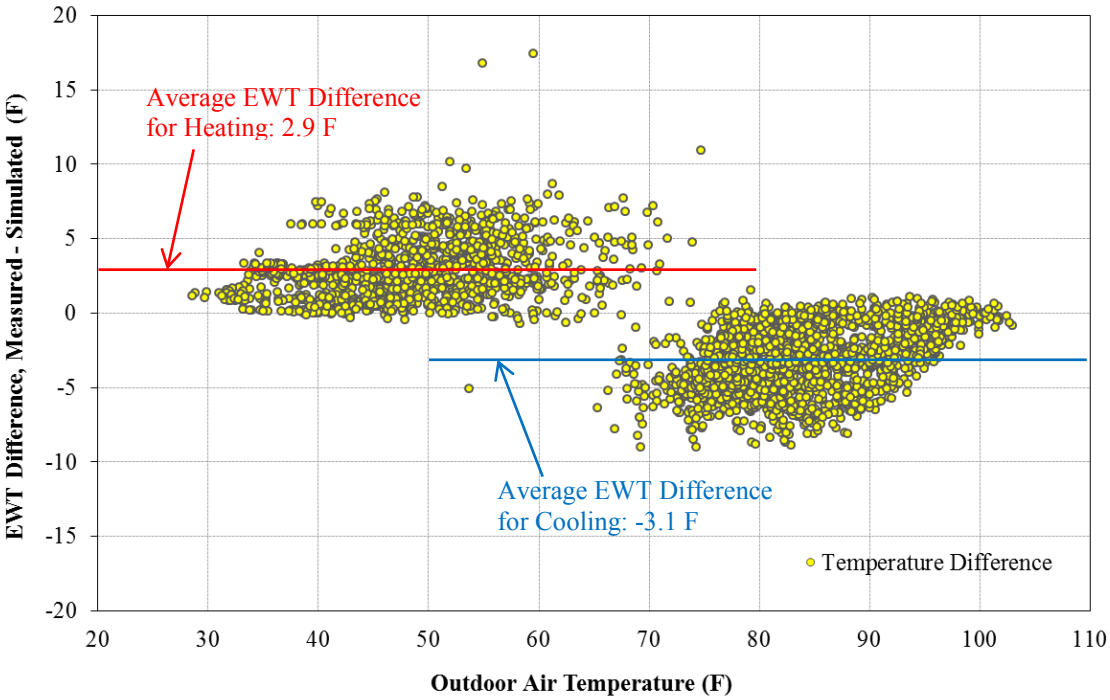

Figure 5-27: EWT Difference against Outdoor Air Temperature

5.1.4. Summary

The water-source heat pump (WSHP) system in the case-study house utilizes the custom-built ground heat exchangers (GHXs), which use a combination of horizontal GHXs and surface water (pond) GHX. To calculate the entering water temperatures (EWTs) from the custom-built GHX at the case-study house, therefore, this study developed the custom-built GHX model which combines the horizontal GHX model and the surface water GHX model.

The Energy Systems Laboratory's Solar Test Bench (STB) weather data were collected from the middle of December 2012 to the end of July 2013, which corresponds to the period when the case-study house temperature measurements were taken. The periods included both the heating season and the cooling season. To calculate the EWTs, this study used the data collected from the ESL's STB and the measured data from the case-study house for the custom-built GHX model.

The calculated EWTs, using the custom-built GHX model, were then compared with the measured EWTs from the case-study house. Based on the comparison between the calculated EWTs and the measured EWTs, this study observed that the average EWT temperature difference was about 3 F for both the heating season and the cooling season.

The calculated EWTs were lower than the measured EWTs for the heating season and higher than the measured EWTs for the cooling season. Therefore, the calculated EWTs might to be slightly over-estimated. However, the resultant EWTs were felt to be acceptable considering the uncertainty of other unknowns such as the pond water level change, exact underground soil condition, and system degradation.

5.2. Vertical Ground Heat Exchanger Model

A vertical ground heat exchanger (GHX) model was developed to determine the entering water temperature (EWT) from a vertical GHX to the heat pump. The vertical GHX model for this study used the g-function approximation, as described in Section 4.2.3.3, to reproduce the g-function values developed by Eskilson (1987), which were further enhanced by Yavuzturk and Spitler (1999). Using the approximated g-function values, the average borehole wall temperature was calculated. Next, the average fluid (water) temperature inside the pipe in the borehole was calculated using a total thermal borehole resistance. Finally, the EWT was determined.

In this study, a simplified residential air-source heat pump (ASHP) base-case model was developed to apply the vertical GHX model. The ASHP base-case model was modified with the vertical GHX model to work like the ground-coupled heat pump (GCHP) base-case model.

This section presents the simulation results: Section 5.2.1 shows the results of the simplified residential ASHP base-case simulation model; Section 5.2.2 shows the results of the simplified residential GCHP base-case simulation model. Section 5.2.3 presents the comparison of the DOE-2.1e base-case model simulation results for ASHP and GCHP against the other simulation programs.

5.2.1. Residential ASHP Base-Case Model

The simplified residential air-source heat pump (ASHP) base-case simulation models were developed using residential home characteristics compliance with the 2009

International Energy Conservation Code (IECC) requirements. The weather files for the residential base-case models are used the Houston and Dallas location in Texas to represent the hot and humid climate of Texas. Therefore, the simulation throughout this study was performed with using Typical Meteorological Year version 2 (TMY2) weather data for Houston and Dallas.

First, to develop the 2009 IECC compliant DOE-2.1e ASHP residential model for Houston, this study used the step-by-step input change procedure described in Section 4.4.1. The step-by-step procedure consists of six categories (30 simulation runs), including the *Project* category (7 simulation runs), the *ASHP System* category (7 simulation runs), the *Construction* category (9 simulation runs), the *Internal Gain* category (2 simulation runs), the *Schedule* category (4 simulation runs), and the *DHW* category (1 simulation run).

The *Project* category defines general structures for the simplified residential building model. The *ASHP System* category defines the input parameters for the ASHP system. The *Construction* category defines the input parameters for the residential building envelope based on the 2009 IECC requirements. The *Internal Gain* category defines the input parameters for the energy use of the lighting and equipment. The *Schedule* category defines the input parameters for simplified schedules for lighting, equipment, infiltration, and interior shading. Finally, the *DHW* category defines an electric DHW system.

The step-by-step procedure began with "RUN 3A[49]". Through the step-by-step procedure, the RUN 3A was modified to become a single-story residential ASHP model for Houston (i.e., RUN_30 in this study). Second, using the residential ASHP base-case model for Houston (i.e., RUN_30), a residential ASHP base-case model for Dallas was developed by modifying the appropriate input parameters for the 2009 IECC requirements from Houston to Dallas.

To evaluate the accuracy of the simulation results from the residential DOE-2.1e ASHP base-case models, comparison against eQUEST and other code-compliant programs (i.e., IC3, EnergyGauge, and REM/Rate) were used. The eQUEST program was used for the comparison throughout the entire step-by-step procedure whereas the other code-compliant programs were only used to compare the final results of the DOE-2.1e ASHP base-case simulation model developed using the step-by-step procedure.

To compare the simulation results between DOE-2.1e and eQUEST for the initial step-by-step development procedure, the "RUN 3A" DOE-2.1e sample file with a variable air volume (VAV) system, which is not typically used for a residential building, was used. In the *Project* category (i.e., RUN_3A through RUN_7, described in Section 4.4.1.1.1), the simulation results from DOE-2.1e and eQUEST were compared using building loads only. After the system type was modified from VAV to RESYS (i.e., RUN_8) in the *ASHP System* category described in Section 4.4.1.1.2, the simulation results were then compared using system energy use.

---

[49] "RUN 3A" is one of the examples for a simple structure in the samp1e.inp file included in the DOE-2.1e program package.

5.2.1.1. Comparison of Building Cooling and Heating Loads

Before comparing the results between the different programs, the building loads should first be matched since differences in the building loads affect the energy use differences of the simulated building system. However, it is not always possible to match the building loads because different programs use different calculation algorithms. Nevertheless, the building load differences between the programs should be reduced as much as possible to then allow for differences in simulation to be evaluated. Therefore, this section presents the comparison of the building's heating and cooling loads for the residential ASHP base-case model for Houston using the DOE-2.1e and eQUEST simulation programs. For the comparison, this study used the building loads and the space peak loads. For the building loads comparison, the annual/monthly simulation results from the Building Monthly Loads Summary (i.e., LS-D output) were used; and for the space peak loads comparison, the simulation results from the Space Peak Loads Summary (i.e., LS-A output) were used. The comparison of the building loads in this section includes:

- Annual cooling and heating building loads resulting from RUN_3A to RUN_7 using the step-by-step procedure,
- Peak cooling and heating loads resulting from RUN_3A to RUN_7 using the step-by-step procedure, and
- Monthly cooling and heating loads resulting from RUN_30, which represents the final residential ASHP base-case model for Houston using the step-by-step procedure.

5.2.1.1.1. *Annual Cooling and Heating Building Loads from RUN_3A to RUN_7*

The annual cooling and heating building loads resulting from RUN_3A to RUN_7 in the *Project* category are shown in Figure 5-28 through Figure 5-30 which shows the annual cooling loads, the annual heating loads, and a sum of heating and cooling loads, respectively, from the LS-D output. Each figure includes plots of the annual building load comparisons and the annual building load differences between DOE-2.1e and eQUEST. The differences were calculated by subtracting from the DOE-2.1e results to the eQUEST results. In addition, Table 5-3 shows the annual cooling and heating building load results from RUN_3A to RUN_7[50] in the *Project* category.

Table 5-3: Annual Cooling/Heating Building Loads from RUN_3A to RUN_7

Run Name	Key Modification	DOE-2.1e			eQUEST		
		Cooling Load (MMBtu/yr)	Heating Load (MMBtu/yr)	Sum of Cooling and Heating Load (MMBtu/yr)	Cooling Load (MMBtu/yr)	Heating Load (MMBtu/yr)	Sum of Cooling and Heating Load (MMBtu/yr)
RUN_3A	Building location change	241.2	9.4	250.6	242.5	8.7	251.2
RUN_1	Reduced number of zones	240.6	6.0	246.6	243.4	6.3	249.7
RUN_2	Reduced space area/fenestration	151.9	3.5	155.4	152.6	3.9	156.4
RUN_3	Overhang removed	153.1	3.4	156.6	154.0	3.8	157.8
RUN_4	Orientation faced south	152.0	3.4	155.4	152.9	3.8	156.6
RUN_5	Number of occupancy	120.7	4.0	124.7	121.7	4.4	126.1
RUN_6	Plenum removed	131.0	7.7	138.7	132.4	7.9	140.4
RUN_7	Door size and location	129.1	8.0	137.0	130.5	8.1	138.6

[50] RUN_3A modified the building location from Chicago to Houston; RUN_1 changed the building space from five zones to a single zone; RUN_2 reduced the building space area from 5,000 ft^2 to 2,500 ft^2 and modified the WFR from 22 % to 15 %; RUN_3 removed the south-facing door overhang; RUN_4 rotated the building orientation so it faced south; RUN_5 changed the occupancy number from 52 to 0; RUN_6 removed the plenum; and, RUN_7 modified the door size and location, from two doors to a single door.

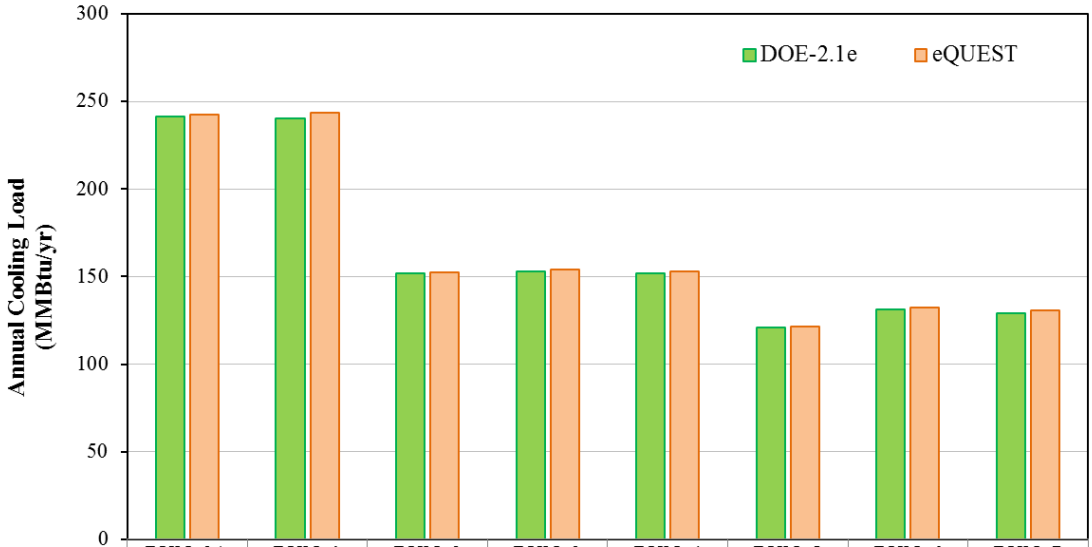

	RUN_3A	RUN_1	RUN_2	RUN_3	RUN_4	RUN_5	RUN_6	RUN_7
DOE-2.1e	241.2	240.6	151.9	153.1	152.0	120.7	131.0	129.1
eQUEST	242.5	243.4	152.6	154.0	152.9	121.7	132.4	130.5

(a) Annual Cooling Building Load

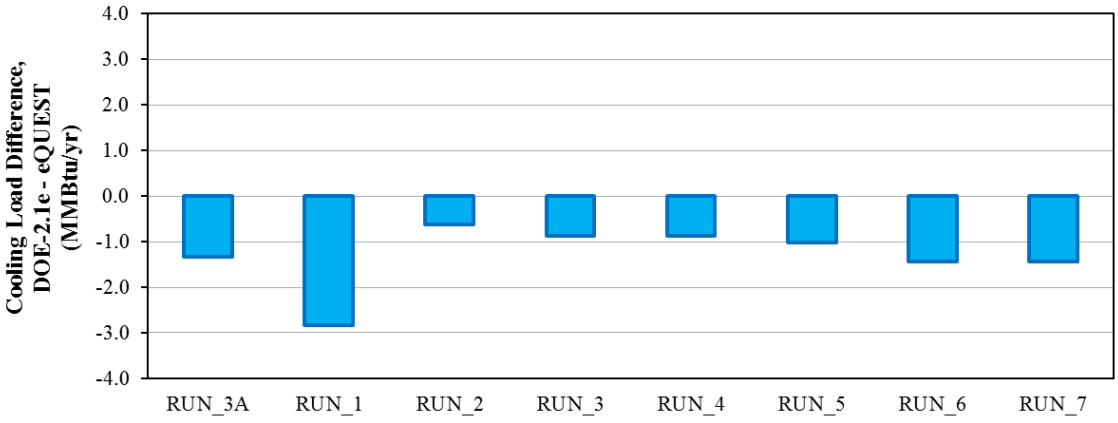

(b) Annual Cooling Building Load Difference

Figure 5-28: Annual Cooling Building Load Comparison from RUN_3A to RUN_7

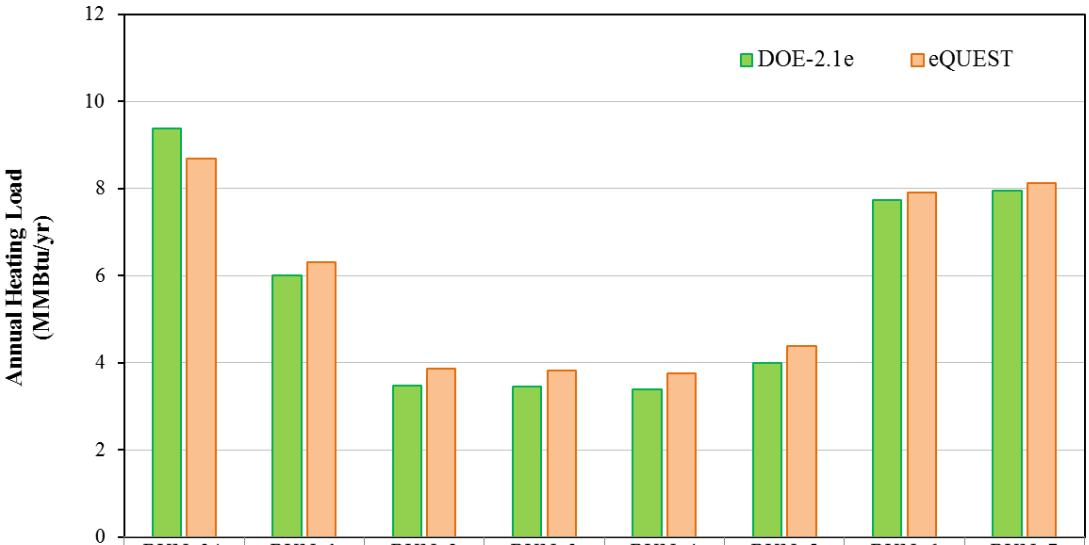

	RUN_3A	RUN_1	RUN_2	RUN_3	RUN_4	RUN_5	RUN_6	RUN_7
DOE-2.1e	9.4	6.0	3.5	3.4	3.4	4.0	7.7	8.0
eQUEST	8.7	6.3	3.9	3.8	3.8	4.4	7.9	8.1

(a) Annual Heating Building Load

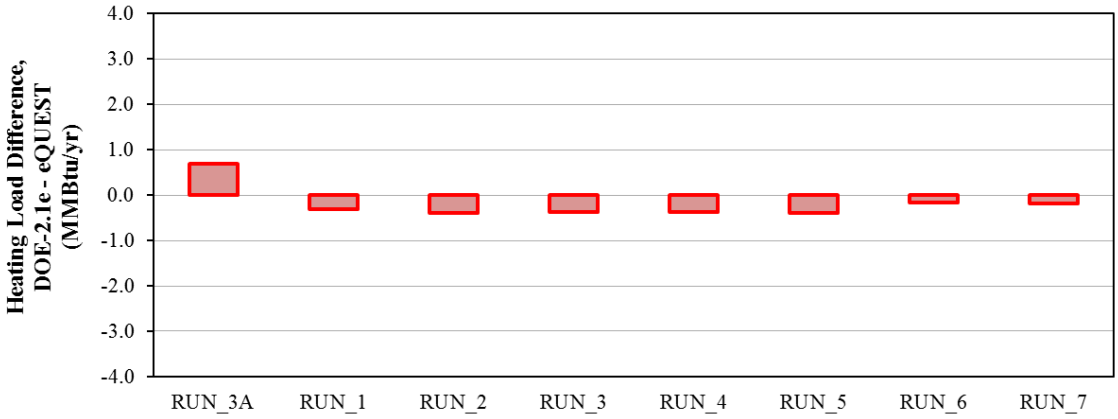

(b) Annual Heating Building Load Difference

Figure 5-29: Annual Heating Building Load Comparison from RUN_3A to RUN_7

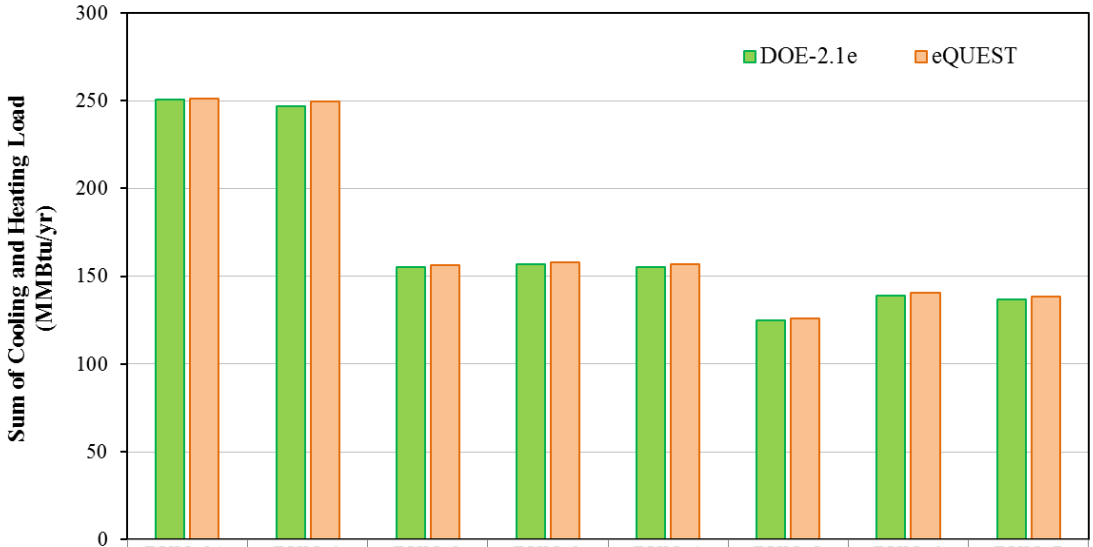

	RUN_3A	RUN_1	RUN_2	RUN_3	RUN_4	RUN_5	RUN_6	RUN_7
DOE-2.1e	250.6	246.6	155.4	156.6	155.4	124.7	138.7	137.0
eQUEST	251.2	249.7	156.4	157.8	156.6	126.1	140.4	138.6

(a) Total Annual Cooling plus Heating Building Load

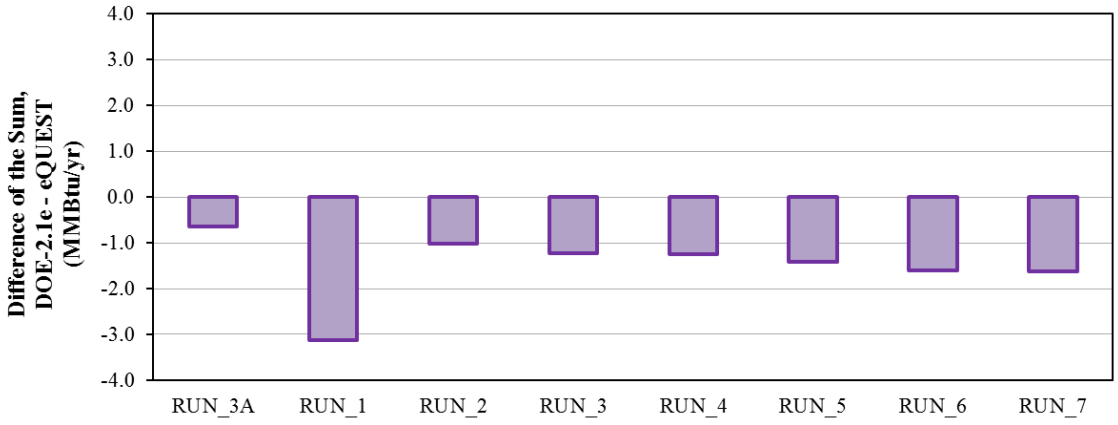

(b) Difference of Total Annual Cooling plus Heating Building Load

Figure 5-30: Total Annual Cooling plus Heating Building Load Comparison from RUN_3A to RUN_7

In general, the results showed the eQUEST simulation had more annual cooling and heating building loads than the DOE-2.1e program. The average differences of the annual building loads between the programs follow as: the cooling was 1.30 MMBtu/yr (0.8%); the heating was 0.36 MMBtu/yr (7.2%); and the sum of the total annual cooling and heating building loads was 1.49 MMBtu/yr (0.9%). The reasons for these loads differences were not resolved.

In the annual cooling building loads, noticeable cooling loads changes occurred in RUN_2 (i.e., reducing conditioned space area from 5,000 ft^2 to 2,500 ft^2), RUN_5 (i.e., removing number of occupancy from 52 to zero), and RUN_6 (i.e., removing plenum space). In the annual heating building loads, noticeable heating loads changes also occurred in RUN_2 and RUN_6. However, the annual heating loads did not have a big change in RUN_5 but had a noticeable change in RUN_1 (i.e., reducing the number of zones from five zones to one single zone).

Not surprisingly, both the cooling loads and the heating loads were significantly decreased in RUN_2, which reduced conditioned space area from 5,000 ft^2 to 2,500 ft^2. In addition, both the annual cooling and heating loads increased in RUN_6, which removed the plenum space. However, the heating loads noticeably decreased in RUN_1, which reduced the space from five zones to one zone, whereas the cooling loads did not have much change. The annual heating loads increased whereas the annual cooling loads decreased in RUN_5, which changed the occupancy number from 52 to zero, due to the reduced people internal heat gain. Other parameter changes (i.e., overhang removal, south-facing orientation, and the door location) in the *Project* category did not result in

large changes for the building cooling and heating loads. The sum of the cooling and heating loads had the similar changes of the annual cooling loads since the cooling loads are a large portion of the total building loads in Houston, a hot and humid climate.

5.2.1.1.2. *Peak Cooling and Heating Loads from RUN_3A to RUN_7*

In this study, the peak cooling and heating loads resulted from RUN_3A to RUN_7 were also compared in Figure 5-31 through Figure 5-33, which present the peak cooling loads, peak heating loads, and total peak cooling and heating loads from the LS-A output, respectively. Each figure includes the peak cooling/heating loads comparison plot and the peak cooling/heating loads difference between DOE-2.1e and eQUEST. The differences were calculated by subtracting from the DOE-2.1e results to the eQUEST results. Table 5-4 summarizes the peak cooling/heating loads resulted from RUN_3A to RUN_7 in the *Project* category, described in Section 4.4.1.1.1.

Table 5-4: Peak Cooling/Heating Loads from RUN_3A to RUN_7

Run Name	Key Modification	DOE-2.1e			eQUEST		
		Peak Cooling Load (kBtu/hr)	Peak Heating Load (kBtu/hr)	Sum of Peak Cooling and Heating Load (kBtu/hr)	Peak Cooling Load (kBtu/hr)	Peak Heating Load (kBtu/hr)	Sum of Peak Cooling and Heating Load (kBtu/hr)
RUN_3A	Building location change	82.4	24.1	106.5	82.8	24.4	107.2
RUN_1	Reduced number of zones	81.9	23.3	105.2	82.8	24.0	106.7
RUN_2	Reduced space area/fenestration	52.7	13.6	66.3	53.1	14.5	67.6
RUN_3	Overhang removed	53.1	13.6	66.7	53.6	14.4	68.0
RUN_4	Orientation faced south	52.1	13.5	65.6	52.5	14.4	66.9
RUN_5	Number of occupancy	40.8	14.2	55.0	41.2	15.0	56.2
RUN_6	Plenum removed	48.1	20.7	68.8	48.6	21.5	70.2
RUN_7	Door size and location	48.0	20.9	68.9	48.6	21.8	70.3

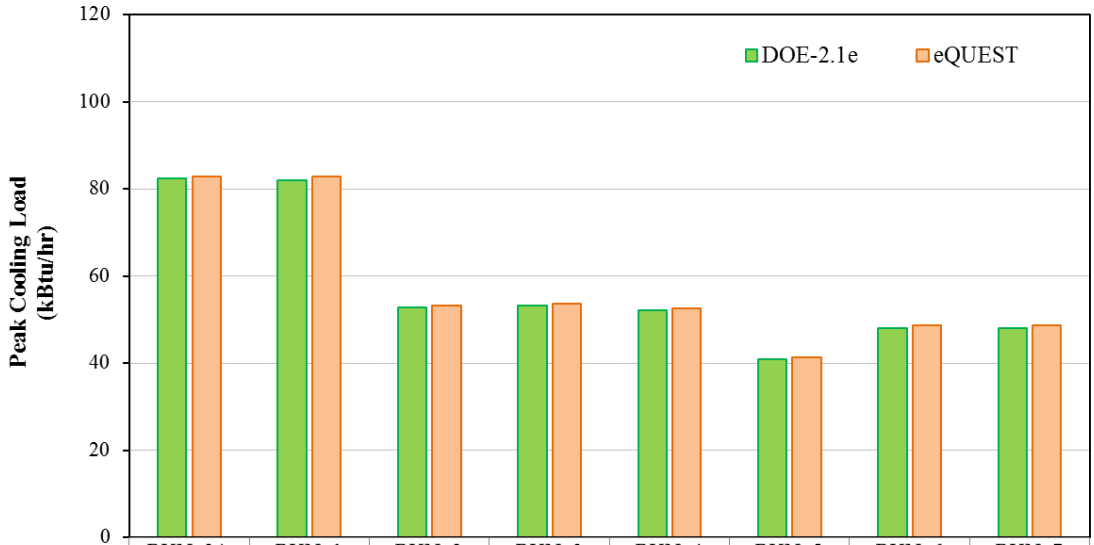

	RUN_3A	RUN_1	RUN_2	RUN_3	RUN_4	RUN_5	RUN_6	RUN_7
DOE-2.1e	82.4	81.9	52.7	53.1	52.1	40.8	48.1	48.0
eQUEST	82.8	82.8	53.1	53.6	52.5	41.2	48.6	48.6

(a) Peak Cooling Building Load

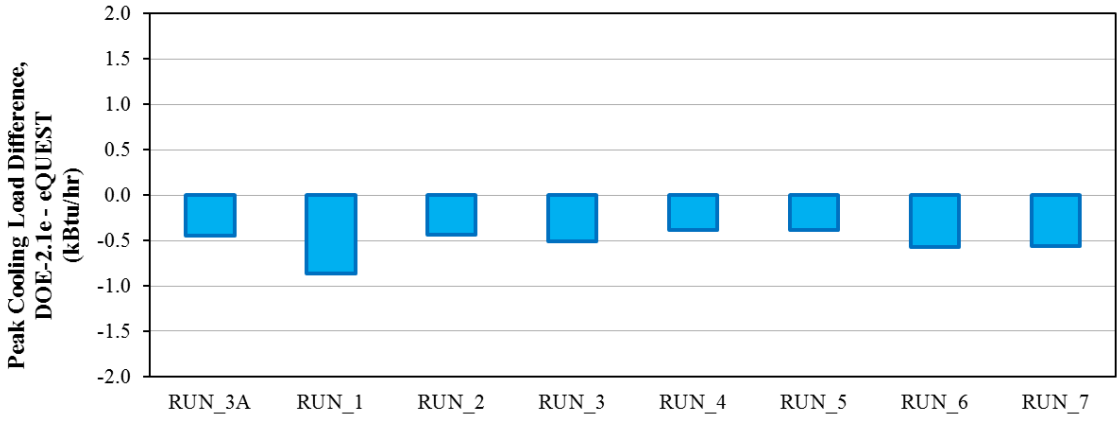

(b) Peak Cooling Building Load Difference

Figure 5-31: Peak Cooling Building Load Comparison from RUN_3A to RUN_7

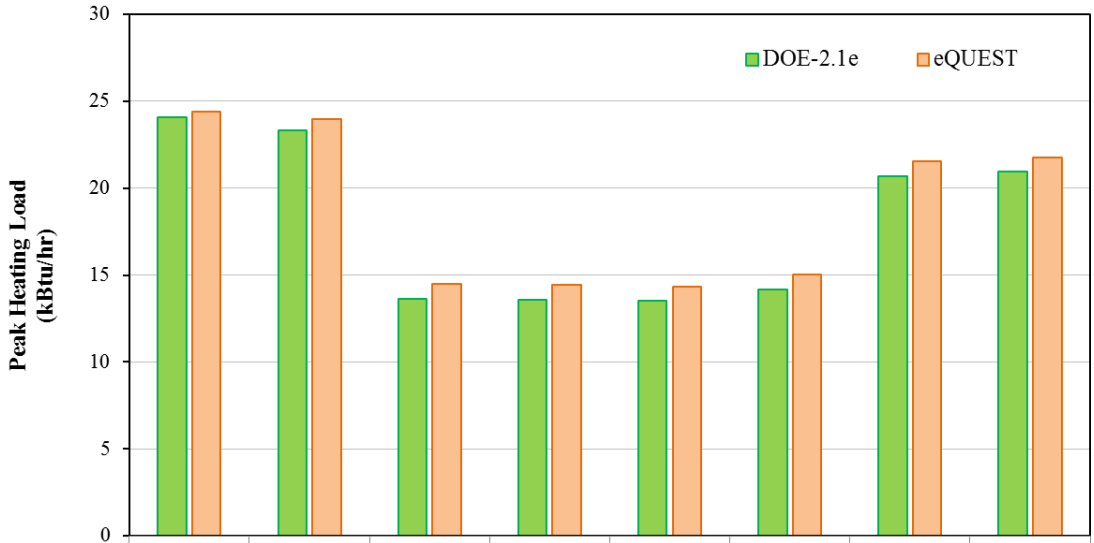

	RUN_3A	RUN_1	RUN_2	RUN_3	RUN_4	RUN_5	RUN_6	RUN_7
DOE-2.1e	24.1	23.3	13.6	13.6	13.5	14.2	20.7	20.9
eQUEST	24.4	24.0	14.5	14.4	14.4	15.0	21.5	21.8

(a) Peak Heating Building Load

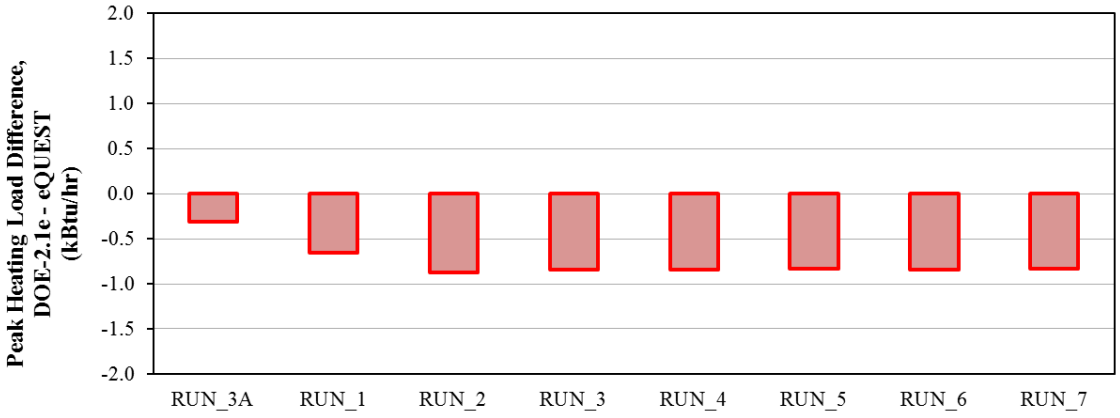

(b) Peak Heating Building Load Difference

Figure 5-32: Peak Heating Building Load Comparison from RUN_3A to RUN_7

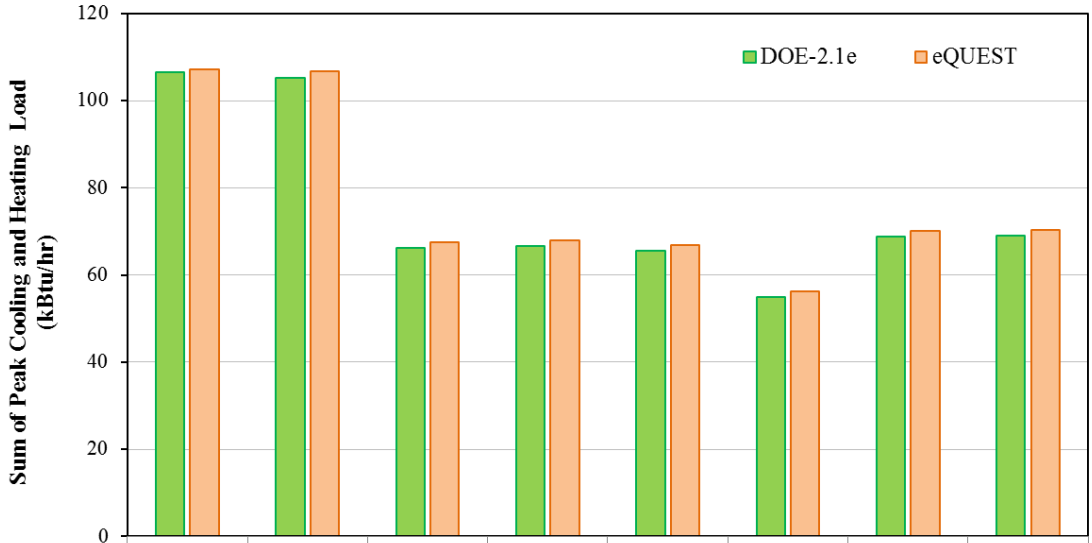

	RUN_3A	RUN_1	RUN_2	RUN_3	RUN_4	RUN_5	RUN_6	RUN_7
DOE-2.1e	106.5	105.2	66.3	66.7	65.6	55.0	68.8	68.9
eQUEST	107.2	106.7	67.6	68.0	66.9	56.2	70.2	70.3

(a) Total Peak Cooling plus Heating Building Load

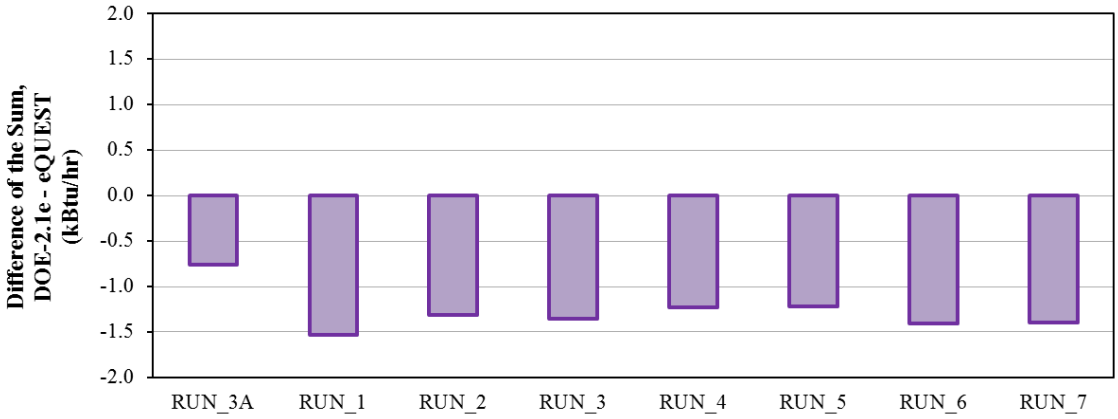

(b) Difference of Total Peak Cooling plus Heating Building Load

Figure 5-33: Total Peak Cooling plus Heating Building Load Comparison from RUN_3A to RUN_7

The eQUEST program had a larger peak hourly load for both cooling and heating than the DOE-2.1e program. The average differences of the peak hourly building loads between the programs follow as: the peak cooling was 0.52 kBtu/hr (0.9%); the peak heating was 0.76 kBtu/hr (4.5%); and the sum of the total peak cooling and heating loads was 1.28 kBtu/hr (1.8%). The reasons for these loads differences were not resolved.

In a similar fashion to the comparison of the annual building loads, noticeable changes for the peak cooling loads occurred in RUN_2 (i.e., reducing conditioned space area from 5,000 ft^2 to 2,500 ft^2), RUN_5 (i.e., removing number of occupancy from 52 to zero), and RUN_6 (i.e., removing plenum space). In addition, noticeable changes for the peak heating loads occurred in RUN_2 and RUN_6. However, the peak heating loads had a little change in RUN_1, which was for reducing the space from five zones to a single zone, unlikely that the annual heating loads had noticeable change.

Both peak cooling and heating loads were significantly decreased after the conditioned space area was reduced from 5,000 ft^2 to 2,500 ft^2 in RUN_2. When the occupancy number changed from 52 to 0 in RUN_5, the peak heating loads increased whereas the peak cooling loads decreased due to the reduced people internal heat gain. When the plenum space was removed in RUN_6, both of the peak loads increased. Other parameter changes (i.e., the reduced number of zones, overhang removal, south-facing orientation, and the door location) in the *Project* category[51] did not result in large changes for both of the peak loads. The sum of the peak cooling and heating loads had the similar changes of the peak cooling loads like the annual building loads comparison.

[51] The *Project* category which defines general structures was described in Section 4.4.1.1.1.

5.2.1.1.3. *Monthly Cooling and Heating Loads Resulted from RUN_30*

The monthly cooling and heating building loads resulted from RUN_30 (i.e., the final residential ASHP base-case model for Houston) are compared in Figure 5-34 through Figure 5-36, which show the monthly cooling loads, the monthly heating loads, and the total monthly cooling and heating loads, respectively. Each figure includes the monthly cooling/heating loads comparison plot and the monthly cooling/heating loads difference between DOE-2.1e and eQUEST. The differences were calculated by subtracting from the DOE-2.1e results to the eQUEST results. Table 5-5 summarizes the resultant monthly cooling and heating loads for RUN_30, which is the residential ASHP base-case model for Houston.

Table 5-5: Monthly Cooling and Heating Building Loads for the Final ASHP Base-Case Model, Houston

Month	DOE-2.1e			eQUEST		
	Cooling Load (MMBtu/month)	Heating Load (MMBtu/month)	Sum of Cooling and Heating Load (MMBtu/month)	Cooling Load (MMBtu/month)	Heating Load (MMBtu/month)	Sum of Cooling and Heating Load (MMBtu/month)
JAN	1.22	4.12	5.34	1.28	4.03	5.31
FEB	1.00	3.92	4.92	1.05	3.82	4.87
MAR	2.24	1.70	3.94	2.33	1.65	3.98
APR	4.06	0.36	4.42	4.17	0.33	4.50
MAY	6.82	0.04	6.86	6.95	0.03	6.98
JUN	9.03	0.00	9.03	9.23	0.00	9.23
JUL	10.73	0.00	10.73	10.90	0.00	10.90
AUG	10.49	0.00	10.49	10.70	0.00	10.70
SEP	8.76	0.00	8.76	8.91	0.00	8.91
OCT	6.05	0.09	6.14	6.28	0.07	6.35
NOV	3.38	0.90	4.27	3.52	0.83	4.35
DEC	1.05	3.53	4.58	1.10	3.40	4.50

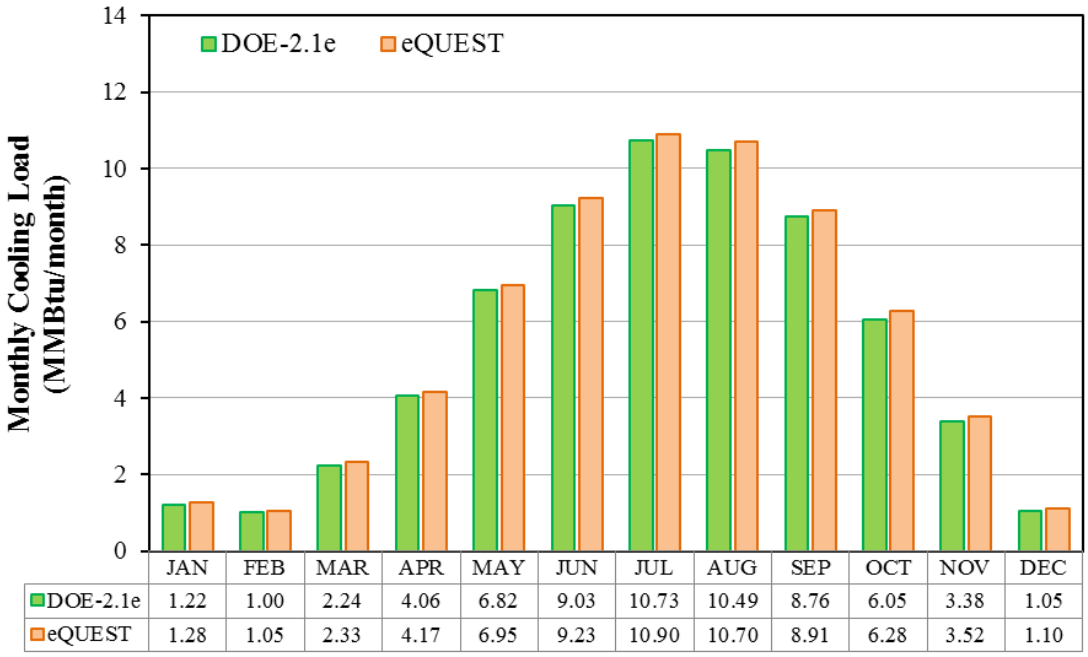

	JAN	FEB	MAR	APR	MAY	JUN	JUL	AUG	SEP	OCT	NOV	DEC
DOE-2.1e	1.22	1.00	2.24	4.06	6.82	9.03	10.73	10.49	8.76	6.05	3.38	1.05
eQUEST	1.28	1.05	2.33	4.17	6.95	9.23	10.90	10.70	8.91	6.28	3.52	1.10

(a) Monthly Cooling Building Load

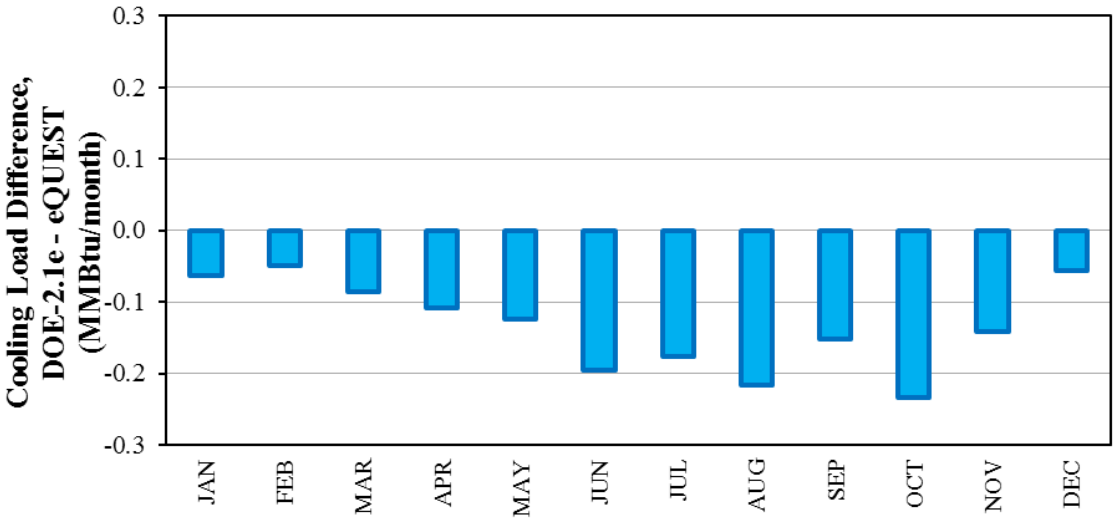

(b) Monthly Cooling Building Load Difference

Figure 5-34: Monthly Cooling Building Load Comparison for RUN_30

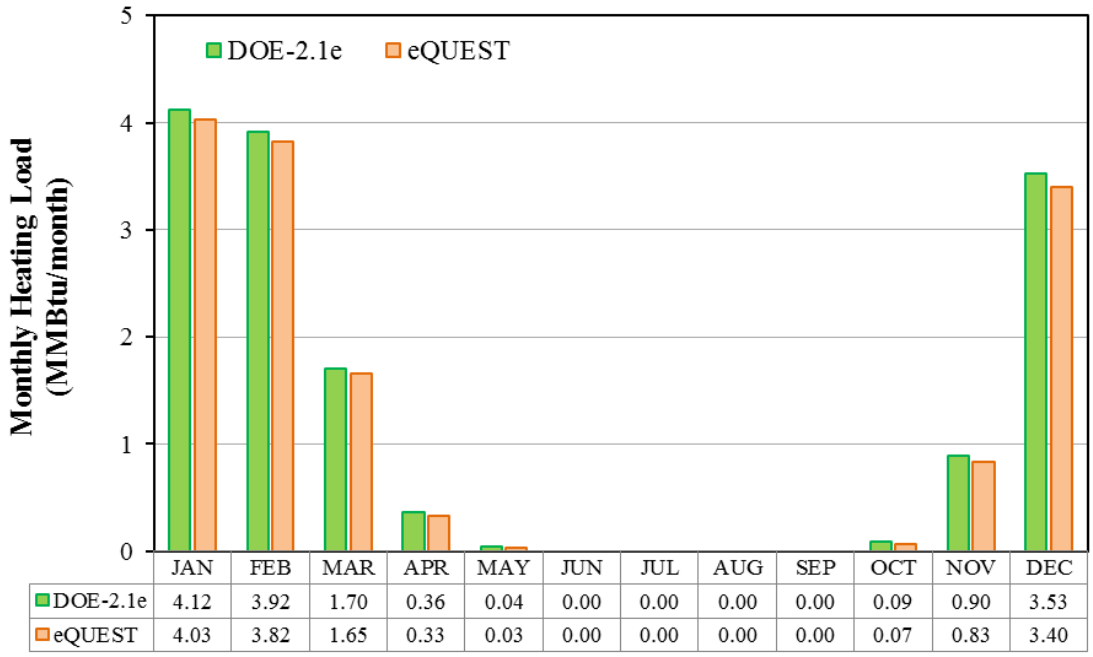

	JAN	FEB	MAR	APR	MAY	JUN	JUL	AUG	SEP	OCT	NOV	DEC
DOE-2.1e	4.12	3.92	1.70	0.36	0.04	0.00	0.00	0.00	0.00	0.09	0.90	3.53
eQUEST	4.03	3.82	1.65	0.33	0.03	0.00	0.00	0.00	0.00	0.07	0.83	3.40

(a) Monthly Heating Building Load

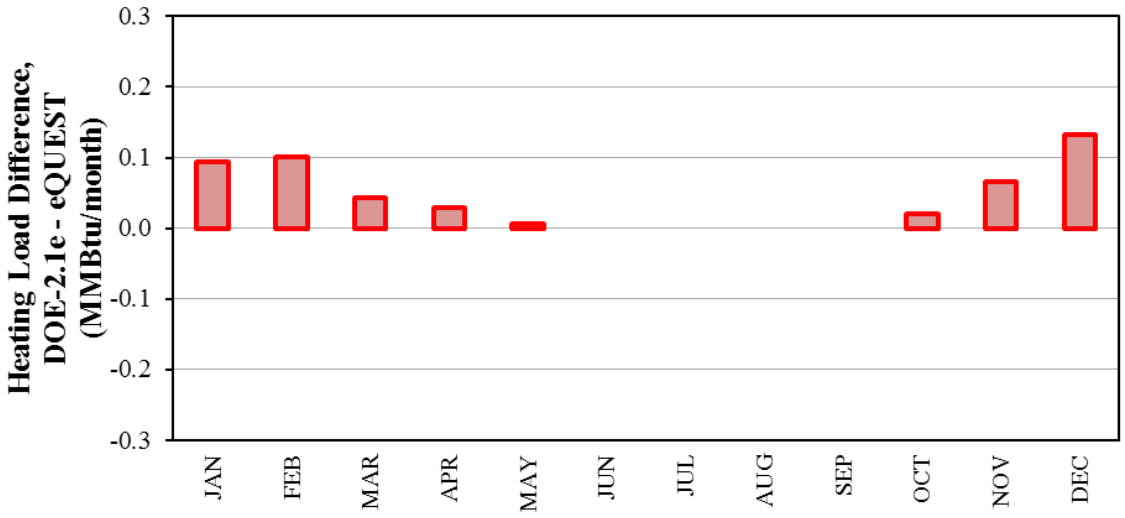

(b) Monthly Heating Building Load Difference

Figure 5-35: Monthly Heating Building Load Comparison for RUN_30

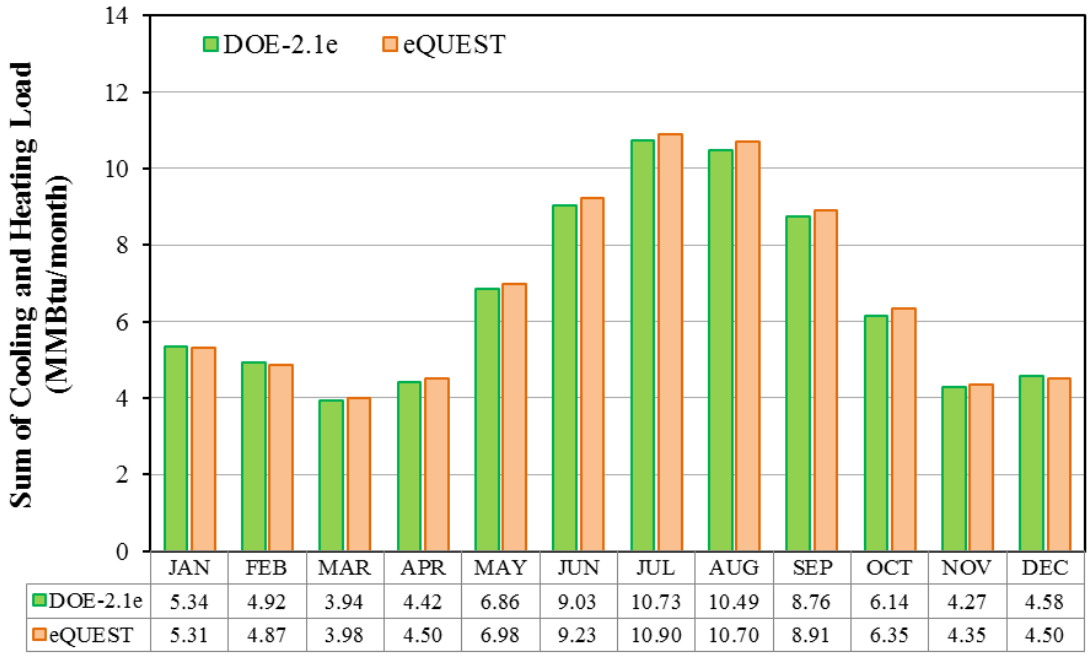

	JAN	FEB	MAR	APR	MAY	JUN	JUL	AUG	SEP	OCT	NOV	DEC
DOE-2.1e	5.34	4.92	3.94	4.42	6.86	9.03	10.73	10.49	8.76	6.14	4.27	4.58
eQUEST	5.31	4.87	3.98	4.50	6.98	9.23	10.90	10.70	8.91	6.35	4.35	4.50

(a) Total Monthly Cooling plus Heating Building Load

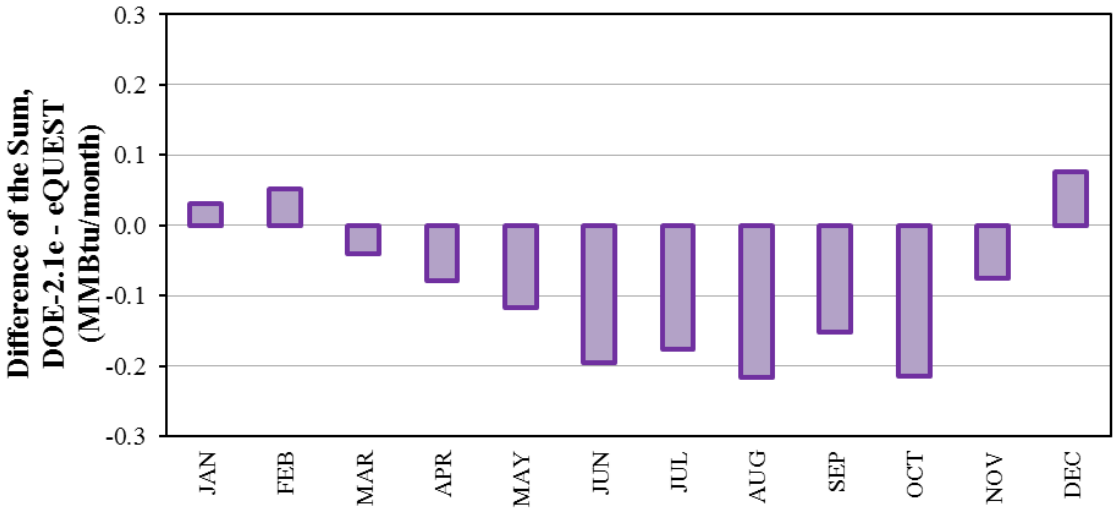

(b) Difference of Total Monthly Cooling plus Heating Building Load

Figure 5-36: Total Monthly Cooling plus Heating Building Load Comparison for RUN_30

The eQUEST program had larger monthly cooling loads than the DOE-2.1e program whereas the eQUEST program had less monthly heating loads than the DOE-2.1e program. In the sum of the monthly cooling and heating loads, the eQUEST program had less heating loads and more cooling loads than the DOE-2.1e program. The average differences of the monthly building loads between the programs follow as: the cooling was 0.13 MMBtu/month (3.3%); the heating was 0.06 MMBtu/month (9.8%); and the sum of the monthly cooling and heating loads was 0.09 MMBtu/month (1.1%). The reasons for the remained loads differences were not resolved in this study.

Based on the comparison of the monthly cooling and heating building loads, it was identified for the ASHP base-case model in Houston that the total cooling and heating building loads from both DOE-2.1e and eQUEST were well-matched within 0.22 MMBtu/month (approximately 2%) of monthly loads differences.

5.2.1.2. Comparison of ASHP System Cooling and Heating Loads

This section presents comparison of the simulated cooling and heating system loads from the residential ASHP base-case model (i.e., RUN_30) for Houston using the DOE-2.1e and eQUEST simulation programs. For the comparison, this study used the monthly system loads from the Heat Pump Cooling/Heating Summary (i.e., SS-Q in both programs). Figure 5-37 through Figure 5-39 shows the monthly system load comparison for the cooling, the heating, and the total cooling and heating, respectively, including plots of the monthly loads comparison and the monthly loads difference. The differences were calculated by subtracting from the DOE-2.1e results to the eQUEST results.

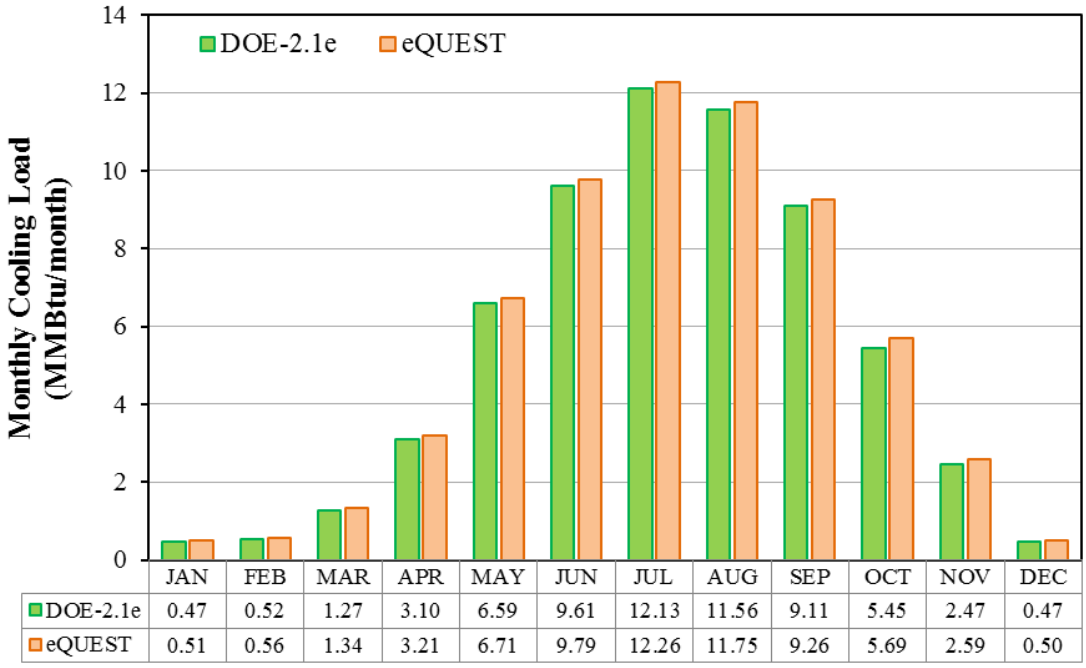

	JAN	FEB	MAR	APR	MAY	JUN	JUL	AUG	SEP	OCT	NOV	DEC
DOE-2.1e	0.47	0.52	1.27	3.10	6.59	9.61	12.13	11.56	9.11	5.45	2.47	0.47
eQUEST	0.51	0.56	1.34	3.21	6.71	9.79	12.26	11.75	9.26	5.69	2.59	0.50

(a) Monthly Cooling System Load

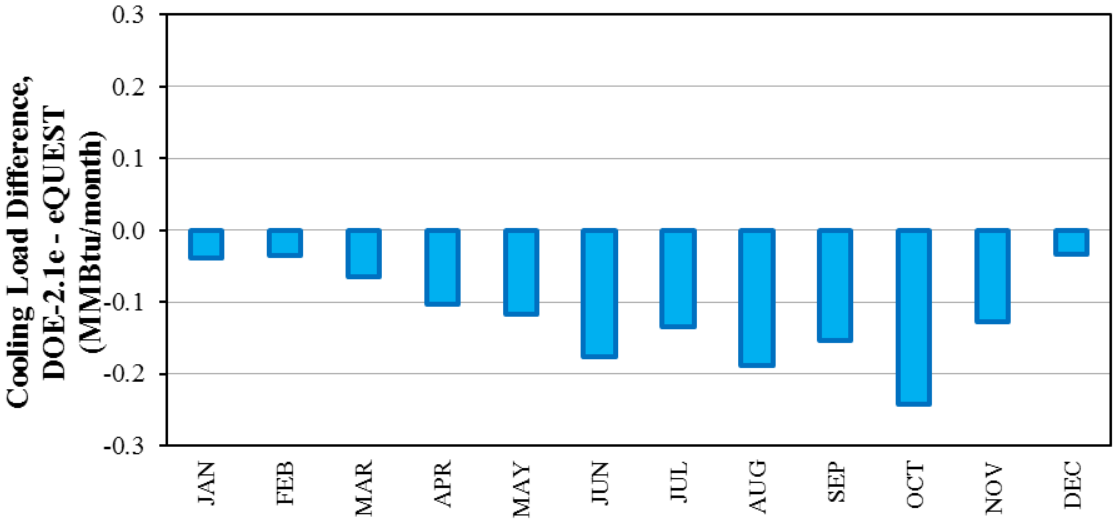

(b) Monthly Cooling System Load Difference

Figure 5-37: Monthly Cooling System Load Comparison for RUN_30

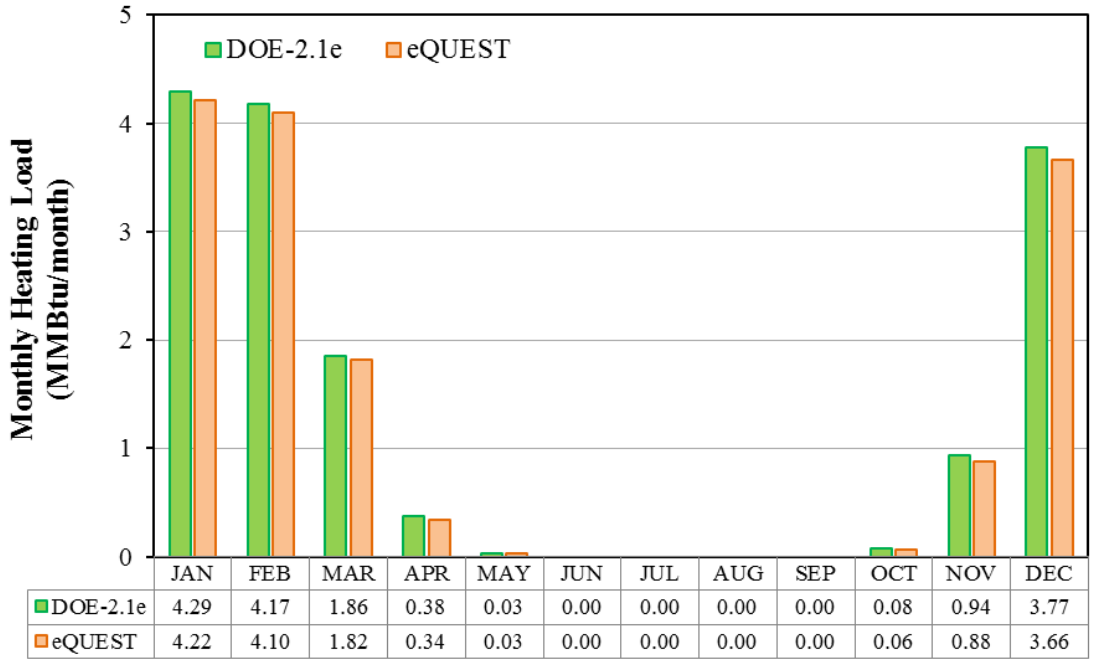

	JAN	FEB	MAR	APR	MAY	JUN	JUL	AUG	SEP	OCT	NOV	DEC
DOE-2.1e	4.29	4.17	1.86	0.38	0.03	0.00	0.00	0.00	0.00	0.08	0.94	3.77
eQUEST	4.22	4.10	1.82	0.34	0.03	0.00	0.00	0.00	0.00	0.06	0.88	3.66

(a) Monthly Heating System Load

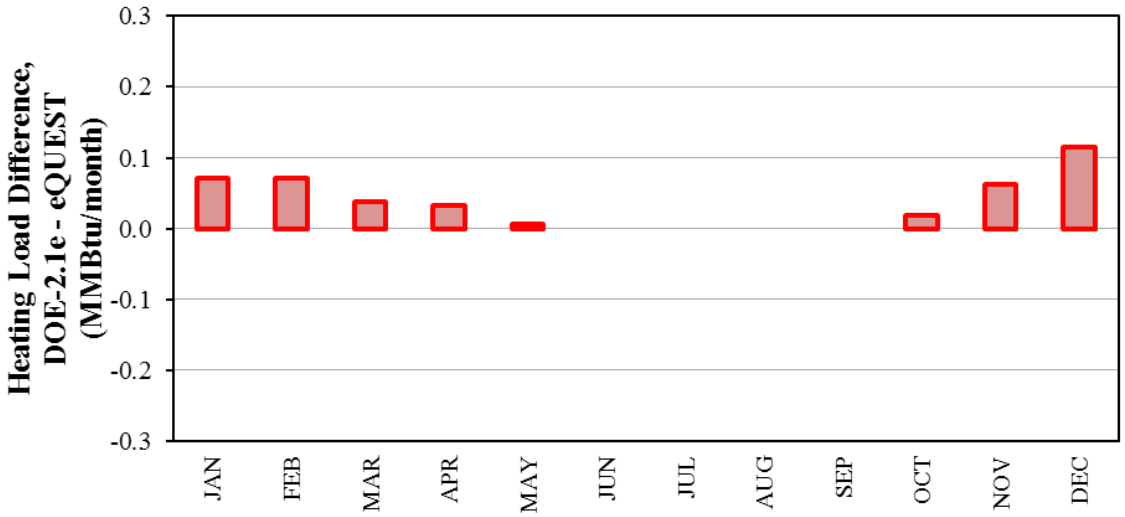

(b) Monthly Heating System Load Difference

Figure 5-38: Monthly Heating System Load Comparison for RUN_30

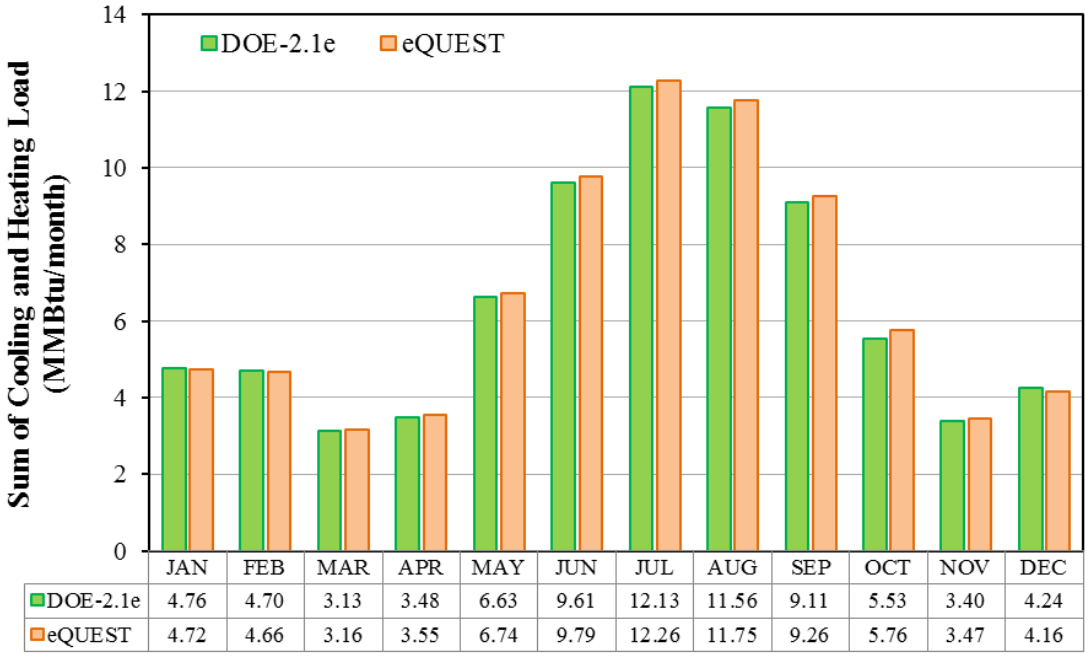

	JAN	FEB	MAR	APR	MAY	JUN	JUL	AUG	SEP	OCT	NOV	DEC
DOE-2.1e	4.76	4.70	3.13	3.48	6.63	9.61	12.13	11.56	9.11	5.53	3.40	4.24
eQUEST	4.72	4.66	3.16	3.55	6.74	9.79	12.26	11.75	9.26	5.76	3.47	4.16

(a) Total Monthly Cooling plus Heating System Load

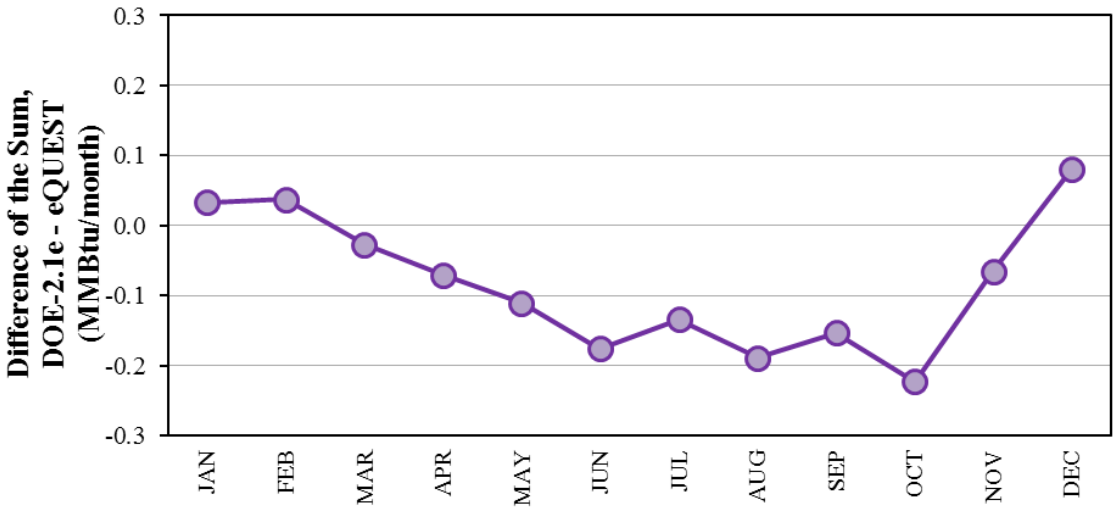

(b) Difference of Total Monthly Cooling plus Heating System Load

Figure 5-39: Total Monthly Cooling plus Heating System Load Comparison for RUN_30

Not surprisingly, the comparison of the system's loads between DOE-2.1e and eQUEST showed similar pattern to the comparison of the building's loads in Section 5.2.1.1. The eQUEST program had more monthly cooling loads and less heating loads than the DOE-2.1e program. In the sum of the monthly cooling and heating loads, the eQUEST program had less heating loads and more cooling loads than the DOE-2.1e program. Table 5-8 summarizes the resultant monthly cooling and heating system loads of RUN_30, which is the residential ASHP base-case model for Houston. In addition, Table 5-6 presents the difference of the resultant monthly cooling and heating system loads of RUN_30 between DOE-2.1e and eQUEST.

Table 5-6: Monthly Cooling/Heating System Loads for the ASHP Base-Case Model, Houston

Month	DOE-2.1e			eQUEST		
	Cooling Load (MMBtu/month)	Heating Load (MMBtu/month)	Sum of Cooling and Heating Load (MMBtu/month)	Cooling Load (MMBtu/month)	Heating Load (MMBtu/month)	Sum of Cooling and Heating Load (MMBtu/month)
JAN	0.47	4.29	4.76	0.51	4.22	4.72
FEB	0.52	4.17	4.70	0.56	4.10	4.66
MAR	1.27	1.86	3.13	1.34	1.82	3.16
APR	3.10	0.38	3.48	3.21	0.34	3.55
MAY	6.59	0.03	6.63	6.71	0.03	6.74
JUN	9.61	0.00	9.61	9.79	0.00	9.79
JUL	12.13	0.00	12.13	12.26	0.00	12.26
AUG	11.56	0.00	11.56	11.75	0.00	11.75
SEP	9.11	0.00	9.11	9.26	0.00	9.26
OCT	5.45	0.08	5.53	5.69	0.06	5.76
NOV	2.47	0.94	3.40	2.59	0.88	3.47
DEC	0.47	3.77	4.24	0.50	3.66	4.16
TOTAL (MMBtu/yr)	62.75	15.52	78.27	64.17	15.10	79.27

Table 5-7: Differences of the Monthly Cooling/Heating System Loads for the ASHP Base-Case Model, Houston

Month	Difference of Monthly Cooling Load		Difference of Monthly Heating Load		Difference of Total Monthly Cooling and Heating Load	
	MMBtu/month	%	MMBtu/month	%	MMBtu/month	%
JAN	-0.04	-8.33%	0.07	1.68%	0.03	0.69%
FEB	-0.04	-6.69%	0.07	1.72%	0.04	0.79%
MAR	-0.06	-5.11%	0.04	2.05%	-0.03	-0.86%
APR	-0.10	-3.32%	0.03	8.53%	-0.07	-2.04%
MAY	-0.12	-1.79%	0.01	21.88%	-0.11	-1.68%
JUN	-0.18	-1.83%	-	-	-0.18	-1.83%
JUL	-0.13	-1.10%	-	-	-0.13	-1.10%
AUG	-0.19	-1.63%	-	-	-0.19	-1.63%
SEP	-0.15	-1.68%	-	-	-0.15	-1.68%
OCT	-0.24	-4.44%	0.02	23.46%	-0.22	-4.03%
NOV	-0.13	-5.15%	0.06	6.62%	-0.06	-1.91%
DEC	-0.03	-7.25%	0.12	3.05%	0.08	1.91%
AVERAGE	-0.12	-4.03%	0.05	8.62%	-0.08	-1.12%
TOTAL (MMBtu/yr)	-1.42	-2.25%	0.42	2.69%	-1.00	-1.28%

Notes:
1. The load differences were calculated by subtracting from DEO-2.1e to eQUEST.
2. The % differences were calculated by dividing the load differences by the DOE-2.1e monthly loads.

The average differences of the monthly system loads between the programs follow as: the monthly cooling loads average difference was 0.12 MMBtu/month (4.03%); the monthly heating loads average difference was 0.05 MMBtu/month (8.62%); and the sum of the monthly cooling and heating loads average difference was 0.08 MMBtu/month (1.12%). In addition, for the annual cooling and heating system loads, the annual cooling loads average difference was 1.42 MMBtu/yr (2.25%); the annual

heating loads average difference was 0.42 MMBtu/yr (2.69%); and the sum of the annual cooling and heating loads average difference was 1.00 MMBtu/yr (1.28%). Based on the comparison of the system loads, it was identified for the ASHP base-case model in Houston that the cooling and heating system loads from both DOE-2.1e and eQUEST were well-matched, although minor, unknown differences still remained.

5.2.1.3. Comparison of Site Energy Use

This section presents the site energy use comparison of the residential ASHP base-case model in Houston between the DOE-2.1e and eQUEST programs, following the procedure of the step-by-step input changes described in Section 4.4.1.1. The simulated site energy uses from RUN_8 to RUN_30 were compared after the system type was modified from VAV (i.e., RUN_3A through RUN_7) to RESYS (i.e., RUN_8 through RUN_30).

The simulated energy use differences between DOE-2.1e and eQUEST were described in six categories: total energy use, area lights, miscellaneous equipment, space heat, space cool, and others which include the pump and fan energy use. In addition, the energy use intensity (EUI) is also included. Table 5-8 and Table 5-9 present the summary table of the annual site energy use and EUI for each simulation, including description of the key modification.

Figure 5-40 and Figure 5-41 show the plots of the resultant site energy use changes in each sector from RUN_8 to RUN_30 to develop the residential ASHP base-case model in Houston, using the DOE-2.1e and eQUEST programs. In addition, Figure

5-42 and Figure 5-43 show the plots of their EUI changes; and, Figure 5-44 presents comparison of the total site energy use differences between the programs.

Table 5-8: DOE-2.1e Site Energy Use Results from RUN_8 to RUN_30

Category	Run Name	Key Modification	Area Lights (MMBtu/yr)	Misc. Equipment (MMBtu/yr)	Space Heat (MMBtu/yr)	Space Cool (MMBtu/yr)	Fan & Pump (MMBtu/yr)	DHW (MMBtu/yr)	Total Site Energy Use (MMBtu/yr)	Energy Use Intensity (kBtu/yr-ft^2)
ASHP System	RUN_8	System from VAVS to ASHP	37.2	22.3	0.3	37.3	25.8	0.0	122.9	49.2
	RUN_9	Cooling efficiency	37.2	22.3	0.3	18.0	25.8	0.0	103.6	41.4
	RUN_10	Heating efficiency	37.2	22.3	0.2	18.0	25.8	0.0	103.5	41.4
	RUN_11	Constant fan schedule	37.2	22.3	0.1	17.5	24.3	0.0	101.4	40.6
	RUN_12	Thermostat heating	37.2	22.3	1.4	17.7	25.1	0.0	103.7	41.5
	RUN_13	Thermostat cooling	37.2	22.3	2.4	31.9	77.9	0.0	171.7	68.7
	RUN_14	Supply air flow	37.2	22.3	2.7	23.7	9.6	0.0	95.5	38.2
Construction	RUN_15	Floor insulation	37.2	22.3	5.8	20.9	8.9	0.0	95.1	38.0
	RUN_16	Roof insulation	37.2	22.3	4.9	20.1	8.5	0.0	93.0	37.2
	RUN_17	Roof absorptance	37.2	22.3	4.9	20.2	8.5	0.0	93.1	37.2
	RUN_18	Wall insulation	37.2	22.3	4.6	20.0	8.4	0.0	92.5	37.0
	RUN_19	Wall absorptance	37.2	22.3	4.6	20.1	8.4	0.0	92.6	37.0
	RUN_20	Door insulation	37.2	22.3	4.5	19.7	8.2	0.0	91.9	36.8
	RUN_21	Glass conductance/SHGC/Frame	37.2	22.3	5.5	15.2	6.6	0.0	86.8	34.7
	RUN_22	Infiltration	37.2	22.3	7.2	18.0	7.0	0.0	91.7	36.7
	RUN_23	Ground reflectance	37.2	22.3	7.1	18.3	7.1	0.0	92.0	36.8
Internal Gain	RUN_24	Lighting power density	4.8	22.3	8.6	12.9	5.3	0.0	53.9	21.6
	RUN_25	Equipment power density	4.8	5.9	9.8	10.5	4.7	0.0	35.7	14.3
Schedule	RUN_26	Lighting schedule	14.6	5.9	8.7	11.7	4.9	0.0	45.8	18.3
	RUN_27	Equipment schedule	14.6	19.7	7.4	13.5	5.3	0.0	60.5	24.2
	RUN_28	Infiltration schedule	14.6	19.7	7.4	13.5	5.3	0.0	60.5	24.2
	RUN_29	Interior shading schedule	14.6	19.7	7.6	12.4	4.9	0.0	59.2	23.7
DHW	RUN_30	DHW system	14.6	19.7	7.6	12.4	4.9	10.8	70.0	28.0

Table 5-9: eQUEST Site Energy Use Results from RUN_8 to RUN_30

Category	Run Name	Key Modification	Area Lights (MMBtu/yr)	Misc. Equipment (MMBtu/yr)	Space Heat (MMBtu/yr)	Space Cool (MMBtu/yr)	Fan & Pump (MMBtu/yr)	DHW (MMBtu/yr)	Total Site Energy Use (MMBtu/yr)	Energy Use Intensity (kBtu/yr-ft^2)
ASHP System	RUN_8	System from VAVS to ASHP	37.1	22.3	0.3	37.1	25.5	0.0	122.3	48.9
	RUN_9	Cooling efficiency	37.1	22.3	0.3	17.9	25.5	0.0	103.1	41.2
	RUN_10	Heating efficiency	37.1	22.3	0.2	17.9	25.5	0.0	103.0	41.2
	RUN_11	Constant fan schedule	37.1	22.3	0.1	17.4	24.1	0.0	101.0	40.4
	RUN_12	Thermostat heating	37.1	22.3	1.1	17.6	24.9	0.0	103.0	41.2
	RUN_13	Thermostat cooling	37.1	22.3	1.7	32.3	77.4	0.0	170.8	68.3
	RUN_14	Supply air flow	37.1	22.3	2.1	25.2	7.3	0.0	94.0	37.6
Construction	RUN_15	Floor insulation	37.1	22.3	5.2	22.6	7.0	0.0	94.2	37.7
	RUN_16	Roof insulation	37.1	22.3	4.3	21.9	6.6	0.0	92.2	36.9
	RUN_17	Roof absorptance	37.1	22.3	4.3	22.0	6.7	0.0	92.4	37.0
	RUN_18	Wall insulation	37.1	22.3	3.9	21.8	6.6	0.0	91.7	36.7
	RUN_19	Wall absorptance	37.1	22.3	3.9	21.9	6.6	0.0	91.8	36.7
	RUN_20	Door insulation	37.1	22.3	4.0	21.4	6.5	0.0	91.3	36.5
	RUN_21	Glass conductance/SHGC/Frame	37.1	22.3	4.8	16.9	5.3	0.0	86.4	34.6
	RUN_22	Infiltration	37.1	22.3	6.4	19.7	6.3	0.0	91.8	36.7
	RUN_23	Ground reflectance	37.1	22.3	6.3	19.9	6.4	0.0	92.0	36.8
Internal Gain	RUN_24	Lighting power density	4.8	22.3	7.7	14.3	5.1	0.0	54.2	21.7
	RUN_25	Equipment power density	4.8	5.9	8.9	11.5	4.4	0.0	35.5	14.2
Schedule	RUN_26	Lighting schedule	14.6	5.9	7.7	12.8	4.6	0.0	45.6	18.2
	RUN_27	Equipment schedule	14.6	19.7	6.3	14.9	5.0	0.0	60.5	24.2
	RUN_28	Infiltration schedule	14.6	19.7	6.3	14.9	5.0	0.0	60.5	24.2
	RUN_29	Interior shading schedule	14.6	19.7	6.5	13.7	4.7	0.0	59.2	23.7
DHW	RUN_30	DHW system	14.6	19.7	6.5	13.7	4.7	10.9	70.1	28.0

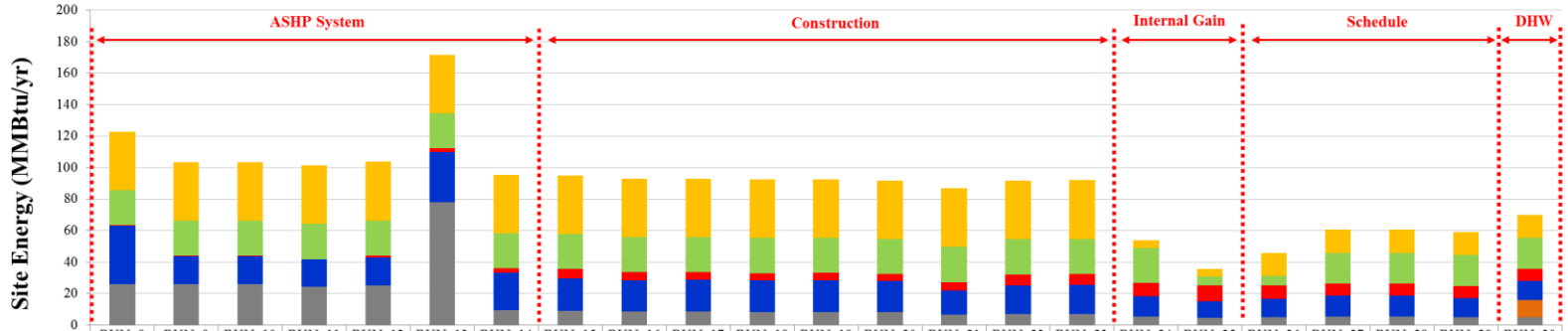

	RUN_8	RUN_9	RUN_10	RUN_11	RUN_12	RUN_13	RUN_14	RUN_15	RUN_16	RUN_17	RUN_18	RUN_19	RUN_20	RUN_21	RUN_22	RUN_23	RUN_24	RUN_25	RUN_26	RUN_27	RUN_28	RUN_29	RUN_30
TOTAL	122.9	103.6	103.5	101.4	103.7	171.7	95.5	95.1	93.0	93.1	92.5	92.6	91.9	86.8	91.7	92.0	53.9	35.7	45.8	60.5	60.5	59.2	70.0
Area Lights	37.2	37.2	37.2	37.2	37.2	37.2	37.2	37.2	37.2	37.2	37.2	37.2	37.2	37.2	37.2	37.2	4.8	4.8	14.6	14.6	14.6	14.6	14.6
Equipment	22.3	22.3	22.3	22.3	22.3	22.3	22.3	22.3	22.3	22.3	22.3	22.3	22.3	22.3	22.3	22.3	22.3	5.9	5.9	19.7	19.7	19.7	19.7
Space Heat	0.3	0.3	0.2	0.1	1.4	2.4	2.7	5.8	4.9	4.9	4.6	4.6	4.5	5.5	7.2	7.1	8.6	9.8	8.7	7.4	7.4	7.6	7.6
Space Cool	37.3	18.0	18.0	17.5	17.7	31.9	23.7	20.9	20.1	20.2	20.0	20.1	19.7	15.2	18.0	18.3	12.9	10.5	11.7	13.5	13.5	12.4	12.4
DHW	0.0	0.0	0.0	0.0	0.0	0.0	0.0	0.0	0.0	0.0	0.0	0.0	0.0	0.0	0.0	0.0	0.0	0.0	0.0	0.0	0.0	0.0	10.8
Fan+Pump	25.8	25.8	25.8	24.3	25.1	77.9	9.6	8.9	8.5	8.5	8.4	8.4	8.2	6.6	7.0	7.1	5.3	4.7	4.9	5.3	5.3	4.9	4.9

Figure 5-40: DOE-2.1e Site Energy Use Resulted from RUN_8 to RUN_30

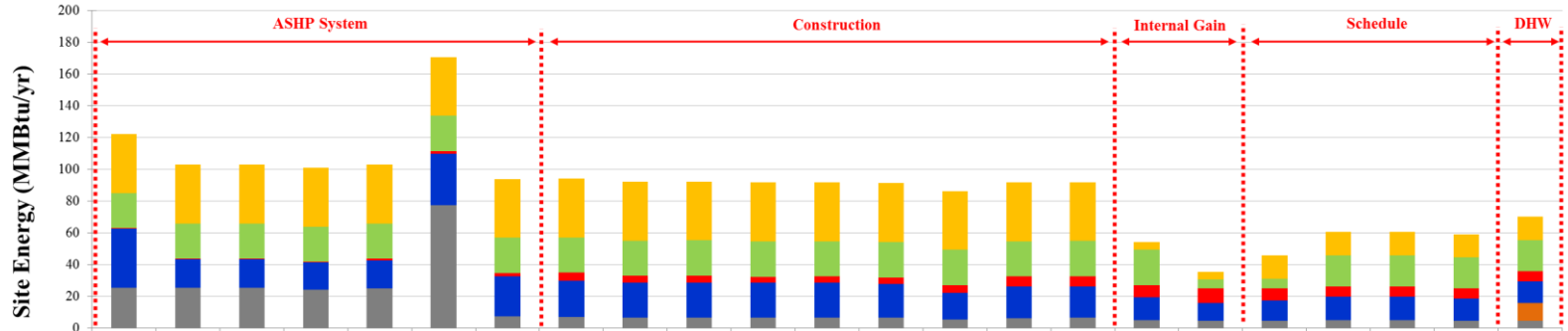

	RUN_8	RUN_9	RUN_10	RUN_11	RUN_12	RUN_13	RUN_14	RUN_15	RUN_16	RUN_17	RUN_18	RUN_19	RUN_20	RUN_21	RUN_22	RUN_23	RUN_24	RUN_25	RUN_26	RUN_27	RUN_28	RUN_29	RUN_30
TOTAL	122.3	103.1	103.0	101.0	103.0	170.8	94.0	94.2	92.2	92.4	91.7	91.8	91.3	86.4	91.8	92.0	54.2	35.5	45.6	60.5	60.5	59.2	70.1
Area Lights	37.1	37.1	37.1	37.1	37.1	37.1	37.1	37.1	37.1	37.1	37.1	37.1	37.1	37.1	37.1	37.1	4.8	4.8	14.6	14.6	14.6	14.6	14.6
Equipment	22.3	22.3	22.3	22.3	22.3	22.3	22.3	22.3	22.3	22.3	22.3	22.3	22.3	22.3	22.3	22.3	22.3	5.9	5.9	19.7	19.7	19.7	19.7
Space Heat	0.3	0.3	0.2	0.1	1.1	1.7	2.1	5.2	4.3	4.3	3.9	3.9	4.0	4.8	6.4	6.3	7.7	8.9	7.7	6.3	6.3	6.5	6.5
Space Cool	37.1	17.9	17.9	17.4	17.6	32.3	25.2	22.6	21.9	22.0	21.8	21.9	21.4	16.9	19.7	19.9	14.3	11.5	12.8	14.9	14.9	13.7	13.7
DHW	0.0	0.0	0.0	0.0	0.0	0.0	0.0	0.0	0.0	0.0	0.0	0.0	0.0	0.0	0.0	0.0	0.0	0.0	0.0	0.0	0.0	0.0	10.9
Fan+Pump	25.5	25.5	25.5	24.1	24.9	77.4	7.3	7.0	6.6	6.7	6.6	6.6	6.5	5.3	6.3	6.4	5.1	4.4	4.6	5.0	5.0	4.7	4.7

Figure 5-41: eQUEST Site Energy Use Resulted from RUN_8 to RUN_30

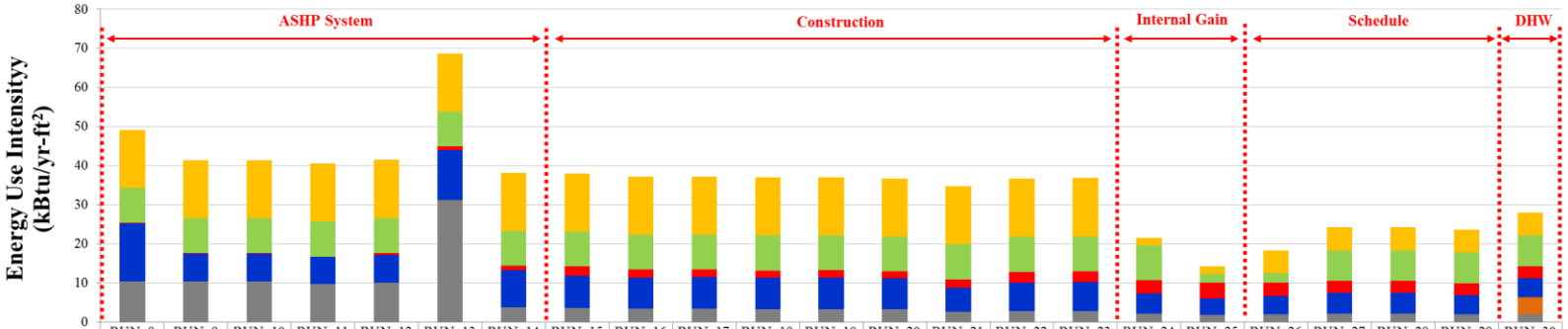

	RUN_8	RUN_9	RUN_10	RUN_11	RUN_12	RUN_13	RUN_14	RUN_15	RUN_16	RUN_17	RUN_18	RUN_19	RUN_20	RUN_21	RUN_22	RUN_23	RUN_24	RUN_25	RUN_26	RUN_27	RUN_28	RUN_29	RUN_30
TOTAL	49.2	41.4	41.4	40.6	41.5	68.7	38.2	38.0	37.2	37.2	37.0	37.0	36.8	34.7	36.7	36.8	21.6	14.3	18.3	24.2	24.2	23.7	28.0
Area Lights	14.9	14.9	14.9	14.9	14.9	14.9	14.9	14.9	14.9	14.9	14.9	14.9	14.9	14.9	14.9	14.9	1.9	1.9	5.8	5.8	5.8	5.8	5.8
Equipment	8.9	8.9	8.9	8.9	8.9	8.9	8.9	8.9	8.9	8.9	8.9	8.9	8.9	8.9	8.9	8.9	8.9	2.4	2.4	7.9	7.9	7.9	7.9
Space Heat	0.1	0.1	0.1	0.0	0.6	1.0	1.1	2.3	2.0	2.0	1.8	1.8	1.8	2.2	2.9	2.8	3.4	3.9	3.5	3.0	3.0	3.0	3.0
Space Cool	14.9	7.2	7.2	7.0	7.1	12.8	9.5	8.4	8.0	8.1	8.0	8.0	7.9	6.1	7.2	7.3	5.2	4.2	4.7	5.4	5.4	5.0	5.0
DHW	0.0	0.0	0.0	0.0	0.0	0.0	0.0	0.0	0.0	0.0	0.0	0.0	0.0	0.0	0.0	0.0	0.0	0.0	0.0	0.0	0.0	0.0	4.3
Fan+Pump	10.3	10.3	10.3	9.7	10.0	31.2	3.8	3.6	3.4	3.4	3.4	3.4	3.3	2.6	2.8	2.8	2.1	1.9	2.0	2.1	2.1	2.0	2.0

Figure 5-42: DOE-2.1e Energy Use Intensity Resulted from RUN_8 to RUN_30

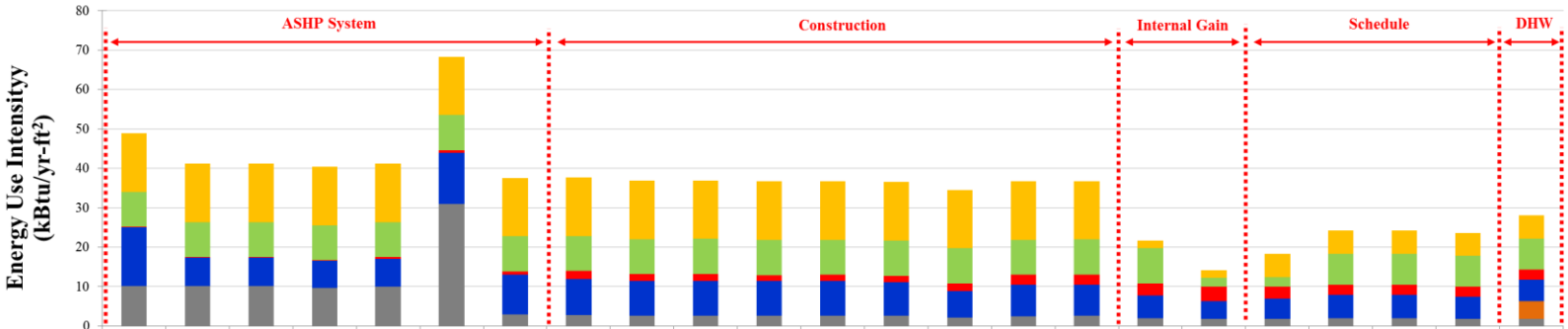

	RUN_8	RUN_9	RUN_10	RUN_11	RUN_12	RUN_13	RUN_14	RUN_15	RUN_16	RUN_17	RUN_18	RUN_19	RUN_20	RUN_21	RUN_22	RUN_23	RUN_24	RUN_25	RUN_26	RUN_27	RUN_28	RUN_29	RUN_30
TOTAL	48.9	41.2	41.2	40.4	41.2	68.3	37.6	37.7	36.9	37.0	36.7	36.7	36.5	34.6	36.7	36.8	21.7	14.2	18.2	24.2	24.2	23.7	28.0
Area Lights	14.8	14.8	14.8	14.8	14.8	14.8	14.8	14.8	14.8	14.8	14.8	14.8	14.8	14.8	14.8	14.8	1.9	1.9	5.8	5.8	5.8	5.8	5.8
Equipment	8.9	8.9	8.9	8.9	8.9	8.9	8.9	8.9	8.9	8.9	8.9	8.9	8.9	8.9	8.9	8.9	8.9	2.4	2.4	7.9	7.9	7.9	7.9
Space Heat	0.1	0.1	0.1	0.0	0.4	0.7	0.8	2.1	1.7	1.7	1.6	1.6	1.6	1.9	2.6	2.5	3.1	3.6	3.1	2.5	2.5	2.6	2.6
Space Cool	14.8	7.2	7.2	7.0	7.0	12.9	10.1	9.0	8.8	8.8	8.7	8.8	8.6	6.8	7.9	8.0	5.7	4.6	5.1	6.0	6.0	5.5	5.5
DHW	0.0	0.0	0.0	0.0	0.0	0.0	0.0	0.0	0.0	0.0	0.0	0.0	0.0	0.0	0.0	0.0	0.0	0.0	0.0	0.0	0.0	0.0	4.4
Fan+Pump	10.2	10.2	10.2	9.6	10.0	31.0	2.9	2.8	2.6	2.7	2.6	2.6	2.6	2.1	2.5	2.6	2.0	1.8	1.8	2.0	2.0	1.9	1.9

Figure 5-43: eQUEST Energy Use Intensity Resulted from RUN_8 to RUN_30

Results from the step-by-step input changes showed that the ASHP base-case model had eight noticeable changes in the total site energy use, which resulted from both the DOE-2.1e and eQUEST programs (Figure 5-40 through Figure 5-43), as follows:

- In RUN_9, which changed the cooling efficiency from SEER 7.3 to 13, the total site energy use decreased due to the lower space cooling energy use;
- In RUN_13, which set the cooling thermostat at a constant 75 F from the cooling thermostat temperature schedule defined in RUN 3A (Figure 4-53), the totCal site energy use increased due to the higher space cooling energy use and fan energy use;
- In RUN_14, which reduced the supply air flow from 7,366 cfm to 1,800 cfm, the total site energy use decreased due to the lower fan energy use;
- In RUN_24, which modified the lighting power density from 1.5 W/ft^2 to 0.1951 W/ft^2, the total site energy use decreased due to the lower lighting energy use and internal gain;
- In RUN_25, which modified the equipment power density from 1.0 W/ft^2 to 0.2632 W/ft^2, the total site energy use decreased due to the lower equipment energy use and internal gain;
- In RUN_26, which set the lighting system to be always on, the total site energy use increased due to the higher lighting energy use and internal gain;
- In RUN_27, which set the equipment system to be always on, the total site energy use increased due to the higher equipment energy use and internal gain; and
- In RUN_30, which defined the residential electric DHW system, the total site energy use increased due to the DHW energy use.

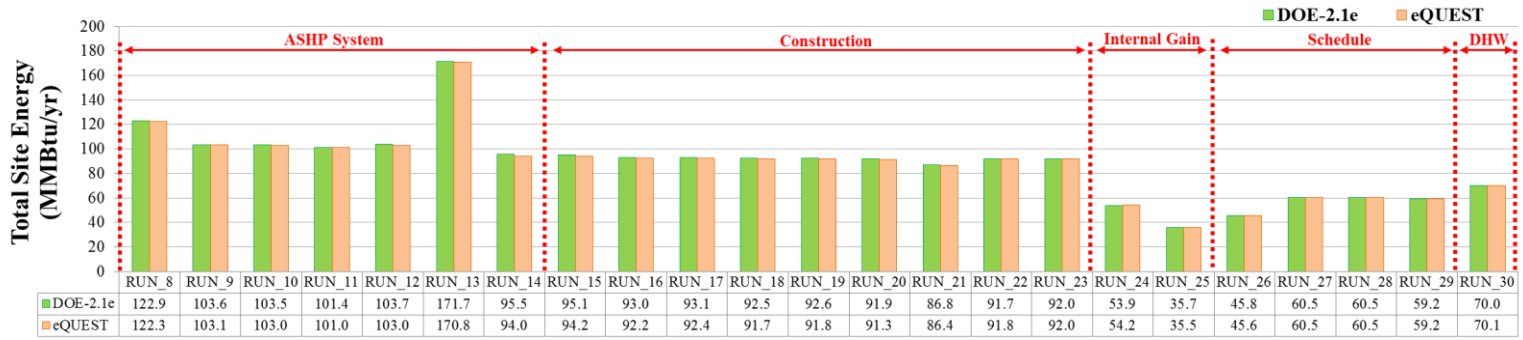

	RUN_8	RUN_9	RUN_10	RUN_11	RUN_12	RUN_13	RUN_14	RUN_15	RUN_16	RUN_17	RUN_18	RUN_19	RUN_20	RUN_21	RUN_22	RUN_23	RUN_24	RUN_25	RUN_26	RUN_27	RUN_28	RUN_29	RUN_30
DOE-2.1e	122.9	103.6	103.5	101.4	103.7	171.7	95.5	95.1	93.0	93.1	92.5	92.6	91.9	86.8	91.7	92.0	53.9	35.7	45.8	60.5	60.5	59.2	70.0
eQUEST	122.3	103.1	103.0	101.0	103.0	170.8	94.0	94.2	92.2	92.4	91.7	91.8	91.3	86.4	91.8	92.0	54.2	35.5	45.6	60.5	60.5	59.2	70.1

(a) Total Site Energy Use Changes

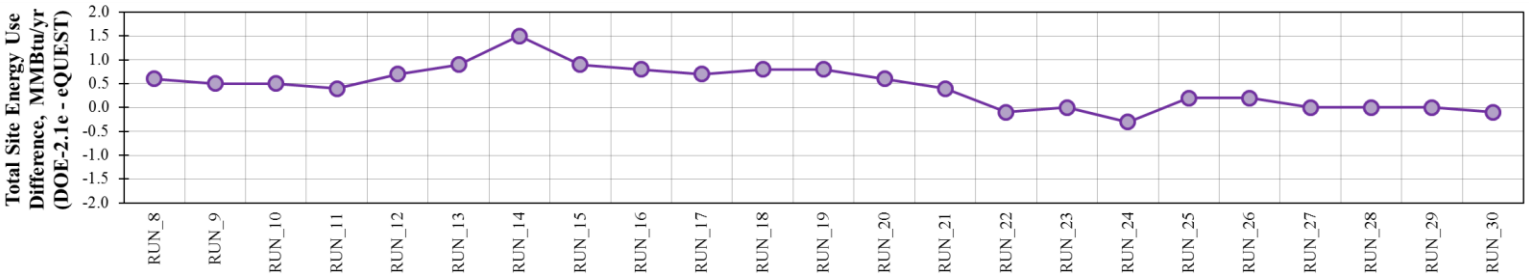

(b) Changes of Differences of Total Site Energy Use

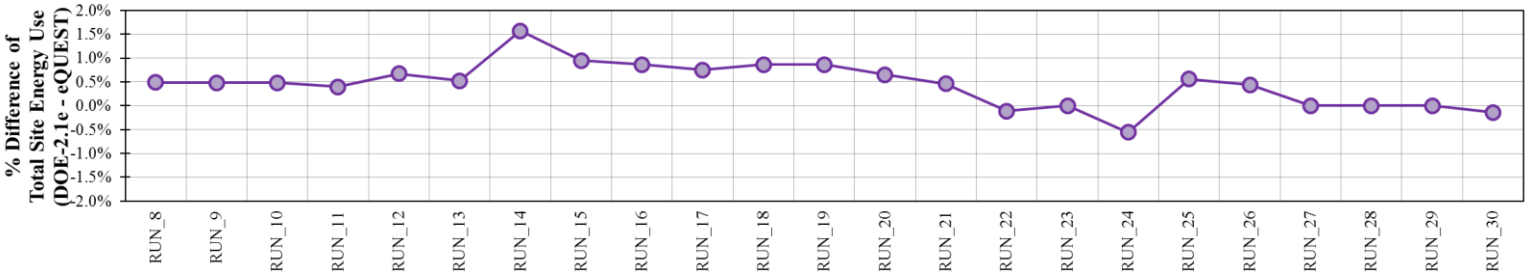

(c) Changes of % Differences of Total Site Energy Use

Figure 5-44: Total Site Energy Use Differences between DOE-2.1e and eQUEST Resulted from RUN_8 to RUN_30

Excluding the previously listed eight input changes, other step-by-step input parameter changes resulted in modest changes to the total site energy use in both DOE-2.1e and eQUEST. At the end of the input change procedure, RUN_30 was modified to represents the residential ASHP model in Houston. The resultant total site energy use from DOE-2.1e in the RUN_30 was well-matched to the eQUEST results within 0.1 MMBtu/yr of annual total site energy use difference, shown in Figure 5-44. The resultant annual total site energy use of RUN_30 from DOE-2.1e was 70.0 MMBtu/yr (28.0 kBtu/yr-ft^2 of EUI), including:

- 14.6 MMBtu/yr, or 20.9% (5.8 kBtu/yr-ft^2 of EUI) for area lights,
- 19.7 MMBtu/yr, or 28.1% (7.9 kBtu/yr-ft^2 of EUI) for equipment,
- 7.6 MMBtu/yr, or 10.9% (3.0 kBtu/yr-ft^2 of EUI) for space heat,
- 12.4 MMBtu/yr, or 17.7% (5.0 kBtu/yr-ft^2 of EUI) for space cool,
- 10.8 MMBtu/yr, or 15.4% (4.3 kBtu/yr-ft^2 of EUI) for DHW, and
- 4.9 MMBtu/yr, or 7.0% (2.0 kBtu/yr-ft^2 of EUI) for other (i.e., fan and pump).

On the other hand, the resultant annual total site energy use of RUN_30 from eQUEST was 70.1 MMBtu/yr (28.0 kBtu/yr-ft^2 of EUI), including:

- 14.6 MMBtu/yr, or 20.8% (5.8 kBtu/yr-ft^2 of EUI) for area lights,
- 19.7 MMBtu/yr, or 28.1% (7.9 kBtu/yr-ft^2 of EUI) for equipment,
- 6.5 MMBtu/yr, or 9.3% (2.6 kBtu/yr-ft^2 of EUI) for space heat,
- 13.7 MMBtu/yr, or 19.5% (5.5 kBtu/yr-ft^2 of EUI) for space cool,
- 10.9 MMBtu/yr, or 15.5% (4.4 kBtu/yr-ft^2 of EUI) for DHW, and
- 4.7 MMBtu/yr, or 6.7% (1.9 kBtu/yr-ft^2 of EUI) for other (i.e., fan and pump).

Based on the residential ASHP model for Houston (i.e., RUN_30), the residential ASHP base-case model for Dallas was developed by modifying the RUN_30 based on the methodology was described in Section 4.4.1.2. The resultant annual total site energy use for the residential ASHP base-case model for Dallas was shown in Figure 5-45, which includes the comparison of the resultant site energy use of the ASHP base-case models for Houston and Dallas, using the DOE-2.1e and eQUEST programs.

The resultant annual total site energy use of the DOE-2.1e ASHP model for Dallas was 72.8 MMBtu/yr (29.1 kBtu/yr-ft^2 of EUI), including:

- 14.6 MMBtu/yr, or 20.1% (5.8 kBtu/yr-ft^2 of EUI) for area lights,
- 19.7 MMBtu/yr, or 27.1% (7.9 kBtu/yr-ft^2 of EUI) for equipment,
- 10.6 MMBtu/yr, or 14.6% (4.2 kBtu/yr-ft^2 of EUI) for space heat,
- 11.2 MMBtu/yr, or 15.4% (4.5 kBtu/yr-ft^2 of EUI) for space cool,
- 11.5 MMBtu/yr, or 15.8% (4.6 kBtu/yr-ft^2 of EUI) for DHW, and
- 5.2 MMBtu/yr, or 7.1% (2.1 kBtu/yr-ft^2 of EUI) for other (i.e., fan and pump).

On the other hand, the resultant annual total site energy use of the eQUEST ASHP model for Dallas was 72.2 MMBtu/yr (28.9 kBtu/yr-ft^2 of EUI), including:

- 14.6 MMBtu/yr, or 20.2% (5.8 kBtu/yr-ft^2 of EUI) for area lights,
- 19.7 MMBtu/yr, or 27.3% (7.9 kBtu/yr-ft^2 of EUI) for equipment,
- 9.2 MMBtu/yr, or 12.7% (3.7 kBtu/yr-ft^2 of EUI) for space heat,
- 12.4 MMBtu/yr, or 17.2% (5.0 kBtu/yr-ft^2 of EUI) for space cool,
- 11.6 MMBtu/yr, or 16.1% (4.6 kBtu/yr-ft^2 of EUI) for DHW, and
- 4.7 MMBtu/yr, or 6.5% (1.9 kBtu/yr-ft^2 of EUI) for other (i.e., fan and pump).

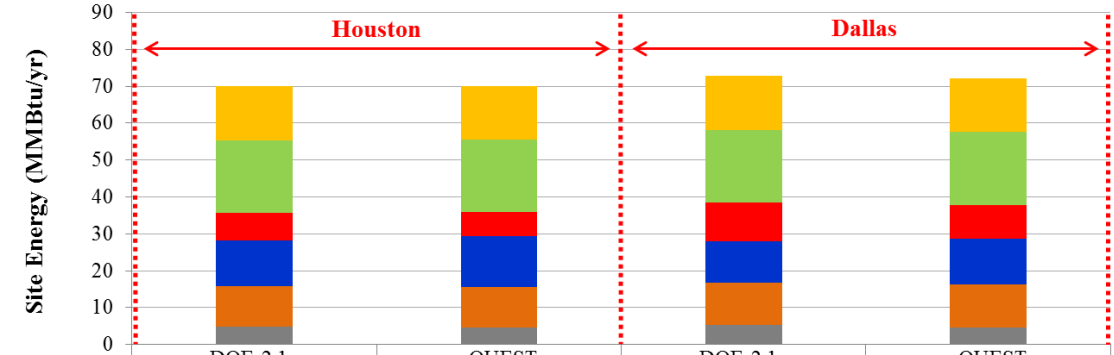

	DOE-2.1e	eQUEST	DOE-2.1e	eQUEST
TOTAL	70.0	70.1	72.8	72.2
Area Lights	14.6	14.6	14.6	14.6
Equipment	19.7	19.7	19.7	19.7
Space Heat	7.6	6.5	10.6	9.2
Space Cool	12.4	13.7	11.2	12.4
DHW	10.8	10.9	11.5	11.6
Fan+Pump	4.9	4.7	5.2	4.7

% Energy Use Difference in ASHP Base-Case Models ((DOE-2.1e - eQUEST) / DOE-2.1e)

	Houston	Dallas
TOTAL	-0.1%	0.8%
Area Lights	0.0%	0.0%
Equipment	0.0%	0.0%
Space Heat	14.5%	13.2%
Space Cool	-10.5%	-10.7%
DHW	-0.9%	-0.9%
Fan+Pump	4.1%	9.6%

Figure 5-45: Site Energy Use Comparison of ASHP Base-Case Model between DOE-2.1e and eQUEST

As shown in Figure 5-45, the total annual site energy use from the DOE-2.1e ASHP model for Houston and Dallas was well-matched to the eQUEST results with 0.1 MMBtu/yr (0.1%) for Houston and 0.6 MMBtu/yr (0.8%) for Dallas. In addition, the annual site energy use for the area lights, equipment, and DHW had good agreement to within 1% differences.

However, it was identified that the percent differences for heating, cooling, and others (i.e., fan and pump) between the programs were 14.5%, 10.5%, and 4.1% for Houston, and 13.2%, 10.7%, and 9.6% for Dallas, respectively.

Table 5-10: ASHP System Design Parameters from the SV-A Report

SV-A Report		HOUSTON		DALLAS	
PARAMETER	UNIT	DOE-2.1e	eQUEST	DOE-2.1e	eQUEST
ASHP System					
Altitude Factor		1.00	1.00	1.02	1.02
Floor Area	(sqft)	2,500	2,500	2,500	2,500
Max People		0	0	0	0
Outside Air Ratio		0	0	0	0
Cooling Capacity	(kBtu/hr)	60	60	60	60
SHR		0.652	0.652	0.678	0.678
Heating Capacity	(kBtu/hr)	-60	-60	-60	-60
Cooling EIR	(Btu/Btu)	0.21	0.21	0.21	0.21
Heating EIR	(Btu/Btu)	0.24	0.24	0.24	0.24
Heat Pump Supp-Heat	(kBtu/hr)	-64.382	-64.382	-64.585	-64.585
Supply Fan	(CFM)	1,800	1,800	1,836	1,836
Fan Elec	(kW)	0.918	0.918	0.918	0.918
Fan Delta-T	(F)	1.6	1.6	1.5	1.5
Space					
Supply Flow	(CFM)	1,800	1,800	1,836	1,836
Exhaust Flow	(CFM)	0	0	0	0
Fan Elec	(kW)	0	0	0	0
Minimum Flow Ratio		1	1	1	1
Outside Air Flow	(CFM)	0	0	0	0
Cooling Capacity	(kBtu/hr)	0	0	0	0
SHR		0	0	0	0
Extraction Rate	(kBtu/hr)	40.17	40.17	40.25	40.25
Heating Capacity	(kBtu/hr)	0	0	0	0
Addition Rate	(kBtu/hr)	-67.77	-67.77	-67.91	-67.91
Multiplier		1	1	1	1

Since the SV-A reports (i.e., the report for the system design parameters) from both programs showed all of the parameters were matched closely as shown in Table 5-10 and the system's annual cooling loads and heating loads between the programs were

very close within 3% as presented in Section 5.2.1.2, reason for the differences in the heating and cooling energy use appears to be due to the differences in system curve-fit[52], shown in Table 5-11. Specifically, big differences between the programs were observed in both curve-fit correlations and type, following: (1) HEAT-CAP-FT and HEAT-EIR-FPLR for heating; (2) COOL-SH-FT for cooling. Different curve-fits may lead to different simulation results.

Table 5-11: RESYS System Default Curve-Fit Correlations

RESYS	Type of Curve	a	b	c	d	e	f
DOE-2.1e							
COOL-CAP-FT	BI-QUAD	0.60034040	0.00228730	-0.00001280	0.00138980	-0.00008060	0.00014120
COOL-EIR-FT	BI-QUAD	-0.96177870	0.04817750	-0.00023110	0.00324390	0.00014880	-0.00029520
COOL-EIR-FPLR	LINEAR	0.12500000	0.87500000	0.00000000	0.00000000	0.00000000	0.00000000
COOL-SH-FT	BI-QUAD	6.52756980	-0.12613750	0.00056880	0.00907570	-0.00004830	-0.00000880
HEAT-CAP-FT	CUBIC	0.29495690	0.01425360	-0.00001170	0.00000060	0.00000000	0.00000000
HEAT-EIR-FT	CUBIC	2.18554780	-0.04947180	0.00070420	-0.00000400	0.00000000	0.00000000
HEAT-EIR-FPLR	CUBIC	0.08565220	0.93881370	-0.18343610	0.15897020	0.00000000	0.00000000
eQUEST[1]							
COOL-CAP-FT	BI-QUAD	0.60034040	0.00228730	-0.00001280	0.00138980	-0.00008060	0.00014120
COOL-EIR-FT	BI-QUAD	-0.96177870	0.04817750	-0.00023110	0.00324390	0.00014880	-0.00029520
COOL-EIR-FPLR	LINEAR	0.12500000	0.87500000	0.00000000	0.00000000	0.00000000	0.00000000
COOL-SH-FT	BI-QUAD	6.52757025	-0.12613751	0.00056879	0.00907575	-0.00004830	-0.00000875
HEAT-CAP-FT	BI-QUAD	0.31392699	0.00000000	0.00000000	0.01184160	0.00005863	0.00000000
HEAT-EIR-FT	BI-QUAD	2.05702496	0.00000000	0.00000000	-0.03322292	0.00022836	0.00000000
HEAT-EIR-FPLR	CUBIC	0.08565220	0.93881370	-0.18343610	0.15897020	0.00000000	0.00000000

Note: 1. The curve-fit correlations were obtained from the eQUEST simulation program (JJH, 2013)

[52] Forms of the System Curve-Fit Equations (LBL, 1993a):
Linear: $z = a + bx$
Cubic: $z = a + bx + cx^2 + dx^3$
Bi-Quadratic: $z = a + bx + cx^2 + dy + ey^2 + fxy$

5.2.2. Residential DOE-2.1e GCHP Base-Case Model with Vertical GHX

This study developed a residential DOE-2.1e ground-coupled heat pump (GCHP) simulation model using a vertical Ground Heat Exchanger (GHX) model. The vertical GHX DOE-2.1e model, which was based on the equations in Section 4.2.3, was developed using the DOE-2.1e input FUNCTION method. The vertical GHX DOE-2.1e input FUNCTION was incorporated into the air-source heat pump (ASHP) simulation module (i.e., RESYS) by modifying the calculation algorithm (i.e., the input file), which was described in Section 4.4.2. In this way, the modified ASHP system module works like the GCHP system model that includes a vertical GHX.

To apply the vertical GHX DOE-2.1e input FUNCTION, this study used the simplified residential ASHP base-case models developed for Houston and Dallas, which were described in Section 4.4.1 and presented the simulation results in Section 5.2.1.

5.2.2.1. g-function Approximation

This section shows the result of the g-function approximation described in Section 4.2.3.3. The g-function is a set of tabulated non-dimensional temperature response factors, which can determine the temperature change at the borehole wall corresponding to a change in the heat extraction/rejection input for a time step.

The g-function method was implemented in the GHXCALC subroutine of the GHX input FUNCTION. First, the approximated g-function calculation was performed for the single borehole. The resultant g-function curve, comparing the Eskilson's long

time-step g-function and Yavuzturk and Spitler's short time-step g-function, is shown in Figure 5-46.

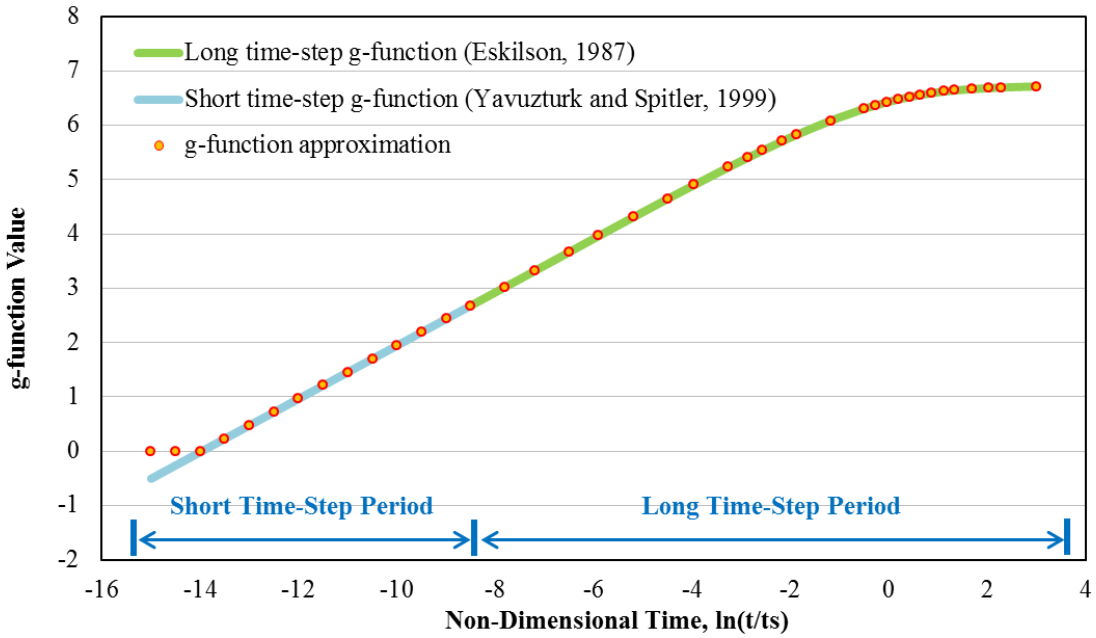

Figure 5-46: g-Function Approximation Result Curve for a Single Borehole

In addition, the approximated g-function calculation was performed for a field with multiple boreholes. The resultant g-function curves, which compare the Eskilson's g-function only, are shown in Figure 5-47 through Figure 5-49.

Figure 5-46 through Figure 5-49 show the comparison of the g-function curves resulted from the g-function approximation and from Eskilson's g-values for several borehole field types (Table 4-1) to be applicable to residential systems which described in Section 4.2.3.3. In addition, the detailed residual plots between the approximated g-function and the Eskilson's g-function for each borehole field type can be found in the Appendix B.

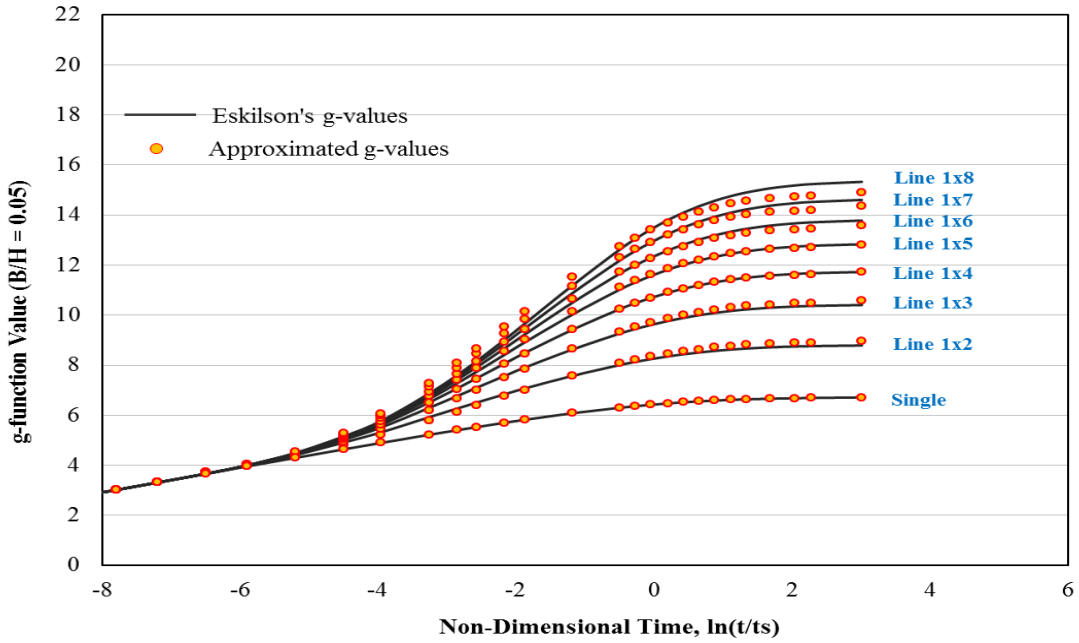

(a) Ratio of Borehole Space and Depth (B/H) = 0.05

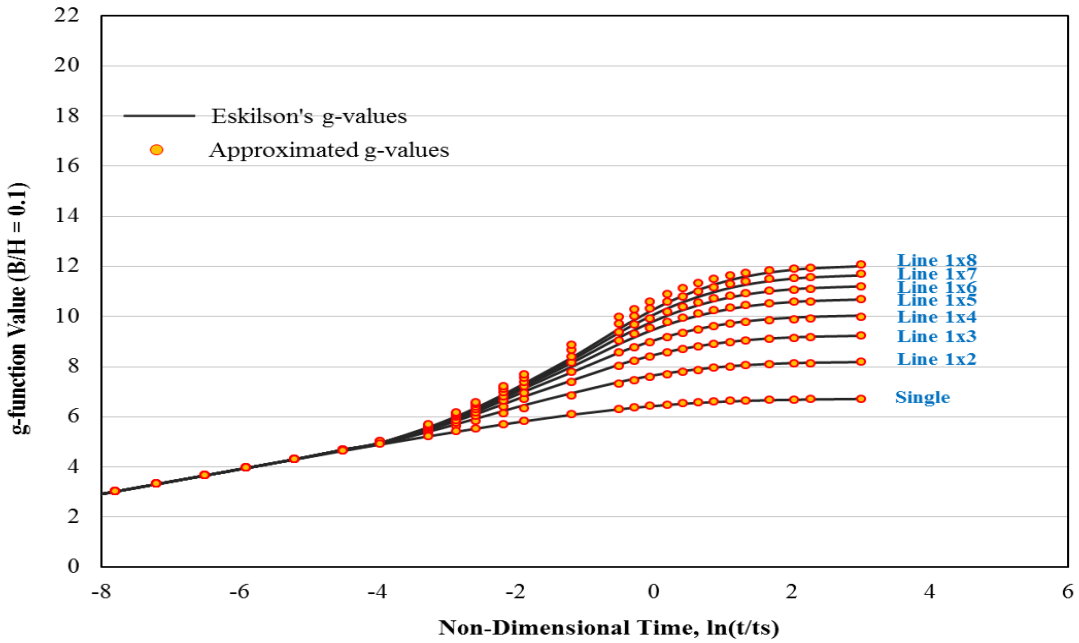

(b) Ratio of Borehole Space and Depth (B/H) = 0.1

Figure 5-47: Approximated g-Function Curve for Line Type Multiple Boreholes

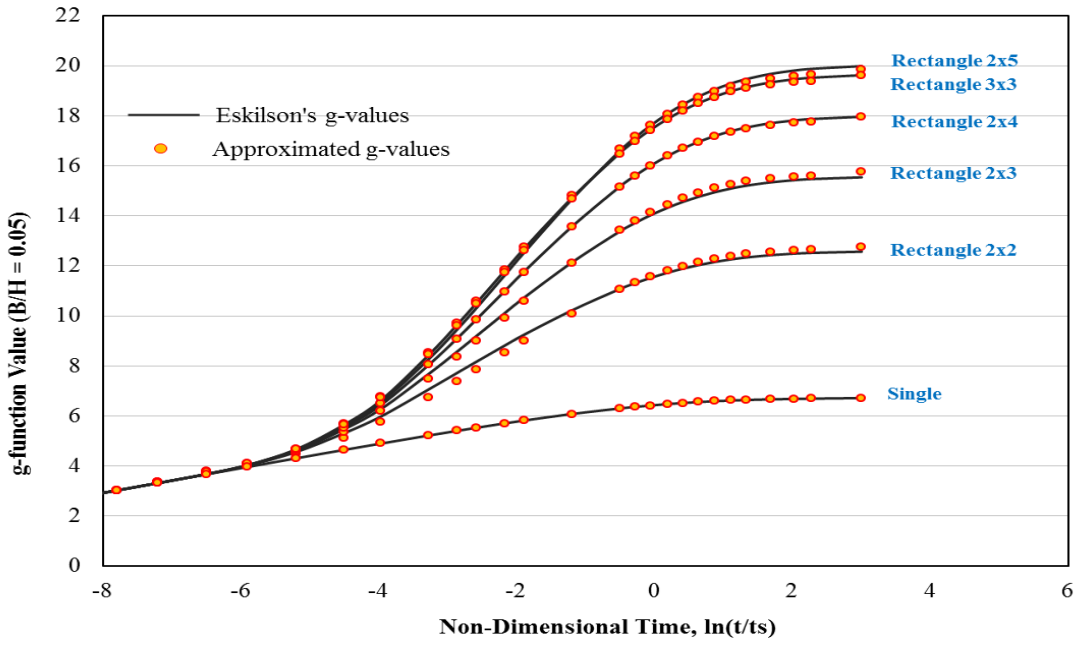

(a) Ratio of Borehole Space and Depth (B/H) = 0.05

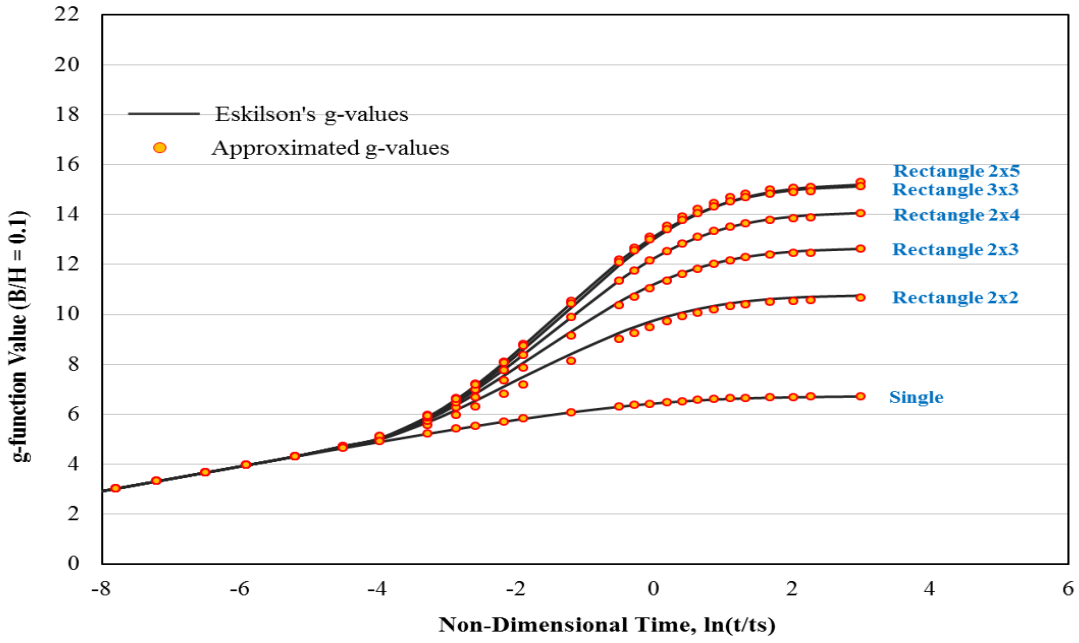

(b) Ratio of Borehole Space and Depth (B/H) = 0.1

Figure 5-48: Approximated g-Function Curve for Rectangle Type Multiple Boreholes

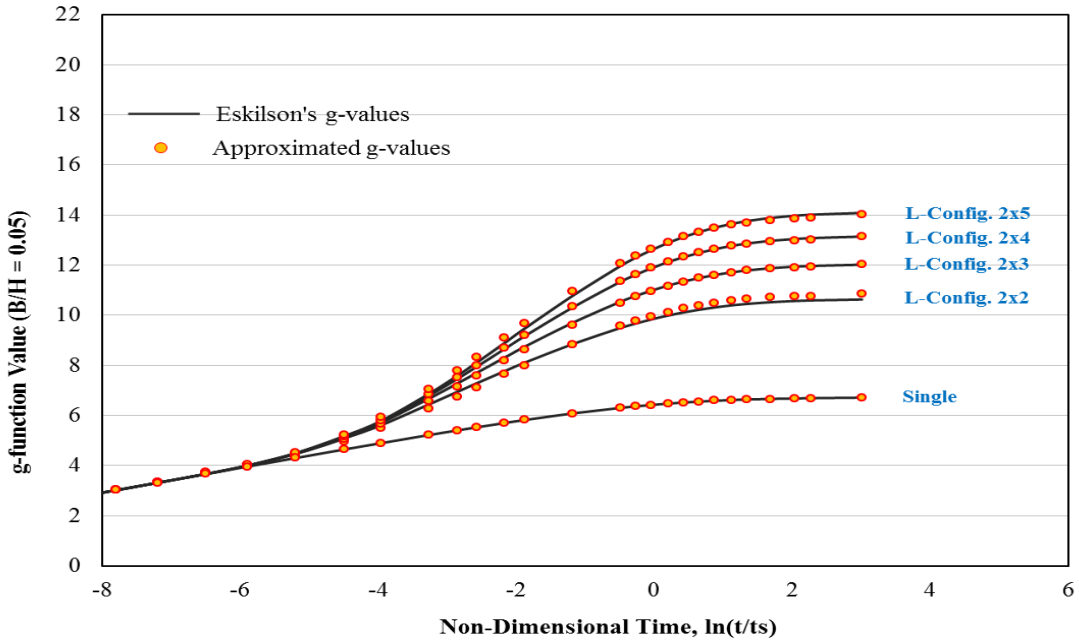

(a) Ratio of Borehole Space and Depth (B/H) = 0.05

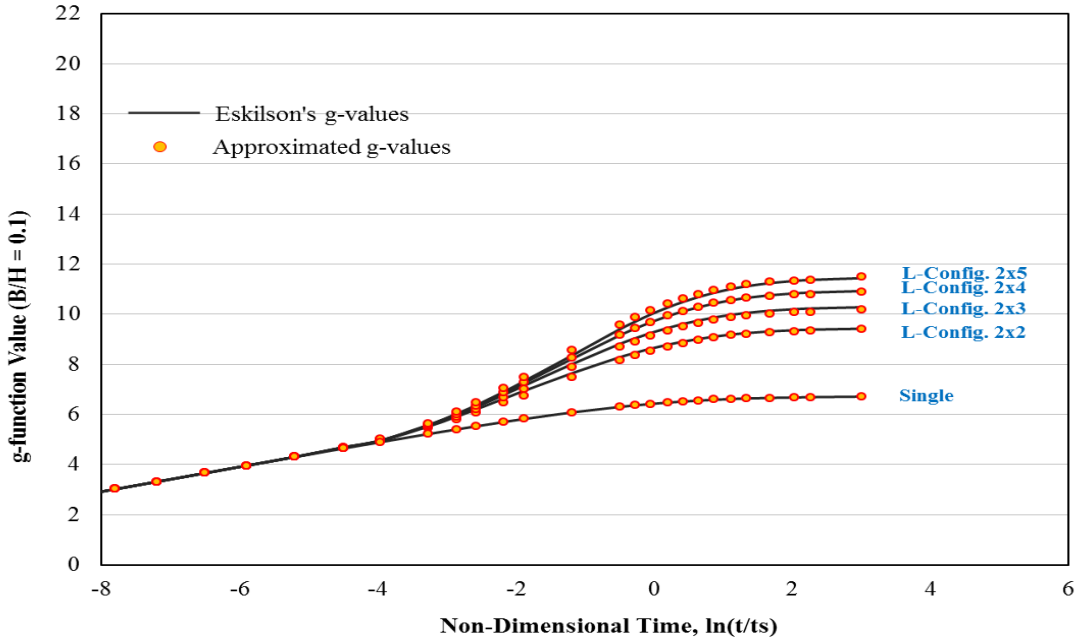

(b) Ratio of Borehole Space and Depth (B/H) = 0.1

Figure 5-49: Approximated g-Function Curve for L-Shape type Multiple Boreholes

Figure 5-47 through Figure 5-49 showed that the approximated g-function values were well-matched overall against the Eskilson's g-function values. The g-function values approximated in this study had less than 0.5 of the average g-function value difference against the Eskilson's g-values. In addition, all of the approximated g-function values were within the ±10% difference range. Especially, for a large value of the B/H parameter, the agreement of the g-function values was very good.

However, it should be noted that the approximated g-function values were over-estimated or under-estimated the Eskilson's g-function in certain non-dimensional time periods and for small values of the B/H. For example, the results of the g-function approximation for the eight boreholes with the line type borehole configuration (Figure 5-47) were over-estimated for small values of the non-dimensional time and were under-estimated for large values of the non-dimensional time. In addition, the approximated g-function values were over-estimated for small values of the ratio of borehole space and borehole depth (B/H). However, it is also worth to mention that the most widely used value of B/H parameter was 0.05 or 0.10. The reason is that typical vertical borehole depth is between 200 ft to 300 ft and the borehole spacing is at least 20 ft which is recommended in the Geothermal Energy Chapter in the ASHRAE Handbook (ASHRAE 2007b). As a result, the g-function values approximated in this study matched well with the Eskilson g-function values, as observed in the Figure 5-46 through Figure 5-49 and the figures in Appendix B.

5.2.2.2. Vertical Ground Heat Exchanger DOE-2.1e Function Model

The vertical GHX model, using the DOE-2 FUNCTION command, which was written in the SYSTEMS section of the DOE-2.1e input file, is used to calculate the entering water temperatures (EWTs). In addition, the vertical GHX input FUNCTION was incorporated within the residential ASHP base-case model for Houston (i.e., RUN_30 in this study) by modifying the calculation algorithm (i.e., the input file). Next, the modified ASHP system module, which works like the GCHP system model using a vertical GHX, calls the DOE-2.1e GCHP base-case model developed for this study.

The vertical GHX input FUNCTION in the DOE-2.1e program included two subroutines (Figure 4-64), which were described in Section 4.4.2.2. The two subroutines were called THERMALLOAD and GHXCALC. The THERMALLOAD subroutine calculates the system's thermal loads before the system operates for cooling and heating. The calculated system loads pass through another subroutine, which named GHXCALC. The calculated system's thermal loads of the GCHP base-case models for Houston and Dallas are shown in Figure 5-50. The negative and positive values in these figures account for the heating loads and the cooling loads in the GCHP system, respectively. Second, the GHXCALC subroutine, which includes the g-function approximation, calculates the EWTs based on the system's thermal loads. The calculated EWTs from the DOE-2.1e GCHP base-case models[53] for Houston and Dallas using the 2009 IECC system efficiency (i.e., EER 13.4 and 3.1 COP) are shown in Figure 5-51. Figure 5-52 shows a comparison of the monthly average EWTs between Houston and Dallas.

[53] The detail of the input parameters was described in Section 4.4.3.

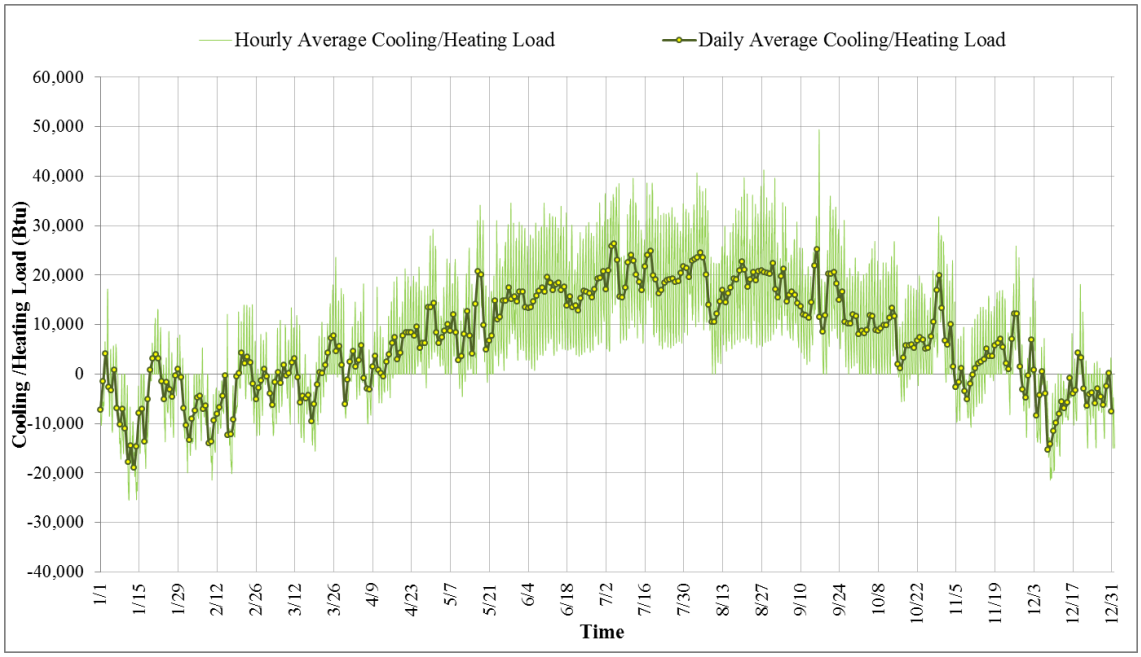

(a) For Houston

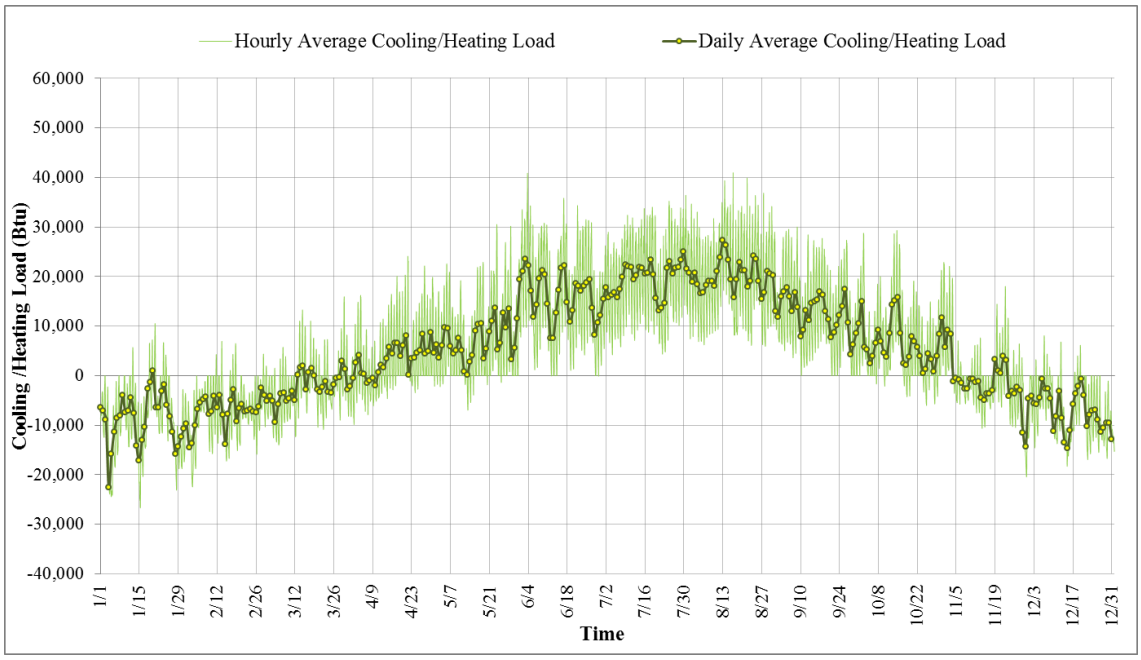

(b) For Dallas

Figure 5-50: System's Thermal Load Calculated from the THERMALLOAD subroutine

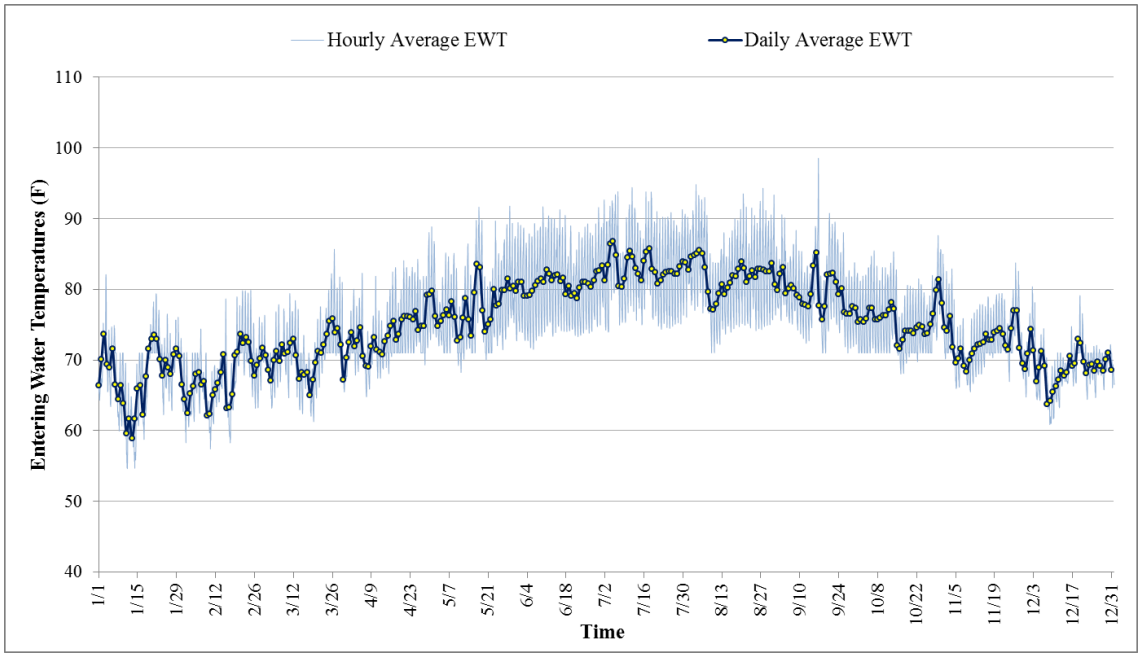

(a) For Houston

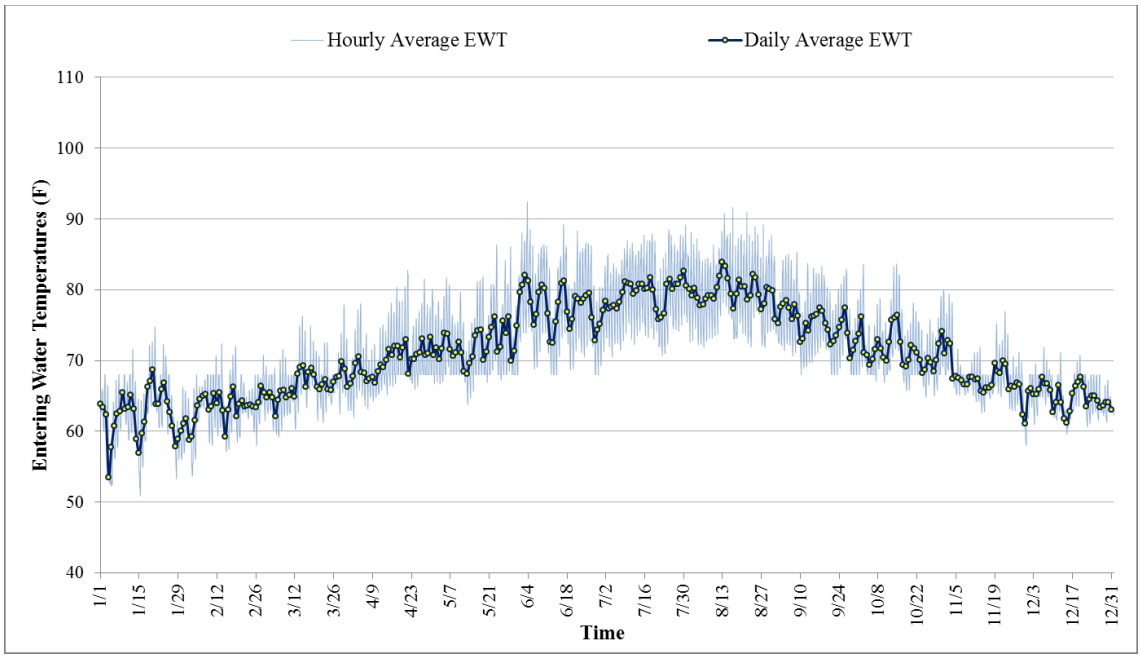

(b) For Dallas

Figure 5-51: Entering Water Temperatures Calculated from the GHXCALC subroutine

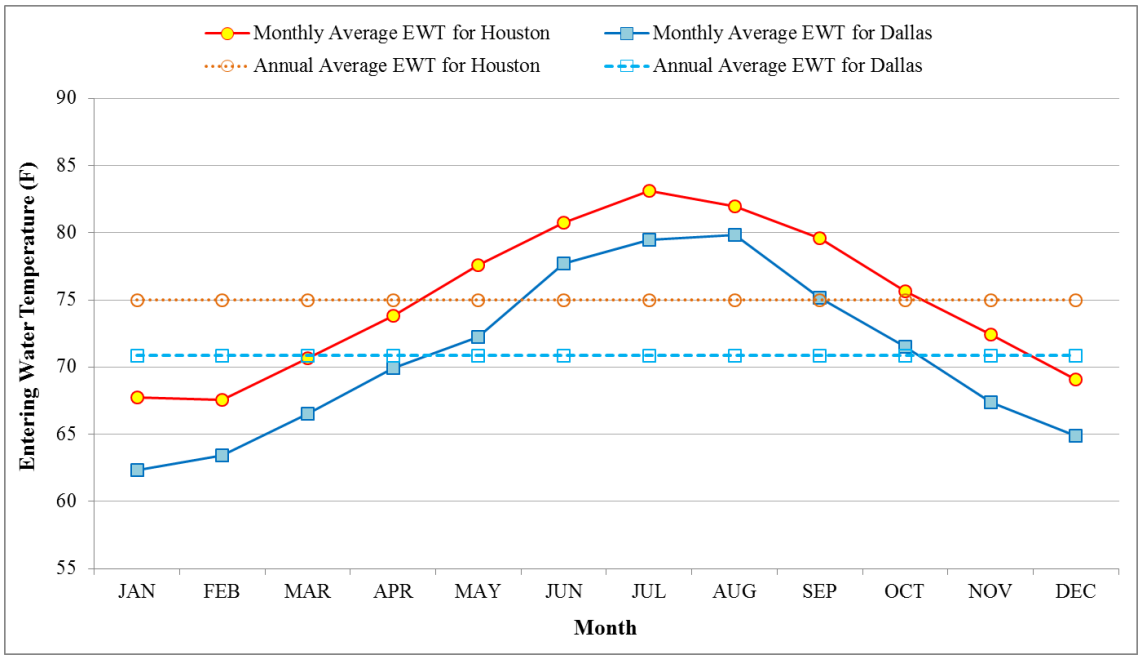

Figure 5-52: Calculated Entering Water Temperatures

Not surprisingly, the GCHP base-case model for Houston had more cooling loads and less heating loads than Dallas (Figure 5-50). The calculated EWTs for Houston were higher than Dallas (Figure 5-51) and the annual average EWT difference resulted in about a 4.1F higher temperature (Figure 5-52). The higher EWTs for the Houston GCHP base-case model were caused by two main factors: one is the input set for the mean ground temperature (i.e., 71F for Houston and 68F for Dallas, presented in Table 4-14). The other is the calculated system's cooling and heating loads. The higher mean ground temperature (3F) for Houston resulted in higher EWTs than Dallas. The increased cooling loads and decreased heating loads for Houston versus Dallas meant that more heat was injected into the ground and less heat was extracted from the ground. As a

result, the EWT for Houston resulted in annual average temperature rise about 1.1 F higher than Dallas.

5.2.2.3. Energy Use of the Residential DOE-2.1e GCHP Base-Case Model

The residential DOE-2.1e GCHP base-case models for Houston and Dallas were developed by modifying the DOE-2.1e RESYS system using the DOE-2.1e input FUNCTION method for the vertical GHX model. This section presents the results of the GCHP system energy use by comparing the resultant ASHP system energy use, shown in Table 5-12. In addition, Figure 5-53 and Figure 5-54 show the plots that compare the resultant monthly cooling and heating energy use between ASHP and GCHP.

Table 5-12: Monthly Cooling/Heating Energy Use for ASHP and GCHP

(MMBtu)	Houston						Dallas					
	ASHP			GCHP			ASHP			GCHP		
Month	Cooling	Heating	Total Cooling and Heating	Cooling	Heating	Total Cooling and Heating	Cooling	Heating	Total Cooling and Heating	Cooling	Heating	Total Cooling and Heating
JAN	0.087	2.061	2.148	0.085	0.572	0.657	0.029	3.111	3.140	0.028	0.848	0.876
FEB	0.100	2.019	2.119	0.094	0.571	0.665	0.015	2.180	2.195	0.015	0.649	0.664
MAR	0.239	0.877	1.116	0.228	0.273	0.501	0.111	1.151	1.262	0.105	0.341	0.446
APR	0.594	0.213	0.807	0.557	0.061	0.618	0.453	0.322	0.775	0.414	0.088	0.502
MAY	1.285	0.024	1.309	1.190	0.006	1.196	0.842	0.074	0.916	0.762	0.018	0.780
JUN	1.929	0.000	1.929	1.753	0.000	1.753	1.959	0.000	1.959	1.698	0.000	1.698
JUL	2.470	0.000	2.470	2.229	0.000	2.229	2.571	0.000	2.571	2.172	0.000	2.172
AUG	2.338	0.000	2.338	2.109	0.000	2.109	2.628	0.000	2.628	2.240	0.000	2.240
SEP	1.779	0.000	1.779	1.636	0.000	1.636	1.576	0.000	1.576	1.390	0.000	1.390
OCT	1.038	0.052	1.090	0.965	0.014	0.979	0.826	0.119	0.945	0.749	0.030	0.779
NOV	0.459	0.483	0.942	0.435	0.143	0.578	0.177	1.094	1.271	0.166	0.303	0.469
DEC	0.088	1.885	1.973	0.082	0.537	0.619	0.023	2.514	2.537	0.022	0.713	0.735
SUM	12.4	7.6	20.0	11.4	2.2	13.5	11.2	10.6	21.8	9.8	3.0	12.8
AVERAGE	1.0	0.6	1.7	0.9	0.2	1.1	0.9	0.9	1.8	0.8	0.2	1.1

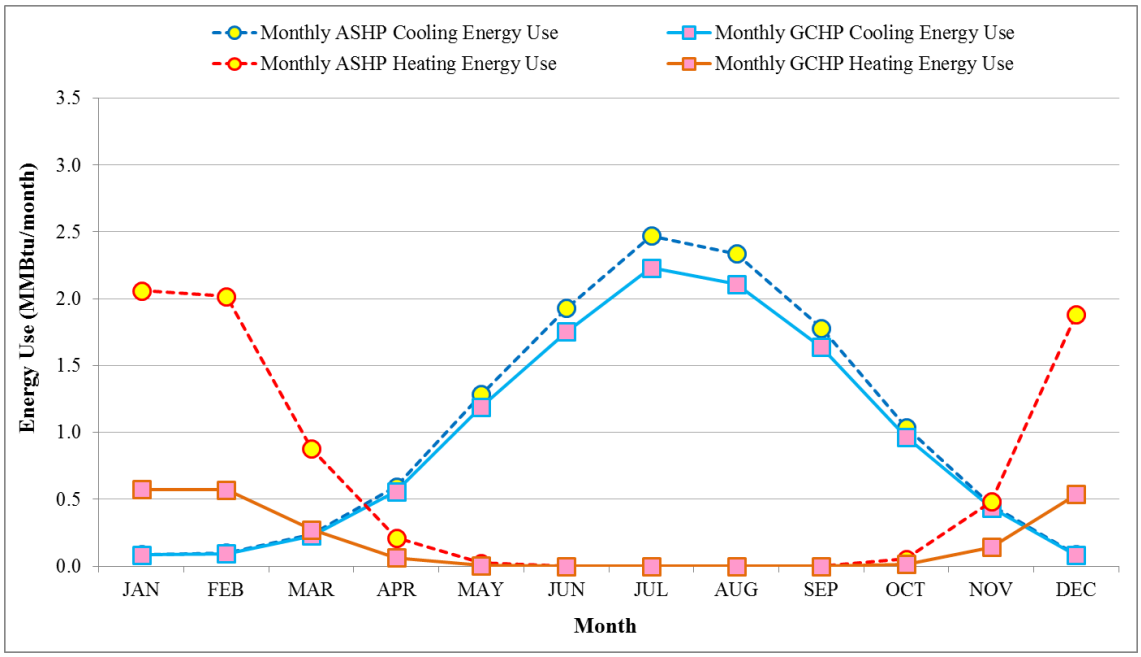

(a) Houston

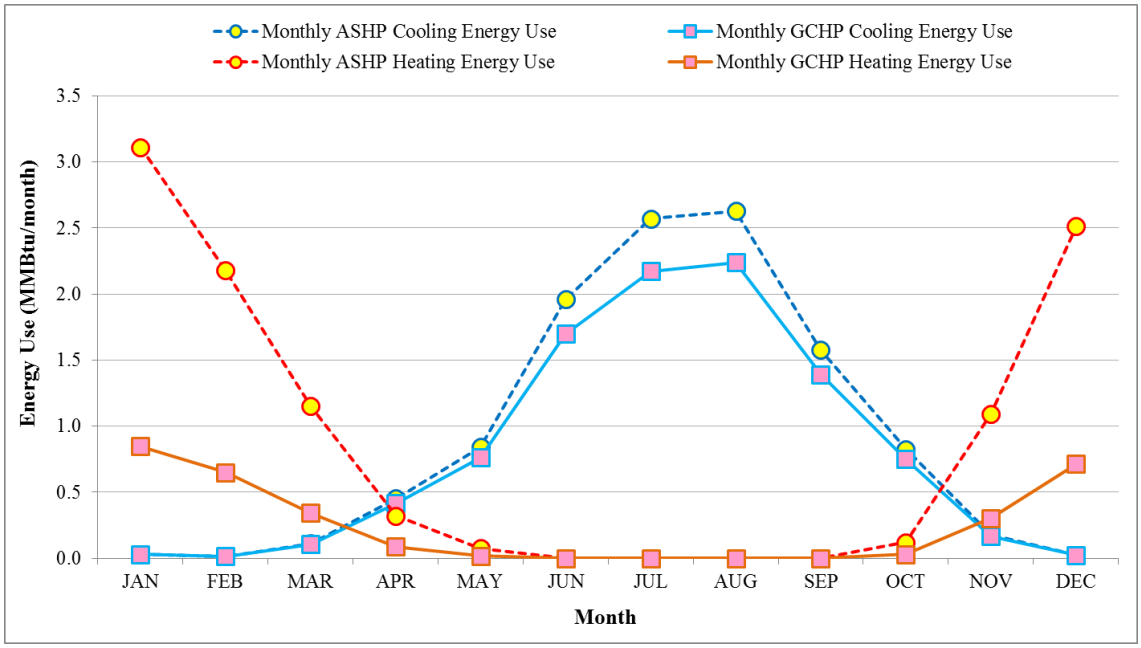

(b) Dallas

Figure 5-53: Cooling and Heating Energy Use for ASHP and GCHP

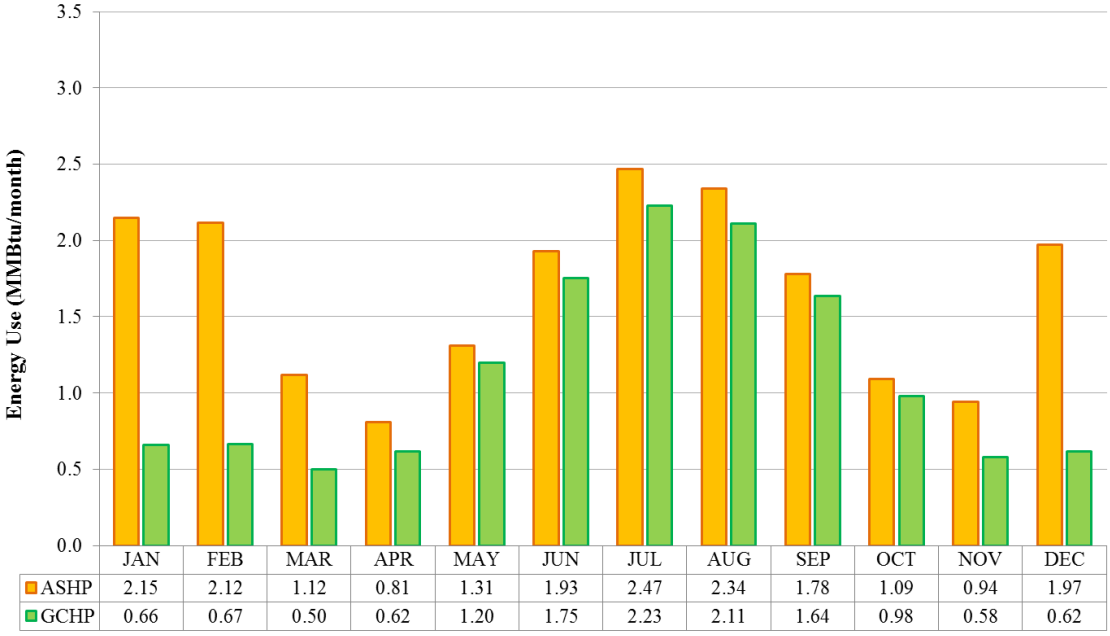

	JAN	FEB	MAR	APR	MAY	JUN	JUL	AUG	SEP	OCT	NOV	DEC
ASHP	2.15	2.12	1.12	0.81	1.31	1.93	2.47	2.34	1.78	1.09	0.94	1.97
GCHP	0.66	0.67	0.50	0.62	1.20	1.75	2.23	2.11	1.64	0.98	0.58	0.62

(a) Houston

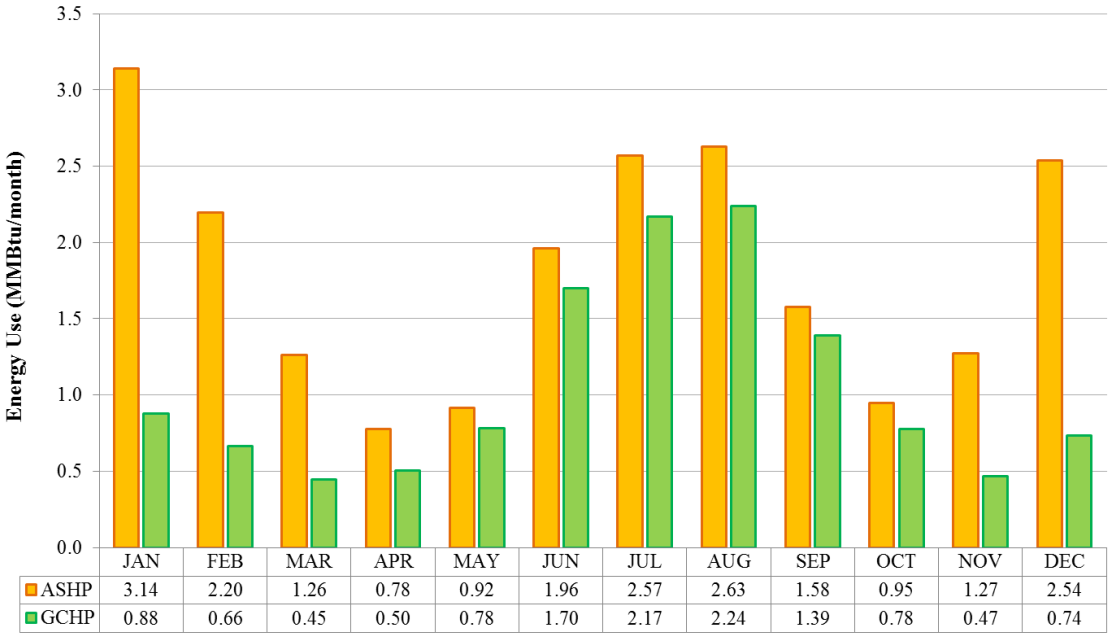

	JAN	FEB	MAR	APR	MAY	JUN	JUL	AUG	SEP	OCT	NOV	DEC
ASHP	3.14	2.20	1.26	0.78	0.92	1.96	2.57	2.63	1.58	0.95	1.27	2.54
GCHP	0.88	0.66	0.45	0.50	0.78	1.70	2.17	2.24	1.39	0.78	0.47	0.74

(b) Dallas

Figure 5-54: Total Cooling plus Heating Energy Use for ASHP and GCHP

The energy use results show that the ASHP system for Houston had more annual cooling energy use (1.2 MMBtu/yr) and less annual heating energy use (3.0 MMBtu/yr) than Dallas. However, it should be noted that the monthly cooling energy use for Dallas was larger than Houston during the cooling season (i.e., June through August). The higher cooling energy use in Dallas resulted from the higher outdoor air (OA) temperatures in Dallas than in Houston, as shown in Figure 5-55.

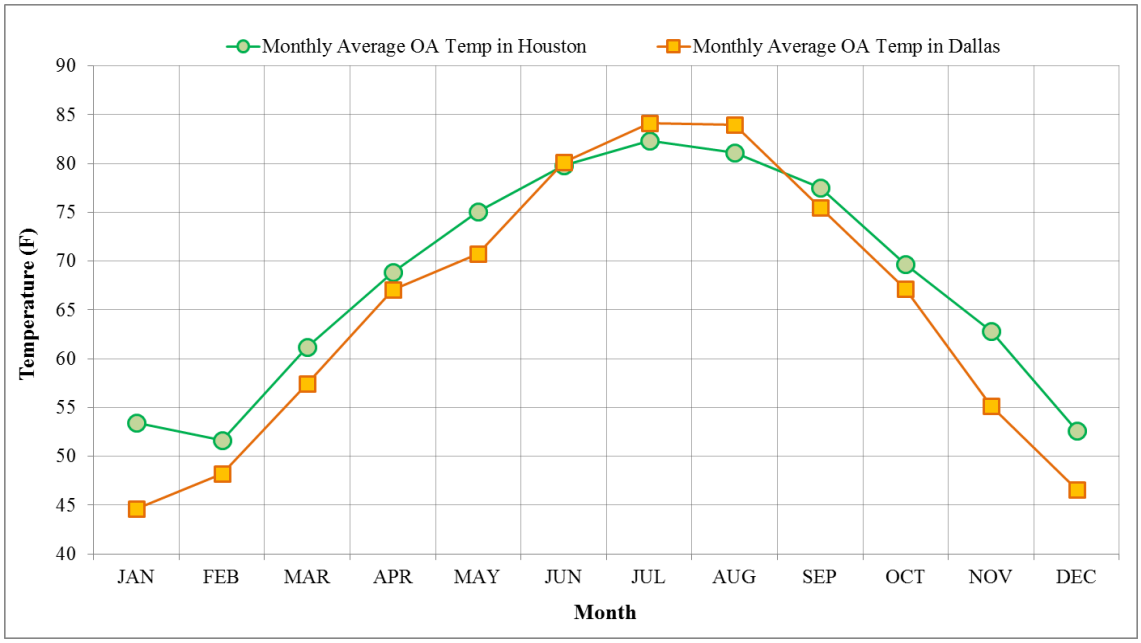

Figure 5-55: OA Temperature from the Houston and Dallas TMY2 Weather Files

As expected, the GCHP base-case models for both Houston and Dallas used less heating energy and cooling energy than the ASHP base-case models. The annual savings of the total cooling and heating energy resulted in 6.5 MMBtu/yr (32.4%) for Houston and 9.0 MMBtu/yr (41.4%) for Dallas. The resultant energy savings for heating and cooling are shown in Table 5-13.

Table 5-13: GCHP Monthly Cooling/Heating Energy Savings against ASHP

Month	GCHP Energy Savings against ASHP											
	Houston						Dallas					
	Cooling	Heating	Total Cooling and Heating	Cooling	Heating	Total Cooling and Heating	Cooling	Heating	Total Cooling and Heating	Cooling	Heating	Total Cooling and Heating
	MMBtu			%			MMBtu			%		
JAN	0.002	1.489	1.491	2.3%	72.2%	69.4%	0.001	2.263	2.264	3.4%	72.7%	72.1%
FEB	0.006	1.448	1.454	6.0%	71.7%	68.6%	0.000	1.531	1.531	0.0%	70.2%	69.7%
MAR	0.011	0.604	0.615	4.6%	68.9%	55.1%	0.006	0.810	0.816	5.4%	70.4%	64.7%
APR	0.037	0.152	0.189	6.2%	71.4%	23.4%	0.039	0.234	0.273	8.6%	72.7%	35.2%
MAY	0.095	0.018	0.113	7.4%	75.0%	8.6%	0.080	0.056	0.136	9.5%	75.7%	14.8%
JUN	0.176	0.000	0.176	9.1%	-	9.1%	0.261	0.000	0.261	13.3%	-	13.3%
JUL	0.241	0.000	0.241	9.8%	-	9.8%	0.399	0.000	0.399	15.5%	-	15.5%
AUG	0.229	0.000	0.229	9.8%	-	9.8%	0.388	0.000	0.388	14.8%	-	14.8%
SEP	0.143	0.000	0.143	8.0%	-	8.0%	0.186	0.000	0.186	11.8%	-	11.8%
OCT	0.073	0.038	0.111	7.0%	73.1%	10.2%	0.077	0.089	0.166	9.3%	74.8%	17.6%
NOV	0.024	0.340	0.364	5.2%	70.4%	38.6%	0.011	0.791	0.802	6.2%	72.3%	63.1%
DEC	0.006	1.348	1.354	6.8%	71.5%	68.6%	0.001	1.801	1.802	4.3%	71.6%	71.0%
SUM	1.0	5.4	6.5	8.4%	71.4%	32.4%	1.4	7.6	9.0	12.9%	71.7%	41.4%
AVERAGE	0.1	0.5	0.5	6.9%	71.8%	31.6%	0.1	0.6	0.8	8.5%	72.6%	38.6%

5.2.3. Comparison of the Residential Base-Case Models with Other Programs

To evaluate the accuracy of the simulation results from the final residential DOE-2.1e ASHP/GCHP base-case models, this study compared the simulated results against other programs. The DOE-2.1e ASHP base-case models for Houston and Dallas were compared against eQUEST, IC3, EnergyGauge, and REM/Rate. The DOE-2.1e GCHP base-case models for Houston and Dallas were also compared against eQUEST, REM/Rate, and EnergyGauge. However, the IC3 program was excluded for the GCHP base-case model comparison since the IC3 program did not have the capability to simulation a GCHP system. The comparison of the results from the residential ASHP and GCHP base-case simulation models was presented in Section 5.2.3.1.

In addition, this study conducted the sensitivity test for the DOE-2.1e GCHP model varying the parameters of GHX field arrangement and GHX length (i.e., depth) and compared the resulted energy use against the eQUEST and REM/Rate programs. The EnergyGauge program was excluded for the GHX sensitivity test since the program does not require any input parameters for a GHX. The comparison of the GHX sensitivity test results was presented in Section 5.2.3.2.

5.2.3.1. Comparison of the Residential ASHP/GCHP Base-Case Models

This section presents comparison of the residential DOE-2.1e ASHP and GCHP base-case models for Houston and Dallas against eQUEST, IC3 only for ASHP, EnergyGauge, and REM/Rate. The inputs for the ASHP and GCHP base-case simulation models were previously described in Section 4.4.3. For the system efficiencies, this study used SEER13 and 7.7 HSPF for the ASHP system and EER 13.4 and 3.1 COP for the GCHP system based on the 2009 IECC requirements. In addition, this study used EER 14.1 and 3.3 COP for the GCHP system efficiency recommended by Oak Ridge National Laboratory (ORNL) (ORNL, 2013). The simulated site energy use was compared between the different programs. To accomplish this, the study calculated the cooling and heating energy use for DOE-2.1e, eQUEST, and IC3 to include the pump and fan energy use. The reason for including the pump and fan energy use was that different programs provide different energy use categories. For example, REM/Rate does not provide the pump and fan energy use separately. In the REM/Rate program, the simulation provides the heating and cooling energy use, which already includes the

pump and fan energy use. In contrast, EnergyGauge provides the pump and fan energy use separately. However, the cooling fan energy use belongs to the cooling category whereas the heating fan and pump belong to the heating category. As a result, the pump and fan energy use in DOE-2.1e, eQUEST, and IC3 were tabulated to be included in the cooling and heating energy use.

The simulated energy use for the ASHP and GCHP base-case models using different programs is shown in Figure 5-56 through Figure 5-58 for Houston and Figure 5-59 through Figure 5-61 for Dallas. Figure 5-56 and Figure 5-59 show the site energy use resulted from the base-case models and include percent energy use differences against DOE-2.1e. Figure 5-57 and Figure 5-60 present the comparison of the heating and cooling energy use only. Figure 5-58 and Figure 5-61 show the energy savings from the GCHP system against the ASHP system.

The ASHP simulation results comparison in Figure 5-56 and Figure 5-59 showed good agreement in the total site energy use within 1.1 MMBtu/yr (1.5%) difference for Houston and 3.4 MMBtu/yr (4.7%) difference for Dallas. However, the comparison showed large differences in individual cooling/heating energy use. In Houston, the cooling differences were between 0.5 MMBtu/yr (3.2%) and 1.6 MMBtu/yr (10.2%) and the heating differences were between 0.4 MMBtu/yr (4.0%) and 1.2 MMBtu/yr (13.1%). In Dallas, the cooling differences were between 0.4 MMBtu/yr (2.9%) and 2.0 MMBtu/yr (13.7%) and the heating differences were between 0.5 MMBtu/yr (4.2%) and 1.6 MMBtu/yr (13.3%). The reasons for these site energy use differences were not resolved.

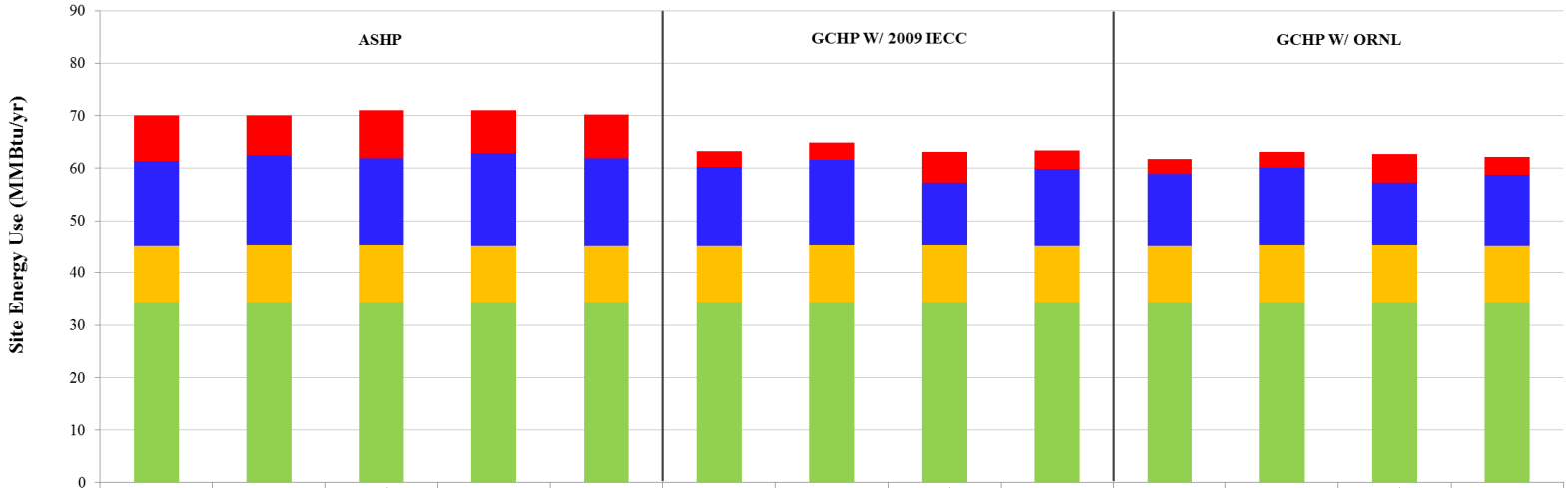

	DOE-2.1e	eQUEST	REM/Rate	EnergyGauge	IC3	DOE-2.1e	eQUEST	REM/Rate	EnergyGauge	DOE-2.1e	eQUEST	REM/Rate	EnergyGauge
TOTAL	70.0	70.1	71.1	71.0	70.3	63.2	64.9	63.1	63.5	61.7	63.2	62.7	62.1
HEATING	8.8	7.6	9.2	8.1	8.4	3.0	3.3	5.8	3.6	2.8	3.1	5.4	3.4
COOLING	16.2	17.3	16.7	17.8	16.8	15.1	16.4	12.1	14.8	13.8	14.9	12.1	13.6
DHW	10.8	10.9	10.9	10.8	10.8	10.8	10.9	10.9	10.8	10.8	10.9	10.9	10.8
Lgt & Appl	34.3	34.3	34.3	34.2	34.3	34.3	34.3	34.3	34.2	34.3	34.3	34.3	34.2

% Energy Use Difference against DOE-2.1e

	DOE-2.1e	eQUEST	REM/Rate	EnergyGauge	IC3	DOE-2.1e	eQUEST	REM/Rate	EnergyGauge	DOE-2.1e	eQUEST	REM/Rate	EnergyGauge
TOTAL		0.1%	1.5%	1.4%	0.3%		2.5%	-0.2%	0.3%		2.3%	1.6%	0.6%
HEATING		-13.1%	5.0%	-7.5%	-4.0%		9.5%	92.8%	20.6%		10.1%	92.3%	22.8%
COOLING		6.9%	3.2%	10.2%	3.5%		8.1%	-20.0%	-2.5%		7.4%	-12.5%	-1.6%
DHW		0.9%	0.9%	0.3%	0.0%		0.9%	0.9%	0.3%		0.9%	0.9%	0.3%
Lgt & Appl		0.0%	0.0%	-0.2%	0.0%		0.0%	0.0%	-0.2%		0.0%	0.0%	-0.2%

Figure 5-56: Comparison of ASHP/GCHP Site Energy Use from Different Programs for Houston

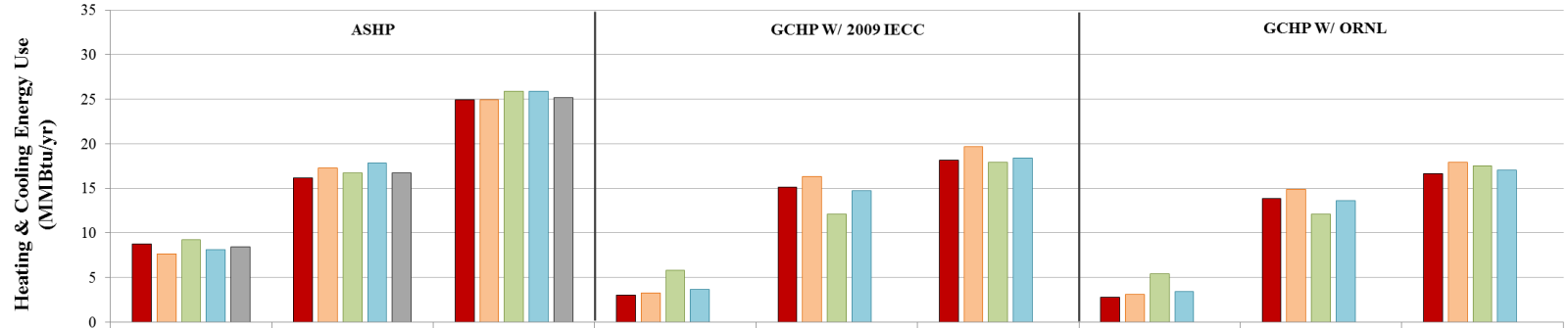

	ASHP			GCHP W/ 2009 IECC			GCHP W/ ORNL		
	HEATING	COOLING	HEATING + COOLING	HEATING	COOLING	HEATING + COOLING	HEATING	COOLING	HEATING + COOLING
DOE-2.1e	8.8	16.2	24.9	3.0	15.1	18.1	2.8	13.8	16.6
eQUEST	7.6	17.3	24.9	3.3	16.4	19.7	3.1	14.9	18.0
REM/Rate	9.2	16.7	25.9	5.8	12.1	17.9	5.4	12.1	17.5
EnergyGauge	8.1	17.8	25.9	3.6	14.8	18.4	3.4	13.6	17.1
IC3	8.4	16.8	25.2						

Figure 5-57: ASHP/GCHP Heating and Cooling Energy Use from Different Programs for Houston

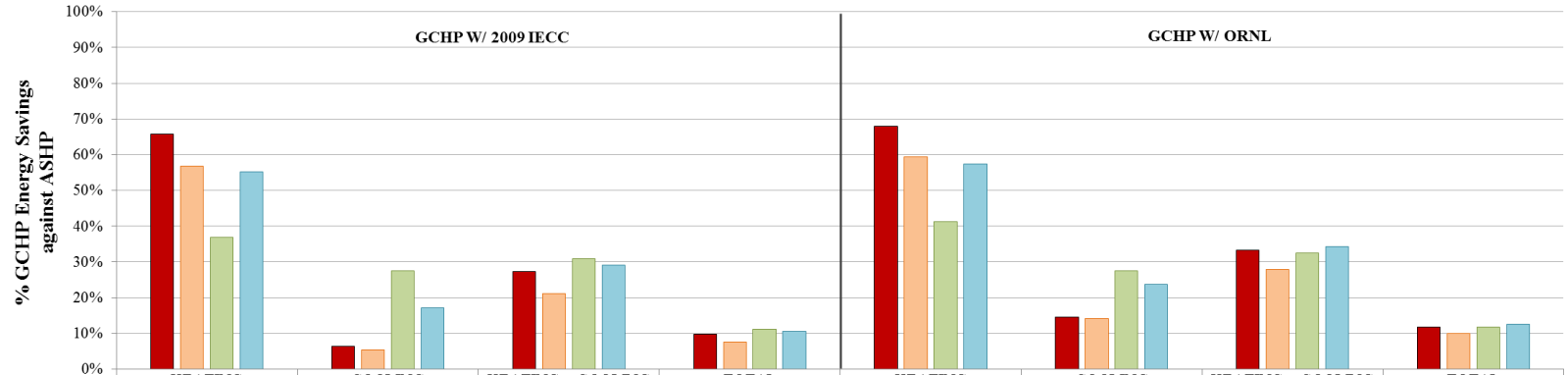

	GCHP W/ 2009 IECC				GCHP W/ ORNL			
	HEATING	COOLING	HEATING + COOLING	TOTAL	HEATING	COOLING	HEATING + COOLING	TOTAL
DOE-2.1e	65.7%	6.5%	27.3%	9.7%	68.0%	14.5%	33.3%	11.9%
eQUEST	56.8%	5.4%	21.1%	7.5%	59.4%	14.1%	27.9%	9.9%
REM/Rate	37.0%	27.5%	30.9%	11.3%	41.3%	27.5%	32.4%	11.8%
EnergyGauge	55.3%	17.2%	29.1%	10.6%	57.4%	23.7%	34.2%	12.5%

Figure 5-58: GCHP Site Energy Savings against ASHP for Houston

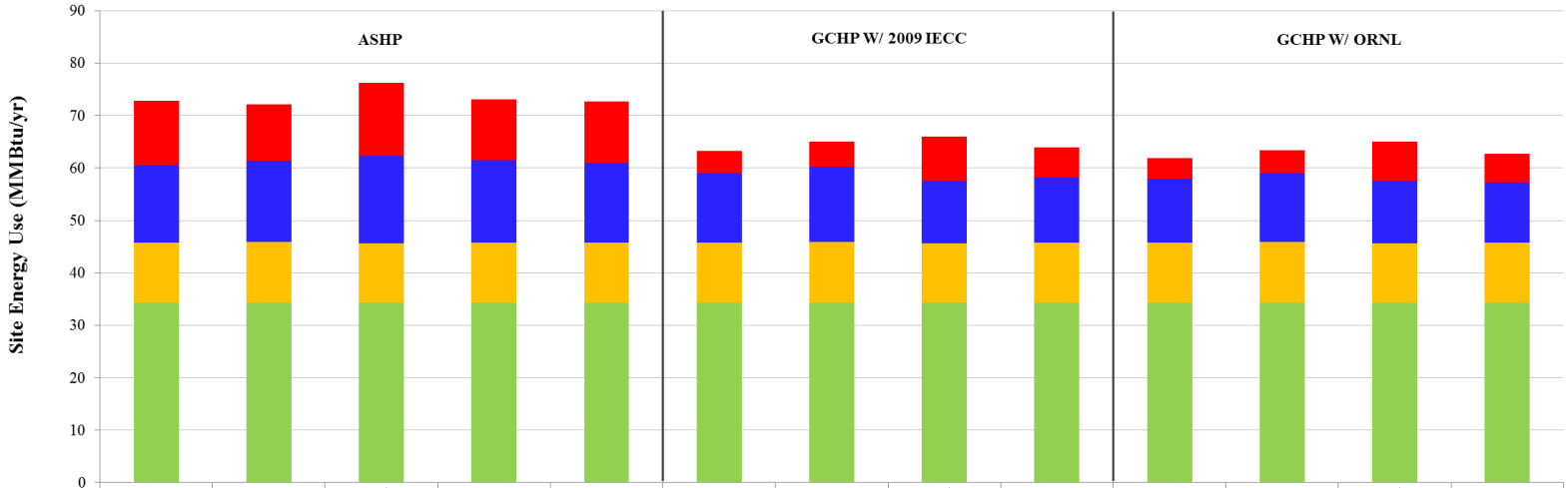

	DOE-2.1e	eQUEST	REM/Rate	EnergyGauge	IC3	DOE-2.1e	eQUEST	REM/Rate	EnergyGauge	DOE-2.1e	eQUEST	REM/Rate	EnergyGauge
TOTAL	72.8	72.2	76.2	73.1	72.7	63.2	65.0	66.0	64.0	61.8	63.4	65.1	62.8
HEATING	12.3	10.8	13.9	11.7	11.8	4.1	4.7	8.5	5.7	3.9	4.4	7.6	5.5
COOLING	14.7	15.5	16.7	15.6	15.1	13.3	14.4	11.9	12.5	12.1	13.1	11.9	11.5
DHW	11.5	11.6	11.3	11.6	11.5	11.5	11.6	11.3	11.6	11.5	11.6	11.3	11.6
Lgt & Appl	34.3	34.3	34.3	34.2	34.3	34.3	34.3	34.3	34.2	34.3	34.3	34.3	34.2

% Energy Use Difference against DOE-2.1e

	DOE-2.1e	eQUEST	REM/Rate	EnergyGauge	IC3	DOE-2.1e	eQUEST	REM/Rate	EnergyGauge	DOE-2.1e	eQUEST	REM/Rate	EnergyGauge
TOTAL		-0.8%	4.7%	0.5%	-0.1%		2.8%	4.4%	1.2%		2.6%	5.3%	1.5%
HEATING		-11.9%	13.3%	-5.0%	-4.2%		13.9%	104.9%	38.2%		12.1%	92.5%	38.2%
COOLING		5.3%	13.7%	6.4%	2.9%		8.4%	-10.4%	-6.3%		8.4%	-1.5%	-5.0%
DHW		0.9%	-1.7%	0.6%	0.0%		0.9%	-1.7%	0.6%		0.9%	-1.7%	0.6%
Lgt & Appl		0.0%	0.0%	-0.2%	0.0%		0.0%	0.0%	-0.2%		0.0%	0.0%	-0.2%

Figure 5-59: Comparison of ASHP/GCHP Site Energy Use from Different Programs for Dallas

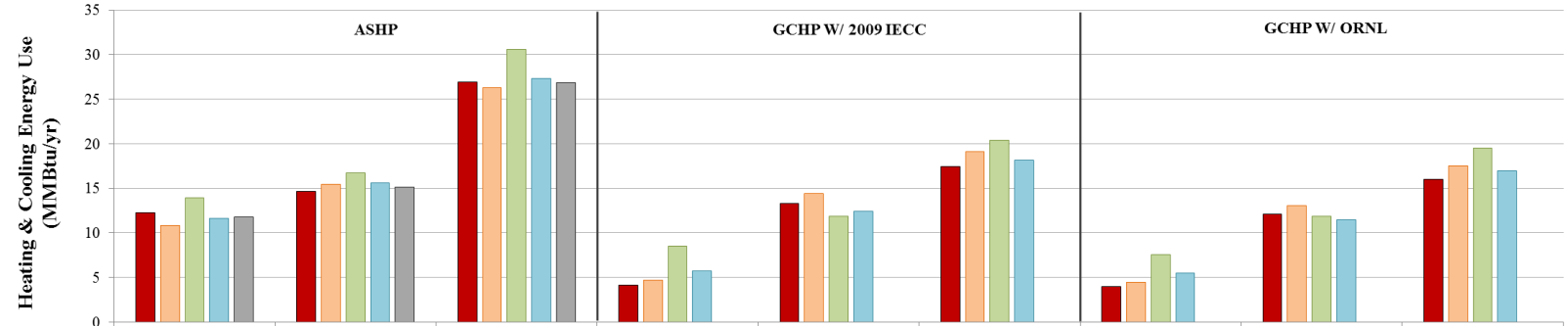

	ASHP			GCHP W/ 2009 IECC			GCHP W/ ORNL		
	HEATING	COOLING	HEATING + COOLING	HEATING	COOLING	HEATING + COOLING	HEATING	COOLING	HEATING + COOLING
DOE-2.1e	12.3	14.7	27.0	4.1	13.3	17.4	3.9	12.1	16.0
eQUEST	10.8	15.5	26.3	4.7	14.4	19.1	4.4	13.1	17.5
REM/Rate	13.9	16.7	30.6	8.5	11.9	20.4	7.6	11.9	19.5
EnergyGauge	11.7	15.6	27.3	5.7	12.5	18.2	5.5	11.5	16.9
IC3	11.8	15.1	26.9						

Figure 5-60: ASHP/GCHP Heating and Cooling Energy Use from Different Programs for Dallas

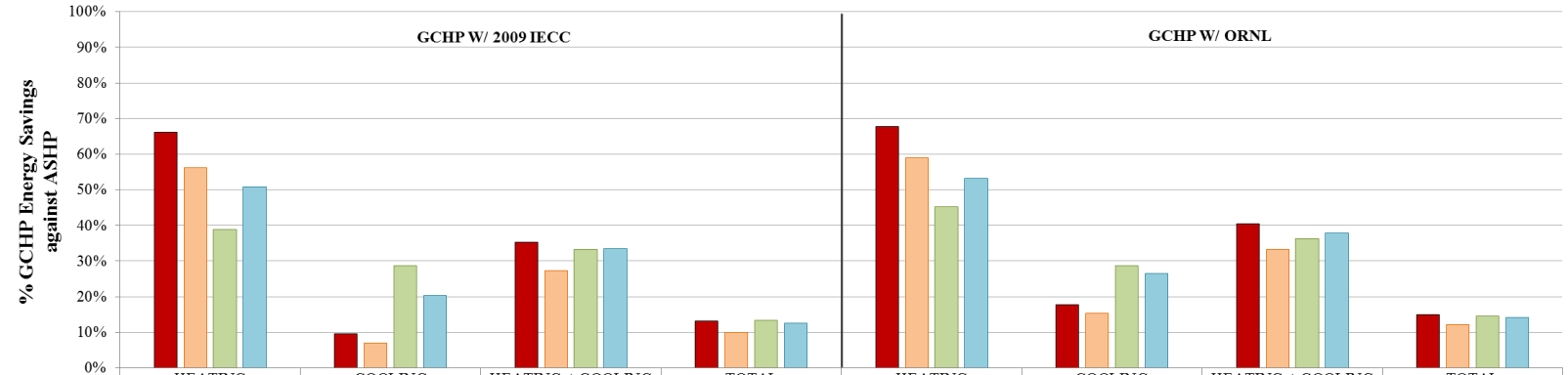

	GCHP W/ 2009 IECC				GCHP W/ ORNL			
	HEATING	COOLING	HEATING + COOLING	TOTAL	HEATING	COOLING	HEATING + COOLING	TOTAL
DOE-2.1e	66.2%	9.6%	35.3%	13.1%	67.8%	17.8%	40.5%	15.0%
eQUEST	56.3%	7.0%	27.2%	9.9%	59.0%	15.4%	33.3%	12.1%
REM/Rate	38.8%	28.7%	33.3%	13.4%	45.3%	28.7%	36.3%	14.6%
EnergyGauge	50.8%	20.4%	33.4%	12.5%	53.2%	26.6%	38.0%	14.2%

Figure 5-61: GCHP Site Energy Savings against ASHP for Dallas

The GCHP simulation used the system efficiencies of the 2009 IECC (EER 13.4 and 3.1 COP) and Oak Ridge National Laboratory (ORNL) recommendation (EER 14.1 and 3.3 COP). The total site energy results between the programs showed good agreement within 1.7 MMBtu/yr (2.5%) differences for Houston and 3.3 MMBtu/yr (5.3%) differences for Dallas, as shown in Figure 5-56 and Figure 5-59.

However, the comparison of the GCHP simulation results showed large differences between the programs in the individual cooling and heating energy use. In particular, it was found that REM/Rate had large differences against DOE-2.1e and eQUEST in the cooling and heating energy use. REM/Rate had more heating energy use, which was about two times, than DOE-2.1e and eQUEST whereas REM/Rate used less cooling energy than DOE-2.1e and eQUEST. In addition, even if the higher cooling system efficiency (from EER 13.4 in the 2009 IECC to EER 14.1 in the ORNL recommendation) was used for the GCHP base-case model, REM/Rate had the same cooling energy use for both EER13.4 and EER 14.1 (12.1 MMBtu/yr for Houston and 11.9 MMBtu/yr for Dallas). In a similar fashion, EnergyGauge had more heating energy use and less cooling energy use than DOE-2.1e and eQUEST. The large energy use differences in cooling and heating may be from different algorithms: REM/Rate uses the simplified input parameters, and EnergyGauge requires limited inputs for rated system efficiencies, which was previously discussed in Section 4.4.3.

On the other hand, in the results of the comparison of the individual cooling and heating energy, eQUEST showed better agreement against DOE-2.1e than REM/Rate and EnergyGauge. In Houston, the cooling energy use differences were 1.3 MMBtu/yr

(8.1%) and 1.1 MMBtu/yr (7.4%) for the 2009 IECC requirement and the ORNL recommendation, respectively. The heating energy use differences were 0.3 MMBtu/yr (9.5%) and 0.3 MMBtu/yr (10.1%) for the 2009 IECC requirement and the ORNL recommendation, respectively. In Dallas, the cooling energy use differences were 1.1 MMBtu/yr (8.4%) and 1.0 MMBtu/yr (8.4%) for the 2009 IECC requirement and the ORNL recommendation, respectively. The heating energy use differences were 0.6 MMBtu/yr (13.9%) and 0.5 MMBtu/yr (12.1%) for the 2009 IECC requirement and the ORNL recommendation, respectively.

Regarding the GCHP system energy savings against the ASHP system, the energy savings are shown in Figure 5-58 for Houston and Figure 5-61 for Dallas. The results include heating, cooling, the sum of heating and cooling, and the total site energy use. In the total site energy savings for Houston, DOE-2.1e showed 9.7% savings with the 2009 IECC requirement (EER 13.4 and 3.1 COP) and 11.9% savings with the ORNL recommendation (EER 14.1 and 3.3 COP). In the total site energy savings for Dallas, DOE-2.1e showed 13.1% savings with the 2009 IECC requirement and 15.0% savings with the ORNL recommendation.

In the sum of the heating and cooling savings for Houston, DOE-2.1e showed 27.3% savings with the 2009 IECC requirement and 33.3% savings with the ORNL recommendation. In the sum of the heating and cooling savings for Dallas, DOE-2.1e showed 35.3% savings with the 2009 IECC requirement and 40.5% savings with the ORNL recommendation. Not surprisingly, it was found that the GCHP system against the ASHP system in Dallas had more energy savings than Houston since the heating

energy savings in Dallas was much larger than Houston. For example, using the 2009 IECC requirement, the amount of the heating energy reduction from the ASHP to the GCHP was 5.8 MMBtu/yr in Houston and 8.2 MMBtu/yr in Dallas whereas the amount of the cooling energy reduction was 1.1 MMBtu/yr in Houston and 1.4 MMBtu/yr in Dallas. These results suggest that a GCHP system works better in the heating dominated location than the cooling dominated location.

Based on the comparison of the ASHP/GCHP base-case models simulation results from the different programs, it was found that DOE-2.1e had the smallest heating energy use of all the other programs. As a result, DOE-2.1e had the largest percent heating energy savings against the other programs. On the other hand, DOE-2.1e had larger cooling energy use than REM/Rate and EnergyGauge, and smaller cooling energy use than eQUEST. As a result, DOE-2.1e had larger percent cooling energy savings than eQUEST and smaller percent cooling energy savings than REM/Rate and EnergyGauge.

Based on the resultant GCHP energy savings with the 2009 IECC requirements using the DOE-2.1e, eQUEST, REM/Rate, and EnergyGauge programs, the average energy savings for Houston and Dallas were calculated and summarized as follow:

- The average savings in the heating energy use were 53.7% (5.8 MMBtu/yr) in Houston and 53.0% (8.2 MMBtu/yr) in Dallas,
- The average savings in the cooling energy use were 14.2% (1.0 MMBtu/yr) in Houston and 16.4% (1.4 MMBtu/yr) in Dallas,
- The average savings that represent the sum of the heating and cooling energy use were 27.1% (6.8 MMBtu/yr) in Houston and 32.3% (9.5 MMBtu/yr) in Dallas, and

- The average savings that represent total site energy use were 9.8% (6.8 MMBtu/yr) in Houston and 12.2% (9.5 MMBtu/yr) in Dallas.

5.2.3.2. GHX Sensitivity Test

In addition to the previous comparison, this study conducted a GHX sensitivity test for the DOE-2.1e GCHP base-case model varying the parameters of borehole field configurations (i.e., arrangement) and GHX length (i.e., depth). The test compared the results against the eQUEST and REM/Rate programs. The EnergyGauge program was excluded from the GHX sensitivity test since the program does not provide any inputs for a GHX unit.

The GHX conductivity test used the GCHP base-case model in Houston and the 2009 IECC requirements (EER 13.4 and 3.1 COP). The vertical GHX length was varied from 100 ft to 300 ft with an interval of 50 ft. Six borehole field configurations[54] were selected, which include: the 1x3 line type, the 1x5 line type, the 2x2 rectangle type, the 2x3 rectangle type, the 2x2 L-shape type, and the 2x3 L-shape type. In the GHX sensitivity test, the selected borehole field configurations were varied in the DOE-2.1e and eQUEST simulations. In addition, the borehole numbers corresponding to the selected borehole field configurations were varied in REM/Rate since the program does not provide inputs for the borehole field configurations but rather the number of boreholes. Therefore, the REM/Rate simulations used the borehole numbers

[54] This study considered a total of the 17 borehole field configurations for residential applications, which include: line type, rectangle type, and L-shape type borehole configurations, presented in Section 4.2.3.3.

corresponding to the configurations, as follow: three for the 1x3 line type, five for the 1x5 line type, four for the 2x2 rectangle type, six for the 2x3 rectangle type, three for the 2x2 L-shape type, and four for the 2x3 L-shape type. The borehole numbers, borehole field array, and the borehole field configurations were previously discussed in Section 4.2.3.3.

Figure 5-62 through Figure 5-65 show the simulated annual energy use from the GHX sensitivity test using DOE-2.1e, eQUEST, and REM/Rate. Figure 5-62 presents the heating energy use comparison; Figure 5-63 presents the cooling energy use comparison; Figure 5-64 presents the comparison of the sum of the heating and cooling energy use; and Figure 5-65 presents the total site energy use comparison. The total site energy use includes the lighting, appliance, and domestic hot water energy use.

As a result of testing the sensitivity of the GHX length and configurations in the annual building site energy use, first in varying the GHX length, DOE-2.1e and eQUEST were sensitive to the variation of the GHX length in the energy use in Figure 5-62 and Figure 5-63. They also had the similar pattern in the energy use (i.e., the building energy use decreased by increasing the GHX length). However, REM/Rate was not sensitive in the cooling energy use when the GHX length was longer than 200 ft, as shown in Figure 5-63. The cooling energy uses simulated with 200 ft, 250 ft, and 300 ft of the GHX length were continuously same as 12.1 MMBtu/yr. In addition, REM/Rate had more heating energy use with 200 ft of the GHX length than 150 ft for the GHX length, as shown in Figure 5-62. It may not be ordinary simulation results since longer GHX length uses less energy until a system meets minimum energy use.

In addition, to the sensitivity test that varied the borehole field configurations, DOE-2.1e and eQUEST were also shown to be sensitive to the variation of the borehole field configurations and had similar site energy use patterns in Figure 5-62 and Figure 5-63. However, when the GHX length was short as 100 ft, the cooling energy use had a reverse pattern in Figure 5-63. For example, for the 1x3 line type, DOE-2.1e had more cooling energy use than eQUEST. For the 1x5 line type, DOE-2.1e had less cooling energy use than eQUEST. The reasons for the difference were not resolved in this study. On the other hand, REM/Rate did not show noticeable energy use changes by varying the borehole number corresponding to the borehole field configurations, especially when the GHX length was longer than 150ft in Figure 5-62 and Figure 5-63. Therefore, it was found that REM/Rate was not sensitive to the borehole number changes.

In general, based on the simulation results of the GHX sensitivity test for the GCHP base-case model in Houston using the 2009 IECC requirements, it was identified that 150 ft of the GHX length was long enough to minimize the heating energy use, as shown in Figure 5-62. However, to minimize the cooling energy use, it was found that 150 ft of the GHX length was not enough since the cooling energy use continuously decreased as the GHX length increased, as shown in Figure 5-63. Therefore, to achieve more cooling energy savings, the GHX length may be extended and/or additional boreholes installed. This phenomenon agrees with that the GCHP base-case model used for the GHX sensitivity test is located in the cooling dominated climate, Houston.

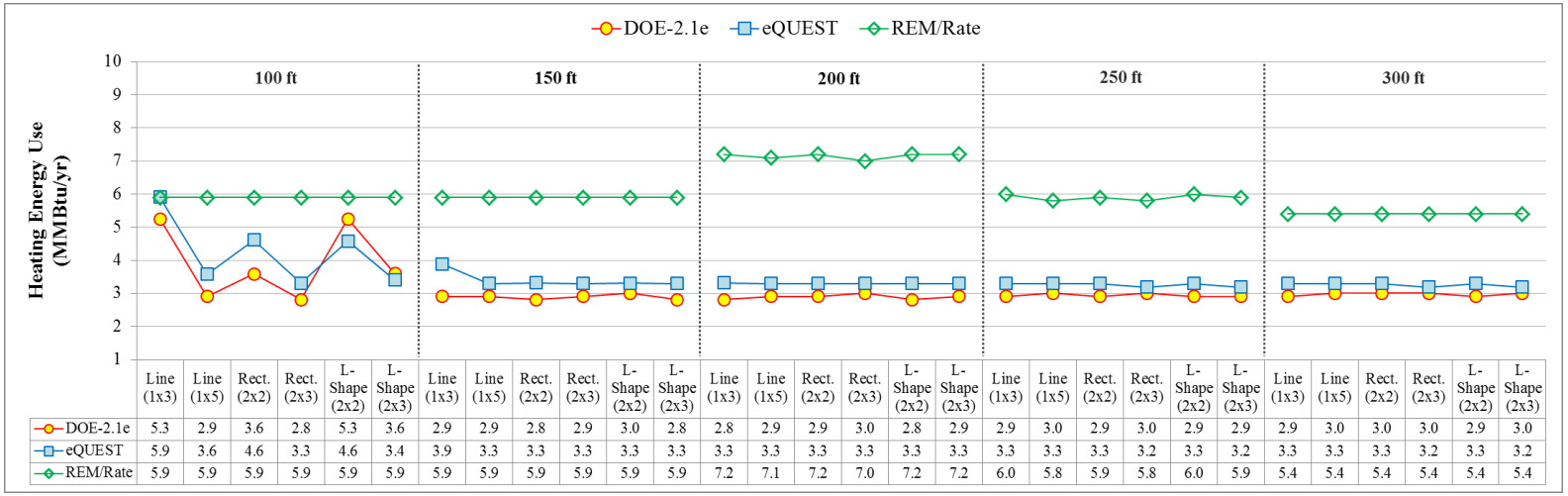

	100 ft						150 ft						200 ft						250 ft						300 ft					
	Line (1x3)	Line (1x5)	Rect. (2x2)	Rect. (2x3)	L-Shape (2x2)	L-Shape (2x3)	Line (1x3)	Line (1x5)	Rect. (2x2)	Rect. (2x3)	L-Shape (2x2)	L-Shape (2x3)	Line (1x3)	Line (1x5)	Rect. (2x2)	Rect. (2x3)	L-Shape (2x2)	L-Shape (2x3)	Line (1x3)	Line (1x5)	Rect. (2x2)	Rect. (2x3)	L-Shape (2x2)	L-Shape (2x3)	Line (1x3)	Line (1x5)	Rect. (2x2)	Rect. (2x3)	L-Shape (2x2)	L-Shape (2x3)
DOE-2.1e	5.3	2.9	3.6	2.8	5.3	3.6	2.9	2.9	2.8	2.9	3.0	2.8	2.8	2.9	2.9	3.0	2.8	2.9	2.9	3.0	2.9	3.0	2.9	2.9	2.9	3.0	3.0	3.0	2.9	3.0
eQUEST	5.9	3.6	4.6	3.3	4.6	3.4	3.9	3.3	3.3	3.3	3.3	3.3	3.3	3.3	3.3	3.3	3.3	3.3	3.3	3.3	3.3	3.2	3.3	3.2	3.3	3.3	3.3	3.2	3.3	3.2
REM/Rate	5.9	5.9	5.9	5.9	5.9	5.9	5.9	5.9	5.9	5.9	5.9	5.9	7.2	7.1	7.2	7.0	7.2	7.2	6.0	5.8	5.9	5.8	6.0	5.9	5.4	5.4	5.4	5.4	5.4	5.4

Figure 5-62: GCHP Heating Energy Use for Different GHX Length and Configuration

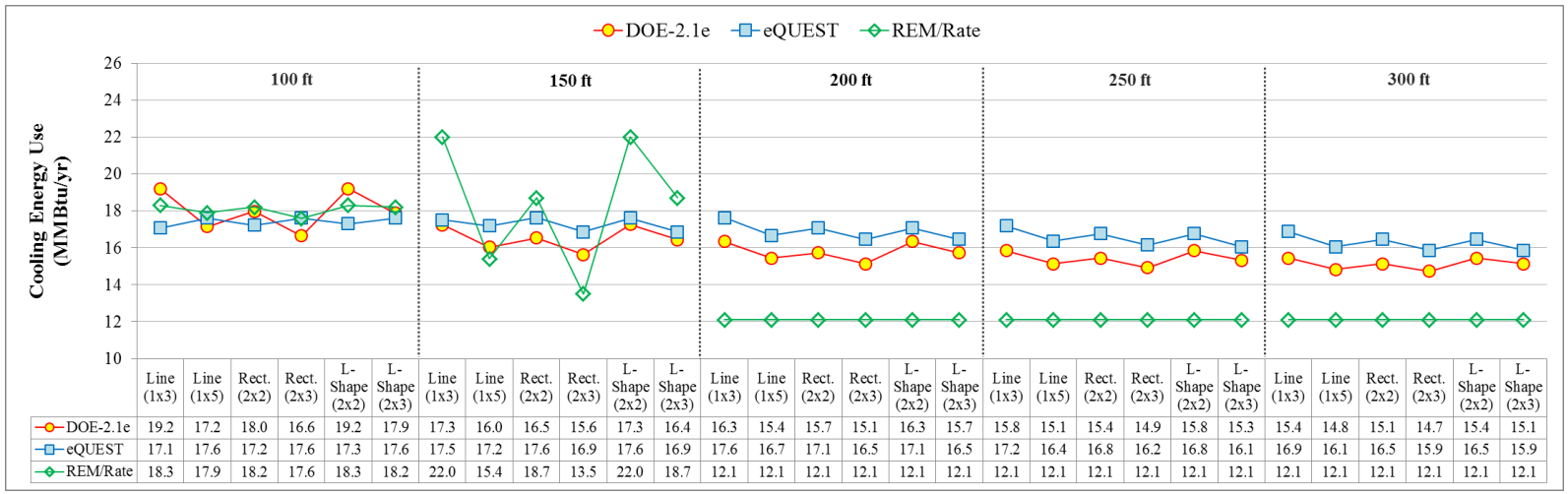

	100 ft						150 ft						200 ft						250 ft						300 ft					
	Line (1x3)	Line (1x5)	Rect. (2x2)	Rect. (2x3)	L-Shape (2x2)	L-Shape (2x3)	Line (1x3)	Line (1x5)	Rect. (2x2)	Rect. (2x3)	L-Shape (2x2)	L-Shape (2x3)	Line (1x3)	Line (1x5)	Rect. (2x2)	Rect. (2x3)	L-Shape (2x2)	L-Shape (2x3)	Line (1x3)	Line (1x5)	Rect. (2x2)	Rect. (2x3)	L-Shape (2x2)	L-Shape (2x3)	Line (1x3)	Line (1x5)	Rect. (2x2)	Rect. (2x3)	L-Shape (2x2)	L-Shape (2x3)
DOE-2.1e	19.2	17.2	18.0	16.6	19.2	17.9	17.3	16.0	16.5	15.6	17.3	16.4	16.3	15.4	15.7	15.1	16.3	15.7	15.8	15.1	15.4	14.9	15.8	15.3	15.4	14.8	15.1	14.7	15.4	15.1
eQUEST	17.1	17.6	17.2	17.6	17.3	17.6	17.5	17.2	17.6	16.9	17.6	16.9	17.6	16.7	17.1	16.5	17.1	16.5	17.2	16.4	16.8	16.2	16.8	16.1	16.9	16.1	16.5	15.9	16.5	15.9
REM/Rate	18.3	17.9	18.2	17.6	18.3	18.2	22.0	15.4	18.7	13.5	22.0	18.7	12.1	12.1	12.1	12.1	12.1	12.1	12.1	12.1	12.1	12.1	12.1	12.1	12.1	12.1	12.1	12.1	12.1	12.1

Figure 5-63: GCHP Cooling Energy Use for Different GHX Length and Configuration

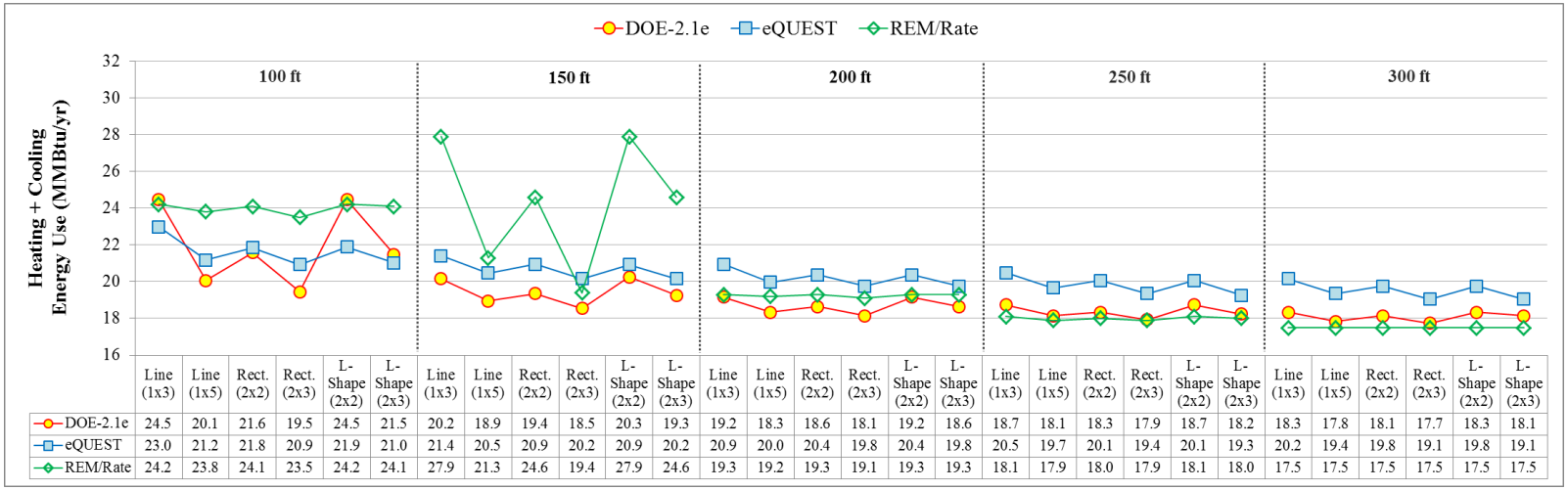

	Line (1x3)	Line (1x5)	Rect. (2x2)	Rect. (2x3)	L-Shape (2x2)	L-Shape (2x3)	Line (1x3)	Line (1x5)	Rect. (2x2)	Rect. (2x3)	L-Shape (2x2)	L-Shape (2x3)	Line (1x3)	Line (1x5)	Rect. (2x2)	Rect. (2x3)	L-Shape (2x2)	L-Shape (2x3)	Line (1x3)	Line (1x5)	Rect. (2x2)	Rect. (2x3)	L-Shape (2x2)	L-Shape (2x3)	Line (1x3)	Line (1x5)	Rect. (2x2)	Rect. (2x3)	L-Shape (2x2)	L-Shape (2x3)
DOE-2.1e	24.5	20.1	21.6	19.5	24.5	21.5	20.2	18.9	19.4	18.5	20.3	19.3	19.2	18.3	18.6	18.1	19.2	18.6	18.7	18.1	18.3	17.9	18.7	18.2	18.3	17.8	18.1	17.7	18.3	18.1
eQUEST	23.0	21.2	21.8	20.9	21.9	21.0	21.4	20.5	20.9	20.2	20.9	20.2	20.9	20.0	20.4	19.8	20.4	19.8	20.5	19.7	20.1	19.4	20.1	19.3	20.2	19.4	19.8	19.1	19.8	19.1
REM/Rate	24.2	23.8	24.1	23.5	24.2	24.1	27.9	21.3	24.6	19.4	27.9	24.6	19.3	19.2	19.3	19.1	19.3	19.3	18.1	17.9	18.0	17.9	18.1	18.0	17.5	17.5	17.5	17.5	17.5	17.5

Figure 5-64: Sum of GCHP Heating and Cooling Energy Use for Different GHX Length and Configuration

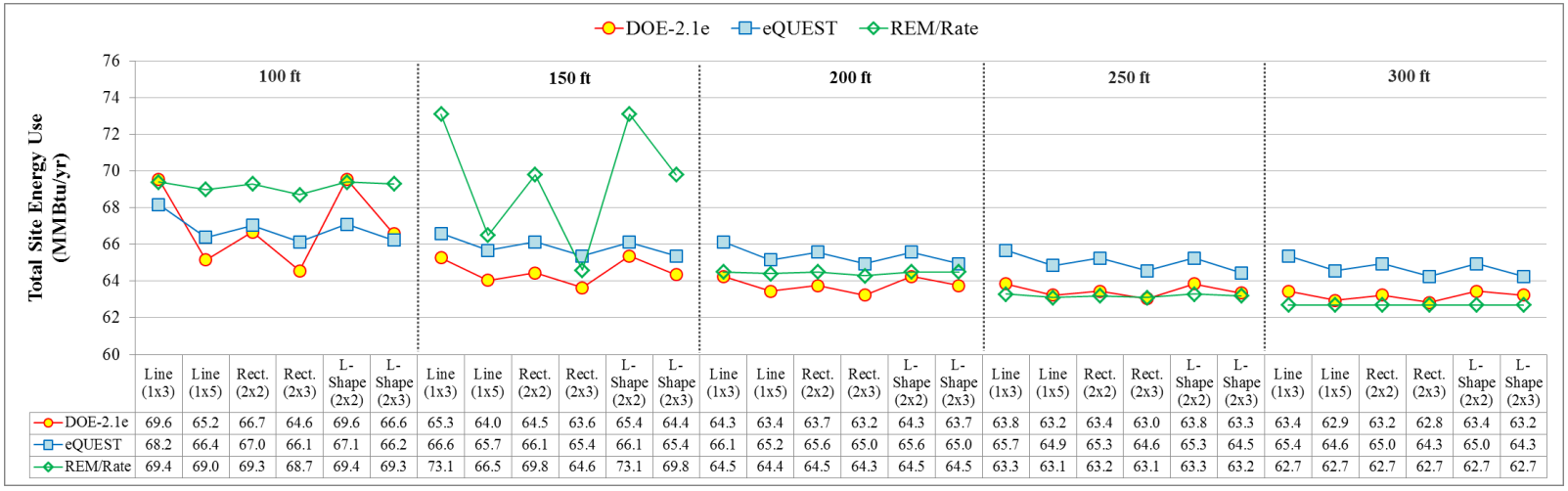

	Line (1x3)	Line (1x5)	Rect. (2x2)	Rect. (2x3)	L-Shape (2x2)	L-Shape (2x3)	Line (1x3)	Line (1x5)	Rect. (2x2)	Rect. (2x3)	L-Shape (2x2)	L-Shape (2x3)	Line (1x3)	Line (1x5)	Rect. (2x2)	Rect. (2x3)	L-Shape (2x2)	L-Shape (2x3)	Line (1x3)	Line (1x5)	Rect. (2x2)	Rect. (2x3)	L-Shape (2x2)	L-Shape (2x3)	Line (1x3)	Line (1x5)	Rect. (2x2)	Rect. (2x3)	L-Shape (2x2)	L-Shape (2x3)
DOE-2.1e	69.6	65.2	66.7	64.6	69.6	66.6	65.3	64.0	64.5	63.6	65.4	64.4	64.3	63.4	63.7	63.2	64.3	63.7	63.8	63.2	63.4	63.0	63.8	63.3	63.4	62.9	63.2	62.8	63.4	63.2
eQUEST	68.2	66.4	67.0	66.1	67.1	66.2	66.6	65.7	66.1	65.4	66.1	65.4	66.1	65.2	65.6	65.0	65.6	65.0	65.7	64.9	65.3	64.6	65.3	64.5	65.4	64.6	65.0	64.3	65.0	64.3
REM/Rate	69.4	69.0	69.3	68.7	69.4	69.3	73.1	66.5	69.8	64.6	73.1	69.8	64.5	64.4	64.5	64.3	64.5	64.5	63.3	63.1	63.2	63.1	63.3	63.2	62.7	62.7	62.7	62.7	62.7	62.7

Figure 5-65: Total GCHP Site Energy Use for Different GHX Length and Configuration

Based on the results of the GHX sensitivity test by varying the borehole field configurations, it was found that different borehole field configurations resulted in different energy use in DOE-2.1e and eQUEST as shown in Figure 5-64 and Figure 5-65. For example, for the different borehole field configurations using 250 ft of the GHX length, the total site energy use resulted from DOE-2.1e (Figure 5-65) was as follow:

- 63.8 MMBtu/yr for three boreholes in the 1x3 line type,
- 63.2 MMBtu/yr for five boreholes in the 1x5 line type,
- 63.4 MMBtu/yr for four boreholes in the 2x2 rectangle type,
- 63.0 MMBtu/yr for six boreholes in the 2x3 rectangle type,
- 63.8 MMBtu/yr for three boreholes in the 2x2 L-shape type, and
- 63.3 MMBtu/yr for four boreholes in the 2x3 L-shape type.

As a result of the simulated energy use using the selected borehole field configurations, six boreholes using the 2x3 rectangle type configuration used the smallest site energy, which was 63.0 MMBtu/yr. Whereas three boreholes using the 1x3 line type configuration and the 2x2 L-shape type configuration used the largest site energy, which was 63.8 MMBtu/yr. Therefore, the number of boreholes was found as an important factor to determine the GCHP system energy use. On the other hand, the 2x2 rectangle type configuration and the 2x3 L-shape type configuration have the same number of boreholes (i.e., four boreholes), However, they produced different total site energy uses: 63.4 MMBtu/yr for the 2x2 rectangle type configuration and 63.3 MMBtu/yr for the 2x3 L-shape type configuration. Therefore, it was found that different

GHX field configurations were also important since they may produce different site energy uses even if the number of boreholes is same.

5.2.4. Summary

This study developed a closed-loop vertical ground heat exchanger (GHX) model for the DOE-2.1e program to determine the entering water temperatures (EWTs) from a vertical GHX to the heat pump. Seventeen borehole field configurations were considered for residential applications and the approximated g-function values (i.e., a set of tabulated non-dimensional temperature response factors) were used for the configurations in this study. A g-function approximation method was used for the vertical GHX DOE-2.1e model using the DOE-2.1e input FUNCTION method. Then, to develop the DOE-2.1e ground-coupled heat pump (GCHP) system model, this study incorporated the vertical GHX DOE-2.1e input FUNCTION within the air-source heat pump (ASHP) simulation module (i.e., RESYS in DOE-2.1e) by modifying the calculation algorithm (i.e., the input file). To accomplish this, this study first developed the simplified residential ASHP base-case models for Houston and Dallas, using a step-by-step input change procedure.

To evaluate the accuracy of the simulation results, the final residential DOE-2.1e ASHP/GCHP base-case model was compared against eQUEST and other code-compliant programs (i.e., IC3 only for ASHP; EnergyGauge and REM/Rate for ASHP and GCHP). The comparison of the simulated ASHP site energy use from these programs showed good agreement for the total site energy use, which were within

1.1MMBtu/yr (1.5%) difference for Houston and 3.4 MMBtu/yr (4.7%) difference for Dallas. In addition, the comparison of the simulated GCHP site energy use[55] from these programs also showed good agreement for the total site energy use, which were within 1.7 MMBtu/yr (2.5%) difference for Houston and 3.3 MMBtu/yr (5.3%) difference for Dallas.

However, the comparison for the ASHP and GCHP base-case models showed larger differences for the individual cooling and heating energy use than for the total site energy use. For example, REM/Rate and EnergyGauge had more heating energy use and less cooling energy use than DOE-2.1e and eQUEST. These differences in the cooling and heating energy use may be caused by the different algorithms using more simplified input parameters in REM/Rate and EnergyGauge than DOE-2.1e. On the other hand, eQUEST had better agreement against DOE-2.1e than REM/Rate and EnergyGauge. This would appear to be due to the fact that eQUEST used input parameters that are similar to DOE-2.1e.

Although DOE-2.1e had smaller heating energy use than the other programs, DOE-2.1e had larger cooling energy use than REM/Rate and EnergyGauge, and smaller cooling energy use than eQUEST. After the DOE-2.1e ASHP and GCHP base-case models with the 2009 IECC requirements were completed, the GCHP system energy savings against the ASHP system were then calculated. The results showed that the GCHP system energy savings in the total site energy use were 9.7% (6.8 MMBtu/yr) in

[55] For system efficiencies, this study used SEER13 and 7.7 HSPF for the ASHP system and EER 13.4 and 3.1 COP for the GCHP system based on the 2009 IECC requirements. In addition, this study used EER 14.1 and 3.3 COP for the GCHP system efficiency recommended by ORNL (ORNL, 2013).

Houston and 13.1% (9.6 MMBtu/yr) in Dallas. The GCHP energy savings in the heating plus cooling energy use were 27.3% (6.8 MMBtu/yr) in Houston and 35.3% (9.6 MMBtu/yr) in Dallas.

Lastly, this study tested the sensitivity of the different GHX length and borehole field configurations using the DOE-2.1e, eQUEST, and REM/Rate programs. The test used the GCHP base-case model with the 2009 IECC requirements. The simulated results from the programs were then compared. As a result of the GHX sensitivity test, it was found that DOE-2.1e and eQUEST showed similar sensitivities for the given GHX length and borehole field configurations. These two programs had similar results for the annual energy use. However, the REM/Rate program appeared to be insensitive to the GHX length and borehole field configurations in the annual energy use comparisons when the GHX length was longer than 200 ft.

In addition, based on the GHX sensitivity test, it was found that 150 ft of the GHX length appeared to be long enough for the residential GCHP simulation model in Houston to minimize the heating energy use. To minimize the cooling energy use, however, the GHX length is required to be longer than 150 ft and/or additional boreholes are required to be installed.

CHAPTER VI

SUMMARY AND FUTURE WORK

6.1. Summary of the Methodology

To improve residential energy efficiency in Texas, an improved simulation tool for home builders and code officers was developed for use in evaluating their design. This study developed the closed-loop ground heat exchanger (GHX) models including a custom-built GHX model and a vertical GHX model.

The case-study house selected in this study used a custom-built GHX, which is a combination of horizontal GHXs and surface water (pond) GHX. This study developed the custom-built GHX model to calculate the entering water temperatures (EWTs) for the case-study house. The custom-built GHX model was then validated using the measured EWT data from the case-study house in Texas[56]. The methodologies used for developing the custom-built GHX model include:

- Calculation of the closed loop GHX models including the horizontal and surface water GHX;
- Development of the custom-built GHX model for the residential case-study building in Texas;
- Collection of the weather data from the Solar Test Bench (STB);

[56] The data were collected from the middle of December 2012 to the end of July 2013. The periods included both the heating season and the cooling season.

- Calibration and installation of the temperature sensors to measure the EWTs for the case-study house;
- Collection of the measured data from the case-study house; and
- Validation of the custom-built GHX model using the measured EWT data from the case-study house.

The vertical GHX model to calculate the EWTs was developed to be used in the DOE-2.1e simulation program by using the DOE-2 FUNCTION command. The g-function approximation method for residential applications developed in this study was used for the vertical GHX DOE-2.1e model. To develop the DOE-2.1e ground-coupled heat pump (GCHP) system model, the vertical GHX DOE-2.1e input FUNCTION was incorporated within the air-source heat pump (ASHP) simulation module by modifying the calculation algorithm (i.e., the input file).

This study also developed simplified residential ASHP/GCHP base-case models for Houston and Dallas, using DOE-2.1e, eQUEST, IC3[57]., REM/Rate, and EnergyGauge. The DOE-2.1e simulation results were then compared for the other programs. The methodologies used for developing the DOE-2.1e GCHP simulation model with a vertical GHX include:

- Calculation of the closed loop vertical GHX model;
- Development of the g-function approximation;

[57] The IC3 program was excluded from the GCHP base-case model development since the current IC3 program did not have the capability to simulation a GCHP system.

- Development of the vertical GHX model to be used in the DOE-2.1e simulation program, using the DOE-2 FUNCTION command;
- Development of the DOE-2.1e GCHP simulation model using the vertical GHX DOE-2.1e input FUNCTION;
- Development of the step-by-step method for studying a simplified residential ASHP base-case model;
- Development of the residential ASHP base-case models for Houston and Dallas using DOE-2.1e, eQUEST, IC3, REM/Rate, and EnergyGauge;
- Development of the residential GCHP base-case models for Houston and Dallas using DOE-2.1e, eQUEST, REM/Rate, and EnergyGauge; and
- Comparison of the simulation results for the GCHP base-case model between the programs.

6.2. Summary of the Results

This section includes two types of results obtained from this study: 1) the results from the custom-built GHX model for the case-study house, and 2) the results from the vertical GHX and GCHP models incorporated within the DOE-2.1e simulation programs.

6.2.1. Summary of the Custom-Built GHX Model Results

The case-study house selected in this study utilizes the custom-built GHXs using a combination of horizontal GHXs and surface water (pond) GHX. The custom-built GHX consists of three GHXs, connecting the first horizontal GHX, the surface water

GHX, and the second horizontal GHX, in sequence. This study developed the custom-built GHX model to calculate the entering water temperatures (EWTs) for the case-study house. To calculate the EWTs using the custom-built GHX model, this study used the weather data collected from the ESL's STB and the measured GCHP/GHX data from the case-study house. The calculated EWTs were then compared with the measured EWTs from the case-study house.

The custom-built GHX model calculated the EWTs for each hour of the simulation using the calculated ground temperatures and pond water temperatures. First, the ground temperatures were calculated for the horizontal GHX type (i.e., the first GHX and the third GHX in the case-study house). A ground depth of 5 ft and 6 ft was used for the first GHX and the third GHX, respectively. The calculated hourly ground temperatures for the measurement period were as follow: 1) for the first GHX, the minimum ground temperature was 62.5 F and the maximum ground temperature was 78.3 F, and 2) for the third GHX, the minimum ground temperature was 63.8 F and the maximum ground temperature was 76.3 F.

Second, the pond water temperatures were calculated for the surface water GHX, which is the second GHX in the case-study house. The pond water temperatures were calculated based on the energy transfer mechanisms including: the solar radiation absorbed by the pond at the pond's surface, the thermal radiation from the pond water to the sky at the pond's surface, the evaporation at the pond's surface, the convection at the pond's surface, the conductive heat transfer to/from the ground in contact with the pond, and the heat transfer between the fluid in the pipe and the pond. In the calculated pond

water temperatures, the lowest pond water temperature was 37.6 F on 16th of January, 2013. The highest pond water temperature was 88.3 F on 29th of June, 2013. In the calculations of the pond water temperatures, it was observed that the absorbed solar radiation was the largest heat transfer amount which was about 43 % of total heat transfer amount.

Third, based on the calculated ground and pond water temperatures, the entering water temperatures (EWTs) were calculated and compared to the measured EWTs data from the case-study house. It was identified that the monthly average EWTs differences between the measured EWTs and the calculated EWTs were observed to be about 2.2 F during the heating season (December, January, and February) and about 3.2 F during the cooling season (May, June, and July). The calculated EWTs were lower than the measured EWTs for the heating season and higher than the measured EWTs for the cooling season. Therefore, this study concluded that the calculated EWTs were slightly over-estimated. However, the calculated EWTs were felt to be acceptable considering the uncertainty of other unknowns such as the pond water level change, exact underground soil condition, and system degradation.

6.2.2. Summary of the Vertical GHX and GCHP DOE-2.1e Models Results

A vertical ground heat exchanger (GHX) model for the DOE-2.1e program was developed to determine the entering water temperature (EWT) from a vertical GHX to a heat pump. To develop the DOE-2.1e ground-coupled heat pump (GCHP), a vertical GHX DOE-2.1e input FUNCTION was incorporated within an air-source heat pump

(ASHP) simulation module (i.e., RESYS in DOE-2.1e) by modifying the calculation algorithm (i.e., the input file). This study developed and compared residential ASHP/GCHP base-case models using DOE-2.1e, eQUEST, IC3 for the ASHP only, REM/Rate, and EnergyGauge. Finally, this study conducted GHX sensitivity tests using DOE-2.1e, eQUEST, and REM/Rate.

The vertical GHX DOE-2.1e model developed for this study used the g-function method, which can determine the temperature change at the borehole wall corresponding to a change in the heat extraction/rejection input for a time step. To use the g-function method, this study approximated the g-function values of seventeen borehole field configurations considered for residential applications in this study, which include: line type, rectangle type, and L-shape type borehole field configurations. The g-function values approximated in this study showed good agreement within the ±10% difference range, which was discussed in section 5.2.2.1 and appendix B, against the g-function values developed by Eskilson (1987), and enhanced by Yavuzturk and Spitler (1999).

The comparison of the simulation results[58] between these programs showed good agreement in the total site energy use. For the ASHP simulation models, the site energy use differences between the programs were identified within 1.1MMBtu/yr (1.5%) for Houston and 3.4 MMBtu/yr (4.7%) for Dallas. On the other hand, the total site energy use differences resulted from the GCHP base-case models were identified within 1.7 MMBtu/yr (2.5%) for Houston and 3.3 MMBtu/yr (5.3%) for Dallas.

---

[58] For system efficiencies, this study used SEER13 and 7.7 HSPF for the ASHP system and EER 13.4 and 3.1 COP for the GCHP system based on the 2009 IECC requirements. In addition, this study used EER 14.1 and 3.3 COP for the GCHP system efficiency recommended by ORNL (ORNL, 2013).

However, the comparisons of the ASHP and GCHP base-case model simulations showed larger difference in the individual cooling and heating energy use than the total site energy use. For example, REM/Rate and EnergyGauge had more heating energy use and less cooling energy use than DOE-2.1e and eQUEST. These differences in the cooling and heating energy use were most likely caused by the different algorithms, which used simplified input parameters for REM/Rate and EnergyGauge versus the more detailed inputs used for this study (DOE-2.1e). On the other hand, eQUEST had better agreement against DOE-2.1e than REM/Rate and EnergyGauge since eQUEST used the similar detailed input parameters with DOE-2.1e.

Regarding the GCHP system energy savings against the ASHP system, in the total site energy use for Houston, this study showed 9.7% savings with the 2009 IECC requirement and 11.9% savings with the ORNL recommendation. For Dallas, this study showed 13.1% savings with the 2009 IECC requirement and 15.0% savings with the ORNL recommendation. When the heating and cooling energy use was added together for Houston, this study showed 27.3% savings with the 2009 IECC requirement and 33.3% savings with the ORNL recommendation. For Dallas, this study showed 35.3% savings with the 2009 IECC requirement and 40.5% savings with the ORNL recommendation.

In addition, this study tested the sensitivity of the GHX length and borehole field configurations in the annual building site energy use by varying these parameters. As a result, it was found that DOE-2.1e and eQUEST were sensitive to both variations of the GHX length and borehole field configurations in the site energy use. However, REM/Rate was not sensitive to the GHX field configuration, especially in the cooling

energy use. By varying the GHX length for the residential GCHP base-case model in Houston, it was found that 150 ft of the GHX length was long enough to minimize the heating energy use. However, to minimize the cooling energy use, more GHX length was required. By varying the borehole field configurations, on the other hand, this study found that the number of boreholes and the borehole field configurations affect to the GCHP system energy use.

6.3. Recommendations for Future Research

This study developed the ground heat exchanger (GHX) models, including the custom-built GHX model for the case-study house and the vertical GHX model used for the DOE-2.1e simulation program. The GHX models developed in this study were limited to the following characteristics:

- A closed-loop GHX;
- A single-family residential building in Texas;
- Custom-built GHX model development and validation;
- Vertical GHX DOE-2.1e model development and application;
- The specially developed g-function approximation method for residential application;
- The specially developed ASHP/GCHP base-case simulation models;
- DOE-2.1e ground-coupled heat pump (GCHP) simulation model development; and
- An hourly energy simulation analysis.

The limitations in this study present a number of opportunities for future study. As a result, the following issues are recommended and presented as follow:

- Recommended future study for an open-loop GHX model: This study was limited to develop the closed-loop GHX model. Since an open-loop GHX may lead to different conclusion, it is recommended that research be aimed to develop the open-loop GHX model, which can then be used to calculate/simulate energy use for a GCHP system using an open-loop GHX.
- Recommended future study for non-residential buildings in Texas: This study was limited to a single-family residential building in Texas. Based on that limitation, the g-function approximation to be used for the vertical GHX model was developed for residential applications. Since a non-residential building requires more boreholes and different borehole field configurations than a residential building because a non-residential building may have more heating and cooling loads. Therefore, it is recommended that research be performed to develop the g-function approximation for non-residential applications.
- Recommended future study for mean ground temperatures in different locations/climates: This study was limited to Texas, which is hot and humid climate. This study also investigated/included the mean ground temperatures at several representative locations in Texas and the mean ground temperatures were then used for the developed GHX models. Since other locations/climates may lead to very different mean ground temperatures, it is recommended that additional research be conducted to investigate mean ground temperatures for other locations/climates, which can then be used to calculate the entering water temperatures (EWTs) for other locations/climates.

- Recommended future study for ground temperature calculation in horizontal GHX model: This study used the algorithm developed by Kusuda and Achenbach (1965) to predict ground temperatures. Unfortunately, the predicted ground temperatures do not account for the weather change such as outdoor air temperature, solar radiation, wind, rain, evaporation, and other variables. As a result, the predicted ground temperatures were overestimated or underestimated, especially during the spring and fall seasons which have rapid temperature variation. Therefore, it is recommended that research be conducted to develop a new better method to calculate the ground temperatures, which can then account for the weather change more accurately.
- Recommended future study for application of the custom-built GHX model: This study was limited to develop and validate the custom-built GHX model (i.e., combining the horizontal and surface water GHX models) using the measured EWTs form the case-study house. However, the custom-built GHX model was not incorporated into a simulation program. Therefore, it is recommended that further research be conducted to allow the custom-built GHX model in a simulation program (i.e., DOE-2.1e), which can then be used to calculate/simulate whole-building energy use. In similar fashion, further research should be conducted to insert a separate horizontal GHX model or a surface water GHX model into a simulation program.
- Recommended future study for monitoring temperatures of the custom-built GHX model and the case-study house: This study developed the custom-built GHX model and measured temperatures of the supply air, return air, leaving water, and entering water to validate the model. However, this study did not measure the source

temperatures including underground for 1st and 3rd GHX units and pond for 2nd GHX unit. Therefore, it is recommended that further research be conducted to measure the source temperatures, which can then give more confidence for the model and allow the model to be improved.

- Recommended future study for validation the DOE-2.1e GCHP model with the vertical GHX: This study developed the DOE-2.1e GCHP simulation model using the vertical GHX input FUNCTION. The simulation results from the DOE-2.1e GCHP model were only compared against the results from other simulation programs. Therefore, it is recommended that research be conducted to validate the DOE-2.1e GCHP simulation results with the measured data from several case-study houses with vertical GHXs or with the data from lab tests, which can then provide more confidence for the DOE-2.1e GCHP simulation model with vertical GHXs.
- Recommended future study for an improvement of IC3: The publicly-funded, web-based, and RESNET-certified code-compliant IC3 program does not have a capability to calculate the GCHP system performance. Therefore, it is recommended that research be conducted to incorporate the vertical GHX DOE-2.1e input FUNCTION developed in this study within the IC3 program, which can then allow the IC3 program to have the GCHP simulation capability. To accomplish this future task, the DOE-2.1e Input MACRO commands need to be studied. In addition, IC3 BDL structure and algorithm need to be fully studied as well. After applying the developed GCHP simulation model into IC3, users can evaluate their design for a

GCHP system and it eventually helps to improve residential energy use efficiency in Texas.

- Recommended future study for benefit analysis of a GCHP system: This study was limited to an energy simulation analysis. As a result, this study did not provide any cost analysis associated with implementing a GCHP system in a residence. Therefore, it is recommended that future research be conducted to quantify all GCHP system implementation cost, which can then allow a cost analysis against other residential heating and cooling systems. In a similar fashion with this matter, it is also recommended that research be conducted to quantify emissions reduction (i.e., CO2, NOx, and SOx) from implementing the GCHP system.
- Recommended future study for a residential base-case model using different systems: This study developed the residential base-case simulation model using a step-by-step input change method. For the base-case model development, this study was limited to an air-source heat pump (ASHP) system. Since different residential heating and cooling system may lead to different energy use, it is recommended that research be conducted to develop residential base-case simulation models using different systems, which can then allow quantifying energy savings by implementing a GCHP system from a different residential system.

REFERENCES

AEC. (2011). *REM/Rate: The Home Energy Rating Tool (Version 12.93)*. Boulder, CO: Architectural Energy Corporation. Retrieved from http://www.archenergy.com/

AES. (2012). Alternative Energy Sources: Geothermal Energy. Retrieved May 20, 2012 from http://faculty.fairfield.edu/mediacenter/nm_webdesign/s_zandan/sz_alt_energy/geothermal_energy.html

AHRI. (1998). *1998 Standard for Ground Source Close-Loop Heat Pumps (AHRI Standard 330-1998)*. Arlington, VA: Air-conditioning, Heating, and Refrigeration Institute.

AHRI. (2008). *2008 Standard for Performance Rating of Unitary Air-Conditioning & Air-Source Heat Pump Equipment (ANSI/AHRI Standard 210/240-2008)*. Arlington, VA: Air-conditioning, Heating, and Refrigeration Institute.

ASCE. (2005). *The ASCE Standardized Reference Evapotranspiration Equation*. Reston, VA: American Society of Civil Engineers.

ASHRAE. (2004). *Method of Test for Determining the Design and Seasonal Efficiencies of Residential Thermal Distribution Systems (ASHRAE Standard 152-2004)*. Atlanta, GA: American Society of Heating, Refrigerating, and Air-conditioning Engineers.

ASHRAE. (2007a). *Energy-Efficient Design of Low-Rise Residential Buildings (ASHRAE Standard 90.2-2007)*. Atlanta, GA: American Society of Heating, Refrigerating and Air-Conditioning Engineers.

ASHRAE. (2007b). *2007 ASHRAE Handbook, Ch. 32: Geothermal Energy*. Atlanta, GA: American Society of Heating, Refrigerating and Air-Conditioning Engineers, Inc.

ASHRAE. (2010). *Standard 62.2, Ventilation and Acceptable Indoor Air Quality in Low-Rise Residential Buildings*, Atlanta, GA: American Society of Heating, Refrigerating and Air Conditioning Engineers.

ASHRAE. (2011). *2011 ASHRAE Handbook, Ch. 5.6: Natatoriums*. Atlanta, GA: American Society of Heating, Refrigerating and Air-Conditioning Engineers, Inc.

ASTM. (1981). *Manual on the Use of Thermocouples in Temperature Measurement*. Philadelphia, PA: American Society for Testing and Materials.

ASTM. (2007). *ASTEM E77-07 Standard Test Method for Inspection and Verification of Thermometers*. West Conshohocken, PA: American Society for Testing and Materials.

Azbil. (2011). Temperature Sensor for Pipe Surface (Pt100 RTD) for Actival^{TM} Plus Model FVY51XX, Specifications/Instructions. AB-6923, Yamatake Corporation Building Systems Company. Retrieved November 18, 2012, from http://www.azbil.com/products/bi/ba/ss/AB-6923.pdf

Banks, D. (2012). *An Introduction to Thermogeology: Ground Source Heating and Cooling (2nd ed.)*. Ames, IA: John Wiley & Sons, Inc.

Beca. (2009). *Technical Report: Geothermal Heat Pump Study*. New Zealand: Beca Carter Hollings & Ferner Ltd. (Beca).

BECP. (2009). *Impacts of the 2009 IECC for Residential Buildings in the State of Texas*. U.S. Department of Energy. Retrieved June 19, 2013, from http://www.energycodes.gov/sites/default/files/documents/Residential_Texas_0.pdf

Bennet, J., Claesson, J., & Hellstrom, G., 1987. *Multipole Method to Compute the Conductive Heat Transfer to and between Pipes in a Composite Cylinder*. Notes on Heat Transfer 3-1987. Lund, Sweden: Department of Building Physics, Lund Institute of Technology.

Bernstein, L., Pachauri, R. K., & Reisinger, A. (2008). *Climate Change 2007: Synthesis Report*. Geneva, Switzerland: Intergovernmental Panel on Climate Change (IPCC).

BLOCON. (2008). *Earth Energy Designer Manual (EED 3.0)*. Lund, Sweden: BLOCON. Retrieved from http://www.buildingphysics.com/manuals/EED3.pdf

Breger, D., Hubbell, J., Hasnaoui, H., & Sunderland, J. (1996). Thermal Energy Storage in the Ground: Comparative Analysis of Heat Transfer Modeling Using U-Tubes and Boreholes. *Solar Energy*, 56(6), 493-503.

Bryant. (2013). *GeoDesigner: Advanced Energy Analysis Software*. Oklahoma City, OK: ClimateMaster. Retrieved from http://www.bryantgeo.com/geodesigner.htm

Campbell Scientific. (2013a). *AM16/32B: 16 or 31 Channel Relay Multiplexer*. Retrieved May 27, 2013, from http://www.campbellsci.com/am16-32b

Campbell Scientific. (2013b). *CR1000, Measurement and Control Datalogger*. Retrieved May 27, 2013, from http://www.campbellsci.com/cr1000

Campbell Scientific. (2013c). *Loggernet: Datalogger Support Software*. Retrieved May 29, 2013, from http://www.campbellsci.com/loggernet

Campbell Scientific. (2013d). *RTMCpro:Real-Time Monitoring and Control Software*. Retrieved May 29, 2013, from http://www.campbellsci.com/rtmcpro

Campbell Scientific. (2013e). *RTMCwebs: RTMC Web Server*. Retrieved May 29, 2013, from http://www.campbellsci.com/rtmc-web-server

Campbell Scientific. (2013f). 034B-L: Wind Set. Retrieved May 29, 2013, from http://www.campbellsci.com/034B

CANMET. (2005). *Clean Energy Project Analysis: RETScreen Engineering & Cases Textbook*. Ottawa, Canada: CANMET Energy Technology Centre - Varennes, Natural Resources Canada.

Carslaw, H. & Jaeger, J. (1947). *Conduction of Heat in Solid*. Oxford, Australia: Claremore Press.

Chiasson, Andrew. D. (1999). *Advances in Modeling of Ground-Source Heat Pump Systems*. M.S. Thesis. Stillwater, OK: Oklahoma State University.

Ching, F. & Winkel, S. (2007). *Building Codes Illustrated: A Guide to Understanding the 2006 International Building Code*. Hoboken, NJ: John Wiley & Sons, Inc.

Do, S., Choi, J., & Haberl, J. (2013). *A Simplified Residential Base-Case Model*. A Project for Texas's Senate Bill 5 Legislation for Reducing Pollution in Nonattainment and Affected Areas. ESL-TR-13-09-01. College Station, TX: Energy Systems Laboratory, Texas A&M University System.

DOE. (1999). *Codes & Standards: The Model Energy Code*. U.S. Department of Energy. Retrieved April 23, 2013, from http://smartenergy.illinois.edu/pdf/Archive/ModelEnergyCode.pdf

DOE. (2009). *Impacts of the 2009 IECC for Residential Buildings at State Level*. U.S. Department of Energy Building Energy Codes Program. Retrieved June 10, 2013, from http://www.energycodes.gov/sites/default/files/documents/Residential_Utah_0.pdf

Dwyer. (2012). *Spirit-Filled Glass Thermometer*. Retrieved December 07, 2012, from http://www.proheatinc.com/products/dwyer/htdocs/temperature/SeriesGTIntro.html

ECW. (2012). *Go Hybrid with HyGCHP*. Madison, WI: Energy Center of Wisconsin (ECW). Retrieved from http://www.ecw.org/project.php?workid=1&resultid=465

EnergyGauge. (2013). *EnergyGauge USA FlaRes 2008 Online Help System*. Retrieved September 13, 2013 from EnergyGauge Website: https://securedb.fsec.ucf.edu/egflacom/support

EnergyLogic. (2010). *OptiMiser: Empowered Energy Audit Software, Version 1.0*. Denver, CO: EnergyLogic Inc. Retrieved from http://optimiserenergy.com/

EPA. (1993). *Space Conditioning: The Next Frontier*. Washington, DC: U.S. Environmental Protection Agency.

EPLAB. (2006). *Black & White Pyranometer, Model 8-48: Instruction Sheet*. Newport, RI: The Eppley Laboratory, Inc.. Retrieved May 29, 2013, from http://go.owu.edu/~chjackso/Climate/8-48_instructions.pdf

EPLAB. (2013a). *Normal Incidence Pyrheliometer*. Retrieved May 29, 2013, from http://www.eppleylab.com/PrdNormIncPyrhelmtr.htm

EPLAB. (2013b). *Precision Spectral Pyranometer*. Retrieved May 29, 2013, from http://www.eppleylab.com/PrdPrecSpectralPyrmtr.htm

Eskilson, P. (1987). *Thermal Analysis of Heat Extraction Boreholes*. Lund, Sweden: Department of Mathematical Physics, University of Lund.

ESL. (2010a). *International Code Compliant Calculator(IC3) (Version 3.9.3)*. College Station, TX: Energy Systems Laboratory, Texas A&M University. Retrieved from http://ic3.tamu.edu

ESL. (2010b). *International Code Compliant Calculator(IC3) Manual*. College Station, TX: Energy Systems Laboratory, Texas A&M University.

Fairey, P., Parker, D., Wilcox, B., Lombardi, M., & Center, F. S. E. (2004). Climate Impacts on Heating Seasonal Performance Factor (HSPF) and Seasonal Energy Efficiency Ratio (SEER) for Air Source Heat Pumps. *ASHRAE Transactions*, 110(2), 178-188.

Fairey, P., Vieira, R., Parker, D., Hanson, B., Broman, P., Grant, J., Fuehrlein, B., & Gu, L. (2002). *EnergyGauge USA: A Residential Building Energy Simulation Design Tool*. Cocoa, FL: Florida Solar Energy Center (FSEC).

Fisher, D. E., Rees, S. J., Padhmanabhan, S. K., & Murugappan, A. (2006). Implementation and Validation of Ground-Source Heat Pump System Models in

an Integrated Building and System Simulation Environment. *International Journal of HVAC&R Research*, 12:S1, 693-710.

Fossa, M., Cauret, O. & Bernier, M. A. (2009). Comparing the Thermal Performance of Ground Heat Exchangers of Various Lengths. Paper presented at the *11th International Conference*, June 14 - 17, 2009, Effstock, Stockholm.

FSEC. (2005). *Development of High Efficiency Air Conditioner Condenser Fans*. Cocoa, FL: Florida Solar Energy Center.

FSEC. (2011). *EnergyGauge USA: Code Compliance and Home Energy Rating Software, Version 2.8.05*. Cocoa, FL: Florida Solar Energy Center.

FSEC. (2012). *Release Notes EnergyGauge USA 3.0.03*. Cocoa, FL: Florida Solar Energy Center. Retrieved from http://www.energygauge.com/USARES/ReleaseNotes_3003.pdf

Gehlin, S. (1998). *Thermal Response Test, In-Situ Measurements of Thermal Properties in Hard Rock*. Licentiate Thesis. Luleå, Sweden: Luleå University of Technology.

GeoKISS. (2013). *Ground Source Heat Pump Design, GshpCalc (Version 5.0.5)*.Northport, AL: GeoKISS. Retrieved from http://www.geokiss.com/gsoftware.htm

Gilman, D., Marshall, K., Liu, Z., Mukhopadhyay, J., Stackhouse, R., Cordes, J., Montgomery, C., McKelvey, K., O'Neal, S., Culp, C., Haberl, J., & Yazdani, B. (2008). *Development of a Residential Code-Compliant Web-Based Energy Efficiency Calculator for Texas*. College Station, TX: Energy Systems Laboratory, Texas A&M University.

Graven, R. M., & Hirsch, P. R. (1977). *CAL-ERDA User's Manual* (ANL/ENG-77-03). Argonne, IL: Argonne National Laboratory.

Haberl, J.S. & Cho, S. 2004. *Literature Review of Uncertainty of Analysis Methods (DOE-2 Program)*. College Station, TX: Energy Systems Laboratory, Texas A&M University.

Hayes, Tony, Song, Li, & Dawson, Micah. (2011). Heat Balance Analysis to Validate the Heat Dissipation Rate of a Man-Made Lake as a Heat Rejection Device in a Power Plant. Proceedings of the *Eleventh International Conference Enhanced Building Operations*.

Hellström, G. (1989). *Duct Ground Heat Storage Model: Manual for Computer Code*. Lund, Sweden: University of Lund.

Hellström, G. & Sanner, B. (2000). *Earth Energy Designer User Manual (Version 2.0)*. Lund, Sweden: University of Lund.

Hellström, G. & Sanner, B. (2001). PC-programs and Modeling for Borehole Heat Exchanger Design. Paper presented at the *International Geothermal Days Germany 2001* (International Summer School on Direct Applications of Geothermal Energy). Skepje, Macedonia.

Henderson, H. I., Parker, D., & Huang, Y. J. (2000). Improving DOE-2's RESYS Routine: User Defined Functions to Provide More Accurate Part Load Energy Use and Humidity Predictions. Paper presented at the *2000 ACEEE Summer Study on Energy Efficiency in Buildings*, August 20-25, 2000 in Pacific Grove, CA.

Henninger, R.H. 1975. *NECAP-NASA'S Energy-Cost Analysis Program, Part I-Users's Mannual*. Washington, DC: National Aeronautics and Space Administration.

Hughes, P. J. (2008). Geothermal (Ground-Source) *Heat Pumps: Market Status, Barriers to Adoption, and Actions to Overcome Barriers*. Oak Ridge, TN: Oak Ridge National Laboratory (ORNL).

Hwang, Y., Lee, J., Jeong, Y., Koo,K., Lee, D., Kim, I., Jin, S., & Kim, S. (2009). Cooling Performance of a Vertical Ground-Coupled Heat Pump System Installed in a School Building. *Renewable Energy*, 34 (2009) 578-582.

ICC. (2006). *2006 International Energy Conservation Code*. Falls Church, VA: International Code Council, Inc.

ICC. (2009a). *2009 International Energy Conservation Code*. Falls Church, VA: International Code Council, Inc.

ICC. (2009b). *2009 International Residential Code for One- and Two-Family Dwellings*. Falls Church, VA: International Code Council, Inc.

IGSHPA. (2012). *GLHEPRO for Windows: The Professional Ground Loop Heat Exchanger Software*. Retrieved April 09, 2012, from http://www.hvac.okstate.edu/glhepro/

IGSHPA. (2012a). *What Is Geothermal: Residential*. Retrieved February 13, 2012, from http://www.igshpa.okstate.edu/geothermal/residential.htm#2

IGSHPA. (2012b). *About Us: History*. Retrieved May 20, 2012, from http://www.igshpa.okstate.edu/about/about_us.htm

Incropera, F. K. & De Witt, D. P. (2001). *Fundamental of Heat and Mass Transfer, 5th Edition*.New York, NY: John Wiley & Sons, Inc.pp. 470.

Ingersoll, L. R., & Zobel, A. C. (1954). *Heat Conduction: With Engineering, Geological, and Other Applications (2nd ed.)*. New York: McGraw-Hill.

James J. Hirsch & Associates (JJH) (2012). *Comparison of DOE-2.1E, DOE-2.2, eQUEST, and PowerDOE.* Retrieved from http://www.doe2.com/compare.html

James J. Hirsch & Associates (JJH) (2013). *The Quick Energy Simulation Tool, eQUEST Software.* Retrieved from http://www.doe2.com/equest/

Karr, M. (2011). *Ground-Source Variable Refrigerant Flow Heat Pumps: A Solution for Affordable Housing, Assisted Living, Hotels and Dorms*. Extension Energy Program, Washington State University.

Kavanaugh, S. P. (1985). *Simulation and Experimental Verification of Vertical Ground-Coupled Heat Pump Systems*. Ph.D. Thesis. Stillwater, OK: Oklahoma State University.

Kavanaugh, S.P. (1991). *Ground and Water Source Heat Pumps: A Manual for the Design and Installation of Ground Coupled, Ground Water and Lake Water Heating and Cooling Systems in Southern Climates*. Energy Information Services, Tuscaloosa.

Kavanaugh, S.P. (2000). Field Tests for Ground Thermal Properties: Methods and impact on GSHP system design. *ASHRAE Transactions* 106(1): DA-00-13-4.

Kavanaugh, S.P. (2001). *Investigation of Methods for Determining Soil Formation Thermal Characteristics from Short Term Field Tests*. Final Report, ASHRAE RP-1118. Atlanta, GA: American Society of Heating, Refrigerating, and Air-conditioning Engineers.

Kavanaugh, S.P., Lambert, S., & Messer, D. (2002). *Development of Guidelines for the Selection and Design of the Pumping/Piping Subsystem for Ground Coupled Heat Pumps*. Final Report, ASHRAE TRP-1217. Atlanta, GA: American Society of Heating, Refrigerating, and Air-conditioning Engineers.

Kavanaugh, S. P., & Rafferty, K. (1997). *Ground-Source Heat Pumps, Design of Geothermal Systems for Commercial and Institutional Buildings*. Atlanta, GA: American Society of Heating, Refrigerating, and Air-conditioning Engineers.

Kelvin, W. (1882). *Mathematical and Physical Papers, Volume 1*. Cambridge, New York: Cambridge University Press.

Klein, S. A., Beckman, W. A., Mitchell, J. W., Duffie, J. A., Duffie, N. A., Freeman, T. L., . . . Duffy, M. J. (2010). *TRNSYS 17: A Transient System Simulation Progra*m. Madison, WI: Solar Energy Laboratory, University of Wisconsin.

Kim, H., Baltazar, J., Haberl, J., Lewis, C., & Yazdani, B. (2011). Cost-Effective Energy Efficiency Measures for 15% Above 2009 IECC Code-Compliant House for Residential Buildings in Texas. Proceedings of the *Eleventh International Conference for Enhanced Building Operations*.

Kim, S. (2006). *An Analysis of International Energy Conservation Code (IECC)-Compliant Single-Family Residential Energy Use*. Ph.D. Thesis. College Station, TX: Texas A&M University.

Kim, S., & Haberl, J. S. (2008). Development of an ASHRAE 152-2004 Duct Model for the Single-Family Residential House. Proceedings of the *Sixteenth Symposium on Improving Building Systems in Hot and Humid Climates*.

Kishore, V.V.N. & Joshi, V. (1984). A Practical Collector Efficiency Equation for Nonconvecting Solar Ponds. *Solar Energy*, 33(5), 391-395.

Kusuda, T., & Achenbach, P. R. (1965). Earth Temperature and Thermal Diffusivity at Selected Stations in the United States. *ASHRAE Transactions*, 71(1), 61-75.

Lamarche, L., Kajl, S., & Beauchamp, B. (2010). A Review of Methods to Evaluate Borehole Thermal Resistances in Geothermal Heat-Pump Systems. *Geothermics*, 39(2), 187-200.

Lamoureux, J (2003). *Heat Transfer in Outdoor Aquaculture Ponds*. M.S. Thesis. Baton Rouge, LA: Louisiana State University

LASL. (1980). *DOE-2 Reference Manual part 1 (Version 2.1).* Los Alamos, NM: Los Alamos Scientific Laboratory.

LBL. (1982a). *DOE-2 Engineers Manual 2.1A* (LBL-11353). Berkeley, CA: Lawrence Berkeley National Laboratory.

LBL. (1982b). *DOE-2 Supplement Version 2.1B* (LBL-8706, Rev.3.Suppl.). Berkeley, CA: Lawrence Berkeley National Laboratory.

LBL. (1984). *DOE-2 Supplement Version 2.1C* (LBL-8706, Rev.4.Suppl.). Berkeley, CA: Lawrence Berkeley National Laboratory.

LBL. (1989). *DOE-2 Supplement Version 2.1D* (LBL-8706, Rev.5.Suppl.). Berkeley, CA: Lawrence Berkeley National Laboratory.

LBL. (1993a). *DOE-2 Supplement Version 2.1E* (LBL-34947). Berkeley, CA: Lawrence Berkeley National Laboratory.

LBL. (1993b). *DOE-2 BDL Summary, Version 2.1E*. Berkeley, CA: Lawrence Berkeley National Laboratory.

LBL. (1993c). *DOE-2 Supplement Version 2.1E* (Preliminary Version). Berkeley, CA: Lawrence Berkeley National Laboratory.

LBL. (1994). *DOE-2 Basics, Version 2.1E*. Berkeley, CA: Lawrence Berkeley National Laboratory.

LBNL. (2010). *Energy Efficient Building Program*. Chapter from Energy & Environment Annual Report 1977: CAL-ERDA (DOE-1), A Computer Program for Energy Analysis of Buildings.LBNL Paper LBL-7842. Berkeley, CA: Lawrence Berkeley National Laboratory.

LBNL. (2013). *DOE-2 Home*. Retrieved August 8, 2013, from http://gundog.lbl.gov/dirsoft/d2whatis.html

Lee, Edwin (2008). *Development, Verification, and Implementation of a Horizontal Buried Pipe Ground Heat Transfer Model in Energyplus*. M.S. Thesis. Stillwater, OK: Oklahoma State University.

Leighton, G.S., Ross, H.D., Lokmanhekim, M., Rosenfeld, A.H., Winkelmann, F.C., & Cumali, Z.O. (1978). *DOE-1: A New State-of-the-Art Computer Program for the Energy Utilization Analysis of Building*. Lawrence Berkeley Laboratory, LBL-7836.

LI-COR. (2013). *Pyranometer Light Sensors*. Retrieved May 29, 2013, from http://www.licor.com/env/products/light/pyranometers/

Liu, X., & Hellström, G. (2006). Enhancements of an Integrated Simulation Tool for Ground-Source Heat Pump System Design and Energy Analysis. Proceedings of the *Tenth International Conference on Thermal Energy Storage*.

Liu, Z., Kim, H., Malhotra, M., Mukhopadhyay, J., Baltazar, J. C., Haberl, J., Culp, C., Yazdani, B., & Montgomery, C. (2010). *Going Beyond a Resnet Certification for Code-Compliant Simulations: A Comparison of Detailed Results of Three Resnet-Certified, Code-Compliant Residential Simulation Programs*. College Station, TX: Energy Systems Laboratory, Texas A&M University.

Liu, Z., Mukhopadhyay, J., Malhotra, M., Haberl, J., Gilman, D., Montgomery, C., McKelvey, K., Culp, C., & Yazdani, B. (2008). Methodology for Residential Building Energy Simulations Implemented in the International Code Compliance

Calculator (IC3). Proceedings of the *Sixteenth Symposium on Improving Building Systems in Hot and Humid Climates*.

Lienau, P., Boyd, T., and Rogers, R. L. (1995). *Ground-source Heat Pump Case Studies and Utility Programs*. Klamath Falls, OR: Geo-Heat Center, Oregon Institute of Technology.

Lund, J., Sanner, B., Rybach, L., Curtis, R., & Hellström, G. (2004). *Geothermal (Ground-Source) Heat Pumps: A World Overview*. Geo-Heat Centre Quarterly Bulletin, 25, 1-10.

Muraya, N. K., O'Neal, D. L., & Heffington, W. M. (1996). Thermal Interference of Adjacent Legs in a Vertical U-Tube Heat Exchanger for a Ground-Coupled Heat Pump. *ASHRAE Transactions*, 102(2), 12-21.

Murugappan, A. (2001). *Implementing Ground Source Heat Pump and Ground Loop Heat Exchanger Models in the Energyplus Simulation Environment*. M.S. Thesis. Stillwater, OK: Oklahoma State University.

Nicholas, J.V. & White, D.R. (1994). *Trasceable Temperatures: An Introduction to Temperature Measurement and Calibration*. Chichester, England: John Wiley & Sons Ltd.

Niles, A. (2012). Commercial Ground Loop Water Source Heat Pump Systems. Paper presented at the *2012 Rocky Mountain Chapter ASHRAE Technical Conference: Leadership in HVAC&R*, April 20, 2012, Lakewood, CO.

NREL. (2004). *Building America Performance Analysis Procedures, Revision1*. NREL/TP-550-35567. National Renewable Energy Laboratory. June, 2004.

NREL. (2005). *Building America Research Benchmark Definition, Version 3.1*. NREL/TP-550-36429. National Renewable Energy Laboratory. January, 2005.

NREL. (2008). *Building America Research Benchmark Definition*. NREL/TP-550-44816. National Renewable Energy Laboratory. December 19, 2008.

Oh, S. (2013). *Origins of Analysis Methods in Energy Simulation Programs Used for High Performance Commercial Buildings*. M.S. Thesis. College Station, TX: Texas A&M Univeristy.

O'Neal, D. L., Gonzalez, J. A. and Aldred, W. (1994). A Simplified Procedure for Sizing Vertical Ground Coupled Heat Pump Heat Exchangers for Residences in Texas. Proceedings of the *Ninth Symposium on Improving Building Systems in Hot and Humid Climates*.

ORNL. (2013). *How to Buy an Energy-Efficient Ground-Source Heat Pump*. Retrieved November 3, 2013, from http://web.ornl.gov/sci/femp/pdfs/gshp-pro-chal.pdf

Pezent, M.C., & Kavanaugh , S.P. (1990). Development and Verification of a Thermal Model of Lakes Used with Water Source Heat Pumps. *ASHRAE Transactions*, 96(1), 574-582.

Rees, S. J., Spitler, J. D., Deng, Z., Orio, C. D., & Johnson, C. N. (2004). A Study of Geothermal Heat Pump and Standing Column Well Performance. *ASHRAE Transactions*, 110(1), 3-13.

Residential Energy Services Network, I. (2006). *Procedures for Verification of RESNET Accredited HERS Software Tools*. RESNET Publication No, 06-002.

RMI. (2011). *Building Energy Modeling Innovation Summit*. Boulder, CO: Rocky Mountain Institute.

Rottmayer, S. P., Beckman, W. A., & Mitchell, J. W. (1997). Simulation of a Single Vertical U-Tube Ground Heat Exchanger in an Infinite Medium. *ASHRAE Transactions*, 103 (2), 651-659.

Rybach, L. (2005). The Advance of Geothermal Heat Pumps–Worldwide. *IEA Heat Pump Center News Letter*, 23(4).

Shonder, J.A. & Hughes, P.J. (1998). Increasing Confidence in Geothermal Heat Pump Design Methods. Proceedings of the *Second Stockton International Geothermal Conference*.

Shonder, J. A. & Beck, J. V. (1999). Determining Effective Soil Formation Thermal Properties from Field Data Using a Parameter Estimation Technique. *ASHRAE Transactions*, 105(1), 458-466.

Simergy. (2013). *Simergy Software (Version Beta 2)*. Berkeley, CA: Lawrence Berkeley National Laboratory. Retrieved from http://simergy-beta.lbl.gov/index.html

Spitler, J. D. (2000). GLHEPRO, A Design Tool for Commercial Building Ground Loop Heat Exchangers. Proceedings of the *Fourth International Heat Pump in Cold Climates Conference*.

Spitler, J. D. (2005). Ground-Source Heat Pump System Research – Past, Present, and Future. *International Journal of HVAC&R Research*, 11 (2), 165-167.

Stamper, E. (1995). ASHRAE's Development of Computerized Energy Calculations for Buildings. *ASHRAE Transactions*, 101 (1), 768-772.

Sukup, M. M., & Johnson, F. (1989). *The Earth-Coupled Heat Pump: Utilizing Innovative Technology in Single Family Rehabilitation Strategies*. City of Houston.

Synergistic Control Systems. (1994). *Software, Installation and Technical Specification for the Model 180 Survey Meter/Recorder*. Metairie, LA: Synergistics Control Systems Inc.

Thornton, J. W., McDowell, T., Shonder, J. A., Hughes, P., Pahud, D., & Hellstrom, G. (1997). Residential Vertical Geothermal Heat Pump System Models: Calibration to Data. *ASHRAE Transactions*, 103 (2), 660-674.

Vaisala. (2013). *HMP45A/D Humidity and Temperature Probe*. Retrieved May 29, 2013, from http://www.iprocessmart.com/vaisala/vaisala_hmp45a.htm

Wagers, H. L., & Wagers, M. C. (1985). The Earth-Coupled or Geothermal Heat Pump Air Conditioning System. Proceedings of the *Second Symposium on Improving Building Systems in Hot and Humid Climates*.

Winkelmann, F., (1998). *Underground Surfaces: How to Get Better Underground Surface Heat Transfer Calculation in DOE-2.1E*, DOE-2 User News, Vol. 19, No. 1, p. 6- 13. Berkeley, CA: Lawrence Berkeley National Laboratory.

Yang, H., Cui, P., & Fang, Z. (2010). Vertical-Borehole Ground-Coupled Heat Pumps: A Review of Models and Systems. *Applied Energy*, 87(1), 16-27.

Yavuzturk, C. (1988). *Modeling of Vertical Ground Loop Heat Exchangers for Ground Source Heat Pump Systems*. Ph.D. Thesis. Stillwater, OK: Oklahoma State University.

Yavuzturk, C., & Spitler, J. 1999. A Short Time Step Response Factor Model for Vertical Ground Loop Heat Exchangers. *ASHRAE Transactions*. 105(2):475-485.

Young, T. R. (2004). *Development, Verification, and Design Analysis of the Borehole Fluid Thermal Mass Model for Approximating Short Term Borehole Thermal Response*. Master's Thesis. Stillwater, OK: Oklahoma State University.

Zeng, H., Diao, N., & Fang, Z. (2003). Heat Transfer Analysis of Boreholes in Vertical Ground Heat Exchangers. *International Journal of Heat and Mass Transfer*, 46(23), 4467-4481.

Zogg, M. (2008). History of Heat Pumps Swiss Contributions and International Milestones. Proceedings of *Nineth International IEA Heat Pump Conference*.

APPENDIX A

CALIBRATION OF MEASURING INSTRUMENTS

Ten thermocouple sensors (T-type) were used to measure the temperatures for the supply air, the return air, leaving water, and entering water. Before installing the thermocouple sensors in the ground-coupled heat pump system, the thermocouple sensors were calibrated to improve the accuracy of the measurement (Nicholas and White, 1994). To develop the correction factor, a calibrated scale and offset must be calculated. To implement the calibration of the thermocouple sensors, the American Society for Testing and Materials (ASTM) Standards E77-07 2007 was used. This appendix presents the detailed calibration results for the thermocouple sensors used in field measurement.

The calibration methodology used in this study compares the temperature readings of the thermocouple sensors with the reference temperature readings. In order to calibrate the ten thermocouple sensors, two ASTM certified liquid-in-glass thermometers, two spirit-filled glass thermometers[59], three Resistance Temperature Detector (RTD) temperature sensors, a Campbell data logger model CR1000 (Campbell Scientific, 2013b), and a portable Synergistic data logger model C180 (Synergistic Control Systems, 1994) were used. Figure A-1 shows the procedure used to calibrate the thermocouple sensors.

---

[59] National Institute of Standards and Technology (NIST)-certified spirit-filled glass thermometers were used.

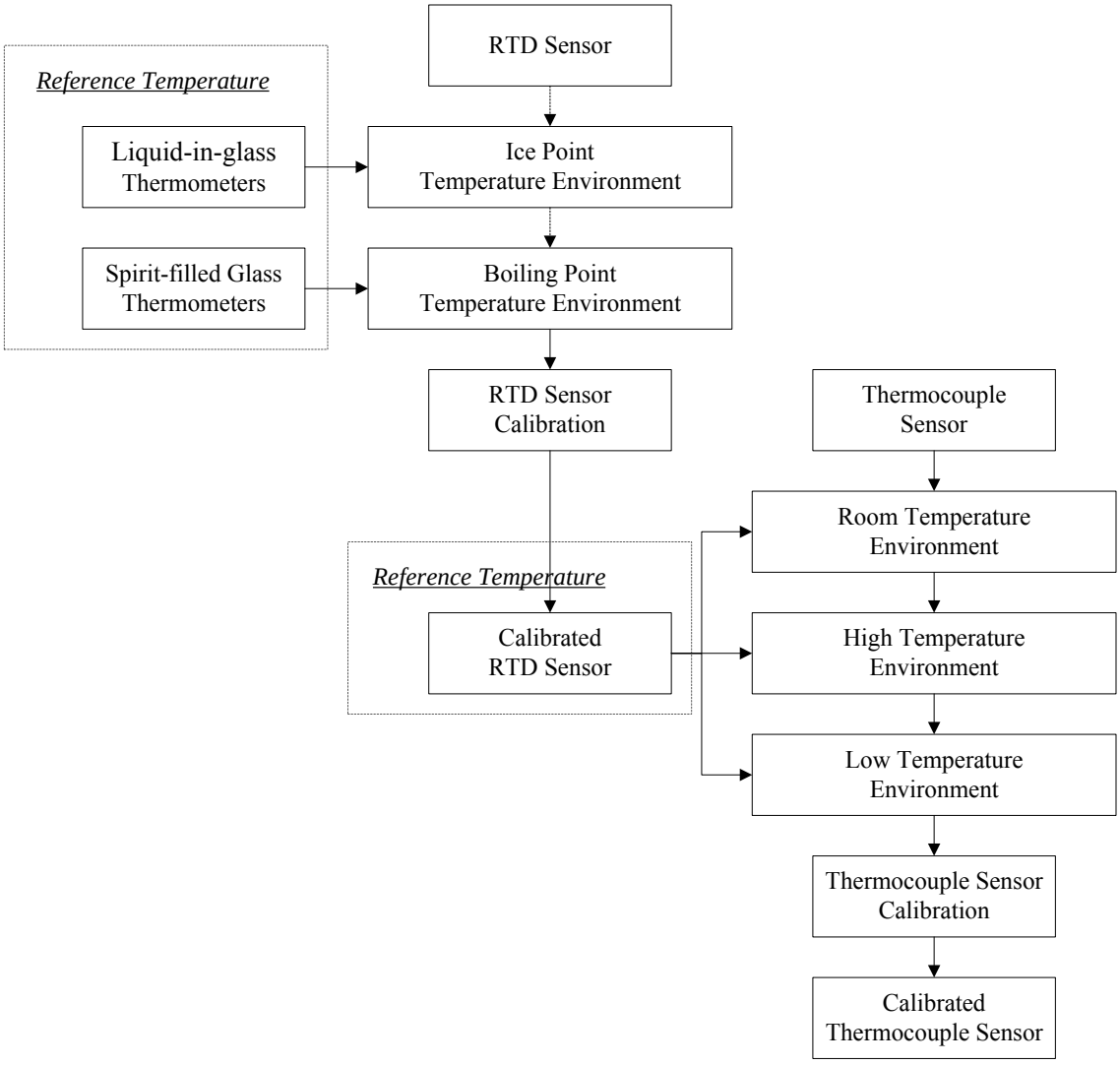

Figure A-1: Calibration Procedure for the Thermocouple Sensors

First, the RTD temperature sensors were calibrated against ASTM certified liquid-in-glass thermometers and spirit-filled glass thermometer. The RTD temperature sensors were connected with a portable Synergistic data logger to read temperatures, shown in Figure A-2. The calibration was conducted under controlled temperature environments including an ice point and a boiling point, shown in Figure 4-29 and

Figure 4-30 in Section 4.3.2.1, using distilled water. Scales and offsets were then determined, based on the RTD temperature readings and the reference temperature readings. The RTD sensors were calibrated according to the scales and offsets. The scales and offsets determined from the calibration can be found in Table A-1. Figure A-3 shows the calibration results of the RTD temperature sensors, including temperature correction and residual plot for before and after calibration.

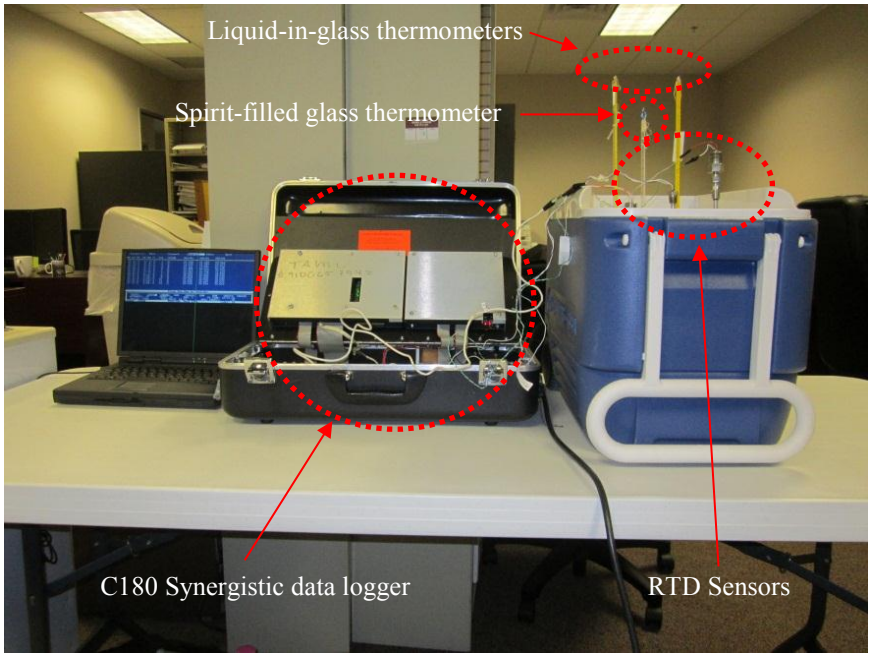

Figure A-2: Experiment Setting for the RTD Sensor Calibration

Table A-1: Scale and Offset Parameters for Temperatures of the RTD Sensors

Sensor Number	Calibration	
	Scale	Offset
RTD Sensor #1	1.0106	2.4968
RTD Sensor #2	1.0397	0.6661
RTD Sensor #3	1.0434	0.7433

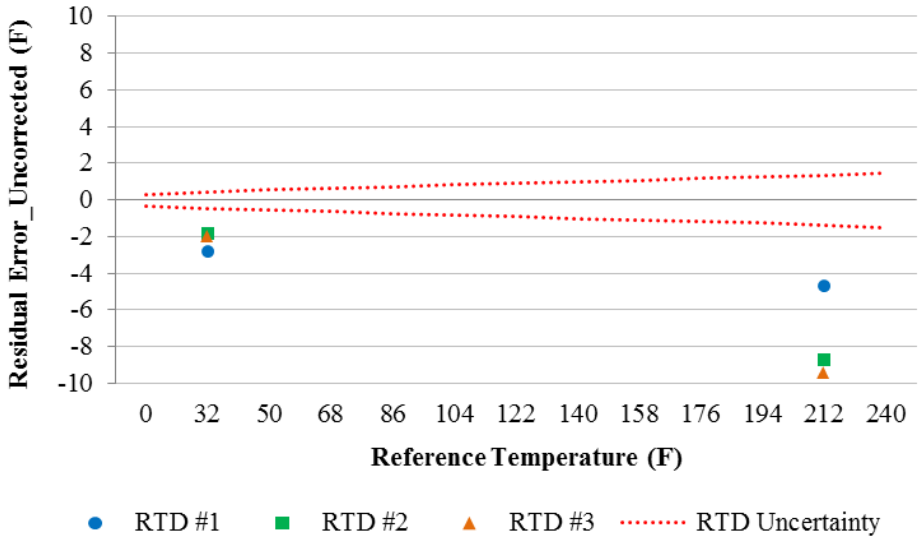

(a) Uncorrected Temperature Difference Before Calibration

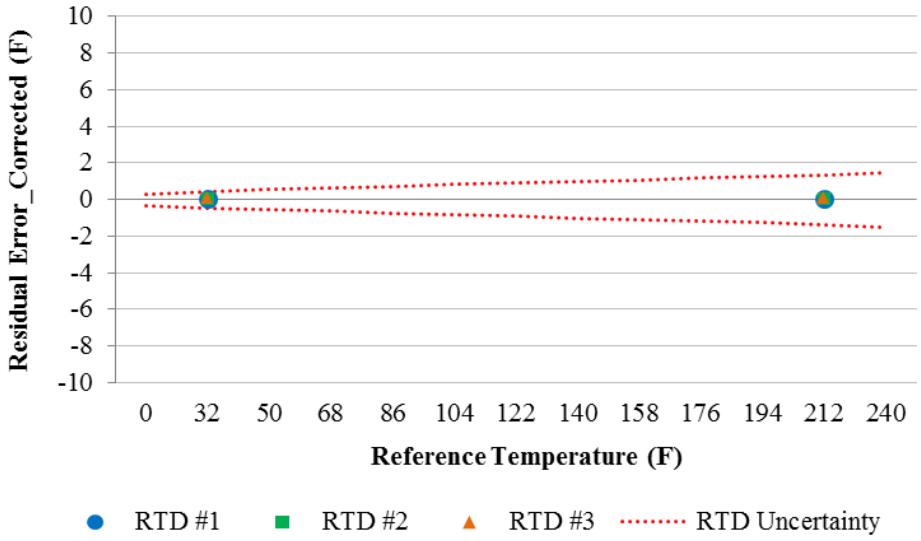

(b) Corrected Temperature Difference After Calibration

Figure A-3: Residual Plot of the RTD Temperature Measured against the ASTM Reference Temperatures with the Manufacturer Specified Sensor Accuracy

After calibrating three RTD temperature sensors, the thermocouple sensors were next calibrated against the calibrated RTD temperature sensors under three different controlled temperature environments, which are general interest in this study: high temperature, room temperature, and low temperature.

Figure A-4 shows the temperature readings from the ten thermocouple sensors and the average temperature readings from the RTD sensors before and after calibration. In addition, Figure A-4 presents the data points used for the calibration of the thermocouple sensors. Table A-2 presents scales and offsets used for calibration temperatures of the thermocouple sensors against the RTD reference temperatures. Figure A-5 through Figure A-14 show residual plots of each thermocouple sensor for before and after calibration.

Table A-2: Scale and Offset Parameters for Temperatures of the Thermocouple Sensors

Sensor Number	Calibration	
	Scale	Offset
Thermocouple Sensor #1	1.0071	-0.1983
Thermocouple Sensor #2	1.0097	-0.4037
Thermocouple Sensor #3	1.0025	0.2290
Thermocouple Sensor #4	1.0123	-0.6594
Thermocouple Sensor #5	1.0077	-0.2625
Thermocouple Sensor #6	1.0133	-0.6600
Thermocouple Sensor #7	1.0103	-0.3907
Thermocouple Sensor #8	1.0001	0.4413
Thermocouple Sensor #9	1.0070	-0.0957
Thermocouple Sensor #10	1.0083	-0.3158

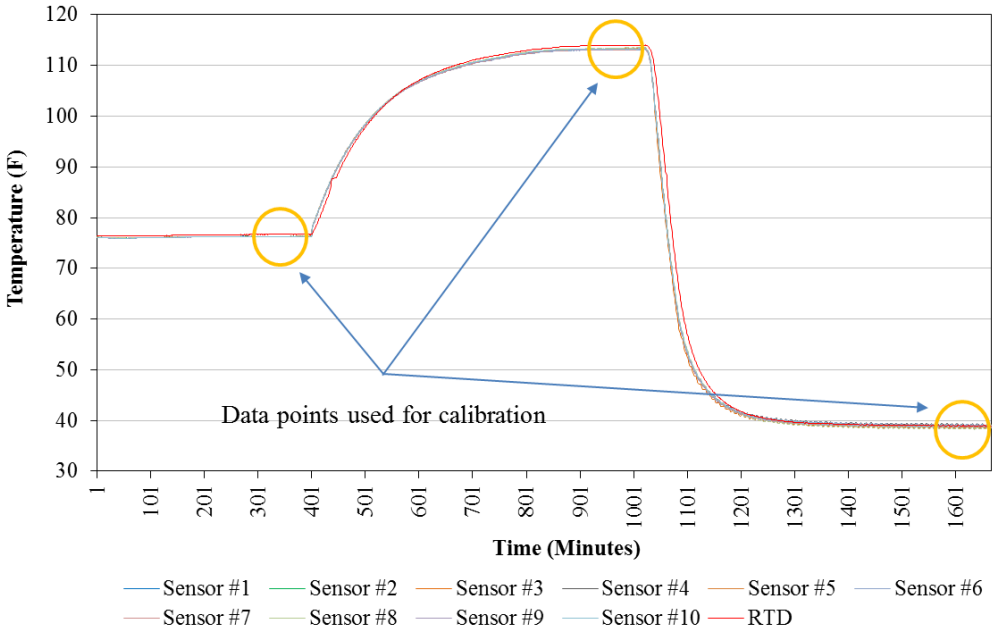

(a) Before Calibration

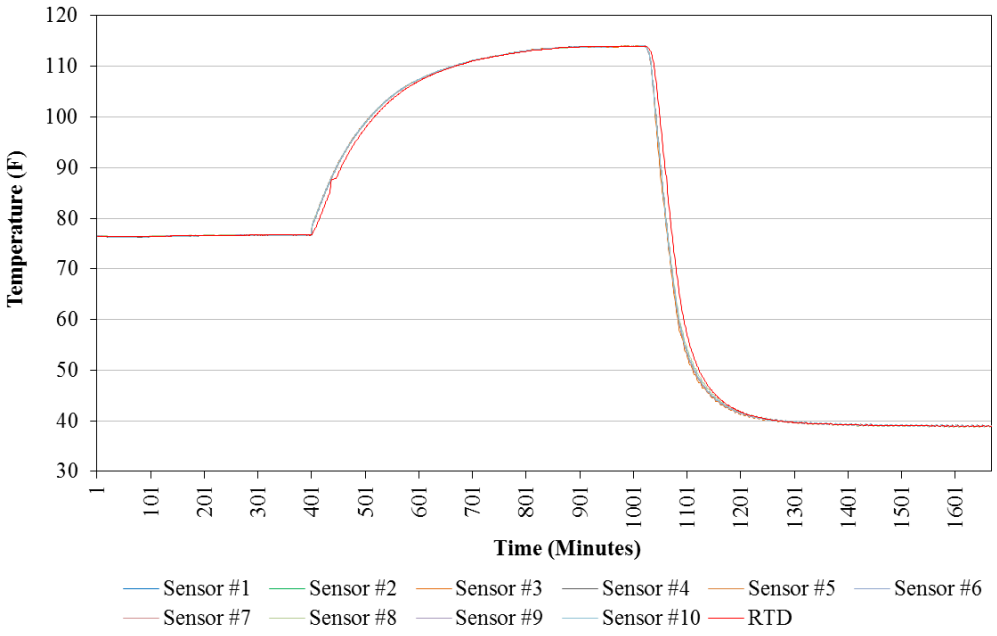

(b) After Calibration

Figure A-4: Time Series Plot of the Ten Thermocouple Sensors and the RTD Sensors after Calibration

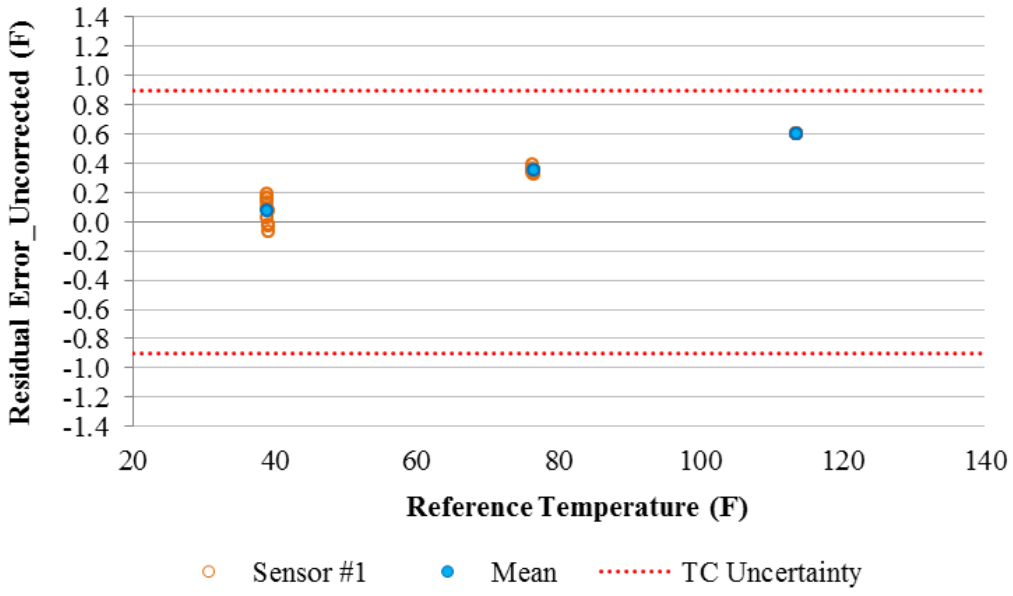

(a) Uncorrected Temperature Difference Before Calibration

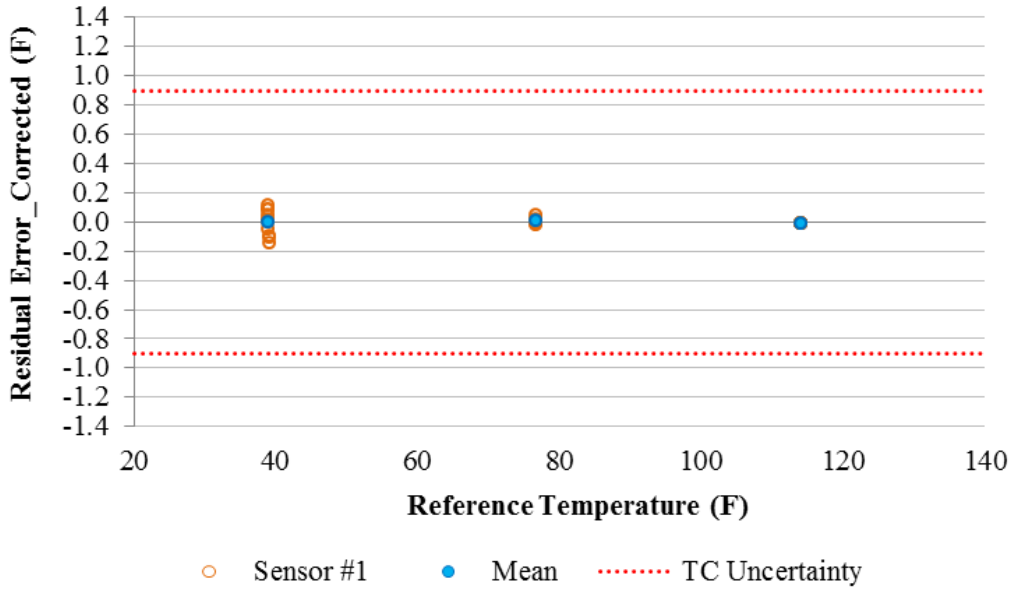

(b) Corrected Temperature Difference After Calibration

Figure A-5: Residual Plot of the Temperatures of Thermocouple Sensor #1 against the RTD Reference Temperatures with the Manufacturer Specified Sensor Accuracy (±0.9F)

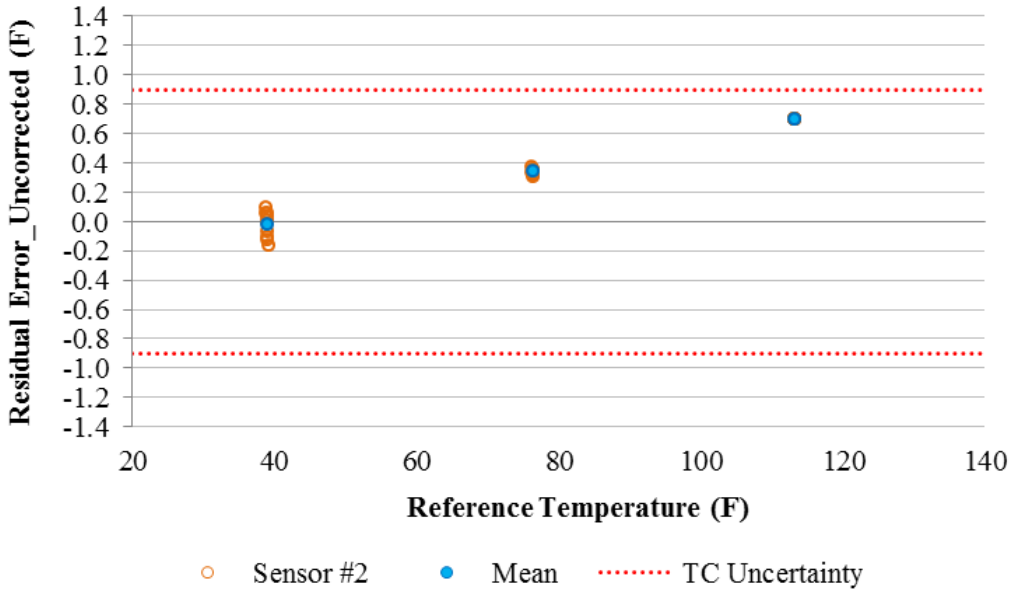

(a) Uncorrected Temperature Difference Before Calibration

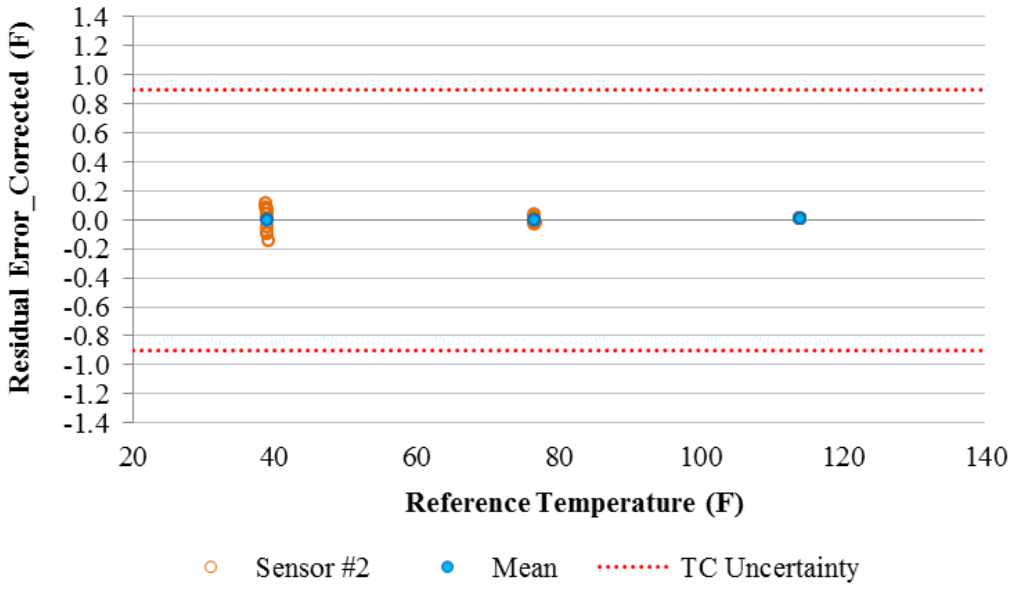

(b) Corrected Temperature Difference After Calibration

Figure A-6: Residual Plot of the Temperatures of Thermocouple Sensor #2 against the RTD Reference Temperatures with the Manufacturer Specified Sensor Accuracy (±0.9F)

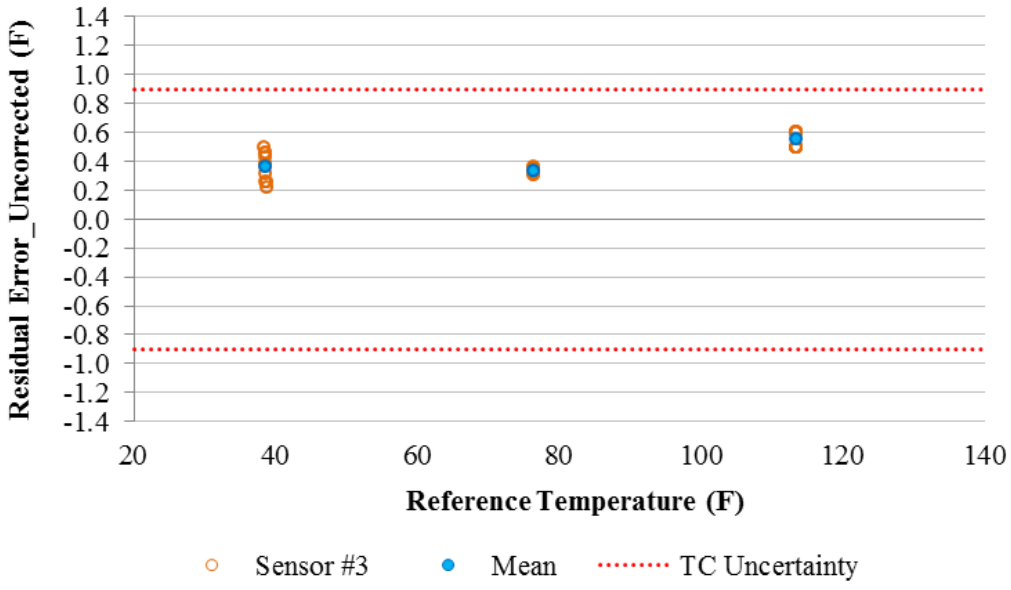

(a) Uncorrected Temperature Difference Before Calibration

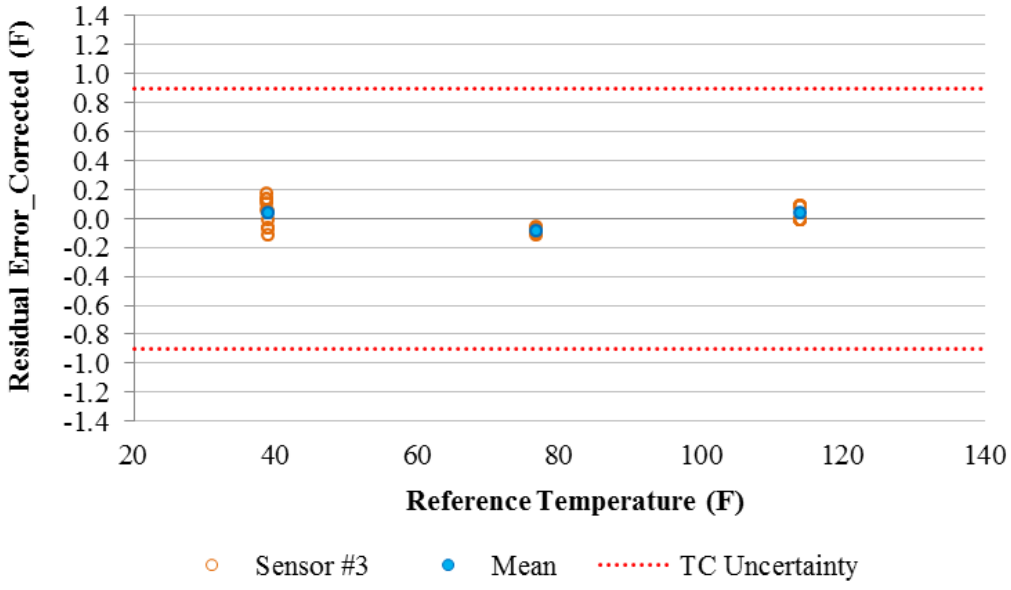

(b) Corrected Temperature Difference After Calibration

Figure A-7: Residual Plot of the Temperatures of Thermocouple Sensor #3 against the RTD Reference Temperatures with the Manufacturer Specified Sensor Accuracy (±0.9F)

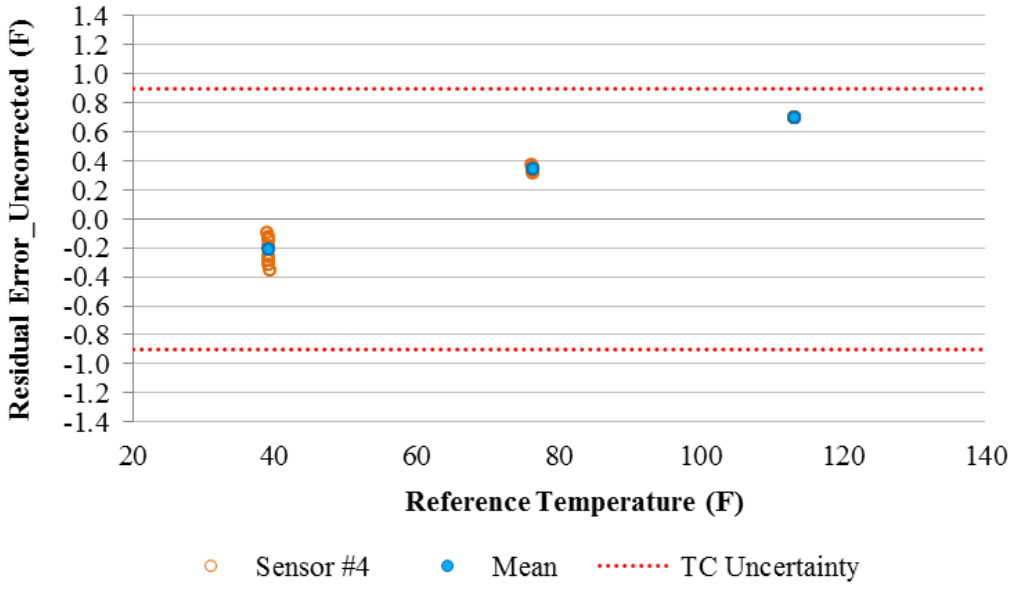

(a) Uncorrected Temperature Difference Before Calibration

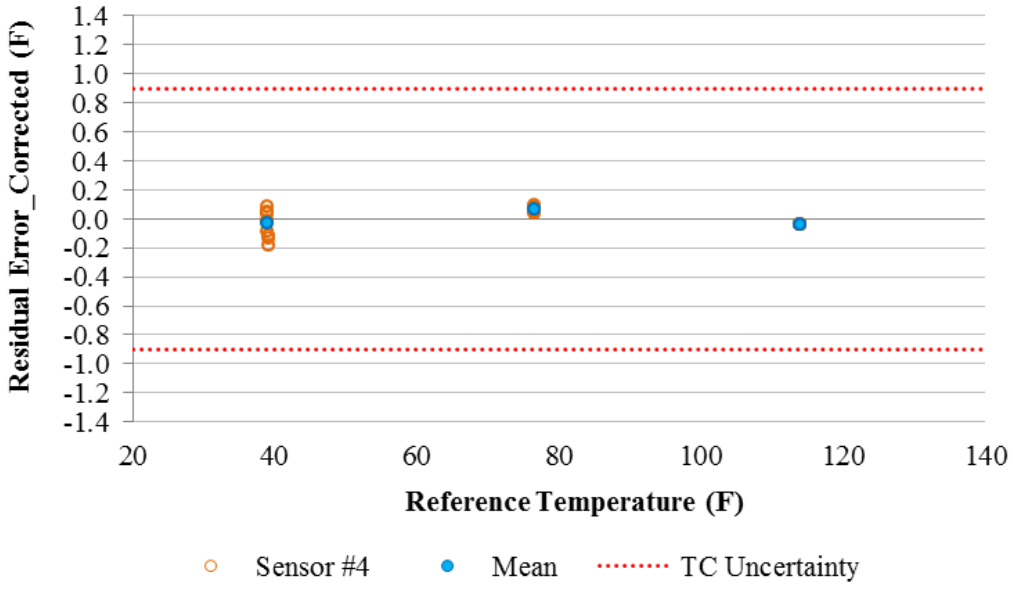

(b) Corrected Temperature Difference After Calibration

Figure A-8: Residual Plot of the Temperatures of Thermocouple Sensor #4 against the RTD Reference Temperatures with the Manufacturer Specified Sensor Accuracy (±0.9F)

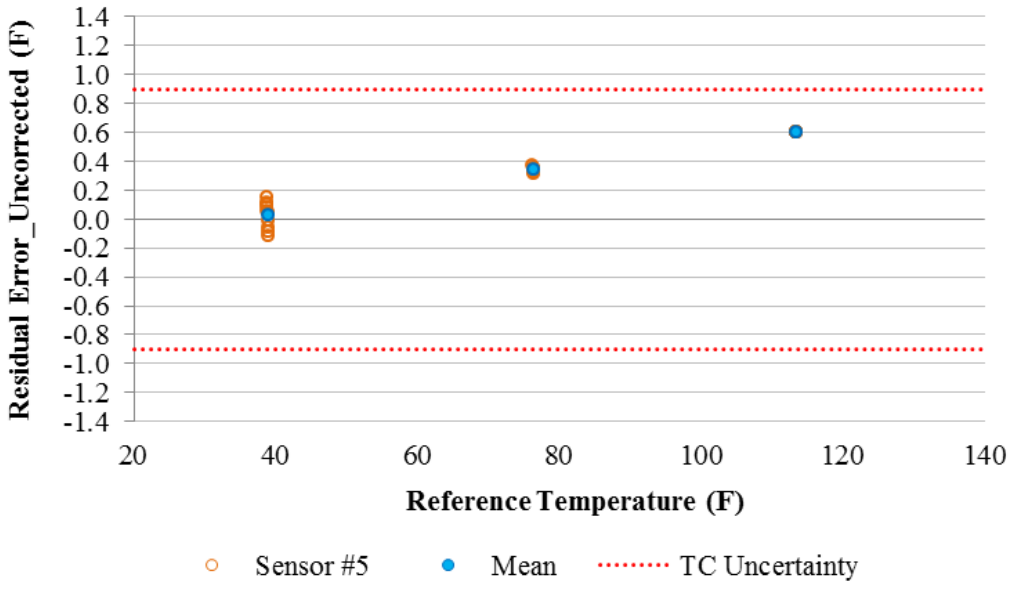

(a) Uncorrected Temperature Difference Before Calibration

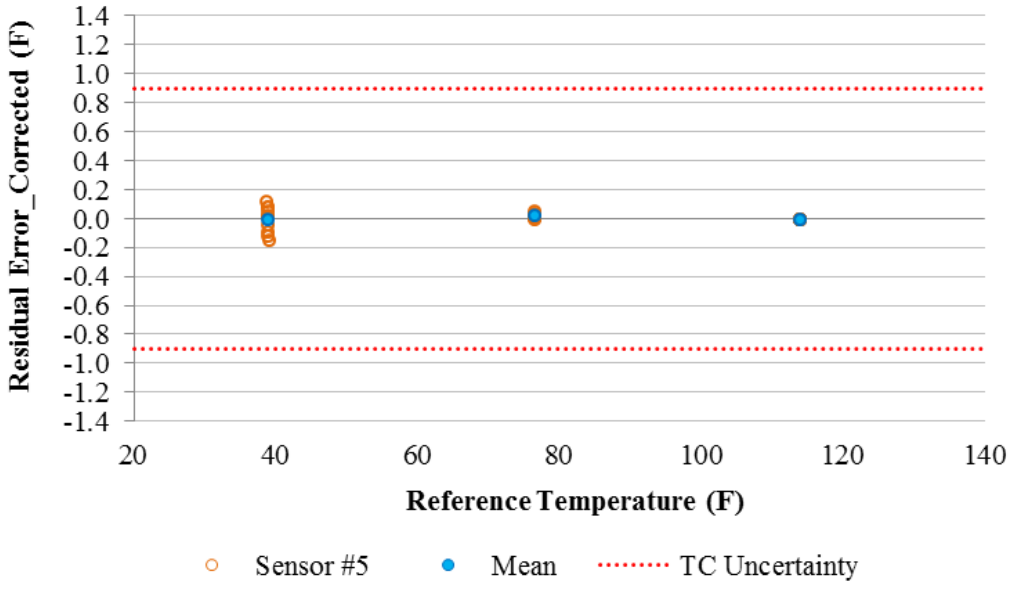

(b) Corrected Temperature Difference After Calibration

Figure A-9: Residual Plot of the Temperatures of Thermocouple Sensor #5 against the RTD Reference Temperatures with the Manufacturer Specified Sensor Accuracy (±0.9F)

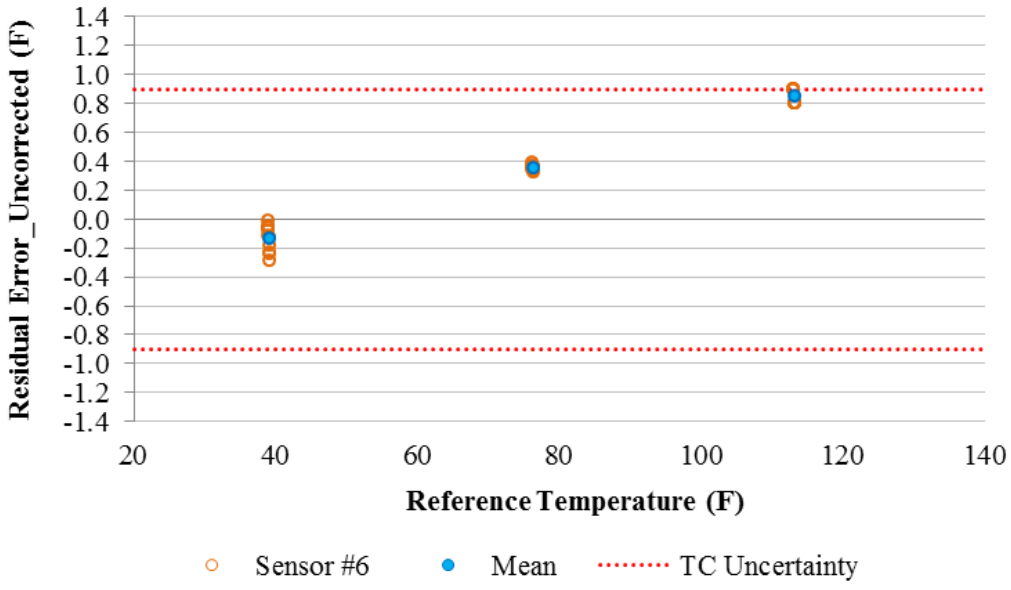

(a) Uncorrected Temperature Difference Before Calibration

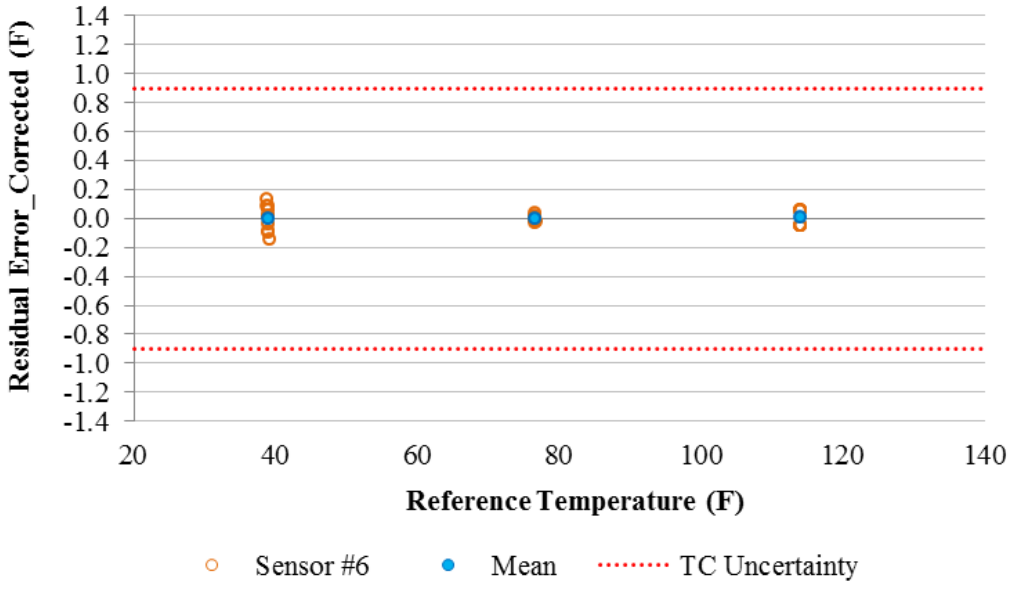

(b) Corrected Temperature Difference After Calibration

Figure A-10: Residual Plot of the Temperatures of Thermocouple Sensor #6 against the RTD Reference Temperatures with the Manufacturer Specified Sensor Accuracy (±0.9F)

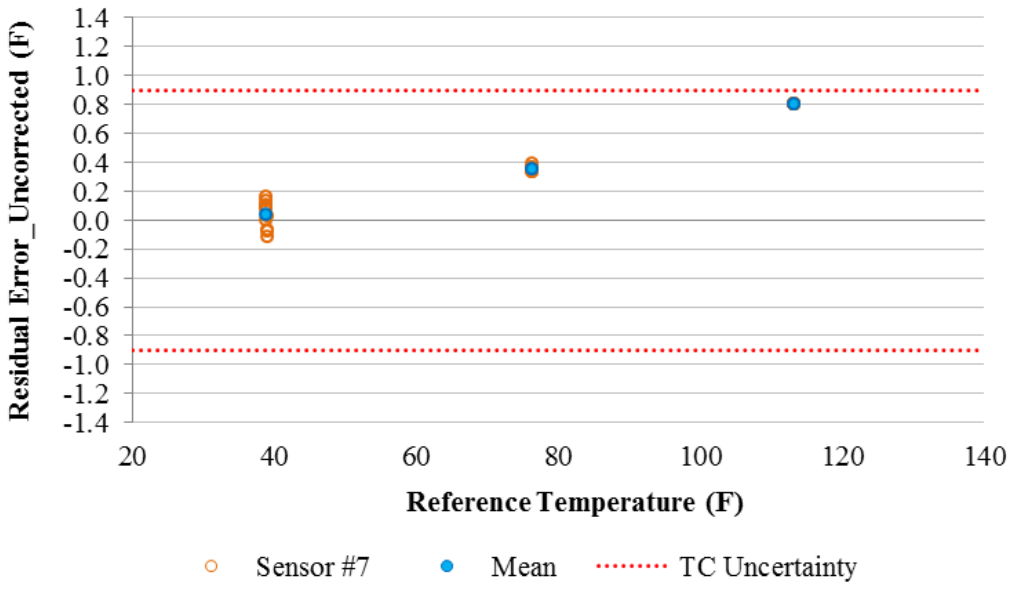

(a) Uncorrected Temperature Difference Before Calibration

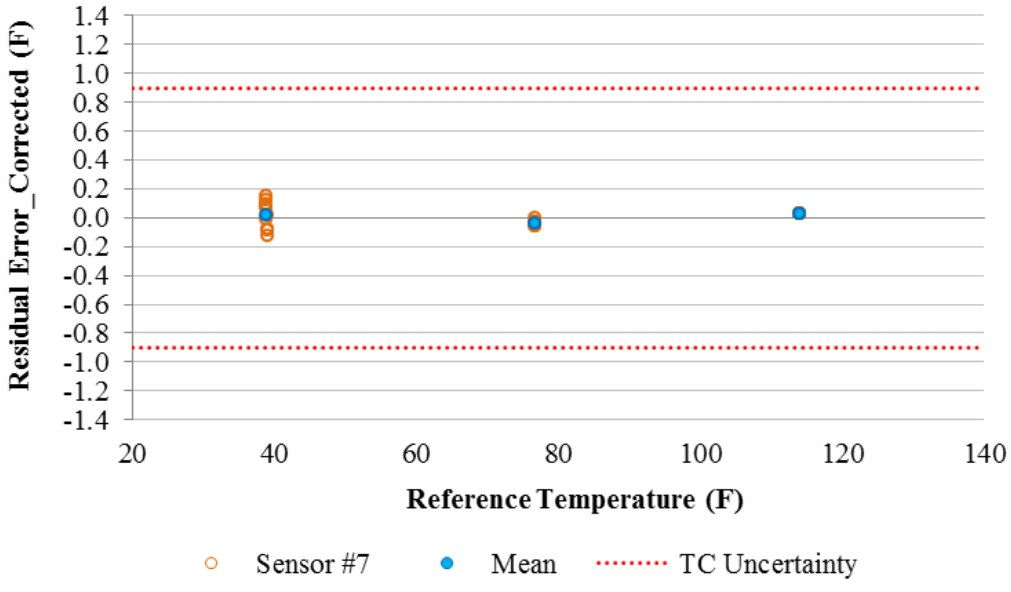

(b) Corrected Temperature Difference After Calibration

Figure A-11: Residual Plot of the Temperatures of Thermocouple Sensor #7 against the RTD Reference Temperatures with the Manufacturer Specified Sensor Accuracy (±0.9F)

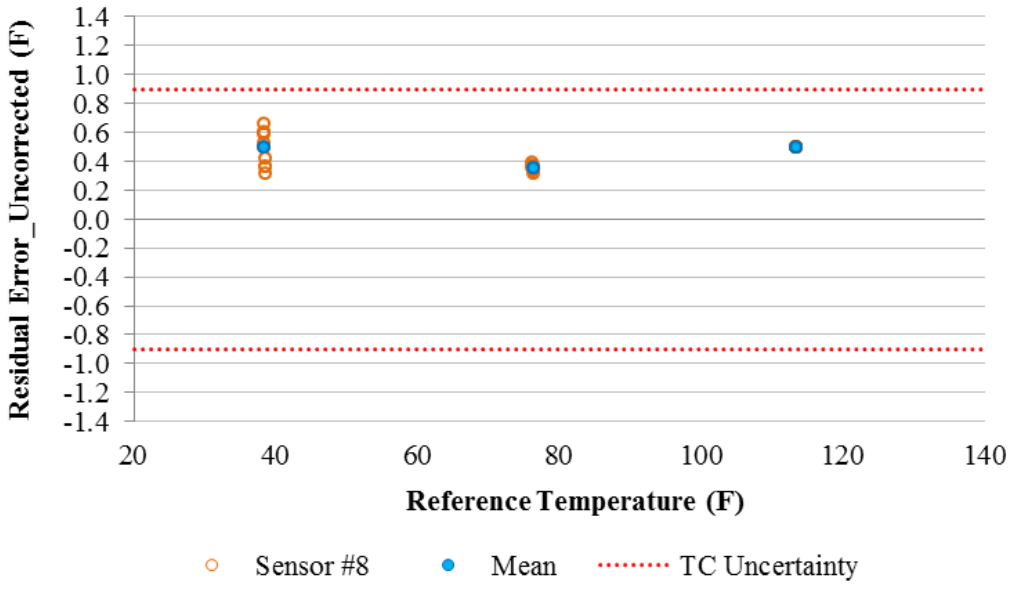

(a) Uncorrected Temperature Difference Before Calibration

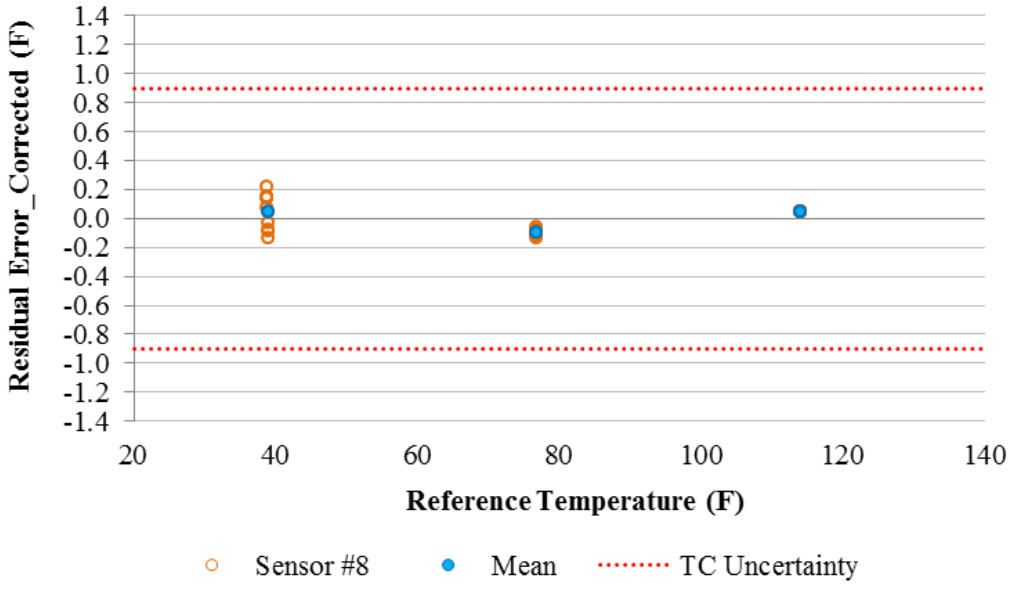

(b) Corrected Temperature Difference After Calibration

Figure A-12: Residual Plot of the Temperatures of Thermocouple Sensor #8 against the RTD Reference Temperatures with the Manufacturer Specified Sensor Accuracy (±0.9F)

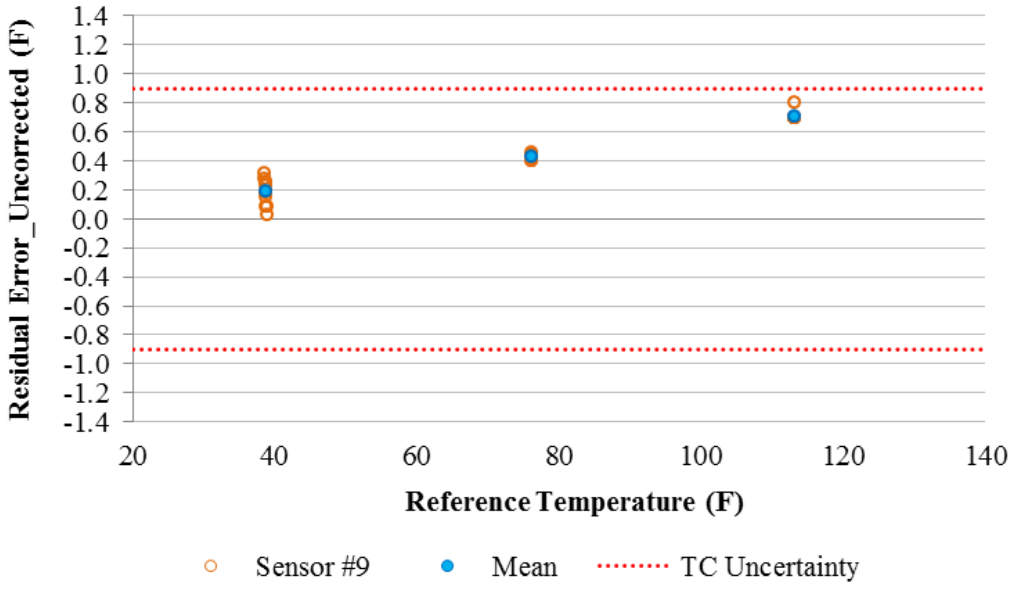

(a) Uncorrected Temperature Difference Before Calibration

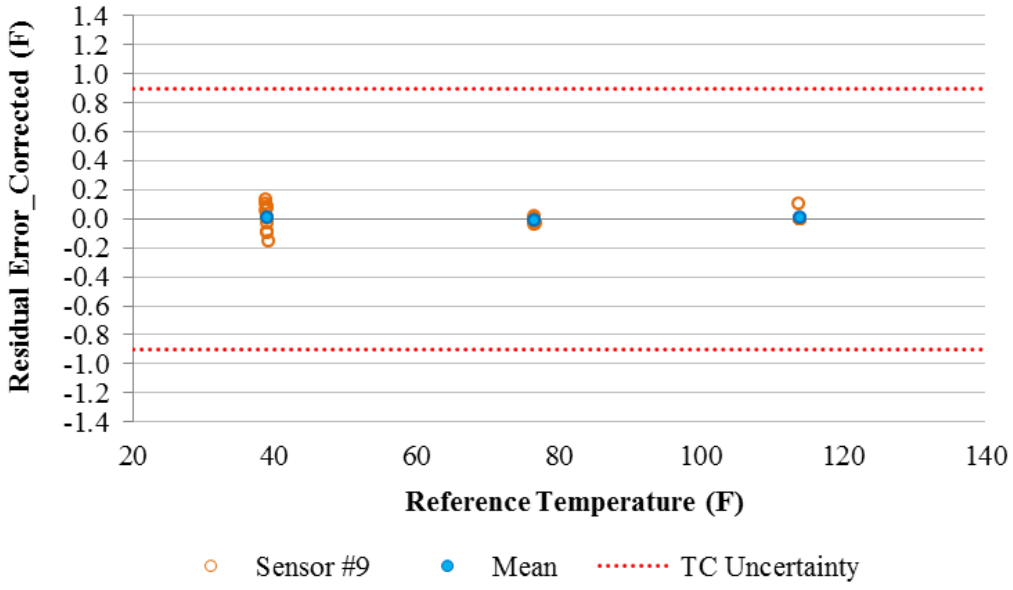

(b) Corrected Temperature Difference After Calibration

Figure A-13: Residual Plot of the Temperatures of Thermocouple Sensor #9 against the RTD Reference Temperatures with the Manufacturer Specified Sensor Accuracy (±0.9F)

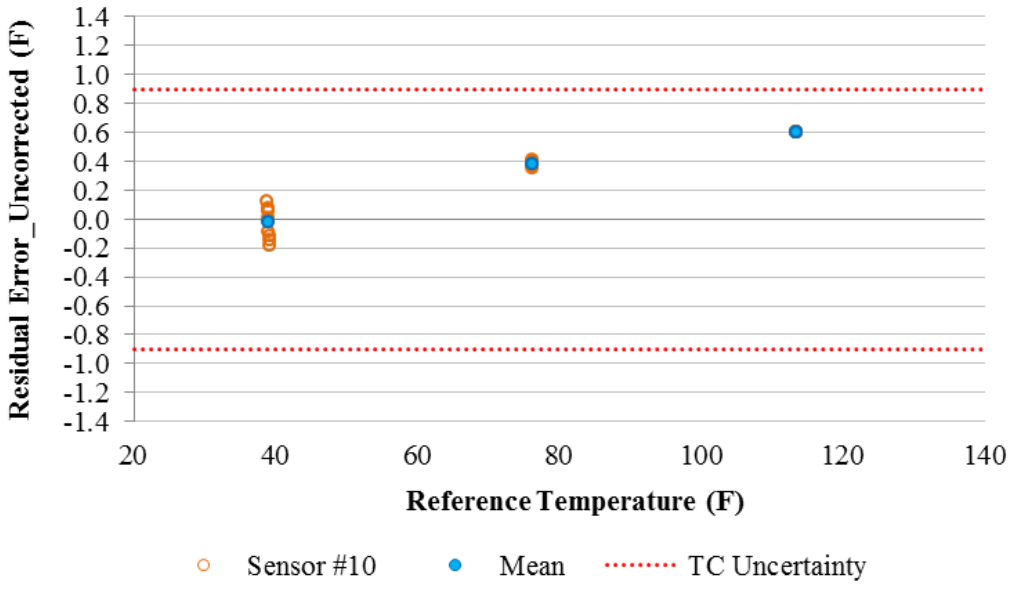

(a) Uncorrected Temperature Difference Before Calibration

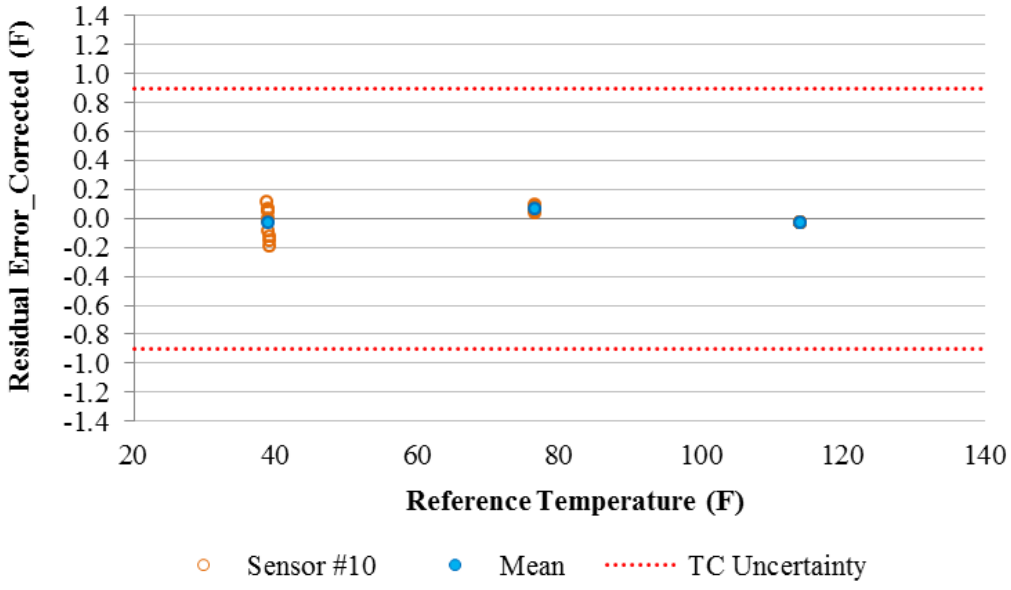

(b) Corrected Temperature Difference After Calibration

Figure A-14: Residual Plot of the Temperatures of Thermocouple Sensor #10 against the RTD Reference Temperatures with the Manufacturer Specified Sensor Accuracy (±0.9F)

APPENDIX B

g-FUNCTION APPROXIMATION

The g-function is a set of tabulated non-dimensional temperature response factors[60], which can determine the temperature change at the borehole wall corresponding to a change in the heat extraction/rejection input for a time step.

The tabulated long time-step g-function, developed by Eskilson, is often displayed using graphs. For example, Figure B-1 shows the long time-step temperature response factor (g-function) curves, which use non-dimensional time for boreholes that have line type and rectangle type configurations. The g-function values corresponding to each borehole configuration have a ratio of 0.1 between the borehole space and depth[61]. Figure B-2 presents long time-step g-function values corresponding to different center-to-center borehole spacing for 3×3 rectangle type borehole configuration. Figure B-1 and Figure B-2 indicate that temperature changes at the borehole wall increases as the number of boreholes increase, time of system operation increases, and borehole spacing decreases.

---

[60] The tabulated g-function values are available from the Bdllib.dat file in the eQUEST program. The file includes g-function values for 42 well configurations. In addition, Eskilson has presented curves of the g-function values for 38 borehole configurations, which can be tabulated (Eskilson, 1987)

[61] t is time, ts is time scale, B is the borehole space, and H is the borehole depth in Figure 4-13.

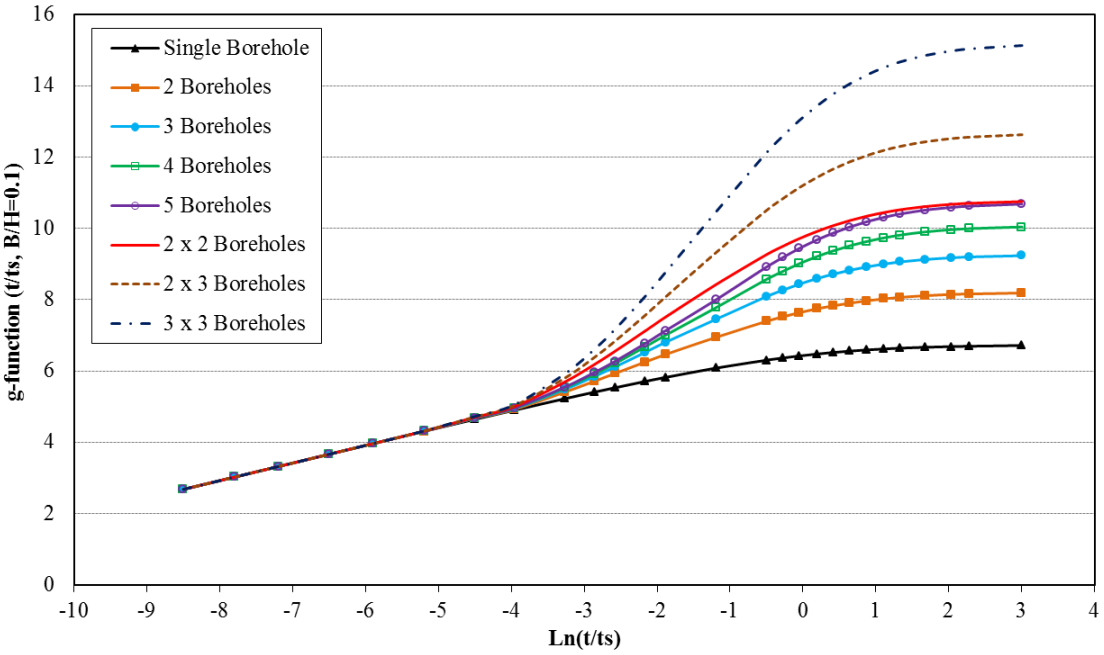

Figure B-1: Long Time-Step g-Function Curves for Straight Line Type and Rectangle Type Borehole Configurations (Eskilson, 1987)

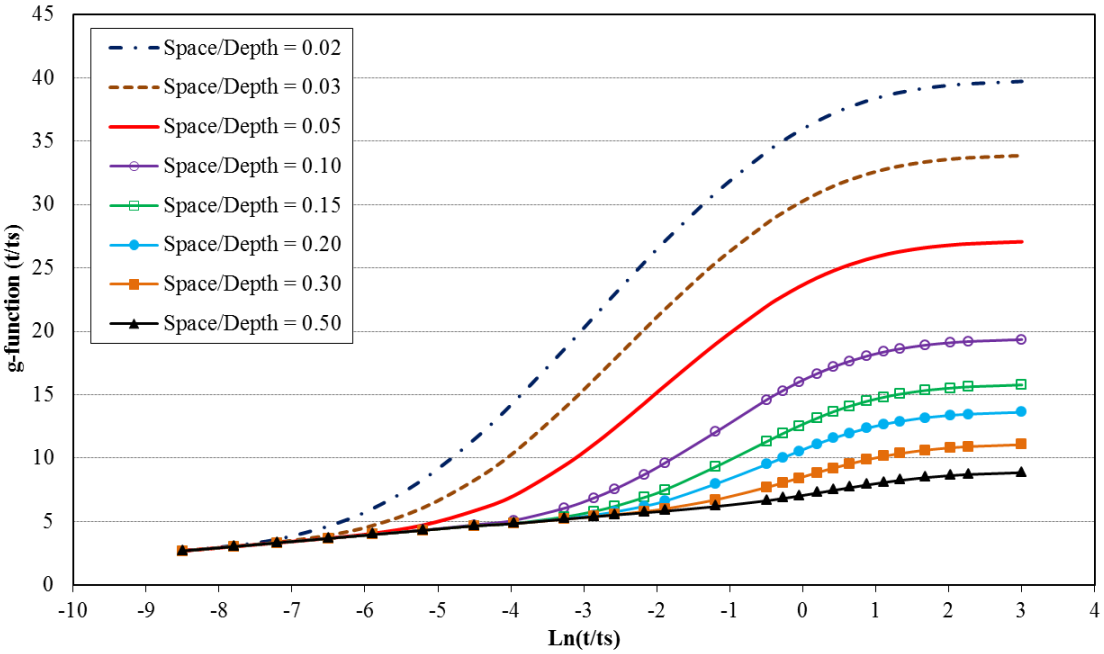

Figure B-2: Long Time-Step g-Function Curves for 3×3 Rectangle Type Borehole Configurations (Eskilson, 1987)

This study considered 17 types of the borehole field configurations for residential applications, which include: line type, rectangle type, and L-shape type borehole configurations. The maximum number of boreholes in the considered configuration types was ten boreholes, assuming that a general rule-of-thumb is 250 feet of borehole length per ton of GCHP capacity (Chiasson, 1999). Table B-1 presents the borehole field configuration types, array, and corresponding to borehole numbers.

Table B-1: Borehole Field Configuration for Residential Application

Configuration	Array	# of Borehole
Line Type 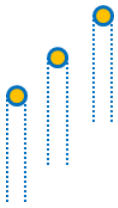	Line 1x1 (Single)	1
	Line 1x2	2
	Line 1x3	3
	Line 1x4	4
	Line 1x5	5
	Line 1x6	6
	Line 1x7	7
	Line 1x8	8
Rectangle Type 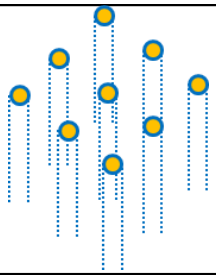	Rec 2x2	4
	Rec 2x3	6
	Rec 2x4	8
	Rec 2x5	10
	Rec 3x3	9
L-Shape Type 	L 2x2	3
	L 2x3	4
	L 2x4	5
	L 2x5	6

In order to use the g-function values for the vertical ground heat exchanger (GHX) model, this study developed the method to approximate the g-function. The g-function approximation utilized polynomial curve-fitting method, and Figure B-3 shows the simplified diagram to approximate the g-function values in this study. The detailed procedure was described in Section 0.

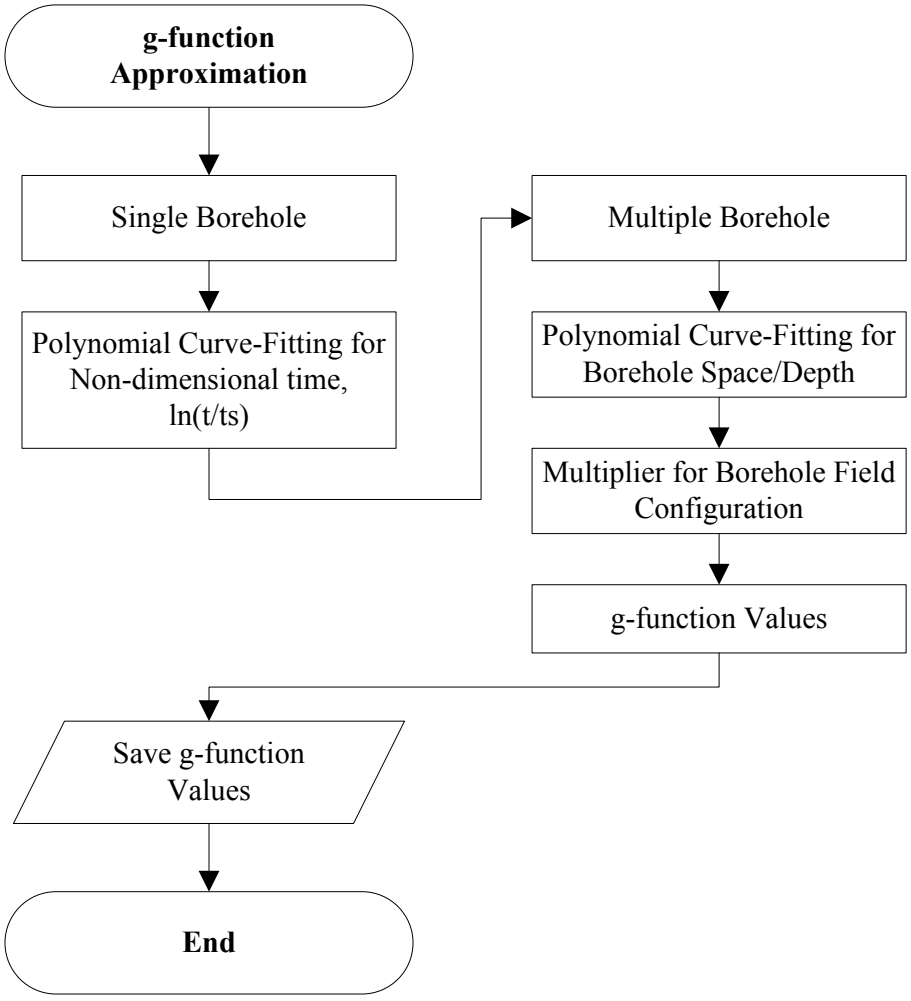

Figure B-3: Diagram of g-Function Approximation Procedure

This appendix presents the comparison of the approximated g-function for multiple boreholes used in this study and the Eskilson's g-function (Eskilson, 1987).

In general, the g-function values approximated in this study had less than 0.5 of the average g-function value difference against the Eskilson's g-function. All the g-function values are within the ±10 % difference range. The difference increases as the B/H parameter has a small value. The agreement of the g-function values is very good for a large value of the B/H parameter. In addition, it is worth mentioning that the most widely used value of B/H parameter is 0.05 or 0.10. The reason is that typical vertical borehole depth is between 200 ft and 300 ft and the borehole spacing is at least 20 ft. In the sense of the facts, the g-function values approximated are matched with the Eskilson g-function very well.

Table B-2 through Table B-17 show the g-function value difference[62] between the approximated g-values and Eskilson's g-values for the multiple boreholes considered in this study, corresponding to the ratio of borehole spacing and depth (B/H) and the non-dimensional time (ln t/ts). In addition, Figure B-4 through Figure B-19 show the residual plots for the difference of the g-function values between them, according to the B/H parameter for each borehole field configuration, including maximum, minimum, and average differences.

[62] The g-function value difference was calculated by subtracting from the Eskilson's g-value to the approximated g-value.

Table B-2: Difference between Approximated g-Values and Eskilson's g-Values for Line Type 1×2 Multiple Boreholes

	B/H							
ln(t/ts)	0.02	0.03	0.05	0.10	0.15	0.20	0.30	0.50
-8.5	0.00	0.00	0.00	0.00	0.00	0.00	0.00	0.00
-7.8	0.02	0.00	0.00	0.00	0.00	0.00	0.00	0.00
-7.2	0.03	0.01	-0.01	0.00	0.00	0.00	0.00	0.00
-6.5	0.07	0.03	-0.02	0.00	0.00	0.00	0.00	0.00
-5.9	0.11	0.07	0.00	0.00	0.00	0.00	0.00	0.00
-5.2	0.14	0.11	0.04	0.00	0.00	0.00	0.00	0.00
-4.5	0.12	0.14	0.10	0.02	-0.02	0.00	0.00	0.00
-3.963	0.08	0.13	0.10	-0.02	-0.07	-0.07	-0.07	-0.07
-3.27	0.00	0.09	0.14	0.06	-0.01	-0.03	-0.04	-0.04
-2.864	-0.06	0.05	0.13	0.09	0.02	0.00	-0.03	-0.03
-2.577	-0.10	0.02	0.12	0.11	0.05	0.02	-0.02	-0.02
-2.171	-0.16	-0.03	0.09	0.13	0.08	0.04	0.00	-0.02
-1.884	-0.20	-0.07	0.07	0.14	0.10	0.06	0.02	-0.01
-1.191	-0.30	-0.16	-0.01	0.10	0.13	0.13	0.07	0.03
-0.497	-0.37	-0.23	-0.06	0.09	0.14	0.15	0.11	0.06
-0.274	-0.39	-0.24	-0.08	0.08	0.13	0.15	0.12	0.07
-0.051	-0.40	-0.26	-0.09	0.07	0.13	0.15	0.13	0.08
0.196	-0.42	-0.27	-0.11	0.06	0.13	0.15	0.13	0.10
0.419	-0.43	-0.29	-0.12	0.05	0.12	0.15	0.14	0.11
0.642	-0.44	-0.29	-0.13	0.04	0.11	0.14	0.14	0.11
0.873	-0.45	-0.30	-0.14	0.03	0.11	0.14	0.13	0.12
1.112	-0.45	-0.31	-0.14	0.03	0.10	0.13	0.13	0.12
1.335	-0.46	-0.31	-0.15	0.02	0.10	0.13	0.13	0.12
1.679	-0.46	-0.31	-0.15	0.03	0.10	0.13	0.12	0.12
2.028	-0.47	-0.31	-0.14	0.03	0.10	0.13	0.12	0.12
2.275	-0.47	-0.31	-0.15	0.03	0.10	0.13	0.12	0.11
3.003	-0.50	-0.35	-0.18	0.00	0.08	0.11	0.11	0.10

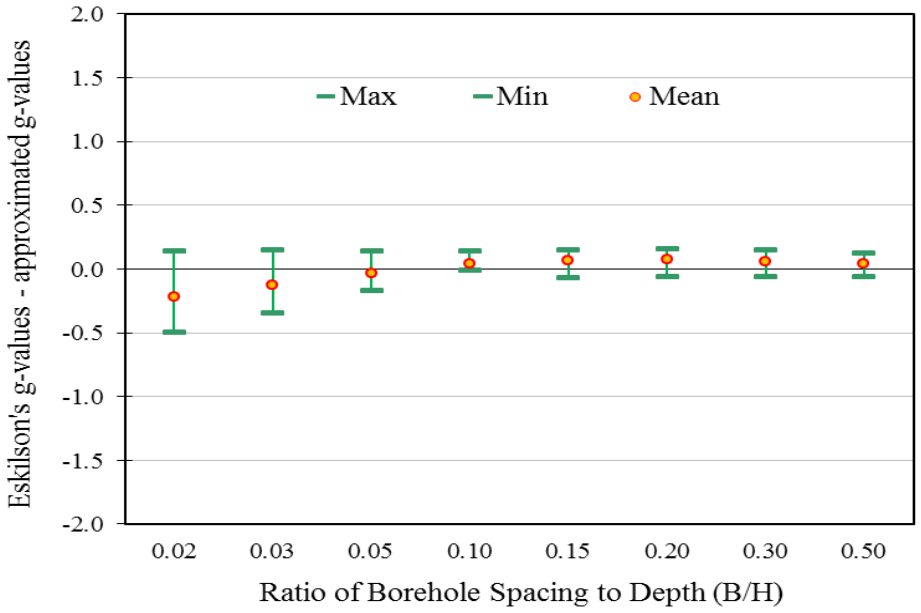

Figure B-4: Residual Plot for Line Type 1×2 Multiple Boreholes

Table B-3: Difference between Approximated g-Values and Eskilson's g-Values for Line Type 1×3 Multiple Boreholes

	B/H							
ln(t/ts)	0.02	0.03	0.05	0.10	0.15	0.20	0.30	0.50
-8.5	0.00	0.00	0.00	0.00	0.00	0.00	0.00	0.00
-7.8	0.03	0.00	0.00	0.00	0.00	0.00	0.00	0.00
-7.2	0.03	0.00	-0.01	0.00	0.00	0.00	0.00	0.00
-6.5	0.05	0.02	-0.03	0.00	0.00	0.00	0.00	0.00
-5.9	0.07	0.05	0.00	0.00	0.00	0.00	0.00	0.00
-5.2	0.10	0.09	0.04	0.00	0.00	0.00	0.00	0.00
-4.5	0.09	0.11	0.08	0.02	-0.03	0.00	0.00	0.00
-3.963	0.06	0.09	0.07	-0.02	-0.08	-0.07	-0.07	-0.07
-3.27	-0.01	0.07	0.11	0.05	-0.01	-0.03	-0.04	-0.04
-2.864	-0.07	0.04	0.10	0.08	0.02	0.00	-0.03	-0.03
-2.577	-0.11	0.01	0.10	0.09	0.04	0.02	-0.01	-0.02
-2.171	-0.17	-0.04	0.07	0.11	0.07	0.04	0.00	-0.02
-1.884	-0.21	-0.07	0.06	0.12	0.08	0.05	0.02	-0.01
-1.191	-0.31	-0.18	-0.02	0.07	0.10	0.12	0.06	0.02
-0.497	-0.37	-0.23	-0.07	0.06	0.10	0.13	0.09	0.05
-0.274	-0.39	-0.25	-0.08	0.06	0.10	0.13	0.10	0.06
-0.051	-0.40	-0.26	-0.09	0.05	0.10	0.13	0.11	0.07
0.196	-0.41	-0.27	-0.11	0.05	0.10	0.14	0.12	0.08
0.419	-0.42	-0.28	-0.12	0.04	0.09	0.13	0.12	0.09
0.642	-0.43	-0.29	-0.13	0.03	0.09	0.13	0.12	0.10
0.873	-0.44	-0.29	-0.13	0.02	0.09	0.13	0.12	0.10
1.112	-0.44	-0.29	-0.13	0.02	0.08	0.12	0.11	0.10
1.335	-0.44	-0.29	-0.13	0.02	0.08	0.12	0.11	0.10
1.679	-0.44	-0.29	-0.13	0.03	0.08	0.12	0.11	0.10
2.028	-0.45	-0.29	-0.12	0.04	0.09	0.12	0.11	0.10
2.275	-0.45	-0.29	-0.12	0.04	0.10	0.12	0.11	0.10
3.003	-0.49	-0.34	-0.16	0.01	0.07	0.11	0.10	0.09

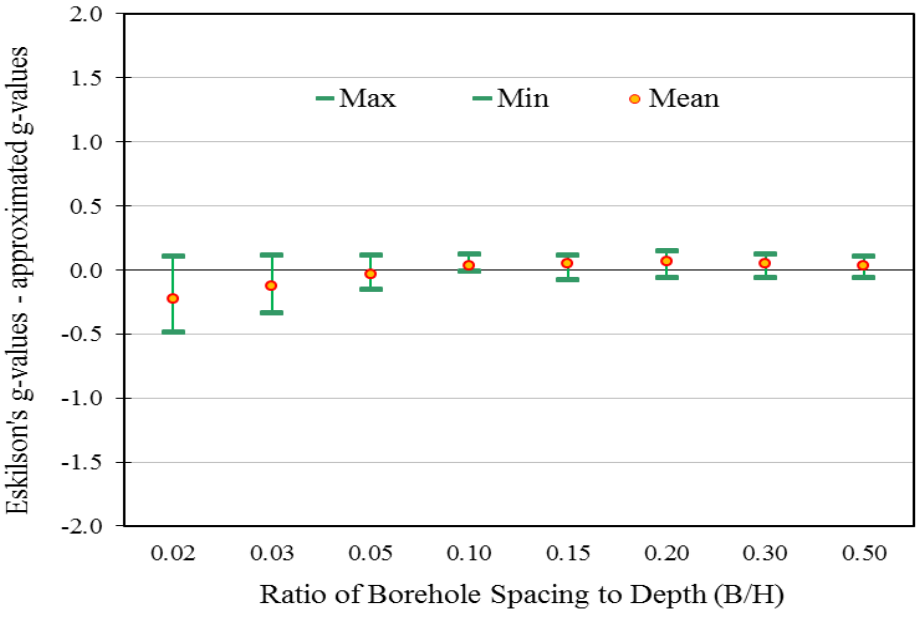

Figure B-5: Residual Plot for Line Type 1×3 Multiple Boreholes

Table B-4: Difference between Approximated g-Values and Eskilson's g-Values for Line Type 1×4 Multiple Boreholes

	B/H							
ln(t/ts)	0.02	0.03	0.05	0.10	0.15	0.20	0.30	0.50
-8.5	0.00	0.00	0.00	0.00	0.00	0.00	0.00	0.00
-7.8	0.03	0.00	0.00	0.00	0.00	0.00	0.00	0.00
-7.2	0.02	0.00	-0.02	0.00	0.00	0.00	0.00	0.00
-6.5	0.02	0.01	-0.04	0.00	0.00	0.00	0.00	0.00
-5.9	0.01	0.02	-0.01	0.00	0.00	0.00	0.00	0.00
-5.2	0.01	0.03	0.02	0.00	0.00	0.00	0.00	0.00
-4.5	0.01	0.03	0.04	0.02	-0.04	0.00	0.00	0.00
-3.963	0.00	0.01	0.01	-0.03	-0.09	-0.07	-0.07	-0.07
-3.27	-0.01	0.02	0.03	0.02	-0.02	-0.02	-0.04	-0.04
-2.864	-0.03	0.01	0.03	0.04	0.01	0.01	-0.03	-0.03
-2.577	-0.04	0.00	0.03	0.04	0.02	0.02	-0.01	-0.02
-2.171	-0.06	-0.01	0.03	0.05	0.03	0.02	0.00	-0.02
-1.884	-0.08	-0.02	0.03	0.05	0.04	0.03	0.01	-0.01
-1.191	-0.11	-0.07	-0.01	0.00	0.03	0.08	0.04	0.02
-0.497	-0.12	-0.08	-0.01	0.03	0.04	0.08	0.05	0.04
-0.274	-0.12	-0.08	-0.01	0.03	0.04	0.08	0.06	0.05
-0.051	-0.12	-0.08	-0.01	0.04	0.04	0.08	0.06	0.05
0.196	-0.12	-0.07	-0.01	0.04	0.05	0.09	0.07	0.06
0.419	-0.12	-0.07	-0.01	0.04	0.05	0.09	0.07	0.06
0.642	-0.12	-0.07	-0.01	0.04	0.05	0.09	0.07	0.06
0.873	-0.12	-0.06	-0.01	0.04	0.06	0.09	0.07	0.06
1.112	-0.11	-0.06	0.00	0.04	0.06	0.08	0.07	0.06
1.335	-0.11	-0.05	0.01	0.05	0.06	0.08	0.07	0.06
1.679	-0.10	-0.04	0.02	0.07	0.07	0.09	0.07	0.06
2.028	-0.10	-0.03	0.04	0.09	0.09	0.10	0.07	0.06
2.275	-0.10	-0.03	0.04	0.10	0.10	0.11	0.08	0.06
3.003	-0.15	-0.09	-0.01	0.05	0.07	0.10	0.07	0.06

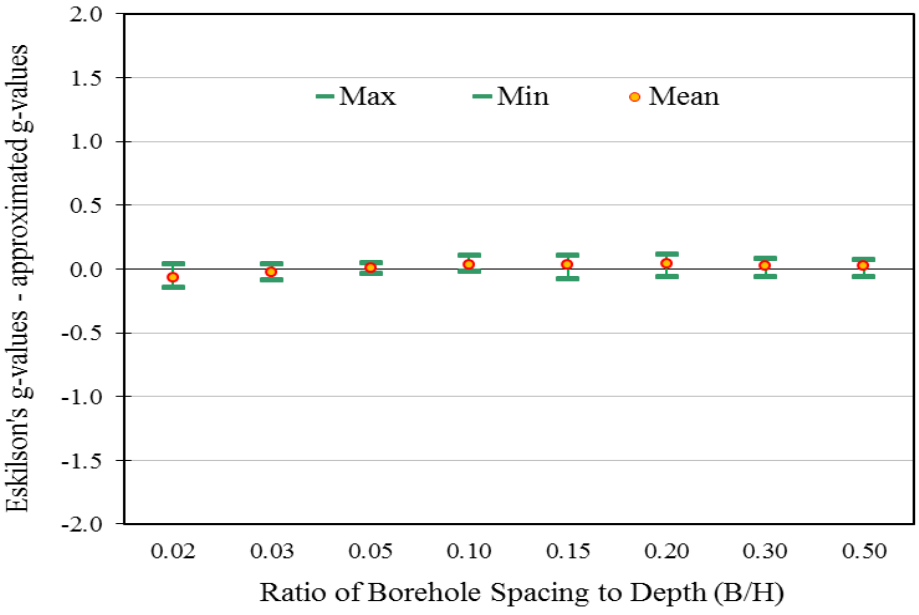

Figure B-6: Residual Plot for Line Type 1×4 Multiple Boreholes

Table B-5: Difference between Approximated g-Values and Eskilson's g-Values for Line Type 1×5 Multiple Boreholes

	B/H							
ln(t/ts)	0.02	0.03	0.05	0.10	0.15	0.20	0.30	0.50
-8.5	0.00	0.00	0.00	0.00	0.00	0.00	0.00	0.00
-7.8	0.03	0.00	0.00	0.00	0.00	0.00	0.00	0.00
-7.2	0.00	0.00	-0.02	0.00	0.00	0.00	0.00	0.00
-6.5	-0.03	0.00	-0.05	0.00	0.00	0.00	0.00	0.00
-5.9	-0.08	-0.01	-0.02	0.00	0.00	0.00	0.00	0.00
-5.2	-0.13	-0.05	0.00	0.00	0.00	0.00	0.00	0.00
-4.5	-0.16	-0.10	-0.01	0.01	-0.05	0.00	0.00	0.00
-3.963	-0.17	-0.15	-0.09	-0.04	-0.09	-0.07	-0.07	-0.07
-3.27	-0.15	-0.15	-0.11	-0.01	-0.02	-0.02	-0.04	-0.04
-2.864	-0.14	-0.15	-0.12	-0.02	-0.01	0.00	-0.03	-0.03
-2.577	-0.13	-0.14	-0.13	-0.04	-0.01	0.01	-0.01	-0.02
-2.171	-0.11	-0.13	-0.13	-0.06	-0.02	0.00	0.00	-0.02
-1.884	-0.09	-0.12	-0.12	-0.07	-0.03	-0.01	0.01	-0.01
-1.191	-0.07	-0.12	-0.12	-0.14	-0.08	0.01	0.01	0.01
-0.497	-0.02	-0.06	-0.08	-0.11	-0.09	-0.03	0.00	0.03
-0.274	0.00	-0.05	-0.07	-0.10	-0.09	-0.03	-0.01	0.02
-0.051	0.02	-0.03	-0.06	-0.09	-0.09	-0.04	-0.01	0.02
0.196	0.03	-0.02	-0.05	-0.08	-0.08	-0.03	-0.01	0.03
0.419	0.05	0.00	-0.04	-0.07	-0.07	-0.03	-0.02	0.02
0.642	0.06	0.01	-0.03	-0.07	-0.07	-0.03	-0.02	0.02
0.873	0.07	0.03	-0.02	-0.06	-0.06	-0.03	-0.02	0.01
1.112	0.08	0.04	0.00	-0.05	-0.06	-0.03	-0.03	0.01
1.335	0.10	0.06	0.01	-0.04	-0.05	-0.03	-0.03	0.00
1.679	0.11	0.08	0.03	-0.01	-0.03	-0.02	-0.03	0.00
2.028	0.12	0.09	0.06	0.02	-0.01	0.00	-0.02	0.00
2.275	0.12	0.10	0.06	0.03	0.01	0.01	-0.01	0.00
3.003	0.07	0.02	0.01	-0.02	-0.02	0.00	-0.02	0.00

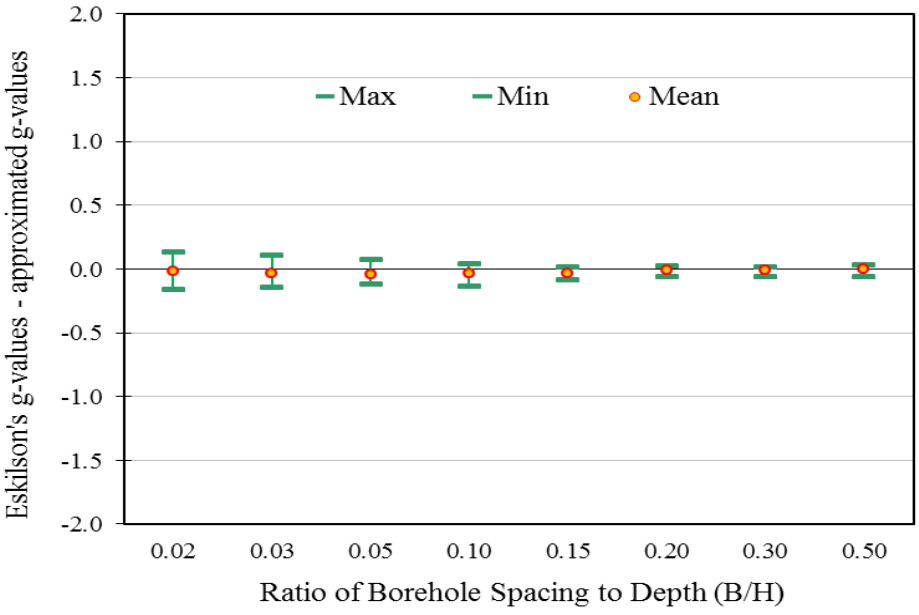

Figure B-7: Residual Plot for Line Type 1×5 Multiple Boreholes

Table B-6: Difference between Approximated g-Values and Eskilson's g-Values for Line Type 1×6 Multiple Boreholes

	B/H							
ln(t/ts)	0.02	0.03	0.05	0.10	0.15	0.20	0.30	0.50
-8.5	0.00	0.00	0.00	0.00	0.00	0.00	0.00	0.00
-7.8	0.03	0.00	0.00	0.00	0.00	0.00	0.00	0.00
-7.2	-0.01	0.00	-0.02	0.00	0.00	0.00	0.00	0.00
-6.5	-0.09	-0.02	-0.06	0.00	0.00	0.00	0.00	0.00
-5.9	-0.18	-0.05	-0.03	0.00	0.00	0.00	0.00	0.00
-5.2	-0.32	-0.14	-0.02	0.00	0.00	0.00	0.00	0.00
-4.5	-0.45	-0.27	-0.07	0.01	-0.06	0.00	0.00	0.00
-3.963	-0.28	-0.26	-0.15	-0.04	-0.09	-0.07	-0.07	-0.07
-3.27	-0.21	-0.26	-0.20	-0.04	-0.03	-0.02	-0.04	-0.04
-2.864	-0.15	-0.24	-0.23	-0.07	-0.02	0.00	-0.03	-0.03
-2.577	-0.09	-0.21	-0.24	-0.09	-0.03	0.00	-0.01	-0.02
-2.171	-0.01	-0.16	-0.23	-0.13	-0.05	-0.02	0.00	-0.02
-1.884	0.05	-0.11	-0.21	-0.16	-0.08	-0.04	0.00	-0.01
-1.191	0.19	-0.01	-0.16	-0.24	-0.16	-0.04	-0.01	0.01
-0.497	0.34	0.13	-0.05	-0.20	-0.18	-0.10	-0.04	0.01
-0.274	0.38	0.17	-0.01	-0.18	-0.18	-0.11	-0.06	0.01
-0.051	0.42	0.21	0.02	-0.15	-0.18	-0.12	-0.07	0.00
0.196	0.46	0.25	0.05	-0.13	-0.16	-0.11	-0.07	0.00
0.419	0.49	0.28	0.08	-0.11	-0.15	-0.11	-0.08	-0.01
0.642	0.52	0.31	0.10	-0.09	-0.14	-0.11	-0.09	-0.02
0.873	0.55	0.34	0.12	-0.08	-0.13	-0.11	-0.09	-0.02
1.112	0.58	0.37	0.15	-0.05	-0.11	-0.10	-0.09	-0.03
1.335	0.60	0.39	0.17	-0.03	-0.10	-0.09	-0.09	-0.04
1.679	0.62	0.42	0.21	0.00	-0.07	-0.08	-0.09	-0.04
2.028	0.64	0.45	0.24	0.04	-0.04	-0.05	-0.07	-0.04
2.275	0.65	0.46	0.25	0.06	-0.02	-0.04	-0.06	-0.04
3.003	0.59	0.38	0.19	0.01	-0.04	-0.04	-0.07	-0.04

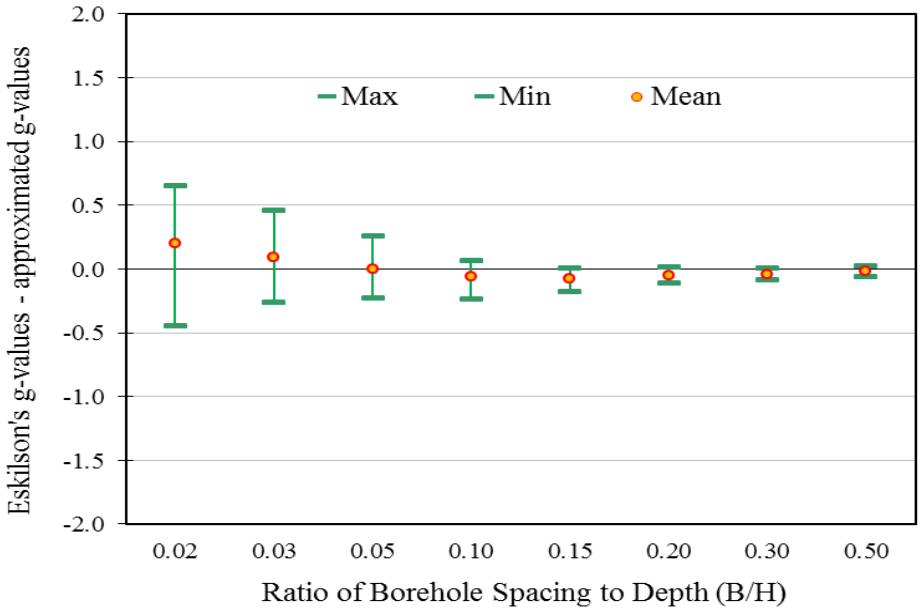

Figure B-8: Residual Plot for Line Type 1×6 Multiple Boreholes

Table B-7: Difference between Approximated g-Values and Eskilson's g-Values for Line Type 1×7 Multiple Boreholes

	B/H							
ln(t/ts)	0.02	0.03	0.05	0.10	0.15	0.20	0.30	0.50
-8.5	0.00	0.00	0.00	0.00	0.00	0.00	0.00	0.00
-7.8	0.03	0.00	0.00	0.00	0.00	0.00	0.00	0.00
-7.2	-0.02	0.00	-0.02	0.00	0.00	0.00	0.00	0.00
-6.5	-0.11	-0.02	-0.06	0.00	0.00	0.00	0.00	0.00
-5.9	-0.22	-0.06	-0.03	0.00	0.00	0.00	0.00	0.00
-5.2	-0.35	-0.17	-0.03	0.00	0.00	0.00	0.00	0.00
-4.5	-0.43	-0.30	-0.09	0.01	-0.07	0.00	0.00	0.00
-3.963	-0.45	-0.41	-0.23	-0.05	-0.10	-0.07	-0.07	-0.07
-3.27	-0.36	-0.43	-0.33	-0.07	-0.03	-0.02	-0.04	-0.04
-2.864	-0.26	-0.40	-0.38	-0.12	-0.03	0.00	-0.03	-0.03
-2.577	-0.17	-0.36	-0.39	-0.16	-0.05	0.00	-0.01	-0.02
-2.171	-0.04	-0.28	-0.39	-0.22	-0.10	-0.03	-0.01	-0.02
-1.884	0.06	-0.20	-0.37	-0.27	-0.14	-0.07	0.00	-0.01
-1.191	0.30	-0.04	-0.28	-0.38	-0.25	-0.10	-0.03	0.01
-0.497	0.54	0.19	-0.12	-0.34	-0.31	-0.19	-0.09	0.00
-0.274	0.61	0.26	-0.06	-0.31	-0.31	-0.21	-0.11	-0.01
-0.051	0.68	0.32	-0.01	-0.28	-0.31	-0.22	-0.13	-0.02
0.196	0.74	0.38	0.04	-0.25	-0.29	-0.22	-0.14	-0.03
0.419	0.79	0.43	0.08	-0.22	-0.28	-0.23	-0.16	-0.04
0.642	0.84	0.47	0.11	-0.20	-0.26	-0.23	-0.17	-0.05
0.873	0.88	0.51	0.15	-0.17	-0.24	-0.22	-0.18	-0.07
1.112	0.92	0.55	0.18	-0.14	-0.23	-0.21	-0.18	-0.08
1.335	0.95	0.59	0.22	-0.11	-0.21	-0.20	-0.18	-0.09
1.679	0.98	0.63	0.26	-0.07	-0.17	-0.18	-0.18	-0.10
2.028	1.01	0.66	0.30	-0.02	-0.13	-0.15	-0.16	-0.10
2.275	1.02	0.67	0.32	0.00	-0.11	-0.14	-0.15	-0.09
3.003	0.96	0.59	0.26	-0.05	-0.13	-0.14	-0.15	-0.09

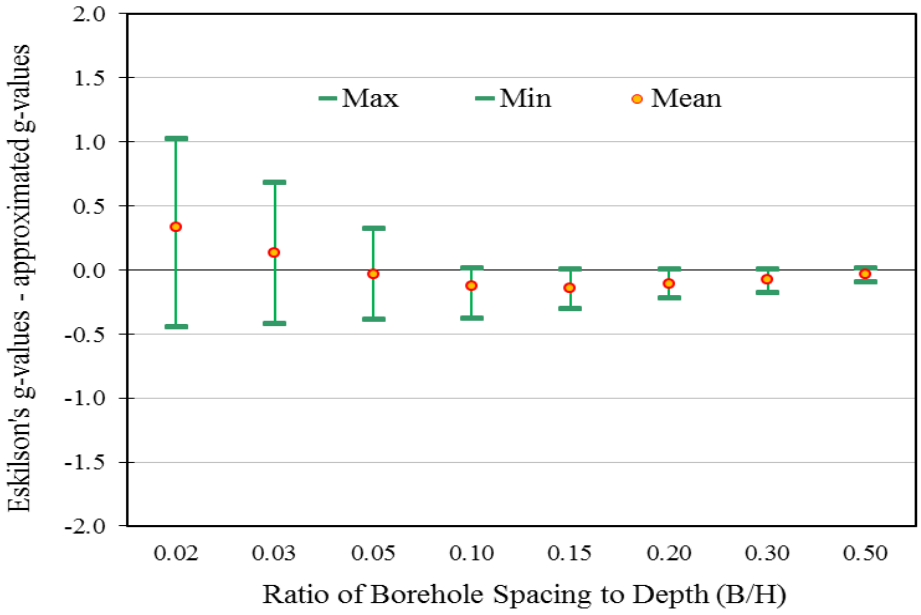

Figure B-9: Residual Plot for Line Type 1×7 Multiple Boreholes

Table B-8: Difference between Approximated g-Values and Eskilson's g-Values for Line Type 1×8 Multiple Boreholes

	B/H							
ln(t/ts)	0.02	0.03	0.05	0.10	0.15	0.20	0.30	0.50
-8.5	0.00	0.00	0.00	0.00	0.00	0.00	0.00	0.00
-7.8	0.03	0.00	0.00	0.00	0.00	0.00	0.00	0.00
-7.2	-0.03	0.00	-0.02	0.00	0.00	0.00	0.00	0.00
-6.5	-0.15	-0.03	-0.07	0.00	0.00	0.00	0.00	0.00
-5.9	-0.30	-0.09	-0.04	0.00	0.00	0.00	0.00	0.00
-5.2	-0.49	-0.23	-0.04	0.00	0.00	0.00	0.00	0.00
-4.5	-0.65	-0.43	-0.14	0.01	-0.07	0.00	0.00	0.00
-3.963	-0.57	-0.51	-0.29	-0.06	-0.10	-0.07	-0.07	-0.07
-3.27	-0.44	-0.54	-0.41	-0.09	-0.04	-0.02	-0.04	-0.04
-2.864	-0.30	-0.51	-0.48	-0.16	-0.04	0.00	-0.03	-0.03
-2.577	-0.17	-0.45	-0.50	-0.21	-0.07	-0.01	-0.01	-0.02
-2.171	0.02	-0.34	-0.50	-0.29	-0.13	-0.05	-0.01	-0.02
-1.884	0.17	-0.23	-0.47	-0.34	-0.18	-0.09	-0.01	-0.01
-1.191	0.53	0.03	-0.35	-0.48	-0.32	-0.14	-0.05	0.00
-0.497	0.89	0.36	-0.12	-0.43	-0.40	-0.26	-0.13	-0.01
-0.274	0.99	0.45	-0.04	-0.40	-0.40	-0.29	-0.15	-0.02
-0.051	1.08	0.54	0.03	-0.36	-0.40	-0.30	-0.18	-0.03
0.196	1.18	0.63	0.10	-0.32	-0.38	-0.31	-0.19	-0.05
0.419	1.25	0.69	0.16	-0.28	-0.36	-0.31	-0.21	-0.06
0.642	1.31	0.76	0.21	-0.25	-0.35	-0.31	-0.23	-0.08
0.873	1.37	0.82	0.26	-0.21	-0.32	-0.30	-0.24	-0.10
1.112	1.42	0.87	0.31	-0.17	-0.30	-0.29	-0.25	-0.11
1.335	1.46	0.91	0.35	-0.13	-0.27	-0.28	-0.25	-0.13
1.679	1.51	0.97	0.41	-0.08	-0.23	-0.25	-0.24	-0.14
2.028	1.55	1.01	0.46	-0.02	-0.18	-0.22	-0.22	-0.14
2.275	1.56	1.03	0.48	0.01	-0.15	-0.19	-0.20	-0.13
3.003	1.50	0.95	0.42	-0.04	-0.17	-0.19	-0.20	-0.13

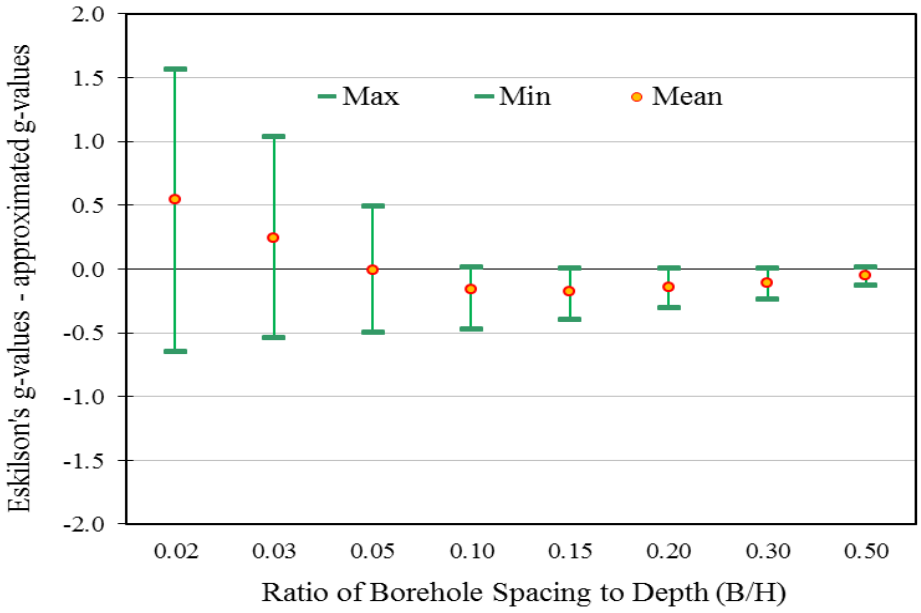

Figure B-10: Residual Plot for Line Type 1×8 Multiple Boreholes

Table B-9: Difference between Approximated g-Values and Eskilson's g-Values for Rectangle Type 2×2 Multiple Boreholes

	B/H							
ln(t/ts)	0.02	0.03	0.05	0.10	0.15	0.20	0.30	0.50
-8.5	0.00	0.00	0.00	0.00	0.00	0.00	0.00	0.00
-7.8	0.04	0.00	0.00	0.00	0.00	0.00	0.00	0.00
-7.2	0.05	0.01	-0.02	0.00	0.00	0.00	0.00	0.00
-6.5	0.13	0.04	-0.05	0.00	0.00	0.00	0.00	0.00
-5.9	0.22	0.11	-0.01	0.00	0.00	0.00	0.00	0.00
-5.2	0.31	0.22	0.07	0.00	0.00	0.00	0.00	0.00
-4.5	0.33	0.32	0.19	0.03	-0.05	0.00	0.00	0.00
-3.963	0.28	0.33	0.22	0.00	-0.09	-0.07	-0.07	-0.07
-3.27	0.16	0.30	0.33	0.13	0.01	-0.02	-0.04	-0.04
-2.864	0.06	0.24	0.34	0.21	0.07	0.02	-0.03	-0.03
-2.577	-0.02	0.19	0.33	0.26	0.11	0.05	-0.01	-0.02
-2.171	-0.13	0.10	0.29	0.31	0.18	0.09	0.02	-0.02
-1.884	-0.21	0.03	0.26	0.33	0.22	0.13	0.04	-0.01
-1.191	-0.39	-0.13	0.13	0.31	0.31	0.25	0.11	0.03
-0.497	-0.52	-0.27	0.02	0.27	0.31	0.29	0.19	0.08
-0.274	-0.56	-0.30	-0.01	0.24	0.31	0.29	0.21	0.10
-0.051	-0.59	-0.33	-0.04	0.22	0.30	0.30	0.23	0.12
0.196	-0.61	-0.36	-0.07	0.20	0.28	0.30	0.25	0.15
0.419	-0.63	-0.38	-0.09	0.17	0.27	0.29	0.25	0.16
0.642	-0.65	-0.40	-0.11	0.15	0.25	0.28	0.25	0.18
0.873	-0.67	-0.41	-0.13	0.14	0.24	0.27	0.25	0.19
1.112	-0.68	-0.41	-0.13	0.13	0.22	0.26	0.24	0.19
1.335	-0.68	-0.42	-0.14	0.13	0.22	0.25	0.24	0.19
1.679	-0.69	-0.41	-0.13	0.13	0.22	0.25	0.23	0.19
2.028	-0.69	-0.41	-0.12	0.15	0.23	0.25	0.23	0.19
2.275	-0.69	-0.41	-0.12	0.16	0.24	0.25	0.24	0.19
3.003	-0.76	-0.50	-0.18	0.10	0.20	0.24	0.22	0.18

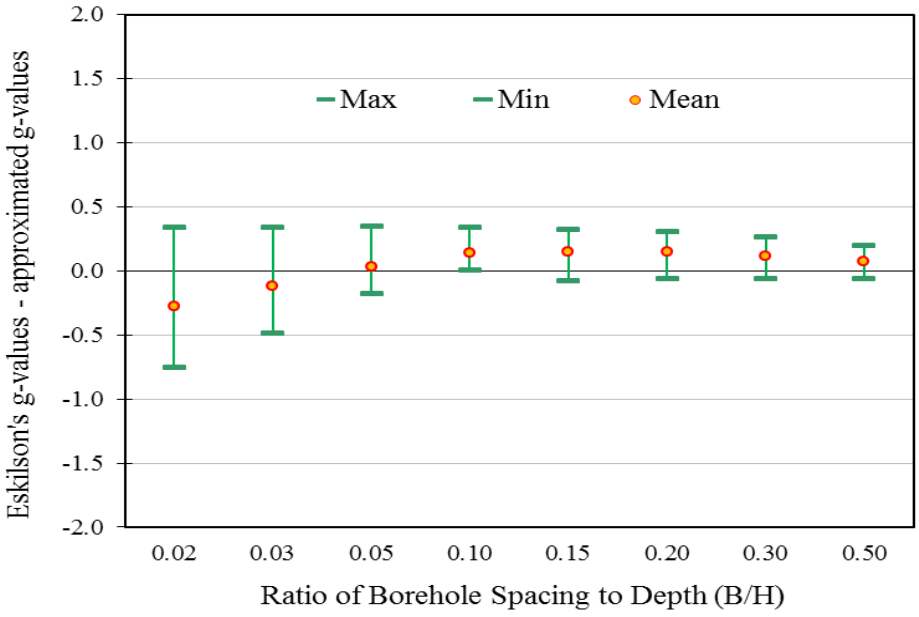

Figure B-11: Residual Plot for Rectangle Type 2×2 Multiple Boreholes

Table B-10: Difference between Approximated g-Values and Eskilson's g-Values for Rectangle Type 2×3 Multiple Boreholes

	B/H							
ln(t/ts)	0.02	0.03	0.05	0.10	0.15	0.20	0.30	0.50
-8.5	0.00	0.00	0.00	0.00	0.00	0.00	0.00	0.00
-7.8	0.05	0.00	0.00	0.00	0.00	0.00	0.00	0.00
-7.2	0.02	0.01	-0.03	0.00	0.00	0.00	0.00	0.00
-6.5	0.04	0.01	-0.07	0.00	0.00	0.00	0.00	0.00
-5.9	0.08	0.05	-0.03	0.00	0.00	0.00	0.00	0.00
-5.2	0.15	0.11	0.04	0.00	0.00	0.00	0.00	0.00
-4.5	0.18	0.17	0.11	0.03	-0.08	0.00	0.00	0.00
-3.963	0.16	0.18	0.09	-0.02	-0.10	-0.07	-0.07	-0.07
-3.27	0.08	0.18	0.19	0.07	-0.01	-0.01	-0.04	-0.04
-2.864	-0.01	0.14	0.20	0.12	0.04	0.03	-0.02	-0.03
-2.577	-0.07	0.10	0.20	0.16	0.07	0.04	0.00	-0.02
-2.171	-0.17	0.03	0.18	0.20	0.10	0.05	0.01	-0.02
-1.884	-0.23	-0.03	0.16	0.21	0.13	0.06	0.03	-0.01
-1.191	-0.40	-0.17	0.05	0.19	0.20	0.16	0.07	0.02
-0.497	-0.50	-0.29	-0.04	0.17	0.20	0.18	0.12	0.05
-0.274	-0.53	-0.32	-0.07	0.14	0.19	0.18	0.13	0.06
-0.051	-0.55	-0.35	-0.10	0.13	0.18	0.18	0.14	0.07
0.196	-0.57	-0.37	-0.13	0.10	0.16	0.19	0.16	0.09
0.419	-0.58	-0.38	-0.15	0.08	0.15	0.18	0.16	0.10
0.642	-0.59	-0.39	-0.16	0.05	0.14	0.17	0.16	0.11
0.873	-0.60	-0.40	-0.17	0.04	0.12	0.16	0.15	0.12
1.112	-0.61	-0.40	-0.18	0.03	0.11	0.15	0.15	0.12
1.335	-0.61	-0.39	-0.17	0.03	0.11	0.14	0.14	0.12
1.679	-0.61	-0.38	-0.16	0.05	0.11	0.14	0.13	0.11
2.028	-0.60	-0.37	-0.14	0.08	0.13	0.15	0.14	0.12
2.275	-0.60	-0.37	-0.13	0.09	0.15	0.16	0.15	0.12
3.003	-0.69	-0.49	-0.22	0.01	0.10	0.14	0.13	0.11

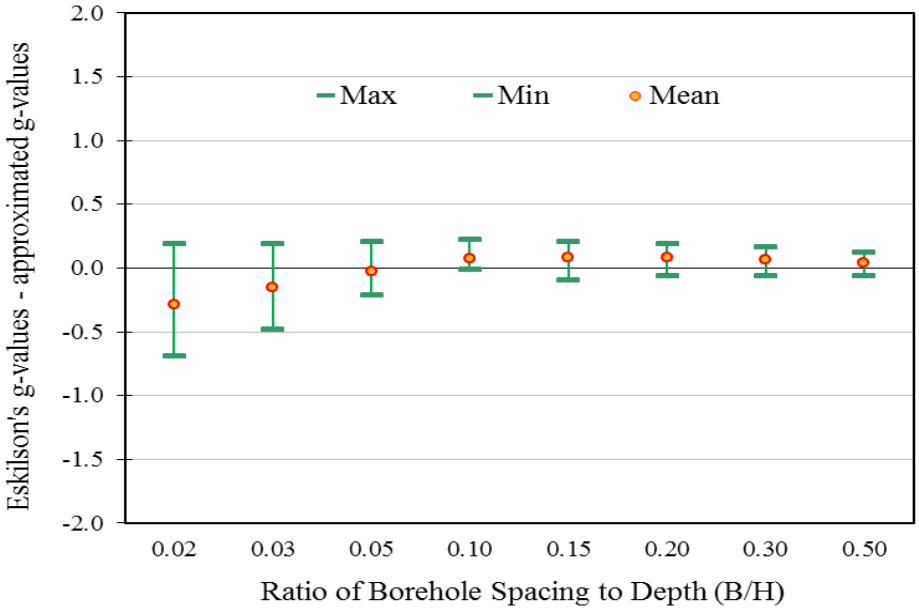

Figure B-12: Residual Plot for Rectangle Type 2×3 Multiple Boreholes

Table B-11: Difference between Approximated g-Values and Eskilson's g-Values for Rectangle Type 2×4 Multiple Boreholes

	B/H							
ln(t/ts)	0.02	0.03	0.05	0.10	0.15	0.20	0.30	0.50
-8.5	0.00	0.00	0.00	0.00	0.00	0.00	0.00	0.00
-7.8	0.05	0.00	0.00	0.00	0.00	0.00	0.00	0.00
-7.2	-0.01	0.00	-0.03	0.00	0.00	0.00	0.00	0.00
-6.5	-0.05	-0.01	-0.09	0.00	0.00	0.00	0.00	0.00
-5.9	-0.07	-0.02	-0.04	0.00	0.00	0.00	0.00	0.00
-5.2	-0.06	-0.03	0.00	0.00	0.00	0.00	0.00	0.00
-4.5	-0.02	-0.02	0.01	0.02	-0.10	0.00	0.00	0.00
-3.963	0.02	-0.02	-0.06	-0.04	-0.11	-0.07	-0.07	-0.07
-3.27	0.04	0.03	0.00	0.01	-0.02	-0.01	-0.04	-0.04
-2.864	0.04	0.04	0.02	0.02	0.01	0.02	-0.02	-0.03
-2.577	0.04	0.04	0.03	0.03	0.01	0.02	0.00	-0.02
-2.171	0.02	0.04	0.04	0.04	0.01	0.01	0.00	-0.02
-1.884	0.01	0.03	0.05	0.05	0.01	0.00	0.01	-0.01
-1.191	-0.02	0.01	0.02	0.03	0.05	0.05	0.02	0.01
-0.497	0.00	-0.01	0.03	0.05	0.04	0.03	0.02	0.02
-0.274	0.01	0.00	0.02	0.04	0.04	0.03	0.02	0.02
-0.051	0.01	0.00	0.02	0.04	0.04	0.03	0.03	0.02
0.196	0.02	0.00	0.01	0.02	0.03	0.04	0.04	0.03
0.419	0.03	0.01	0.01	0.01	0.03	0.04	0.04	0.03
0.642	0.04	0.02	0.01	0.00	0.02	0.03	0.03	0.03
0.873	0.05	0.03	0.01	0.00	0.01	0.03	0.03	0.03
1.112	0.06	0.04	0.02	0.00	0.01	0.02	0.02	0.03
1.335	0.07	0.06	0.04	0.02	0.01	0.02	0.01	0.03
1.679	0.09	0.09	0.07	0.05	0.03	0.02	0.02	0.02
2.028	0.11	0.12	0.10	0.09	0.06	0.04	0.03	0.03
2.275	0.11	0.12	0.12	0.11	0.08	0.06	0.04	0.03
3.003	0.01	-0.02	0.01	0.02	0.03	0.04	0.03	0.03

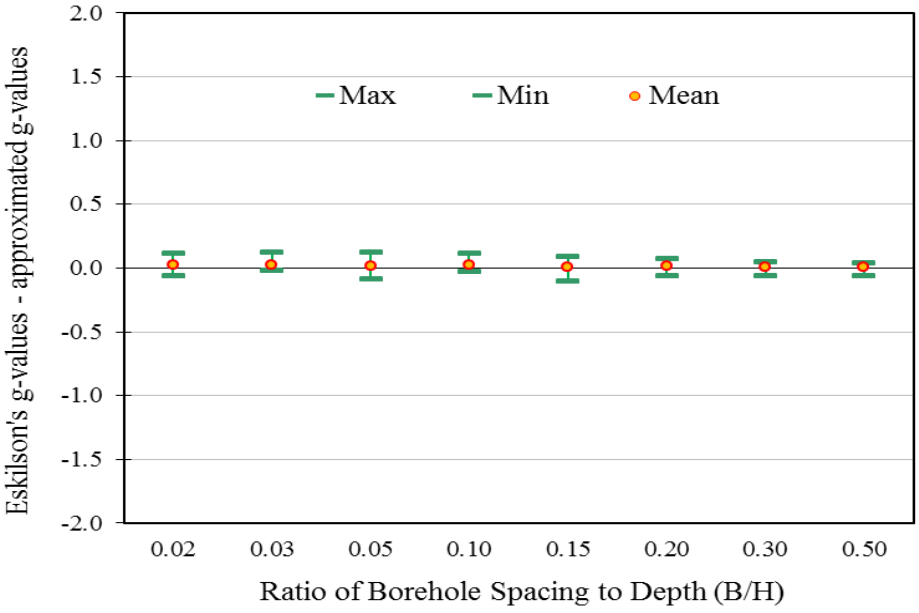

Figure B-13: Residual Plot for Rectangle Type 2×4 Multiple Boreholes

Table B-12: Difference between Approximated g-Values and Eskilson's g-Values for Rectangle Type 2×5 Multiple Boreholes

	B/H							
ln(t/ts)	0.02	0.03	0.05	0.10	0.15	0.20	0.30	0.50
-8.5	0.00	0.00	0.00	0.00	0.00	0.00	0.00	0.00
-7.8	0.06	0.00	0.00	0.00	0.00	0.00	0.00	0.00
-7.2	-0.04	0.00	-0.04	0.00	0.00	0.00	0.00	0.00
-6.5	-0.15	-0.04	-0.11	0.00	0.00	0.00	0.00	0.00
-5.9	-0.25	-0.09	-0.06	0.00	0.00	0.00	0.00	0.00
-5.2	-0.31	-0.18	-0.04	0.00	0.00	0.00	0.00	0.00
-4.5	-0.31	-0.26	-0.09	0.02	-0.12	0.00	0.00	0.00
-3.963	-0.26	-0.30	-0.23	-0.06	-0.12	-0.07	-0.07	-0.07
-3.27	-0.15	-0.25	-0.25	-0.07	-0.03	-0.01	-0.04	-0.04
-2.864	-0.08	-0.21	-0.26	-0.10	-0.03	0.02	-0.02	-0.03
-2.577	-0.02	-0.17	-0.25	-0.12	-0.05	0.00	0.00	-0.02
-2.171	0.07	-0.11	-0.22	-0.15	-0.09	-0.04	0.00	-0.02
-1.884	0.13	-0.06	-0.19	-0.17	-0.12	-0.07	0.00	-0.01
-1.191	0.26	0.05	-0.15	-0.23	-0.15	-0.08	-0.03	0.00
-0.497	0.41	0.16	-0.05	-0.19	-0.20	-0.16	-0.08	-0.02
-0.274	0.46	0.20	-0.02	-0.19	-0.20	-0.17	-0.10	-0.03
-0.051	0.50	0.23	0.00	-0.17	-0.20	-0.18	-0.11	-0.03
0.196	0.55	0.27	0.02	-0.18	-0.20	-0.17	-0.11	-0.04
0.419	0.58	0.30	0.04	-0.17	-0.19	-0.17	-0.12	-0.04
0.642	0.62	0.33	0.05	-0.17	-0.20	-0.18	-0.13	-0.05
0.873	0.65	0.36	0.07	-0.16	-0.20	-0.18	-0.14	-0.06
1.112	0.68	0.39	0.10	-0.14	-0.19	-0.18	-0.15	-0.07
1.335	0.71	0.43	0.13	-0.12	-0.18	-0.18	-0.16	-0.08
1.679	0.74	0.47	0.17	-0.08	-0.15	-0.17	-0.16	-0.09
2.028	0.77	0.51	0.22	-0.02	-0.11	-0.14	-0.14	-0.09
2.275	0.77	0.52	0.24	0.01	-0.08	-0.11	-0.12	-0.08
3.003	0.67	0.37	0.13	-0.09	-0.13	-0.13	-0.13	-0.08

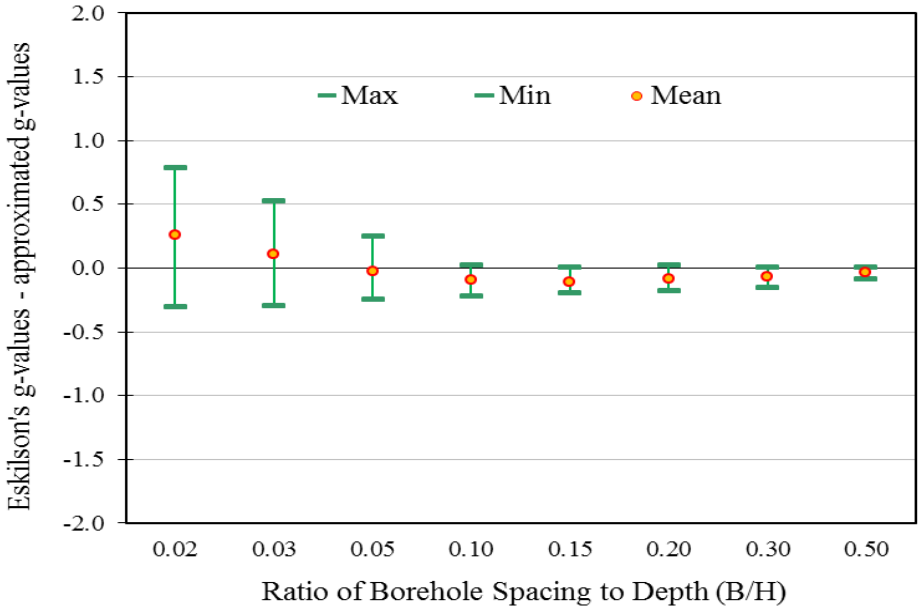

Figure B-14: Residual Plot for Rectangle Type 2×5 Multiple Boreholes

Table B-13: Difference between Approximated g-Values and Eskilson's g-Values for Rectangle Type 3×3 Multiple Boreholes

	B/H							
ln(t/ts)	0.02	0.03	0.05	0.10	0.15	0.20	0.30	0.50
-8.5	0.00	0.00	0.00	0.00	0.00	0.00	0.00	0.00
-7.8	0.06	0.00	0.00	0.00	0.00	0.00	0.00	0.00
-7.2	-0.02	0.00	-0.04	0.00	0.00	0.00	0.00	0.00
-6.5	-0.09	-0.02	-0.11	0.00	0.00	0.00	0.00	0.00
-5.9	-0.13	-0.05	-0.05	0.00	0.00	0.00	0.00	0.00
-5.2	-0.10	-0.07	-0.02	0.00	0.00	0.00	0.00	0.00
-4.5	-0.02	-0.04	-0.02	0.02	-0.11	0.00	0.00	0.00
-3.963	0.05	-0.04	-0.10	-0.05	-0.12	-0.07	-0.07	-0.07
-3.27	0.10	0.06	-0.02	-0.02	-0.03	-0.01	-0.04	-0.04
-2.864	0.10	0.09	0.01	-0.01	-0.01	0.02	-0.02	-0.03
-2.577	0.10	0.10	0.04	0.00	-0.01	0.01	0.00	-0.02
-2.171	0.08	0.09	0.07	0.02	-0.02	-0.01	0.00	-0.01
-1.884	0.07	0.09	0.09	0.04	-0.02	-0.03	0.01	-0.01
-1.191	0.03	0.05	0.06	0.03	0.03	0.02	0.01	0.00
-0.497	0.03	0.03	0.06	0.06	0.03	0.01	-0.01	0.00
-0.274	0.04	0.02	0.05	0.05	0.04	0.01	0.00	0.00
-0.051	0.04	0.02	0.04	0.05	0.03	0.01	0.00	0.00
0.196	0.05	0.02	0.03	0.03	0.03	0.03	0.02	0.01
0.419	0.06	0.03	0.02	0.02	0.03	0.03	0.02	0.01
0.642	0.07	0.04	0.02	0.00	0.01	0.02	0.02	0.01
0.873	0.08	0.05	0.02	-0.01	0.00	0.02	0.02	0.01
1.112	0.09	0.06	0.03	-0.01	0.00	0.01	0.01	0.01
1.335	0.10	0.08	0.04	0.00	0.00	0.00	0.00	0.00
1.679	0.12	0.11	0.07	0.03	0.01	0.01	0.00	0.00
2.028	0.13	0.14	0.11	0.08	0.05	0.03	0.01	0.01
2.275	0.14	0.14	0.13	0.11	0.07	0.05	0.03	0.01
3.003	0.02	-0.01	0.01	0.00	0.02	0.02	0.01	0.01

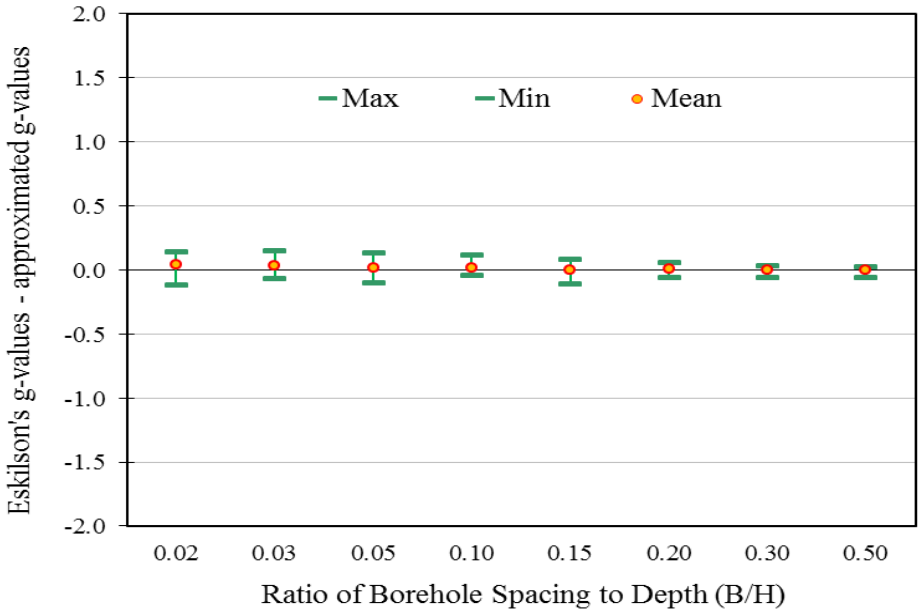

Figure B-15: Residual Plot for Rectangle Type 3×3 Multiple Boreholes

Table B-14: Difference between Approximated g-Values and Eskilson's g-Values for L-Shape Type 2×2 Multiple Boreholes

	B/H							
ln(t/ts)	0.02	0.03	0.05	0.10	0.15	0.20	0.30	0.50
-8.5	0.00	0.00	0.00	0.00	0.00	0.00	0.00	0.00
-7.8	0.03	0.00	0.00	0.00	0.00	0.00	0.00	0.00
-7.2	0.03	0.01	-0.01	0.00	0.00	0.00	0.00	0.00
-6.5	0.08	0.02	-0.03	0.00	0.00	0.00	0.00	0.00
-5.9	0.13	0.07	-0.01	0.00	0.00	0.00	0.00	0.00
-5.2	0.18	0.13	0.05	0.00	0.00	0.00	0.00	0.00
-4.5	0.17	0.18	0.11	0.02	-0.03	0.00	0.00	0.00
-3.963	0.12	0.18	0.13	-0.01	-0.08	-0.07	-0.07	-0.07
-3.27	0.02	0.14	0.18	0.07	-0.01	-0.03	-0.04	-0.04
-2.864	-0.06	0.09	0.18	0.12	0.03	0.01	-0.03	-0.03
-2.577	-0.12	0.05	0.17	0.15	0.06	0.02	-0.01	-0.02
-2.171	-0.20	-0.02	0.14	0.18	0.10	0.05	0.00	-0.02
-1.884	-0.26	-0.07	0.11	0.19	0.13	0.07	0.02	-0.01
-1.191	-0.40	-0.20	0.01	0.16	0.19	0.16	0.08	0.02
-0.497	-0.50	-0.30	-0.07	0.13	0.19	0.18	0.13	0.06
-0.274	-0.53	-0.33	-0.10	0.12	0.18	0.18	0.14	0.07
-0.051	-0.55	-0.35	-0.12	0.10	0.17	0.18	0.15	0.09
0.196	-0.57	-0.37	-0.14	0.08	0.16	0.19	0.16	0.11
0.419	-0.59	-0.38	-0.16	0.07	0.15	0.18	0.17	0.12
0.642	-0.60	-0.40	-0.17	0.05	0.14	0.17	0.17	0.13
0.873	-0.61	-0.41	-0.18	0.04	0.13	0.17	0.16	0.13
1.112	-0.62	-0.41	-0.18	0.04	0.12	0.16	0.16	0.13
1.335	-0.62	-0.41	-0.19	0.03	0.12	0.15	0.15	0.13
1.679	-0.63	-0.41	-0.18	0.04	0.12	0.15	0.15	0.13
2.028	-0.63	-0.41	-0.18	0.05	0.12	0.15	0.15	0.13
2.275	-0.64	-0.41	-0.18	0.05	0.13	0.15	0.15	0.13
3.003	-0.68	-0.47	-0.23	0.01	0.10	0.14	0.14	0.12

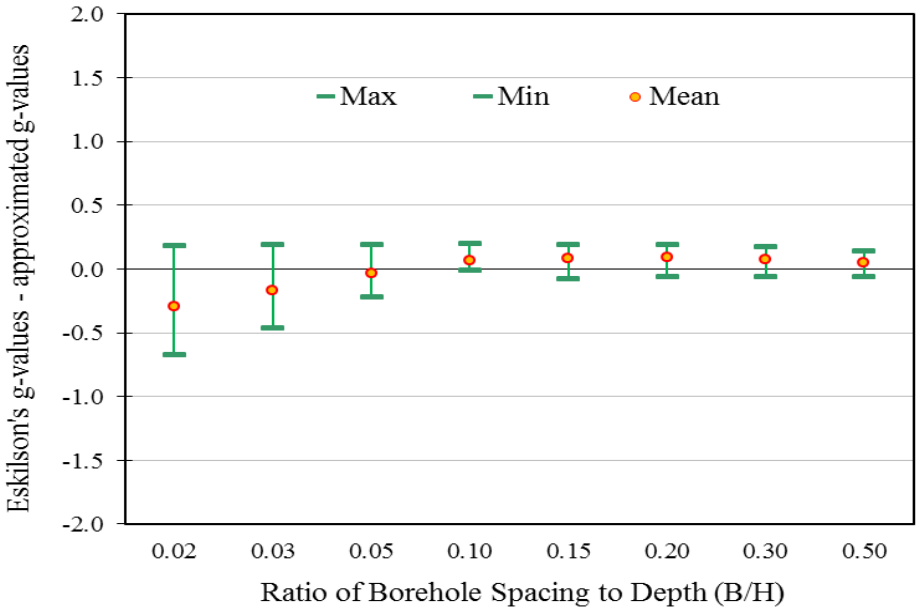

Figure B-16: Residual Plot for L-Shape Type 2×2 Multiple Boreholes

Table B-15: Difference between Approximated g-Values and Eskilson's g-Values for L-Shape Type 2×3 Multiple Boreholes

	B/H							
ln(t/ts)	0.02	0.03	0.05	0.10	0.15	0.20	0.30	0.50
-8.5	0.00	0.00	0.00	0.00	0.00	0.00	0.00	0.00
-7.8	0.03	0.00	0.00	0.00	0.00	0.00	0.00	0.00
-7.2	0.01	0.00	-0.02	0.00	0.00	0.00	0.00	0.00
-6.5	-0.01	0.00	-0.04	0.00	0.00	0.00	0.00	0.00
-5.9	-0.04	0.01	-0.02	0.00	0.00	0.00	0.00	0.00
-5.2	-0.12	-0.01	0.01	0.00	0.00	0.00	0.00	0.00
-4.5	-0.29	-0.08	0.02	0.01	-0.05	0.00	0.00	0.00
-3.963	0.11	0.11	0.05	-0.02	-0.09	-0.07	-0.07	-0.07
-3.27	0.07	0.12	0.12	0.04	-0.02	-0.02	-0.04	-0.04
-2.864	0.04	0.11	0.13	0.07	0.02	0.01	-0.03	-0.03
-2.577	0.01	0.09	0.13	0.09	0.04	0.02	-0.01	-0.02
-2.171	-0.04	0.06	0.13	0.12	0.06	0.03	0.00	-0.02
-1.884	-0.07	0.03	0.12	0.13	0.08	0.04	0.01	-0.01
-1.191	-0.15	-0.04	0.07	0.13	0.13	0.11	0.05	0.02
-0.497	-0.19	-0.08	0.04	0.13	0.14	0.13	0.08	0.05
-0.274	-0.20	-0.09	0.03	0.13	0.15	0.14	0.09	0.05
-0.051	-0.21	-0.11	0.02	0.13	0.14	0.14	0.10	0.06
0.196	-0.22	-0.11	0.01	0.11	0.14	0.15	0.12	0.08
0.419	-0.22	-0.12	0.01	0.11	0.14	0.15	0.12	0.08
0.642	-0.23	-0.12	0.00	0.10	0.14	0.15	0.12	0.09
0.873	-0.23	-0.12	0.00	0.10	0.13	0.15	0.12	0.09
1.112	-0.23	-0.12	0.00	0.10	0.13	0.14	0.12	0.09
1.335	-0.23	-0.11	0.01	0.10	0.13	0.14	0.12	0.10
1.679	-0.22	-0.10	0.02	0.12	0.14	0.14	0.12	0.10
2.028	-0.22	-0.09	0.03	0.13	0.15	0.15	0.12	0.10
2.275	-0.22	-0.09	0.04	0.14	0.16	0.16	0.13	0.10
3.003	-0.28	-0.16	-0.02	0.10	0.13	0.14	0.12	0.09

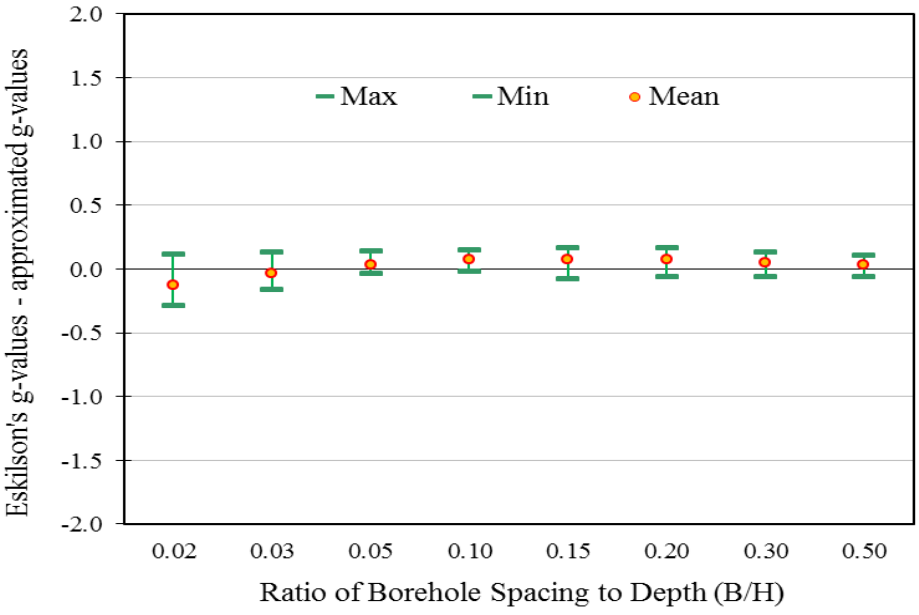

Figure B-17: Residual Plot for L-Shape Type 2×3 Multiple Boreholes

Table B-16: Difference between Approximated g-Values and Eskilson's g-Values for L-Shape Type 2×4 Multiple Boreholes

	B/H							
ln(t/ts)	0.02	0.03	0.05	0.10	0.15	0.20	0.30	0.50
-8.5	0.00	0.00	0.00	0.00	0.00	0.00	0.00	0.00
-7.8	0.03	0.00	0.00	0.00	0.00	0.00	0.00	0.00
-7.2	0.00	0.00	-0.02	0.00	0.00	0.00	0.00	0.00
-6.5	-0.03	0.00	-0.05	0.00	0.00	0.00	0.00	0.00
-5.9	-0.05	-0.01	-0.02	0.00	0.00	0.00	0.00	0.00
-5.2	-0.07	-0.02	0.01	0.00	0.00	0.00	0.00	0.00
-4.5	-0.08	-0.05	0.01	0.02	-0.06	0.00	0.00	0.00
-3.963	-0.07	-0.07	-0.06	-0.04	-0.09	-0.07	-0.07	-0.07
-3.27	-0.06	-0.06	-0.04	0.00	-0.02	-0.02	-0.04	-0.04
-2.864	-0.07	-0.05	-0.05	0.00	0.00	0.01	-0.03	-0.03
-2.577	-0.07	-0.05	-0.04	0.00	0.00	0.01	-0.01	-0.02
-2.171	-0.08	-0.06	-0.04	-0.01	0.00	0.00	0.00	-0.02
-1.884	-0.08	-0.06	-0.04	-0.01	-0.01	0.00	0.01	-0.01
-1.191	-0.09	-0.07	-0.05	-0.03	0.00	0.03	0.02	0.01
-0.497	-0.07	-0.06	-0.03	-0.01	0.00	0.01	0.02	0.03
-0.274	-0.07	-0.06	-0.03	-0.01	0.00	0.01	0.02	0.03
-0.051	-0.06	-0.05	-0.02	-0.01	0.00	0.01	0.02	0.03
0.196	-0.05	-0.05	-0.02	-0.01	0.00	0.02	0.02	0.03
0.419	-0.05	-0.04	-0.02	-0.01	0.00	0.02	0.02	0.04
0.642	-0.04	-0.03	-0.02	-0.01	0.00	0.02	0.02	0.03
0.873	-0.03	-0.02	-0.01	0.00	0.00	0.02	0.02	0.03
1.112	-0.02	-0.01	0.00	0.00	0.01	0.02	0.01	0.03
1.335	-0.02	0.00	0.01	0.01	0.01	0.02	0.01	0.03
1.679	0.00	0.02	0.03	0.03	0.03	0.03	0.01	0.03
2.028	0.00	0.03	0.05	0.06	0.05	0.04	0.02	0.03
2.275	0.00	0.04	0.06	0.07	0.06	0.05	0.03	0.03
3.003	-0.06	-0.04	0.00	0.02	0.03	0.04	0.02	0.03

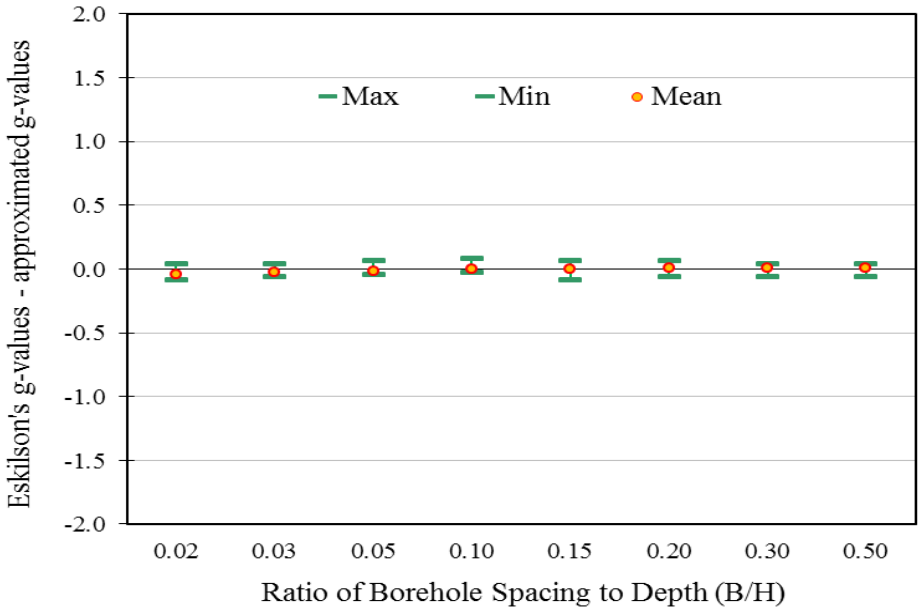

Figure B-18: Residual Plot for L-Shape Type 2×4 Multiple Boreholes

Table B-17: Difference between Approximated g-Values and Eskilson's g-Values for L-Shape Type 2×5 Multiple Boreholes

	B/H							
ln(t/ts)	0.02	0.03	0.05	0.10	0.15	0.20	0.30	0.50
-8.5	0.00	0.00	0.00	0.00	0.00	0.00	0.00	0.00
-7.8	0.03	0.00	0.00	0.00	0.00	0.00	0.00	0.00
-7.2	-0.01	0.00	-0.02	0.00	0.00	0.00	0.00	0.00
-6.5	-0.07	-0.01	-0.06	0.00	0.00	0.00	0.00	0.00
-5.9	-0.15	-0.04	-0.03	0.00	0.00	0.00	0.00	0.00
-5.2	-0.22	-0.10	-0.01	0.00	0.00	0.00	0.00	0.00
-4.5	-0.26	-0.18	-0.05	0.01	-0.06	0.00	0.00	0.00
-3.963	-0.25	-0.24	-0.15	-0.05	-0.10	-0.07	-0.07	-0.07
-3.27	-0.21	-0.24	-0.19	-0.04	-0.03	-0.02	-0.04	-0.04
-2.864	-0.17	-0.22	-0.21	-0.07	-0.02	0.00	-0.03	-0.03
-2.577	-0.13	-0.20	-0.22	-0.09	-0.03	0.00	-0.01	-0.02
-2.171	-0.09	-0.17	-0.21	-0.12	-0.05	-0.02	0.00	-0.02
-1.884	-0.05	-0.14	-0.20	-0.14	-0.08	-0.04	0.00	-0.01
-1.191	0.03	-0.08	-0.17	-0.19	-0.11	-0.04	-0.01	0.01
-0.497	0.13	0.00	-0.09	-0.16	-0.15	-0.10	-0.04	0.01
-0.274	0.16	0.03	-0.07	-0.16	-0.15	-0.11	-0.05	0.01
-0.051	0.19	0.05	-0.05	-0.14	-0.15	-0.11	-0.06	0.00
0.196	0.21	0.08	-0.03	-0.13	-0.14	-0.11	-0.07	0.00
0.419	0.24	0.11	-0.02	-0.12	-0.13	-0.11	-0.07	-0.01
0.642	0.26	0.13	0.00	-0.11	-0.13	-0.11	-0.08	-0.01
0.873	0.28	0.15	0.02	-0.10	-0.12	-0.10	-0.08	-0.02
1.112	0.30	0.17	0.04	-0.09	-0.11	-0.10	-0.09	-0.03
1.335	0.31	0.19	0.06	-0.07	-0.10	-0.10	-0.09	-0.04
1.679	0.34	0.22	0.09	-0.04	-0.08	-0.08	-0.09	-0.04
2.028	0.35	0.24	0.12	0.00	-0.05	-0.06	-0.07	-0.04
2.275	0.35	0.25	0.13	0.02	-0.03	-0.05	-0.06	-0.04
3.003	0.29	0.16	0.06	-0.04	-0.06	-0.06	-0.07	-0.04

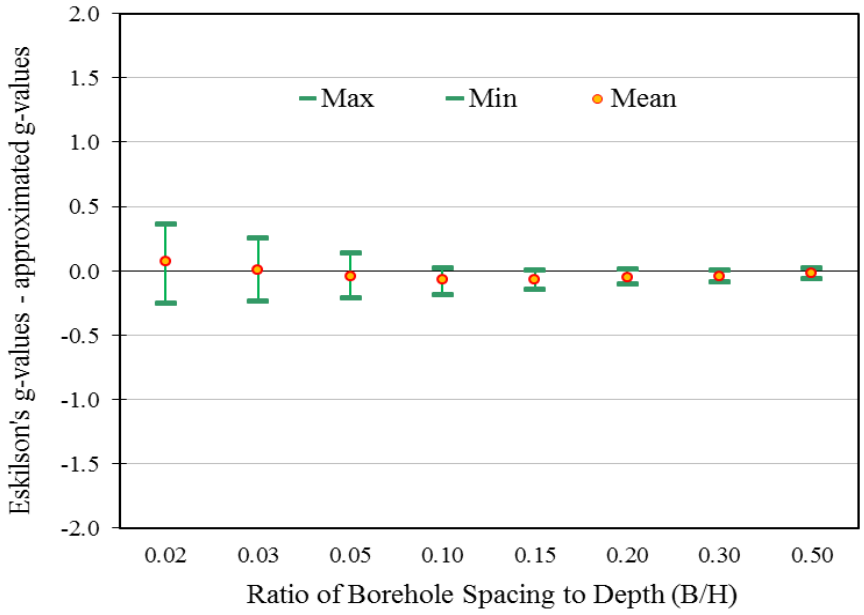

Figure B-19: Residual Plot for L-Shape Type 2×5 Multiple Boreholes